

# **SILICATE AND ALUMINATE BASED DIELECTRIC CERAMICS FOR MICROWAVE COMMUNICATION**

THESIS SUBMITTED TO COCHIN UNIVERSITY OF SCIENCE  
AND TECHNOLOGY IN PARTIAL FULFILMENT OF  
REQUIREMENT FOR THE DEGREE OF  
**DOCTOR OF PHILOSOPHY IN PHYSICS**

**SHERIN THOMAS**

*Under the guidance and supervision of*  
**Dr. M. T. Sebastian (Supervisor)**



**NATIONAL INSTITUTE FOR INTERDISCIPLINARY SCIENCE  
AND TECHNOLOGY (CSIR), THIRUVANANTHAPURAM**

**AUGUST 2010**

# **SILICATE AND ALUMINATE BASED DIELECTRIC CERAMICS FOR MICROWAVE COMMUNICATION**

THESIS SUBMITTED TO COCHIN UNIVERSITY OF SCIENCE  
AND TECHNOLOGY IN PARTIAL FULFILMENT OF  
REQUIREMENT FOR THE DEGREE OF  
**DOCTOR OF PHILOSOPHY IN PHYSICS**

**SHERIN THOMAS**

*Under the guidance and supervision of*  
**Dr. M. T. Sebastian (Supervisor)**



**NATIONAL INSTITUTE FOR INTERDISCIPLINARY SCIENCE  
AND TECHNOLOGY (CSIR), THIRUVANANTHAPURAM**

**AUGUST 2010**

## **DECLARATION**

I hereby declare that the matter presented in the thesis entitled “**SILICATE AND ALUMINATE BASED DIELECTRIC CERAMICS FOR MICROWAVE COMMUNICATION**” is the outcome of investigations carried out by me under the supervision of Dr. M. T. Sebastian, Scientist ‘G’, Materials and Minerals Division, National Institute for Interdisciplinary Science and Technology (Formerly Regional Research Laboratory) (CSIR), Thiruvananthapuram, India and the results embodied here has not been submitted elsewhere for the award of any other degree.

**Thiruvananthapuram**

**Sherin Thomas**

**Dated:**

**Dedicated to my family**



<http://w3.rrlt.csir.res.in>

Fax: ++91-(0) 471-2491712  
Phone: 4712515294 (O), 471-2446901 (R)  
E-Mail: mailadils@yahoo.com.  
mtsebastian@niist.res.in

**Council of Scientific & Industrial Research**  
**NATIONAL INSTITUTE FOR INTERDISCIPLINARY**  
**SCIENCE AND TECHNOLOGY**  
**THIRUVANANTHAPURAM- 695019. INDIA**

---

**Dr. M. T. SEBASTIAN**  
Scientist-G & Deputy Director

## **CERTIFICATE**

**This is to certify that this thesis entitled “SILICATE AND ALUMINATE BASED DIELECTRIC CERAMICS FOR MICROWAVE COMMUNICATION” is an authentic record of the investigations carried out by Ms. Sherin Thomas at the Materials and Minerals Division of National Institute for Interdisciplinary Science and Technology (Formerly Regional Research Laboratory) (CSIR), Thiruvananthapuram, India, under my supervision and guidance. This thesis or any part thereof has not been submitted elsewhere for the award of any other degree.**

**Dr. M. T. Sebastian**

**Thiruvananthapuram**

**Dated**

**(Supervisor)**

# CONTENTS

## PREFACE

## ACKNOWLEDGEMENTS

## CHAPTER 1

### INTRODUCTION

|     |  |    |    |    |
|-----|--|----|----|----|
| 1.1 | INTRODUCTION   | 2  |    |    |
| 1.2 | MICROWAVE DIELECTRIC CERAMICS  | 5  |    |    |
|     | 1.2.1 INTRODUCTION   |    | 5  |    |
|     | 1.2.2 MICROWAVE DIELECTRIC RESONATORS                                      |    |    | 5  |
|     | 1.2.2.1 HISTORICAL DEVELOPMENT OF DIELECTRIC RESONATORS                    |    |    | 6  |
| 1.3 | PHYSICS OF DIELECTRIC RESONATORS   | 9  |    |    |
|     | 1.3.1 POLARIZATION MECHANISMS IN DIELECTRICS                               |    |    | 9  |
|     | 1.3.2 CLAUSIUS - MOSSOTTI EQUATION   |    | 11 |    |
|     | 1.3.3 WORKING PRINCIPLE OF DIELECTRIC RESONATORS                           |    |    | 12 |
|     | 1.3.4 RESONANCE  | 13 |    |    |
|     | 1.3.5 MODES AND MODE NOMENCLATURE  |    | 14 |    |
| 1.4 | MATERIAL REQUIREMENTS FOR DR APPLICATIONS                                  | 16 |    |    |
|     | 1.4.1 RELATIVE PERMITTIVITY ( $\epsilon_r$ )                               | 16 |    |    |
|     | 1.4.2 HIGH QUALITY FACTOR (Q)  | 18 |    |    |
|     | 1.4.3 SMALL TEMPERATURE COEFFICIENT OF RESONANT FREQUENCY ( $\Delta f/f$ ) | 20 |    |    |
| 1.5 | FACTORS AFFECTING MICROWAVE DIELECTRIC PROPERTIES                          | 21 |    |    |
|     | 1.5.1 EFFECT OF POROSITY   |    | 22 |    |
|     | 1.5.2 EFFECT OF HUMIDITY   |    | 24 |    |
| 1.6 | APPLICATIONS OF DIELECTRIC RESONATORS                                      | 25 |    |    |
|     | 1.6.1 DIELECTRIC RESONATOR OSCILLATORS                                     |    |    | 25 |
|     | 1.6.2 DIELECTRIC RESONATOR FILTERS   |    |    | 26 |
|     | 1.6.3 DIELECTRIC RESONATOR ANTENNAS  |    |    | 27 |
| 1.7 | SUBSTRATES   | 27 |    |    |
| 1.8 | LOW TEMPERATURE CO-FIRED CERAMICS  | 29 |    |    |
|     | 1.8.1 INTRODUCTION   |    | 29 |    |
|     | 1.8.2 HISTORICAL DEVELOPMENTS IN LTCC TECHNOLOGY                           |    |    | 30 |
|     | 1.8.3 MATERIAL SELECTION AND REQUIREMENTS                                  |    |    | 33 |

|           |   |    |    |
|-----------|---|----|----|
| 1.8.3.1   | DENSIFICATION TEMPERATURE LESS THAN 950                                   | 33 |    |
| 1.8.3.2   | GLASS-CERAMIC COMPOSITES  |    | 34 |
| 1.8.3.3   | DIELECTRIC PROPERTIES   |    | 37 |
| 1.8.3.3.1 | RELATIVE PERMITTIVITY ( $\epsilon_r$ )                                    | 37 |    |
| 1.8.3.3.2 | DIELECTRIC LOSS ( $\tan \delta$ )   | 37 |    |
| 1.8.3.3.3 | TEMPERATURE STABILITY OF DIELECTRIC PROPERTIES                            |    | 38 |
| 1.8.3.4   | THERMAL PROPERTIES  |    | 38 |
| 1.8.3.4.1 | THERMAL CONDUCTIVITY  |    | 39 |
| 1.8.3.4.2 | THERMAL EXPANSION   |    | 39 |
| 1.8.3.5   | CHEMICAL COMPATIBILITY WITH ELECTRODE MATERIAL                            |    | 40 |
| 1.8.4     | APPLICATIONS OF LTCC TECHNOLOGY   |    | 41 |
| 1.9       | COMPOSITES  | 41 |    |
| 1.9.1     | INTRODUCTION  |    | 41 |
| 1.9.2     | POLYMER-CERAMIC COMPOSITES  |    | 42 |
| 1.9.3     | CONNECTIVITY  |    | 44 |
| 1.9.4     | MATERIAL REQUIREMENTS FOR ELECTRONIC PACKAGING AND SUBSTRATE APPLICATIONS |    | 45 |
| 1.9.4.1   | DIELECTRIC PROPERTIES   |    | 45 |
| 1.9.4.2   | THERMAL AND THERMO-MECHANICAL PROPERTIES                                  |    | 45 |
| 1.9.4.3   | MECHANICAL PROPERTIES   |    | 46 |
| 1.9.4.4   | CHEMICAL PROPERTIES   |    | 46 |
| 1.9.5     | ADVANTAGES OF POLYMER/CERAMIC COMPOSITES                                  |    | 47 |
| 1.10      | REFERENCES  | 48 |    |

## CHAPTER 2

### SYNTHESIS AND CHARACTERISATION

|           |   |    |    |
|-----------|---|----|----|
| 2.1       | CERAMIC PROCESSING                      | 55 |    |
| 2.1.1     | INTRODUCTION                            |    | 55 |
| 2.1.2     | SOLID STATE SYNTHESIS OF CERAMICS       |    | 56 |
| 2.1.2.1   | SELECTION AND WEIGHING OF RAW MATERIALS |    | 57 |
| 2.1.2.2   | STOICHIOMETRIC MIXING                   |    | 58 |
| 2.1.2.3   | CALCINATION                             |    | 59 |
| 2.1.2.4   | GRINDING                                |    | 59 |
| 2.1.2.5   | ADDITION OF POLYMERIC BINDER            |    | 59 |
| 2.1.2.6   | POWDER COMPACTION (UNIAXIAL PRESSING)   |    | 60 |
| 2.1.2.7   | SINTERING                               | 61 |    |
| 2.1.2.7.1 | SOLID STATE SINTERING                   |    | 62 |
| 2.1.2.7.2 | LIQUID PHASE SINTERING                  |    | 65 |

|     |   |    |    |
|-----|---|----|----|
| 2.2 | PREPARATION OF GLASS                            | 67 |    |
| 2.3 | SYNTHESIS OF POLYMER-CERAMIC COMPOSITES         | 67 |    |
|     | 2.3.1 POWDER PROCESSING METHOD                  |    | 67 |
|     | 2.3.2 SIGMA BLEND METHOD                        |    | 68 |
| 2.4 | STRUCTURAL AND MICROSTRUCTURAL CHARACTERIZATION | 69 |    |
|     | 2.4.1 X-RAY DIFFRACTOMETER                      |    | 69 |
|     | 2.4.2 SCANNING ELECTRON MICROSCOPE              |    | 70 |
|     | 2.4.3 TRANSMISSION ELECTRON MICROSCOPY          |    | 71 |
| 2.5 | MICROWAVE CHARACTERIZATION                      | 73 |    |
|     | 2.5.1 INTRODUCTION                              |    | 73 |
|     | 2.5.2 NETWORK ANALYZER                          |    | 74 |
|     | 2.5.3 MEASUREMENT OF RELATIVE PERMITTIVITY (    | 75 |    |
|     | 2.5.4 MEASUREMENT OF UNLOADED QUALITY FACTOR (Q | 78 |    |
|     | 2.5.5 MEASUREMENT OF TEMPERATURE COEFFICIENT OF |    |    |
|     | RESONANT FREQUENCY (                            | 79 |    |
|     | 2.5.6 CAVITY PERTURBATION METHOD                |    | 80 |
|     | 2.5.7 SPLIT-POST DIELECTRIC RESONATOR METHOD    |    | 82 |
| 2.6 | RADIO FREQUENCY DIELECTRIC MEASUREMENTS         | 84 |    |
| 2.7 | ERROR CALCULATIONS IN DIELECTRIC PROPERTY       |    |    |
|     | MEASUREMENTS                                    | 85 |    |
| 2.8 | THERMAL CHARACTERIZATION TOOLS                  | 85 |    |
|     | 2.8.1 THERMO GRAVIMETRIC ANALYSIS (TGA)         |    | 85 |
|     | 2.8.2 THERMO MECHANICAL ANALYSIS (TMA)          |    | 86 |
|     | 2.8.3 THERMAL CONDUCTIVITY MEASUREMENT          |    | 86 |
| 2.9 | REFERENCES                                      | 87 |    |

### CHAPTER 3

#### STRUCTURE AND MICROWAVE DIELECTRIC PROPERTIES OF $RE_4Si_3O_{13}$ [A= Sr, Ca, Ba; RE=Rare Earths] CERAMICS

|     |                   |    |
|-----|-------------------|----|
| 3.1 | INTRODUCTION      | 91 |
| 3.2 | APATITE STRUCTURE | 91 |
| 3.3 | EXPERIMENTAL      | 93 |



|         |   |     |
|---------|---|-----|
| 3.4     | RESULTS AND DISCUSSION  | 94  |
| 3.4.1   | MICROWAVE DIELECTRIC PROPERTIES OF SRRE<br>[RE= LA, PR, ND, SM, EU, GD, TB, DY, ER, TM, YB AND Y] | 94  |
| 3.4.1.1 | TAILORING THE TiO <sub>2</sub> ADDITION   | 109 |
| 3.4.2   | MICROWAVE DIELECTRIC PROPERTIES OF (Ca, Ba)RE<br>[RE= RARE EARTHS]                                | 112 |
| 3.5     | CONCLUSIONS   | 117 |
| 3.6     | REFERENCES  | 119 |

## CHAPTER 4

### MICROWAVE DIELECTRIC PROPERTIES OF NOVEL RARE EARTH SILICATE CERAMICS

|         |  |     |
|---------|--|-----|
| 4.1     | SYNTHESIS AND MICROWAVE DIELECTRIC PROPERTIES<br>OF SM <sub>2</sub> Si <sub>2</sub> O <sub>7</sub>                                       | 123 |
| 4.1.1   | INTRODUCTION   | 123 |
| 4.1.2   | EXPERIMENTAL   | 125 |
| 4.1.2.1 | SOLID STATE SYNTHESIS OF CERAMICS  | 125 |
| 4.1.2.2 | CHEMICAL SYNTHESIS OF CERAMICS   | 125 |
| 4.1.3   | RESULTS AND DISCUSSION   | 126 |
| 4.1.3.1 | STRUCTURE AND DIELECTRIC PROPERTIES OF SM <sub>2</sub> Si <sub>2</sub> O <sub>7</sub>  | 126 |
| 4.1.3.2 | PROPERTIES OF Na <sub>2</sub> SiO <sub>3</sub> CERAMIC   | 131 |
| 4.1.3.3 | EFFECT OF GLASS ADDITION ON CERAMIC  | 133 |
| 4.2     | MICROWAVE DIELECTRIC PROPERTIES OF NOVEL<br>RARE EARTH BASED SILICATES: RE <sub>2</sub> Tl <sub>2</sub> SiO <sub>9</sub> [RE=LA, PR, ND] | 142 |
| 4.2.1   | INTRODUCTION   | 142 |
| 4.2.2   | EXPERIMENTAL   | 143 |
| 4.2.3   | RESULTS AND DISCUSSION   | 144 |
| 4.3     | CONCLUSIONS  | 151 |
| 4.4     | REFERENCES   | 153 |

## CHAPTER 5

### POLYMER-CERAMIC COMPOSITES FOR MICROELECTRONIC APPLICATIONS

|     |   |     |     |
|-----|---|-----|-----|
| 5.1 | INTRODUCTION  | 157 |     |
| 5.2 | THEORETICAL MODELLING   | 160 |     |
|     | 5.2.1 RELATIVE PERMITTIVITY   |     | 160 |
|     | 5.2.2 COEFFICIENT OF THERMAL EXPANSION (CTE)  |     | 161 |
|     | 5.2.3 THERMAL CONDUCTIVITY  |     | 162 |
| 5.3 | EXPERIMENTAL  | 164 |     |
| 5.4 | RESULTS AND DISCUSSION  | 166 |     |
|     | 5.4.1 PTFE/ $\text{SM}_2\text{Si}_2\text{O}_7$ COMPOSITES   |     |     |
|     | 5.4.1.1 EFFECT OF COUPLING AGENT ON THE PROPERTIES OF PTFE/ $\text{SM}_2\text{Si}_2\text{O}_7$ COMPOSITES |     | 172 |
|     | 5.4.1.2 EFFECT OF PARTICLE SIZE ON THE PROPERTIES OF PTFE/ $\text{SM}_2\text{Si}_2\text{O}_7$ COMPOSITES  |     | 180 |
|     | 5.4.2 $\text{SM}_2\text{Si}_2\text{O}_7$ FILLED POLYETHYLENE AND POLYSTYRENE COMPOSITES                   |     | 187 |
| 5.5 | CONCLUSIONS   | 197 |     |
| 5.6 | REFERENCES  | 199 |     |

## CHAPTER 6

### ALUMINATE BASED COMPOSITES FOR LTCC AND ELECTRONIC PACKAGING APPLICATIONS

|     |  |     |     |
|-----|--|-----|-----|
| 6.1 | SYNTHESIS AND CHARACTERIZATION OF $0.83 \text{ZnAl}_2\text{O}_4$ - $0.17 \text{TiO}_2$ /GLASS COMPOSITES FOR LTCC APPLICATIONS | 204 |     |
|     | 6.1.1 INTRODUCTION   | 204 |     |
|     | 6.1.1.1 SPINELS  |     | 205 |
|     | 6.1.2 EXPERIMENTAL   | 207 |     |
|     | 6.1.3 RESULTS AND DISCUSSION   | 207 |     |
|     | 6.1.3.1 PHASE ANALYSIS   |     | 209 |

|         |  |     |
|---------|--|-----|
| 6.1.3.2 | SINTERING AND DENSIFICATION  | 210 |
| 6.1.3.3 | MICROSTRUCTURAL ANALYSIS   | 212 |
| 6.1.3.4 | MICROWAVE DIELECTRIC PROPERTIES  | 214 |
| 6.2     | POLYMER/0.83ZNA $\frac{1}{2}$ IO <sub>4</sub> -0.17TIO <sub>2</sub> COMPOSITES FOR ELECTRONIC PACKAGING APPLICATIONS | 222 |
| 6.2.1   | INTRODUCTION   | 222 |
| 6.2.2   | EXPERIMENTAL   | 223 |
| 6.2.3   | RESULTS AND DISCUSSION   | 224 |
| 6.3     | CONCLUSION   | 233 |
| 6.4     | REFERENCES   | 235 |

## CHAPTER 7

|  |     |
|--|-----|
| <b>CONCLUSIONS AND SCOPE FOR FUTURE WORK</b> | 238 |
|--|-----|

|                      |     |
|----------------------|-----|
| LIST OF PUBLICATIONS | 245 |
|----------------------|-----|

## **PREFACE**

Recently, microwave telecommunication has been developed for a wide range of applications, such as mobile phone, wireless LAN and Intelligent Transport System (ITS). Utilized microwave frequency has also increased from microwave to millimeter range in order to transmit large quantity of information with high speed. Microwave dielectric materials are continuing to play a very important role in the microwave communication systems. As a result, a large number of ceramic dielectric materials have been developed for use as dielectric resonators, capacitors, substrates and electronic packages. The key material requirements for microwave dielectric materials to be used for high frequency applications are: optimum relative permittivity, high quality factor and near-zero temperature coefficient of resonant frequency. The development of low-temperature co-fired ceramics (LTCC) has been stimulated by the benefits offered for the fabrication of miniature multilayer devices and for high level of passive integration involving the co-firing of dielectric and highly conductive metals, such as silver and copper. The present thesis entitled **“SILICATE AND ALUMINATE BASED DIELECTRIC CERAMICS FOR MICROWAVE COMMUNICATION”** is the outcome of a detailed investigation performed on the synthesis, characterization and microwave dielectric properties of some novel rare earth based silicates and aluminate. Accordingly the thesis is divided into seven chapters.

The first chapter gives a general introduction on low loss microwave dielectric ceramics and its importance in various areas of interest such as dielectric resonators, low temperature cofired ceramics, substrates and electronic packaging. A brief discussion about the relevance of polymer ceramic composites in microelectronic industry is also included. The major scientific and technological aspects, material requirements and applications of the dielectric ceramics are also given.

Chapter 2 presents the details of the preparation techniques adopted for the synthesis of dielectric resonators, LTCC materials and polymer ceramic composites. A brief description about the various characterization techniques used for the structural, microstructural and dielectric characterization in the purview of this thesis is also presented.

Chapter 3 gives a general idea on the importance of silicate materials for microwave applications and throws light into a new group of materials  $ARE_4Si_3O_{13}$  [ $A=Ca, Sr$  and  $Ba$ ;  $RE=rare\ earths$ ] belonging to the 'apatite' family for high frequency applications. The synthesizing conditions of these materials are optimized for the best properties. The structural investigations using XRD refinements and TEM revealed that they belong to  $P6_3/m$  space group with hexagonal symmetry. The materials exhibited a relative density less than 94 % which was improved to certain extent by the addition of a small amount of glass. The microwave dielectric properties of these materials are reported for the first time. The sintered ceramics has a relative permittivity ( $\epsilon_r$ ) less than about 20 and quality factor  $Q_u \times f$  up to 30000 GHz. The high  $f$  value (-46 ppm/ $^{\circ}C$ ) of  $SrLa_4Si_3O_{13}$  is tuned to a near zero value by the addition of suitable amount of  $TiO_2$ . The mixture rules are used to calculate the density,  $\epsilon_r$  and  $f$  of these ceramics and the theoretical values agree well with the experimental ones.

Chapter 4 highlights the synthesis, characterization and microwave dielectric properties of two novel rare earth based silicates [ $Sm_2Si_2O_7$  and  $RE_2Ti_2SiO_9$  ( $RE=La, Pr$  and  $Nd$ )] ceramics. The  $Sm_2Si_2O_7$  ceramics has a tetragonal symmetry whereas  $RE_2Ti_2SiO_9$  ( $RE=La, Pr$  and  $Nd$ ) dielectric ceramics possess a monoclinic symmetry. The  $Sm_2Si_2O_7$  ceramics sintered at  $1375^{\circ}C/2h$  exhibit excellent dielectric properties:  $\epsilon_r = 10$  and  $\tan \delta = 0.006$  measured at 9 GHz. The effect of various low loss glass addition on the sintering, densification and microwave dielectric properties of  $Sm_2Si_2O_7$  is

studied. The  $\text{Sm}_2\text{Si}_2\text{O}_7$  ceramics mixed with 15 wt% LBS glass lowered the sintering temperature to  $975^\circ\text{C}$ , whereas the 15 wt% LMZBS glass addition lowered sintering temperature of  $950^\circ\text{C}$ . The pure  $\text{Sm}_2\text{Si}_2\text{O}_7$  ceramics and that mixed with 15 wt% LMZBS glass did not show much variation in relative permittivity with temperature. The  $\text{RE}_2\text{Ti}_2\text{SiO}_9$  ( $\text{RE}=\text{La}, \text{Pr}$  and  $\text{Nd}$ ) ceramics exhibited a relative permittivity less than 20 and relatively low  $\tau_f$  value. A maximum value of  $Q_u \times f$  of 33500 GHz is shown by  $\text{Pr}_2\text{Ti}_2\text{SiO}_9$  ceramics. It is seen that Pr substitution for La favored the formation of solid solution in the whole range obeying Vegard's law while Nd substitution resulted in the formation of additional phases. As the Pr content increases, an improvement in the quality factor is noted whereas the  $\tau_f$  value is not much affected.

Chapter 5 discusses in detail the synthesis and characterization of various polymer ceramic composite using  $\text{Sm}_2\text{Si}_2\text{O}_7$  ceramics as filler for electronic packaging applications. The polymers used in the investigation are PTFE, Polyethylene and Polystyrene. The dielectric, thermal and mechanical properties of these polymer-ceramic composites has been investigated. The effects of coupling agent and filler particle size on the above properties of PTFE/ $\text{Sm}_2\text{Si}_2\text{O}_7$ -composites are also studied. For a filler loading of 0.5  $v_f$ , PTFE composite has  $\epsilon_r = 3.82$  and  $\tan \delta = 0.0136$  (at 9 GHz),  $k_c = 1.76 \text{ W/m}^\circ\text{C}$ ,  $\alpha_c = 36 \text{ ppm}/^\circ\text{C}$ , Vickers' microhardness of  $13 \text{ kgf/mm}^2$ ; PE composite has  $\epsilon_r = 5.28$  and  $\tan \delta = 0.0091$  (at 9 GHz),  $k_c = 2.97 \text{ W/m}^\circ\text{C}$ ,  $\alpha_c = 60 \text{ ppm}/^\circ\text{C}$ , Vickers' microhardness of  $17 \text{ kgf/mm}^2$  and PS composite has  $\epsilon_r = 4.60$  and  $\tan \delta = 0.0110$  (at 9 GHz),  $k_c = 0.29 \text{ W/m}^\circ\text{C}$ ,  $\alpha_c = 36 \text{ ppm}/^\circ\text{C}$ , Vickers' microhardness of  $56 \text{ kgf/mm}^2$ . Several theoretical model approaches have been employed to predict the relative permittivity, thermal conductivity and coefficient of linear expansion of the composite systems and the results were compared with that of

*experimental data. All theoretical predictions were found to be valid for low filler contents.*

*Chapter 6 outlines the applicability of 0.83 ZnAl<sub>2</sub>O<sub>4</sub>-0.17 TiO<sub>2</sub> (ZAT) dielectric ceramic based glass and polymer composites for LTCC substrate and electronic packaging applications respectively. The ZAT dielectric ceramic possess excellent thermal and microwave dielectric properties but with a high sintering temperature of 1450°C. The first section of the Chapter 6 discusses the efforts taken to reduce the sintering temperature by glass addition for use as LTCC substrate material. Among the various glasses added, BBSZ is found to lower the sintering temperature without much affecting the microwave dielectric properties. The XRD and SEM of BBSZ glass added ZAT composites suggested the existence of no additional secondary phases. The addition of 10 wt% BBSZ glass reduced the sintering temperature to 950°C with reasonably good microwave dielectric properties. The composites also possessed high chemical compatibility with silver. The results bring out the possibility of using ZAT/10 wt% BBSZ composites for LTCC substrate applications. The second section of this chapter compares the physical, dielectric and thermal properties of ZAT loaded PTFE and PE composites. The PE/ZAT composites possessed a high relative density when compared with the PTFE/ZAT composites. For lower filler content the fillers are uniformly dispersed in the matrix and as the filler content increased the agglomeration also increased and resulted in porosity. The dielectric properties of both the composites showed that ZAT loaded with PE composites exhibited good dielectric properties and also a very low water absorption value of less than 0.1 %. The results show that ZAT filler loaded composites have better properties than that loaded with Sm<sub>2</sub>Si<sub>2</sub>O<sub>7</sub> filler and can be used for electronic packaging applications.*

*The seventh chapter gives the conclusion of the thesis and scope for future work.*

**\*\*\*\*\*ACKNOWLEDGEMENTS\*\*\*\*\***

*I present this report, in the name of God, the Almighty, who kindly showers HIS unperturbed concern, grace and blessings throughout my life.*

*I wish to express my deepest sense of gratitude to Dr. M. T. Sebastian, (Scientist 'G', National Institute for Interdisciplinary Science and Technology, Thiruvananthapuram), my guide, mentor and supervisor. I am deeply indebted to him for suggesting this research problem and for his efficient guidance, creative discussions, constant encouragement and support.*

*I am grateful to Dr. Suresh Das, Director, National Institute for Interdisciplinary Science and Technology (NIIST), Dr. B. C. Pai and Prof. T. K. Chandrasekhar, (Former Directors, NIIST, Thiruvananthapuram) for kindly providing the facilities to carry out my research work.*

*I wish to express my sincere thanks to Dr. Manoj Raama Varma (Scientist E-II, NIIST, Thiruvananthapuram) and Dr. Jose James (Scientist F, NIIST, Thiruvananthapuram) for their fruitful scientific discussions and advices during my work.*

*I am indebted to Dr. K. G. K. Warriar (Head, Materials and Minerals Division, NIIST, Thiruvananthapuram), Dr. U. Shyama Prasad, Dr. P. Prabhakar Rao (Scientists, MMD, NIIST, Thiruvananthapuram) and Dr. Peter Koshy for their help rendered during the course of this work.*

*I wish to express my heartiest thanks to Prof. P. Mohanan (Department of Electronics, CUSAT, Kochi) for dielectric measurements and Prof. Jacob Philip (Director, Sophisticated Testing and Instrumentation Centre, CUSAT, Kochi) for thermal conductivity measurements for the present study.*

*I want to record thanks to Mr. P. Chandran, Mr. P. Gurusamy, Mr. Robert Philip and Mr. P. Mukundan for extending the XRD, SEM, TEM and thermal measurement facility for this research work. I am thankful to all the office and library staff at NIIST for all the help and cooperation.*

*I have been privileged to collaborate with Dr. Rick Uvic and Dr. Lii-Cherng Leu, Boise State University, USA, and extend my sincere thanks for the Transmission Electron Microscopy of the ceramics presented in the thesis.*

*The creative suggestions and valuable advice given by my seniors in the lab, Dr. N. Santha, Dr. K. P. Surendran (University of Aviero, Portugal), Dr. P. V. Bijumon (Research in Motion, Canada), Dr. L. A. Khalam (Sel. Grade Lecturer, Iqbal College, Thiruvananthapuram), Dr. G. Subodh (University of Stuttgart, Germany) and Dr. H. Sreemoolanadhan (Scientist, VSSC,) are thankfully*



## *Acknowledgements*

*remembered. I would like to thank Dr. P. S. Anjana, (Lecturer, All Saints College, Thiruvananthapuram) for the invaluable support, timely advices and suggestions rendered throughout this period.*

*I would like to thank all my colleagues and friends in the Materials and Minerals Division of NIIST especially, Dr. Sumesh George, Mr. Tony Joseph, Ms. K. S. Deepa, Ms. T. S. Sasikala, Ms. P. Nisha, Ms. C. P. Resmi, Mr. Dhanesh Thomas, Ms. P. Neenulekshmi, Mr. K. M. Manu, Ms. K. Anlin Lazar, Ms. K. T. Rethika and Dr. Savitha S. Pillai for their support, love and positive criticism. I would like to thank Mr. Jithesh Kavil for rendering all the help, support and suggestions during chemical synthesis. The constant support, help and companionship offered by Ms. J. Chameswary is also thankfully remembered. I am also thankful to Ms. Asha Pramod, Ms. L. Shamlam, Dr. P. C. Rajath Varma, Ms. R. Rejini, Ms. B. R. Priya Rani, Ms. K. S. Sandhya, Ms. S. Renjini, Ms. Ali Fathima, Ms. V. Madhumitha, Mr. Sudeep, Mr. M. A. Sanoj and Mr. Suresh who helped me in many ways during my research work. At this venture I would also like to thank all the M. Sc and M. Tech. project students especially Ms. B. Sayoojyam, Mr. V. K. Sajith, Mr. Vineeth Venugopal and Mr. Jobin Varghese.*

*The help and support given by Ms. M. N. Suma, Mr. V. Deepu, Mr. Sujith Raman (Department of Electronics, CUSAT), Dr. Manjusha, Ms. V. Viji and Ms. Uma (STIC, CUSAT) are greatly acknowledged.*

*I would like to thank Defence Research and Development Organisation (DRDO) and Council of Scientific and Industrial Research (CSIR), Government of India for providing me the research fellowship.*

*I owe an unlimited debt of gratitude to my parents, my sister and my brother-in-law who have enlighten my paths with their invaluable advice, support and encouragement that contributed a lot to shape my career. My husband has shown indefinable patience, love and support which helped me a lot for the successful completion of this work.*

*Last but not least, I offer my regards to all of those who supported me in any respect during the completion of this work. I remember that the care and support from all these people gave me the confidence, their encouragement means so much to me throughout those countless hard-working days and nights.*

**Sherin Thomas**

# CHAPTER 1

## INTRODUCTION

*This chapter gives an introduction and overview of progress of research in dielectric resonators (DR) and low temperature co-fired ceramics (LTCC). The various scientific and technological features of polymer-ceramic composites for substrate and electronic packaging applications are also discussed. The fundamental physical aspects, working principle and some of the practical applications of DR's are briefly depicted. The chapter also cites the important characteristics required for a material for LTCC, electronic packaging and substrate applications.*

## 1.1 INTRODUCTION

COMMUNICATION IS THE FUNDAMENTAL ASPECT OF SOCIAL INTERACTION. THE PROGRESSIVE TECHNOLOGICAL ADVANCES OF THE 19TH CENTURY BROUGHT PROFOUND CHANGES IN COMMUNICATION WHICH WERE PREVIOUSLY LIMITED TO PRIMITIVE HAND-DELIVERY OF MESSAGES. THE 'SEMAPHORE'. THE INTRODUCTION OF ELECTRICITY LED TO THE DEVELOPMENT OF THE TELEGRAPH. THE BIRTH OF THE TELECOMMUNICATIONS INDUSTRY IN 1895, WHEN GUGLIELMO MARCONI OPENED THE WAY FOR MODERN WIRELESS COMMUNICATION BY TRANSMITTING THE THREE DOTS AND DASH CODE FOR THE LETTER 'S' OVER A DISTANCE OF THREE KILOMETERS USING ELECTROMAGNETIC WAVES. THAT THE WIRELESS COMMUNICATION DEVELOPED INTO A KEY ELEMENT OF MODERN COMMUNICATION. THE LAST FEW DECADES HAVE WITNESSED A PROLIFERATION OF INTERPERSONAL COMMUNICATION TECHNOLOGIES. DEMAND WITHIN THE ELECTRONICS AND TELECOMMUNICATION INDUSTRIES HAS GROWN RAPIDLY WITH CONTINUAL REQUIREMENTS FOR LOWER COST AND BETTER PERFORMANCE. THE END USER. THE WIRELESS TECHNOLOGY HAS BEEN THE FASTEST-GROWING INDUSTRY IN THE WORLD UNTIL NOW. A PRIME EXAMPLE IS MOBILE TECHNOLOGY, WHICH HAS SEEN A RAPID EXPANSION OVER THE LAST TEN YEARS, AND WITH REDUCTION IN COST OF SYSTEMS, THE TECHNOLOGY IS NOW READILY AVAILABLE TO ALL. EVEN OUR COUNTRY HAVE WITNESSED THE RAPID GROWTH OF MOBILE PHONE WIZARD THAN ANY OTHER NEW TECHNOLOGICAL INNOVATIONS, BOTH IN RURAL AND URBAN AREAS ATTRACTING PEOPLE BY THE AFFORDABILITY AND MANY OTHER BENEFITS AND FACILITIES. ACCORDING TO A RECENT SURVEY, THE INDIAN TELECOMMUNICATION INDUSTRY IS ONE OF THE WORLD'S FASTEST-GROWING INDUSTRIES AND THE SECOND LARGEST TELECOMMUNICATION NETWORK IN THE WORLD (BEING CHINA) WITH ABOUT 654 MILLION TELEPHONE SUBSCRIBERS AND ABOUT 620 MILLION MOBILE PHONE CONNECTIONS. IT IS PROJECTED THAT INDIA WILL HAVE NEARLY 1.16 BILLION MOBILE PHONE SUBSCRIBERS BY 2013 [1]. MOBILE PHONE NETWORKS ALLOW COMMUNICATION FROM ANYWHERE VIA ANTENNAS LOCATED ON MASTS AND ASSOCIATED BASE STATIONS.

TODAY, MICROWAVES ARE EMPLOYED BY TELECOMMUNICATION INDUSTRIES IN THE FIELD OF BOTH TERRESTRIAL RELAYS AND SATELLITE COMMUNICATIONS. THE TECHNOLOGY USED IN MICROWAVE COMMUNICATION WAS DEVELOPED IN THE EARLY 1940'S BY WESTERN UNION. THE FIRST MICROWAVE MESSAGE WAS SENT IN 1945 FROM TOWERS LOCATED IN NEW YORK AND PHOENIX. FOLLOWING THIS SUCCESSFUL ATTEMPT, MICROWAVE COMMUNICATION BECAME THE MOST COMMONLY USED DATA TRANSMISSION METHOD FOR TELECOMMUNICATIONS SERVICES.

FREQUENCIES RANGING FROM 300 MHz-30 GHz ARE USUALLY CALLED "MICROWAVE". FREQUENCIES ABOVE ABOUT 30 MHz CAN PASS THROUGH THE IONOSPHERE AND SO ARE USED FOR COMMUNICATING WITH SATELLITES AND OTHER EXTRA-TERRESTRIAL SOURCES. AT HIGH FREQUENCIES, MICROWAVES HAVE THE ADVANTAGE OF BEING ABLE TO CARRY MORE INFORMATION THAN ORDINARY RADIO WAVES AND ARE CAPABLE OF BEING BEAMED DIRECTLY FROM ONE PLACE TO ANOTHER. FIG. 1.1 SHOWS THE MICROWAVE FREQUENCY SPECTRUM AND THE APPLICATIONS IN THE VARIOUS FREQUENCY BANDS [2]. WITH CONTINUING ADVANCES IN MICROWAVE DEVICES, NEW SYSTEMS ARE BEING DEVELOPED FOR MILLIMETER PORTION OF THE MICROWAVE BAND.

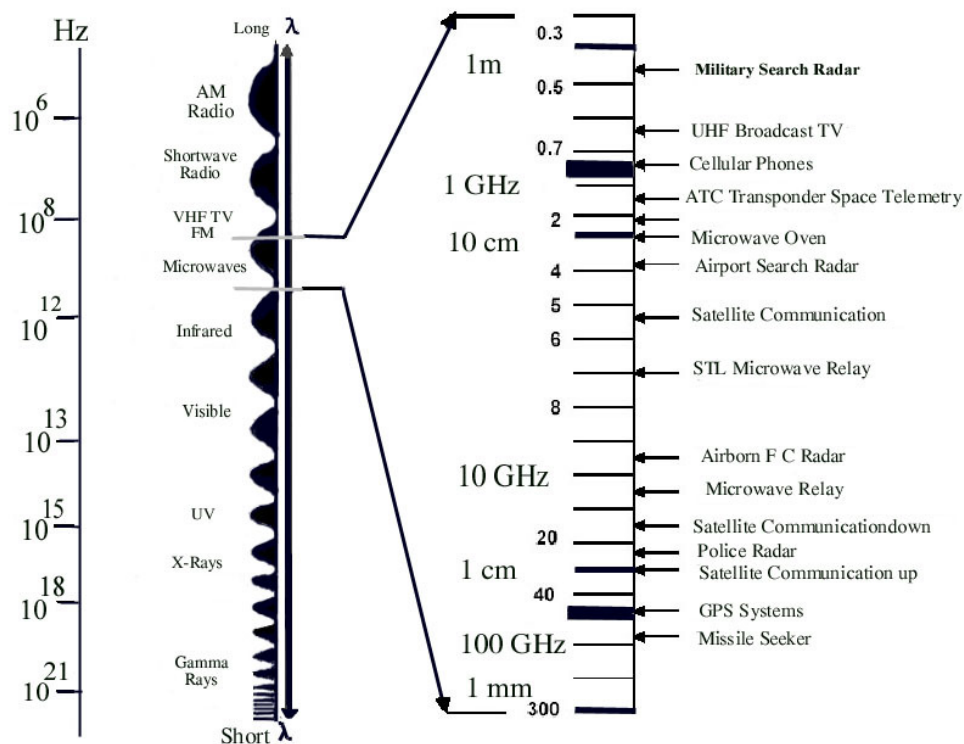


Fig. 1.1 Microwave spectra and its applications.

THE DEMAND FOR CERAMICS IN ELECTRONIC EQUIPMENTS IS GROWING RAPIDLY AND THIS IS DUE TO THE SUPERIOR PHYSICAL PROPERTIES AND IMMENSE TECHNOLOGICAL APPLICATIONS OF CERAMICS. IN THE PAST FIVE YEARS, CERAMICS HAVE UNDERGONE A REVOLUTION ALMOST AS DRAMATIC AS THE REVOLUTION THAT TOOK PLACE IN FAMILIAR ONE IN ELECTRONICS. NOVEL APPROACHES FOR PREPARING AND PROCESSING CERAMICS HAVE BEEN DEVELOPED. TODAY'S ADVANCED CERAMICS REPRESENT DEVELOPMENTS IN

THE IMAGINATION OF EVEN THE FEW FARSIGHTED SCIENTISTS OF 25 YEARS AGO WHO FIRST REALIZED THE REMARKABLE POTENTIAL OF CERAMIC SOLIDS AND ESTABLISHED DUCTILE ENGINEERING AS A SUITABLE OBJECTIVE FOR MATERIALS RESEARCHERS TO PURSUE. DESIGNERS ARE NOW USING CERAMIC SOLUTIONS IN ELECTRICAL SYSTEMS, AND THE MATERIAL OFTEN PROVIDES AN AFFORDABLE SOLUTION TO MANY OF THE ISSUES THAT NEED TO BE OVERCOME. THE WORD CERAMIC ORIGINATED FROM THE GREEK WORD 'KERAMOS' ~~CAN BE DEFINED AS~~, *but may be other inorganic elements in combination with well-defined crystal lattice structures. They are generally hard, brittle and have very high melting points* [3].

DIELECTRIC CERAMIC MATERIALS HAVE BEEN STUDIED FOR DECADES DUE TO BOTH THEIR USES IN IMPORTANT TECHNOLOGIES AND THE FUNDAMENTALLY INTERESTING RELATIONSHIPS BETWEEN CRYSTAL CHEMISTRY, CRYSTAL STRUCTURES AND PHYSICAL PROPERTIES. THE PERFORMANCE OF MICROELECTRONIC DEVICES DEPENDS INCREASINGLY ON A SOPHISTICATED CERAMIC IN WHICH INDIVIDUAL COMPONENTS ARE LOCATED ON COMPLEX SUBSTRATES COMBINED WITH NECESSARY POWER DISTRIBUTION LINES AND INTERCONNECTS. THESE SUBSTRATES COMBINE MULTIPLE LAYERS OF CERAMIC, METAL AND THIN FILM ORGANIC INSULATORS. THE FABRICATION OF THESE SUBSTRATES IS MADE DIFFICULT BY A NUMBER OF PROBLEMS, PROMINENT AMONG WHICH IS ENSURING ADHESION BETWEEN THE DIFFERENT COMPONENTS. THE MOST COMMONLY USED CERAMIC IN MICROELECTRONICS IS ALUMINA. IT HAS A HIGH RELATIVE PERMITTIVITY WHICH REDUCES THE LOSS OF THE ELECTRICAL SIGNAL TRANSMISSION. CERAMICS WITH LOWER RELATIVE PERMITTIVITY ARE PREFERABLE BUT NONE OF THE PRESENT ALTERNATIVES IS AS EASILY PROCESSED AS ALUMINA. MICROELECTRONIC PACKAGING REQUIREMENTS FOR LOW TEMPERATURE SINTERING, HIGH PERMITTIVITY AND CONTROLLED THERMAL EXPANSION CANNOT BE MET BY CONVENTIONAL CERAMIC MATERIALS SUCH AS ALUMINA. NEW MULTIPHASE COMPOSITES OFFER MANY OF THE DESIRED PROPERTIES, BUT THE RELATIONSHIPS BETWEEN STRUCTURE AND PROPERTY ARE HIGHLY COMPLEX. THUS THE ELECTRONIC CERAMIC INDUSTRY IS MOVING TOWARDS CHEMICALLY SYNTHESIZED CERAMIC POWDERS IN WHICH SOL-GEL AND OTHER INNOVATIVE TECHNIQUES YIELD MATERIALS THAT CAN BE FORMED AND SINTER MORE READILY AND YIELD MORE ACCEPTABLE PHYSICAL PROPERTIES.

## 1.2 MICROWAVE DIELECTRIC CERAMICS

### 1.2.1 INTRODUCTION

THE REVOLUTION IN WIRELESS COMMUNICATIONS AND INFORMATION ACCESS IS MOST DRAMATIC CHANGES IN TECHNOLOGY IN THE PAST DECADE. AS IN ALL TECHNOLOGY THE BASIS OF THESE REVOLUTIONARY CHANGES IS ADVANCES IN MATERIALS. WITH THE GENERATION OF MICROELECTRONIC DEVICES NEW AND MORE STRINGENT DEMANDS ARE BEING PLACED ON THE MATERIALS BEING USED. AMONG THE VARIOUS BRANCHES OF FUNCTIONAL CERAMICS, THE CERAMIC INDUSTRY IS OF PRIMARY INTEREST CHARACTERIZED BY RAPID INNOVATION AND TECHNOLOGICAL ADVANCES. ONE OF THE MAJOR ACHIEVEMENTS OF ELECTRONIC CERAMICS IS THE RECOGNITION OF POTENTIAL USEFULNESS OF DIELECTRIC MATERIALS AS ENERGY STORAGE DEVICES, OSCILLATORS AND FILTERS FOR THE MICROWAVES CARRYING THE DESIRED INFORMATION. THESE APPLICATIONS NOW CONSTITUTE THE MAJOR MARKET FOR ADVANCED CERAMICS USED AS SUBSTRATES, CAPACITORS, PIEZOELECTRICS AND RESISTORS. THESE MATERIALS ARE NOW EMPLOYED AS BULK CERAMICS IN MICROWAVE COMMUNICATION DEVICES; THEY ARE NOT INTEGRATED INTO THE MICROELECTRONICS BUT ARE FOUND AS DISCRETE COMPONENTS. SOME OF THE APPLICATIONS OF ELECTRONIC CERAMICS IN TELECOMMUNICATION INDUSTRY ARE DISCUSSED BELOW.

### 1.2.2 MICROWAVE DIELECTRIC RESONATORS

THE NEED FOR COMMUNICATION SYSTEMS USING MICROWAVES ARE INCREASING DUE TO THE INCREASE IN DEMAND FOR EXCHANGE OF INFORMATION VIA WIRELESS COMMUNICATIONS. DIELECTRIC RESONATORS ARE IMPORTANT COMPONENTS IN MICROWAVE COMMUNICATION CIRCUITS. THEY FORM AN IMPORTANT PART OF RADIO RECEIVERS AND CELL PHONES. A MICROWAVE CIRCUIT WORKS WHEN THE DIELECTRIC RESONATOR VIBRATES OR “RESONATES” AT A SPECIFIC FREQUENCY. TYPICALLY MADE OF QUARTZ OR CERAMIC, THESE DEVICES PERFORM THE CRITICAL FUNCTION OF PICKING OUT THE FREQUENCY OF THE DESIRED SIGNAL FROM THE CACOPHONY OF TRANSMISSIONS IN THE AIRWAVES. HOWEVER, QUARTZ RESONATORS ARE UNATTRACTIVE AT MICROWAVE FREQUENCIES DUE TO THE SMALL SIGNAL TO NOISE RATIO, FREQUENCY MULTIPLICATION AND THEIR BULKY NATURE. ONE CAN NO LONGER RELY ON QUARTZ CHOICES BUT HAS TO SEARCH FOR ALTERNATIVES. THUS THE METALLIC CAVITY RESONATOR WAS DEVELOPED, WHICH ALSO PROVED TO BE BULKY AND NON-INTEGRABLE FOR MICROWAVE COMMUNICATION CIRCUITS (MIC). LATER ON MICROSTRIP RESONATORS EMERGED WHICH HAD POOR THERMAL

AND HIGH DIELECTRIC LOSS. THUS THE MINIATURIZATION WAS POSSIBLE IN COMMUNICATIONS BY COMPROMISING ON THE QUALITY FACTOR AND TEMPERATURE STABILITY. NEXT AT THE USE OF CERAMIC PIECES WHICH ARE DESIGNED TO BE DIELECTRIC RESONATORS, RESONANT FREQUENCY OF THE CARRIER SIGNAL TO ALLOW THAT SIGNAL TO BE EFFICIENTLY SEPARATED FROM OTHER SIGNALS IN THE MICROWAVE BAND. THIS LED TO A BOOMING DEVELOPMENT OF NOVEL MICROWAVE DIELECTRIC RESONATORS. A Dielectric Resonator (DR) CAN BE DEFINED AS “*electromagnetic component, which is a ceramic puck that exhibits resonance with useful properties for a narrow range of frequencies.*” THE RESONANT FREQUENCY OF THE DIELECTRIC RESONATOR COMPONENT DEPENDS ON THE RELATIVE PERMITTIVITY OF THE DIELECTRIC AND THE SIZE OF THE RESONATOR [4]. CERAMIC DIELECTRIC MATERIALS ARE USED TO FORM THERMALLY STABLE DIELECTRIC RESONATORS AS KEY COMPONENTS IN A NUMBER OF MICROWAVE SUBSYSTEMS WHICH ARE USED IN A RANGE OF CONSUMER AND COMMERCIAL MARKET PRODUCTS. THE SIZE OF THE RESONATOR AT A PARTICULAR FREQUENCY DEPENDS ON THE INVERSE OF THE SQUARE ROOT OF THE RELATIVE PERMITTIVITY ( $\epsilon_r$ ) OF THE MATERIAL. THUS DIELECTRIC CERAMIC MATERIALS ARE GENERALLY REQUIRED TO HAVE A HIGH RELATIVE PERMITTIVITY TO MEET A DEMAND FOR SIZE REDUCTION OF DEVICES, A SMALL DIELECTRIC LOSS IN HIGH FREQUENCY REGIONS AND A SMALL CHANGE IN RESONANT FREQUENCY WITH TEMPERATURE CHANGE. UNTIL RECENTLY, THE OXIDE AND NITRIDE OF SILICON HAVE BEEN USED EXCLUSIVELY FOR DIELECTRIC APPLICATIONS. NOW, BOTH LOW AND HIGH PERMITTIVITY CERAMICS ARE NEEDED FOR DIFFERENT APPLICATIONS.

### 1.2.2.1 HISTORICAL DEVELOPMENT OF DIELECTRIC RESONATORS

THE TERM “DIELECTRIC RESONATOR” WAS FIRST USED IN 1939 BY RICHTMEYER AT STANFORD UNIVERSITY WHO SUGGESTED THE POSSIBILITY OF USING UNMETALLIZED DIELECTRIC RESONATORS. HE INVESTIGATED THEORETICALLY THE RESONANT PROPERTIES OF TOROIDAL AND RING SHAPED DIELECTRIC MATERIALS. HOWEVER, HIS THEORETICAL INVESTIGATIONS FAILED TO ATTRACT SIGNIFICANT INTEREST AND PRACTICALLY NOTHING HAPPENED IN THIS AREA FOR OVER 15 YEARS. IN 1953, SCHLICHE [6] REPORTED THE APPLICATION OF SUPER-HIGH RELATIVE PERMITTIVITY CERAMICS ( $\epsilon_r \sim 1000$ ) AS CAPACITORS IN LOW RADIO FREQUENCIES. IN THE 1960'S, SEVERAL WORKERS INVESTIGATED THE BEHAVIOR OF DIELECTRICS AT MICROWAVE FREQUENCIES AND TRIED TO APPLY THEM TO THE MICROWAVE DEVICES. FOR EXAMPLE, THE DIELECTRIC CERAMICS AT MICROWAVE

FREQUENCY WAS MEASURED AND ITS MECHANISM WAS DISCUSSED BY SILVERMAN FAR INFRARED DISPERSION WAS INVESTIGATED BY SPATZER AND BARASH REPORTED X-BAND UNLOAD Q OF 9000 AT ROOM TEMPERATURE FOR RUTILE RESONATORS. THE STUDIES OF RESONATOR MATERIALS COMMENCED WITH THE WORK OF COHN [9] IN THE RUTILE ( $\text{TiO}_2$ ) CRYSTALS WHICH EXHIBITED RELATIVE PERMITTIVITY VALUE AND HIGH HOWEVER, THE FILTER USING IT WAS NOT PUT INTO PRACTICAL USE BECAUSE OF ITS LARGE TEMPERATURE VARIATION OF RESONANT FREQUENCY. ABOUT THE 1950s DURING INVESTIGATIONS BY BOLTON [10] ON HIGH PERMITTIVITY TUNGSTEN BRONZE-STRUCTURE  $\text{LN}_2\text{O}_3\text{-TiO}_2$  ACHIEVED TEMPERATURE STABILITY AND RELATIVE PERMITTIVITIES OF 60–80 *et al.* [11] NOTED THAT THE WORK OF BOLTON WAS RARELY ACKNOWLEDGED IN SUBSEQUENT BUT PROVIDED THE TECHNICAL FOUNDATION FOR THE INVESTIGATIONS OF TUNGSTEN BRONZE TYPE MATERIALS.

BY THE LATE 1970'S AND EARLY 1980'S THERE WAS INTEREST IN A RANGE OF MATERIALS INCLUDING  $\text{MgTiO}_3$ ,  $(\text{Zr,Sn})\text{TiO}_3$  AND  $\text{BaTiO}_3$  [12]. TEMPERATURE STABLE MICROWAVE DRs WERE DEVELOPED BY KONISHI [13] AND PLOUDRE [14] UTILIZING THE COMPOSITE STRUCTURE OF POSITIVE AND NEGATIVE TEMPERATURE COEFFICIENTS. HOWEVER, THE DR RESONATOR WAS NOT USED IN PRACTICE, BECAUSE OF TOO PRECISE AND CARE NECESSARY MATERIAL PREPARATION PROCESS, MACHINING AND ASSEMBLING. PLOURDE AND REN [15] REPORTED THAT THE MAXIMUM QUALITY FACTOR WAS AROUND 36,000 GHZ, WITH TEMPERATURE COEFFICIENT OF 40. LATER, A MODIFIED BARIUM TETRATITANATE WITH IMPROVED PERFORMANCE WAS REPORTED FROM BELL LABORATORIES [16]. THE NEXT MAJOR BREAKTHROUGH CAME WHEN THE MURATA MANUFACTURING COMPANY [17] PRODUCED DRs. SINCE THEN THEY OFFERED ADJUSTABLE COMPOSITIONS SO THAT THE TEMPERATURE COEFFICIENT COULD VARY BETWEEN +10 AND -22 PPM. THESE COMPONENTS BECAME COMMERCIALY AVAILABLE AT REASONABLE PRICES. AFTERWARDS, THE EXPERIMENTAL AND THEORETICAL WORK AS WELL AS DRs EXPANDED RAPIDLY.

THE GROWTH OF THE MOBILE COMMUNICATIONS MARKET IN THE 1990'S STIMULATED RESEARCH IN MICROWAVE DIELECTRICS, PARTICULARLY FOR HIGH RELATIVE PERMITTIVITY (~75–90) FOR MOBILE TELEPHONE HANDSET APPLICATIONS AND VERY HIGH PERMITTIVITY (AT 3 GHZ) FOR BASE STATION APPLICATIONS. FOR THE FORMER TUNGSTEN BRONZE



STRUCTURED MATERIALS (FOR EXAMPLE, B1) REMAINED THE PRIMARY CHOICE, WHILST COMPLEX PEROVSKITES (FOR EXAMPLE, B4-29) PROVIDED THE HIGHEST Q VALUES FOR THE BASE STATIONS. A STRIKING FEATURE IS THE GAP IN THE MATERIALS WITHIN THE RANGE 45-75. REANEY AND IDDLES [18] HIGHLIGHTED THE FACT MATERIALS WITH 45-75, WITH HIGH Q VALUE AND ZERO LOSS DO NOT CURRENTLY EXIST. TODAY ABOUT MORE THAN 1500 MICROWAVE DIELECTRIC CERAMICS HAVE BEEN INVESTIGATED FOR APPLICATIONS [2]. CURRENTLY AVAILABLE FOR PRACTICAL PURPOSES WHICH POSSESS EXCELLENT DIELECTRIC PROPERTIES INCLUDE,  $[(\text{Mg}, \text{Fe})_{1-x}(\text{Sn}, \text{Mg})_x \text{Ta}_{2/3}] \text{O}_3$  [19],  $\text{Ba}(\text{Mg}_{1-x}\text{Ta}_{2/3})\text{O}_3$  [20],  $(\text{Zr}, \text{Sn})\text{TiO}_3$  [21],  $\text{Ba}_2\text{Tl}_9\text{O}_{20}$  [22],  $(\text{Ba}, \text{Sr})\text{O}-\text{REO}_3-\text{TiO}_2$  [23],  $\text{Ba}[(\text{Zn}_{0.7}\text{Co}_{0.3})_{1/3}\text{Nb}_{2/3}]\text{O}_3$  ETC. IT IS NOTEWORTHY THAT STILL DR MATERIALS ARE NEEDED WITH A WIDE VARIETY OF DIELECTRIC PROPERTIES TO MEET THE EVER-GROWING DEMAND FOR WIRELESS DEVICES. HENCE SEARCH IS CONTINUING TO FIND NEW MATERIALS AS WELL AS IMPROVE PROPERTIES OF EXISTING MATERIALS.

AS A RESULT OF THE VAST DEVELOPMENT IN THE TELECOMMUNICATION INDUSTRY, UTILIZED FREQUENCY HAS ALSO INCREASED FROM MICROWAVE TO MILLIMETER-WAVE. A LARGE QUANTITY OF INFORMATION MUST BE TRANSPORTED WITH HIGH SPEED. DIELECTRIC MATERIALS FOR MILLIMETER-WAVE USE ARE REQUIRED TO HAVE HIGH Q, LOW QUALITY FACTOR, RELATIVE PERMITTIVITY AND SMALL TEMPERATURE COEFFICIENT OF RESONANT FREQUENCY. HENCE NEW MATERIALS WITH LOW RELATIVE PERMITTIVITY NEED TO BE EXPLORED. FROM THIS PERSPECTIVE MANY ALUMINATE AND SILICATE BASED DIELECTRIC CERAMICS HAVE ATTRACTED ATTENTION.  $\text{ZnAl}_2\text{O}_4$  [24],  $\text{MgAl}_2\text{O}_4$  [25],  $\text{Mg}_2\text{SiO}_4$  [26],  $\text{Zn}_2\text{SiO}_4$  [27-28],  $\text{Al}_2\text{O}_3$  [29-30],  $\text{Mg}_4\text{Nb}_2\text{O}_9$  [31-32] AND  $\text{Sr}_3\text{Mg}_2\text{O}_{12}$  [33] GARNET CERAMICS HAVE BEEN INVESTIGATED AS POTENTIAL CANDIDATE MATERIALS FOR MILLIMETER-WAVE DEVICES. THE NEXT GENERATION OF SPECTRAL CROWDING AND COMMERCIAL REALITIES CREATE A CONTINUOUS NEED TO REDUCE DIELECTRIC LOSS AND LOWER THE COST OF CERAMIC RESONATORS AND FILTERS. THESE ARE IMPORTANT CHALLENGES TO MATERIALS SCIENTISTS BECAUSE THE FUNDAMENTAL PHYSICS OF THE RISE TO THE DESIRED PROPERTIES, ESPECIALLY DIELECTRIC LOSS, IS NOT WELL UNDERSTOOD. FURTHERMORE, THE DIELECTRIC LOSS OF A MATERIAL, WHICH LIMITS FREQUENCY RESPONSE, IS HEAVILY INFLUENCED BY EXTRINSIC FACTORS SUCH AS MICROSTRUCTURE, DEFECTS

FUNDAMENTAL UNDERSTANDING OF MICROWAVE CERAMICS IS NEEDED TO IMPROVE MATERIALS AND DISCOVER NEW MATERIALS FOR ADVANCED APPLICATIONS.

## 1.3 PHYSICS OF DIELECTRIC RESONATORS

### 1.3.1 POLARIZATION MECHANISMS IN DIELECTRICS

DIELECTRIC PROPERTIES ARE OF SPECIAL IMPORTANCE WHEN CERAMICS OR GLASS, EITHER AS A CAPACITIVE ELEMENT IN ELECTRONIC APPLICATIONS OR AS INSULATION. PERMITTIVITY, DIELECTRIC LOSS AND DIELECTRIC STRENGTH USUALLY DETERMINE THE PARTICULAR MATERIAL FOR SUCH APPLICATIONS. VARIATION OF DIELECTRIC PROPERTIES WITH FREQUENCY, FIELD STRENGTH AND OTHER CIRCUIT VARIABLES INFLUENCE THE DEVICE DESIGN. THESE DIELECTRIC PROPERTIES ARE MAINLY CONTROLLED BY MECHANISMS ARISING FROM THE ELECTRICAL RESPONSE OF INDIVIDUAL MOLECULES OF A MEDIUM. THERE ARE FOUR BASIC KINDS OF POLARIZATION MECHANISMS VIZ. INTERFACIAL, DIPOLAR, IONIC AND SPACE CHARGE. EACH DIELECTRIC MECHANISM HAS A CHARACTERISTIC "CUTOFF FREQUENCY." AS FREQUENCY INCREASES, THE SLOW MECHANISMS DROP OUT IN TURN, LEAVING THE FASTER ONES TO DOMINATE. THE LOSS FACTOR ( $\tan \delta$ ) WILL CORRESPONDINGLY PEAK AT EACH CRITICAL FREQUENCY. THE MAGNITUDE AND "CUT OFF FREQUENCY" OF EACH MECHANISM IS UNIQUE FOR DIFFERENT MATERIALS.

(i) **SPACE CHARGE/INTERFACIAL POLARIZATION:** IN ELECTRICALLY HETEROGENEOUS MATERIALS THE MOTION OF CHARGE CARRIERS MAY OCCUR MORE EASILY THROUGH ONE PHASE AND BE CONFINED AT THE PHASE BOUNDARIES. SPACE CHARGE OR INTERFACIAL POLARIZATION OCCURS WHEN CHARGE CARRIERS ARE IMPEDED BY PHYSICAL BARRIERS SUCH AS GRAIN BOUNDARIES, DISLOCATIONS, SURFACE BOUNDARY ETC. THAT INHIBITS CHARGE MIGRATION LEADING TO PILING UP OF CHARGE AT THE BARRIERS. WHEN AN AC FIELD OF SUFFICIENTLY LOW FREQUENCY IS APPLIED, A NET OSCILLATION OF CHARGE IS PRODUCED BETWEEN THE BARRIERS AS FAR APART AS 1 CM. THIS TYPE INVOLVES A LONG TIME CONSTANT AND VERY LARGE CAPACITANCE AND RELATIVE PERMITTIVITY. THIS TYPE INVOLVES A LONG TIME CONSTANT AND MAY EXTEND TO 10<sup>10</sup> HZ.

(ii) **ORIENTATIONAL/DIPOLAR POLARIZATION:** THIS TYPE OF POLARIZATION OCCURS ONLY IN POLAR SUBSTANCES. THE DIPOLAR POLARIZATION, OTHERWISE KNOWN AS ORIENTATIONAL POLARIZATION, CONTRIBUTES TO THE DIELECTRIC PROPERTIES IN THE SUB-INFRARED RANGE OF FREQUENCIES.

ELECTRIC FIELD, THE DIPOLES WILL BE RANDOMLY ORIENTED AND THUS CARRY NO NET MOMENT. WHEN AN ELECTRIC FIELD IS APPLIED, THE DIPOLES WILL TEND TO ALIGN IN THE DIRECTION OF THE APPLIED FIELD AND THE MATERIALS WILL ACQUIRE A NET MOMENT. IN OTHER WORDS, THE EFFECT OF THERMAL MOTION OF THE IONIC OR MOLECULAR DIPOLES, PRODUCES A NET DIPOLE MOMENT IN THE DIRECTION OF THE APPLIED FIELD. TWO MECHANISMS CAN BE OPERATIVE IN THIS CASE. (A) IN LINEAR DIELECTRICS (NON-FERROELECTRICS) DIPOLAR POLARIZATION RESULTS FROM THE DISPLACEMENT OF CHARGED IONS BETWEEN THE INTERSTITIAL POSITIONS IN IONIC STRUCTURES PARALLEL TO THE FIELD DIRECTION. THE MECHANISM IS ACTIVE IN THE MEDIUM FREQUENCY RANGE. (B) MOLECULES HAVING PERMANENT DIPOLE MOMENT MAY BE ROTATED ABOUT AN EQUILIBRIUM POSITION AGAINST A RESTORING POSITION. ITS FREQUENCY OF RELAXATION IS VERY HIGH OF THE ORDER OF  $10^{12}$  TO  $10^{14}$  Hz. DUE TO THE RANDOMIZING EFFECT OF THE THERMAL VIBRATIONS, ORIENTATIONAL POLARIZATION IS MORE EFFECTIVE AS THE TEMPERATURE IS DECREASED AND IT GIVES RISE TO A TEMPERATURE DEPENDENT RELATIVE PERMITTIVITY.

(iii) **IONIC POLARIZATION** IONIC POLARIZATION IS DUE TO A RELATIVE DISPLACEMENT OF POSITIVE AND NEGATIVE IONS IN A MATERIAL WITH RESPECT TO EACH OTHER, IN THE PRESENCE OF AN ELECTRIC FIELD. IN THIS CASE THE MATERIAL SHOULD HAVE AN IONIC CHARACTER. THE BUILT IN DIPOLES CANCEL EACH OTHER AND ARE UNABLE TO ROTATE. THE APPLIED EXTERNAL FIELD DISPLACES THEM SLIGHTLY FROM THEIR REST POSITIONS AND THEREBY INDUCING NET DIPOLES. THIS MECHANISM CONTRIBUTES TO THE RELATIVE PERMITTIVITY AT INFRARED FREQUENCY RANGE ( $\sim 10^3$  TO  $10^5$  Hz).

(iv) **ELECTRONIC POLARIZATION** ELECTRONIC POLARIZATION IS PRESENT IN ALL MATERIALS AND DOES NOT CONTRIBUTE TO CONDUCTIVITY OR DIELECTRIC LOSS IN MOST DIELECTRICS. IT ARISES FROM A SHIFT OF THE CENTRE OF MASS OF THE NEGATIVE ELECTRON CHARGE CLOUD FROM THE POSITIVE ATOMIC NUCLEUS UNDER THE INFLUENCE OF AN ELECTRIC FIELD. THIS MECHANISM IS ACTIVE AT FREQUENCIES OF ABOUT  $10^{15}$  TO  $10^{17}$  Hz. THE RELATIVE PERMITTIVITY AT OPTICAL FREQUENCIES IS CONTRIBUTED ALMOST ENTIRELY FROM THE ELECTRONIC POLARIZABILITY.

FIGURE 1.2 SHOWS THE VARIATION OF DIELECTRIC LOSS AND PERMITTIVITY WITH FREQUENCY. AT MICROWAVE FREQUENCIES THE MECHANISMS DUE TO IONIC AND ELECTRONIC POLARIZATION CONTRIBUTES TO THE DIELECTRIC PROPERTIES. THE DIELECTRIC PROPERTIES OF A MATERIAL DEPEND ON IT BY THE TEMPERATURE. THIS DEPENDENCE IS DUE TO THE EFFECT OF TEMPERATURE UPON THE DIFFERENT POLARIZATION MECHANISMS. ELECTRONIC POLARIZATION IS RELATIVELY UNAFFECTED BY TEMPERATURE.

HOWEVER, ATOMIC POLARIZATION IS AFFECTED SINCE THE BINDING FORCES BETWEEN IONS CHANGES WITH TEMPERATURE. IT IS FOUND TO INCREASE WITH TEMPERATURE DUE TO THE CHARGE CARRIERS AND ION MOBILITY. THE ABILITY OF A DIPOLE TO ROTATE IN AN ELECTRIC FIELD IS ALSO TEMPERATURE DEPENDENT AND SO ORIENTATIONAL POLARIZATION WILL BE TEMPERATURE DEPENDENT. ORIENTATIONAL POLARIZATION IS OPPOSED BY THERMAL AGITATION, SO THE RELATIONSHIP GOES DOWN AS THE TEMPERATURE INCREASES. FINALLY, SINCE CHARGE MOBILITY IS TEMPERATURE DEPENDENT, THE INTERFACIAL MECHANISM WILL ALSO BE TEMPERATURE DEPENDENT.

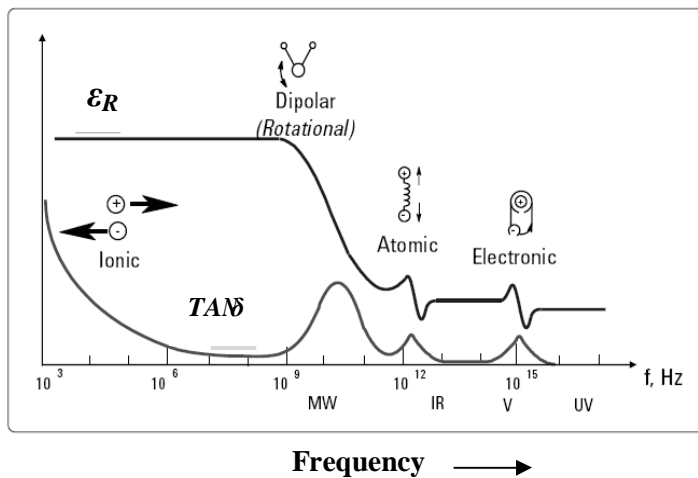


Fig. 1.2 Frequency response of dielectric mechanisms. (en.wikipedia.org/wiki/Dielectric\_spectroscopy)

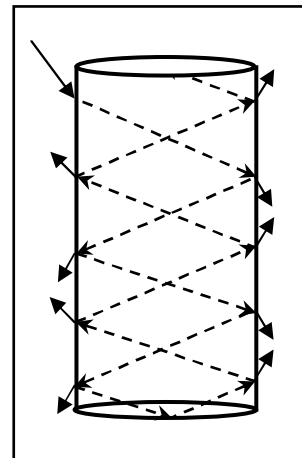


Fig. 1.3 Sketch of multiple total internal reflections in DR.

### 1.3.2 CLAUSIUS - MOSSOTTI EQUATION

THE RELATIVE PERMITTIVITY OF AN INSULATOR IS RELATED TO THE POLARIZABILITY OF THE MATERIALS COMPRISING IT. THE PERMITTIVITY CAN BE CALCULATED THEORETICALLY USING CLAUSIUS-MOSSOTTI EQUATION FOR CUBIC OR ISOTROPIC MATERIALS [34]

$$\frac{\epsilon_r - 1}{\epsilon_r + 2} = \left( \frac{4}{3} \right) \left( \frac{D}{V_m} \right) \tag{1.1}$$

REARRANGING WE GET,  $\epsilon_r = \frac{3V_m + 8}{3V_m - 4} \frac{D}{D}$  (1.2)

WHERE  $\epsilon_m$  IS THE MOLAR VOLUME AND THE SUM OF THE DIELECTRIC POLARIZABILITIES OF INDIVIDUAL IONS. THE DIELECTRIC MATERIAL CAN BE OBTAINED FROM X-RAY DIFFRACTION STUDIES. IT DEPENDS ON THE DIELECTRIC POLARIZABILITY OF THE CONSTITUENT IONS AND CRYSTAL STRUCTURE. BASED ON THE ADDITIVITY RULE, SHANNON STATES THAT THE DIELECTRIC POLARIZABILITY OF A COMPLEX MATERIAL CAN BE BROKEN UP INTO THE MOLECULAR POLARIZABILITIES OF SIMPLER COMPOUNDS BY [35]

$$\epsilon_D(A_2A'O_4) = 2 \epsilon_D(AO) + \epsilon_D(A'O_2) \quad (1.3)$$

WHERE A ARE THE CATIONS. FURTHERMORE, IT IS POSSIBLE TO BREAK UP THE MOLECULAR POLARIZABILITIES OF COMPLEX COMPOUNDS INTO IONS ACCORDING TO

$$\epsilon_D(A_2A'O_4) = 2 \epsilon_D(A^{2+}) + \epsilon_D(A^{4+}) + 4 \epsilon_D(O^{2-}) \quad (1.4)$$

THE DIELECTRIC POLARIZABILITIES OF SEVERAL IONS ARE REPORTED BY SHANNON [35]. HIS CALCULATIONS USUALLY AGREE WELL WITH POROSITY-CORRECTED EXPERIMENTAL VALUES FOR BEHAVED CERAMICS. IT MAY BE NOTED THAT DEVIATIONS FROM CALCULATED VALUES ARE DUE TO DEVIATIONS FROM CUBIC SYMMETRY, PRESENCE OF IONIC OR ELECTRONIC CONDUCTIVITY, CO<sub>2</sub> IN CHANNELS, RATTLING OF IONS, PRESENCE OF DIPOLAR IMPURITIES OR FERROELECTRICITY AND ALSO THE FACT THAT THE SAMPLE IS CERAMIC AND NOT A SINGLE CRYSTAL. THE DISCREPANCY BETWEEN REPORTED VALUES OF DIELECTRIC POLARIZABILITY AND EVEN A SMALL ERROR IN DETERMINING VOLUME CAN SIGNIFICANTLY AFFECT THE CALCULATED VALUE OF THE PERMITTIVITY.

### 1.3.3 WORKING PRINCIPLE OF DIELECTRIC RESONATORS

A PIECE OF DIELECTRIC WITH HIGH RELATIVE PERMITTIVITY CAN CONFINE MICROWAVE ENERGY AT A FEW DISCRETE FREQUENCIES THROUGH TOTAL MULTIPLE INTERNAL REFLECTIONS AT THE DIELECTRIC-AIR INTERFACE, PROVIDED THAT THE ENERGY IS FED IN THE APPROPRIATE DIRECTION (SEE FIGURE 1.1). AN ELECTROMAGNETIC WAVE MOVING FROM THE ELECTRICALLY DENSE HIGH DIELECTRIC MEDIUM TO AN ELECTRICALLY THIN AIR MEETS VERY HIGH IMPEDANCE AT THE DIELECTRIC-AIR INTERFACE AND REFLECTS BACK TO THE DIELECTRIC ITSELF. AS THE RELATIVE PERMITTIVITY INCREASES THE IMPEDANCE MISMATCH BY THE BOUNDARY ALSO INCREASES TO ALLOW BETTER CONFINEMENT OF ENERGY WITHIN THE DIELECTRIC BODY.

THE REFLECTION COEFFICIENT APPROACHES UNITY WHEN THE RELATIVE PERMITTIVITY APPROACHES INFINITY. THE TRAPPED ELECTROMAGNETIC WAVES WILL FORM STANDING WAVES AND GENERATE RESONANCE. A HIGH RELATIVE PERMITTIVITY MATERIAL CAN CONFINES MOST OF THE ELECTROMAGNETIC WAVE WITHIN ITS VOLUME. IF THE TRANSVERSE DIMENSIONS OF THE DIELECTRIC ARE COMPARABLE TO THE WAVE LENGTH OF THE MICROWAVE, THEN CERTAIN FIELD DISTRIBUTIONS WILL SATISFY MAXWELL'S EQUATIONS AND BOUNDARY CONDITIONS [36] AND ONLY THOSE MODES SATISFYING THIS CONDITION WILL BE EXCITED. THE FREQUENCY OF THE GENERATED MODES DEPENDS ON THE DIMENSIONS AND RELATIVE PERMITTIVITY OF THE DIELECTRIC. FOR MICROWAVES, THE FREE SPACE WAVELENGTH IS OF THE ORDER OF A FEW CENTIMETERS AND ON ENTERING THE MATERIAL WITH A RANGE 20-100, THE WAVELENGTH INSIDE THE DIELECTRIC WILL BE IN MILLIMETERS. THE ELECTROMAGNETIC FIELD IN THE DIELECTRIC SAMPLE DECAYS RAPIDLY. ONE CAN PREVENT RADIATION LOSSES BY PLACING THE DIELECTRIC IN A SMALL ENCLOSED METALLIC ENCLOSURE. SINCE ONLY A SMALL RADIATION FIELD SEES THE METALLIC SURFACE, CONDUCTION LOSS WILL BE TOO SMALL AND CAN BE NEGLECTED [37].

### 1.3.4 RESONANCE

A BULK DIELECTRIC MATERIAL EXCITED FOR RESONANCE USING MICROWAVE IS EQUIVALENT TO A PARALLEL RESONANT CIRCUIT. HENCE THE ALTERNATING FIELD WILL BE PURELY INDUCTIVE, CAPACITIVE AND RESISTIVE COMPONENTS. ALL THE THREE COMPONENTS, CAPACITOR, INDUCTOR AND OHMIC RESISTANCE IN THE CIRCUIT HAVE A COMMON VOLTAGE  $V \cos \omega t$ . FROM THE FUNDAMENTAL RULES OF RESONANT ELECTRICAL CIRCUITS, THE ENERGY STORED IN THE CAPACITOR IS GIVEN AS [38]

$$W_e(t) = \frac{1}{2} C [v(t)]^2 = \frac{1}{2} C |V|^2 \cos^2 \omega t \quad (1.5)$$

AND MAGNETIC ENERGY STORED IN THE INDUCTOR IS

$$W_m(t) = \frac{1}{2} L [I(t)]^2 = \frac{|V|^2}{2 \omega^2 L} \sin^2 \omega t \quad (1.6)$$

THE STORED ELECTRIC ENERGY IS THUS PROPORTIONAL TO THE STORED MAGNETIC ENERGY IS PROPORTIONAL TO THE SQUARE OF TIME. AS FUNCTIONS OF TIME, THE STORED ENERGY  $W_e(t)$  AND  $W_m(t)$  FLUCTUATE BETWEEN ZERO AND THEIR MAXIMUM VALUES. THEIR AVERAGE VALUES  $W_e$  AND  $W_m$  ARE EQUAL TO ONE HALF OF THE CORRESPONDING MAXIMUM VALUES. AT RESONANCE, CAPACITIVE AND INDUCTIVE REACTANCES BECOME EQUAL AND OPPOSITE. HENCE THE IMPEDANCE OF THE CIRCUIT EQUALS THE OHMIC RESISTANCE AND MAXIMUM ENERGY STORAGE TAKES PLACE WITHIN THE BODY OF THE DIELECTRIC RESONATOR.

AT THIS CONDITION,

$$\omega = \omega_{res} = \frac{1}{\sqrt{LC}} \quad (1.7)$$

THE MAXIMUM STORED ENERGY WILL BE THE SUM OF THE STORED ENERGY IN CAPACITOR (  $W_{e,max}$  ) AND INDUCTOR (  $W_{m,max}$  ) SINCE THE AVERAGE ENERGY VALUES ARE EQUAL TO ONE HALF OF THE MAXIMUM VALUES,

$$W_{max} = 2W_e = 2W_m = W_e + W_m \quad (1.8)$$

IN TERMS OF THE AVERAGE STORED ENERGIES, RESONANCE BECOMES [39]

$$Q = \left[ \frac{(W_e + W_m)}{P_d} \right]_{\omega = \omega_{res}} \quad (1.9)$$

WHERE  $P_d$  IS THE AVERAGE POWER DISSIPATED IN THE RESONATOR. IF THE RESONANT FREQUENCY IS NOT EQUAL TO THE RESONANT FREQUENCY, THE PEAK OF THE STORED ELECTRIC ENERGY IS NOT EQUAL TO THE PEAK OF THE STORED MAGNETIC ENERGY. THEREFORE, THERE IS NO DISCREPANCY IN ANY FREQUENCY OTHER THAN  $\omega_{res}$ .

### 1.3.5 MODES AND MODE NOMENCLATURE

A MICROWAVE RESONATOR HAS INFINITE NUMBER OF MODES, EACH OF THEM CORRESPONDING TO A PARTICULAR RESONANT FREQUENCY, AT WHICH THE ELECTRIC ENERGY IS EQUAL TO THE MAGNETIC ONE. THE EXCITED MODES CAN BE CLASSIFIED INTO THREE D

TE, TM AND HYBRID. THE FIELD FORM MODES ARE AXISYMMETRIC WHEREAS HYBRID MODES ARE AZIMUTHALLY DEPENDENT. THE HYBRID MODES CAN AGAIN BE CATEGORIZED INTO HE AND EH. ACCORDING TO THE MODE NOMENCLATURE DESCRIBED BY KOBAYASHI VARIATION OF FIELDS ALONG THE AZIMUTHAL DIRECTION INSIDE THE RESONATOR, ARE DENOTED BY ADDING MODE INDICES AS SUBSCRIPTS TO EACH FAMILY OF MODE NOMENCLATURE IS HISTORICALLY BASED ON THE MODE NOMENCLATURE OF CYLINDRICAL WAVEGUIDES. THE TM, HE AND EH MODES ARE CLASSIFIED AS  $TM_{nmp+\Delta}$ ,  $HE_{nmp+\Delta}$  AND  $EH_{nmp+\Delta}$  RESPECTIVELY. THE FIRST INDEX DENOTES THE NUMBER OF FIELD VARIATIONS IN AZIMUTHAL DIRECTION (THE INDEX...) DENOTES THE ORDER OF VARIATION OF THE FIELD ALONG THE RADIAL DIRECTION AND THE INDEX DENOTES THE ORDER OF VARIATION OF THE FIELD ALONG THE

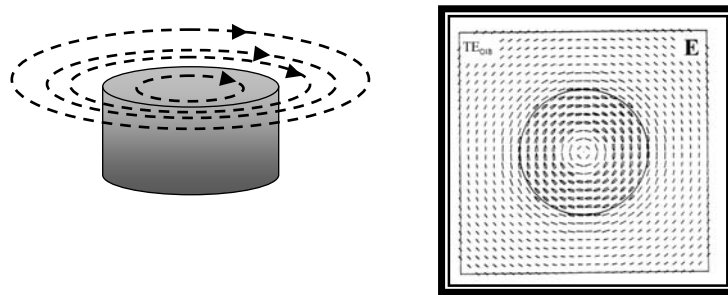


Fig. 1.4 Electric field distribution of  $TE_{01\Delta}$  mode in equatorial plane.

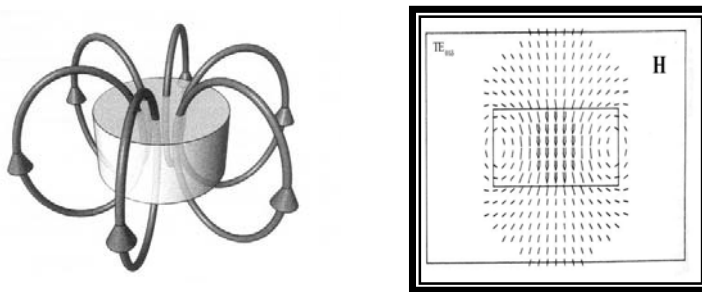


Fig. 1.5 Magnetic field distribution of  $TE_{01\Delta}$  in the meridian plane.

THE RESONANT MODE MOST OFTEN USED IN SHIELDED MICROWAVE CIRCUITS IS TRANSVERSE ELECTRICAL MODE HAVING AZIMUTHAL SYMMETRY WITH A HALF CYCLE VARIATION IN FIELD IN THE Z-DIRECTION. HERE, THE THIRD INDEX, DENOTES THE



DIELECTRIC RESONATOR IS SHORTER THAN ONE-HALF WAVELENGTH DEPENDS ON THE RELATIVE PERMITTIVITY OF THE RESONATOR AND THE SUBSTRATE, AND ON THE PRO AND BOTTOM CONDUCTOR PLATES. FIGS. 1.4 AND 1.5 RESPECTIVELY SHOWS THE TYPE DISTRIBUTIONS FOR FEA CYLINDRICAL DIELECTRIC RESONATOR [39]. THE MAGNITUDE OF ELECTRICAL FIELD COMPONENT IS ZERO AT THE CENTRE OF THE RESONATOR AND HAS A AT AROUND  $r/3$  WHERE  $r$  IS THE RADIUS OF THE DISK. OUTSIDE THE RESONATOR, THE FIELD DECAYS EXPONENTIALLY. THE FIELD VARIATION AS A FUNCTION OF RADIAL DISTANCE REMAINS DIFFERENT PLANES PARALLEL TO THE EQUATORIAL PLANE [41].

## 1.4 MATERIAL REQUIREMENTS FOR DR APPLICATIONS

AS IN ALL TECHNOLOGICAL SYSTEMS, THE BASIC FUNCTIONAL REQUIREMENTS IN WIRELESS COMMUNICATION IS ADVANCES IN MATERIALS. THESE UNIQUE TECHNOLOGIES DEMAND MATERIALS WHICH HAVE THEIR OWN SPECIALIZED REQUIREMENTS AND FUNCTIONS. THE IMPULSE FOR MINIATURIZATION CANNOT BE OVEREMPHASIZED IN ANY HAND-HELD COMMUNICATION DEVICE AND CAN BE SEEN IN THE DRAMATIC DECREASE IN THE SIZE AND WEIGHT OF DEVICES. THE NEED FOR MINIATURIZATION PROVIDES A CONTINUING DRIVING FORCE FOR THE DISCOVERY AND DEVELOPMENT OF INCREASINGLY SOPHISTICATED MATERIALS TO PERFORM THE SAME FUNCTION WITH DECREASED SIZE AND WEIGHT. THERE ARE THREE KEY PROPERTIES THAT CHARACTERIZE THE DIELECTRIC RESONATORS AND THEY ARE DISCUSSED IN DETAIL IN THE FOLLOWING SECTIONS.

### 1.4.1 RELATIVE PERMITTIVITY ( $\epsilon_r$ )

THE RELATIVE PERMITTIVITY CHARACTERIZES A MATERIAL'S ABILITY TO STORE CHARGE. A DIELECTRIC RESONATOR (DR) CAN CONFINE ELECTROMAGNETIC WAVES THROUGH TOTAL INTERNAL REFLECTIONS AT THE DIELECTRIC-AIR INTERFACE. IF THE DR IS RESONATING AT A FREQUENCY  $f_o$  THEN THE MAXIMUM WAVELENGTH IT CAN HAVE IS RELATED TO THE RELATIVE PERMITTIVITY OF THE MATERIAL BY THE FOLLOWING EQUATION;

$$f_o \approx \frac{c}{D\sqrt{\epsilon_r}} \approx \frac{c}{D\sqrt{\epsilon_r}} \quad (1.10)$$

WHERE  $v$  IS THE VELOCITY OF LIGHT IN VACUUM AND  $\lambda$  IS THE WAVELENGTH OF THE STANDING WAVE ALONG THE DIAMETER OF A RESONATOR. CONSEQUENTLY, IF THE PERMITTIVITY IS INCREASED, THE SIZE OF THE RESONATOR MAY BE DECREASED WHILE STILL MAINTAINING A SPECIFIC FREQUENCY. IN THE MICROWAVE FREQUENCY RANGE, IONIC POLARIZATION IS THE MAJOR CONTRIBUTOR TOWARDS THE RELATIVE PERMITTIVITY. HENCE MATERIALS CONTAINING HIGH IONIC POLARIZABILITIES ARE NEEDED FOR SUPERCONDUCTING HIGH CLASSICAL DISPERSION THEORY, THE CRYSTAL IS APPROXIMATED AS A SYSTEM OF DAMPED OSCILLATORS WITH AN APPROPRIATE FREQUENCY AND DIPOLE MOMENT. THE REAL AND IMAGINARY PARTS OF THE RELATIVE PERMITTIVITY AS FUNCTIONS OF FREQUENCY (WHERE  $\omega = 2\pi f$ ) ARE GIVEN BY

$$\epsilon'(\omega) = \epsilon_{\infty} + \sum_j \frac{4 f_j (\omega_j^2 - \omega^2) \omega_j^2}{(\omega_j^2 - \omega^2)^2 + (\omega_j \gamma_j)^2} \quad (1.11)$$

WHERE  $f_j$  IS THE OSCILLATOR STRENGTH,  $\omega_j$  IS THE RESONANT ANGULAR FREQUENCY OF THE OSCILLATOR,  $\epsilon_{\infty}$  IS THE RELATIVE PERMITTIVITY CAUSED BY ELECTRONIC POLARIZATION AT HIGH FREQUENCIES AND  $\gamma_j$  IS THE DAMPING CONSTANT WHICH IS GIVEN BY THE WIDTH OF THE PEAK. THE SUMMATION IS OVER ALL RESONANCES IN THE SPECTRUM. EACH RESONANCE IS CHARACTERIZED BY ITS DISPERSION PARAMETERS. FOR

$$\epsilon'(\omega) = \epsilon_{\infty} + \sum_j 4 f_j \quad (1.12)$$

THE ABOVE EQUATION SHOWS THAT RELATIVE PERMITTIVITY IS INDEPENDENT OF FREQUENCY IN THE MICROWAVE FREQUENCY REGION. FOR AN IDEAL DIELECTRIC RESONATOR TO BE MINIATURIZED IN THE MICROWAVE FREQUENCY RANGE, THE RELATIVE PERMITTIVITY MUST BE HIGH IN ORDER TO ACHIEVE MINIATURIZATION. HOWEVER, DUE TO THE CROWDING OF CHANNELS, THE APPLICATIONS OF DIELECTRIC RESONATORS TO HIGHER FREQUENCIES. THUS LOW RELATIVE PERMITTIVITY IS ESSENTIAL FOR MILITARY APPLICATIONS.

### 1.4.2 HIGH QUALITY FACTOR

ONE OF THE MOST PERSISTENT PROBLEMS IN MATERIALS IS THE DIELECTRIC LOSS. DIELECTRIC LOSS WAS FIRST MEASURED BY RUBENS AND HERTZ [42] IN 1912 AND, TEN YEARS LATER, EWALD [43] SUGGESTED THAT ITS ORIGIN WAS THE ANHARMONIC INTERACTION BETWEEN THE ELECTROMAGNETIC FIELD AND THE THERMAL LATTICE VIBRATIONS. WHEN THE ELECTROMAGNETIC FIELD IS COUPLED TO THE LATTICE VIBRATIONS, A MUTUAL PERTURBATION RESULTS AS IN THE COUPLING OF ANY TWO SYSTEMS. AT MICROWAVE FREQUENCIES, THE COUPLING OF THE FIELD WITH THE LATTICE VIBRATIONS IS FAR FROM RESONANCE. HOWEVER, THE MUTUAL PERTURBATION IS STILL NOTICEABLE. SOME MECHANICAL LATTICE VIBRATIONS ACQUIRE A SMALL FRACTION OF THE ENERGY OF THE ELECTROMAGNETIC FIELD. THEN, DUE TO THE THIRD AND HIGHER ORDER TERMS IN THE EXPANSION OF THE ENERGY OF THE LATTICE, THIS SMALL FRACTION OF EXTRA ENERGY GRADUALLY DIFFUSES THROUGH THE MODES IN THE LATTICE AND ULTIMATELY APPEARS AS HEAT.

THE FIGURE OF MERIT FOR ASSESSING THE PERFORMANCE OR QUALITY OF A RESONATOR IS THE QUALITY FACTOR. IT IS THE EFFICIENCY OF A RESONANT CIRCUIT TO CONFINE ELECTROMAGNETIC ENERGY INSIDE A RESONATOR STORE ENERGY AT THE RESONANT FREQUENCY WHERE EQUAL STORAGE OF ELECTRIC AND MAGNETIC ENERGIES OCCUR. THUS QUALITY FACTOR IS A MEASURE OF ENERGY STORED IN THE FIELDS INSIDE THE RESONATOR PER CYCLE AS COMPARED TO THE ENERGY DISSIPATED PER CYCLE. THE QUALITY FACTOR IS DEFINED BY [44]

$$Q = \frac{\text{Maximum Energy Stored per cycle}}{\text{Average Energy Dissipated per cycle}}$$

$$Q = \frac{2 W_0}{PT} = \frac{W_0}{P} \quad (1.13)$$

WHERE  $W_0$  IS THE STORED ENERGY, P IS POWER DISSIPATION,  $\omega_0$  IS THE RESONANT RADIANT FREQUENCY AND T IS PERIOD  $T = \frac{2\pi}{\omega_0}$ . IN THE CASE OF BULK CERAMICS ENERGIZED BY ELECTROMAGNETIC WAVES,

THE QUALITY FACTOR IS ROUGHLY THE INVERSE OF DIELECTRIC LOSS OF THE MATERIAL. FOR AN ELECTRICAL RESONANT SYSTEM, THE QUALITY FACTOR REPRESENTS THE EFFECT OF ELECTRICAL RESISTANCE. FOR ELECTROMECHANICAL RESONATORS SUCH AS QUARTZ CRYSTALS IT REPRESENTS THE MECHANICAL LOSS. IN MICROWAVE COMMUNICATIONS, QUALITY FACTOR IS DETERMINED AS THE RESONANT

$(f_o)$  DIVIDED BY THE BANDWIDTH, MEASURED AT 3 DB BELOW THE MAXIMUM HEIGHT AT RESONANCE.

$$Q = \frac{f_o}{\Delta f} = \frac{f_o}{\Delta f} \quad (1.14)$$

IT IS THEREFORE A DIRECT MEASURE OF THE ABILITY OF THE RESONATING BODY TO STORE ENERGY AT A PARTICULAR FREQUENCY. THE DIELECTRIC QUALITY FACTOR FOR HOMOGENEOUS DIELECTRIC MATERIAL IS GIVEN BY

$$Q_d = \frac{1}{\tan \delta} \quad (1.15)$$

WHEN A RESONANT CIRCUIT OR CAVITY IS USED AS A LOAD IN A MICROWAVE CIRCUIT, DIFFERENT QUALITY FACTORS CAN BE DEFINED. FIRST IS THE UNLOADED QUALITY FACTOR ( $Q_u$ ), NEXT EXTERNAL QUALITY FACTOR ( $Q_e$ ) WHICH IS THE QUALITY FACTOR FOR EXTERNAL LOSSES. WHEN THE RESONATOR IS USED OR ATTACHED TO SOME EXTERNAL CIRCUIT THERE ARISES A QUALITY FACTOR ( $Q_L$ ) WHICH IS THE OVERALL QUALITY FACTOR AND INCLUDES BOTH INTERNAL AND EXTERNAL LOSSES. FOR CAVITY RESONATORS, POWER LOSS BY CONDUCTORS, DIELECTRIC FILLS AND RADIATION LOSS CONtribute TO UNLOADED QUALITY FACTOR. CONDUCTOR LOSS IS DUE TO THE CURRENT ON THE SURFACE OF THE CAVITY AND DR, RADIATION LOSS IS DUE TO THE EVANESCENT FIELD DECAYING OUT OF THE SURFACE AND DIELECTRIC LOSS IS THE INTRINSIC LOSS OF THE MATERIAL.

$$\frac{1}{Q_u} = \frac{1}{Q_c} + \frac{1}{Q_d} + \frac{1}{Q_r} \quad (1.16)$$

WHERE  $Q_c$  IS THE CONDUCTOR QUALITY FACTOR,  $Q_d$  IS THE DIELECTRIC QUALITY FACTOR AND  $Q_r$  IS THE RADIATION QUALITY FACTOR. WHEN THE RESONATOR IS CONNECTED TO LOAD

$$\frac{1}{Q_L} = \frac{1}{Q_e} + \frac{1}{Q_u} \quad (1.17)$$

WHERE  $Q_L$  IS THE LOADED QUALITY FACTOR,  $Q_e$  IS THE EXTERNAL QUALITY FACTOR AND  $Q_u$  IS THE UNLOADED QUALITY FACTOR. IT SHOULD ALSO BE NOTED THAT IN THE CASE OF AN ISOLATED DR,  $Q_e$  IS INFINITE. HOWEVER, THE QUALITY FACTOR OF A DR CAN ONLY BE MEASURED BY THE LOADED VOLTAGE

KEEPING IN AN EXTERNAL CIRCUIT. HENCE IT IS NECESSARY TO HAVE A RELATION BETWEEN FORMS OF QUALITY FACTOR (AND IS REPRESENTED AS

$$Q_u = Q_L(1 + \kappa) \quad (1.18)$$

WHERE  $\kappa$  IS TERMED AS THE COUPLING COEFFICIENT GIVEN BY

$$\kappa = \frac{P_e}{P_u} \quad (1.19)$$

$P_e$  IS THE POWER LOSS DUE TO EXTERNAL FACTORS AND THAT DUE TO CONDUCTOR, DIELECTRIC AND RADIATION.

CLASSICAL DISPERSION THEORY [45] PREDICTS THAT AT MICROWAVE FREQUENCIES PERMITTIVITY IS INDEPENDENT OF FREQUENCY AND PROPORTIONAL TO FREQUENCY (

$$\tan \delta = \left( \frac{\nu}{\nu_r} \right)^2 f \quad (1.20)$$

WHERE  $\nu$  IS THE DAMPING FACTOR AND  $\nu_r$  IS THE RESONANT FREQUENCY OF THE OPTICAL MODE OF LATTICE VIBRATION.  $\tan \delta$  INCREASES WITH INCREASING FREQUENCY AND IS THEREFORE OFTEN QUOTED WHILE COMPARING CERAMICS.

### 1.4.3 SMALL TEMPERATURE COEFFICIENT OF RESONANT FREQUENCY (

THE TEMPERATURE COEFFICIENT OF RESONANT FREQUENCY IS A MEASURE OF THE STABILITY OF THE RESONATOR. IT INDICATES THE “DRIFT” OF RESONANT FREQUENCY WITH TEMPERATURE. THE FREQUENCY OF STANDING WAVE WITHIN THE RESONATOR IS GIVEN BY (1.10). WHEN TEMPERATURE CHANGES, THEN THE RESONANT FREQUENCY VARIES DUE TO THE VARIATION IN LENGTH OF THE DIELECTRIC MATERIAL. DIFFERENTIATING WITH RESPECT TO TEMPERATURE GIVES

$$\frac{1}{f_0} \cdot \frac{\Delta f_0}{\Delta T} = \frac{-1}{L} \cdot \frac{\Delta L}{\Delta T} - \frac{1}{2} \cdot \frac{1}{r} \cdot \frac{\Delta r}{\Delta T} \quad (1.21)$$

WHERE  $\frac{1}{f_o} \frac{\Delta f}{\Delta T}$  IS THE TEMPERATURE COEFFICIENT OF RESONANT FREQUENCY AND

EXPANSION COEFFICIENT AND  $\frac{1}{\epsilon_r} \frac{\Delta \epsilon_r}{\Delta T}$  IS THE TEMPERATURE COEFFICIENT OF PERMITTIVITY (1.21)

SUBSTITUTING THESE VALUES IN THE ABOVE EQUATION, BECOMES

$$f = - \left( L + \frac{1}{2} \right) \quad (1.22)$$

THE  $f$  CAN BE DEFINED MATHEMATICALLY IN TERMS OF RESONANT FREQUENCY AND TEMPERATURE

$$f = \frac{1}{f_o} \times \frac{\Delta f}{\Delta T} \quad (1.23)$$

WHERE  $f$  IS THE RESONANT FREQUENCY AND VARIATION OF RESONANT FREQUENCY WITH CHANGE IN TEMPERATURE IS USUALLY EXPRESSED IN PARTS PER MILLION PER DEGREE CELSIUS (PPM/°C).

THE VALUE OF  $f$  SHOULD BE NEAR TO ZERO FOR PRACTICAL APPLICATIONS. IT IS SELF EVIDENT THAT A MATERIAL WITH A SIGNIFICANT  $f$  IS UNSUITABLE FOR A MICROWAVE CIRCUIT AS IT CANNOT MAINTAIN ITS RESONANT FREQUENCY AS THE BASE STATION OPERATING TEMPERATURE VARIATION. HOWEVER, IN REALITY, A SMALL NON-ZERO VALUE OF  $f$  IS REQUIRED TO COMPENSATE FOR THERMAL EXPANSION OF THE MICROWAVE CAVITY AND OTHER COMPONENTS IN THE CIRCUIT.

## 1.5 FACTORS AFFECTING MICROWAVE DIELECTRIC PROPERTIES

MICROWAVE DIELECTRIC PROPERTIES ARE INFLUENCED BY A NUMBER OF FACTORS SUCH AS PERMITTIVITY [46], ONSET OF PHASE TRANSITIONS [47-48], PROCESSING CONDITIONS, RAW MATERIAL IMPURITIES [49] AND ORDER/DISORDER BEHAVIOR AND POROSITY [50]. THE DIELECTRIC LOSS IS THE RESULT OF A COMBINED CONTRIBUTION OF THE DEGREE OF CRYSTAL STRUCTURE ORDER, MICROSTRUCTURAL INHOMOGENITY AND INTERACTION OF PHONONS. BOTH A HIGH PURITY AND GOOD PROCESSING AND THUS GOOD MICROSTRUCTURE ARE REQUIRED FOR A LOW LOSS. MICROSTRUCTURAL INHOMOGENITIES SUCH AS SPACE CHARGES OR DIPOLES WHICH LIE IN

MATRIX GRAINS AND INCLUSIONS OR AT GRAIN BOUNDARIES HAVE HIGHER LOSS. INHOMOGENITIES MAY ARISE DUE TO SECONDARY PHASES, IMPURITY SEGREGATION, DENSIFICATION ETC. IT IS FOUND THAT THE QUALITY FACTOR OF A CERAMIC IS INCREASED IN BULK DENSITY, PROVIDED THE DENSIFICATION IS PROMOTED BY SOLID STATE MECHANISM. HENCE GLASSY PHASE FORMATION SHOULD BE AVOIDED DURING SINTERING TO IMPROVE QUALITY FACTOR. BECAUSE OF THE NATURAL DIFFICULTIES INVOLVED IN GETTING REPRODUCIBLE MICROSTRUCTURES, IT IS ESSENTIAL THAT THE CERAMIC IS AT LEAST A SINGLE PHASE WITH HOMOGENEOUS MICROSTRUCTURE AS FAR AS POSSIBLE.

THE STRUCTURAL FACTORS THAT ARE INVOLVED IN LOSS MECHANISM INCLUDE LOSS OF SYMMETRY, MASS OF IONS, CATION ORDERING ETC. THE DIELECTRIC LOSS IN MICROWAVE DIELECTRICS IS BROUGHT ABOUT BY THE EFFECT OF ANHARMONIC TERMS IN THE POTENTIAL ENERGY ON THE MEAN SEPARATION OF A PAIR OF ATOMS AND IS INCREASED BY IMPERFECTIONS IN THE CRYSTAL. THE DIELECTRIC LOSS CAUSED BY THE ANHARMONIC TERMS IS MORE SIGNIFICANT AT HIGHER TEMPERATURES. THE RANDOM DISTRIBUTION OF IONS IS ALSO CONSIDERED TO BE AN IMPERFECTION. THE QUALITY FACTOR OF THE ORDERED CERAMICS WOULD BE MUCH GREATER THAN THAT OF UNORDERED CERAMICS. ANY TYPE OF DEFECTS SUCH AS GRAIN BOUNDARIES, STACKING FAULTS OR STRUCTURAL DISORDER, POINT DEFECTS, PLANAR DEFECTS, LINE DEFECTS, INCLUSIONS, PHASES, TWINNING, POROSITY ETC. CONTRIBUTE TO DIELECTRIC LOSSES. IN THE MICROWAVE RANGE THE INTRINSIC LOSS IS MAINLY DUE TO THE INTERACTION OF THE APPLIED FIELD WITH THE LATTICE WHICH LEADS TO DAMPENING OF THE PHONON MODES OF FUNDAMENTAL LATTICE.

### 1.5.1 EFFECT OF POROSITY

#### (a) Relative permittivity

THE VARIATION OF RELATIVE PERMITTIVITY WITH POROSITY HAS BEEN CONSIDERED BY A NUMBER OF APPROXIMATIONS [51]. THE MODELS CONSIDER THE DIELECTRICS AS A COMPOSITE SYSTEM OF TWO PHASES (DIELECTRIC MATERIAL AND POROSITY) WITH DIFFERENT PERMITTIVITIES. THE SIMPLEST MODEL IS TO CONSIDER THE DIELECTRIC AS PARALLEL CONNECTION OF TWO DIELECTRICS HAVING VOLUME FRACTIONS  $V_1$  AND  $V_2$  AND RELATIVE PERMITTIVITIES  $\epsilon_1$  (  $\epsilon_1 = \epsilon_m$ , DIELECTRIC PHASE) AND  $\epsilon_2$  (  $\epsilon_2 = 1$ , POROSITY) RESPECTIVELY. THEN THERE ARE TWO POSSIBLE CONFIGURATIONS

(A) ELECTRIC FIELD IS PERPENDICULAR TO THE PLANE OF THE PLATES [51]. THEN

$$\epsilon' = \epsilon_m - P(\epsilon_m - 1) \quad (1.24)$$

(B) IF ELECTRIC FIELD IS PARALLEL TO THE PLANE OF THE PLATES,

$$\epsilon' = \frac{\epsilon_m}{P(\epsilon_m - 1) + 1} \quad (1.25)$$

MAXWELL DERIVED A REALISTIC MODEL OF SPHERICAL PARTICLES OF RELATIVE PERMITTIVITY  $\epsilon_m$  IN A DIELECTRIC MATRIX OF RELATIVE PERMITTIVITY  $\epsilon_d$ . THE RELATIVE PERMITTIVITY OF THE MIXTURE IS GIVEN BY

$$\epsilon' = \frac{V_m \epsilon_m \left( \frac{2}{3} + \frac{d}{3 \epsilon_m} \right) + V_d \epsilon_d}{V_m \left( \frac{2}{3} + \frac{d}{3 \epsilon_m} \right) + V_d} \quad (1.26)$$

IF THE SPHERES ARE PORES AND APPLYING A LINEARIZED APPROXIMATION [52] FOR THEN THE ABOVE EQUATION BECOMES

$$\epsilon' = \epsilon_m \left( 1 - \frac{3P(\epsilon_m - 1)}{2 \epsilon_m + 1} \right) \quad (1.27)$$

**(b) Dielectric loss (tan  $\delta$ )**

THE COMPLEX PERMITTIVITY OF A MATERIAL IS GIVEN BY

$$\epsilon = \epsilon' - i \epsilon'' \quad (1.28)$$

REAL COMPONENT IS RELATIVE PERMITTIVITY AND IMAGINARY COMPONENT DESCRIBES THE DISSIPATION OF THE ELECTRIC FIELD.

DIELECTRIC LOSS TANGENT,  $\tan \delta = \frac{\epsilon''}{\epsilon'}$  (1.29)

QUALITY FACTOR,  $Q = \frac{1}{\tan \delta}$  (1.30)



THE LOSS INCREASES WITH POROSITY AND THEREFORE  $\tan \delta$  IS INTRODUCED. PLOT OF  $\tan \delta$  AGAINST POROSITY ON A LOG-LOG PLOT SUGGESTED WHICH WOULD GIVE A DEPENDENCE OF THE FORM,

$$\tan \delta = (1-P) \tan \delta_0 + AP^n \quad (1.31)$$

$\tan \delta_0$  IS THE LOSS TANGENT OF FULLY DENSE MATERIAL ON WHICH AMOUNT OF MATERIAL PRESENT IE., IT SHOULD DEPEND ON THE POROSITY. THE ABOVE EQUATION CAN BE PUT IN LAW OF MIXTURES AS

$$\tan \delta = (1-P) \tan \delta_0 + P(AP^{n-1}) \quad (1.32)$$

THE LOSS MAY BE RELATED TO THE SURFACE AREA OF THE PORE VOLUME,

$$\tan \delta = (1-P) \tan \delta_0 + P(A'S) \quad (1.33)$$

AS PER THE SINTERING THEORY, SURFACE AREA OF THE PORES VARIES WITH POROSITY AS

$$S \propto \left( \frac{P}{1-P} \right)^{2/3} \quad (1.34)$$

SUBSTITUTING THE ABOVE EQUATION IN EQ. (1.33), WE GET [53]

$$\tan \delta = (1-P) \tan \delta_0 + A'P \left[ \frac{P}{1-P} \right]^{2/3} \quad (1.35)$$

## 1.5.2 EFFECT OF HUMIDITY

THE  $\tan \delta$  INCREASES WITH INCREASING POROSITY DUE TO MOISTURE IN THE PORES. HUMIDITY EFFECTS ON LOW FREQUENCY DIELECTRIC PROPERTIES OF POROUS MATERIALS HAVE BEEN STUDIED [54]. JONSCHER [55] IDENTIFIED LOW FREQUENCY LOSS MECHANISM IN MATERIALS IN THE PRESENCE OF MOISTURE AND STUDIED THE EFFECT IN SOME MATERIALS AT MICROWAVES. IT IS CLEAR THAT THE RELAXATION PROCESS CENTERED AT MICROWAVE RANGE IS RESPONSIBLE FOR HIGH DIELECTRIC LOSS OVER A WIDE FREQUENCY RANGE EXTENDING TO MICROWAVE RANGE. THE HUMIDITY EFFECTS ON LOW FREQUENCY DIELECTRIC PROPERTIES

MATERIALS HAVE BEEN ASSOCIATED TO THE LIBERATION FOUND IN THE DRY CONDITION. IN CONTACT WITH AN ADSORBED WATER FILM, THESE IONS BECOME FREE TO MOVE OVER REGIONS. THIS MECHANISM WOULD PRODUCE AN INTERFACIAL POLARIZATION PROCESS A LOW FREQUENCY PEAK. CHARGE CARRIERS COULD ALSO BE PRODUCED BY AN ELECTROLYTIC PROCESS OF DISSOCIATION OF WATER INTO A PROTON AND A HYDROXYL ION [57].

## 1.6 APPLICATIONS OF DIELECTRIC RESONATORS

WITH THE ADVENT OF TEMPERATURE STABLE DIELECTRIC RESONATORS HAVE EMERGED AS A HIGHLY CONVENIENTLY SIZED ELEMENT FOR APPLICATIONS IN MICROWAVE INTEGRATED CIRCUITS (MICS) FOR THE ENTIRE MICROWAVE FREQUENCY RANGE. THEY FORM FILTERS, OSCILLATORS, TRIPLEXERS, AND OTHER CIRCUITS DUE TO THEIR RELATIVELY HIGH Q FACTOR (VALUES AND GOOD FREQUENCY STABILITY. SOME APPLICATIONS OF MICROWAVE DIELECTRIC RESONATORS ARE BRIEFLY DISCUSSED BELOW.

### 1.6.1 DIELECTRIC RESONATOR OSCILLATORS

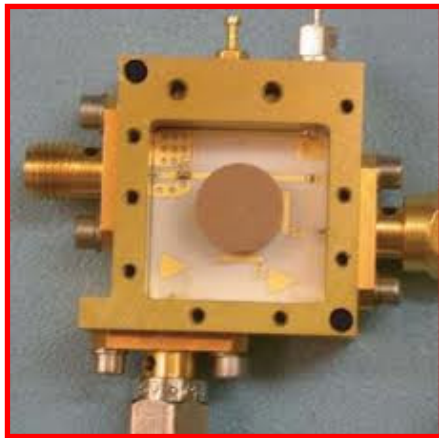


Fig. 1.6 Tuneable dielectric resonator oscillator.  
([www.londonmet.ac.uk/londonmet/library](http://www.londonmet.ac.uk/londonmet/library))

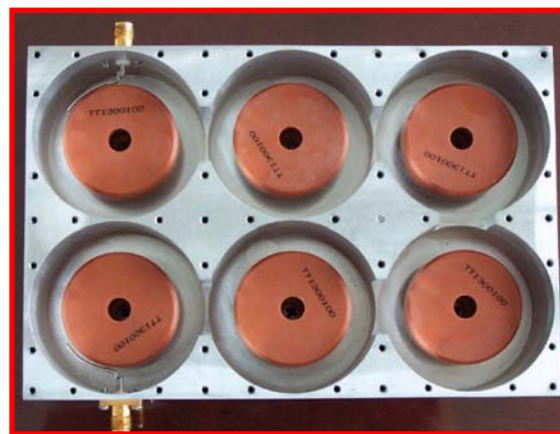


Fig. 1.7 A typical dielectric resonator filter. (BL microwave Ltd.)

OSCILLATORS REPRESENT THE BASIC MICROWAVE ENERGY SOURCE FOR ALL SYSTEMS SUCH AS RADARS, COMMUNICATIONS, NAVIGATION OR ELECTRONIC WARFARE. A MICROWAVE OSCILLATOR CONSISTS OF AN ACTIVE DEVICE (A DIODE OR TRANSISTOR)

FREQUENCY DETERMINING RESONANT ELEMENT. ADVANCEMENT OF TECHNOLOGY, THERE HAS BEEN AN INCREASING NEED FOR BETTER PERFORMANCE. THE EMPHASIS HAS NOISE, SMALL SIZE, LOW COST, HIGH EFFICIENCY, HIGH TEMPERATURE STABILITY AND DIELECTRIC RESONATOR OSCILLATORS (DRO) OFFER THE SYSTEM DESIGNER A VIABLE ALTERNATIVE. EFFORT TO MEET THESE CHALLENGES. THE APPLICATIONS OF DRO'S INCLUDE LOCAL OSCILLATORS FOR COMMUNICATION SYSTEMS, THE LARGEST APPLICATION OF WHICH MAY BE IN DIRECT TV. THE APPLICATION OF DR AS OSCILLATOR ELEMENT WAS FIRST PROPOSED BY DAY IN 1964. SUBSEQUENTLY, IN 1977, A 4 GHz BARRETT RESONATOR INTEGRATED WITH SI BIPOLAR TRANSISTOR WAS USED AS A FIXED FREQUENCY OSCILLATOR. THESE FUNDAMENTAL FIXED FREQUENCY OSCILLATORS ARE SIGNIFICANTLY SIMPLER AND EFFICIENT WITH 10–20 DB LOWER PHASE NOISE THAN CONVENTIONAL ELECTRONIC OSCILLATORS [59]. FIG. 1.6 SHOWS A TYPICAL TUNABLE DRO.

## 1.6.2 DIELECTRIC RESONATOR FILTERS

OWING TO THE SUPERIOR PERFORMANCE CHARACTERISTICS OF DIELECTRIC RESONATORS, THE USE OF DIELECTRIC RESONATORS HAS BECOME WIDESPREAD, PARTICULARLY IN HIGHLY SELECTIVE FILTERS. DIELECTRIC RESONATOR FILTERS ARE A CLASS OF STABLE MICROWAVE FILTERS FREQUENTLY USED IN RADAR AND COMMUNICATION SYSTEMS. A TYPICAL DIELECTRIC RESONATOR FILTER (SEE FIG. 1.7) CONSISTS OF CERAMIC RESONATOR DISCS MOUNTED IN A PARTICULAR WAVELENGTH METAL CAVITY. DIELECTRIC RESONATORS ARE OFTEN UTILIZED IN FILTER CIRCUITS BECAUSE OF THEIR INTRINSICALLY HIGH Q FACTOR. THE DIELECTRIC RESONATOR, OPERATING FREQUENCY, IS TUNABLE OVER A NARROW BANDWIDTH AND FREQUENCY FINE TUNING MUST BE ACCOMPLISHED WITHOUT AFFECTING THE Q OF THE RESONATOR. THESE CHARACTERISTICS ALLOW A DESIGNER EMPLOYING A DIELECTRIC RESONATOR TO HAVE EXCELLENT FREQUENCY STABILITY WITH A SMALL AMOUNT OF FREQUENCY DRIFT OVER A WIDE RANGE OF TEMPERATURES AND ENVIRONMENTAL CONDITIONS. UNLIKE METALLIC RESONATORS, DIELECTRIC RESONATORS YIELD LITTLE LOSS AND IMPEDANCE ELECTRIC FIELDS WHEN THEY ARE OPERATED IN DESIRED OPERATING MODES. DIELECTRIC RESONATORS EMPLOYED IN FILTERS COULD BE UTILIZED IN A VARIETY OF MODES, SUCH AS TEMPERATURE AND HEM (HYBRID ELECTROMAGNETIC) MODES. AT THE PRESENT TIME, DIELECTRIC RESONATOR FILTERS ARE EMERGING AS THE BASELINE DESIGNS FOR THE MAJORITY OF RF FILTERS USED IN COMMUNICATION SATELLITE APPLICATIONS. THE Q OF THESE FILTERS IS WITH A RELATIVE LOSS COEFFICIENT RATIO IN

COMPARISON WITH ANY OTHER KNOWN FILTER TECHNOLOGY. IF RECONFIGURABLE RF FILTERS ARE EMPLOYED IN WIRELESS BASE STATIONS AND SATELLITE SYSTEMS, TUNABLE DIELECTRIC FILTERS STAND TO BE THE OPTIMUM SOLUTION.

### 1.6.3 DIELECTRIC RESONATOR ANTENNAS

DIELECTRIC RESONATOR ANTENNAS (DRAS) ARE MADE FROM CERAMICS OR ANOTHER DIELECTRIC MEDIUM FOR MICROWAVE FREQUENCIES. DIELECTRIC RESONATOR ANTENNAS ARE FABRICATED ENTIRELY FROM LOW LOSS DIELECTRIC MATERIALS AND ARE TYPICALLY MADE AS FLAT PLATES. THEIR RADIATION CHARACTERISTICS ARE A FUNCTION OF THE MODE OF OPERATION OF THE DRA. THE MODE IS GENERALLY CHOSEN BASED UPON THE OPERATIONAL REQUIREMENTS. DIELECTRIC RESONATOR ANTENNAS OFFER SEVERAL ADVANTAGES OVER OTHER ANTENNAS: SMALL SIZE, HIGH RADIATION EFFICIENCY AND SIMPLIFIED COUPLING SCHEMES FOR VARIOUS TRANSMISSION LINES. THE BANDWIDTH CAN BE CONTROLLED OVER A WIDE RANGE BY THE CHOICE OF DIELECTRIC PERMITTIVITY AND THE GEOMETRIC PARAMETERS OF THE RESONATOR. DIELECTRIC RESONATOR ANTENNAS CAN ALSO BE MADE IN LOW PROFILE CONFIGURATIONS, MAKING THEM MORE AESTHETIC THAN STANDARD WHIP, HELICAL, OR OTHER UPRIGHT ANTENNAS.

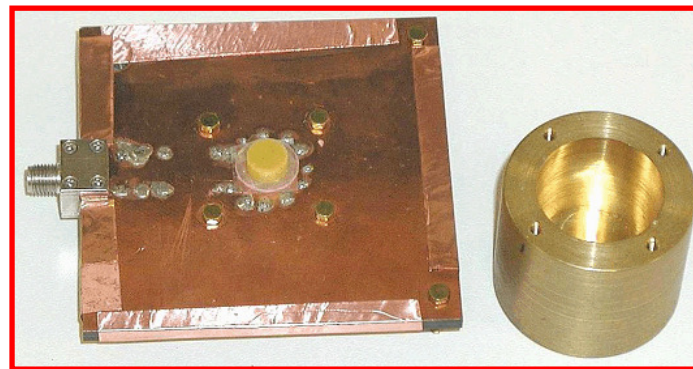


Fig. 1.8 A dielectric resonator antenna with a cap for measuring the radiation efficiency.  
([www.ee.olemiss.edu/researchbriefs/resonator.bmp](http://www.ee.olemiss.edu/researchbriefs/resonator.bmp))

## 1.7 SUBSTRATES

SUBSTRATES PROVIDE THE MECHANICAL BASIS AND DIELECTRIC MEDIUM ON WHICH THICK-FILM MATERIALS ARE FABRICATED. THEY MAY FUNCTION AS A SIMPLE PASS

PROVIDING STRENGTH AS IN MANY HYBRID MICROELECTRONIC MAY BE A KEY ACTIVE COMPONENT OF THE CIRCUIT AS IN SILICON SOLAR CELLS. ALL THICK-FILM SUBSTRATES ABILITY TO WITHSTAND HIGH TEMPERATURES AND HAVE HIGH ELECTRICAL RESISTIVE STRENGTH, DIELECTRIC BREAKDOWN VOLTAGE AND THERMAL SHOCK RESISTANCE. IN A GENERAL REQUIREMENTS, OTHER IMPORTANT PROPERTIES THAT DEPEND ON THE APPLIED THERMAL CONDUCTIVITY, THERMAL EXPANSION, SURFACE SMOOTHNESS, RELATIVE PERMITTIVITY AND DIELECTRIC LOSS. TABLE 1.1 LISTS THE KEY PHYSICAL AND DIELECTRIC PROPERTIES OF THESE SUBSTRATES.

**Table 1.1 Physical properties of selected substrate materials.**

| Property   | Al <sub>2</sub> O <sub>3</sub> | BeO     | AlN     | Silicon | Borosilicate glass |
|--|--------------------------------|---------|---------|---------|--------------------|
| CTE (PPM/°C)   | 6.6                            | 7.2-8.0 | 3.8-4.4 | 3.5     | 3.3                |
| THERMAL CONDUCTIVITY (WM <sup>-1</sup> K <sup>-1</sup> ) | 29-37                          | 260-290 | 140-260 | 125     | 1.2                |
| ε <sub>R</sub> (AT 1 MHZ)                                | 9.7-10.5                       | 6.5-7.0 | 8.0-9.2 | 11.8    | 4                  |
| TAN δ (AT 1 MHZ)   | 0.0002                         | 0.0004  | 0.0005  | 0.005   | 0.0004             |

CERAMIC SUBSTRATES ARE THE PREFERRED SUBSTRATE FOR MOST THICK-FILM APPLICATIONS DUE TO DIMENSION STABILITY AND INERTNESS AT TYPICAL THICK-FILM FIRING TEMPERATURES. HIGH ELECTRICAL RESISTIVITIES IN THE ORDER OF 10<sup>13</sup> OHM-CM AND DIELECTRIC BREAKDOWN VOLTAGES IN EXCESS OF 500 V/MIL, MAKING THEM IDEAL FOR HIGH-VOLTAGE CIRCUITRY. AMONG THE COMMERCIALY AVAILABLE SUBSTRATE MATERIALS, ALUMINA HAS BECOME THE MOST COMMON ONE BECAUSE IT COMBINES ELECTRICAL, MECHANICAL AND ECONOMICAL ADVANTAGES. ALUMINA IN ITS PURE FORM HAS A VERY HIGH SINTERING TEMPERATURE ABOVE 1700°C. IT ALSO POSSESS A HIGH THERMAL CONDUCTIVITY VALUE (AN ORDER OF MAGNITUDE HIGHER THAN SILICON). THE COMBINATION OF HIGH STRENGTH AND THERMAL CONDUCTIVITY GIVE BEO A GOOD THERMAL SHOCK RESISTANCE. THE CTE VALUE IS SLIGHTLY HIGHER THAN ALUMINA AND RELATIVE PERMITTIVITY IS SLIGHTLY LOWER. THE DISADVANTAGES WITH BERYLIA ARE THE HIGH COST AND POTENTIAL TOXICITY PROBLEM ASSOCIATED WITH ITS USE. THE HIGH THERMAL CONDUCTIVITY OF ALN CANNOT BE UTILIZED FOR SUBSTRATE APPLICATIONS, HOWEVER, THEY ALSO POSSESS A HIGH

TEMPERATURE. ALSO, THEY ARE REACTIVE TO SOME GLASS VITRIFIERS THUS CAUSING DIFFICULTIES IN CO-FIRING PROCESS. THUS SEARCH FOR NEW MATERIALS WITH GOOD DIELECTRIC PROPERTIES AND ALSO HAVING GOOD CO-FIRING PROPERTIES ARE STILL IN PROGRESS.

## 1.8 LOW TEMPERATURE CO-FIRED CERAMICS

### 1.8.1 INTRODUCTION

THE CURRENT TREND IN THE MICROELECTRONICS INDUSTRY IS TO REDUCE THE OVERALL SIZE OF ELECTRONIC PACKAGES. THIS MEANS THAT MORE COMPLEX PACKAGES HAVE TO BE DESIGNED WITH HIGHER INTERCONNECT DENSITY, SMALLER COMPONENTS BUT WITH SAME OR GREATER FUNCTIONALITY. AMONG THE VARIOUS FABRICATION METHODS OF ELECTRONIC DEVICES, LOW TEMPERATURE CO-FIRED CERAMIC (LTCC) TECHNOLOGY HAS BECOME AN ATTRACTIVE MANUFACTURING PLATFORM DUE TO ITS SPEED AND GOOD FUNCTIONALITY FOR COMPACT, LIGHT WEIGHT AND INTEGRATED ELECTRONIC COMPONENTS, MODULES, SUBSTRATES AND DEVICES OF LAMINATES AND PASSIVE COMPONENTS. INTEGRATION ON HIGH OHMIC SILICON, LTCC IS AN ESTABLISHED TECHNOLOGY FOR THE FABRICATION OF HIGHLY INTEGRATED MODULES FOR MOBILE COMMUNICATION DEVICES. TO REALIZE MINIATURIZED RF MODULES, ONE TECHNOLOGY TREND IS TO DECREASE THE LINEWIDTH OF METAL LINES TO REACH A HIGHER WIRING DENSITY. ANOTHER TREND IS TO INCREASE THE NUMBER OF THE PROCESSES IN ORDER TO ENABLE THE SUBSTRATE INTEGRATION OF FUNCTIONALITY TO MEET THE DEMAND OF ACCURACY. NEXT TO THESE PROCESSING TRENDS LTCC TECHNOLOGY OFFERS THE ABILITY TO COMBINE DIFFERENT TYPES OF CERAMIC MATERIALS INTO ONE MULTILAYER BOARD. LTCC TECHNOLOGY HAS THE ABILITY TO INTEGRATE PASSIVE COMPONENTS SUCH AS RESISTORS, CAPACITORS AND INDUCTORS INTO A MONOLITHIC PACKAGE [62-64], THEREBY FREEING VALUABLE CERAMIC AREAS FOR ACTIVE COMPONENTS. FOR THE MINIATURIZATION OF THESE FUNCTIONS, A CERAMIC MATERIAL WITH A REASONABLY HIGH RELATIVE PERMITTIVITY, INHERENT LOW LOSS AT HIGH FREQUENCIES AND EXCELLENT TEMPERATURE STABILITY IS REQUIRED. NEW LOW LOSS CERAMIC MATERIALS HAVE TO BE COMPATIBLE WITH RESPECT TO FIRING, DIELECTRIC, MAGNETIC AND MECHANICAL PROPERTIES WITH THE COMMERCIAL GLASS CERAMIC LTCC TAPES AND METALS. THAT MECHANICALLY RELIABLE MULTILAYER STRUCTURES WITH THE DESIRED ELECTRICAL PROPERTIES CAN BE MANUFACTURED. THE TARGET FIRING TEMPERATURE USED IN THESE TRENDS IS 850-940 °C IS THE MOST SUITABLE RANGE FOR COMMERCIAL LTCC METAL PASTES AND TAPES.

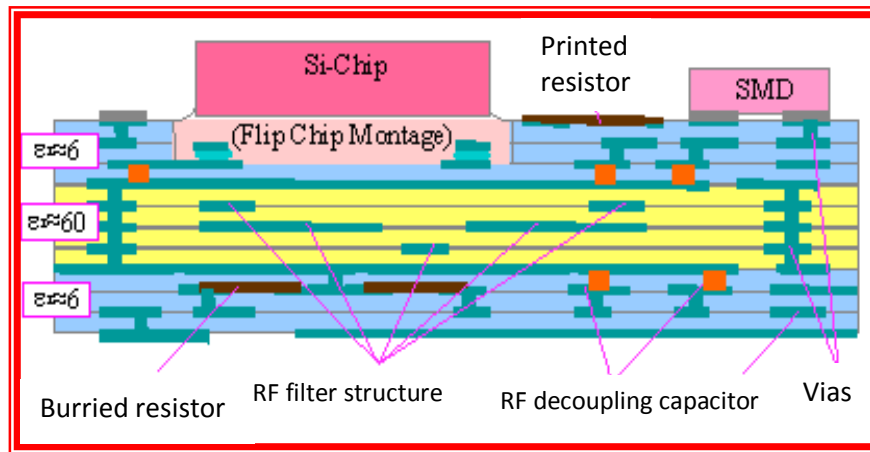


Fig. 1.9 LTCC multilayer module for telecommunication.

THE SIZE, COST AND PERFORMANCE OF INTEGRATION, PACKAGING AND INTERCONNECT TECHNOLOGIES ARE CRITICAL FACTORS FOR THE SUCCESS OF A MICROWAVE PRODUCT IN MILITARY AND COMMERCIAL APPLICATIONS, LOWER WEIGHT AND SMALLER SIZE REQUIREMENTS NECESSITATING INCREASED DENSITY IN ELECTRONICS PACKAGING. CROSS-TALK NOISE AND ELECTRIC SIGNAL DELAY ARE SUPPRESSED BY POSITIONING THE ELECTRIC-SIGNAL COMPONENTS IN ALTERNATING MATERIAL LAYERS. DOWNSIZING OR LOWERING SUBSTRATE LOSS (EG. DECREASE NUMBER OF CAPACITANCE LAYERS) CAN BE ACHIEVED BY FORMING INTERDIGITAL CAPACITORS ON HORIZONTAL LAYERS. ONE WAY TO ACHIEVE GREATER DENSITY IS THROUGH INTEGRATION OF DIFFERENT COMPONENTS WITHIN A SINGLE PACKAGE FIG. 1.9 SHOWS THE STRUCTURE OF AN LTCC MODULE. LTCC HAS THE UNIQUE ABILITY TO INTEGRATE A BROAD VARIETY OF COMPONENTS SUCH AS INDUCTORS, CAPACITORS AND FILTERS INTO A VERY COMPACT ARRANGEMENT.

## 1.8.2 HISTORICAL DEVELOPMENTS IN LTCC TECHNOLOGY

THE DEVELOPMENT OF MULTI CHIP INTEGRATED CIRCUITS WAS DRIVEN BY THE NEED FOR INCREASED INTERCONNECT DENSITY, HIGHER SIGNAL TRANSMISSION AND CLOCK SPEEDS IN MICROWAVE ELECTRONICS IN THE EARLY 1990'S. ALTHOUGH MCIC, IN GENERAL, WAS

MILITARY, SPACE APPLICATIONS ETC., LTCC-BASED TECHNOLOGY MADE ITS OWN BREAKTHROUGH IN THE TELECOMMUNICATION FIELD, WHICH IS ONE OF THE FASTEST GROWING IN THE CONSUMER ELECTRONICS INDUSTRY. THE HISTORY OF LTCC TECHNOLOGY ACCELERATED BACK TO EARLY 80'S, WHEN IT WAS FIRST DEVELOPED BY HUGHES AND DUPONT FOR COMMUNICATION SYSTEMS. THE ORIGIN OF MULTILAYER CERAMIC SUBSTRATE TECHNOLOGY IS AT RCA COMMUNICATIONS IN THE LATE 1950'S AND THE BASES OF CURRENT PROCESS TECHNOLOGIES WERE DISCOVERED [66-68]. PROGRESS WAS MADE USING THESE TECHNOLOGIES WITH IBM TAKING THE LEAD IN MULTILAYER CIRCUIT BOARD FOR IBM'S MAINFRAME COMPUTER COMMERCIALIZED IN THE EARLY 1980'S AS AN INHERITANCE [69-70]. SINCE THIS MULTILAYER BOARD WAS COFIRED AT THE HIGH TEMPERATURE (1600°C WITH THE ALUMINA INSULATING MATERIAL (ALN OR ALN-MO-MN)), IT IS CALLED HIGH TEMPERATURE COFIRED CERAMIC. FROM THE MIDDLE OF THE 1980'S, EFFORTS TO INCREASE THE SPEED OF MAINFRAME COMPUTERS ACCELERATED, AND AS THE KEY TO IMPROVE COMPUTER PERFORMANCE, FURTHER IMPROVEMENTS ARE MADE TO MULTILAYER CERAMIC SUBSTRATES FOR HIGH DENSITY MOUNTING APPLICATIONS. FINE WIRES WERE USED IN ORDER TO INCREASE WIRING DENSITY IN CIRCUIT BOARDS FOR HIGH DENSITY MOUNTING. BUT ATTENUATION OF SIGNALS DUE TO THE ELECTRICAL RESISTANCE OF THE WIRING. HENCE IT IS NECESSARY TO USE MATERIALS WITH LOW ELECTRICAL RESISTANCE (LIKE CU OR AU). IN ADDITION, WITH THE FLIP CHIP METHOD OF MOUNTING BARE LSI COMPONENTS DIRECTLY, POOR CONNECTION OF THE INTERCONNECTS MAY OCCUR DUE TO THERMAL EXPANSION OF THE BOARD IS NOT CLOSE TO THAT OF THE SILICON (3.5 PPM/°C). THEREFORE, AN INSULATING MATERIAL WITH LOW THERMAL EXPANSION (CERAMIC) IS DESIRABLE. FURTHERMORE, FOR HIGH SPEED TRANSMISSION OF SIGNALS, IT IS NECESSARY THAT THE CERAMIC HAS A LOW PERMITTIVITY. IN THE EARLY 1990'S, MANY JAPANESE AND AMERICAN ELECTRONIC AND CERAMIC MANUFACTURERS HAD DEVELOPED MULTILAYER BOARDS THAT MET THESE REQUIREMENTS. AMONG THEM, FUJITSU AND IBM WERE THE FIRST TO SUCCEED WITH COMMERCIAL APPLICATIONS OF MULTILAYER SUBSTRATES USING COPPER AS WIRING MATERIAL AND LOW RELUCTANCE CERAMICS. FROM THE LATTER HALF OF THE 1990'S TO THE PRESENT, THE FOCUS OF APPLICATIONS HAS SHIFTED TO HIGH FREQUENCY WIRELESS FOR THE ELECTRONIC COMPONENTS, MODULES AND SYSTEMS IN MOBILE COMMUNICATION DEVICES. FOR THE MULTILAYER CIRCUIT BOARD, THE LOW THERMAL EXPANSION OF CERAMICS WAS ITS BIGGEST MERIT FOR THE PURPOSE OF HIGH DENSITY MOUNTING.



LSI COMPONENTS. FOR HIGH FREQUENCY APPLICATIONS, TRANSMISSION LOSS IS ITS KEY FEATURE, AND THE LOW DIELECTRIC LOSS OF CERAMIC GIVES IT AN ADVANTAGE OVER O

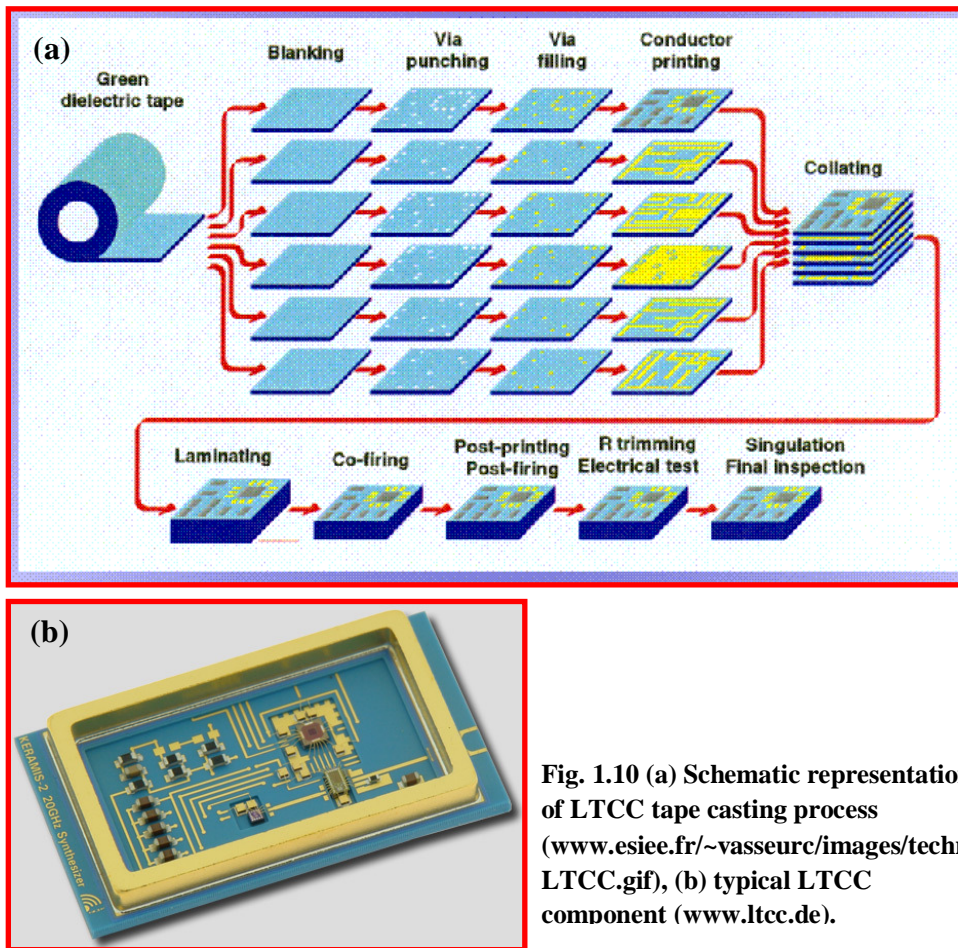


Fig. 1.10 (a) Schematic representation of LTCC tape casting process ([www.esiee.fr/~vasseurc/images/techno-LTCC.gif](http://www.esiee.fr/~vasseurc/images/techno-LTCC.gif)), (b) typical LTCC component ([www.ltcc.de](http://www.ltcc.de)).

DURING THE LATE 1980'S, U.S. AND JAPANESE MANUFACTURERS OF COMPUTER CERAMIC MATERIALS CONDUCTED EXTENSIVE RESEARCH AND DEVELOPMENT OF LTCC THAT IS NOW CRUCIAL TO PRESENT DAY AND FUTURE COMMUNICATION TECHNOLOGIES. 15 YEARS SCIENTISTS WORLD OVER HAVE DEVELOPED A LARGE NUMBER OF NEW DIELECTRIC MATERIALS (ABOUT 400) FOR HIGH FREQUENCY APPLICATIONS WITH LOW SINTERING TEMPERATURES AND BETTER PROPERTIES OF KNOWN MATERIALS. ABOUT 1000 PAPERS AND ABOUT 500 PATENTS HAVE BEEN PUBLISHED IN THE AREA OF LTCC MATERIALS AND RELATED TECHNOLOGIES. FOR DETAILS OF THE LTCC TECHNOLOGY, THE READER IS REFERRED TO THE RECENT REVIEW BY SEBASTIAN AND JANTUNEN [1].

GENERATION ELECTRONICS SYSTEMS WILL DEMAND THE PERFORM, LIGHTER WEIGHT AND AFFORDABILITY THAT LTCC TECHNOLOGY CAN PROVIDE.

### 1.8.3 MATERIAL SELECTION AND REQUIREMENTS

IN THE DEVELOPMENT OF LTCC APPLICATIONS SEVERAL PROPERTIES NEED TO BE TAKEN INTO ACCOUNT. THE ELECTRICAL PROPERTIES OF THE DIELECTRIC AND THE CONDUCTIVE PHASE ARE THE BASIC ISSUE, BUT DESIGNERS SHOULD ALSO BE AWARE OF THE EFFECTS OF THERMOMECHANICAL PROPERTIES, PRODUCTION COSTS AND VARIATION RANGE OF ELECTRICAL PROPERTIES [65]. THE IMPORTANT CHARACTERISTICS REQUIRED FOR AN IDEAL LTCC MATERIAL ARE LISTED BELOW.

#### 1.8.3.1 DENSIFICATION TEMPERATURE LESS THAN 950

AS THE NAME ITSELF SUGGESTS, LTCC IS A CERAMIC WITH METAL WIRING AT LOW TEMPERATURE, AND ITS CONSTITUENT MATERIALS ARE METAL AND CERAMIC. THE TYPICAL METALS USED IN LTCCS ARE THOSE WITH HIGH ELECTRICAL CONDUCTIVITY SUCH AS AG, AU, CU AND TI AND THEY ALL POSSESS A MELTING POINT WHICH IS NECESSARY TO CO-FIRE THE CERAMICS MATERIAL WITH THESE METALS, EXTREME PRECISION IS REQUIRED TO KEEP THE TEMPERATURE BELOW THEIR MELTING POINT (900). IN ORDER TO LOWER THE SINTERING TEMPERATURE SEVERAL METHODS CAN BE ADOPTED SUCH AS ADDITION OF LOW MELTING, LOW LOSS GLASS PHASE, CHEMICAL SYNTHESIS OF THE CERAMICS [74] AND USING STARTING MATERIALS WITH SMALL PARTICLE SIZE. AMONG THESE METHODS, LOW LOSS GLASS ADDITION SEEMS TO BE MUCH EFFECTIVE. IT IS NOTED THAT ANY DENSIFICATION OR CRYSTALLISATION OF THE COMPOSITE AT LOW TEMPERATURES SUCH AS BELOW 800 IS UNDESIRABLE AS THIS CAN PREVENT THE EVAPORATION OF ORGANICS AND SOLVENTS USED IN CONDUCTIVE PASTES AND BINDER AND PLASTICIZERS CAUSING CARBON TRACES IN THE MICROSTRUCTURE [60, 77]. ANY RESIDUAL CARBON THAT MAY BE LEFT FROM BINDER DECOMPOSITION IF LEFT IN THE LTCC WOULD ADVERSELY AFFECT THE DIELECTRIC PROPERTIES. THUS THE DENSIFICATION OF THE CERAMIC SHOULD START ABOVE THIS TEMPERATURE.

### 1.8.3.2 GLASS-CERAMIC COMPOSITES

IN THE FABRICATION OF DESIRABLE LTCC SUBSTRATES, SUFFICIENT DENSIFICATION AND SUFFICIENT CRYSTALLIZATION ARE GENERALLY NECESSARY TO ACHIEVE THE REQUIRED DIELECTRIC PROPERTIES. POROSITY AND LOW DEGREE OF CRYSTALLINITY WOULD LEAD TO POOR MECHANICAL PROPERTIES AND RESIDUAL GLASS WOULD DECREASE WITH INCREASING FREQUENCY. ATTEMPTS TO ACHIEVE THE ABOVE REQUIREMENTS ARE THE USE OF GLASSES INCLUDING A HIGH SOFTENING GLASS, NUCLEATING AGENTS, SINTERING AIDS AND PROCESS STRUCTURE MODIFIERS [78-81]. THREE APPROACHES HAVE BEEN USED TO OBTAIN GLASS-CERAMIC COMPOSITIONS SUITABLE FOR FABRICATING SELF-SUPPORTING LTCC SUBSTRATES. IN THE FIRST TYPE, THE GLASS-CERAMICS (GC), FINE POWDER OF A SUITABLE GLASS COMPOSITION IS USED TO OBTAIN A GLASS WITH THE ABILITY TO SINTER WELL TO FULL DENSITY IN THE GLASSY STATE AND SIMULTANEOUSLY CRYSTALLINE PHASES BECOME GLASS-CERAMIC. THE CRYSTALLINE PHASES MAKE THE GLASS-CERAMIC VERY STABLE TO FURTHER TEMPERATURE TREATMENTS SUCH AS POST FIRING PROCESSES. A TYPICAL EXAMPLE IS THE GLASS SYSTEM  $MgO-CO_2$  HAVING CORDIERITE AS THE PRINCIPAL CRYSTALLINE PHASE [82].

THE SECOND TYPE, THE GLASS-CERAMIC COMPOSITES (GCC), CONSISTS OF A MIXTURE OF A SUITABLE GLASS AND ONE OR FEW CERAMIC POWDERS, SUCH AS ALUMINA IN NEARLY EQUAL PROPORTIONS [83]. USUALLY A VOLUME CONTENT OF MORE THAN 50% OF A GLASS WITH A SOFTENING TEMPERATURE OF  $900^\circ\text{C}$  OR BELOW THE SINTERING TEMPERATURE OF THE COMPOSITE IS USED. THE GLASS SERVES AS A FLOW MEDIUM, IE., SINTERING OR DENSIFICATION IS CAUSED BY A VISCOUS FLOW, DISPERSING AND REARRANGING OF THE CRYSTALLINE PARTICLES IN THE GLASS MELT. ADDITIONAL PROCESSES SUCH AS DISSOLUTION AND PRECIPITATION OCCUR AT THE GLASS CERAMIC INTERFACE. THESE ARE NOT ESSENTIAL FOR THE DENSIFICATION PROCESS, IE., DENSIFICATION IS DUE TO LIQUID PHASE SINTERING. IN MOST CASES, THE REACTION BETWEEN THE GLASS AND THE CERAMIC POWDERS LEADS TO THE FORMATION OF NEW CRYSTALLINE PHASES WHICH AFFECTS THE PROPERTIES OF THE GLASS-CERAMIC. IN THE THIRD TYPE, THE GLASS BONDED CERAMICS (GBC), LOW VOLUME FRACTION (5-15%) OF A GLASS WITH A VERY LOW SOFTENING TEMPERATURE ( $< 400^\circ\text{C}$ ) IS USED TO DENSELY SINTER THE COMPOSITE. IN THIS CASE, IT IS NECESSARY THAT THE PARTICLE SIZE OF THE CRYSTALLINE PHASES BE VERY LOW. COMPARED TO THE SECOND CASE, THE GLASS FLOW CHARACTERISTICS WHICH MUST BE MET TO ACHIEVE FULL DENSIFICATION ARE VERY SOPHISTICATED. T

SPECIAL DEVELOPMENT OF SUITABLE GLASSES FOR BONDING CERAMICS IS ALWAYS NECESSARY. SOME OF THE LTCC MATERIALS BELONGING TO THE ABOVE MENTIONED CATEGORIES AND THEIR PROPERTIES ARE GIVEN IN TABLE 1.2.

Table 1.2 Some of the common LTCC dielectric and their main properties.

| LTCC dielectric material                             | $\epsilon_r$ (1 MHz) | CTE (ppm/ $^{\circ}$ C) | Bending strength (MPa) | $T_s$ ( $^{\circ}$ C) | Cond. material   | Company     |
|--|----------------------|-------------------------|------------------------|-----------------------|------------------|-------------|
| <b>Glass-ceramics</b>                                |                      |                         |                        |                       |                  |             |
| MGO- $Al_2O_3$ - $SiO_2$                             | 5.3-5.7              | 2.4-5.5                 | 180-230                | 850-950               | CU               | IBM         |
| CAO- $Al_2O_3$ - $SiO_2$ - $B_2O_3$                  | 6.7                  | 4.8                     | 250                    | 950                   | CU, NI           | TAIYO YUDEN |
| <b>Glass-ceramic composites</b>                      |                      |                         |                        |                       |                  |             |
| $SiO_2$ - $B_2O_3$ + $Al_2O_3$                       | 5.6                  | 4.0                     | 240                    | 1000                  | CU               | FUJITSU     |
| MGO- $Al_2O_3$ - $SiO_2$ - $B_2O_3$ + SILICA         | 4.3-5.0              | 3-8                     | 150                    | 850-950               | AG, AG/PD        | HITACHI     |
| <b>Glass-bonded ceramic</b>                          |                      |                         |                        |                       |                  |             |
| $BaTi_4O_{12}$ + $Bi_2O_3$ - $B_2O_3$ - $SiO_2$ -ZNO | 60                   | 9-10                    | 300                    | 900                   | AG, AU, AG/PD/PT | SIEMENS     |

THE EFFECTIVENESS OF SINTERING AIDS DEPENDS ON SEVERAL FACTORS SUCH AS TEMPERATURE, VISCOSITY, SOLUBILITY AND GLASS WETTABILITY [84]. IN ALL THESE COMPOSITES, THE DENSIFICATION IS ACHIEVED BY THE PROCESS OF LIQUID PHASE SINTERING. THE MAIN REQUIREMENT FOR LIQUID PHASE SINTERING IS THAT THE LIQUID PHASE SHOULD VISCOSITY OF THE CERAMICS. GENERALLY THE CHEMICAL REACTION BETWEEN SINTERING AIDS AND CERAMIC CAN PROVIDE THE BEST WETTING CONDITION [85]. HOWEVER, A CHEMICAL REACTION REACTION FORMATION OF THE SECONDARY PHASE. IT WAS SHOWN THAT ONE CAN EXPLOIT DIFFERENT MECHANISMS OF LIQUID PHASE SINTERING DEPENDING ON THE AMOUNT OF THE GLASS PHASE IN THE COMPOSITE MIXTURE. TO OBTAIN FULL DENSITY IN THE CERAMIC GLASS COMPOSITE, A CERTAIN QUANTITY OF GLASS (20-50 %) IS REQUIRED. TOO LITTLE GLASS CAN RESULT IN POOR DENSIFICATION.

WHICH PRODUCES LOW MECHANICAL STRENGTH AND ONLY FOR INTERNAL PRODUCTS. TOO MUCH GLASS (> 50%) IS ALSO UNDESIRABLE, BECAUSE IT CAUSE SHAPE DISTORTION DURING SINTERING AND ALSO DETERIORATES THE MICROWAVE DIELECTRIC PROPERTIES.

IT HAS BEEN REPORTED THAT THE GLASS MATERIALS FORM PARTICLE-PARTICLE CONTACTS DURING SINTERING. THESE CONTACTS CAN DISINTEGRATE THE SOLID PARTICLES INTO SMALLER GRAINS BY THE LIQUID PENETRATING MECHANISM. THE INTERACTION AND RESULTANT LIQUID-SOLID INTERFACE PROPERTIES ARE KNOWN TO BE HIGHLY DEPENDENT UPON CHEMICAL COMPOSITION OF THE LIQUID PHASE, IT IS STILL DIFFICULT TO MAKE PRECISE PREDICTIONS ABOUT THE LIQUID PHASE SINTERING MECHANISM. LOW MELTING GLASSES SUCH AS  $\text{B}_2\text{O}_3$ -ZNO GLASS AND  $\text{D}_3\text{BAO-SiO}_2$  GLASS HAVE BEEN CONSIDERED BASED ON SEVERAL ATTRIBUTES RELATED TO SINTERING TEMPERATURE, VISCOSITY, SOLUBILITY AND WETTABILITY. THESE GLASSES FORM COFIRED CERAMICS. THE CONSTITUENT OXIDES IN GLASS COMPOSITION ARE BROADLY DIVIDED INTO OXIDES THAT MAKE NETWORKS, MODIFIER OXIDES THAT BREAK NETWORK AND INTERMEDIATE OXIDES THAT CAN BECOME OXIDES OF EITHER TYPE. SINCE MODIFIER OXIDES BREAK NETWORKS, THEY LOWER THE SOFTENING POINT OF THE GLASS AND INCREASE ITS SOLUBILITY. BOROXYGEN AND A FEW OTHERS ARE THE COMMON NETWORK FORMERS. GLASSES MADE SOLELY FROM NETWORK FORMERS OFTEN HAVE LIMITED UTILITY. FOR EXAMPLE, PURE  $\text{SiO}_2$  IS NOT WATER RESISTANT AND PURE  $\text{SiO}_2$  GLASS WHILE VALUED FOR ITS CHEMICAL AND THERMAL SHOCK RESISTANCE, POSSESS HIGH PROCESSING TEMPERATURES (ABOUT 1700°C). MOST OF USEFUL GLASSES CONTAIN ADDITIVES THAT SERVE TO ALTER THE PROCESSING AND PROPERTIES. THESE ADDITIVES COMMONLY TERMED AS NETWORK MODIFIERS AND INTERMEDIATES. NETWORK MODIFIERS BRING EXTRA OXYGEN IONS BUT DO NOT PARTICIPATE IN THE NETWORK, THEREBY RAISING THE SOFTENING POINT OF THE GLASS. THE EXTRA OXYGEN ALLOWS THE BRIDGING OXYGEN BETWEEN TWO TETRAHEDRONS TO BE DISRUPTED AND TWO NON-BRIDGING OXYGEN TO TERMINATE EACH TETRAHEDRON. NETWORK MODIFIERS ARE DIRECTLY ANALOGOUS TO THE INTERMEDIATE OXIDES OBSERVED IN CRYSTALLINE SILICATES WITH INCREASING O/SI RATIO. IN GLASSES THE LOSS OF CONNECTIONS BETWEEN TETRAHEDRONS IN GREATLY DECREASED VISCOSITY FOR MODIFIED SILICATES AND REDUCES THE PROCESSING TEMPERATURES OF SILICATE GLASSES INTO MORE PRACTICAL RANGES, WHILE ALKALINE EARTH OXIDES ( $\text{CaO}$ ,  $\text{SrO}$ ,  $\text{BaO}$ ,  $\text{Li}_2\text{O}$ ,  $\text{K}_2\text{O}$ ) ARE VERY EFFECTIVE MODIFIERS, THEY RESULT IN GLASSES THAT ARE NOT CHEMICALLY DURABLE.

### 1.8.3.3 DIELECTRIC PROPERTIES

#### 1.8.3.3.1 Relative Permittivity ( $\epsilon_r$ )

LTCCS ARE BASICALLY COMPOSITE STRUCTURES OF CERAMICS AND METALS. THEREFORE, CONTROLLING THEIR RELATIVE PERMITTIVITY DEPENDS LARGELY ON THE COMBINATIONS OF MATERIALS OF THE COMPOSITE AND ITS MATERIAL COMPOSITION. GENERALLY, LOW PERMITTIVITY MATERIALS ARE USED FOR SUBSTRATE LAYERS WHILE HIGH PERMITTIVITY MATERIALS ARE OPTED TO ENABLE MINIATURISED, EMBEDDED CAPACITORS, INDUCTORS AND ANTENNAS [72, 86]. IN THE CASE OF CERAMIC PACKAGES, THE RELATIVE PERMITTIVITY OF CERAMIC OVER AND WITHIN THE METAL LINES GOVERNS THE PROPAGATION DELAY (BY [69]

$$t_d = \frac{l\sqrt{\epsilon_r}}{c} \quad (1.36)$$

WHERE  $l$  IS THE LINE LENGTH,  $\epsilon_r$  IS THE RELATIVE PERMITTIVITY OF THE SUBSTRATE AND  $c$  IS THE SPEED OF LIGHT. THUS SUBSTRATES WITH LOW RELATIVE PERMITTIVITY ARE REQUIRED TO INCREASE THE SPEED OF THE SIGNAL.

#### 1.8.3.3.2 Dielectric Loss ( $\tan \delta$ )

IN ORDER TO REDUCE THE DIELECTRIC LOSS IN LTCCS, IT IS NECESSARY TO CONSTRUCT THEM WITH LOW DIELECTRIC LOSS MATERIALS. THE DIELECTRIC LOSS VALUE OF LTCC MATERIALS, AS EXPRESSED BY  $\tan \delta$  (=  $t \cdot \delta$ ) MULTIPLIED BY THE MEASUREMENT FREQUENCY, WHICH SHOULD BE GREATER THAN 1000. SINCE THE DIELECTRIC LOSS OF GLASSES IS A MAJOR CONCERN IN THESE COMPOSITES, AT LEAST THREE TYPES OF DIELECTRIC GLASSES HAVE BEEN DISTINGUISHED: RESONANCE TYPE VIBRATIONAL LOSSES AT VERY HIGH FREQUENCIES, IONIC MIGRATION LOSSES CAUSED BY THE MOVEMENT OF MOBILE IONS AND DEFORMATION OF THE BASIC SILICON OXIDE NETWORK [87]. RESONANCE TYPE VIBRATIONAL LOSSES ARE PARTICULARLY IMPORTANT IN THE MICROWAVE REGION. AMONG THE GLASSES, FUSED QUARTZ HAS THE LOWEST DIELECTRIC LOSS IN THE MICROWAVE REGION [87-88]. THE DIELECTRIC LOSS OF FUSED QUARTZ IS LESS THAN 0.001 IN THE FREQUENCY RANGE FROM 10<sup>3</sup> TO 10<sup>10</sup> Hz. ALTHOUGH THE LOSS LEVEL IS ATTRACTIVE, SILICA IS NOT AN EFFECTIVE FLUX FOR MICROWAVE DIELECTRIC GLASSES ALONE. TO LOWER THE MELTING POINT, THE RIGID NETWORK IS BROKEN BY MODIFIERS,

PARTICULARLY ALKALI IONS, BUT THIS LOSS IS SIGNIFICANT FOR BINARY GLASSES BASED ON  $\text{SiO}_2$ .  $\tan \delta$  FOR BOROSILICATE IS ABOUT 0.001 AT 3 GHz. GLASSES BASED ON BOROSILICATES ALSO SHOWS LOW LOSS IN THE MICROWAVE REGION. SOME OF THE ALUMINA-BASED GLASSES SUCH AS CORDIERITE AND CELSIAN ALSO SHOW LOW LOSS FACTORS IN THE MICROWAVE REGION. THE LOSS TANGENT FOR CORDIERITE GLASS CERAMICS AT 10 GHz INCREASES WITH INCREASING DEGREE OF REDUCTION OF THE GLASS-CERAMIC. THE MINERAL CELSIAN WHICH CONTAINS TITANIUM DECREASED AT 10 GHz WITH INCREASING TEMPERATURE. THIS WAS PROBABLY DUE TO A DECREASE IN THE RESIDUAL GLASSY PHASE WHICH CONTRIBUTES TO INTERFACIAL POLARIZATION [91]. TABLE 1.3 GIVES THE PHYSICAL AND DIELECTRIC PROPERTIES OF VARIOUS GLASSES USED IN THE PRESENT INVESTIGATION.

#### 1.8.3.3 Temperature Stability of Dielectric Properties ( $\tau_f$ AND $\tau_\epsilon$ )

THE TEMPERATURE DEPENDENCE OF THE RESONANT FREQUENCY FOR LTCC'S IS SIGNIFICANT BECAUSE THE VARIOUS COMPONENTS BASED ON NON-COMPENSATED DIELECTRIC MATERIALS REQUIRE ADDITIONAL MECHANICAL AND ELECTRICAL DESIGN TO ENSURE SATISFACTORY ELECTRIC PERFORMANCE OF THE DEVICE OVER ITS OPERATING TEMPERATURE [92-93]. THE COEFFICIENT OF TEMPERATURE VARIATION OF THE RESONANT FREQUENCY OF 10 PPM/°C CAUSES A 0.11 % SHIFT OF THE RESONANT FREQUENCY (5.5 MHz AT 5.2 GHz) WITHIN THE TEMPERATURE RANGE -30°C TO +30°C. THOUGH NOVEL LTCC MATERIALS WITH ZERO COEFFICIENT (CT2000, 10 PPM/°C) HAVE BEEN DEVELOPED, THE COMPONENT DESIGNER MUST BE AWARE THAT THE STRUCTURAL DEFECTS CAN AFFECT ITS

#### 1.8.3.4 THERMAL PROPERTIES

THE CIRCUIT BOARDS AND PACKAGES UNDERGOING ASSEMBLY PROCESSES SUCH AS IN SOLDER REFLOW WHEN LSI COMPONENTS AND OTHER ELECTRONIC PARTS ARE ATTACHED TO THEM AND WHEN RELIABILITY TESTS ARE PERFORMED BEFORE PRODUCT SHIPMENT AND DURING DEVICE OPERATION. THUS IN ADDITION TO THE DIELECTRIC PROPERTIES, DESIGNERS MUST ALSO CONSIDER THE THERMAL PROPERTIES OF THE LTCC COMPOSITES.

#### 1.8.3.4.1 THERMAL CONDUCTIVITY

THE THERMAL CONDUCTIVITY OF LTCC MATERIALS IS RELATIVELY GOOD. THE REMOVAL OF HEAT GENERATED BY THE DEVICE DURING OPERATION IS CRITICAL FOR FUNCTIONING OF THE PACKAGE. IT IS THEREFORE NECESSARY TO MAINTAIN THE TEMPERATURE AT 100°C FOR EFFICIENT AND RELIABLE OPERATION. THE REQUIREMENT OF HEAT REMOVAL HAS BECOME EVEN MORE CRITICAL IN RECENT YEARS BECAUSE OF THE EVER-GROWING NEED TO PACK MORE DENSITY AND HIGH POWER DEVICES THAT CAN OPERATE AT HIGH SPEED. ADVANCED TECHNOLOGY AND THE CONTINUING TRENDS TOWARD MINIATURIZATION OF DEVICES IN PLACE EVEN MORE STRINGENT REQUIREMENTS ON HEAT DISSIPATION CHARACTERISTICS IN PACKAGING LTCC. THE THERMAL CONDUCTIVITY OF AN LTCC IS 2 W/MK, VERSUS 0.5 W/MK FOR ORGANIC MATERIALS. A COMMON METHOD TO IMPROVE THERMAL DISSIPATION IS TO USE A SPREADER, BUT A MORE ADVANTAGEOUS ALTERNATIVE PROVIDED BY LTCC TECHNOLOGY IS METALLIC VIA ARRAYS (THERMAL CONDUCTIVITY 50 W/MK) UNDER HIGH POWER COMPONENTS.

#### 1.8.3.4.2 THERMAL EXPANSION

THE COEFFICIENT OF THERMAL EXPANSION (CTE) IS A MEASURE OF THE CHARACTERISTIC CHANGE IN ITS DIMENSION FOR EACH DEGREE CHANGE IN TEMPERATURE. IF A MATERIAL IS UNIFORMLY HEATED OR COOLED. THUS, CTE CAN BE WRITTEN AS:

$$\alpha = \frac{\Delta l}{l_0 \Delta T} \quad (1.37)$$

WHERE  $\Delta l$  REPRESENTS THE CHANGE IN LENGTH OVER A TEMPERATURE RANGE FROM AN INITIAL LENGTH  $l_0$ . IT IS STRONGLY TEMPERATURE DEPENDENT. FOR MOST CERAMIC INSULATORS A NEAR LINEAR RANGE CAN BE DEFINED BETWEEN 0°C AND APPROXIMATELY 250°C, WHICH THE EXPANSION COEFFICIENT VARIES LITTLE. THE CTE IS AN IMPORTANT PARAMETER THAT AFFECTS THE SI BASED ICS ATTACHED. THEREFORE, THE SUBSTRATE IS EXPECTED TO HAVE VALUES CLOSE TO THAT OF SI IN ORDER TO AVOID DEFORMATIONS SUCH AS CRACK, DELAMINATION BETWEEN THE SUBSTRATE AND THE ATTACHED COMPONENTS DUE TO SHRINKAGE MISMATCH. THE EXPANSION COEFFICIENT IS A DIRECTIONAL OR ANISOTROPIC FACTOR BECAUSE OF ITS DEPENDENCE ON THE CRYSTAL STRUCTURE, BOND STRENGTH AND DENSITY.



### 1.8.3.5 CHEMICAL COMPATIBILITY WITH ELECTRODE MATERIAL

THE LTCC SHOULD NOT REACT WITH THE CONDUCTIVE MATERIAL. THE FORMATION OF ADDITIONAL PHASES IN THE CERAMIC SHOULD BE MINIMISED SINCE THE REACTION OF THE CERAMIC WITH THE CONDUCTING ELECTRODE, DEGRADES THE PERFORMANCE OF THE MICROWAVE DEVICE. A CRITICAL ISSUE IN MANUFACTURING LTCC MICROELECTRONICS IS THE PRECISE AND ACCURATE CONTROL OF SHRINKAGE ON SINTERING. IN THE SCREEN-PRINTING OF THE CONDUCTIVE PASTE INSTEAD OF PURE METALS, PASTES CONTAINING CONDUCTIVE PARTICLES IN GLASS MATRICES AND ADDITIVES ARE USED. THUS WHEN DEVELOPING LTCC MATERIALS, ONE HAS TO TAKE INTO ACCOUNT REACTIONS NOT ONLY WITH THE CONDUCTIVE MATERIAL LIKE SILVER BUT ALSO WITH THE CERAMIC AND THE CONDUCTOR PASTE.

**Table 1.3 Common LTCC glasses and their physical and dielectric properties.**

| Glass Code | Glass  | Density (g/cm <sup>3</sup> ) | T <sub>s</sub> (°C) | $\epsilon_r$ | TAN $\delta$ (1 MHz) | Ref. |
|------------|--|------------------------------|---------------------|--------------|----------------------|------|
| B          | B <sub>2</sub> O <sub>3</sub>  | 2.46                         | 450                 | 2.5          | 0.00550              | [95] |
| ZB1        | ZNO:B <sub>2</sub> O <sub>3</sub> (50:50)  | 3.65                         | 582                 | 6.9          | 0.00012              | [96] |
| ZB2        | ZNO:B <sub>2</sub> O <sub>3</sub> (71:29)  | 2.19                         | 567                 | 4.2          | 0.00330              | [97] |
| AS         | Al <sub>2</sub> O <sub>3</sub> :SiO <sub>2</sub> (50:50)   | 2.60                         | 850                 | 8.1          | 0.00970              | [97] |
| MAS        | MGO-Al <sub>2</sub> O <sub>3</sub> -SiO <sub>2</sub> (22:22:66)                                      | 2.30                         | 1350                | 4.5          | 0.00074              | [97] |
| MBS        | MGO-B <sub>2</sub> O <sub>3</sub> -SiO <sub>2</sub> (40:40:20)                                       | 3.18                         | 950                 | 5.0          | 0.00230              | [97] |
| BBS        | BAO-B <sub>2</sub> O <sub>3</sub> -SiO <sub>2</sub> (30:60:10)                                       | 3.40                         | 627                 | 7.2          | 0.00440              | [97] |
| ZBS        | ZNO-B <sub>2</sub> O <sub>3</sub> -SiO <sub>2</sub> (50:40:10)                                       | 3.55                         | 611                 | 6.9          | 0.00950              | [97] |
| LBS        | Li <sub>2</sub> O-B <sub>2</sub> O <sub>3</sub> -SiO <sub>2</sub><br>(35.14:31.66:33.2)              | 2.34                         | 513                 | 6.4          | 0.00360              | [75] |
| BBSZ       | B <sub>2</sub> O <sub>3</sub> -Bi <sub>2</sub> O <sub>3</sub> -SiO <sub>2</sub> -ZNO<br>(27:35:6:32) | 4.30                         | 950                 | 8.8          | 0.00130              | [98] |
| LMZBS      | Li <sub>2</sub> O-MGO-ZNO-B <sub>2</sub> O <sub>3</sub> -SiO <sub>2</sub><br>(20:20:20:20:20)        | 2.75                         | 900                 | 6.9          | 0.00200              | [99] |

## 1.8.4 APPLICATIONS OF LTCC TECHNOLOGY

NOWADAYS THERE ARE MANY NEW MICROELECTRONIC AND MESO SCALE APPLICATIONS OF THE LTCC TECHNOLOGY. LTCC IS VERY GOOD FOR HIGH VOLTAGE, HIGH PRESSURE OR VACUUM APPLICATIONS. THE TECHNOLOGY IS APPLIED TO BUILD MICROFLUIDIC DEVICES FOR MINIATURE FUEL CELL ENERGY CONVERSION SYSTEMS, DRUG DELIVERY, BIOLOGICAL MONITORING, GAS OR LIQUID CHROMATOGRAPHS, COOLING AND HEAT EXCHANGE DEVICES, MEMS SEPARATORS, POLYMERASE CHAIN REACTION (PCR) [101], MICRO TOTAL ANALYSIS SYSTEMS ( $\mu$ TAS), PHOTONIC DEVICES, MOEMS AND MEMS PACKAGING [102]. IMPORTANT NEW APPLICATIONS OF LTCC ARE MICROFLUIDIC SYSTEMS [103] USED MOSTLY FOR CHEMICAL ANALYSIS AND MICRO-HIGH PERFORMANCE LIQUID CHROMATOGRAPHY ( $\mu$ -HPLC) MADE IN LTCC DEMONSTRATING THE VERY GOOD PROPERTIES OF CERAMICS AT HIGH PRESSURES. THE PROPERTIES OF LTCC/CHINA SMART CHANNELS ARE COMPARABLE TO THE PERFORMANCE OF SILICON-BASED ONE. A MICRODISCHARGE DEVICE HAS BEEN DEVELOPED AND OPERATED IN NE GAS [104]. THE DEVICE CAN BE USED AS UV SOURCE IN BIOMOLECULE ASSAY OPERATIONS WHERE THE TARGET MOLECULES FLUORESCED IN THE UV LIGHT. LTCC STRUCTURE CAN BE USED AS A FOCUSING ELECTRODE FOR FIELD EMITTER ARRAYS [105]. LTCC MATERIALS ARE APPLIED FOR FIBER OPTIC AND ELECTRONIC PACKAGES [106]. SILICON MEMS PACKAGING IS ANOTHER VERY WIDE FIELD OF LITHOGRAPHY APPLICATION [107]. ANOTHER INTERESTING APPLICATION OF LTCC IS THREE-DIMENSIONAL PRINTING USED FOR EXAMPLE IN SPHERICAL STEPPER MOTOR [108] OR RADAR SENSOR.

## 1.9 COMPOSITES

### 1.9.1 INTRODUCTION

THE TREND FOR MICROELECTRONIC DEVICES IS HISTORICALLY CONTINUE TO BE, TOWARDS SMALLER FEATURE SIZE, FASTER SPEEDS, MORE COMPLEXITY, HIGHER POWER DENSITY AND LOWER COST. THE MOTIVATING FORCE BEHIND THESE ADVANCES TRADITIONALLY HAS BEEN MICROPROCESSOR WITH THE TREMENDOUS GROWTH OF WIRELESS TELECOMMUNICATION, RF APPLICATIONS BEGINNING TO DRIVE MANY AREAS OF MICROELECTRONICS TRADITIONALLY LED BY THE MICROPROCESSOR. AN INCREASINGLY DOMINANT FACTOR IN RF MICROELECTRONIC PACKAGING AND THE MATERIALS NEEDED TO CREATE THE PACKAGE, BECAUSE THE MATERIALS STRONGLY AFFECT THE PERFORMANCE OF THE RF ELECTRONICS. THE CONT

IN ELECTRONIC PACKAGING DENSITY HAS ~~BEFORE~~ ~~REQUIREMENTS~~ WITH HIGH THERMAL CONDUCTIVITIES. IN ADDITION, TO MINIMIZE THERMAL STRESSES THAT CAN CAUSE C SOLDER FAILURE, PACKAGING MATERIALS MUST HAVE COEFFICIENT OF THERMAL EXPAN WITH THOSE OF CERAMIC SUBSTRATES AND SEMICONDUCTORS. FURTHER, LOW DENSITY MANY APPLICATIONS, INCLUDING PORTABLE SYSTEMS SUCH AS LAP-TOP COMPUTERS TELEPHONES AND AVIONICS. REDUCING WEIGHT ALSO MINIMIZES POTENTIALLY DAMAG RESULTING FROM SHOCK LOADS THAT CAN OCCUR DURING SHIPPING AND FROM OTHE COST IS ALSO A KEY CONSIDERATION. AS TRADITIONAL MATERIALS USED IN ELECTRONI NOT MEET ALL OF THESE REQUIREMENTS, NEW COMPOSITE MATERIALS HAVE BEEN AND A TO BE DEVELOPED.

THE TERM 'COMPOSITES' DESCRIBES A MIXT~~URE OF~~ ~~DIFFERENT~~ ~~MATERIALS~~, EACH BEING PRESENT IN SIGNIFICANT QUANTITIES AND EACH IMPARTING A UNIQUE PROPERTY TO TH USE AND POTENTIAL FOR COMPOSITES IN ELECTRONIC PACKAGING IS VERY BROAD. BY C OR MORE CONSTITUENTS, IT IS POSSIBLE TO CREATE MATERIALS WITH UNIQUE COM PROPERTIES THAT CANNOT BE ACHIEVED IN ANOTHER WAY. THE BEST EXAMPLE IS PR BOARDS (PCBS), FOR WHICH DIELECTRIC PROPERTIES AND THE CTE ARE CRITICAL. POLY COMPOSITES IN THE FORM OF E-GLASS FIBER-REINFORCED POLYMER PCBS ARE WELL I PACKAGING MATERIALS. SIMILARLY, A VARIETY OF PARTICLES ARE ADDED TO POLYMER CTE AND INCREASE THE THERMAL CONDUCTIVITY, OR BOTH. THESE MATERIALS ARE USI TO AS PARTICLE-REINFORCED POLYMER-MATRIX COMPOSITES.

### 1.9.2 POLYMER-CERAMIC COMPOSITES

THE IMPORTANCE OF POLYMERS IN ELECTRONIC APPLICATION THAT, THOUGH THEY ARE NOT INTRINSICALLY FUNCTIONAL, THEY CAN BE DOPED AND MADE FUNCTION OR PLIABLE NATURE ENABLES FLEXIBLE FREE-STANDING SUBSTRATES IN A VARIETY OF UNTIL NOW, THE NEEDS OF SUBSTRATE MATERIALS WERE COVERED BY SOFT THERMOPL POLYTETRAFLUOROETHYLENE (PTFE) OR CERAMIC SUBSTRATES, BUT NEITHER SATIS REQUIRED DIELECTRIC AND MECHANICAL CHARACTERISTICS. THE PRESENCE OF TE FORMULATION OF SUCH POLYMERIC SUBSTRATES MAKES THE METALLIZATION PROC MANUFACTURE OF LARGE SIZED BOARDS DIFFICULT. IN ADDITION, THERE IS A POLYMER

ROOM TEMPERATURE, SO THE VARIATION OF THE RELATIVE TEMPERATURE IS NOT LINEAR. RECENTLY, THERE HAS BEEN A HUGE INTEREST IN POLYMER CERAMIC COMPOSITES. THEY ENABLE INEXPENSIVE INDUSTRIAL LEVEL REALIZATION OF 3-D MICROWAVE DEVICES AND PACKAGES WITH ADVANCED ELECTRIC AND MECHANICAL PROPERTIES. PARTICULARLY, POLYMERS USING THERMOPLASTIC POLYMERS SUCH AS PTFE, POLYETHYLENE, POLYSTYRENE, SILICONES, ETC HAVE DRAWN MUCH INDUSTRIAL AND ACADEMIC INTEREST BECAUSE THEY HAVE THE ADVANTAGE OF A SIMPLE, 3-D FABRICATION PROCESS SUCH AS INJECTION MOULDING OF COMPLEX COMPONENTS.

THE ALMOST LIMITLESS POSSIBILITIES TO COMBINE TWO OR MORE MATERIALS AT THE MICRO OR NANOSCOPIC LEVEL LEAD TO A LARGE RANGE OF PROPERTIES. POLYMER – CERAMIC COMPOSITES CONSISTING OF CERAMIC PARTICLES FILLED IN A POLYMER MATRIX ARE NOW WIDELY USED IN THE ELECTRONIC INDUSTRY AS SUBSTRATES FOR HIGH FREQUENCY USES, SINCE THEY COMBINE THE ELECTRICAL PROPERTIES OF CERAMICS AND THE MECHANICAL FLEXIBILITY, CHEMICAL STABILITY AND PROCESSING POSSIBILITY OF POLYMERS [109]. THE PRESENCE OF FILLER IN A SEMICRYSTALLINE POLYMER CAN CAUSE MANY CHANGES TO THE PHYSICAL PROPERTIES OF THE POLYMER. MANY REPORTS ARE AVAILABLE WHICH INVESTIGATES THE USE OF SILICA FILLED POLYMER COMPOSITES FOR PACKAGING APPLICATIONS. HOWEVER, BECAUSE OF THE LOW THERMAL CONDUCTIVITY OF CERAMICS, RESEARCHERS ARE EXTENDING THEIR WORK TO DEVELOP NEW FILLERS WITH HIGH THERMAL AND ELECTRICAL PERFORMANCE [110]. THERE ARE MANY POSSIBLE CANDIDATES FOR CERAMIC FILLERS HAVING BOTH HIGH THERMAL CONDUCTIVITY AND HIGH ELECTRICAL RESISTIVITY SUCH AS ALUMINA, BERYLLIA, BORON NITRIDE, ALUMINUM NITRIDE ETC. THE THERMAL PROPERTIES OF THE POLYMER CAN BE IMPROVED WITH A SUFFICIENTLY HIGH (> 40%) VOLUME PERCENTAGE OF FILLER. HOWEVER, HIGHER FILLER CONTENT RESULTS IN LOW STRENGTH, POOR FLUIDITY, POOR PROCESSABILITY, DEFECTS IN THE COMPOSITE AND HAVE ADVERSE EFFECT ON THE DIELECTRIC PROPERTIES. WITH THE PROPER DESIGN OF THESE COMPOSITES, WE CAN UTILIZE THE EASE OF PROCESSING OF POLYMERS, THE RELATIVE PERMITTIVITY OF POLYMERS AND HIGH THERMAL CONDUCTIVITY, LOW THERMAL EXPANSION COEFFICIENT AND THERMAL STABILITY OF CERAMICS.

### 1.9.3 CONNECTIVITY

MAKING CERAMIC POLYMER COMPOSITES NOT ONLY INVOLVES WEIGHT MATERIAL BUT ALSO COUPLING THEM WITH BEST POSSIBLE DESIGN. THE CONCEPT OF CONNECTIVITY ESTABLISHED BY NEWMAN [112]. CONNECTIVITY IS A KEY FEATURE IN THE DEVELOPMENT OF MULTI PHASE SOLIDS SINCE THE PHYSICAL PROPERTIES CAN BE CHANGED IN DIFFERENT MAGNITUDE DEPENDING ON HOW CONNECTIONS ARE MADE [113]. THE INTERSPATIAL RELATIONSHIP IN A MULTIPHASE MATERIAL HAS MAXIMUM IMPORTANCE BECAUSE IT CONTROLS THE FLOW OF ELECTRICAL, MAGNETIC AND THERMAL FLUXES BETWEEN THE PHASES. IN A COMPOSITE PHASE MAY BE SELF-CONNECTED IN EITHER ONE, TWO OR THREE DIMENSIONS. IN A TWO PHASE SYSTEM THERE ARE 10 DIFFERENT COMBINATIONS OF CONNECTIVITY AND THEY ARE 0-0, 0-1, 0-2, 0-3, 1-1, 1-2, 1-3, 2-2, 2-3 AND 3-3 CONNECTIVITY. THESE CONNECTIVITY PATTERNS ARE ILLUSTRATED IN FIG. 1.11 USING CUBE AS BUILDING BLOCK. THE MOST COMMONLY STUDIED COMPOSITES ARE 0-3 AND 3-3 CONFIGURATIONS. 0-3 CONFIGURATION CAN BE EASILY PREPARED AT RELATIVELY LOW

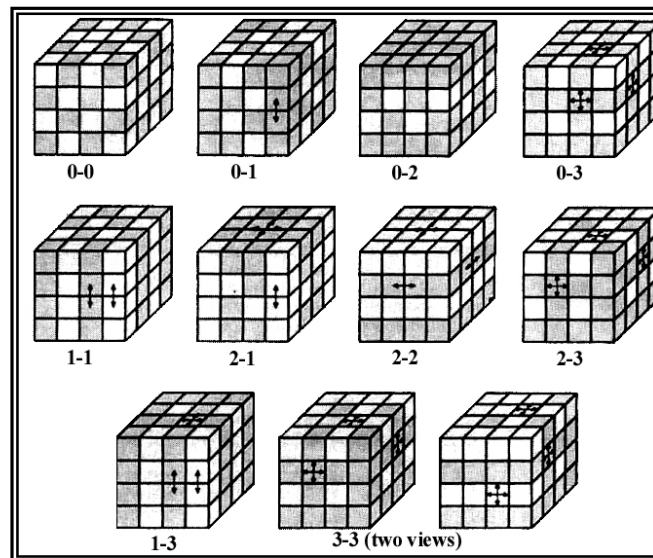


Fig. 1.11 Connectivity patterns in a di-phasic composites systems [112].

## 1.9.4 MATERIAL REQUIREMENTS FOR ELECTRONIC PACKAGING AND SUBSTRATE APPLICATIONS

THE SELECTION OF A PROPER RF SUBSTRATE MATERIAL IS INFLUENCED BY THE MATERIAL CHARACTERISTICS, PARTICULARLY ITS DIELECTRIC PROPERTIES, SINCE THEY SHOULD MATCH THE OTHER COMPONENTS. IN COMMERCIAL HIGH-FREQUENCY SUBSTRATES, BASED ON COMPOSITES OF CERAMIC OR WOVEN QUARTZ FILLERS AND HYDROCARBON RESINS OR MICROFIBERS MATRICES, IT IS DIFFICULT TO FIND TEMPERATURE-COMPENSATING MATERIALS WITH PERMITTIVITIES AROUND 10 AND LOW DIELECTRIC LOSSES [115].

### 1.9.4.1 DIELECTRIC PROPERTIES

DIELECTRIC PROPERTIES OF PACKAGING MATERIALS INFLUENCE THE PERFORMANCE OF HIGH SPEED MICROELECTRONIC DEVICES. ELECTRICAL CHARACTERISTICS OF MICROELECTRONIC DEVICES, SUCH AS SIGNAL ATTENUATION, PROPAGATION VELOCITY, AND REFLECTION COEFFICIENTS ARE INFLUENCED BY THE DIELECTRIC PROPERTIES OF THE PACKAGE SUBSTRATE AND THE WIRING MATERIAL. THE ELECTRICAL PROPERTIES IN MATERIAL SELECTION INCLUDE RELATIVE PERMITTIVITY, LOSS TANGENT, FREQUENCY AND TEMPERATURE STABILITY OF DIELECTRIC PROPERTIES, DIELECTRIC STRENGTH AND ELECTRICAL RESISTIVITY. AN IMPORTANT ROLE OF PACKAGING MATERIALS IS TO PROVIDE ELECTRICAL INSULATION OF THE SILICON CHIP AND OF CIRCUIT PINS. IDEALLY, A LOW LOSS FACTOR IS NEEDED TO AVOID CURRENT LEAKAGE, A LOW RELATIVE PERMITTIVITY TO MINIMIZE CAPACITIVE COUPLING EFFECTS AND REDUCE SIGNAL DELAY AND A LOW LOSS FACTOR TO REDUCE SIGNAL ATTENUATION [116]. THE TEMPERATURE COEFFICIENT OF THE RELATIVE PERMITTIVITY OF MICROWAVE SUBSTRATES IS VERY IMPORTANT IN MANY OUTDOOR WIRELESS APPLICATIONS FOR THE REDUCTION OF TEMPERATURE-INDUCED DRIFT IN CIRCUIT OPERATING CHARACTERISTICS [117]. HIGH ELECTRICAL RESISTIVITY AND DIELECTRIC STRENGTH ARE ALSO REQUIRED FOR MICROELECTRONIC APPLICATIONS.

### 1.9.4.2 THERMAL AND THERMO-MECHANICAL PROPERTIES

AN ELECTRONIC MATERIAL EXPERIENCES A RANGE OF TEMPERATURES, TEMPERATURE GRADIENTS, RATES OF TEMPERATURE CHANGE, TEMPERATURE CYCLING AND THERMAL SHOCKS THROUGH MANUFACTURING, STORAGE AND OPERATION. THERMAL PROPERTIES

SIGNIFICANT IN ENDURING SUCH LIFE CYCLE DEPENDENT PROPERTIES AS CONDUCTIVITY/DIFFUSIVITY, SPECIFIC HEAT CAPACITY AND COEFFICIENT OF THERMAL EXPANSION.

#### 1.9.4.3 MECHANICAL PROPERTIES

THE MECHANICAL PROPERTIES AFFECT THE MATERIALS UNDER LOADS DUE TO VIBRATIONS, SHOCK AND THERMOMECHANICAL STRESSES DURING MANUFACTURE, ASSEMBLY AND OPERATION. KEY PROPERTIES THAT ARE OF IMPORTANCE FOR ELECTRONIC PACKAGING INCLUDE THE MODULUS OF ELASTICITY, TENSILE STRENGTH, POISSON'S RATIO, FLEXURAL STIFFNESS, FRACTURE TOUGHNESS, CREEP RESISTANCE AND FATIGUE STRENGTH.

#### 1.9.4.4 CHEMICAL PROPERTIES

CHEMICAL PROPERTIES OF THE SUBSTRATE MATERIALS ARE IMPORTANT BECAUSE OF THE NEED TO SURVIVE MANUFACTURING, STORAGE, HANDLING AND OPERATING ENVIRONMENTS. PROPERTIES OF SIGNIFICANCE ARE WATER ABSORPTION, FLAMMABILITY AND CORROSION. THE ELECTRICAL PROPERTIES OF ELECTRONIC MATERIALS OFTEN CHANGE AS A RESULT OF WATER ABSORPTION, SWELLING AND OTHER DIMENSIONAL INSTABILITIES. THE CORROSION FORMATION OF MORE STABLE COMPOUNDS AND CAN DEGRADE THE PHYSICAL PROPERTIES OF MATERIALS.

THE KEY PROPERTIES OF THE COMPOSITE MATERIAL VIZ. THE RELATIVE PERMITTIVITY, CONDUCTIVITY AND COEFFICIENT OF THERMAL EXPANSION ARE DEPENDENT ON VARIOUS FACTORS AS THE NUMBER OF COMPONENTS OR PHASES, VOLUME FRACTION OF THE FILLER, THE PROPERTIES OF THE PHASES, PREPARATION METHOD AND THE INTERACTION BETWEEN THE FILLER AND MATRIX. HOWEVER, A LIMITATION FOR CERAMIC LOADING EXISTS FOR POLYMER-CERAMIC COMPOSITES WHICH IS ONE OF THE BIGGEST CONSTRAINTS TO IMPROVE ITS THERMAL, MECHANICAL AND ELECTRICAL PROPERTIES. BASED ON THE PRESENT TECHNOLOGY, A CERAMIC LOADING OF ABOVE 80% IS IMPRACTICABLE. HENCE BY THE PROPER DESIGN OF THESE COMPOSITES, WE CAN UTILIZE THE ADVANTAGES OF PROCESSING AND LOW RELATIVE PERMITTIVITY OF POLYMERS AND HIGH THERMAL CONDUCTIVITY, LOW THERMAL EXPANSION COEFFICIENT AND THERMAL STABILITY OF CERAMICS. VARIOUS TYPES OF COUPLING AGENTS AND DISTRIBUTIONS CAN OFFER DIFFERENT SURFACE ENERGIES THAT MAY FACILITATE THE BONDING BETWEEN THE POLYMER CHAINS [60, 119]. THE COUPLING AGENTS PROMOTE A CHANGE OF INTERFACIAL

PROPERTIES OF THE FILLER PARTICLES, FITTING BETWEEN THE FILLER AND THE POLYMER BINDER AND ULTIMATELY TO THE INCREASED PHYSICAL STRENGTH OF THE COMPOSITE [121].

### 1.9.5 ADVANTAGES OF POLYMER/CERAMIC COMPOSITES

COMPOSITE MATERIALS ARE TRADITIONALLY DESIGNED FOR ALL MATERIALS. WITH THE RAPID GROWTH OF THE ELECTRONICS INDUSTRY, COMPOSITE MATERIALS ARE BEING USED IN MORE AND MORE ELECTRONIC APPLICATIONS. THE DESIGN CRITERIA FOR THESE GROUP OF COMPOSITES ARE DIFFERENT BECAUSE OF THE VAST DIFFERENCE IN PROPERTY REQUIREMENTS BETWEEN STRUCTURAL COMPOSITES AND ELECTRONIC COMPOSITES. WHILE STRUCTURAL COMPOSITES EMPHASIZE HIGH STRENGTH AND HIGH MODULUS, ELECTRONIC COMPOSITES EMPHASIZE HIGH THERMAL STABILITY, LOW THERMAL EXPANSION, LOW RELATIVE PERMITTIVITY, HIGH/LOW ELECTRICAL CONDUCTIVITY, EFFECTIVE ELECTROMAGNETIC INTERFERENCE (EMI) SHIELDING EFFECTIVENESS, DEPENDING ON THE SPECIFIC ELECTRONIC APPLICATION. THE APPLICATIONS OF POLYMER-CERAMIC COMPOSITES IN MICROELECTRONICS INCLUDE INTERCONNECTIONS, PRINTED CIRCUIT BOARDS, ENCAPSULATIONS, INTERLAYER DIELECTRICS, DIE ATTACH, ELECTRICAL CONTACTS, COUPLERS, INTERFACE MATERIALS, HEAT SINKS, LIDS AND HOUSINGS. THE APPLICATIONS OF PRINTED CIRCUIT BOARDS CAN BE DIVIDED INTO TWO AREAS: INFORMATION TECHNOLOGY AND COMMUNICATIONS INDUSTRIES. BOTH APPLICATIONS HAVE IDENTICAL TECHNICAL DEMANDS FOR THE FUTURE OF HIGH-FREQUENCY APPLIANCES. AS THE WORKING FREQUENCY OF ELECTRONIC APPLIANCES INCREASES, SIGNAL INTENSITY LOSSES BECOME MORE SENSITIVE. CIRCUIT SUBSTRATES WITH POOR ELECTRICAL PROPERTIES WILL MAINTAIN AN UNFAVOURABLE SIGNAL CONVEYING EFFICIENCY. THEREFORE, THERE IS HIGH DEMAND IN HIGH FREQUENCY APPLIANCE MARKETS FOR SMALL RELATIVE PERMITTIVITY AND LOW DISSIPATION ENERGY SUBSTRATES. POLYMER-CERAMIC COMPOSITES ALSO OFFER EXCELLENT ELECTRICAL CHARACTERISTICS INCLUDING LOW TEMPERATURE PROCESSABILITY, FLEXIBILITY, HIGH THERMAL RESISTANCE, OUTSTANDING SOLVENT RESISTANCE ETC.



## 1.10 REFERENCES

1. [http://en.wikipedia.org/wiki/Communications\\_in\\_India#cite\\_note-informatm\\_india2013-6](http://en.wikipedia.org/wiki/Communications_in_India#cite_note-informatm_india2013-6).
2. M. T. SEBASTIAN, "Dielectric Materials for Wireless Communication", ELSEVIER SCIENCE PUBLISHERS, OXFORD, (2008).
3. W. D. KINGERY, "Introduction to Ceramics", JOHN WILEY AND SONS, NEW YORK, (1960).
4. R. J. CAVAJ, *Mater. Chem.*, **11**, 54-62, (2001).
5. R. D. RICHTMYER, *Appl. Phys.*, **10**, 391-398, (1939).
6. H. M. SCHLICKER, *Appl. Phys.*, **24**, 187-191, (1953).
7. B. D. SILVERMAN, *Phys. Rev.*, **125**, 1921, (1962).
8. W. G. SPITZER, R. C. MILLER, D. A. KLEINMAN AND L. E. HOWARTH, *Phys. Rev.*, **126**, 1710, (1962).
9. S. B. COHN, *IEEE Trans. Microwave Theory Tech.*, **16**, 218- 227, (1968).
10. R. L. BOLTON, *Ph.D Thesis, University of Illinois, Urbana-Champaign, IL*, (1968).
11. T. NEGAS, G. YEAGER, S. BELL AND R. AMBERLY, "and properties of temperature compensated microwave dielectrics", PROC. INT. CONF. CHEM. ELECTRON. CERAM. MATER. NIST SPECIAL PUBLICATION 804, 1990.
12. D. J. MASSE, R. A. PURCEL, D. W. READY, E. A. MAGUIRE AND C. DRÖBNER, *IEEE Trans.*, **59**, 1628, (1971).
13. Y. KONISHI, *Techn. Rep. NHK, TOKYO JAPAN*, **11**, (1971).
14. J. K. PLOURDE, *IEEE MTT-S Digest*, 202-205, (1973).
15. J. K. PLOURDE AND R. CHUNG, *IEEE Trans. Microwave Theory Tech.*, **29**, 754-770, (1981).
16. J. K. PLOURDE, D. F. LINN, H. M. O'BRYAN JR. AND J. THOMSON JR., *Ceram. Soc.*, **58**, 418-420, (1975).
17. K. WAKINO, M. KATSUBE, H. TAMURA, T. NISHIKAWA AND T. NISHIKAWA, *Int. Conf. Conv. Rec.*, PAPER **235**, (1977).
18. I. M. REANEY AND D. IDLER, *Ceram. Soc.*, **89**, 2063-2072, (2006).
19. H. TAMURA, T. KONOIKE AND K. WAKINO, *3rd U.S-Japan Seminar Dielectric Piezoelectr. Ceram.*, **69**, (1984).
20. H. TAMURA, T. KONOIKE, Y. SAKABE AND K. WAKINO, *Ceram. Soc.*, **67**, C59-C61, (1984).
21. K. WAKINO, K. MINAI AND H. TAMURA, *Ceram. Soc.*, **67**, 278-281, (1984).

22. H. M. O'BRYAN JR., J. THOMPSON JR. AND J. K. FLOURNOY, *IEEE Trans. Electron Devices*, **21**, 450-453, (1974).
23. Y. I. S. NISHIKAWA, J. HATTORI AND Y. IIDA, *IEEE Electron. Inf. Commun. Eng*, **J27-C-1**, 650, (1989).
24. K. P. SURENDRAN, M. T. SEBASTIAN, M. V. MANJUSHA, AND A. P. PHILLIP, *IEEE Appl. Phys. Lett.*, **98**, 44101-44105, (2005).
25. K. P. SURENDRAN, P. V. BIJUMON, P. MOHANAN AND M. T. SEBASTIAN, *IEEE Appl. Phys. Lett.*, **81**, 823-826, (2005).
26. T. TSUNOOKA, T. SUGIYAMA, H. OHSATO, K. KAKIMOTO, M. ANDOU, Y. HIGASHIDA AND H. SUGIURA, *Electroceramics in Japan VII*, **269**, 199-202, (2004).
27. Y. GUO, H. OHSATO AND K.-I. KAKIMOTO, *IEEE Ceram. Soc.*, **26**, 1827-1830, (2006).
28. N. H. NGUYEN, J. B. LIM, S. NAHM, J. H. PAIK AND J. H. KIM, *Ceram. Soc.*, **90**, 3127-3130, (2007).
29. T. T. H. OHSATO, M. ANDO, Y. OHISHI, Y. MIYAUCHI AND K. KAKIMOTO, *Ceram. Soc.*, **40**, 350-3, (2003).
30. T. T. H. OHSATO, A. KAN, Y. OHISHI, Y. MIYAUCHI, Y. TOHDO, T. OKAWA, K. KAKIMOTO AND H. OGAWA, *Key Eng. Mater.*, **269**, 195-8, (2004).
31. H. OGAWA, A. KAN, S. ISHIHARA AND Y. HIGASHIDA, *Ceram. Soc.*, **23**, 2485-2488, (2003).
32. L. A. KHALAM, S. THOMAS AND M. T. SEBASTIAN, *Appl. Ceram. Technol.*, **4**, 359-366, (2007).
33. J. C. KIM, M. H. KIM, J. B. LIM, S. NAHM, J. H. PAIK AND J. H. KIM, *Ceram. Soc.*, **90**, 641-644, (2007).
34. H. FROHLICH, *Theory of Dielectrics*, CLARENDON PRESS, OXFORD, (1950).
35. R. D. SHANNON, *Appl. Phys.*, **73**, 348-366, (1993).
36. D. KAJFEZ, *Q factor*, VECTOR FIELDS, OXFORD, (1994).
37. L. A. TRINOGGA, G. KAIZHOU AND I. C. HUNTER, *Microstrip Circuit Design*, ELLIS HORWOOD, BOSTON, (1991).
38. P. J. HARROLD, *Dielectrics*, BUTTERWORTH, LONDON, (1972).
39. D. KAJFEZ AND P. GUILLOM, *Dielectric Resonators*, NOBLE PUBLISHING CORP. ATLANTA, (1998).
40. Y. KOBAYASHI AND S. TANAKA, *Trans. Microwave Theory Tech.*, **MTT-28**, 1077-85, (1980).
41. S. K. KAUL, *Millimeterwaves and Optical Dielectric Integrated Circuits*, WILEY, NEW YORK, (1997).

42. H. RUBENS AND G. HERTZ, *Zn. Ber.*, **14**, 256, (1912).
43. P. P. EWALD, *Naturwissenschaften*, **10**, 1057, (1922).
44. I. J. BAHL AND P. BHARTIYA, "Microwave Solid State Circuit Design", WILEY, NEW YORK, (1988).
45. K. WAKINO, M. MURATA AND H. TAMURA, *IEE Proc. & Trans. Microw. & Antennas Propag.*, **69**, 34-37, (1986).
46. P. J. HARROP, *Mater. Sci.*, **4**, 370-374, (1969).
47. E. L. COLLA, I. M. REANEY AND N. SETTER, *Semicond. Sci. Technol.*, **74**, 3414-3425, (1993).
48. I. M. REANEY, E. L. COLLA, AND N. SETTER, *Appl. Phys. Part 1*, **33**, 3984-3990, (1994).
49. A. TEMPLETON, X. R. WANG, S. J. PENN, S. J. WEBB, L. F. COHEN AND N. M. ALFORD, *Ceram. Soc.*, **83**, 95-100, (2000).
50. D. A. SAGALA AND S. NAMBI, *Ceram. Soc.*, **75**, 2573-2575, (1992).
51. W. D. KINGERY, H. K. BOWEN AND D. R. UHLMANN, "Introduction to Ceramics", 2ND ED., WILEY, NEW YORK, (1976).
52. R. HEIDINGER AND S. NAZARE, *Metall. Int.*, **20**, 30 (1988).
53. S. J. PENN, N. M. ALFORD, A. TEMPLETON, X. R. WANG, M. S. XU, M. REECE AND K. SCHRAPPEL, *Am. Ceram. Soc.*, **80**, 1885-1888, (1997).
54. R. F. FIELD, *Appl. Phys.*, **17**, 318-325, (1946).
55. A. K. JONSCHER, "Universal Relaxation Law", CHELSEA DIELECTRIC, LONDON, (1996).
56. W. R. TINGA, W. A. G. VOSS AND D. F. BLOSSOM, *J. Appl. Phys.*, **44**, 3897-3902, (1973).
57. J. MOLLA, M. GONZALEZ, R. VILA AND J. A. BARRO, *IEEE Trans. Microw. & Antennas Propag.*, **85**, 1727-1730, (1999).
58. W. R. DAY, *IEEE MTT-S Int. Microwave Symp. Dig.*, **24** (1970).
59. J. K. PLOURDE, D. F. LINN, I. TATSUGUCHI AND C. E. SWANSON, *IEEE MTT-S Int. Microwave Symp. Dig.*, **273** (1977).
60. R. R. TUMMALA, *Am. Ceram. Soc.*, **74**, 895-908, (1991).
61. M. T. SEBASTIAN AND H. JANTUNEN, *IEEE Mater. Rev.*, **53**, 57-90, (2008).
62. J. L. SPRAGUE, *IEEE Trans. Compon. Hyb. Manuf. Technol.*, **13**, 390-396, (1990).
63. L. GOLDBERG, *Electronic Design*, **43**, 40, (1995).
64. J. ALEXANDER, *International Symposium on Microelectronics*, **2105**, 204-208, (1993).
65. H. JANTUNEN, T. KANGASVIERI, J. VÄHÄKANGAS AND R. LEPPÄWÄRD, *IEEE Proc. Soc.*, **23**, 2541-2548, (2003).
66. H. W. STETSON, *Ceramics and Civilization*, **3**, 307 (1987).
67. W. J. GYUVK, U. S. PATENT NO. 3, 192, 086, (1965).

68. H. STESON, U. S. PATENT NO. 3, 189, 978, (1965).
69. B. SCHWARTZ, *Ceram. Soc. Bull.*, **63**, 577 (1984).
70. A. J. BLODGETT AND D. R. BARRIBOUR, *Res. Dev.*, **26**, 30, (1982),
71. Y. IMANAKA, *Multilayered Low Temperature Cofired Ceramics (LTCC) Technology*”, SPRINGER SCIENCE, U.S.A., (2005).
72. H. KAGATA, T. INOUE, J. KATO AND I. KAMEYAMA, *J. Appl. Phys. Part 1*, **31**, 3152-3155, (1992).
73. D. W. KIM, J. R. KIM, S. H. YOON, K. S. HONG AND C. K. KIM, *Ceram. Soc.*, **85**, 2759-2762, (2002).
74. Y. XU, G. HUANG AND Y. CHEN, *Ceram. Int.*, **31**, 21-25, (2005).
75. J. H. PARK, Y. J. CHOI AND J. G. PARK, *Chem. Phys.*, **88**, 308-312, (2004).
76. O. A. SHLYAKHTIN, A. V. ORLOV AND Y. ELCHERAM, *J. Electroceram.*, **17**, 405-413, (2006).
77. V. GEKTIN, A. BAR-COHEN AND S. WITZMAN, *Trans. Compon. Packag. Manuf. Technol. Part A*, **21**, 577-584, (1998).
78. J. H. JEAN AND T. K. GUPTA, *J. Mater. Sci.*, **27**, 1575-1584, (1992).
79. J. H. JEAN AND J. I. SHEN, *J. Appl. Phys. Part 1*, **35**, 3942-3946, (1996).
80. J. H. JEAN AND C. R. CHANG, *Ceram. Soc.*, **80**, 3084-3092, (1997).
81. J. H. JEAN AND J. I. SHEN, *J. Mater. Sci.*, **31**, 4289-4295, (1996).
82. S. H. KNICKERBOCKER, A. H. KUMAR AND L. WAHLERS, *Ceram. Soc. Bull.*, **72**, 90-95, (1993).
83. A. H. KUMAR, P. W. MCMILLAN AND R. R. TUMMALAR, U. S. PATENT NO. 4 301 324, (1981).
84. W. D. KINGERY, *J. Appl. Phys.*, **30**, 301-306, (1959).
85. J. H. JEAN AND S. C. LIN, *Am. Ceram. Soc.*, **83**, 1417-1422, (2000).
86. R. L. WAHLERS, S. J. STEIN, Y. D. HUANG AND M. R. HEINZ, *Multilayer Dielectric System for Telecommunications*”, TECHNICAL PUBLICATIONS OF ELECTRO-SCIENCE LABORATORIES, PRUSSIA, PA, USA.
87. L. NAVIAS AND F. L. GREENE, *J. Appl. Phys.*, **29**, 267-276, (1946).
88. E. B. SHAND, *Properties of Glass*”, GLASS ENGINEERING HANDBOOK, MCGRAW-HILL, NEW YORK, (1958).
89. A. R. VON HIPPEL, *Dielectric Materials and Applications*”, TECHNOLOGY PRESS OF MIT, CAMBRIDGE, MA AND JOHN WILEY AND SONS, NEW YORK, (1954).
90. D. L. KINSER, *Electrical Conduction in Glass and Glass-Ceramics*”, PHYSICS OF ELECTRONIC CERAMICS PART A, MARCEL DEKKER, NEW YORK, 523-37, (1971).

91. T. TAKADA, S. F. WANG, S. YOSHIKAWA, S. J. JANG AND R. E. NEWHAM, *Soc.*, **77**, 2485-2488, (1994).
92. C. WANG AND K. A. ZAKKEE *MMT-S Intern. Microwave Symp. Digest*, **3**, 1041 (1993).
93. H. JANTUNEN AND A. TURUNEN *Internat*, **5**, 302-924 (1994).
94. B. M. J.P. SOMMER, U. GOEBEL AND J. JELONNEK, *Inter Society Conference on Thermal and Thermomechanical Phenomena in Electronic systems, IOTHERM*, 360 (2000).
95. L. NAVIAS AND R. L. GREEN, *Ceram. Soc.*, **29**, 267, (1946).
96. J.-M. WU AND H.-L. HUANG, *Non-Cryst. Solids*, **260**, 116-124, (1999).
97. K. P. SURENDRAN, P. MOHANAN, AND M. T. SEBASTIAN, *Chem.*, **177**, 4031-4046, (2004).
98. O. DERNOVSEK, A. NAEINI, G. PREU, W. WERSING, M. EBERSTEIN AND W. SCHILLER, *Ceram. Soc.*, **21**, 1693-1697, (2001).
99. S. N. RENJINI, S. THOMAS, M. T. SEBASTIAN, S. R. KIRAN AND V. R. MURPHY, *Ceram. Technol.*, **6**, 286-294, (2009).
100. L. J. GOLONKA, A. MARKOWSKI, H. ROGUSZCZAK AND T. ZAWADA, *Elektronika*, **45**, 13-14, (2004).
101. C. F. CHOU, R. CHANGRANI, P. ROBERTS, D. SADLER, J. BURDON, F. ZENHAUSERN, S. LIN, A. MULHOLLAND, N. SWAMI AND R. TERBRUGGEN, *Eng.*, **61-62**, 921-925, (2002).
102. J. W. SOUCY, J. F. HALEY AND T. F. MARINIS, *International Symposium on Microelectronics*, **4339**, 768-771, (2000).
103. R. E. BRUZETTI LEMINSKI, *IMAPS/AcerS 1st Int. Conf. and Exhib. on Ceramic Interconnect and Cer. Microsystem Technologies (CICMT)*, BALTIMORE (USA), 337-342, (2005).
104. B. A. VOJAK, S. J. PARK, C. J. WAGNER, J. G. EMMORIELLA, J. BURDON, F. ZENHAUSERN AND D. L. WILCOX, *Appl. Phys. Lett.*, **78**, 1340-1342, (2001).
105. X. CHENGGANG, W. YI AND B. G. SNEHT, *Trans. Electron. Devices*, **49**, 324-328, (2002).
106. P. S. W. BUSS, W. BRODE, A. HEYMEL, F. BECHTOLD, E. MUELLER, T. BARTNITZEK, B. PAWLOWSKI, AND K. KASCHLICK, *13th European Microel. and Pack. Conf.*, BRUGGE (BELGIUM), 325-328, (2005).
107. L. J. GOLONKA, A. DZIEDZIC, J. DZIUBAN, J. KITA AND T. ZAWADA, "A Design for MEMS device", OPTOELECTRONIC AND ELECTRONIC SENSORS V, ED. W. KALITA, PROCEEDINGS SPIE 5124, 115-119, (2003).

108. J. LI AND G. K. ANANTHASUBRAMANIAM, *J. Mech. Microeng.*, **12**, 198-203, (2002).
109. D. S. SOANE AND Z. MARTYNEK, *Encyclopedia in Microelectronics: Fundamentals and Applications*, ELSEVIER, NEW YORK, (1989).
110. M. T. SEBASTIAN AND H. JANUEN, *J. Appl. Ceram. Technol.*, **7**, 415-434, (2010).
111. S. YU, P. HING AND X. HU, *J. Appl. Phys.*, **88**, 398-404, (2000).
112. R. E. NEWNHAM, D. P. SKINNER AND L. E. CROSS, *J. Res. Natl. Bur. Stand. Sect. A*, **82**, 525-536, (1978).
113. D. S. MALACHLAN, M. BLASZKIEWICZ AND R. E. NEWNHAM, *J. Appl. Phys.*, **73**, 2187 (1990).
114. C. J. DIAS AND D. K. DAS-GUPTA, *IEEE Trans. Dielectr. Electr. Insul.*, **3**, 706-734, (1996).
115. E. MOTYL AND B. LOW, *J. Appl. Phys.*, **92**, 379-385, (2002).
116. Y. Y. SUN, Z. Q. ZHANG AND C. P. WONG, *J. Appl. Phys.*, **46**, 2297-2305, (2005).
117. L. M. WALPITA, P. N. CHEN, H. A. GOLDBERG, A. HARRIS AND C. ZIPP, U.S. PATENT NO. 5739193 (1998).
118. G. M. G. PECHT, R. AGARWAL, P. MCCLUSKEY, T. DISHONGH, S. JAVADPOUR AND R. MAHAJAN, *Electronic Packaging Materials and there Properties*, CRC PRESS, LONDON, (1999).
119. Y. C. CHEN, H. C. LIN AND Y. D. LEE, *J. Polym. Res.*, **10**, 247-258, (2003).
120. M. G. TODD AND F. G. SHI, *J. Appl. Phys.*, **94**, 4551-4557, (2003).
121. L. RAMAJO, M. S. CASTRO AND M. M. REREDDO, *J. Appl. Phys.*, **38**, 1852-1859, (2007).

## **CHAPTER 2**

### **SYNTHESIS AND CHARACTERISATION**

*This chapter emphasizes the various steps involved in the synthesis of dielectric ceramics and its composites. A brief description of the instrumentation techniques used for studying the structural, microstructural, microwave dielectric properties and thermal characteristics of low loss materials is also presented.*

## 2.1 CERAMIC PROCESSING

### 2.1.1 INTRODUCTION

REMARKABLE PROGRESS IN SYNTHETIC CHEMISTRY AND RELATED FIELDS HAS LED TO ADVANCES IN MATERIAL SCIENCE. DURING THE PAST 100 YEARS SCIENTISTS AND ENGINEERS HAVE ACQUIRED A MUCH BETTER UNDERSTANDING OF CERAMIC MATERIALS AND THEIR PROCESSING. THEY HAVE FOUND THAT NATURALLY OCCURRING MINERALS COULD BE REFINED OR NEW COMPOSITES COULD BE DEVELOPED TO ACHIEVE UNIQUE PROPERTIES. HIGHLY HOMOGENEOUS AND STABLE INDUSTRIAL CERAMICS, WHICH EXISTING IN NATURE HAVE BEEN COMMERCIALY PRODUCED BY THE USE OF ARTIFICIAL STARTING MATERIALS. THE CREATION OF THESE ARTIFICIAL MATERIALS REQUIRED THE DEVELOPMENT OF CERAMIC PROCESSING FROM A TECHNOLOGY TO A SCIENCE. THIS DEVELOPMENT HAS SET THE BASIS OF SO-CALLED 'FINE OR ADVANCED CERAMICS'. FINE CERAMICS INCLUDES INORGANIC, NONMETALLIC SOLID MATERIALS OF POLYCRYSTALLINE SINTERED BODIES, FINE POWDERS, NONCRYSTALLINE MATERIALS, THICK OR THIN FILMS AND FIBERS WITH VARIOUS MORPHOLOGIES. THE FUNCTIONS OF THESE MATERIALS DEPEND ON THEIR MORPHOLOGY, OVER WHICH CONTROL HAS BEEN GAINED THROUGH ADVANCES IN PRODUCTION PROCESSES. CERAMIC FABRICATION IS THE APPLICATION OF VARIOUS PROCESS TECHNOLOGIES TO PRODUCE MONOLITHIC OR COMPOSITE CERAMIC PARTS WITHIN A GIVEN SHAPE, SIZE AND MICROSTRUCTURE PROPERTY BOUNDS FOR A GIVEN APPLICATION [1]. THE CERAMICS ARE IN GENERAL COMPOUNDS OF THE ELECTROPOSITIVE AND ELECTRONEGATIVE ELEMENTS OF THE PERIODIC TABLE. THEY ARE POLYCRYSTALLINE MATERIALS, WHICH CONSIST OF POLYCRYSTALLINE GRAINS, GRAIN BOUNDARIES, IMPURITIES SEGREGATED IN THE GRAIN BOUNDARIES, AS WELL AS THE GRAINS, PORES IN THE GRAINS, GRAIN BOUNDARIES AND IMPERFECTIONS.

MOST OF THE SYNTHESIS METHODS OF ORGANIC AND METALS ARE GENERALLY NOT SUITABLE FOR CERAMICS, DUE TO THE BRITTLINESS AND THE REFRACTORY NATURE OF THESE MATERIALS. THE PROCESSING OF CERAMICS INTO USEFUL PRODUCTS REQUIRES THE TRANSFORMATION OF POWDERED RAW MATERIALS TO A DENSE, UNIFORM BODY THROUGH THE APPLICATION OF CONSOLIDATION TECHNIQUES AND SUBSEQUENT THERMAL PROCESSING OR SINTERING. INSTEAD OF GLASS TECHNOLOGY, CERAMIC FORMING TECHNIQUES ARE GENERALLY BASED ON THE PROCESSING WITH POWDER SYNTHESIS, FORMING AND SINTERING. THE SYNTHESIS OF CERAMIC POWDERS AND BETTER CONTROL OF CHEMICAL AND PHYSICAL CHARACTERISTICS OF CERAMICS



ALLOW OBTAINING IMPROVED AND/OR REPRODUCIBLE PROPERTIES. SEVERAL METHODS ARE USED FOR THE PREPARATION OF CERAMIC POWDERS. THE METHODS CAN BE DIVIDED INTO TWO CATEGORIES: (A) MECHANICAL METHODS AND (B) SOLID STATE REACTION METHODS AND OTHER METHODS. IN THE MECHANICAL METHODS, SMALL PARTICLES ARE PRODUCED FROM LARGER PARTICLES BY MECHANICAL FORCES, A PROCESS REFERRED TO AS COMMINUTION. THE PROCESS OF COMMINUTION INVOLVES OPERATIONS SUCH AS CRUSHING, GRINDING AND MILLING. POWDERS OF CERAMICS ARE GENERALLY PREPARED BY MECHANICAL METHODS FROM NATURALLY OCCURRING MATERIALS.

### 2.1.2 SOLID STATE SYNTHESIS OF CERAMICS

THE SOLID STATE OXIDE ROUTE IS CONSIDERED TO BE ONE OF THE OLDEST AND MOST COMMON MATERIALS SYNTHESIZING TECHNIQUES FOR THE SYNTHESIS OF COMPLEX OXIDE MATERIALS. MIXED OXIDES CONTAINING MORE THAN ONE TYPE OF CATION ARE OF INTEREST FROM BOTH AN ACADEMIC AND COMMERCIAL POINT OF VIEW. THIS IS BECAUSE COMPLEX METAL OXIDES EXHIBIT A NUMBER OF UNIQUE FEATURES THAT ARE NOT FOUND IN SIMPLE OXIDES. FOR EXAMPLE, MIXED METAL OXIDES STABILIZE BOTH HIGH AND MIXED OXIDATION STATES OF TRANSITION METAL ELEMENTS [3].

THE CONVENTIONAL CERAMIC APPROACH INVOLVES BASICALLY THREE STEPS: (A) MIXING OF THE STOICHIOMETRIC OXIDES, (B) HIGH TEMPERATURE FIRING AND (C) FINISH GRINDING.

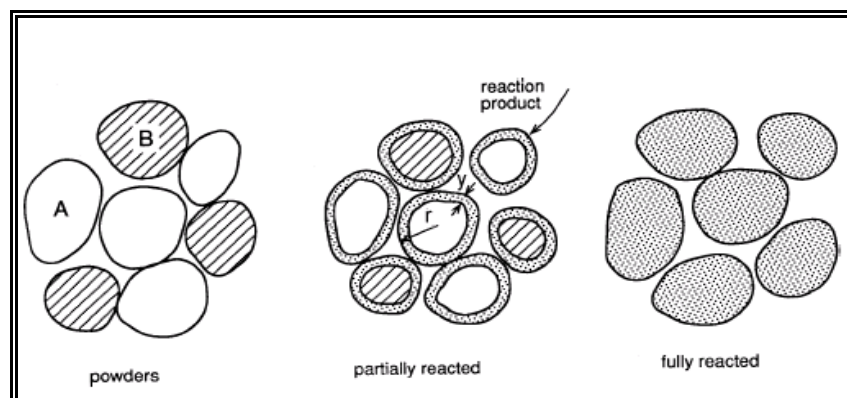


Fig. 2. 1 Reaction between two kinds of particles to form a product at the points of contact.

ON HEATING AT HIGH TEMPERATURES, A NEW MATERIAL IS FORMED (SEE FIG. 2.1) THROUGH THE FREE ENERGY, AT THE POINTS OF CONTACT THROUGH SOLID STATE DIFFUSION. THE PRODUCT LAYER (OF A NEW MATERIAL) EVENTUALLY ACTS AS A POTENTIAL BARRIER BETWEEN TWO GRAINS, IMPEDING FURTHER GRAIN TO GRAIN MATERIAL TRANSPORT. THIS DEMANDS THE NEED FOR NEW POINTS OF CONTACT TO BE INTRODUCED WHICH IS USUALLY ACHIEVED THROUGH GRINDING OF THE PRODUCT. THIS FREQUENT GRINDING COUPLED WITH MULTIPLE CALCINATION MAXIMIZES THE REACTANT RATIO.

THE REACTANT PARTICLES ARE SCHEMATICALLY ILLUSTRATED TO EMPHASIZE THAT REGARDLESS OF THE MATTER WHAT THE PARTICLE SIZE IS, EACH REACTANT PARTICLE CONTAINS ONLY ONE MOLECULE. UNDER THE SEVERE REACTION CONDITIONS ARE NECESSARY TO OBTAIN SINGLE PHASE PRODUCTS. DUE TO THE DIFFUSIONAL LIMITATIONS OF THE SOLID STATE REACTIONS, INITIAL REACTION IS FAST BUT AS THE REACTION GOES SLOWER AND SLOWER AS THE PRODUCT LAYER BUILDS UP AND THE PARTICLE BECOMES LONGER. A FINE POWDER OF APPROXIMATELY 10,000 Å PARTICLE SIZE STILL REPRESENTS DIFFUSION DISTANCES OF THE ORDER OF 10,000 UNIT CELL DIMENSIONS [4]. SOLUTION SYNTHESIS IMPROVES THE REACTIVITY OF THE COMPONENT OXIDES OR SALTS. SOLUTION METHODS CAN GIVE INITIAL CRYSTALLITES OF THE ORDER OF ONLY A FEW HUNDRED Å. THIS MEANS THAT DIFFUSION MUST OCCUR ACROSS 10 TO 50 UNIT CELL DIMENSIONS IN SOLUTION SYNTHESIS TECHNIQUES. COST EFFECTIVENESS AND SIMPLICITY OF SYNTHESIS ARE THE MAJOR ADVANTAGES OF THE SOLID STATE REACTION METHOD. THE MAJOR DISADVANTAGE OF SOLID STATE SYNTHESIS IS OBVIOUSLY THE HIGH TEMPERATURE NEEDED TO FORM THE PRODUCT WHICH LEADS TO AGGLOMERATED PARTICLES WITH POOR SURFACE AREA [5].

THE SOLID-STATE REACTION METHOD, WHICH IS EMPLOYED IN THE PRESENT WORK, INVOLVES THE FOLLOWING STEPS:

### 2.1.2.1 SELECTION AND WEIGHING OF RAW MATERIALS

TO SELECT A CERAMIC RAW MATERIAL, IT IS NECESSARY TO KNOW THE FINAL PROPERTIES DEMANDED OF THE CERAMIC PRODUCT. IN ORDER TO PREVENT SEGREGATION IN CERAMICS GREEN BODY, RAW MATERIALS WITH SIMILAR PARTICLE MORPHOLOGICAL DISTRIBUTIONS SHOULD BE USED. THE NEXT STEP IN THE SOLID-STATE REACTION METHOD IS TO SELECT THE DIFFERENT POWDERS WHICH ACT AS REACTANTS, ACCORDING TO THE STOICHIOMETRY.

PRESENCE OF IMPURITIES IN THE RAW MATERIALS CAN AFFECT REACTIVITY AS WELL AS THE PROPERTIES OF THE FIRED CERAMICS. THE RAW MATERIAL PURITY OF GREATER THAN 99% IS ESSENTIAL FOR OBTAINING PHASE PURE COMPOUNDS. ELECTRONIC BALANCE IS USED FOR WEIGHING WITH AN ACCURACY UP TO FOUR DECIMAL PLACES.

### 2.1.2.2 STOICHIOMETRIC MIXING

THE RAW MATERIALS NEED TO BE INTIMATELY MIXED TO INCREASE THE POINTS OF CONTACT BETWEEN REACTANT OXIDES, WHICH IN TURN ACT AS 'PRODUCT LAYER FORMATION'. THOROUGH MIXING AND MILLING ELIMINATES AGGLOMERATES AND REDUCES PARTICLE SIZE. IF AGGLOMERATES ARE PRESENT THEY DENSIFY MORE RAPIDLY RESULTING IN PORES. DURING THE MIXING AND MILLING AGGLOMERATES ARE BROKEN AND DEFECTS ARE INTRODUCED INTO THE GRAINS THAT IMPAIRS THE SINTERING MECHANISM. THEREFORE THE MIXTURE OF POWDERS IS GROUND WELL AND THOROUGHLY WETTED USING DISTILLED WATER OR ACETONE. BALL MILLS ARE USED FOR THE MIXING PURPOSE. IN THIS INVESTIGATION, THE MIXTURE OF CONSTITUENT POWDERS TAKEN IN POLYTHENE BOTTLES WAS THOROUGHLY MILLED FOR SUFFICIENT DURATION IN DISTILLED WATER MEDIUM USING YTTRIA STABILIZED ZIRCONIA (YSZ) BALLS. IN THE MILLING PROCESS, THE PARTICLES EXPERIENCE MECHANICAL STRESS AT CONTACT POINTS DUE TO COMPRESSION, IMPACT OR SHEAR WITH THE MILLING MEDIUM. OVER TIME, THE PARTICLES [6]. THE MECHANICAL STRESS LEADS TO ELASTIC AND INELASTIC DEFORMATION. IF THE STRESSES EXCEED ULTIMATE STRENGTH OF THE PARTICLE, IT WILL FRACTURE. THE MECHANICAL ENERGY SUPPLIED TO THE PARTICLE IS USED NOT ONLY TO CREATE NEW SURFACES BUT ALSO TO PRODUCE OTHER PHYSICAL CHANGES IN THE PARTICLE [7]. THE RATE OF MILLING IS DEPENDENT ON THE RELATIVE SIZE, SPECIFIC GRAVITY AND HARDNESS OF THE MEDIA AND PARTICLES. THE MILLING MEDIA (BALLS) IS AN IMPORTANT FACTOR IN BALL MILLING AS IT DETERMINES THE PARTICLE SIZE DISTRIBUTION. USING SPHERICAL BALL THE SIZE DISTRIBUTION IS BROAD SINCE THERE IS ONLY ONE POINT OF CONTACT BETWEEN THEM. ON THE OTHER HAND USING CYLINDRICAL BALLS WITH 'DOVE ENDS' THE PARTICLE SIZE DISTRIBUTION IS MORE UNIFORM WITH NARROW DISTRIBUTION [8]. THIS IS DUE TO THE FACT THAT CYLINDRICAL BALLS OFFER A LINE OF CONTACT BETWEEN THEM.

### 2.1.2.3 CALCINATION

CALCINATION IS THE INTERMEDIATE HEAT TREATMENT AT A LOWER TEMPERATURE THAN SINTERING. CALCINATION PROCESSES ARE ENDOTHERMIC DECOMPOSITION REACTIONS. AN OXYSALT, SUCH AS A CARBONATE OR HYDROXIDE, DECOMPOSES, LEAVING AN OXIDE AS A PRODUCT AND LIBERATING A GAS. THE KINETICS OF SOLID STATE REACTIONS OCCURRING DURING CALCINATION MAY BE CONTROLLED BY ANY ONE OF THE THREE PROCESSES: (I) THE REACTION AT THE INTERFACE BETWEEN THE REACTANT AND THE SOLID PRODUCT, (II) HEAT TRANSFER TO THE REACTION SURFACE OR (III) GAS DIFFUSION OR PERMEATION FROM THE REACTION SURFACE THROUGH THE SOLID PRODUCT LAYER. THE CALCINATION CONDITIONS SUCH AS TEMPERATURE, DURATION AND ATMOSPHERE ARE IMPORTANT FACTORS CONTROLLING SHRINKAGE DURING SINTERING. IF THE PHASES OF INTEREST MAY NOT BE COMPLETELY FORMED, THE CALCINATION YIELDS A DEFECTIVE PRODUCT.

### 2.1.2.4 GRINDING

THE CALCINED POWDERS ARE INVARIABLY AGGLOMERATED WHICH NEED TO BE GRINDED TO A FINE POWDER. GRINDING CAN BE ACCOMPLISHED BY ANY SUITABLE MEANS. IT PREPARES A FINER MATERIAL FOR CERAMIC FORMING. THE GRINDING ALSO HELPS TO HOMOGENISE THE COMPOSITION AND VARIATIONS THAT MAY STILL EXIST OR THAT MAY ARISE DURING CALCINATION. GRINDING IS DONE DOWN TO SOMEWHERE AROUND 10 MICROMETERS. IT IS NOT ADVISABLE. IF THE GRIND IS COARSER THE CERAMIC PARTICLE CAN HAVE LARGER INTERGRANULAR VOIDS AND LOWER FIRED DENSITY. IF GRINDING IS TOO FINE, COLLOIDAL PROPERTIES MAY INTERFERE WITH SUBSEQUENT FORMING OPERATIONS [9]. FOR GRINDING PURPOSE BALL MILL OR MORTAR WITH PESTLE IS USED. THE MILLING PROCESS CAN DRAMATICALLY IMPROVE THE QUALITY OF THE POWDER, IMPROVING THE BULK DENSITY AND ENHANCING SINTERING. IN LARGE SCALE OPERATION A GRINDING MEDIUM IS CHOSEN WHICH CAUSES VERY LITTLE WEAR.

### 2.1.2.5 ADDITION OF POLYMERIC BINDER

THE PRINCIPAL FUNCTIONS OF A CERAMIC BINDER ARE TO IMPART SUFFICIENT STRENGTH AND APPROPRIATE ELASTIC PROPERTIES FOR HANDLING AND SHAPING DURING THE POST FERING. THEY COAT THE CERAMIC PARTICLES AND PROVIDE LUBRICATION DURING PRESSING AND

BOND AFTER PRESSING. THE SELECTION OF BINDER AND OTHER ADDITIVES MUST BE CO THE CHEMISTRY OF THE CERAMIC AND THE PURITY REQUIREMENTS OF THE APPLICATI CERAMICS TECHNOLOGY, IN DIE PRESSING, A NARROW RANGE OF WATER-SOLUBLE OR SUCH AS POLY VINYL ALCOHOL IS MOST OFTEN APPLIED TO IMPROVE THE RHEOLOGICAL THE POWDER COMPACT [10]. THE POLYMERIC DISPERSIONS AND ORGANIC BINDERS PR PRESSED CERAMIC POWDERS WITH OPTIMAL PROPERTIES FROM THE POINT OF VIEW OF ABILITIES AND MECHANICAL STRENGTH OF THE PRESSED SAMPLES [11]. THE COMM POLYMERS FOR CERAMIC BINDING PURPOSE ARE POLY VINYL ALCOHOL (PVA), POLY ETH (PEG), CARBOXYMETHYL CELLULOSE ETC. MOST OF WHICH ARE WATER THINNABLE DISPERSIONS. THE AMOUNT OF ORGANIC BINDER REQUIRED FOR PRESSING IS QUITE LO RANGING FROM 0.5 TO 5 WT%. THE BINDER CONCENTRATION FOR EACH PROCESS IS ABOUT PROCESS, 3-17 % IN WET PROCESSING AND 7-20 % IN PLASTIC FORMING [12]. THE RE RESEARCH TRENDS SUGGEST THAT THE PVA AND PEG ARE IDEAL BINDER ADDITIVES FOR MICROWAVE DIELECTRIC CERAMICS [13].

THE BINDER MUST BE REMOVED PRIOR TO DENSIFICATION. ORGANIC BINDERS CAN BE REMOVED BY THERMAL DECOMPOSITION. FOR EXAMPLE, PVA BUR HEATING ABOVE 400°C REACTION BETWEEN THE BINDER AND THE CERAMIC OCCURS BEL BINDER DECOMPOSITION TEMPERATURE OR IF THE CERAMIC DENSIFIES BELOW THIS TEM FINAL PART WILL BE CONTAMINATED OR MAY EVEN BE CRACKED OR BLOATED. IF THE RAISED TOO RAPIDLY OR IF THE ATMOSPHERE IN THE FURNACE IS REDUCING, THE BIN RATHER THAN DECOMPOSE, LEAVING CARBON.

#### **2.1.2.6 POWDER COMPACTION (UNIAXIAL PRESSING)**

MOST CERAMIC-FORMING PROCESSES START WITH A POWDER AND CONSIST OF CO THE POWDER INTO A DESIRED SHAPE. THE MAIN OBJECTIVE IS USUALLY TO ACHIEVE A DEGREE OF PARTICLE PACKING AND A HIGH DEGREE OF HOMOGENEITY. A TYPICAL OPERATION HAS THREE BASIC STEPS: (I) FILLING THE MOULD OR DIE WITH POWDER (II) THE POWDER TO A SPECIFIC SIZE AND SHAPE AND (III) EJECTING THE COMPACT FROM T THE MOST COMMON AND WIDELY USED METHOD OF POWDER COMPACTION IS UNIAXIAL INVOLVES THE COMPACTION OF POWDER INTO A RIGID DIE BY APPLYING PRESSURE IN A

DIRECTION THROUGH A RIGID PUNCH OR PISTON [15-16]. COMPACTION IS DONE SLOWLY TO AVOID THE ESCAPE OF THE ENTRAPPED AIR.

THE PRESSURE GRADIENT IN POWDER COMPACT AS A FUNCTION OF THE DISTANCE FROM THE UPPER PUNCH IS GIVEN BY THE FORMULA

$$P_x = P_a \text{EXP} \left[ -4 K \frac{L}{D} \right] \quad (2.1)$$

WHERE  $K$  IS THE COEFFICIENT OF FRICTION,  $P_a$  IS THE APPLIED PRESSURE,  $L$  IS THE LENGTH AND  $D$  IS THE DIAMETER OF THE POWDER COMPACT. IT IS EVIDENT THAT THE PRESSURE DISTRIBUTION IN THE POWDER COMPACT IS MORE UNIFORM WHEN THE LENGTH TO DIAMETER RATIO IS SMALL. IN MICROWAVE DIELECTRIC MEASUREMENTS WE PREPARE SAMPLES WITH  $D/L$  RATIO = 2.0. IN THIS CASE THE PRESSURE DISTRIBUTION IS MORE OR LESS UNIFORM IN THE POWDER COMPACTS. PRESSURE OF 150 MPA IS IDEAL IN CERAMIC FORMING.

FRICTION BETWEEN THE POWDER AND DIE WALL DECREASES THE PRESSURE AVAILABLE FOR COMPACTION WITH INCREASING DISTANCE FROM THE PRESSING PUNCH. SINCE COMPACTION IS DIRECTLY RELATED TO FORMING PRESSURE, A FORMING PRESSURE GRADIENT BECOMES A PRESSURE GRADIENT IN THE COMPACT. THIS GRADIENT IS INFLUENCED BY THE DIE MATERIAL, THE NATURE OF THE POWDER AND THE ORGANIC ADDITIVES USED. INTERNAL LUBRICANTS SUCH AS ACID DISSOLVED IN PROPANE 2-OL, CAN AID PROCESSING.

### 2.1.2.7 SINTERING

THE FIRING PROCESS OR SINTERING IS USUALLY THE FINAL STAGE IN CERAMIC MANUFACTURE. SINTERING REFERS TO THE DENSIFICATION OF A PARTICULATE CERAMIC COMPACT BY THE COLLAPSE OF PORES BETWEEN THE STARTING PARTICLES (ACCOMPANIED BY SHRINKAGE OF THE COMPACT) WHICH IS COMBINED WITH GROWTH TOGETHER AND STRONG BONDING BETWEEN ADJACENT PARTICLES. IT IS SUBJECTED TO HIGH TEMPERATURES [18]. IT INVOLVES HEAT TREATMENT OF POWDER AT ELEVATED TEMPERATURES, WHERE DIFFUSIONAL MASS TRANSPORT IS APPRECIABLE WITHIN THE COMPACT TO FORM A DENSE POLYCRYSTALLINE SOLID [19]. THE CRITERIA THAT SHOULD BE MET BEFORE SINTERING ARE (I) A MECHANISM FOR MATERIAL TRANSPORT MUST BE PRESENT (II) A SOURCE OF ENERGY TO ACTIVATE AND SUSTAIN THIS MATERIAL TRANSPORT MUST BE PRESENT. THE PRIMARY MECHANISMS OF MATERIAL TRANSPORT ARE DIFFUSION AND VISCOUS FLOW. HEAT IS THE PRIMARY SOURCE OF ENERGY.

CONJUNCTION WITH ENERGY GRADIENTS DUE TO PARTICLE-PARTICLE CONTACT AND THERMODYNAMICALLY, SINTERING IS AN IRREVERSIBLE PROCESS IN WHICH A FREE ENERGY IS BROUGHT ABOUT BY A DECREASE IN SURFACE AREA. THE PRINCIPAL GOAL OF SINTERING IS REDUCTION OF COMPACT POROSITY. THE DEVELOPMENT OF MICROSTRUCTURE AND DENSITY DURING SINTERING IS A DIRECT CONSEQUENCE OF MASS TRANSPORT THROUGH SEVERAL PATHS AND ONE OF THESE PATHS IS USUALLY PREDOMINANT AT ANY GIVEN STAGE OF SINTERING. THE PATHS ARE (I) EVAPORATION/CONDENSATION (II) SOLUTION/PRECIPITATION (III) LATTICE DIFFUSION (IV) SURFACE DIFFUSION OR GRAIN BOUNDARY DIFFUSION. SEVERAL VARIABLES INFLUENCE SINTERING. SOME OF THEM ARE INITIAL DENSITY, MATERIAL, PARTICLE SIZE, SINTERING TEMPERATURE, TIME AND HEATING RATE. THE SINTERING PHENOMENA ARE OF TWO TYPES: DENSIFICATION SINTERING, WHERE ALL DENSIFICATION IS ACHIEVED THROUGH CHANGES IN PARTICLE SIZE, PARTICLE REARRANGEMENT OR THE PRESENCE OF LIQUID AND LIQUID-PHASE SINTERING. LIQUID THAT IS PRESENT AT SINTERING TEMPERATURES AIDS COMPACTION.

#### 2.1.2.7.1 SOLID STATE SINTERING

SOLID-STATE SINTERING INVOLVES MATERIAL TRANSPORT BY VOLUME DIFFUSION. IT MAY CONSIST OF MOVEMENT OF ATOMS OR VACANCIES ALONG A SURFACE OR GRAIN BOUNDARY THROUGH THE VOLUME OF THE MATERIAL. SURFACE DIFFUSION (VAPOUR –PHASE TRANSPORT) RESULT IN SHRINKAGE WHEREAS, VOLUME DIFFUSION ALONG GRAIN BOUNDARIES OR DISLOCATIONS RESULT IN SHRINKAGE [20]. THE DRIVING FORCE FOR SOLID-STATE SINTERING IS THE DIFFERENCE IN FREE ENERGY OR CHEMICAL POTENTIAL BETWEEN THE FREE SURFACES AND THE POINTS OF CONTACT BETWEEN ADJACENT PARTICLES. THE LINEAR SHRINKAGE CAUSED BY THE LATTICE DIFFUSION FROM LINE OF CONTACT BETWEEN TWO PARTICLES IN A REGION CAN BE EXPRESSED AS:

$$\frac{\Delta L}{L_0} = \left( \frac{K a^3 D t}{k T d^n} \right)^m \quad (2.2)$$

WHERE  $\Delta L/L_0$  = LINEAR SHRINKAGE (EQUIVALENT TO THE SINTERING STRAIN); A = ATOMIC VOLUME OF THE DIFFUSING VACANCY; D = SELF-DIFFUSION COEFFICIENT; K =

CONSTANT;  $T$  = TEMPERATURE;  $D$  = PARTICLE DIAMETER;  $t$  = TIME AND  $K$  = CONSTANT D  
 GEOMETRY. THE EXPONENT  $N$  IS CLOSE TO 3 AND  $M$  IS GENERALLY IN THE RANGE OF 0.3 TO 0.5.  
 FROM EQ. (2.2) IT CAN BE CLEARLY UNDERSTOOD THAT THE PARTICLE DIAMETER HAS A  
 ON THE RATE OF SINTERING. THE SMALLER THE PARTICLES, THE GREATER THE SINTERING  
 PARTICLE SIZE POWDER CAN BE SINTERED MORE RAPIDLY AT A LOWER TEMPERATURE.  
 POWDER. THE VARIOUS STAGES INVOLVED IN THE SINTERING PROCESS ARE AS FOLLOWS

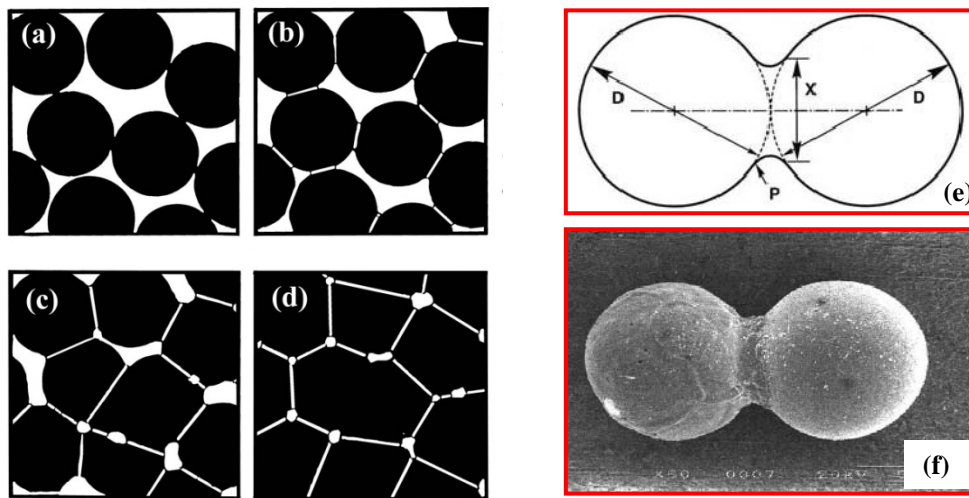


**Fig. 2.2 (a) & (b) Initial stage, (c) Intermediate stage and (d) Final stage of sintering (e) Neck formation during first stage and (f) SEM picture of neck formation in sintered alumina.**

**(A) INITIAL STAGE OF SINTERING:**

IT INVOLVES REARRANGEMENT OF PARTICLES AND INITIAL NECK FORMATION AT THE POINTS OF CONTACT BETWEEN EACH PARTICLE. THE REARRANGEMENT CONSISTS OF SLIGHT MOVEMENT OF PARTICLES AND ADJACENT PARTICLES TO INCREASE THE NUMBER OF POINTS OF CONTACT. BONDING OCCURS AT THESE POINTS OF CONTACT WHERE MATERIAL TRANSPORT CAN OCCUR AND WHERE SURFACE ENERGY IS REDUCED. AFTER THE INITIAL STAGE, THE DENSIFICATION OF THE SINTERING COMPONENT INCREASES RAPIDLY AND IT IS REACHED VERY QUICKLY (SECONDS OR MINUTES) AFTER EXPOSING POWDER TO THE SINTERING TEMPERATURE BECAUSE OF THE LARGE SURFACE AREA AND THE HIGH DRIVING FORCE FOR SINTERING [21].



**(B) INTERMEDIATE STAGE OF SINTERING:**

THE SECOND STAGE OF SINTERING IS REFERRED TO AS INTERMEDIATE SINTERING. THE CHANGES THAT OCCUR AT THIS STAGE ARE: THE SIZE OF THE NECKS BETWEEN THE PARTICLES INCREASES AND THE POROSITY DECREASES AND THE CENTERS OF THE ORIGINAL PARTICLES MOVE CLOSER TOGETHER. GRAIN BOUNDARIES BEGIN TO MOVE SO THAT ONE GRAIN BEGINS TO GROW WHILE THE OTHER IS CONSUMED. THIS ALLOWS GEOMETRY CHANGES THAT ARE NECESSARY TO ACCOMMODATE NECK GROWTH AND REMOVAL OF POROSITY. INTERMEDIATE SINTERING CONTINUES AS LONG AS CHANNELS ARE INTERCONNECTED AND ENDS WHEN PORES BECOME ISOLATED. MOST OF THE SHRINKAGE DURING SINTERING OCCURS DURING THIS STAGE. THE SHRINKAGE IN THE INTERMEDIATE STAGE RESULT IN ADDITIONAL DENSIFICATION BY AS MUCH AS 25%, OR TO A TOTAL OF ABOUT 90% OF (THEORETICAL DENSITY) [22].

**(C) FINAL STAGE OF SINTERING:**

IT INVOLVES THE FINAL REMOVAL OF POROSITY BY VACANCY DIFFUSION ALONG GRAIN BOUNDARIES. THEREFORE THE PORES MUST REMAIN CLOSE TO THE GRAIN BOUNDARIES AND VACANCY DIFFUSION ARE AIDED BY THE MOVEMENT OF GRAIN BOUNDARIES AND GRAIN GROWTH. HOWEVER, IF GRAIN GROWTH IS TOO RAPID, THE GRAIN BOUNDARIES MOVE FASTER THAN THE PORES AND LEAVE THEM ISOLATED INSIDE THE GRAIN. AS THE GRAIN CONTINUES TO GROW, THE PORE BECOMES FURTHER SEPARATED FROM THE GRAIN BOUNDARY AND HAS DECREASED CHANCE OF BEING ELIMINATED. THEREFORE, GRAIN GROWTH MUST BE CONTROLLED TO ACHIEVE COMPLETE REMOVAL OF POROSITY.

THE FINAL SINTERING STAGE BEGINS AT ABOUT 93-95% OF THEORETICAL DENSITY. POROSITY IS ALREADY ISOLATED [23]. IDEALLY, AT THE END OF THIS STAGE ALL POROSITY IS ELIMINATED. THE COMPLETE ELIMINATION OF POROSITY IN THE FINAL STAGE OF SINTERING CAN ONLY BE ACHIEVED IF ALL PORES ARE CONNECTED TO FAST, SHORT DIFFUSION PATHS ALONG GRAIN BOUNDARIES. OTHERWISE, EQUIVALENTLY, IF THE GRAIN BOUNDARIES REMAIN ATTACHED TO THE PORES).

OTHER FACTORS WHICH AFFECT THE RATE OF SINTERING ARE PARTICLE PACKING, PARTICLE SIZE AND PARTICLE SIZE DISTRIBUTION. IF PARTICLE PACKING IS NOT UNIFORM IN THE GREEN BODY, IT WILL BE DIFFICULT TO ELIMINATE ALL THE POROSITY DURING SINTERING. IF THE CONCENTRATION OF PARTICLES IS HIGH, IT CAN RESULT IN BRIDGING DURING THE FORMING PROCESS PRO

IRREGULARLY SHAPED PORES THAT ARE DIFFICULT TO REMOVE AFTER SINTERING. PARTICLES ARE DIFFICULT TO PACK EFFICIENTLY AND THEY FORM COMPACTS WITH LARGE PORE VOLUME PERCENTAGE OF POROSITY. HOWEVER, COMMONLY AVAILABLE POWDER HAS PARTICLE SIZES FROM SUBMICRON UPWARD. BETTER OVERALL PACKING CAN BE ACHIEVED BY COMPACTION, BUT ISOLATED PORES DUE TO BRIDGING AND AGGLOMERATION ARE USUALLY REMOVED AND RESULT EITHER IN POROSITY OR LARGE GRAIN SIZE AFTER SINTERING.

#### **2.1.2.7.2 LIQUID PHASE SINTERING**

LIQUID-PHASE SINTERING (LPS) IS AN IMPORTANT MEANS OF MANUFACTURING DENSE CERAMIC COMPONENTS FROM POWDER COMPACTS. IT INVOLVES THE PRESENCE OF A LIQUID AT THE SINTERING TEMPERATURE AND IS THE PRIMARY DENSIFICATION MECHANISM FOR TWO PHASE SYSTEMS. IN TWO PHASE SYSTEMS INVOLVING MIXED POWDERS, LIQUID FORMATION OCCURS BECAUSE OF DIFFERENT MELTING RANGES FOR THE COMPONENTS OR THE FORMATION OF A LIQUID PHASE, INCLUDING A GLASSY PHASE. THE MAJOR ADVANTAGES OF LPS ARE ENHANCED SINTERING KINETICS AND TAILORED PROPERTIES. HOWEVER, APART FROM THESE MERITS, THE CERAMICS MADE BY LPS ARE SUSCEPTIBLE TO SHAPE DEFORMATION. IN ORDER TO ATTAIN DENSIFICATION, CERTAIN CRITERIA MUST BE SATISFIED. THEY ARE (I) A LIQUID MUST BE PRESENT AT THE SINTERING TEMPERATURE, (II) THERE MUST BE GOOD WETTING OF THE LIQUID ON SOLID OR THE CONTACT ANGLE MUST BE LOW AND (III) THERE MUST BE APPRECIABLE SOLUBILITY OF SOLID IN LIQUID. IN TWO PHASE CERAMICS TEND TO HAVE A SMALL AMOUNT OF REACTIVE LIQUID THAT ACCELERATES SINTERING RATHER THAN FACILITATE VISCOUS FLOW. WHEN THE LIQUID COATS EACH GRAIN, THE COMPACTS OFTEN BE SINTERED TO A HIGHER DENSITY AT A LOWER TEMPERATURE WITH LESS OF VISCOUS EXAGGERATED GRAIN GROWTH. LESS THAN 1 VOLUME % OF THE LIQUID PHASE IS SUFFICIENT TO WET THE GRAINS IF THE LIQUID IS DISTRIBUTED UNIFORMLY AND THE GRAIN SIZE IS ABOUT 1 MICRON. THE LIQUID MUST HAVE A SOLUBILITY FOR THE SOLID. FINALLY, THE DIFFUSIVE TRANSPORT OF ATOMS DISSOLVED IN THE LIQUID SHOULD BE HIGH ENOUGH TO ENSURE RAPID SINTERING. THE WETTING LIQUID CONCENTRATES AT THE PARTICLE CONTACTS AND FORMS A MENISCUS WHICH EXERCISES AN EFFECTIVE COMPRESSIVE PRESSURE ON THE COMPACT RESULTING IN A RAPID REARRANGEMENT OF PARTICLES INTO A HIGHER DENSITY CONFIGURATION.

DENSIFICATION DURING LPS CAN BE ACHIEVED BY THE FOLLOWING THREE RATE-  
MECHANISMS:

**PARTICLE REARRANGEMENT** IN THE INITIAL STAGES OF LIQUID PHASE SINTERING, A NUMBER OF CONSECUTIVE AND SIMULTANEOUS PROCESSES SUCH AS MELTING, WETTING, SPREADING, REDISTRIBUTION ETC. MAY OCCUR. BOTH SOLID AND LIQUID ARE SUBJECTED TO REARRANGEMENT BECAUSE OF THE UNBALANCED CAPILLARY FORCES. LIQUID FILMS BETWEEN THE PARTICLES ACT AS A LUBRICANT AND THE PARTICLE REARRANGEMENT TAKES PLACE IN THE DIRECTION OF REDUCING THE DRIVING FORCE FOR THE REARRANGEMENT ARISES DUE TO THE IMBALANCE IN CAPILLARY FORCES AS A RESULT OF PARTICLE SIZE DISTRIBUTION, IRREGULAR PARTICLE SHAPE, LOCAL DENSIFICATION IN THE POWDER COMPACT AND ANISOTROPIC MATERIAL PROPERTIES. AS THE DENSIFICATION ADVANCES, PARTICLES EXPERIENCE INCREASING RESISTANCE TO FURTHER REARRANGEMENT DUE TO THE CONTACT OF NEIGHBORING PARTICLES UNTIL THE FORMATION OF A CLOSE PACKED STRUCTURE.

**SOLUTION-PRECIPIATION** WHEN THE REARRANGEMENT BECOMES INSIGNIFICANT, ADDITIONAL DENSIFICATION CAN BE ACHIEVED BY DISSOLUTION OF THE SOLID AT GRAIN CONTACTS DURING THE CENTER-TO-CENTER APPROACH OF PARTICLES. THE MAIN DRIVING FORCE FOR THIS PROCESS IS CAPILLARY FORCES. THE DISSOLVED SOLUTE TRANSFERS TO THE UNCOMPRESSED PARTICLE CONTACT STRUCTURE BY DIFFUSION THROUGH A LIQUID PHASE. THIS MASS TRANSFER RESULTS IN CONTACT FLATTENING AND CORRESPONDING LINEAR SHRINKAGE IN THE POWDER COMPACT. THE CURVATURE OF THE SOLID DECREASES AS THE CONTACT AREA INCREASES DUE TO SIMULTANEOUSLY INCREASING EFFECTIVE STRESS AT THE CONTACT AREA. AT THE LATER STAGE OF SOLUTION PRECIPITATION, INTERCONNECTED PORE STRUCTURES PINCH OFF TO FORM ISOLATED OR CLOSED PORES.

**PORE REMOVAL** THIS IS THE FINAL STAGE OF LPS WHICH STARTS AFTER PORE CLOSURE. IN THIS STAGE A MAXIMUM RELATIVE DENSITY UPTO 95% IS ATTAINED. THE CLOSED PORES CONTAIN GASEOUS SPECIES FROM SINTERING ATMOSPHERE, VAPORIZED LIQUID AND UNREACTED SOLID. SEVERAL PROCESSES CAN OCCUR SIMULTANEOUSLY DURING THE FINAL STAGE OF LPS WHICH INCLUDES GROWTH AND COALESCENCE OF GRAINS AND PORES, DISSOLUTION OF LIQUID PHASE TRANSFORMATIONS AND FORMATION OF REACTION PRODUCTS BETWEEN LIQUID AND SOLID.

## 2.2 PREPARATION OF GLASS

MOST OF THE CERAMICS POSSESS HIGH SINTERING TEMPERATURES (ABOVE 1200°C) AS DISCUSSED IN CHAPTER 1, THE MOST EFFECTIVE METHOD TO LOWER THE PROCESSING TEMPERATURE OF THE CERAMIC IS TO ADD LOW MELTING, LOW LOSS GLASSES. TRADITIONALLY, GLASSES ARE FORMED BY COOLING A LIQUID FAST ENOUGH TO PREVENT DETECTABLE CRYSTALLIZATION. FROM A SCIENTIFIC POINT OF VIEW, GLASS FORMATION CAN BE CONSIDERED AS ~~THE~~ *Anti-crystallization*. IN THE PRESENT INVESTIGATION, MULTI COMPONENT GLASSES SUCH AS ZBS, BBSZ, LBS, BBS, LMZBS ETC. ARE SELECTED. INITIALLY HIGH PURITY ~~OXIDES SUCH AS ZBO,~~  $\text{ZnO}$ ,  $\text{BaCO}_3$ ,  $\text{Bi}_2\text{O}_3$  AND  $(\text{MgCO}_3)_x(\text{Mg}(\text{OH})_2 \cdot 5\text{H}_2\text{O})_{1-x}$  (99.9 % ALDRICH CHEMICAL COMPANY, U.S.A) ARE ACCURATELY WEIGHED AND THOROUGHLY MIXED. AFTER MIXING THEY ARE DRIED IN PLATINUM CRUCIBLES ABOVE THEIR MELTING POINTS. THE HIGH TEMPERATURE FAVOURS THEM TO REACT WITH ONE ANOTHER AND ALSO ENCOURAGES THE ESCAPE OF GAS BUBBLES WHICH IS USUALLY REFERRED TO AS REFINING THE GLASS. UPON COMPLETION OF THE PROCESS, THE GLASS IS SUDDENLY COOLED FROM THE MELTING TEMPERATURE TO ROOM TEMPERATURE (PROCESS KNOWN AS QUENCHING) WHERE THE GLASS HAS HIGHER VISCOSITY. FINALLY THE GLASS IS POWDERED FOR FURTHER MIXING WITH CERAMICS.

## 2.3 SYNTHESIS OF POLYMER-CERAMIC COMPOSITES

### 2.3.1 POWDER PROCESSING METHOD

IN THE PRESENT STUDY, PTFE/CERAMIC COMPOSITES WERE PREPARED BY POWDER PROCESSING TECHNOLOGY. DIFFERENT VOLUME FRACTIONS (0 TO 0.5) OF CERAMIC POWDERS WERE DISPERSED IN ETHYL ALCOHOL USING ULTRASONIC MIXER FOR ABOUT 2 HOURS. DRY POWDER MIXTURE WAS OBTAINED BY REMOVING THE SOLVENT BY ~~DRYING~~ *vacuum drying*. THESE HOMOGENEOUSLY MIXED PTFE/CERAMIC COMPOSITE POWDERS WERE THEN COMPACTED UNDER UNIAxIAL PRESSURE OF 50 MPa FOR 1 MINUTE. THE CYLINDRICAL AND RECTANGULAR SAMPLES OBTAINED WERE KEPT FOR 24 HRS.

### 2.3.2 SIGMA BLEND METHOD

THIS METHOD IS USED FOR LOW MELTING, LOW VISCOUS POLYMERS POLYETHYLENE/POLYSTYRENE. THE POLYMER AND CERAMIC WERE MIXED THOROUGHLY IN A KNEADING MACHINE. THE KNEADING MACHINE CONSISTS OF VARIABLE SPEED MIXER MOTOR, HEATING FACILITY AND COUNTER ROTATING SIGMA BLADES WITH A GEAR RATIO OF 1:1.2 AND HEATING FACILITY. THE COUNTER ROTATING SIGMA BLADES ENSURE FINE MIXING BY APPLYING HIGH SHEAR TO THE DOUGH-LIKE MIXTURE. INITIALLY THE DESIRED AMOUNT OF POLYMER IS MELTED AT A CERTAIN POINT. DIFFERENT VOLUME FRACTIONS CERAMICS WERE ADDED TO THE MELTED POLYMER AND BLENDED AT SUITABLE TEMPERATURE FOR 30 MINUTES. THUS OBTAINED COMPOSITES WERE THERMOLAMINATED UNDER A PRESSURE OF 200 MPA AND OPTIMIZED TEMPERATURE FOR 15 MINUTES. AFTER THERMOLAMINATION, THE COMPOSITES WITH DESIRED SHAPES WERE POLISHED FOR MEASUREMENTS. FIG. 2.3 SHOWS THE PICTURE OF THE KNEADING MACHINE AND THE SIGMA BLADES USED FOR MIXING.



**Fig. 2.3** Kneading machine used in melt mixing technique. Inset figure shows the sigma blades.

## 2.4 STRUCTURAL AND MICROSTRUCTURAL CHARACTERIZATION

### 2.4.1 X-RAY DIFFRACTOMETER

X-RAY DIFFRACTION (XRD) IS A VERSATILE, NON-DESTRUCTIVE TECHNIQUE THAT PROVIDES DETAILED INFORMATION ABOUT THE CHEMICAL COMPOSITION AND CRYSTALLOGRAPHIC STRUCTURE OF MATERIALS. AN X-RAY INCIDENT UPON A SAMPLE WILL EITHER BE TRANSMITTED, IN WHICH CASE IT WILL CONTINUE ALONG ITS ORIGINAL DIRECTION, OR IT WILL BE SCATTERED BY THE ATOMS IN THE MATERIAL. ALL THE ATOMS IN THE PATH OF THE X-RAY BEAM SCATTER X-RAYS. IN GENERAL, THE SCATTERED WAVES DESTRUCTIVELY INTERFERE WITH EACH OTHER, WITH THE EXCEPTION OF SPECIAL ORIENTATIONS AT WHICH BRAGG'S LAW IS SATISFIED. THE PHENOMENON OF X-RAY DIFFRACTION OCCURS WHEN PENETRATING RADIATION, SUCH AS X-RAYS, ENTERS A CRYSTALLINE SOLID AND IS PARTIALLY SCATTERED. THE DIRECTION AND INTENSITY OF THE SCATTERED (DIFFRACTED) BEAMS DEPEND ON THE ORIENTATION OF THE CRYSTAL LATTICE WITH RESPECT TO THE INCIDENT BEAM [24]. A CRYSTAL LATTICE CONSISTS OF PARALLEL ROWS OF ATOMS SEPARATED BY A UNIQUE PERIODIC SPACING), WHICH ARE CAPABLE OF DIFFRACTING X-RAYS. IN ORDER FOR A BEAM TO BE CONSIDERED DIFFRACTED, THE DISTANCE IT TRAVELS BETWEEN ROWS OF ATOMS AT THE ANGLE OF INCIDENCE MUST BE EQUAL TO AN INTEGRAL MULTIPLE OF THE WAVELENGTH OF THE INCIDENT BEAM [25].

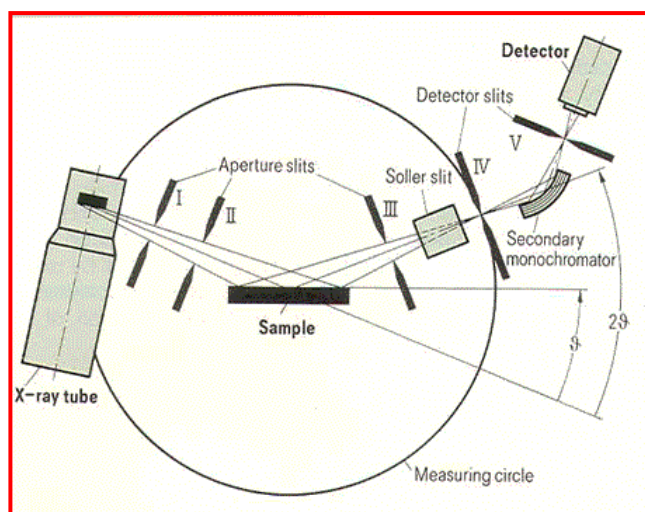


Fig. 2.4 Schematic diagram of an X-ray diffractometer.

AN X-RAY DIFFRACTOMETER UTILIZES A POWDERED SAMPLE, A GONIOMETER, AN POSITION DETECTOR TO MEASURE THE DIFFRACTION PATTERNS OF UNKNOWN (SEE . POWDERED SAMPLE PROVIDES (THEORETICALLY) ALL POSSIBLE ORIENTATIONS OF THE THE GONIOMETER PROVIDES A VARIETY OF ANGLES OF INCIDENCE, AND THE DETECTOR INTENSITY OF THE DIFFRACTED BEAM. THE RESULTING ANALYSIS IS DESCRIBED GRAPHIC PEAKS WITH % INTENSITY ON THE Y-AXIS AND GONIOMETER ANGLE ON THE X-AXIS. ANGLE AND INTENSITY OF A SET OF PEAKS IS UNIQUE TO THE CRYSTAL STRUCTURE E [26]. THE X-RAY DIFFRACTION METHOD IS MOST USEFUL FOR QUALITATIVE, RATIO QUANTITATIVE, ANALYSIS (ALTHOUGH IT CAN BE USED FOR BOTH). THE MONOCHROMA ENSURE THAT A SPECIFIC WAVELENGTH REACHES THE DETECTOR, ELIMINATING FLUOR THE RESULTING TRACE CONSISTS OF RECORDING THE INTENSITY, THE GONIOMETER ANGLE CAN THEN BE USED TO IDENTIFY THE PHASES PRESENT IN THE SAMPLE. DIFFRACTION DA MATERIALS HAVE BEEN RECORDED IN A COMPUTER SEARCHABLE POWDER DIFFRACTION FILE). MATCHING THE OBSERVED DATA IN THE PDF ALLOWS THE PHASES IN THE SAM IDENTIFIED [27-28].

## 2.4.2 SCANNING ELECTRON MICROSCOPE

THE SCANNING ELECTRON MICROSCOPE (SEM) IS THE MOST WIDELY USED FOR ELECTRON MICROSCOPE IN THE FIELD OF MATERIAL SCIENCE. IN LIGHT MICROSCOPY, A VIEWED THROUGH A SERIES OF LENSES THAT MAGNIFY THE VISIBLE-LIGHT IMAGE. H SCANNING ELECTRON MICROSCOPE DOES NOT ACTUALLY VIEW A TRUE IMAGE OF THE RATHER PRODUCES AN ELECTRONIC MAP OF THE SPECIMEN THAT IS DISPLAYED ON A CA THE SEM IS A MICROSCOPE THAT USES ELECTRONS INSTEAD OF VISIBLE LIGHT TO FOR THE SCANNING ELECTRON MICROSCOPE HAS MANY ADVANTAGES OVER T MICROSCOPES. THE SEM HAS A LARGE DEPTH OF FIELD, WHICH ALLOWS MORE OF A SPEC IN FOCUS AT ONE TIME [29]. THE SEM ALSO HAS MUCH HIGHER RESOLUTION, SO CLOSE SPECIMENS CAN BE MAGNIFIED AT MUCH HIGHER LEVELS. BECAUSE THE SEM ELECTROMAGNETS RATHER THAN LENSES, THE RESEARCHER HAS MUCH MORE CONTROL MAGNIFICATION.

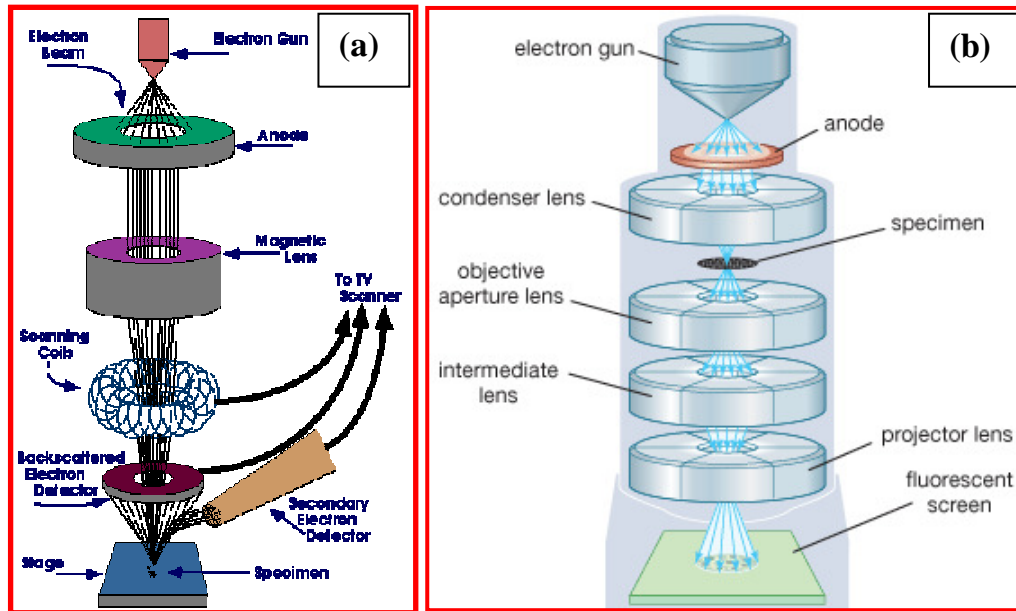


Fig. 2.5 Schematic diagram of (a) SEM ([www.purdue.edu/REM/rs/sem.htm](http://www.purdue.edu/REM/rs/sem.htm)) (b) TEM ([www.britannica.com](http://www.britannica.com))

A BEAM OF ELECTRONS IS PRODUCED AT THE TOP OF THE MICROSCOPE BY AN ELECTRON GUN. THE ELECTRON BEAM FOLLOWS A VERTICAL PATH THROUGH THE MICROSCOPE, WITHIN A VACUUM. THE BEAM TRAVELS THROUGH ELECTROMAGNETIC FIELDS AND IS FOCUSED DOWN TOWARD THE SAMPLE. ONCE THE BEAM HITS THE SAMPLE, ELECTRONS ARE EJECTED FROM THE SAMPLE (SEE FIG. 2.5 (A)). DETECTORS COLLECT THE BACKSCATTERED ELECTRONS, AND SECONDARY ELECTRONS AND CONVERT THEM INTO SIGNALS SENT TO A SCREEN SIMILAR TO A TELEVISION SCREEN. THIS PRODUCES THE FINAL IMAGE. METALS ARE CONDUCTIVE AND REQUIRE NO PREPARATION BEFORE BEING USED. ALL NON-METALS ARE MADE CONDUCTIVE BY COVERING THE SAMPLE WITH A THIN LAYER OF CONDUCTIVE GOLD [30].

### 2.4.3 TRANSMISSION ELECTRON MICROSCOPY

IN TRANSMISSION ELECTRON MICROSCOPY (TEM) A THIN SLICE OF THE MATERIAL TO BE STUDIED (0.1 TO  $10\mu\text{m}$  THICK) IS USED AND AN ENERGETIC ELECTRON BEAM IS PASSED DIRECTLY THROUGH THE SAMPLE. ON THE EXIT SIDE OF THE SPECIMEN SEVERAL DIFFRACTED BEAMS ARE PRODUCED IN ADDITION TO THE TRANSMITTED BEAM AND ARE FOCUSED BY AN OBJECTIVE LENS TO



ITS BACK FOCAL PLANE. THIS DIFFRACTION PATTERN IS ALSO MAGNIFIED BY OTHER TEM. ELECTRON DIFFRACTION PATTERN CAN BE USED TO GAIN QUANTITATIVE INFORMATION OF PHASES AND THEIR ORIENTATION, SPACE GROUPS, ORDER/DISORDER, MAGNETIC DOMAINS. FIG. 2.5 (B) SHOWS THE SCHEMATIC DIAGRAM OF TEM. ONE OF THE DISADVANTAGES OF ELECTRON DIFFRACTION IS THE SECONDARY DIFFRACTION WHICH OCCURS COMMONLY. SECONDARY DIFFRACTION OCCURS WHEN THE DIFFRACTED BEAMS BECOMES INCIDENT BEAM AND INTERACTS WITH ANOTHER SET OF PLANES. THE TWO UNDESIRABLE CONSEQUENCES OF SECONDARY DIFFRACTION ARE OCCURRENCE OF EXTRA SPOTS IN THE DIFFRACTION PATTERN AND THE INTENSITIES OF THE INCIDENT BEAM ARE UNRELIABLE AND CANNOT BE USED FOR CRYSTAL STRUCTURE DETERMINATION.

SELECTED AREA (ELECTRON) DIFFRACTION, ABBREVIATED AS SAD (SAED), IS A CRYSTALLOGRAPHIC EXPERIMENTAL TECHNIQUE THAT CAN BE PERFORMED INSIDE A TEM. IN ELECTRON MICROSCOPY, A THIN CRYSTALLINE SPECIMEN IS SUBJECTED TO A PARALLEL BEAM OF HIGH-ENERGY ELECTRONS. AS TEM SPECIMENS ARE TYPICALLY ~100 NM THICK, ELECTRONS TYPICALLY HAVE ENERGY OF 100-400 KILOELECTRON VOLTS, THE ELECTRONS PASS THROUGH THE SAMPLE EASILY. THE WAVELENGTH OF HIGH-ENERGY ELECTRONS IS A FRACTION OF THE SPACINGS BETWEEN ATOMS IN A SOLID IS ONLY SLIGHTLY LARGER, THE ATOMS ACT AS A DIFFRACTION GRATING TO THE ELECTRONS. THAT IS, SOME FRACTION OF THEM WILL BE DEFLECTED AT PARTICULAR ANGLES, DETERMINED BY THE CRYSTAL STRUCTURE OF THE SAMPLE, WHILE SOME WILL GO TO PASS THROUGH THE SAMPLE WITHOUT DEFLECTION. AS A RESULT, THE IMAGE ON THE TEM WILL BE A SERIES OF SPOTS, THE SELECTED AREA DIFFRACTION PATTERN, SADP. IF THE SAMPLE IS TILTED, THE SAME CRYSTAL WILL STAY UNDER ILLUMINATION, BUT DIFFERENT DIFFRACTION CONDITIONS WILL BE ACTIVATED, AND DIFFERENT DIFFRACTION SPOTS WILL APPEAR ON THE TEM. IN THE PRESENT INVESTIGATION SELECTED AREA DIFFRACTION PATTERN HAS BEEN EMPLOYED TO DETERMINE THE CORRECT SPACE GROUP OF THE CERAMICS. SAMPLES FOR TEM IN THE PRESENT STUDY WERE PREPARED BY THINNING PELLETS TO ELECTRON TRANSPARENCY BY CONVENTIONAL TEM THINNING TECHNIQUES FOLLOWED BY ION THINNING (MODEL 600, GATAN, PLEASANTON, CALIFORNIA). THE TEM WITH ELECTRON TRANSPARENCY FOR OBSERVATION IN THE TEM (JEM-2100 HR, JEOL, JAPAN).

## 2.5 MICROWAVE CHARACTERIZATION

### 2.5.1 INTRODUCTION

MICROWAVE MEASUREMENTS AND THE DIELECTRIC PROPERTIES OF MATERIALS ARE OF INCREASING APPLICATION IN MANY AREAS OF SOLID-STATE PHYSICS, MATERIALS SCIENCE AND ELECTRONIC ENGINEERING. THE INCREASING DEMAND FOR THE DEVELOPMENT OF HIGH FREQUENCY CIRCUITS AND SYSTEMS REQUIRE A COMPLETE UNDERSTANDING OF THE DIELECTRIC PROPERTIES OF MATERIALS FUNCTIONING AT MICROWAVE FREQUENCIES. IN GENERAL, THE MICROWAVE CHARACTERIZATION METHODS FALL INTO TWO CATEGORIES: NON-RESONANT METHODS AND RESONANT METHODS. NON-RESONANT METHODS ARE OFTEN USED TO GET A GENERAL KNOWLEDGE OF ELECTROMAGNETIC PROPERTIES OVER A FREQUENCY RANGE, WHILE RESONANT METHODS ARE USED TO GET ACCURATE KNOWLEDGE OF DIELECTRIC PROPERTIES AT A SINGLE FREQUENCY OR A NARROW BAND OF FREQUENCIES. THE GENERALLY ADOPTED METHODS FOR MEASURING THE MICROWAVE DIELECTRIC PROPERTIES OF MATERIALS ARE (I) PERTURBATION METHODS, (II) OPTICAL METHODS, (III) TRANSMISSION LINE METHODS, (IV) REFLECTION METHODS AND (V) EXACT RESONANCE METHODS. THE CHOICE OF METHOD OR COMBINATION OF METHODS WILL DEPEND ON THE LOSS TANGENT VALUE OF THE MATERIAL, THE FACTOR, THE AMOUNT OF MATERIAL AVAILABLE, THE ACCURACY REQUIRED AND WHETHER THE MEASUREMENT IS REQUIRED FOR RESEARCH OR ROUTINE MEASUREMENTS.

**Perturbation Technique:** THE PERTURBATION METHODS ARE HIGHLY SUITABLE FOR MEASURING THE DIELECTRIC PROPERTIES OF MATERIALS OF SMALL SIZE SINCE THE MATERIAL SHOULD NOT ALTER THE FIELD DISTRIBUTION OF THE WAVEGUIDE CONSIDERABLY. THESE TECHNIQUES ARE SUITABLE FOR RELATIVE PERMITTIVITIES IN THE RANGE 1.0 TO 10.0 ALTHOUGH THIS RANGE CAN BE EXTENDED BY AN EXACT SOLUTION OF THE RESONANT MODES OF THE SPECIMEN [32]. HENCE THIS TECHNIQUE IS NOT COMMONLY USED FOR DR CHARACTERISATION.

**Optical Methods:** OPTICAL METHODS ARE APPLICABLE FOR WAVELENGTH BELOW 100 MICROMETRE. SINCE THIS METHOD REQUIRES LARGE AMOUNT OF MATERIAL IT IS NOT SUITABLE FOR SMALL SAMPLES [33].

**Transmission line techniques:** THIS TECHNIQUE HAS A SERIOUS DISADVANTAGE OF THE NEED FOR VERY SMALL WAVEGUIDE SIZE USED BELOW 4 MM, WHICH GIVES RISE TO PRACTICAL DIFFICULTIES [34]. MORE OVER IMPERFECTIONS IN THE SAMPLE DIMENSIONS PRODUCE ERRORS IN THE MEASUREMENTS.

MEASUREMENT. IT WAS REPORTED THAT THE ACCURACY OF TRANSMISSION MODE MEASUREMENT OF THE DIELECTRIC PROPERTIES IS MORE IN WEAK COUPLING CONDITIONS [35].

**Reflection methods:** IN REFLECTION METHODS, WAVES REFLECTED FROM THE DIELECTRIC SURFACES ARE STUDIED. WHEN THE RELATIVE PERMITTIVITY BECOMES LARGE, THERE OCCURS COMPLICATIONS IN THE MEASUREMENT OF COMPLEX VOLTAGE REFLECTION COEFFICIENT [36].

**Resonance methods:** EXACT RESONANCE METHOD IS THE MOST ACCURATE METHOD FOR THE MEASUREMENT OF DRs. COMPARED TO THE ABOVE-MENTIONED METHODS FOR THE MEASUREMENT OF DRs. IN TRANSMISSION MODE, THE EXACT RESONANT FREQUENCY OF THE RESONATOR IS MEASURED USING DIFFERENT TECHNIQUES. FROM THE RESONANT CHARACTERISTICS, PARAMETERS ARE DETERMINED. SPECIAL TECHNIQUES OF EXACT RESONANCE METHODS ARE USED IN THE PRESENT STUDY, WHICH ARE DESCRIBED IN DETAIL IN THE FOLLOWING SECTIONS.

## 2.5.2 NETWORK ANALYZER

IN MICROWAVE ENGINEERING, NETWORK ANALYZERS ARE THE BASIC INSTRUMENTS USED TO ANALYZE A WIDE VARIETY OF MATERIALS, COMPONENTS, CIRCUITS AND SYSTEMS. A NETWORK ANALYZER MEASURES THE REFLECTION FROM AND/OR TRANSMISSION THROUGH A MATERIAL ALONG WITH KNOWING ITS PHYSICAL DIMENSIONS PROVIDES THE INFORMATION TO CHARACTERIZE THE PERMITTIVITY AND PERMEABILITY OF THE MATERIAL. NETWORK ANALYZER IS A SWEPT FREQUENCY MEASUREMENT EQUIPMENT TO COMPLETELY CHARACTERIZE THE COMPLEX NETWORK PARAMETERS IN THE SHORTEST TIME, WITHOUT ANY DEGRADATION IN ACCURACY AND PRECISION. TWO TYPES OF NETWORK ANALYZERS ARE AVAILABLE, SCALAR AND VECTOR NETWORK ANALYZERS. SCALAR NETWORK ANALYZER MEASURES ONLY THE MAGNITUDE OF REFLECTION AND TRANSMISSION COEFFICIENTS WHILE VECTOR NETWORK ANALYZER MEASURES BOTH THE MAGNITUDE AND PHASE. BOTH THE MAGNITUDE AND PHASE BEHAVIOR OF A COMPONENT CAN BE CRITICAL TO THE PERFORMANCE OF A COMMUNICATION SYSTEM. A VECTOR NETWORK ANALYZER CAN PROVIDE INFORMATION ON A WIDE RANGE OF DEVICE TYPES, FROM ACTIVE DEVICES SUCH AS AMPLIFIERS AND TRANSISTORS, TO PASSIVE DEVICES SUCH AS CAPACITORS AND FILTERS.

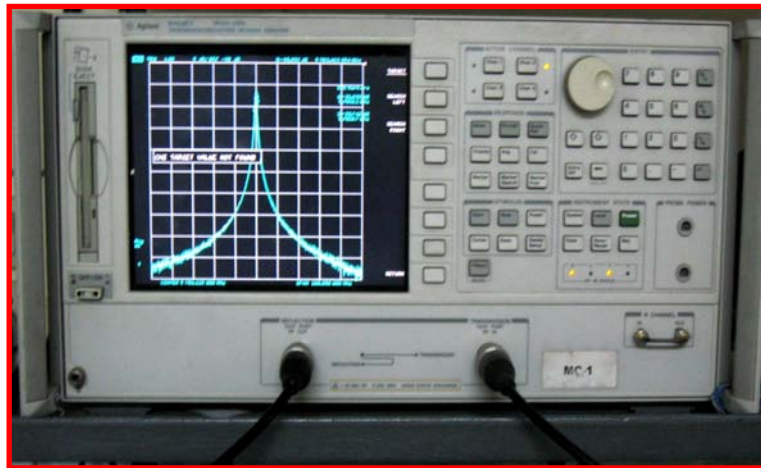


Fig. 2.6 Picture of HP 8753 ET Vector Network Analyzer.

A BASIC NETWORK ANALYZER IS DESIGNED TO SHOW GRAPHICALLY, A PLOT OF GAIN OR LOSS OF A NETWORK VERSUS FREQUENCY. THE NETWORK ANALYZER MEASURES THE MAGNITUDE, PHASE, AND GROUP DELAY OF TWO-PORT NETWORKS TO CHARACTERIZE THEIR BEHAVIOUR. A NETWORK ANALYZER CONSISTS OF A SWEPT FREQUENCY SOURCE THAT IS CONNECTED TO THE NETWORK UNDER TEST AND TWO RECEIVERS. THE FIRST RECEIVER IS USED TO ACCURATELY MEASURE THE REFLECTION OR INPUT VOLTAGE TO THE NETWORK. THE SECOND RECEIVER IS CALLED THE TRANSMISSION CHANNEL AND IS USED TO MEASURE THE OUTPUT OF THE NETWORK UNDER TEST. THE RATIO OF THE OUTPUT TO THE INPUT LEVEL IS DISPLAYED AS DB AND IS THE VOLTAGE GAIN OR LOSS OF THE NETWORK. THE NETWORK ANALYZER USED IN THE PRESENT STUDY IS SHOWN IN FIG. 2.6.

### 2.5.3 MEASUREMENT OF RELATIVE PERMITTIVITY ( $\epsilon_r$ )

IN THIS METHOD DEVELOPED BY HAKKI AND COURMAN [38], A DISC OF MATERIAL TO BE MEASURED IS INSERTED BETWEEN TWO MATHEMATICALLY INFINITE CONDUCTING PLATES, AS SHOWN IN FIG 2.7. IF THE DIELECTRIC MATERIAL IS ISOTROPIC THEN THE CHARACTERISTIC EQUATION OF THIS RESONANT STRUCTURE OPERATING IN THE TM<sub>010</sub> MODE IS WRITTEN AS

$$\frac{J_0(\beta_0)}{J_1(\beta_0)} = - \frac{K_0(\beta_0)}{K_1(\beta_0)} \quad (2.3)$$

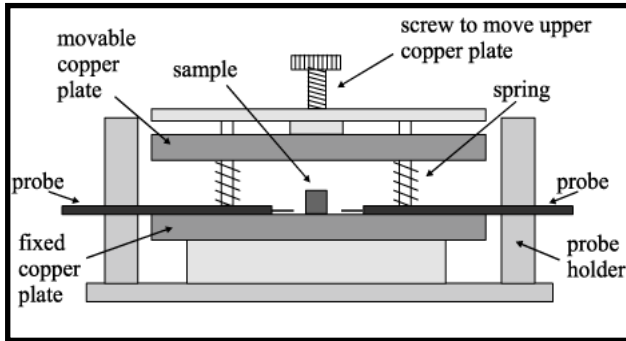


Fig. 2. 7 A dielectric rod kept end shorted between two mathematically infinite conducting plates

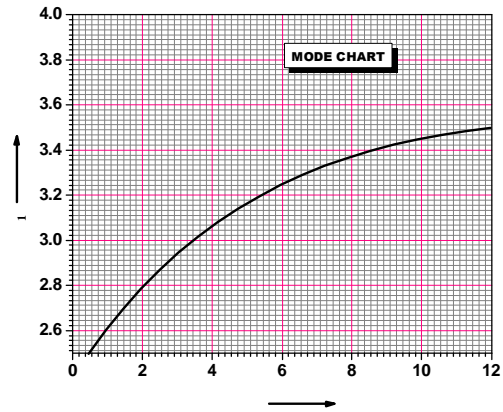


Fig. 2.8 Mode charts of Hakki and Coleman giving  $\beta_1$  as functions of  $l/2L$ .

WHERE  $J_0(\alpha)$  AND  $J_1(\beta)$  ARE BESSEL FUNCTIONS OF THE FIRST KIND OF ORDERS ZERO AND ONE RESPECTIVELY  $K_0(\alpha)$  AND  $K_1(\beta)$  ARE THE MODIFIED BESSEL FUNCTIONS OF THE SECOND KIND OF ORDER ZERO AND ONE RESPECTIVELY. THE FUNDAMENTAL ON THE GEOMETRY, THE RESONANT WAVELENGTH INSIDE AND OUTSIDE THE DR RESPECTIVELY AND DIELECTRIC CONSTANT OF THE DR. THUS,

$$\alpha = \frac{D}{\lambda_0} \left[ r - \left( \frac{l}{2L} \right)^2 \right]^{1/2} \tag{2.4}$$

$$\beta = \frac{D}{\lambda_0} \left[ \left( \frac{l}{2L} \right)^2 - 1 \right]^{1/2} \tag{2.5}$$

WHERE

$l$  = THE LONGITUDINAL VARIATIONS OF THE FIELD ALONG THE AXIS

$L$  = LENGTH OF THE DR

$D$  = DIAMETER OF THE DR

$\lambda_0$  = FREE SPACE RESONANT WAVE LENGTH

THE CHARACTERISTIC EQUATION IS A TRANSCENDENTAL EQUATION AND HENCE SOLUTION IS NECESSARY. CORRESPONDING TO EACH ARE INFINITE NUMBER OF ( THAT SOLVES THE CHARACTERISTIC EQUATION. HAKKI AND COLEMAN OBTAINED A SHOWING THE VARIATION OF AS A FUNCTION AND ARE SHOWN IN FIG. 2.7. THE RELATIVE PERMITTIVITY OF THE RESONATOR CAN BE CALCULATED USING THE MODE ( (  $\beta_1$  AND  $\beta_2$ ), THE RESONANT FREQUENCY, THE DIMENSIONS OF THE DIELECTRIC PUCK USING THE EQUATION

$$\epsilon_r = 1 + \left[ \frac{c}{Df_r} \right]^2 (\beta_1^2 + \beta_2^2) \quad (2.6)$$

THE HORIZONTALLY ORIENTED E-FIELD PROBES FOR COUPLING MICROWAVES TO T PROPOSED BY COURTNEY WHICH ENABLED TO SPAN A WIDE RANGE OF FREQUENCIES, S THERE IS NO CUT-OFF FREQUENCY FOR COAXIAL MODE USED FOR THE MEASUREMENTS SINCE THIS MODE PROPAGATES INSIDE THE SAMPLE BUT IS EVANESCENT THEREFORE A LARGE AMOUNT OF ELECTRICAL ENERGY CAN BE STORED IN THE HIGH RESONATORS [40]. HOWEVER, IN THE OPEN SPACE POST RESONATORS SETUP, A PART OF ENERGY IS RADIATED OUT AS EVANESCENT FIELD AND HENCE THE AXIAL MODE NUMBER EXPRESSED SINCE IT IS LESS THAN 1 (I.E. IN THE END SHORTED CONDITION THE E FIELD BECOMES ZERO CLOSE TO THE METAL WALL AND ELECTRIC ENERGY VANISHES IN THE AIR

IN THE EXPERIMENTAL SETUP, A VECTOR NETWORK ANALYZER (MODEL 8753 ET, A TECHNOLOGIES, HEWLETT-PACKARD, PALO ALTO, CA) IS USED FOR TAKING MEASUREMENTS OF MICROWAVE FREQUENCIES. THE HP 9000, 300 SERIES INSTRUMENTATION COMPUTER, IN WITH NETWORK ANALYSER MAKES THE MEASUREMENT QUICKER AND ACCURATE. THE PROBES ARE PLACED APPROXIMATELY SYMMETRICAL WITH THE TWO PROBES. THE RESONANT FREQUENCY IS VISUALISED BY GIVING A WIDE FREQUENCY RANGE BY ADJUSTING THE NETWORK ANALYZER TO SELECT THE RESONANCE FROM THE SEVERAL MODES HAVE COMMON EXISTENCE. SINCE THE UPPER METAL PLATE IS SLIGHTLY TILTED TO INTRODUCE AN AIR GAP. AS THE PLATE IS TILTED, THE TM MODES MOVE RAPIDLY TO THE HIGHER FREQUENCIES WHERE THEY REMAIN ALMOST STATIONARY. IT IS WELL KNOWN THAT IN EXACT RESONANCE IS DISTURBED BY THE SURROUNDINGS. AFTER IDENTIFYING THE RESONANT FREQUENCY OR CENTRAL FREQUENCY (  $f_r$ )

THE SPAN  $\Delta f$  IS REDUCED AS MUCH AS POSSIBLE TO GET MAXIMUM RESOLUTION. THE BANDWIDTH OF THE CURVE DECREASES AND A STAGE OF SATURATION IS REACHED WHEN  $\Delta f$  REMAINS THE LEAST POSSIBLE. THE COUPLING LOOPS ARE FIXED AT THIS POSITION AND A FREQUENCY CAN BE NOTED CORRESPONDING TO THE MAXIMUM. THE DIAMETER 'D' AND LENGTH 'L' OF THE SAMPLE ARE CALCULATED USING EQ. (2.5). FROM THE MODE CHART THE VALUE OF  $\beta$  CORRESPONDING TO  $\beta_{max}$  IS NOTED. THE RELATIVE PERMITTIVITY IS CALCULATED USING EQ. (2.6).

#### 2.5.4 MEASUREMENT OF UNLOADED QUALITY FACTOR (Q)

THERE ARE VARIOUS METHODS WHICH ENABLES MEASUREMENTS OF THE MICROWAVE RESONATORS [42-45]. HOWEVER, NOT ALL OF THEM TAKE INTO ACCOUNT EFFECTS INTRODUCED BY A REAL MEASUREMENT SYSTEM SUCH AS NOISE, CROSSTALK, TRANSMISSION LINE DELAY, AND IMPEDANCE MISMATCH. INADEQUATE ACCOUNTING OF THESE MAY LEAD TO SIGNIFICANT UNCERTAINTY IN THE OBTAINED.

FOR A DR, THE QUALITY FACTOR MEASUREMENT USING THE PARALLEL PLATE ROD RESONATOR IS VERY LOW SINCE THERE OCCURS LOSSES DUE TO CONDUCTING PLATES UNDER END SHORTED CONDITION. IN ORDER TO REDUCE THESE EFFECTS, IN THE PRESENT UNLOADED QUALITY FACTOR OF THE DRS IS MEASURED USING A TRANSMISSION MODE CAVITY PROPOSED BY KRUPKA [46]. THE SPECIMEN WAS PLACED ON A LOW LOSS QUARTZ SPACER OF HEIGHT 8 MM INSIDE A COPPER CAVITY OF INNER DIAMETER 40 MM AND HEIGHT 22 MM. THE INNER SIDE WAS FINELY POLISHED AND SILVER PLATED TO REDUCE RADIATION LOSS. THE LOSS SINGLE CRYSTAL QUARTZ SPACER REDUCES THE EFFECT OF LOSSES DUE TO THE SURFACE OF THE CAVITY. SAMPLES WITH DIAMETER RANGING FROM 1.8 - 2.2 IS PREFERABLE TO GET MAXIMUM MODE SEPARATION AND TO AVOID INTERFERENCE FROM OTHER MODES. ALSO THE FIELD IS SYMMETRIC WITH THE GEOMETRY OF THE SAMPLE AND THE CAVITY, WHICH HELPS TO AVOID THE SOURCES OF LOSS DUE TO CAVITY. AS SEEN IN FIG. 2.9 (A), THE SAMPLE IS ISOLATED BY QUARTZ SPACER, FROM THE EFFECTS OF LOSSES DUE TO THE FINITE RESISTIVITY OF THE PLATES. MICROWAVES ARE FED INTO THE SAMPLE USING TWO LOOP COAXIAL ANTENNA WHICH PROVIDES A MAGNETIC COUPLING TO EXCITE THE TRANSMISSION MODE RESONANCE

DIELECTRIC CYLINDER. THE COUPLING IS ADJUSTED TO BE OPTIMUM (WEAK COUPLING AND STRONG COUPLING FOR LOSSY SAMPLES) BY OBSERVING RESONANCE FREQUENCY SPECTRUM. IN PRINCIPLE THE CAVITY HAS INFINITE NUMBER OF MODES, WHEN EXCITED WITH MULTIFREQUENCY SPECTRUM OF FREQUENCIES, ONE MODE IS IDENTIFIED AS THE FUNDAMENTAL MODE WITH LEAST PERTURBATION WHEN THE TUNABLE TOP LID IS ADJUSTED PROPERLY. AFTER IDENTIFYING THE FUNDAMENTAL MODE, THE LID IS FINE TUNED TO GET MAXIMUM SEPARATION BETWEEN NEARBY CAVITY MODES, TO ATTAIN MAXIMUM POSSIBLE ACCURACY IN MEASUREMENT OF  $TE_{01\Delta}$  MODE FREQUENCY AND THE 3 DB BANDWIDTH FROM THE RESONANCE SPECTRUM (B)) TO CALCULATE  $Q$  FACTOR USING THE EQ. 1.14.

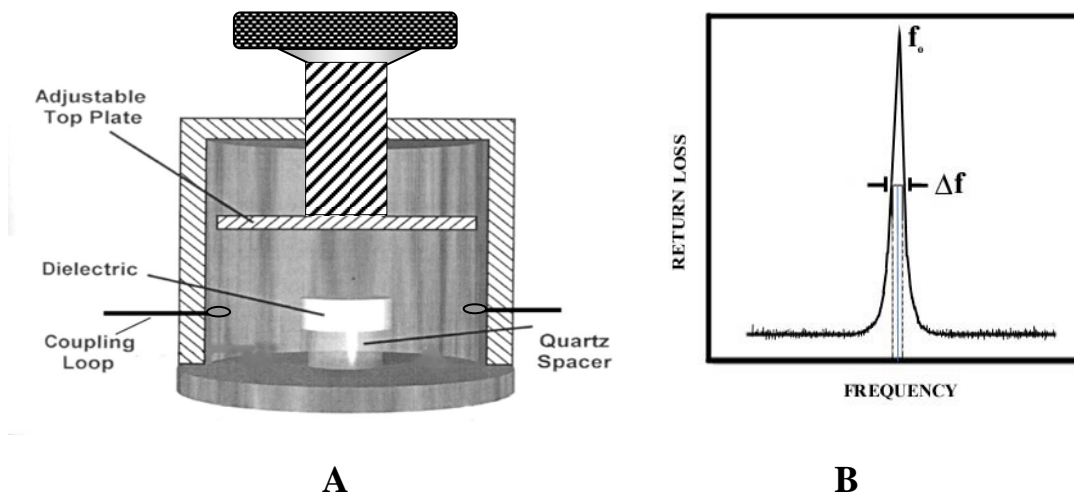


Fig. 2. 9 (A) The cavity set up for the measurement of  $Q$  factor and (B) the method of calculating from resonant mode using Eq. 1.14.

### 2.5.5 MEASUREMENT OF TEMPERATURE COEFFICIENT OF RESONANT FREQUENCY

THE TEMPERATURE COEFFICIENT OF RESONANT FREQUENCY IS AN IMPORTANT PARAMETER THAT DETERMINES THE PERFORMANCE OF THE DEVICE. SINCE RESONATORS ARE USED IN COMMUNICATION SYSTEMS TEMPERATURE STABILITY IS AN IMPORTANT FACTOR AND SHOULD BE AS CLOSE TO ZERO.



THE  $f$  CAN BE MEASURED BY THE CAVITY METHOD USED FOR MEASURING THE FACTOR. THE USE OF INVARIANT CAVITY CAN MINIMIZE THE INACCURACY CAUSED DUE TO EXPANSION OF THE CAVITY WHILE HEATING. THE CAVITY IS KEPT AND THE ENTIRE SYSTEM IS INSULATED IN AN ISOTHERMAL ENCLOSURE. THE SET UP IS THEN SLOWLY HEATED ( $\sim 1^\circ\text{C}/\text{MINUTE}$ ) IN THE RANGE 25 TO 100°C. THE PROBE OF THE THERMOCOUPLE IS KEPT JUST INSIDE THE ISOTHERMAL ENCLOSURE SO THAT IT DOES NOT DISTURB THE RESONANT FREQUENCY. THE RESONANT FREQUENCY MODE IS NOTED AT EVERY INCREMENT IN TEMPERATURE. THE VARIATION OF RESONANT FREQUENCY IS PLOTTED AS FUNCTION OF TEMPERATURE.  $Q$  IS CALCULATED FROM THE SLOPE OF THE CURVE USING THE EQ. (2.7).

$$Q = \frac{1}{f} \frac{\Delta f}{\Delta T} \quad (2.7)$$

### 2.5.6 CAVITY PERTURBATION METHOD

IT IS KNOWN THAT THE COMPLEX PERMITTIVITY OF MATERIALS USUALLY CHANGES ON THE FREQUENCY, TEMPERATURE AND COMPOSITIONS. THEREFORE, IN DESIGNING OF MICROWAVE DEVICES, IT IS VERY IMPORTANT TO STUDY THE TEMPERATURE DEPENDENT PERMITTIVITY OF MATERIALS OVER THE WIDE TEMPERATURE RANGE. ONE OF THE USUAL METHODS TO OBTAIN COMPLEX PERMITTIVITY OF MATERIALS IS THE PERTURBATION METHOD USING A CAVITY RESONATOR. CAVITY PERTURBATION METHODS ARE WIDELY USED IN THE STUDY OF ELECTROMAGNETIC PROPERTIES OF DIELECTRICS, SEMICONDUCTORS, MAGNETIC MATERIALS AND COMPOSITE MATERIALS. IT WORKS WELL FOR THE DETERMINATION OF THE DIELECTRIC PROPERTIES OF THIN SHEET SAMPLES OF LOW AND MEDIUM DIELECTRIC LOSS [47]. WHEN THE PERTURBATION METHOD IS APPLIED, IT IS NECESSARY TO SATISFY TWO CONDITIONS. ONE OF THEM IS THAT THE VOLUME OF DIELECTRIC MATERIAL COMPARED WITH THE VOLUME OF THE CAVITY RESONATOR, AND THE OTHER IS THAT THE ELECTROMAGNETIC FIELD DISTRIBUTION IS NOT CHANGED AFTER INSERTION OF DIELECTRIC MATERIAL INTO THE CAVITY. IN A RESONANT PERTURBATION METHOD, THE SAMPLE IS INTRODUCED TO A RESONANT CAVITY, AND THE ELECTROMAGNETIC PROPERTIES OF THE SAMPLE ARE DEDUCED FROM THE CHANGE OF RESONANT FREQUENCY AND QUALITY FACTOR OF THE CAVITY.

IN THE CAVITY PERTURBATION TECHNIQUE, A SMALL PIECE OF THE MATERIAL UNDER TEST IN THE FORM OF A DISK OR SHEET IS PLACED IN A METALLIC RESONANT CAVITY OPERATING IN A SINGLE MODE. THE MATERIAL CHARACTERISTICS ARE ESTIMATED FROM THE SHIFT IN THE RESONANT FREQUENCY AND CHANGE IN ~~Q~~ OF THE SYSTEM [48]. THIS TECHNIQUE WAS PIONEERED BY SLATER [49] AND DEVELOPED A SUITABLE METHOD FOR MEASURING THE DIELECTRIC PROPERTIES OF MATERIALS WITH PERMITTIVITY LESS THAN 10. THE CAVITY PERTURBATION METHOD IS NOT A SWEEPED FREQUENCY MEASUREMENT. MEASUREMENT FREQUENCIES ARE DETERMINED BY THE CAVITY AS WELL AS THE DRIVING SIGNAL. HENCE IT CAN BE USED ONLY FOR DISCRETE FREQUENCY MEASUREMENTS. IN THIS METHOD, A RECTANGULAR WAVE GUIDE WITH A SMALL SLOT AT THE BROADER WALL AT THE MIDDLE OF THE CAVITY IS EXCITED WITH OPTIMUM IRIS COUPLING AND THE RESONANT FREQUENCY AND Q FACTOR OF THE EMPTY CAVITY IS DETERMINED FOR DIFFERENT CAVITY MODES. THEN THE SAMPLE IS INSERTED AND POSITIONED AT THE E-FIELD ANTINODE. IF THE SAMPLE IS PURELY DIELECTRIC, THE MAXIMUM ELECTRIC FIELD CAN BE EASILY DETERMINED BY SIMPLY MOVING THE SAMPLE ALONG THE SLIT. THE MODE WILL SHIFT TO LOW FREQUENCY SIDE AND RETRACES FROM THERE. IF THE SAMPLE IS KEPT AT THE RETRACING POSITION, THIS IS THE ELECTRIC FIELD MAXIMUM POSITION. IN THIS METHOD, THE MAGNETIC THE PERMITTIVITY CAN BE MEASURED ONLY FOR THE ODD MODES BY KEEPING THE SAMPLE IN THE MIDDLE OF THE CAVITY. THE NEW RESONANT FREQUENCY AND Q FACTOR IS AGAIN MEASURED. THE COMPLEX RELATIVE PERMITTIVITY OF THE SAMPLE IS CALCULATED [47, 50] USING THE FOLLOWING EQ. (2.8 - 2.10) [51].

$$\epsilon_r' = 1 + \left[ \frac{V_c(f_o - f_s)}{2V_s f_s} \right] \quad (2.8)$$

$$\epsilon_r'' = \frac{V_c(Q_o - Q_s)}{4V_s Q_o Q_s} \quad (2.9)$$

$$\tan \delta = \frac{\epsilon_r''}{\epsilon_r'} \quad (2.10)$$

WHERE  $f_o$  = RESONANT FREQUENCY OF THE EMPTY CAVITY,  $f_s$  = RESONANT FREQUENCY OF THE CAVITY WITH SAMPLE,  $V_c$  = VOLUME OF THE CAVITY,  $V_s$  = VOLUME OF THE SAMPLE,  $Q_o$  = THE QUALITY FACTOR OF THE EMPTY CAVITY AND  $Q_s$  = THE QUALITY FACTOR OF THE CAVITY WITH SAMPLE.

EXPERIMENTAL ERROR WAS FOUND TO BE LESS THAN 2 % IN CASE OF PERMITTIVITY AND CASE OF DIELECTRIC LOSS. THE MAIN ADVANTAGE OF THIS METHOD IS THE EASINESS OF THE PERMITTIVITY AND LOSS USING SIMPLE DEVICE WITH MODERATE ACCURACY.

### 2.5.7 SPLIT-POST DIELECTRIC RESONATOR METHOD

SPLIT- RESONATOR METHODS ARE SUITABLE FOR THE CHARACTERIZATION OF DIELECTRIC SAMPLES, INCLUDING DIELECTRIC SUBSTRATES FOR PLANAR CIRCUITS [52]. THE RESONATOR CONSISTS OF TWO DIELECTRIC DISCS IN A METAL ENCLOSURE. THE DIELECTRIC DISCS ARE OF A HEIGHT OF METAL ENCLOSURE IS RELATIVELY SMALL, SO THE EVANESCENT ELECTRIC FIELD CHARACTER IS STRONG NOT ONLY IN THE AIR-GAP REGION FOR RADII GREATER THAN THE DIELECTRIC RESONATOR. IN A SPLIT-POST DIELECTRIC RESONATOR (SPDR) METHOD, THE MEASUREMENT FIXTURE USUALLY HAS A CYLINDRICAL STRUCTURE WORKING AT A TEMPERATURE. THE RESONATOR IS SPLIT INTO TWO PARTS AT THE ELECTRIC CURRENT NODE ALONG A PLANE PERPENDICULAR TO THE CYLINDER AXIS. THE SAMPLE UNDER TEST IS PLACED IN THE GAP BETWEEN THE TWO DIELECTRIC RESONATOR, AND USUALLY THE SAMPLE IS AT THE PLACE OF MAXIMUM ELECTRIC FIELD. THE PRESENCE OF A DIELECTRIC SHEET SAMPLE CHANGES THE RESONANT PROPERTIES OF A SPLIT RESONATOR. THE DIELECTRIC PROPERTIES OF THE SAMPLE CAN BE DERIVED FROM THE RESONANT PROPERTIES OF THE RESONATOR LOADED WITH SAMPLE AND THE DIMENSIONS OF THE RESONATOR AND THE

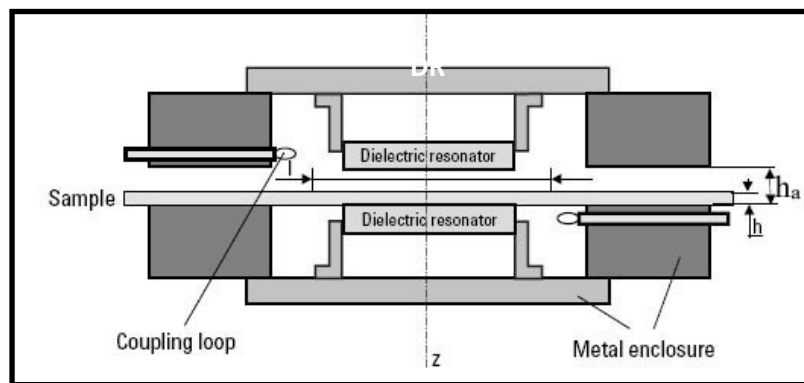


Fig. 2.10 Schematic representation of SPDR.

THE PROPOSED GEOMETRY OF A SPLIT-DIELECTRIC RESONATOR FIXTURE FOR THE OF THE COMPLEX PERMITTIVITY OF DIELECTRIC SHEET SAMPLES IS SHOWN IN FIG. 2.10. DIELECTRIC RESONATOR USUALLY OPERATES WITH THE H- MODE WHICH HAS ONLY AZHIMUTHAL ELECTRIC FIELD COMPONENT, SO THE ELECTRIC FIELD REMAINS CONTINUOUS ON THE INTERFACES. THE FIELD DISTRIBUTIONS ARE AFFECTED BY THE INTRODUCTION OF THE SAMPLE. THE RESONANT FREQUENCY, AND THE QUALITY FACTOR OF THE RESONATOR CHANGE TURN CHANGES THE RESONANT FREQUENCY, AND THE QUALITY FACTOR OF THE RESONATOR. THE DIELECTRIC PROPERTIES OF THE SAMPLE ARE DERIVED FROM THE CHANGES OF RESONANT AND UNLOADED QUALITY FACTOR DUE TO THE INSERTION OF THE SAMPLE. FOR LOW-LOSS SAMPLES, THE INFLUENCE OF LOSSES ON THE RESONANT FREQUENCIES IS NEGLIGIBLE, SO THE PERMITTIVITY OF THE SAMPLE UNDER TEST IS RELATED TO THE RESONANT FREQUENCY AND DIMENSIONS OF THE CAVITY AND SAMPLE ONLY. IN THIS METHOD, CALIBRATION TECHNIQUE IS USED AND WE COMPARE THE DIFFERENCE OF RESONANT FREQUENCY OF THE SPLIT DIELECTRIC RESONATOR BEFORE AND AFTER THE SAMPLE IS INSERTED. THE RELATIVE PERMITTIVITY OF THE SAMPLE IS DETERMINED BY ITERATIVE SOLUTION TO THE FOLLOWING EQUATION [54]

$$\epsilon_r = 1 + \frac{f_o - f_s}{hf_o K_1(\epsilon_r, h)} \quad (2.11)$$

WHERE  $f_o$  IS THE THICKNESS OF THE SAMPLE UNDER TEST,  $f_s$  IS THE RESONANT FREQUENCY OF EMPTY RESONANT FIXTURE,  $K_1$  IS THE RESONANT FREQUENCY OF THE RESONATOR WITH SAMPLE, IS A FUNCTION OF  $\epsilon_r$  AND  $h$ . THE DIELECTRIC LOSS TANGENT OF THE SAMPLE CAN BE DETERMINED BY

$$\tan \delta = \frac{1}{p_{es}} \left( \frac{1}{Q} - \frac{1}{Q_{DR}} - \frac{1}{Q_c} \right) \quad (2.12)$$

WITH

$$p_{es} = h K_1(\epsilon_r, h) \quad (2.13)$$

$$Q_c = Q_{c0} K_2(\epsilon_r, h) \quad (2.14)$$

$$Q_{DR} = Q_{DR0} \cdot \frac{f_o}{f_s} \cdot \frac{P_{eDR0}}{P_{eDR}} \quad (2.15)$$

WHERE  $p_{es}$  AND  $p_{eDR}$  ARE THE ELECTRIC-ENERGY FILLING FACTORS FOR THE SAMPLE AND FOR THE RESONATOR RESPECTIVELY,  $p_{eDR}$  IS THE ELECTRIC-ENERGY FILLING FACTOR OF THE DIELECTRIC RESONATOR FOR EMPTY RESONANT FIXTURE,  $Q_{DR}$  IS THE QUALITY FACTOR DEPENDING ON METAL ENCLOSURE LOSSES FOR EMPTY RESONANT FIXTURE,  $Q_{DR}$  IS THE QUALITY FACTOR DEPENDING ON DIELECTRIC LOSSES IN DIELECTRIC RESONATORS FOR EMPTY RESONANT FIXTURE; AND  $Q_{DR}$  IS THE QUALITY FACTOR OF THE RESONANT FIXTURE CONTAINING THE DIELECTRIC SAMPLE. THE  $p_{es}$  AND  $Q_{DR}$  FOR A GIVEN RESONANT STRUCTURE CAN BE CALCULATED USING NUMERICAL METHODS. IN TERMS OF SAMPLE GEOMETRY, THE REQUIREMENTS ARE THAT THE SAMPLE MUST EXTEND TO THE FULL DIAMETER OF THE TWO CAVITY SECTIONS AND THE SAMPLE MUST BE FLAT. THIS PAPER DESCRIBES THE ACCURACY OF A RESONATOR TECHNIQUE WITHOUT HAVING TO MACHINE THE SAMPLE. THE UNCERTAINTY OF THE PERMITTIVITY MEASUREMENTS OF A SAMPLE OF THICKNESS  $h$  IS  $\Delta \epsilon / \epsilon = \pm (0.0015 + \Delta h/h)$  AND UNCERTAINTY IN LOSS TANGENT MEASUREMENTS IS  $\Delta \tan \delta / \tan \delta = \pm (0.0015 + \Delta h/h)$ .

## 2.6 RADIO FREQUENCY DIELECTRIC MEASUREMENTS

LCR METERS ARE GENERALLY USED FOR MEASUREMENTS OF CAPACITANCE AND LOSS TANGENT AND DISSIPATION FACTOR OF CAPACITORS IN THE RADIO FREQUENCY REGION BY THE WELL-KNOWN PARALLEL PLATE CAPACITOR METHOD. THIS WILL GIVE AN APPROXIMATE VALUE OF CAPACITANCE WHICH HELPS TO CALCULATE THE APPROXIMATE RESONANT FREQUENCY AND SIZE OF THE DRUM. THE Q-FACTOR. THE PARALLEL PLATE CAPACITOR METHOD INVOLVES SANDWICHING A THIN SLICED MATERIAL BETWEEN TWO ELECTRODES TO FORM A CAPACITOR. THE CAPACITANCE OF THIS CAPACITOR IN VACUUM IS COMPARED WITH ONE IN THE PRESENCE OF THE MATERIAL. THE DIELECTRIC PROPERTIES ARE TO BE MEASURED. THEN RELATIVE PERMITTIVITY IS CALCULATED USING EQ. (2.16) [21].

$$C = \frac{\epsilon_r \epsilon_0 A}{d} \quad (2.16)$$

WHERE  $C$  IS THE CAPACITANCE OF MATERIAL,  $\epsilon_r$  ARE THE RELATIVE PERMITTIVITIES OF MATERIAL AND FREE SPACE RESPECTIVELY. IN THE PRESENT STUDY, THE DIELECTRIC PROPERTIES AT RADIO FREQUENCY ARE MEASURED USING LCR METER (HIOKI 3532-50 LCR HI TESTER, JAPAN).

## 2.7 ERROR CALCULATIONS IN DIELECTRIC PROPERTY MEASUREMENTS

THE MEASUREMENT OF MICROWAVE DIELECTRIC PROPERTIES TO TWO DECIMAL POINT ACCURACY. USUALLY THREE SAMPLES WERE PREPARED IN A BATCH CORRESPONDING TO PARTICULAR COMPOSITION AND THE MEASUREMENTS WERE MADE AT LEAST TWO SPECIMEN. THE ERRORS WERE CALCULATED USING THE ROOT SUM OF SQUARES (RSS) METHOD. THE ACCURACY OF MEASUREMENT IS RESTRICTED TO THE ACCURACY IN MEASUREMENT OF FREQUENCY AND DIMENSIONS OF THE SAMPLE. THE MEASUREMENT IS LESS THAN THE POSSIBLE ERRORS IN THE MEASURED VARIABLES. THE ERRORS INCLUDE THE ERROR ASSOCIATED WITH THE SAMPLE SIZE, LENGTH AND RESONANT FREQUENCY GIVEN BY

$$\Delta\epsilon_r = \left[ \left( \frac{\partial}{\partial L} \Delta L \right)^2 + \left( \frac{\partial}{\partial r} \Delta r \right)^2 + \left( \frac{\partial}{\partial f_r} \Delta f_r \right)^2 \right]^{1/2} \quad (2.17)$$

IF THE INDEPENDENT SOURCES OF ERROR CORRESPOND TO ONE STANDARD DEVIATION, THEN THE ERROR WILL ALSO CORRESPOND TO ONE STANDARD DEVIATION [55]. THE ERRORS IN QUALITY FACTOR AND TEMPERATURE COEFFICIENT OF RESONANT FREQUENCY CAN BE CALCULATED USING RSS METHOD BY TAKING PARTIAL DERIVATIVE OF THESE PARAMETERS WITH RESPECT TO INDEPENDENT VARIABLES.

## 2.8 THERMAL CHARACTERIZATION TOOLS

THERMAL ANALYSIS INCORPORATES THOSE TECHNIQUES IN WHICH SOME PHYSICAL PARAMETER OF THE SYSTEM IS DETERMINED AND RECORDED AS A FUNCTION OF TEMPERATURE. THERMAL CHARACTERIZATION METHODS ADOPTED IN THE PRESENT INVESTIGATION ARE LISTED BELOW.

### 2.8.1 THERMO GRAVIMETRIC ANALYSIS (TGA)

THERMO GRAVIMETRIC ANALYSIS IS A TECHNIQUE WHEREBY A SUBSTANCE, IN AN ENVIRONMENT HEATED OR COOLED AT A CONTROLLED RATE, IS RECORDED AS A FUNCTION OF TEMPERATURE. THUS THE BASIC REQUIREMENTS FOR THE MEASUREMENT ARE A HEATING SOURCE, A MEANS OF WEIGHING. THE TG CURVE GIVES INFORMATION ABOUT

- (I) THE THERMAL STABILITY OF THE MATERIAL.
- (II) THE PROCEDURAL DECOMPOSITION TEMPERATURE AT WHICH THE CUMULATIVE MASS CHANGE REACHES A MAGNITUDE THAT THE THERMOANALYZER CAN DETECT.
- (III) THE TEMPERATURE AT WHICH THE REACTION IS COMPLETE AND THE REACTION IS COMPLETE.

### 2.8.2 THERMO MECHANICAL ANALYSIS (TMA)

IN THIS TECHNIQUE, DIMENSIONAL CHANGES IN THE SAMPLE ARE PRIMARILY MEASURED, WITH NEGLIGIBLE FORCE ACTING ON IT, WHILE THE SAMPLE IS HEATED, COOLED, OR STABILIZED AT A CONSTANT TEMPERATURE. IT IS PARTICULARLY SUITED TO POLYMER MATERIALS BUT A WIDE RANGE OF MATERIALS CAN BE EXAMINED [56]. IN THE PRESENT STUDY, TMA (TMA- 60 H, SHIMADZU, KYOTO, JAPAN) IS USED TO DETERMINE THE THERMAL EXPANSION COEFFICIENT AND SOFTENING TEMPERATURE (UNDER APPLICATION OF LOAD AND HEMISPHERE-PLUGS) OF COMPOSITES. TMA IS ALSO USED TO DETERMINE THE SOFTENING AND MELTING TEMPERATURE OF GLASS-CERAMIC COMPOSITES USED FOR HIGH TEMPERATURE CO-FIRED CERAMIC APPLICATIONS.

### 2.8.3 THERMAL CONDUCTIVITY MEASUREMENT

AN IMPROVED PHOTOPYROELECTRIC TECHNIQUE [57-58] WAS USED TO DETERMINE THE THERMAL CONDUCTIVITY OF THE POLYMER COMPOSITES. A 70 MW HE-CD LASER OF WAVELENGTH 442 NM, INTENSITY MODULATED BY A MECHANICAL CHOPPER (MODEL SR540) WAS USED AS OPTICAL HEATING SOURCE. A PVDF FILM OF THICKNESS 2 μm COATING ON BOTH SIDES, IS USED AS PYROELECTRIC DETECTOR. THE OUTPUT SIGNAL IS MEASURED USING A PREAMPLIFIER (MODEL SR 830). MODULATION FREQUENCY IS KEPT ABOVE 60 HZ TO ENSURE THE DETECTOR, THE SAMPLE AND BACKING MEDIUM ARE THERMALLY THIN DURING MEASUREMENT. THERMAL THICKNESS OF THE COMPOSITES WAS VERIFIED BY PLOTTING PHOTOPYROELECTRIC SIGNAL AMPLITUDE AND PHASE WITH FREQUENCY AT ROOM TEMPERATURE. THERMAL DIFFUSIVITY AND THERMAL EFFUSIVITY (E) WERE ALSO MEASURED FROM PPE SIGNAL PHASE AND AMPLITUDE. FROM THE VALUES OF E THE THERMAL CONDUCTIVITY AND SPECIFIC HEAT CAPACITY OF THE COMPOSITE SAMPLES WERE OBTAINED. IN THE PRESENT INVESTIGATION THERMAL CONDUCTIVITY MEASUREMENTS WERE MADE ON POLYMER CERAMIC COMPOSITES USED FOR MICROWAVE SUBSTRATES AND ELECTRONIC APPLICATIONS.

## 2.9 REFERENCES

1. R. RICE, *Ceramic Fabrication Technology*, MARCEL DEKKER, BOSTON, (2003).
2. D. SEAGAL, *Chemical Synthesis of Advanced Ceramic materials*, CAMBRIDGE UNIVERSITY PRESS, CAMBRIDGE, (1991).
3. R. E. CARTER, *Chem. Phys.*, **34**, 2010–15 (1961).
4. J. BERETKA, *Am. Ceram. Soc.*, **67**, 9-12, (1984).
5. S. F. HUBERT, *Br. Ceram. Soc. J.*, **6**, 11-20 (1967).
6. C. C. HARRIS, *Trans. AIME.*, **238**, 17, (1967).
7. B. BEKE, *Principles of Communiton*, AKADEMI KIADO, BUDAPEST, (1964).
8. H. E. ROSE AND R. M. E. SULLIVAN, *Treatise on the Internal Mechanics of Ball, Tube and Rod mills*, CHEMICAL PUBLISHING, BOSTON, (1958).
9. L. M. SHEPPARD, *Ceram. Int.*, **149**, 51-63, (1999).
10. G. Y. ONODA AND L. L. HENCH, *Ceramic Processing before Firing*, WILEY INTERSCIENCE, NEW YORK (1973).
11. P. WINIEWSKI, M. SZAFRAN AND G. ROKICKI, *Mater., Euro Ceramics – VIII*, **264**, 428-32, (2000).
12. A. E. MCHALE, *Processing Additives*, ENGINEERING MATERIALS HANDBOOK, CERAMICS AND GLASSES, VOLUME- 4, THE MATERIALS INFORMATION SOCIETY, SC, (1991).
13. N. M. ALFORD, X. WANG, S. J. PENN, M. POOLE AND B. JONES, *Br. Ceram. Soc. Trans.*, **99**, 212-14, (2000).
14. S. JILL GLASS AND K. G. EWERS, *WISIBulletin*, (1997).
15. N. ICHINOSHITA, *Introduction to Fine Ceramics*, JOHN WILEY AND SONS, NEW YORK, (1987).
16. D. W. RICHESON, *Modern Ceramic Engineering, Properties, Processing, and use in design*, (2006).
17. D. F. CASTRO, *Sintering Course, Presented at Centro de Estudios e Investigaciones Técnicas de Gipuzkoa Centro de Estudios e Investigaciones Técnicas de Gipuzkoa, San Sebastián.*, (JUNE 2000).
18. W. D. KINGERY, *Introduction to Ceramics*, JOHN WILEY AND SONS, NEW YORK, (1960).
19. S.-J. L. KANG, *Sintering, Densification, Grain Growth and Microstructure*, ELSEVIER, AMSTERDAM, (2002).
20. R. L. COBLE, *Appl. Phys.*, **32**, 787-792, (1961).
21. W. D. KINGERY AND M. BERGER, *Appl. Phys.*, **26**, 1205-1212, (1955).
22. T. K. GUPTA, *Am. Ceram. Soc.*, **61**, 191-95, (1978).



23. W. D. KINGER, *Am. Ceram. Soc.*, **37**, 42-45, (1954).
24. D. M. MOORE AND R. C. REYNOLDS, *Diffraction and the Identification and Analysis of Clay Minerals*, OXFORD UNIVERSITY PRESS, NEW YORK, (1989).
25. C. HAMMOND, *The Basics of Crystallography and Diffraction*, 2ND EDN., OUP.
26. G. E. BACON, *X-ray and Neutron Diffraction*, PERGAMON PRESS, AMSTERDAM, (1966).
27. B. D. CULLITY, *Elements of X-ray diffraction*, 2 ED.: ADDISON-WESLEY PUBLISHING COMPANY, (1978).
28. D. L. BISH AND J. E. POSNER, *Modern Powder Diffraction. Reviews in Mineralogy*, 20, MINERALOGICAL ASSOCIATION OF AMERICA, BOSTON, (1989).
29. L. REIMER, *Scanning Electron Microscopy, Physics of Image Formation and Microanalysis*, SPRINGER SERIES IN OPTICAL SCIENCES, 45, SPRINGER, BERLIN, (1985).
30. J. W. EDINGTON, *Operation and Calibration of the Electron Microscope*, MACMILLAN PRESS, LONDON, (1974).
31. A. R. WEST, *Solid State Chemistry and it's Applications*, JOHN WILEY AND SONS.
32. G. BIRNBAUM AND J. FRANK, *Phys.*, **20**, 817-18, (1949).
33. J. MUSSIL AND F. ZACHAR, *Microwave Measurement of Complex Permittivity by Free Space Methods and Applications*, ELSEVIER, NEW YORK, (1986).
34. K. LEONG, *Precise Measurements of Surface Resistance of HTS Thin Films using A Novel Method of Q-Factor Computations for Sapphire Dielectric Resonators in the Transmission Mode*, PH. D. THESIS, JAMES COOK UNIVERSITY, (2000).
35. K. LEONG AND J. MAZIER, *Supercond.*, **14**, 93-103, (2001).
36. D. KAJFEZ, *Q-Factor*, VECTOR FIELDS, OXFORD, (1994).
37. K. WAKINO, *Proc. of The Second Sendai Inter. Conference, YAGI Symposium on Advanced Technology Bridging the Gap between Light and Microwaves*, P. 187-196, (1990).
38. B. W. HAKKI AND P. D. COLEMAN, *IRE Trans. Microwave Theory Tech.*, **8**, 402-410, (1960).
39. W. E. COURTNEY, *IEEE Trans. Microwave Theory Tech.*, **MTT-18**, 476-485 (1970).
40. Y. KOBAYASHI AND S. TANAKA, *Trans. Microwave Theory Tech.*, **MTT-28**, 1077-85, (1980).
41. S. B. COHN AND K. C. KELLEY, *IEEE Trans. Microwave Theory Tech.*, **MTT-14**, 406 -10, (1966).
42. E. L. GINZTON, *Microwave Measurements*, MCGRAW HILL BOOK CO., BOSTON, (1957).

43. E. J. VANZURA AND J. E. ROEBERS, *IEEE Conference on Instrumentation and Measurement Technology*, MAY 14-16, ATLANTA, (1991).
44. T. T. T. MIURA, M. KOBAYASHI, *IEEE Transactions on Electronics*, E7 7-C, 900-07, (1994).
45. M. C. SANCHEZ, *IEEE Proceedings*, 134, Part. H, **243-46** (1987).
46. J. KRUPKA, K. DERZAKOWSKI, B. RIDDLE AND J. BAKER-JARVIS, *IEEE Trans. Electron. Dev.*, **9**, 1751-1756, (1998).
47. A. PARKASH, J. K. VAID AND A. MANSINGH, *IEEE Trans. Microwave Theory Tech.*, **27**, 791-795, (1979).
48. Y. BEERS AND S. WEISBERG, *Rev. Mod. Phys.*, **91**, 1014, (1953).
49. J. C. SLATER, *Rev. Mod. Phys.*, **18**, 441, (1946).
50. M. T. SEBASTIAN, *"Dielectric Materials for Wireless Communication"*, ELSEVIER SCIENCE PUBLISHERS, OXFORD, (2008).
51. L. DAIQING, C. E. FREE, K. E. G. PITT AND P. G. BARNWELL, *Microwave Wireless Compon. Lett.*, **11**, 118-120, (2001).
52. J. KRUPKA, S. A. GABELICH, K. DERZAKOWSKI AND B. RIDDLE, *IEEE Technol.*, 10, 1004-1008, (1999).
53. J. KRUPKA, *Mater. Chem. Phys.*, **79**, 195-198, (2003).
54. J. KRUPKA, A. P. GREGORY, O. C. ROCHARD, R. N. CLARKE, B. RIDDLE AND J. BAKER-JARVIS, *Eur. Ceram. Soc.*, **21**, 2673-2676, (2001).
55. R. G. G. J. B. JARVIS, J. H. GROSVENOR JR., M. D. JANEZIC, C. A. JONES, B. RIDDLE, C. M. WEIL AND J. KRUPKA, *IEEE Trans. Dielectr. Electr. Insul.*, **5**, 571-77, (1998).
56. K. P. MENARD, *"Dynamic Mechanical Analysis; A Practical Introduction"*, CRC PRESS, BOCA RATON, (1999).
57. C. P. MENON AND J. PHILIP, *IEEE Sci. Technol.*, **11**, 1744-1749, (2000).
58. F. M. M. MARINELLI, M. G. MECOZZI AND S. MARTELLI, *IEEE Phys. Mater. Sci. Proc.*, **51**, 387 (1990).
59. M. T. SEBASTIAN, C. P. MENON, J. PHILIP AND R. WZSCHWARZ, *IEEE Phys.*, **94**, 3206-3211, (2003).

## CHAPTER 3

### **STRUCTURE AND MICROWAVE DIELECTRIC PROPERTIES OF $ARE_4Si_3O_{13}$ [A=Sr, Ca, Ba; RE=Rare Earths] CERAMICS**

*This chapter deals with the synthesis, characterization and microwave dielectric properties of a series of rare earth silicate based materials  $ARE_4Si_3O_{13}$  [A=Ca, Sr and Ba; RE=rare earths] with apatite structure. The structure and microstructure of these compounds were confirmed using XRD and SEM analysis. All of them belong to  $P6_3/m$  with a hexagonal symmetry. A detailed structural analysis was performed for  $SrRE_4Si_3O_{13}$  series using refinement studies and TEM analysis. The microwave dielectric properties of  $ARE_4Si_3O_{13}$  materials showed a relative permittivity in the range 10-20, reasonably good quality factor and relatively low value of  $\tau_f$ . The  $\tau_f$  value of  $SrLa_4Si_3O_{13}$  was tailored by the addition of proper amount of  $TiO_2$ . The microwave dielectric properties of these compounds were investigated for the first time.*

### 3.1 INTRODUCTION

THE RAPID DEVELOPMENT IN THE MICROELECTRONIC TECHNOLOGIES SUCH AS WIRELESS COMMUNICATIONS, INTELLIGENT TRANSPORT SYSTEM (ITS) AND MICROWAVE INTEGRATED CIRCUITS (MIC) HAS CREATED AN INCREASING DEMAND FOR NOVEL CERAMIC MATERIALS FOR BEING USED AS DIELECTRIC MATERIALS AT MICROWAVE FREQUENCIES. TO MEET THIS REQUIREMENT MATERIALS WITH RELATIVE PERMITTIVITY  $> 10$  ARE PREFERRED DUE TO THE SMALL SIZE OF THESE MATERIALS AT HIGH FREQUENCIES, LOW CROSS COUPLING EFFECT AS WELL AS HIGH SIGNAL PROPAGATION VELOCITY [1-3]. WITH THE RAPID PROGRESS OF MICROWAVE DEVICES, THE DIELECTRIC MATERIALS USED FOR HIGHER FREQUENCY APPLICATIONS HAVE ATTRACTED MUCH ATTENTION. MANY MICROWAVE CERAMICS WITH LOW DIELECTRIC LOSS AND RELATIVE PERMITTIVITY AS WELL AS LOW TEMPERATURE COEFFICIENT OF RESONANT FREQUENCY HAVE BEEN EXTENSIVELY STUDIED FOR SPECIFIC APPLICATIONS [3-5]. HOWEVER, THE SPECIFIC REQUIREMENTS ON DIELECTRIC PROPERTIES LIMIT THE NUMBER OF MATERIALS AVAILABLE FOR HIGH FREQUENCY APPLICATIONS. THE DETAILED RESEARCH ON FLUORITE AND PEROVSKITE STRUCTURES HAS ESSENTIALLY REACHED THE STATE OF ART THAT CAN BE ACHIEVED IN SUCH STRUCTURES. AS NEW HIGH PERFORMANCE MATERIALS, SILICATES ARE CATCHING MUCH ATTENTION [4, 5]. SILICATES FORM THE LARGEST SINGLE GROUP OF MINERALS. IT IS COMMON PRACTICE TO CLASSIFY SILICATES AS WELL AS OTHER MINERALS ACCORDING TO THE KINDS OF THEIR COORDINATION POLYHEDRA. IN THESE POLYHEDRA ARE LINKED. BY CONTRAST, THE SILICA AND QUARTZ POLYHEDRA ARE THE ONLY [SiO<sub>4</sub>] POLYHEDRA KNOWN TO EXIST IN SILICATES. MANY STUDIES WERE REPORTED ON THE MICROWAVE DIELECTRIC PROPERTIES OF VARIOUS SILICATE BASED SYSTEMS [8-11] FOR SUB-MILLIMETER WAVE APPLICATIONS.

### 3.2 APATITE STRUCTURE

AMONG THE VARIOUS SILICATES INVESTIGATED SO FAR, RARE EARTH BASED OXYPHOSPHATES HAVE RECEIVED MUCH ATTENTION DUE TO THE WIDE VARIETY OF PROPERTIES POSSESSED BY THEM. THEY FORM A LARGE FAMILY OF ISOMORPHOUS COMPOUND WITH GENERAL FORMULA  $A_3B_5(CO_4)_3X_3$  WHERE A REPRESENTS A DIVALENT CATION, B A TRIVALENT OR TETRAVALENT ANION. ONE OF THE MOST CHARACTERISTIC OF THE APATITE STRUCTURE IS THAT IT ALLOWS A LARGE NUMBER OF SUBSTITUTIONS AT ALL THE THREE SITES. SOME OF THESE SUBSTITUTIONS CAN BE REALIZED WITHOUT A CHANGE IN CATIONIC OR ANIONIC CHARGE. IT IS POSSIBLE TO SUBSTITUTE THE BIVALENT CATION WITH

CATION AND TRIVALENT ANION (PO<sup>4</sup>-) AND TETRAVALENT ANION (SiO<sub>4</sub><sup>4-</sup>). AN EARLIER REPORT ALSO CONFIRMS THAT A SOLID SOLUTION EXISTS BETWEEN PHOSPHATE AND SILICATE. MINERALS OF THE APATITE GROUP ARE CHARACTERIZED BY A HIGH RESISTANCE TO CHEMICAL DEGRADATION IN NEUTRAL TO ALKALINE ENVIRONMENTS AND BY THEIR POTENTIAL FOR RESTORING BONE DAMAGES. FIG. 3.1 SHOWS A TYPICAL APATITE STRUCTURE. IN THE APATITE STRUCTURE, CALCIUM CATIONS ARE LOCATED IN TWO DIFFERENT SITES: 4F WITH 9-FOLD COORDINATION AND 6H WITH 6-FOLD COORDINATION [14-15]. THE LARGE DIFFERENCE BETWEEN THESE TWO SITES IS THAT THE 4F POSITION IS COORDINATED TO AN O(4) OXYGEN ION THAT IS PRESENT IN THE CHANNELS AND IS SOMETIMES CALLED 'FREE OXYGEN ION'. THIS OXYGEN ATOM DOES NOT BELONG TO A SILICATE GROUP AND THE BINDING STRENGTH OF THE O(4) ION IS NOT SATURATED. THE NINE OXYGENS COORDINATED TO THE 4F SITE ALL BELONG TO THE SILICATE GROUP. THIS DIFFERENCE LEADS TO AN INCREASE OF THE AVERAGE COVALENCY OF THE 6H SITE. ACCORDING TO FELSCH [15], IN HYDROXYAPATITE, THE Mg<sup>2+</sup> IONS ARE ASSUMED TO BE IN THE 6H SITES. ON THE OTHER HAND, BLASSE [16] PROPOSED THAT THE ALKALINE EARTH METALS MAY BE FOUND IN THE 4F SITES IF THEIR IONIC RADIUS IS TOO LARGE AND THE RARE EARTH IONS WHICH ARE TOO SMALL WERE ALSO EXPECTED TO BE FOUND IN 6H. HE ALSO PREDICTED THAT BY DOPING THESE COMPOUNDS WITH RARE EARTH IONS IN THE 6H SITES IN ME<sub>2</sub>LA<sub>8</sub>(SiO<sub>4</sub>)<sub>6</sub>O<sub>2</sub> AND 4F SITES IN ME<sub>2</sub>Y<sub>8</sub>(SiO<sub>4</sub>)<sub>6</sub>O<sub>2</sub> [ME=Mg, Ca] RESPECTIVELY. THIS IS DUE TO THE FACT THAT THE RARE EARTH IONS ARE SMALLER THAN AND LARGER THAN WATER REPORTS, THE DOPING RARE EARTH IONS (Ce<sup>3+</sup>) HAVE BEEN FOUND TO OCCUPY BOTH THE 4F AND 6H SITES IN ME<sub>2</sub>Y<sub>8</sub>(SiO<sub>4</sub>)<sub>6</sub>O<sub>2</sub> [ME=Mg, Ca, Sr] BY LUMINESCENCE SPECTROSCOPY [17-18].

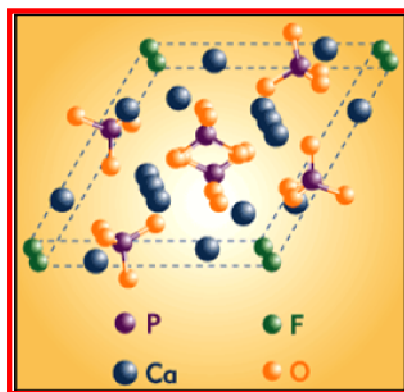


Fig. 3.1 The crystal structure of apatite.  
([www.cea.fr/.../Clefs46/pagesg/clefs46\\_52.html](http://www.cea.fr/.../Clefs46/pagesg/clefs46_52.html))

THE AREAS OF POTENTIAL APPLICATION FOR APATITE MATERIALS ARE WIDELY KNOWN IN BIOMATERIALS, BIOCERAMICS, LUMINESCENT HOST LATTICES, ETC. IN RECENT TIMES, CONSIDERABLE ATTENTION HAS BEEN GIVEN TO THE RARE EARTH CONTAINING SILICATE AND GERMINATE APATITES DUE TO THEIR HIGH IONIC CONDUCTIVITY. THE APATITE BASED SILICATES FIND MUCH INTEREST IN TECHNOLOGICAL APPLICATIONS SUCH AS FUEL CELLS, OXYGEN SENSORS AND IMPROVED ELECTROLYTES FOR USE IN SOFC CELLS [19-22]. THE DOPED APATITE COMPOUNDS HAVE BEEN ESTABLISHED AS PROMISING CANDIDATES FOR USE IN FLUORESCENT LAMP PHOSPHORS AND LASER TECHNOLOGY. RESEARCHERS HAVE ALREADY DEALT WITH THE OXYAPATITE MATERIALS. SOME OF THEM REPORT THE EFFECT OF CATIONIC SUBSTITUTIONS WITH SEVERAL LANTHANIDES OR DIVALENT CATIONS. THESE STUDIES INDICATE THAT THE HIGHEST IONIC CONDUCTIVITY VALUES IN OXYAPATITES ARE CAUSED BY THE FACILE OXYGEN MIGRATION ALONG A NON-LINEAR PATHWAY. HOWEVER, NO ATTEMPT HAS BEEN MADE TO EXPLORE THE MICROWAVE DIELECTRIC PROPERTIES OF THIS GROUP OF MATERIALS. IN THIS STUDY WE FOCUS OUR ATTENTION ON THE SINTERABILITY, STRUCTURE AND DIELECTRIC PROPERTIES OF  $\text{RE}_4\text{Si}_3\text{O}_{13}$  [A = SR, CA AND BA; RE = RARE EARTHS] CERAMICS.

### 3.3 EXPERIMENTAL

THE  $\text{RE}_4\text{Si}_3\text{O}_{13}$  [A = SR, CA AND BA; RE = RARE EARTHS] CERAMICS WERE PREPARED BY THE CONVENTIONAL SOLID STATE CERAMIC ROUTE, USING  $\text{SrCO}_3$ ,  $\text{CaCO}_3$ ,  $\text{BaCO}_3$  (ALDRICH CHEMICAL COMPANY INC., MILWAUKEE, WI; 99.999%),  $\text{SiO}_2$  (SIGMA-ALDRICH INC., ST. LOUIS, MO; 99.9%), RARE EARTH OXIDES  $\text{RE}_2\text{O}_3$ ,  $\text{Eu}_2\text{O}_3$ ,  $\text{Gd}_2\text{O}_3$ ,  $\text{Tb}_2\text{O}_3$ ,  $\text{Dy}_2\text{O}_3$ ,  $\text{Er}_2\text{O}_3$ ,  $\text{Tm}_2\text{O}_3$ ,  $\text{Y}_2\text{O}_3$  (TREIBACHER INDUSTRIES AG-9330, AITHOFFEN, AUSTRIA; 99.999%),  $\text{La}_2\text{O}_3$  AND  $\text{Sm}_2\text{O}_3$  (IRE, 99.9 %) CHEMICALS WERE MIXED BY BALL MILLING FOR 24 HOURS IN DISTILLED WATER MEDIUM USING ZIRCONIA BALLS. AFTER DRYING THE SLURRY, THE POWDERS WERE CALCINED AT 700°C AND THEN GROUND WELL IN AN AGATE MORTAR. THE POWDERS WERE THEN MIXED WITH 4 WT % POLYVINYL ALCOHOL (PVA), DRIED AND UNIAXIALY UNDER 150 MPa PRESSURE INTO PELLETS OF 20 MM DIAMETER AND 10 MM THICK FOR MICROWAVE MEASUREMENTS. THE SINTERING WAS DONE IN THE TEMPERATURE RANGE 1650°C FOR 4 HOURS. THE BULK DENSITIES OF THE POLISHED SAMPLES WERE MEASURED BY ARCHIMEDEAN DIMENSIONAL METHOD. IN THE CASE OF THOSE SAMPLES WITH POOR SINTERABILITY, A S

(0.5 WT %) OF ZINC BOROSILICATE (50ZNO10SiO<sub>2</sub>) GLASS WAS ADDED TO THE CALCINED POWDER AND THE PELLETS WERE PREPARED AS BEFORE.

THE SINTERED SAMPLES WERE POWDERED AND USED TO ANALYZE THE CRYSTAL PHASE PURITY BY X-RAY DIFFRACTION METHOD. ADDITIONAL SAMPLES TO BE EXAMINED VIA THE TRANSMISSION ELECTRON MICROSCOPE (JEOL JEM-2100HR,) WERE PREPARED BY THINNING PELLETS TO ELECTRON TRANSPARENCY USING CONVENTIONAL CERAMOGRAPHY FOLLOWED BY PRECISION ION POLISHING (GATAN MODEL 691). RIETVELD STRUCTURE ANALYSIS WAS CONDUCTED USING THE BRUKER DIFFRACPLUS TOPAS 4.2 PROGRAM. SILICON 650 STANDARD POWDER FROM NATIONAL INSTITUTE OF STANDARDS AND TECHNOLOGY WAS USED AS THE INSTRUMENT PARAMETERS USING A SIMPLE AXIAL MODEL. BACKGROUND WAS REFINED USING CHEBYCHEV FUNCTION, FOLLOWED BY REFINEMENT ON PEAK SHIFTS, INTENSITY SCALING, SAMPLE CONVOLUTIONS, CELL PARAMETERS, CRYSTAL SIZE AND ATOMIC POSITIONING. CELL PARAMETERS AND SITE OCCUPANCIES WERE FIXED DURING THE REFINEMENT PROCESS DUE TO LOW SENSITIVITY ON OXYGEN SITES FOR XRD DATA. THE SINTERED SAMPLES WERE ETCHED AT A TEMPERATURE BELOW THE SINTERING TEMPERATURE FOR 30 MINUTES AND THE SURFACE MORPHOLOGY WAS RECORDED USING SCANNING ELECTRON MICROSCOPE. THE SINTERED AND POLISHED SAMPLES WERE USED FOR MICROWAVE DIELECTRIC PROPERTY MEASUREMENTS USING AN AGILENT NETWORK ANALYZER AS DESCRIBED IN CHAPTER 2.

### 3.4 RESULTS AND DISCUSSION

#### 3.4.1 MICROWAVE DIELECTRIC PROPERTIES OF [S, P, RE = LA, PR, ND, SM, EU, GD, TB, DY, ER, TM, YB AND Y]

THE CALCINATION AND SINTERING TEMPERATURES OF THESE CERAMICS ARE OPTIMIZED FOR THE BEST DENSIFICATION AND MICROWAVE DIELECTRIC PROPERTIES. CALCINATION TEMPERATURE IS OPTIMIZED AT 1000°C. FIG. 3.25 SHOWS THE OPTIMIZATION OF SINTERING TEMPERATURE OF A REPRESENTATIVE MATERIAL (SRL2A) IT IS SEEN THAT AS THE SINTERING TEMPERATURE INCREASES, THE DENSITY INCREASES, REACHING A MAXIMUM VALUE AT 1625°C AND THEREAFTER DECREASES. AT THIS TEMPERATURE THE RELATIVE DENSITY WAS REPORTED EARLIER THAT APATITE BASED MATERIALS ARE DIFFICULT TO SINTER. PERMITTIVITY VARIATION WITH THE SINTERING TEMPERATURE ALSO SHOWS A SIMILAR

RELATIVE PERMITTIVITY IS DEPENDENT ON THE RELATIVE DENSITY. THUS A MAXIMUM PERMITTIVITY OF 14.2 IS EXHIBITED BY FIG. 3.2 (B) SHOWS THE DEPENDENCE OF QUALITY FACTOR OF  $\text{SrLa}_4\text{Si}_3\text{O}_{13}$  CERAMICS WITH SINTERING TEMPERATURE. IT WAS REPORTED BY IDDL [28] THAT ABNORMAL GRAIN GROWTH WAS MORE IMPORTANT FACTOR THAN THE PORE QUALITY FACTOR OF MICROWAVE CERAMICS OVER 90% RELATIVE DENSITY. THE EFFECT CAUSED BY THE DEFECTS IN CERAMICS EG. CRYSTAL DEFECTS, PORE, SUBSTITUTION OR BOUNDARIES, SECONDARY PHASES ETC DOMINATES IN DETERMINING THE CHANGE IN A FUNCTION OF SINTERING TEMPERATURE IN THE MICROWAVE REGION. WHEN THE TEMPERATURE INCREASED THE  $Q_{u,xf}$  INCREASES INITIALLY AND THEN DECREASES. WITH THE INCREASE IN SINTERING TEMPERATURE, FIRST THE PORES SHRINK AND THE GRAINS GROW LARGER WHICH LEADS TO AN INCREASE IN THE QUALITY FACTOR. SRILASIT FORMS A MAXIMUM QUALITY FACTOR OF NEARLY 26300 GHZ AT A SINTERING TEMPERATURE OF 1325°C. THE SINTERING TEMPERATURE OF  $\text{SrLa}_4\text{Si}_3\text{O}_{13}$  IS OPTIMIZED AT 1325°C IN A SIMILAR MANNER THE SINTERING TEMPERATURES OF OTHER MATERIALS IN THE SERIES ARE ALSO OPTIMIZED. TABLE 3.1 GIVES THE OPTIMIZED SINTERING TEMPERATURES OF THE SERIES = LA, PR, ND, SM, EU, GD, TB, DY, ER, TM, YB AND Y] CERAMICS. THE SINTERING TEMPERATURES ARE FOUND TO BE IN THE RANGE 1325 – 1650°C. TO BE NOTED THAT FOR RARE EARTH IONS HAVING LOWER IONIC RADIUS THE MATERIALS REQUIRE HIGHER SINTERING TEMPERATURE (> 1500°C).

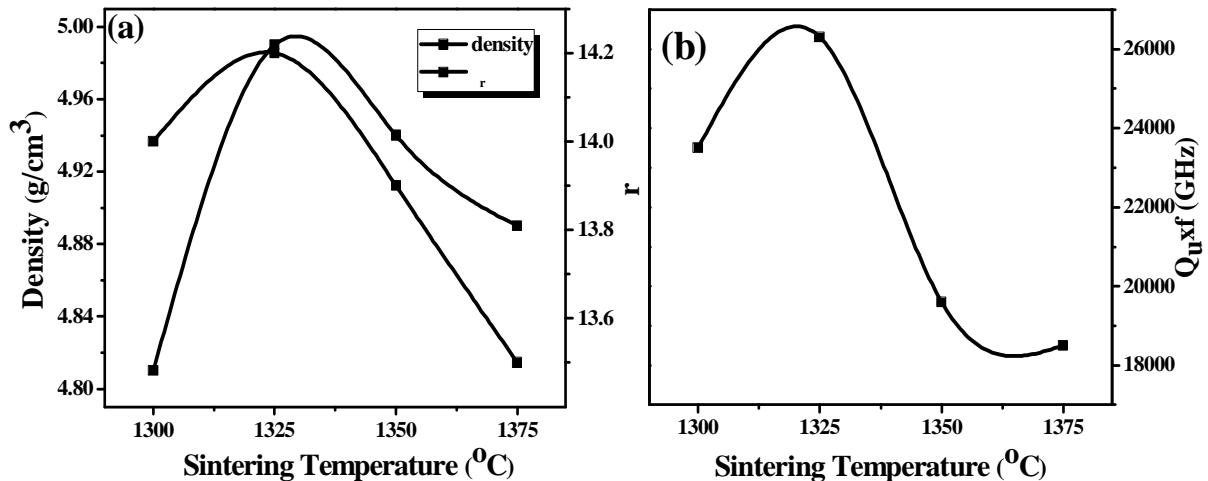


Fig. 3.2 The variation of (a) density,  $\epsilon_r$  and (b)  $Q_{u,xf}$  of  $\text{SrLa}_4\text{Si}_3\text{O}_{13}$  with sintering temperature.



FIGURE 3.3 SHOWS THE XRD PATTERNS OF SrRE<sub>4</sub>Si<sub>3</sub>O<sub>13</sub> [RE = LA, PR, ND, SM, EU, GD, TB, DY, ER, TM, YB AND Y] CERAMICS SINTERED AT THEIR RESPECTIVE OPTIMIZED SINTERING TEMPERATURES. THE STRUCTURAL REFINEMENTS FOR SrRE<sub>4</sub>Si<sub>3</sub>O<sub>13</sub> BASED ON XRD DATA HAVE BEEN REPORTED [29-30], AND THEY HAVE HEXAGONAL (P63/C2) GROUP AS SUCH, A SIMILAR HEXAGONAL UNIT CELL WAS ASSUMED HERE, AND DIFFRACTION INDEXED ACCORDINGLY.

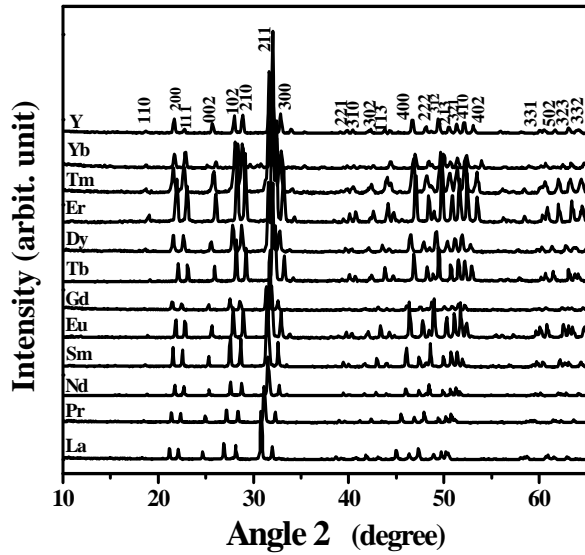


Fig. 3.3 XRD patterns of SrRE<sub>4</sub>Si<sub>3</sub>O<sub>13</sub> [RE = La, Pr, Nd, Sm, Eu, Gd, Tb, Dy, Er, Tm, Yb and Y] ceramics.

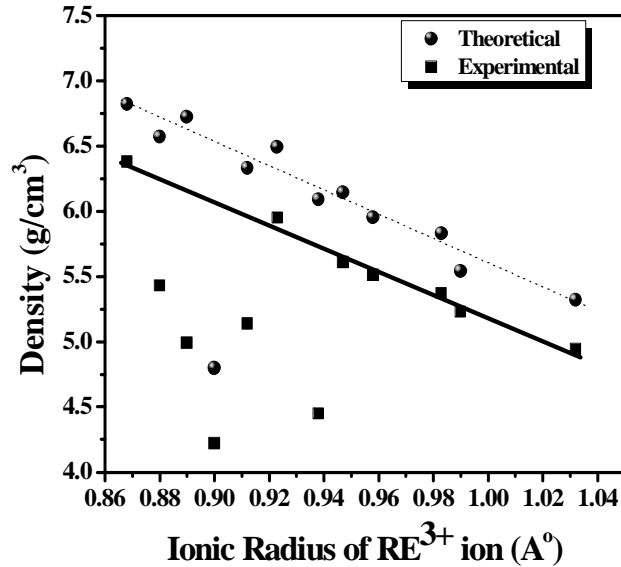


Fig. 3.4 The variation of theoretical and experimental density of SrRE<sub>4</sub>Si<sub>3</sub>O<sub>13</sub> [RE = La, Pr, Nd, Sm, Eu, Gd, Tb, Dy, Er, Tm, Yb and Y] ceramics with the RE<sup>3+</sup> ionic radius.

THE LATTICE PARAMETERS CALCULATED FROM THE XRD PATTERNS ARE TABULATED IN TABLE 3.1. IT CAN BE SEEN THAT THE ‘A’ AND ‘C’ VALUES VARY FROM 9.6752 Å TO 9.2875 Å AND 7.011 Å TO 6.816 Å RESPECTIVELY WITH NO APPRECIABLE DEPENDENCE ON THE IONIC RADIUS OF THE RARE EARTH ION. A GRADUAL DECREASE IN THE LATTICE PARAMETER WITH THE IONIC RADIUS OF THE RARE EARTH ION IS EXPECTED. THE VARIATION IN ‘C’ IS SEEN TO BE MUCH MORE REGULAR THAN THE VARIATION IN ‘A’. HOWEVER, THE RESULTS OBTAINED IN THE PRESENT STUDY ARE, TO SOME EXTENT, NOT IN AGREEMENT WITH THE EARLIER REPORTS ON THE DEPENDENCE OF THE LATTICE PARAMETERS ON THE IONIC RADIUS OF THE RARE EARTH IONS [15]. ONE OF THE REASONS FOR THIS ANOMALY MAY BE DUE TO THE VARIATION IN THE COORDINATION NUMBER EXHIBITED BY THE IONS. SINCE THE EFFECTIVE RADIUS OF ANY ION DEPENDS ON BOTH THE COORDINATION NUMBERS OF THE CATION AND ANION. IT

APATITE BASED MATERIALS THE IONS CAN OCCUPY DIFFERENT SITES EXHIBITING COORDINATION NUMBERS [14-15]. HOWEVER, MORE DETAILED STRUCTURAL STUDIES ARE NEEDED TO EXPLAIN THIS PHENOMENON.

**Table 3.1** The optimised sintering temperature, relative density and lattice parameters of  $\text{SrRE}_4\text{Si}_3\text{O}_{13}$  [RE = La, Pr, Nd, Sm, Eu, Gd, Tb, Dy, Er, Tm, Yb and Y] ceramics.

| $\text{SrRE}_4\text{Si}_3\text{O}_{13}$ | Sintering Temp. ( $^{\circ}\text{C}$ ) | Ionic Radius of $\text{RE}^{3+}$ ( $\text{\AA}$ ) | Relative Density (%) | Lattice parameters ( $\text{\AA}$ ) |        |
|---|--|---|----------------------|-------------------------------------|--------|
|   |  |   |                      | a                                   | c      |
| $\text{SrLa}_4\text{Si}_3\text{O}_{13}$ | 1325 $^{\circ}\text{C}/4\text{H}$      | 1.032   | 93                   | 9.6752                              | 7.1983 |
| $\text{SrPr}_4\text{Si}_3\text{O}_{13}$ | 1325 $^{\circ}\text{C}/4\text{H}$      | 0.990   | 94                   | 9.5885                              | 7.1072 |
| $\text{SrNd}_4\text{Si}_3\text{O}_{13}$ | 1400 $^{\circ}\text{C}/4\text{H}$      | 0.983   | 92                   | 9.4698                              | 7.0207 |
| $\text{SrSm}_4\text{Si}_3\text{O}_{13}$ | 1375 $^{\circ}\text{C}/4\text{H}$      | 0.958   | 93                   | 9.4962                              | 7.0071 |
| $\text{SrEu}_4\text{Si}_3\text{O}_{13}$ | 1450 $^{\circ}\text{C}/4\text{H}$      | 0.947   | 91                   | 9.4073                              | 6.9657 |
| $\text{SrGd}_4\text{Si}_3\text{O}_{13}$ | 1525 $^{\circ}\text{C}/4\text{H}$      | 0.938   | 73                   | 9.5232                              | 7.0087 |
| $\text{SrTb}_4\text{Si}_3\text{O}_{13}$ | 1500 $^{\circ}\text{C}/4\text{H}$      | 0.923   | 92                   | 9.3327                              | 6.8903 |
| $\text{SrDy}_4\text{Si}_3\text{O}_{13}$ | 1475 $^{\circ}\text{C}/4\text{H}$      | 0.912   | 81                   | 9.4699                              | 6.9551 |
| $\text{SrY}_4\text{Si}_3\text{O}_{13}$  | 1575 $^{\circ}\text{C}/4\text{H}$      | 0.900   | 85                   | 9.2875                              | 6.8160 |
| $\text{SrEr}_4\text{Si}_3\text{O}_{13}$ | 1500 $^{\circ}\text{C}/4\text{H}$      | 0.890   | 74                   | 9.3501                              | 6.8493 |
| $\text{SrTm}_4\text{Si}_3\text{O}_{13}$ | 1650 $^{\circ}\text{C}/4\text{H}$      | 0.880   | 83                   | 9.4544                              | 6.8874 |
| $\text{SrYb}_4\text{Si}_3\text{O}_{13}$ | 1525 $^{\circ}\text{C}/4\text{H}$      | 0.868   | 92                   | 9.4109                              | 6.8057 |

FIG. 3.4 SHOWS THE VARIATION OF THEORETICAL AND EXPERIMENTAL DENSITY WITH IONIC RADIUS OF THE RARE EARTH IONS. THE THEORETICAL AND EXPERIMENTAL DENSITIES INCREASE IN THE IONIC RADII DUE TO (I) THE REPLACEMENT OF THE RARE EARTH ION WITH HEAVIER IONS AND (II) THE INCREASE IN THE UNIT CELL VOLUME. THE DENSITY IS LOWER THAN THAT OF OTHER RARE EARTH SILICATES. THIS IS DUE TO THE FACT THAT YTTRIUM IS LIGHTER THAN THE RARE EARTH ELEMENTS AND DOES NOT BELONG TO THE LANTHANIDE GROUP. FROM FIG. 3.4 IT CAN BE SEEN THAT  $\text{SrRE}_4\text{Si}_3\text{O}_{13}$  [RE=LA, PR, ND, SM, EU, TB, YB] SHOWS A RELATIVE DENSITY ABOVE 90 % WHILE  $\text{SrRE}_4\text{Si}_3\text{O}_{13}$  [RE=GD, DY, ER, TM, Y] SHOWS LOW VALUE OF RELATIVE DENSITY (< 85 %). NUMEROUS REPORTS ARE AVAILABLE BASED ON THE EFFECT OF GLASS

THE SINTERABILITY OF DIELECTRIC MATERIALS [31-32]. ADDITION OF SMALL AMOUNT (0.5 WT%) OF ZINC BOROSILICATE (ZBS) GLASS IMPROVED THE DENSITY OF THESE MATERIALS CONSIDERABLY.

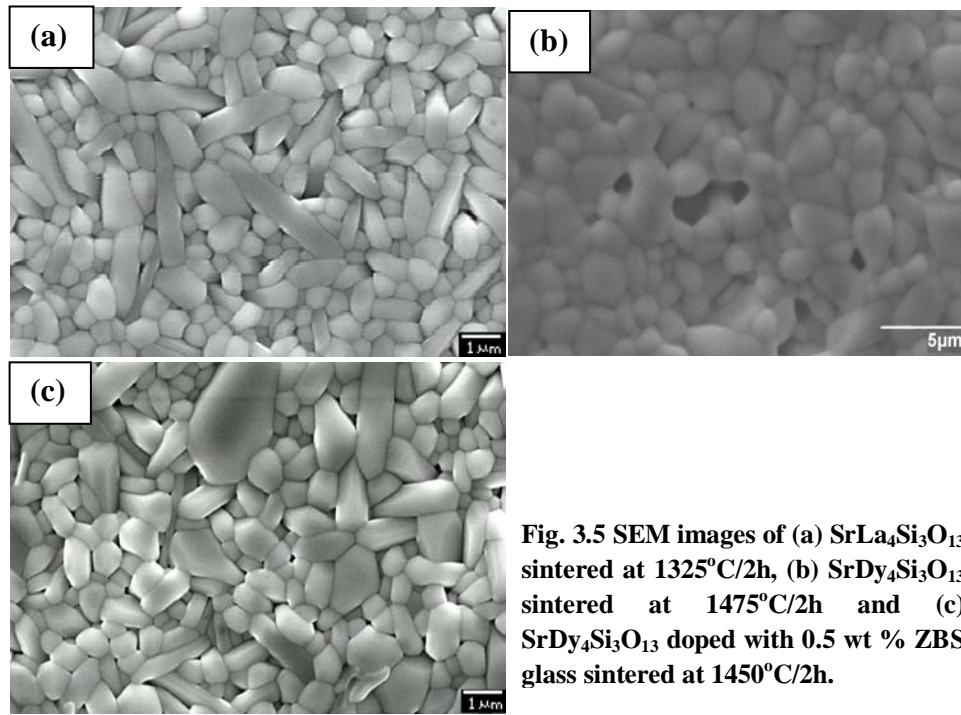


Fig. 3.5 SEM images of (a) SrLa<sub>4</sub>Si<sub>3</sub>O<sub>13</sub> sintered at 1325°C/2h, (b) SrDy<sub>4</sub>Si<sub>3</sub>O<sub>13</sub> sintered at 1475°C/2h and (c) SrDy<sub>4</sub>Si<sub>3</sub>O<sub>13</sub> doped with 0.5 wt % ZBS glass sintered at 1450°C/2h.

FIGURES 3.5 (A) AND (B) SHOW THE SEM IMAGES OF SrLa<sub>4</sub>Si<sub>3</sub>O<sub>13</sub> AND SrDy<sub>4</sub>Si<sub>3</sub>O<sub>13</sub> SINTERED AT 1325°C AND 1475°C RESPECTIVELY. BOTH THE MICROSTRUCTURES REVEAL THE SINGLE PHASE NATURE OF THE MATERIALS. SrLa<sub>4</sub>Si<sub>3</sub>O<sub>13</sub> SHOWS A DENSE MICROSTRUCTURE WITH GRAIN SIZES VARYING FROM 1 TO 3 μM. THE MICROSTRUCTURE SHOWS A RELATIVELY POROUS BEHAVIOUR WHICH IS IN AGREEMENT WITH THE MEASURED DENSITY. FIG. 3.5 (C) SHOWS SEM IMAGE OF 0.5 WT% ZINC BOROSILICATE (ZBS) GLASS DOPED SrDy<sub>4</sub>Si<sub>3</sub>O<sub>13</sub>. IT CAN BE SEEN THAT THE PORES HAVE BEEN ELIMINATED BY LIQUID PHASE SINTERING RESULTING IN THE DENSITY. NO SECONDARY PHASES ARE OBSERVED WHILE AN INCREASE IN THE DENSITY IS NOTED BY THE ADDITION OF GLASS FRITS.

FIGURE 3.6 SHOWS THE TEM IMAGES OF SrLa<sub>4</sub>Si<sub>3</sub>O<sub>13</sub> AND SrDy<sub>4</sub>Si<sub>3</sub>O<sub>13</sub> CERAMICS. THESE SAMPLES SHOW LARGE GRAINS AND CLEAR GRAIN BOUNDARIES, ALTHOUGH THERE IS INTERGRANULAR POROSITY (FIG. 3.6 (B)), WHICH REFLECTS A SOMEWHAT POOR DENSIFICATION. THIS AGREES WELL WITH THE RESULTS IN TABLE 3.1.

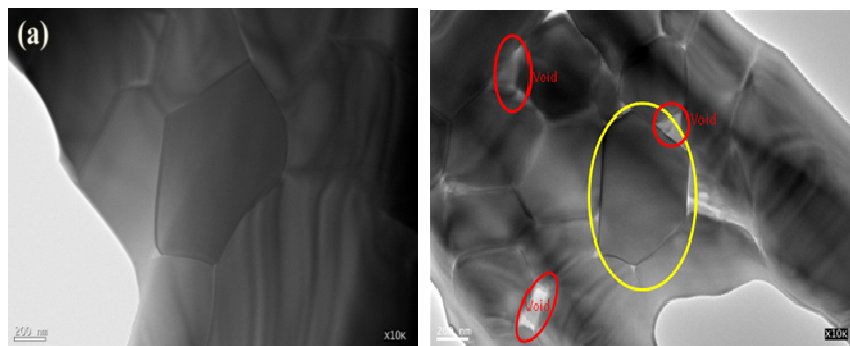


Figure 3.6 TEM images of (a)  $\text{SrY}_4\text{Si}_3\text{O}_{13}$  and (b)  $\text{SrPr}_4\text{Si}_3\text{O}_{13}$ .

FIGURE 3.7 SHOWS SELECTED AREA ELECTRON DIFFRACTION PATTERNS (SAD) REPRESENTATIVE MATERIALS OBTAINED WITH THE BEAM PARALLEL TO (A) [110], (B) [011], (C) [120] AND (D) [001]. THE DIFFRACTION PATTERNS ARE IDENTICAL FOR ALL THE MATERIALS. SIX-FOLD SYMMETRY SHOWN IN THE [001] ELECTRON DIFFRACTION PATTERN SUGGESTS A HEXAGONAL CRYSTAL SYSTEM. CUBIC SPACE GROUPS ARE NOT CONSIDERED BECAUSE OF FOURFOLD SYMMETRY IN PATTERNS. THERE ARE 25 TRIGONAL SPACE GROUPS AND 2 HEXAGONAL ONES. THE DIFFRACTION PATTERNS TAKEN PARALLEL TO [100] AND [120] SHOW CONSISTENT SYSTEMATIC ABSENCE:

$$00l: l = 2n$$

THE XRD OF THESE SAMPLES INDICATES THAT THE  $P6_3/m$  SPACE GROUP SHOULD BE EXCLUDED SINCE  $\{111\}$  REFLECTIONS ARE ALLOWED AND KINEMATICALLY PRESENT, AS SHOWN IN FIGURE 3.7 (B). MOREOVER, THE SYSTEMATIC ABSENCE OF REFLECTION [FIG. 3.7 (C) & (D)] LEAVES ONLY THE POSSIBLE SPACE GROUP,  $P6_3$  (HEXAGONAL, NO.176) OR  $P6_3/22$  (NO.182). OF THESE GROUPS ONLY (NO. 176) IS CENTROSYMMETRIC. AS DIELECTRIC LOSS MEASUREMENTS DO NOT SUGGEST PIEZOELECTRICITY, A CENTROSYMMETRIC SPACE GROUP IS THE MOST PROBABLE SOLUTION. TO FURTHER CONFIRM THE CRYSTAL STRUCTURE, RIETVILDT REFINEMENTS WERE CARRIED OUT ON THE POWDER X-RAY DIFFRACTION DATA.

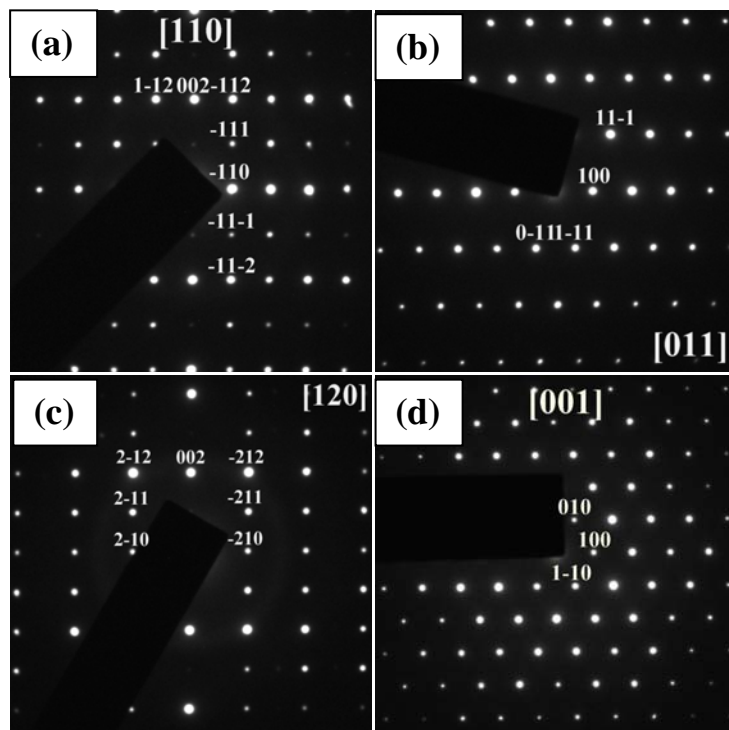
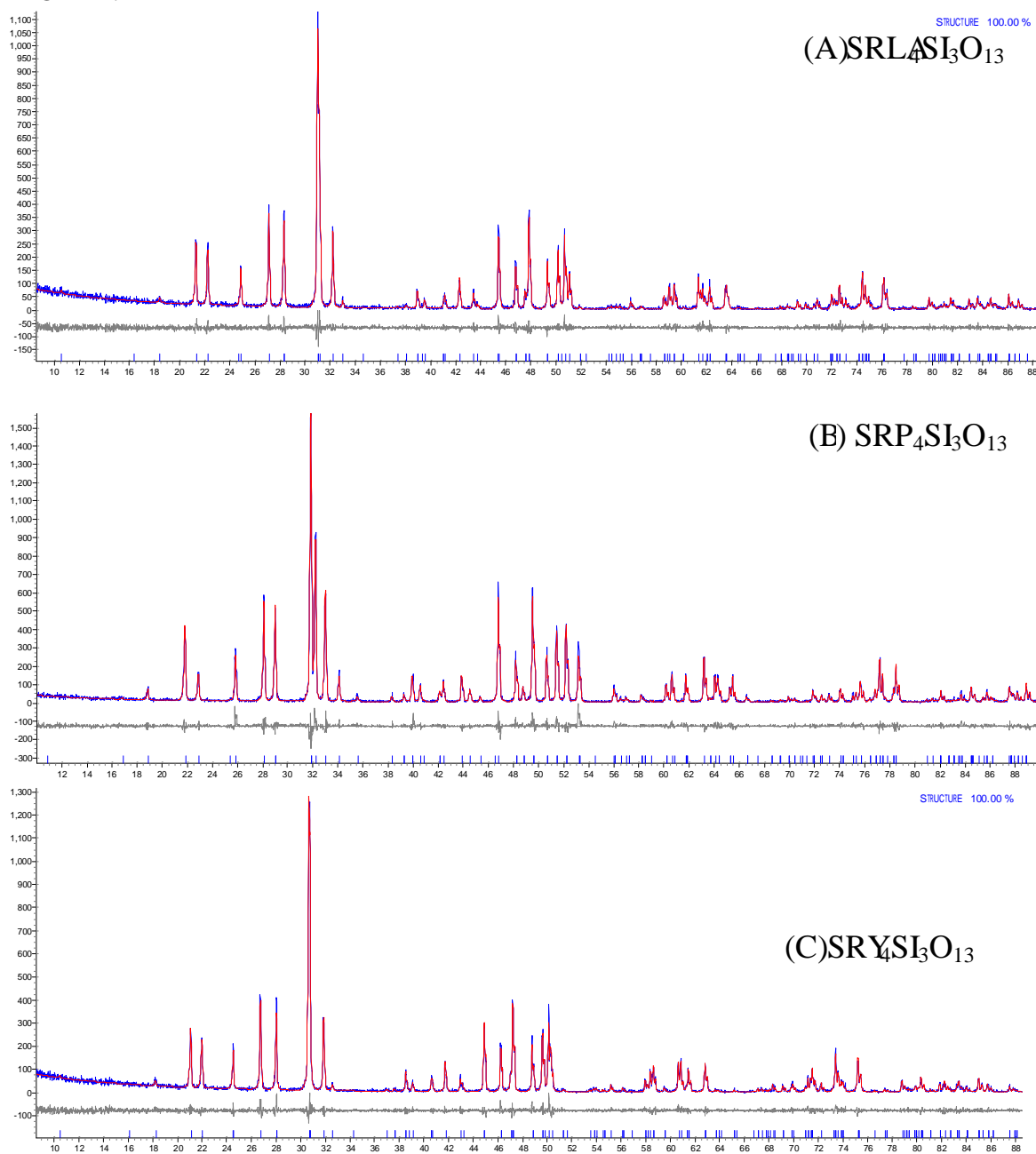


Fig. 3.7 Electron diffractions of  $\text{SrY}_4\text{Si}_3\text{O}_{13}$  taken at (a) [110], (b) [011], (c) [120] and (d) [001].

THE FINAL REFINEMENT PARAMETERS AND ATOMIC COORDINATES FOR SAMPLES S<sub>1</sub> TO S<sub>5</sub> (RE = Y, LA, PR, TB OR YB) ARE SUMMARIZED IN TABLES 3.2 AND 3.3. THE CORRESPONDING FITTED DIFFRACTION PROFILES ARE SHOWN IN FIG. 3.8. THE RESULTS SUGGEST A HEXAGONAL STRUCTURE (NO.176) AND ARE IN GOOD AGREEMENT WITH THOSE OF MASUBUCHI [33] AND SHEN *et al.* [29]. BOTH LATTICE CONSTANTS SHOW A LINEAR RELATIONSHIP WITH THE IONIC RADIUS OF THE RARE-EARTH ELEMENT (LA = 0.99 Å, Y<sup>3+</sup> = 0.9 Å [39]). AS SUCH, THE CELL VOLUME INCREASES WITH INCREASING IONIC RADIUS. THE SUMMARY OF LENGTH AND BOND VALENCE FOR AN AND SI-O POLYHEDRA AND BOND ANGLE OF O-SI-O TETRAHEDRA FROM RIETVELD REFINEMENT IS GIVEN IN TABLE 3.4. RE AND SR CATIONS S<sub>1</sub> SITES AND FORM OCTAHEDRA WITH 6 OXYGEN IONS, INCLUDING THREE O1 AND THREE O2 SITE OCCUPIED ENTIRELY BY RE IONS IS COORDINATED TO SEVEN OXYGEN IONS, INCLUDING ONE O2, FOUR O3 AND ONE O4. THE SI ION IS COORDINATED TO FOUR OXYGEN IONS, WHICH FORM TETRAHEDRON WITH TWO OXYGEN IONS RESIDING ON O3 SITES AND THE OTHERS AT O1. THE DETAIL OF THE CRYSTAL STRUCTURE IS SHOWN IN FIG. 3.9. NOTE THAT RE IONS ARE ALL

(TABLE 3.4), WHEREAS MOST SR IONS (EXCEPT IN THE CASE OF  $\text{Sr}_3\text{O}_2$ ) ARE OVER-BONDED. THESE DISCREPANCIES MIGHT BE ATTRIBUTED TO THE LACK OF ACCURACY IN THE REFINEMENT OF OXYGEN POSITIONS VIA XRD; HOWEVER, THE REFINEMENTS PRESENTED HERE ARE BASED ON THE OBTAINED FROM NEUTRON DIFFRACTION DATA BY MASUBUCHI AND THE RESULTS ARE IN GOOD AGREEMENT WITH THE MODEL.



**Fig. 3.8** Fitted diffraction profiles of (a)  $\text{SrLa}_4\text{Si}_3\text{O}_{13}$  (b)  $\text{SrPr}_4\text{Si}_3\text{O}_{13}$  and (c)  $\text{SrY}_4\text{Si}_3\text{O}_{13}$ , showing observed (blue), calculated (red), and difference (lower) profiles.

**Table 3.2 Refined structure parameters for SrRE<sub>4</sub>Si<sub>3</sub>O<sub>13</sub> (RE=La, Pr and Y) at room temperature.**

| Compound                               | SrLa <sub>4</sub> Si <sub>3</sub> O <sub>13</sub> | SrPr <sub>4</sub> Si <sub>3</sub> O <sub>13</sub> | SrY <sub>4</sub> Si <sub>3</sub> O <sub>13</sub> |
|--|---|---|--|
| R <sub>WP</sub> (%)                    | 19.53   | 19.84   | 18.76  |
| R <sub>BRAC</sub> (%)                  | 3.787   | 3.757   | 4.557  |
| GOF                                    | 1.10  | 1.09  | 1.20   |
| SPACE GROUP                            | <i>P</i> 6 <sub>3</sub> / <i>m</i>                | <i>P</i> 6 <sub>3</sub> / <i>m</i>                | <i>P</i> 6 <sub>3</sub> / <i>m</i>               |
| CELL MASS (G)                          | 1870.98   | 1887.01   | 1470.98  |
| CELL VOLUME (Å <sup>3</sup> )          | 590.12 (2)  | 571.15 (2)  | 524.26 (2)                                       |
| CRYSTALLITE SIZE                       | 1741.9  | 1837.3  | 1624.8   |
| CRYSTALLITE D.<br>(G/CM <sup>3</sup> ) | 5.2648 (2)  | 5.4863 (2)  | 4.6592 (2)                                       |
| LATTICE PARAM                          |   |   |  |
| A (Å)                                  | 9.7035 (2)  | 9.6098 (2)  | 9.3825 (1)                                       |
| C (Å)                                  | 7.2369 (2)  | 7.1415 (2)  | 6.8767 (1)                                       |

**Table 3.3 Refined atomic positions for SrRE<sub>4</sub>Si<sub>3</sub>O<sub>13</sub> (RE= La, Pr and Y) at room temperature.**

| Compound                  | SrLa <sub>4</sub> Si <sub>3</sub> O <sub>13</sub> | SrPr <sub>4</sub> Si <sub>3</sub> O <sub>13</sub> | SrY <sub>4</sub> Si <sub>3</sub> O <sub>13</sub> |
|---------------------------|---|---|--|
| RE1/SR1, 4F (1/3, 2/3, Z) |   |   |  |
| X                         | 0.3333  | 0.3333  | 0.3333   |
| Y                         | 0.6667  | 0.6667  | 0.6667   |
| Z                         | 0.0007 (9)  | 0.0012 (11)                                       | -0.0008 (7)                                      |
| SITE OCCUPAN<br>(RE/SR)   | (0.5/0.5)   | (0.5/0.5)   | (0.5/0.5)  |
| RE2, 6H (X, Y, 1/2)       |   |   |  |
| X                         | 0.0135 (4)  | 0.0102 (4)  | 0.0053 (4)                                       |
| Y                         | 0.2445 (3)  | 0.2431 (3)  | 0.2376 (3)                                       |
| Z                         | 0.2500  | 0.2500  | 0.2500   |
| SITE OCCUPAN              | 1   | 1   | 1  |
| SI, 6H (X, Y, 1/2)        |   |   |  |
| X                         | 0.4033 (13)                                       | 0.3987 (14)                                       | 0.3953 (8)                                       |
| Y                         | 0.3686 (14)                                       | 0.3710 (15)                                       | 0.3697 (8)                                       |
| Z                         | 0.2500  | 0.2500  | 0.2500   |
| SITE OCCUPAN              | 1   | 1   | 1  |
| O1, 6H (X, Y, 1)          |   |   |  |
| X                         | 0.3243 (29)                                       | 0.3201 (30)                                       | 0.3132 (16)                                      |
| Y                         | 0.4773 (27)                                       | 0.4788 (29)                                       | 0.4839 (16)                                      |
| Z                         | 0.2500  | 0.2500  | 0.2500   |
| SITE OCCUPAN              | 1   | 1   | 1  |
| O2, 6H (X, Y, 1/2)        |   |   |  |
| X                         | 0.5973 (29)                                       | 0.5871 (29)                                       | 0.5926 (16)                                      |
| Y                         | 0.4675 (29)                                       | 0.4634 (30)                                       | 0.4753 (16)                                      |
| Z                         | 0.2500  | 0.2500  | 0.2500   |
| SITE OCCUPAN              | 1   | 1   | 1  |
| O3, 12I (X, Y, 1/2)       |   |   |  |

TABLE 3.3 CONTINUED...

| Compound           | SrLa <sub>4</sub> Si <sub>3</sub> O <sub>13</sub> | SrPr <sub>4</sub> Si <sub>3</sub> O <sub>13</sub> | SrY <sub>4</sub> Si <sub>3</sub> O <sub>13</sub> |
|--------------------|---|---|--|
| X                  | 0.3475 (18)                                       | 0.3409 (19)                                       | 0.3352 (11)                                      |
| Y                  | 0.2587 (20)                                       | 0.2555 (20)                                       | 0.2466 (11)                                      |
| Z                  | 0.0777 (20)                                       | 0.0688 (21)                                       | 0.0661 (11)                                      |
| SITE OCCUPANCIES   | 1   | 1   | 1  |
| O4, 2A (0, 0, 1/4) |   |   |  |
| X                  | 0   | 0   | 0  |
| Y                  | 0   | 0   | 0  |
| Z                  | 0.2500  | 0.2500  | 0.2500   |
| SITE OCCUPANCIES   | 1   | 1   | 1  |

Table 3.4 Selected bond lengths, bond valence and bond angles for SrRE<sub>4</sub>Si<sub>3</sub>O<sub>13</sub> (RE=La, Pr and Y).

| Compound                             | SrLa <sub>4</sub> Si <sub>3</sub> O <sub>13</sub> | SrPr <sub>4</sub> Si <sub>3</sub> O <sub>13</sub> | SrY <sub>4</sub> Si <sub>3</sub> O <sub>13</sub> |
|--------------------------------------|---|---|--|
| BOND LENGTH (Å) <sup>I</sup> (4F)-O  |   |   |  |
| A <sup>I</sup> -O1 X 3               | 2.545 (21)  | 2.492 (22)  | 2.372 (12)                                       |
| A <sup>I</sup> -O2 X 3               | 2.513 (24)  | 2.510 (25)  | 2.473 (13)                                       |
| BOND LENGTH (Å) <sup>II</sup> (6H)-O |   |   |  |
| A <sup>II</sup> -O1 X 1              | 2.718 (21)  | 2.704 (22)  | 2.648 (12)                                       |
| A <sup>II</sup> -O2 X 1              | 2.535 (24)  | 2.550 (24)  | 2.386 (13)                                       |
| A <sup>II</sup> -O3 X 2              | 2.536 (15)  | 2.426 (16)  | 2.337 (9)  |
| A <sup>II</sup> -O3 X 2              | 2.612 (17)  | 2.569 (18)  | 2.415 (10)                                       |
| A <sup>II</sup> -O4 X 1              | 2.310 (3)   | 2.288 (4)   | 2.205 (3)  |
| BOND LENGTH (Å) OF SI-               |   |   |  |
| SI-O1                                | 1.585 (37)  | 1.555 (38)  | 1.602 (20)                                       |
| SI-O2                                | 1.630 (27)  | 1.557 (27)  | 1.605 (20)                                       |
| SI-O3 X 2                            | 1.551 (17)  | 1.615 (17)  | 1.612 (9)  |
| BOND ANGLES (°) OF O-                |   |   |  |
| O1-SI-O2                             | 114.1 (15)  | 115.5 (16)  | 112.3 (8)  |
| O1-SI-O3                             | 109.8 (11)  | 110.1 (11)  | 111.5 (6)  |
| O2-SI-O3                             | 107.9 (11)  | 106.9 (11)  | 108.9 (6)  |
| O3-SI-O3                             | 106.9 (14)  | 107.1 (14)  | 103.3 (7)  |
| BOND VALENCE OF                      |   |   |  |
| RE-O ON Å(4F)                        | 1.144   | 1.125   | 1.018  |
| SR-O ON Å(4F)                        | 0.989   | 1.066   | 1.330  |
| RE-O ON Å <sup>I</sup> (4F)          | 2.649   | 2.754   | 2.691  |
| SI-O                                 | 4.531   | 4.453   | 4.180  |



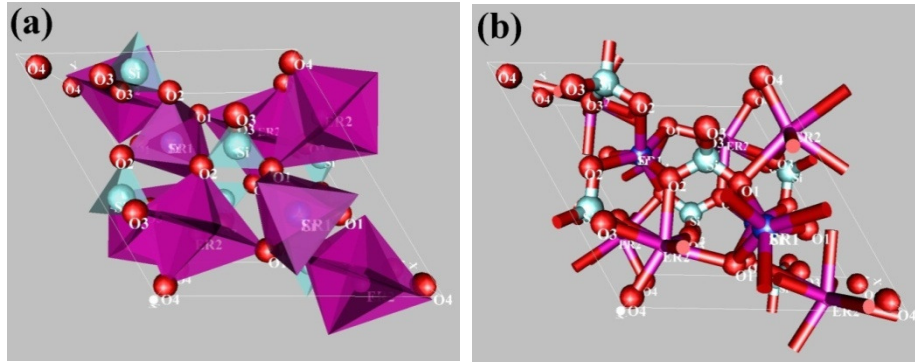


Fig. 3.9 The crystal structure of SrRE<sub>4</sub>Si<sub>3</sub>O<sub>13</sub> showing (a) polyhedral and (b) cation-oxygen bonds.

TABLE 3.5 GIVES THE MICROWAVE DIELECTRIC PROPERTIES OF LARRE, ND, SM, EU, GD, TB, DY, ER, TM, YB AND Y] CERAMICS. FROM THE TABLE IT IS SEEN THAT EXPERIMENTAL RELATIVE PERMITTIVITY VARIES FROM 9.6 TO 15.6. THE CERAMIC COMPOUNDS OF RARE EARTH CERAMICS WITH HIGHER IONIC RADIUS EXHIBITED A HIGHER RELATIVE PERMITTIVITY THAN THE OTHERS. AT MICROWAVE FREQUENCY, THE RELATIVE PERMITTIVITY IS DEPENDENT ON POLARIZABILITY, DENSITY AND PRESENCE OF SECONDARY PHASES. THE RELATIVE PERMITTIVITY OF SRRE<sub>4</sub>Si<sub>3</sub>O<sub>13</sub> AND MINIMUM FOR SrO<sub>13</sub> CERAMICS. SrO<sub>13</sub> CERAMIC HAS A LOW RELATIVE PERMITTIVITY WHEN COMPARED TO SrO<sub>13</sub> AND SrO<sub>13</sub> DUE TO THE HIGH IONIC POLARIZABILITY VALUE OF Sr<sup>2+</sup> WITH RESPECT TO LARRE *et al.* REPORTED [34] THAT A MORE CORRECT VALUE OF THE DIELECTRIC POLARIZABILITY OF LA IS 4.82 INSTEAD OF 3.5 REPORTED BY SHANNON [35]. IN ORDER TO NULLIFY THE EFFECT OF POROSITY ON THE RELATIVE PERMITTIVITY VALUE, PENN [36] PROPOSED A CORRECTION FACTOR WHICH IS GIVEN AS:

$$\epsilon_r = \epsilon_r' \left[ 1 - \frac{3P(\epsilon_r' - 1)}{2\epsilon_r' + 1} \right] \quad (3.1)$$

WHERE  $\epsilon_r$  IS THE RELATIVE PERMITTIVITY OF THE COMPOSITE WHICH CONTAINS A POROSITY,  $\epsilon_r'$  IS THE ACTUAL RELATIVE PERMITTIVITY OF THE DIELECTRIC. THE RELATIVE PERMITTIVITIES OF THE MATERIALS CONSIDERED ARE CORRECTED FOR POROSITY AND ARE GIVEN IN TABLE 3.5. THE POROSITY OF THESE MATERIALS VARIES FROM 12.9 TO A MAXIMUM VALUE OF 15.6. THE RELATIVE PERMITTIVITY IS NOT ONLY DEPENDENT ON THE IONIC POLARIZABILITIES, BUT ALSO ON THE RATTLING EFFECT WHICH COULD BE EXPLAINED BASED ON THE BOND VALENCE OF THE

THE BASIS OF THE REFINED CRYSTAL STRUCTURE PARAMETERS AND BOND VALENCE T STRENGTH AND COVALENCE OF THE CATION-OXYGEN BONDS ARE DETERMINED USING EQUATIONS [37]:

$$V_{ij} = \sum_j S_{ij} \quad (3.2)$$

$$S_{ij} = \text{EXP} \left[ \frac{(R_{ij} - d_{ij})}{b} \right] \quad (3.3)$$

$$f_c = a S_{ij}^M \quad (3.4)$$

WHERE  $R_{ij}$  IS THE BOND VALENCE PARAMETER,  $d_{ij}$  IS THE BOND LENGTH IN Å AND  $b$  IS THE UNIVERSAL CONSTANT. THE COVALENCE AND  $M$  ARE EMPIRICALLY DETERMINED PARAMETERS AND DEPEND ON THE NUMBER OF CORE ELECTRONS IN THE CATION. PREVIOUSLY REPORTED BOND VALENCE PARAMETERS ARE USED [37]. THE AVERAGE BOND STRENGTH CAN BE CALCULATED WITH THE AVERAGE BOND VALENCE SUM DIVIDED BY THE AVERAGE CATION NUMBER. THE AVERAGE BOND STRENGTH AND COVALENCE OF  $\text{Sr}_2\text{Si}_2\text{O}_7$  AND  $\text{Sr}_2\text{Si}_3\text{O}_{13}$  ARE SHOWN IN TABLE 3.6. IT IS CLEAR FROM THE TABLE THAT THE SI-O BOND STRENGTH IS MUCH LARGER WHEN COMPARED WITH THE RE-O AND SR-O. THE BOND VALENCE IS NOT ONLY A MEASURE OF NUMBER OF ELECTRONS ASSOCIATED WITH A BOND, BUT ALSO THE DEGREE OF COVALENCE. THE COVALENCE OF THE VARIOUS BONDS ARE CALCULATED BY THE METHOD PROPOSED BY SHANNON [38]. FROM THE TABLE IT IS SEEN THAT THE SI-O BOND SHOWS A COVALENCE CHARACTER OF ABOUT 59% FOR  $\text{SrSiO}_3$  WHICH DECREASES GRADUALLY WITH INCREASE IN  $x$  IN  $\text{Sr}_{1-x}\text{Ca}_x\text{Si}_2\text{O}_7$ . THUS WITH THE DECREASE IN COVALENCE AN INCREASE IN RELATIVE PERMITTIVITY IS OBSERVED. HOWEVER, THIS IS NOT SATISFACTORY IF WE CONSIDER THE POROSITY CORRECTED VALUE. THUS IT CAN BE CONCLUDED THAT BOTH THE POLARIZABILITY AND BOND STRENGTH ARE CONTRIBUTING TO THE RELATIVE PERMITTIVITY OF THESE MATERIALS.

**Table 3.5 The optimised microwave dielectric properties of SrRE<sub>4</sub>Si<sub>3</sub>O<sub>13</sub> [RE = La, Pr, Nd, Sm, Eu, Gd, Tb, Dy, Er, Tm, Yb and Y] ceramics.**

| SrRE <sub>4</sub> Si <sub>3</sub> O <sub>13</sub> | $Q \times F$<br>(GHz) | Relative<br>permittivity<br>( $\epsilon_r$ ) | Corrected<br>Relative<br>permittivity<br>( $\epsilon_{RCOR}$ ) | $\tau_f$<br>(ppm/°C) |
|---|-----------------------|--|--|----------------------|
| SRL <sub>4</sub> Si <sub>3</sub> O <sub>13</sub>  | 26300                 | 14.2   | 15.7   | -46                  |
| SRP <sub>4</sub> Si <sub>3</sub> O <sub>13</sub>  | 12200                 | 15.6   | 17.0   | -9                   |
| SRNd <sub>4</sub> Si <sub>3</sub> O <sub>13</sub> | 21000                 | 15.5   | 17.4   | -29                  |
| SRSm <sub>4</sub> Si <sub>3</sub> O <sub>13</sub> | 20800                 | 13.5   | 14.9   | -28                  |
| SREu <sub>4</sub> Si <sub>3</sub> O <sub>13</sub> | 20700                 | 14.8   | 17.8   | -24                  |
| SRGd <sub>4</sub> Si <sub>3</sub> O <sub>13</sub> | 8800                  | 12.6   | 18.2   | -20                  |
| SRTb <sub>4</sub> Si <sub>3</sub> O <sub>13</sub> | 19300                 | 14.3   | 16.1   | 6                    |
| SRDy <sub>4</sub> Si <sub>3</sub> O <sub>13</sub> | 9200                  | 9.6  | 12.9   | 28                   |
| SRY <sub>4</sub> Si <sub>3</sub> O <sub>13</sub>  | 20500                 | 12.6   | 15.8   | -18                  |
| SREr <sub>4</sub> Si <sub>3</sub> O <sub>13</sub> | 18100                 | 10.4   | 16.1   | -24                  |
| SRTm <sub>4</sub> Si <sub>3</sub> O <sub>13</sub> | 14400                 | 11.2   | 14.5   | -20                  |
| SRYb <sub>4</sub> Si <sub>3</sub> O <sub>13</sub> | 11400                 | 13.1   | 14.7   | -25                  |

**Table 3.6 The average bond strength and covalence of RE-O, Sr-O, Si-O bonds in SrRE<sub>4</sub>Si<sub>3</sub>O<sub>13</sub> [RE=La, Pr and Y] ceramics.**

| Material   | Average bond strength        |                                 |                            |                            | Covalence (v. u)* |                   |                   |                   |
|--|------------------------------|---------------------------------|----------------------------|----------------------------|-------------------|-------------------|-------------------|-------------------|
|  | $\langle S_{RE-O}^I \rangle$ | $\langle S_{RE-O}^{II} \rangle$ | $\langle S_{SR-O} \rangle$ | $\langle S_{SI-O} \rangle$ | $Fc^I, RE-O$      | $Fc^{II}, RE-O$   | $Fc, SR-O$        | $Fc, SI-O$        |
| SRL <sub>4</sub> Si <sub>3</sub> O <sub>13</sub> | 0.1271                       | 0.3784                          | 0.1099                     | 1.1328                     | 0.0192<br>(15.1%) | 0.1066<br>(28.2%) | 0.0153<br>(13.9%) | 0.6625<br>(58.5%) |
| SRP <sub>4</sub> Si <sub>3</sub> O <sub>13</sub> | 0.1250                       | 0.3934                          | 0.1184                     | 1.1133                     | 0.0187<br>(15%)   | 0.1133<br>(28.8%) | 0.0172<br>(14.5%) | 0.6439<br>(57.8%) |
| SRY <sub>4</sub> Si <sub>3</sub> O <sub>13</sub> | 0.1131                       | 0.3844                          | 0.1478                     | 1.045                      | 0.0160<br>(14.2%) | 0.1092<br>(28.4%) | 0.0244<br>(16.5%) | 0.5804<br>(55.5%) |

\*THE PERCENTAGE COVALENCIES ARE SHOWN IN PARENTHESES.

SRRE<sub>4</sub>Si<sub>3</sub>O<sub>13</sub> (RE=LA, ND, SM, EU AND Y) SHOWED A REASONABLY GOOD (20000 GHZ) WITH A MAXIMUM VALUE OF 26300 GHZ FOR SrRE<sub>4</sub>Si<sub>3</sub>O<sub>13</sub> CERAMIC. THE

DIELECTRIC LOSSES AT MICROWAVE FREQUENCIES ARISE MAINLY FROM THREE MECHANISMS: (I) INTRINSIC LOSSES DUE TO ANHARMONIC LATTICE FORCES IN PERFECT CRYSTAL, (II) EXTRINSIC LOSSES DUE TO SECONDARY PHASES, GRAIN BOUNDARIES AND INCLUSIONS IN REAL INHOMOGENEOUS CRYSTALS, (III) LOSSES IN REAL BUT HOMOGENEOUS CRYSTALS CAUSED BY POINT DEFECTS SUCH AS INTERSTITIAL ATOMS AND VACANCIES [39]. AMONG THESE THE FORMER IS RELATED TO THE CRYSTAL BONDING CHARACTER OF THE MATERIAL. IN GENERAL, STRONGER BOND INDICATES A LOWER DAMPING CONSTANT IF THE NATURE OF BOND IS SIMILAR IN THE SAME SERIES. A LARGER FORCE CONSTANT IMPLIES A LOWER DAMPING CONSTANT RESULTING IN A LOWER DIELECTRIC LOSS. ALSO BY SCHLOMANN [40] SHOWS THAT THE RANDOM DISTRIBUTION OF DIVALENT AND TRIVALENT IONS ON EQUIVALENT SITE CONTRIBUTES TO THE DIELECTRIC LOSSES EVEN WHEN ELECTROLYTIC CONDUCTION ARE COMPLETELY SUPPRESSED. THESE MATERIALS WITH APATITE STRUCTURE WITH RANDOM DISTRIBUTION OF IONS IN THE 4F AND 6H SITES WHICH MAY CONTRIBUTE TO DIELECTRIC LOSSES. IN THE PRESENT CASE ALMOST ALL MATERIALS EXCEPT SRGDSHOW

A  $Q_u \times f$  OF NEARLY 20000 GHZ WITH A LOW RELATIVE DENSITY LESS THAN 94 %. HOWEVER SRGDS  $Q_u \times f$  OF 8800 AND 9200 GHZ RESPECTIVELY. ONE OF THE REASONS MAY BE DUE TO THE POOR DENSIFICATION OF THESE COMPOUNDS (SEE TABLE 3.6)

IT IS WELL KNOWN THAT THE TEMPERATURE COEFFICIENT OF RESONANT FREQUENCY IS POSITIVE FOR TEMPERATURE DEPENDENCE OF RELATIVE PERMITTIVITY AND THERMAL EXPANSION COEFFICIENT [42]. LOW PERMITTIVITY MATERIALS GENERALLY HAVE POSITIVE TEMPERATURE COEFFICIENT OF PERMITTIVITY MATERIALS ( $> 20$ ) HAVE A MORE NEGATIVE TEMPERATURE COEFFICIENT OF PERMITTIVITY. IT IS PROPOSED THAT THE ION COORDINATION NUMBER AND BONDING CHARACTER ARE THE MAIN SOURCES OF THE DIELECTRIC LOSS. ADDITIONALLY, LEVINSKY [43] REPORTED LOWER VALENCE AND MORE UNDERBONDED (SMALL BOND VALENCE SUM) IONS INFLUENCE A MORE NEGATIVE TEMPERATURE COEFFICIENT OF PERMITTIVITY. FROM TABLE 3.6 IT IS CLEAR THAT SRGDS CERAMICS EXHIBITS A HIGH VALUE OF BOND VALENCE SUM WHEN COMPARED TO THAT OF SRND AND SRYSI<sub>3</sub>O<sub>13</sub> CERAMICS AND IT EXHIBITS A LOW VALUE OF -9 PPM/K AS FAR AS THE DIELECTRIC CERAMICS ARE CONCERNED, WHICH IS INDEPENDENT ON TEMPERATURE Owing TO THE NEGLIGIBLE MAGNITUDE OF THERMAL EXPANSION COEFFICIENT. ACCORDING TO BOSMAN AND HAVINGA [44] [45] THERMAL EFFECTS CONTRIBUTE TO THE TEMPERATURE DEPENDENCE OF RELATIVE PERMITTIVITY. AMONG THESE VOLUME-DEPENDENT CONTRIBUTION PLAYS A DOMINATING ROLE. AS CELL VOLUME INCREASES THE NUMBER OF POLARIZABLE PARTICLES PER UNIT VOLUME DECREASES LEADING TO THE

POLARIZABILITY. HENCE THE RELATIVE PERMITTIVITY DECREASES AND RESULTS TO POSITIVE SIDE.

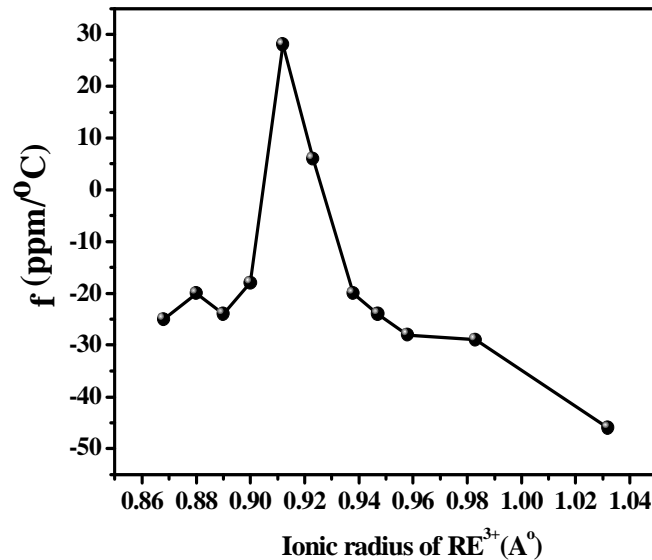


Fig. 3.10 The variation of  $\tau_f$  of  $\text{SrRE}_4\text{Si}_3\text{O}_{13}$  with ionic radius of rare earth ions.

THE TEMPERATURE COEFFICIENT OF RESONANT FREQUENCY OF FIRS AS A FUNCTION OF THE IONIC RADIUS IN FIG. 3.10.  $\tau_f$  VALUE INCREASES TO POSITIVE VALUE (-25 TO +28 PPM/°C) WITH THE IONIC RADIUS UP TO 0.912 Å AND THEN INCREASES TO NEGATIVE VALUE (+6 TO -46 PPM/°C) UP TO  $r_{La} = 1.032$  Å. THIS IS IN ACCORDANCE WITH THE VARIATION OBSERVED IN  $\text{Ca}(\text{B}'_{1/2}\text{TA}_{1/2})\text{O}_3$  [B'=LANTHANIDES, Y AND IN] BY KHALIL ET AL. WHERE THEY NOTED AN INTERSUBSTITUTION BETWEEN THE CA AND THE B' IONS. IN THE PRESENT CASE THE D CAN OCCUPY DIFFERENT SITES AS MENTIONED EARLIER. THE REFINEMENT STUDIES ALSO INTERSUBSTITUTION BETWEEN THE SR

THE DENSITIES OF THESE SAMPLES BY THE ADDITION OF DIFFERENT (0.2, 0.5, 1, 3) W% VARIOUS GLASSES SUCH AS ZBS ARE MEASURED. IT WAS OBSERVED THAT THE SAMPLE SHOWED A MAXIMUM DENSIFICATION AND GOOD DIELECTRIC PROPERTY FOR 0.5 WT% ADDITION. FURTHER INCREASE IN THE AMOUNT OF GLASS DETERIORATED THE QUALITY. ADDITION OF SMALL WEIGHT % OF ZBS GLASS IMPROVED THE DENSITY OF THE MATERIAL TO SOME EXTENT. THE SINTERING TEMPERATURE, RELATIVE DENSITY AND MICROWAVE DIELECTRIC PROPERTIES OF GLASS ADDED CERAMICS ARE GIVEN IN TABLE 3.7. THE SINTERING TEMPERATURE LOWERS BY 100°C BY GLASS ADDITION. A MARKABLE INCREASE IN DENSITY IS NOTED FOR SRTM  $\text{Sr}_4\text{Si}_3\text{O}_{13}$  WHICH CAN BE ATTRIBUTED TO THE LIQUID PHASE SINTERING OCCURRING

COMPOSITES. HOWEVER, ONLY A MARGINAL RISE IS OBTAINED FOR SURE (Y AND ER). THE RELATIVE PERMITTIVITY OF THE GLASS ADDED COMPOSITES ALSO SHOWS AN INCREASE DUE TO THE INCREASE IN RELATIVE DENSITY. IN THE DECREASE IN RELATIVE PERMITTIVITY IS NOTED WHICH MAY BE DUE TO THE DECREASE IN DENSITY. IT IS NOTED THAT GLASSES IN GENERAL HAS A LOW RELATIVE PERMITTIVITY [47]. FROM THE TABLE IT IS SEEN THAT  $Q_{UF}$  FOR  $SrLa_4Si_3O_{13}$  INCREASES FROM 19300 TO 23500 GHZ AND THAT FOR  $SrTm_4Si_3O_{13}$  INCREASES FROM 14400 TO 16500 GHZ. IT MAY BE NOTED THAT IN THE CASE OF THESE MATERIALS WITH ONLY SLIGHT IMPROVEMENT IN DENSITY, THE QUALITY FACTOR IS IMPROVED. THE RELATIVE DENSITY INCREASES FROM 74 TO 77 % WITH AN IMPROVEMENT IN  $Q_{UF}$  VALUE FROM 18100 TO 21000 HOWEVER,  $\tau_f$  OF THE MATERIALS ARE NOT MUCH AFFECTED BY THE GLASS ADDITION.

**Table 3.7** The optimised sintering temperature, density and microwave dielectric properties of glass added  $SrRE_4Si_3O_{13}$  [RE = La, Nd, Sm, Eu, Tb, Dy, Er, Tm, Yb and Y] ceramics.

| $SrRE_4Si_3O_{13} + 0.5 \text{ wt\% ZBS}$ | Sintering Temp. ( $^{\circ}\text{C}$ ) | Relative Density (%) | $Q_{UF}$ (GHz) | Relative permittivity ( $\epsilon_r$ ) | $\tau_f$ (ppm/ $^{\circ}\text{C}$ ) |
|---|--|----------------------|----------------|--|-------------------------------------|
| $SrLa_4Si_3O_{13}$                        | 1300 $^{\circ}\text{C}/4\text{H}$      | 95                   | 25800          | 14.7                                   | -40                                 |
| $SrNd_4Si_3O_{13}$                        | 1350 $^{\circ}\text{C}/4\text{H}$      | 90                   | 20500          | 13.9                                   | -33                                 |
| $SrSm_4Si_3O_{13}$                        | 1350 $^{\circ}\text{C}/4\text{H}$      | 92                   | 21800          | 13.9                                   | -28                                 |
| $SrEu_4Si_3O_{13}$                        | 1425 $^{\circ}\text{C}/4\text{H}$      | 92                   | 19800          | 14.2                                   | -22                                 |
| $SrTb_4Si_3O_{13}$                        | 1425 $^{\circ}\text{C}/4\text{H}$      | 92                   | 23500          | 14.3                                   | 10                                  |
| $SrDy_4Si_3O_{13}$                        | 1425 $^{\circ}\text{C}/4\text{H}$      | 86                   | 9500           | 13.0                                   | 28                                  |
| $SrY_4Si_3O_{13}$                         | 1475 $^{\circ}\text{C}/4\text{H}$      | 90                   | 21500          | 13.5                                   | -18                                 |
| $SrEr_4Si_3O_{13}$                        | 1475 $^{\circ}\text{C}/4\text{H}$      | 77                   | 21000          | 11.2                                   | -20                                 |
| $SrTm_4Si_3O_{13}$                        | 1575 $^{\circ}\text{C}/4\text{H}$      | 92                   | 16500          | 12.8                                   | -26                                 |
| $SrYb_4Si_3O_{13}$                        | 1425 $^{\circ}\text{C}/4\text{H}$      | 92                   | 12000          | 12.9                                   | -27                                 |

### 3.4.1.1 TAILORING THE $\tau_f$ BY $TiO_2$ ADDITION

IT IS EVIDENT FROM TABLE 3.2 THAT  $SrLa_4Si_3O_{13}$  CERAMICS HAS A RELATIVELY HIGH  $Q_{UF}$  OF 26300 GHZ,  $\epsilon_r$  OF 14.2 AND A  $\tau_f$  OF -46 PPMC. IT IS POSSIBLE TO TUNE  $\tau_f$  TO ZERO

BY THE ADDITION OF SUITABLE AMOUNT OF MICROPARTICLES SUCH AS TiO<sub>2</sub> RUTILE HAS  $\epsilon_r$  OF 104,  $Q_u \times f$  OF 26900 GHz AND  $\tau_f$  OF +411 PPMC [3]. SINCE TiO<sub>2</sub> IS WELL KNOWN AS A SINTERING AID TO IMPROVE THE SINTERABILITY OF THE BASE CERAMIC MATERIALS, THE SINTERING TEMPERATURE OF SrLa<sub>4</sub>Si<sub>3</sub>O<sub>13</sub> CERAMIC DECREASES FROM 1325°C WITH INCREASE IN TiO<sub>2</sub> CONTENT. THE XRD PATTERNS OF SrLa<sub>4</sub>Si<sub>3</sub>O<sub>13</sub> MIXED WITH 8 WT % TiO<sub>2</sub> AND SINTERED AT 1225°C/4H IS SHOWN IN FIG. 3.11. THE FIGURE INDICATES THE NON-REACTIVITY OF SrLa<sub>4</sub>Si<sub>3</sub>O<sub>13</sub> WITH TiO<sub>2</sub>. THE TiO<sub>2</sub> PHASES ARE INDEXED BASED ON THE JCPDS FILE NO. 76-1934. THE DENSITY OF THE MIXTURE IS CALCULATED ACCORDING TO THE EQUATION:

$$\rho_{mixture} = \frac{V_1}{\rho_1} + \frac{V_2}{\rho_2} \quad (3.5)$$

WHERE  $\rho_{mixture}$  IS THE CALCULATED THEORETICAL DENSITY OF THE MIXTURE,  $V_1$  AND  $V_2$  ARE THE VOLUME FRACTIONS AND DENSITIES OF SrLa<sub>4</sub>Si<sub>3</sub>O<sub>13</sub> AND TiO<sub>2</sub> RESPECTIVELY. THE VARIATION OF THEORETICAL AND EXPERIMENTAL DENSITIES OF THE MIXTURE AS A FUNCTION OF THE TiO<sub>2</sub> ADDITION IS SHOWN IN FIG. 3.12. THE THEORETICAL DENSITY DECREASES WITH TiO<sub>2</sub> ADDITION DUE TO THE LOWER DENSITY POSSESSED BY TiO<sub>2</sub> COMPARED TO THAT OF SrLa<sub>4</sub>Si<sub>3</sub>O<sub>13</sub> (3.2 G/CM<sup>3</sup>). HOWEVER, A SMALL INCREASE IN THE EXPERIMENTAL DENSITY IS OBSERVED FOR 5 WT% TiO<sub>2</sub>. THE RELATIVE DENSITY REACHES A MAXIMUM VALUE OF 95 % AT THIS COMPOSITION AND THEN DECREASES.

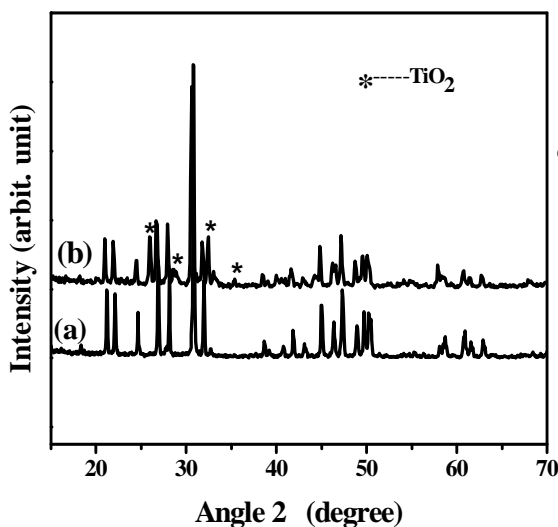


Fig. 3.11 XRD patterns of (a) SrLa<sub>4</sub>Si<sub>3</sub>O<sub>13</sub> ceramics sintered at 1325°C and (b) SrLa<sub>4</sub>Si<sub>3</sub>O<sub>13</sub> + 8 wt% TiO<sub>2</sub> sintered at 1225°C.

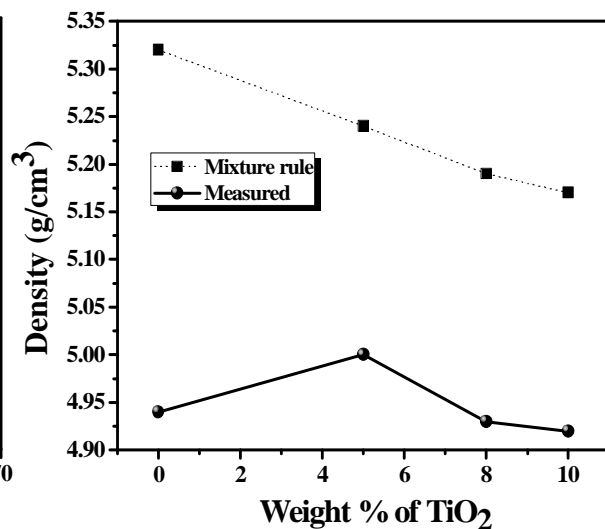


Fig. 3.12 The variation of theoretical and experimental densities of SrLa<sub>4</sub>Si<sub>3</sub>O<sub>13</sub> with TiO<sub>2</sub> addition.

FIGURE 3.13 SHOWS THE VARIATION OF THE MICROWAVE DIELECTRIC PROPERTIES OF  $\text{SrLa}_4\text{Si}_3\text{O}_{13}$  AS A FUNCTION OF THE AMOUNT OF  $\text{TiO}_2$  ADDITION. THE RELATIVE PERMITTIVITY OF THE MIXTURE SHOWS A LINEAR INCREASE AS THE AMOUNT OF  $\text{TiO}_2$  INCREASES AS SHOWN IN FIG. 3.13 (A). THIS IS EXPECTED SINCE THE  $\epsilon_r$  IS MUCH HIGHER AS COMPARED WITH  $\text{SrLa}_4\text{Si}_3\text{O}_{13}$ . THE  $\epsilon_r$  INCREASES FROM 14.2 TO 23.4 AS THE AMOUNT OF  $\text{TiO}_2$  REACHES 10 WT%.  $\epsilon_r$  OF THE MIXTURE IS CALCULATED USING THE SERIAL MIXING RULE GIVEN AS:

$$\epsilon_{\text{mixture}} = V_1 \epsilon_1 + V_2 \epsilon_2 \quad (3.6)$$

WHERE  $\epsilon_{\text{mixture}}$ ,  $\epsilon_1$  AND  $\epsilon_2$  ARE THE RELATIVE PERMITTIVITY OF THE MIXTURE,  $\text{SrLa}_4\text{Si}_3\text{O}_{13}$  AND  $\text{TiO}_2$  RESPECTIVELY. FIG. 3.13 (A) ALSO COMPARES THE CALCULATED AND MEASURED PERMITTIVITIES OF THE MIXTURE AS A FUNCTION OF THE AMOUNT OF  $\text{TiO}_2$ . THE CALCULATED VALUES ARE FOUND TO DEVIATE SLIGHTLY FROM THE EXPERIMENTAL VALUES. THIS IS BECAUSE THE MODEL DOES NOT INCLUDE THE POROSITY IN THE COMPOSITE. THE UNLOADED QUALITY FACTOR OF  $\text{SrLa}_4\text{Si}_3\text{O}_{13}$  IS PLOTTED AS A FUNCTION OF THE AMOUNT OF  $\text{TiO}_2$  IN FIG. 3.13 (A). AS THE AMOUNT OF  $\text{TiO}_2$  INCREASES FROM 0 TO 10 WT%,  $Q_u \times f$  OF THE MIXTURE ADUALLY DECREASES FROM 26000 TO 12000 GHZ. IT IS TO BE NOTED AT THIS POINT OF DISCUSSION THAT THE PROPERTIES OF THE MIXTURE DOES NOT FOLLOW ANY MIXTURE RULE.

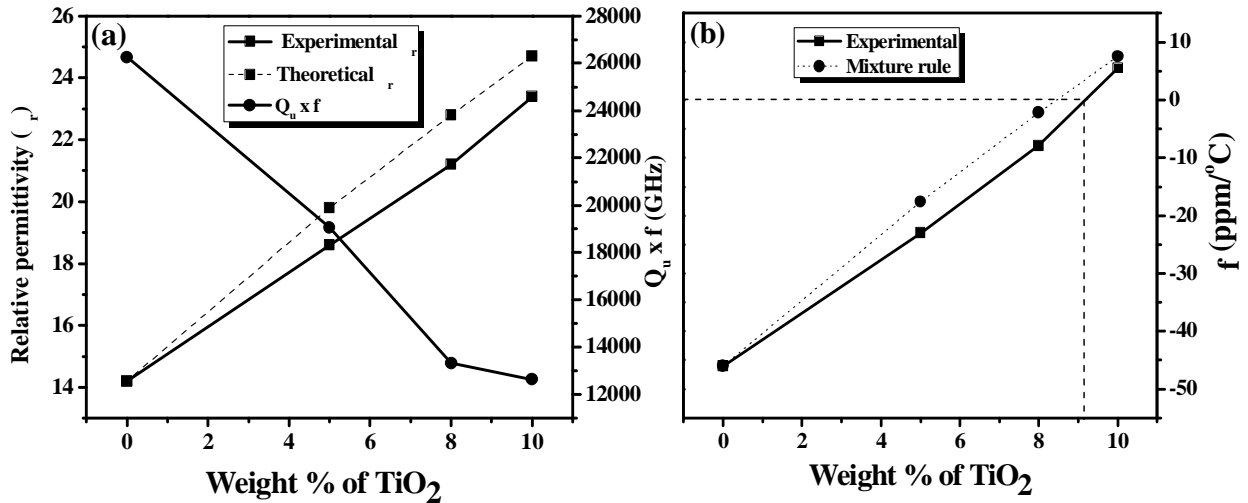


Fig. 3.13 The variation of (a) relative permittivity,  $Q_u \times f$  and (b)  $\tau_f$  of  $\text{SrLa}_4\text{Si}_3\text{O}_{13}$  with  $\text{TiO}_2$  addition.



THE DEPENDENCE OF THE AMOUNT OF  $\text{Sr}^{2+}$  IONS SHOWN IN FIG. 3.13 (B). THE  $\tau_F$  OF  $\text{Ba}_{1-x}\text{Sr}_x\text{Si}_3\text{O}_{13}$  BECOMES LESS NEGATIVE WITH THE INCREASE IN  $x$  DUE TO THE HIGH POSITIVE VALUE OF  $\tau_F$  OF  $\text{SrSi}_3\text{O}_{13}$  (TO 400 PPM/°C). THE  $\tau_F$  OF THE MIXTURE PHASES IS COMPUTED USING THE GENERAL MIXING FORMULA [48]:

$$\tau_{f,mixture} = V_1 \tau_{f1} + V_2 \tau_{f2} \quad (3.7)$$

WHERE  $\tau_{f,mixture}$ ,  $\tau_{f1}$  AND  $\tau_{f2}$  ARE THE TEMPERATURE COEFFICIENT OF RESONANT FREQUENCY OF MIXTURE,  $\text{SrSi}_3\text{O}_{13}$  AND  $\text{BaSi}_3\text{O}_{13}$  RESPECTIVELY. THE EXPERIMENTAL AND MEASURED  $\tau_F$  ARE COMPARED IN FIG. 3.13 (B). BOTH ARE FOUND TO BE MATCHING. THE  $\tau_F$  OF THE MIXTURE VARIES FROM -46 PPM/°C TO A MAXIMUM OF +7.5 PPM/°C FOR 10 WT%  $\text{SrSi}_3\text{O}_{13}$  ADDITION. FROM THE CURVE IT CAN BE INFERRED THAT  $\tau_F$  IS NEARLY ZERO FOR A  $\text{Sr}^{2+}$  CONTENT OF 9 WT%.

### 3.4.2 MICROWAVE DIELECTRIC PROPERTIES OF $(\text{Ca}_{1-x}\text{Sr}_x)\text{Ba}_{1-y}\text{RE}_y\text{Si}_3\text{O}_{13}$ RARE EARTHS]

FIGURES 3.14 (A) AND (B) RESPECTIVELY SHOW THE X-RAY DIFFRACTION PATTERNS OF  $(\text{Ca}_{1-x}\text{Sr}_x)\text{Ba}_{1-y}\text{RE}_y\text{Si}_3\text{O}_{13}$  [RE = LA, PR, ND, SM, EU, TB, DY, TM, YB AND Y] AND  $\text{Ba}_{1-y}\text{RE}_y\text{Si}_3\text{O}_{13}$  [RE = LA, PR, ND, SM] CERAMICS. ALL THE PEAKS ARE INDEXED COMPARING WITH THAT OF THE PEAKS OF  $\text{CaSi}_3\text{O}_{13}$  (JCPDS 71-1368) WITH HEXAGONAL SYMMETRY. IT CAN BE SEEN THAT ALL THE COMPOUNDS IN THE SERIES BELONG TO THE HEXAGONAL SYMMETRY WITH SPACE GROUP  $P6_3/m$  AS SEEN IN THE CASE OF  $\text{SrSi}_3\text{O}_{13}$ . HOWEVER, IT IS INTERESTING TO NOTE THAT AS THE IONIC RADIUS OF A-SITE ION DECREASES FROM BA TO CA, DEFINITE CHANGES ARE VISIBLE FOR THE XRD PATTERNS OF  $\text{Ba}_{1-y}\text{RE}_y\text{Si}_3\text{O}_{13}$  SERIES TO SR SERIES AND FINALLY DISAPPEARS. EVEN THOUGH THE PRESENT STUDY REVEALS THAT SINGLE PHASE COMPOUNDS ARE OBTAINED IN THIS SYSTEM, FURTHER STUDIES ARE CLEARLY NEEDED TO ELUCIDATE THE EXACT CRYSTAL STRUCTURE OF THE COMPOUNDS. THE LATTICE PARAMETERS OF  $(\text{Ca}_{1-x}\text{Sr}_x)\text{Ba}_{1-y}\text{RE}_y\text{Si}_3\text{O}_{13}$  [RE = LA, PR, ND, SM, EU, TB, DY, TM, YB AND Y] AND  $\text{Ba}_{1-y}\text{RE}_y\text{Si}_3\text{O}_{13}$  [RE = LA, PR, ND, SM] CERAMICS ARE DETERMINED FROM THE XRD PATTERNS AND ARE GIVEN RESPECTIVELY IN TABLES 3.8 AND 3.9. IT IS EXPECTED THAT AS THE IONIC RADIUS OF THE RARE EARTH DECREASES FROM LA TO YB, THE LATTICE PARAMETERS (A AND C) WILL DECREASE. HOWEVER, THE VALUES DEVIATE CONSIDERABLY FROM THE LINEAR TREND WHICH

SHOWS AN ALMOST REGULAR DECREASE WITH THE IONIC RADIUS. THIS CAN BE DUE TO SITE OCCUPANCY OF VARIOUS IONS WHICH IS FOUND IN APATITE TYPE STRUCTURES AND CONFIRMED IN  $\text{SrRE}_4\text{Si}_3\text{O}_{13}$  SERIES IN THE PREVIOUS SECTION.

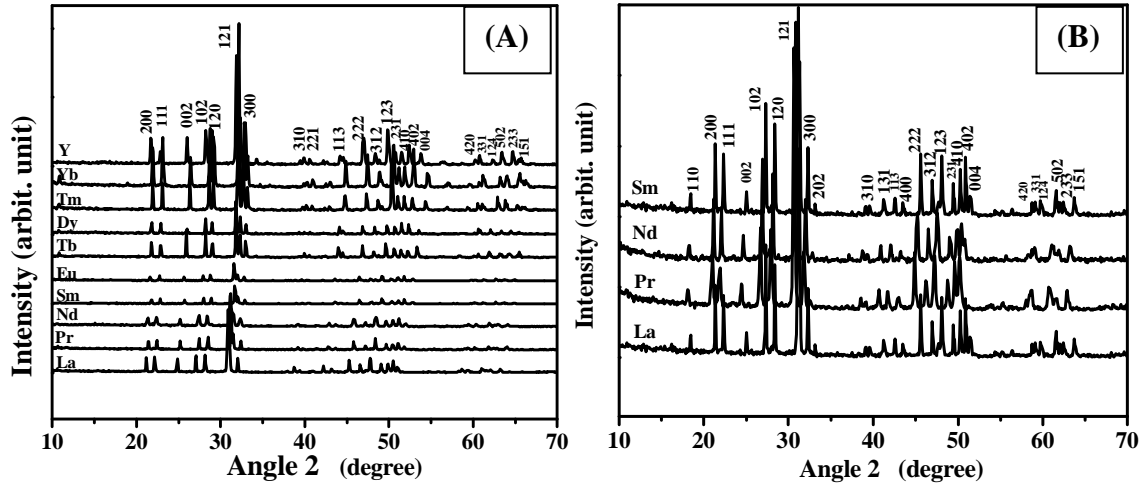


Fig. 3.14 XRD patterns of (A)  $\text{CaRE}_4\text{Si}_3\text{O}_{13}$  [RE = La, Pr, Nd, Sm, Eu, Tb, Dy, Tm, Yb and Y] and (B)  $\text{BaRE}_4\text{Si}_3\text{O}_{13}$  [RE = La, Pr, Nd, Sm] ceramics.

THE DENSITY DEPENDENCE ON IONIC RADIUS IS SIMILAR TO THAT OBSERVED IN THE CASE OF  $\text{SrRE}_4\text{Si}_3\text{O}_{13}$ . AS THE IONIC RADIUS OF THE RARE EARTH ION DECREASES, THE THEORETICAL DENSITY AS THE EXPERIMENTAL DENSITIES INCREASES. HOWEVER, THE RELATIVE DENSITIES OF THIS SERIES EXHIBITED A BETTER VALUE WHEN COMPARED WITH THAT OF OTHER SERIES. A RELATIVE DENSITY VALUE GREATER THAN 90% IS OBSERVED FOR  $\text{CaRE}_4\text{Si}_3\text{O}_{13}$  AND  $\text{CaNd}_4\text{Si}_3\text{O}_{13}$ . A MAXIMUM VALUE OF RELATIVE DENSITY OF ABOUT 94% IS EXHIBITED BY  $\text{CaEu}_4\text{Si}_3\text{O}_{13}$  AND  $\text{CaSm}_4\text{Si}_3\text{O}_{13}$ . A RELATIVELY LOWER RELATIVE DENSITY OF ABOUT 87% IS SHOWN BY  $\text{CaTm}_4\text{Si}_3\text{O}_{13}$ . THE ATTEMPTS TO IMPROVE THE DENSIFICATION BY GLASS ADDITION RESULTED IN AN INCREASE IN THE DIELECTRIC LOSS AND RESULTED IN NON-RESONANT BEHAVIOR. IT IS CLEAR FROM THE TABLES THAT THE BA-COMPOSITIONS EXHIBIT HIGHER DENSITY WITH THAT OF SR AND CA BASED COMPOSITIONS, WHICH IS DUE TO THE HIGHER MASS OF BARIUM. ALSO A COMPARATIVE STUDY ON THE RELATIVE DENSITIES SHOWS THAT BARE COMPOSITIONS POSSESS A HIGHER RELATIVE DENSITY WITH A MAXIMUM OF 98% EXCEPT FOR BALA

**Table 3.8 The optimized sintering temperature, physical and microwave dielectric properties of  $\text{CaRE}_4\text{Si}_3\text{O}_{13}$  [RE = La, Pr, Nd, Sm, Eu, Tb, Dy, Tm, Yb and Y] ceramics.**

| $\text{CaRE}_4\text{Si}_3\text{O}_{13}$ | Sintering Temp. ( $^{\circ}\text{C}$ ) | Lattice parameter  |                    | Theor. Density ( $\text{g}/\text{cm}^3$ ) | Relative density (%) | $Q_U X F$ (GHz) | $\epsilon_R$ | $\epsilon_{RCORR}$ | $\tau_F$ (ppm/ $^{\circ}\text{C}$ ) |
|---|--|--------------------|--------------------|---|----------------------|-----------------|--------------|--------------------|-------------------------------------|
|   |  | a ( $\text{\AA}$ ) | c ( $\text{\AA}$ ) |   |                      |                 |              |                    |                                     |
| $\text{CaLa}_4\text{Si}_3\text{O}_{13}$ | 1350/4F                                | 9.6481             | 7.1343             | 5.13                                      | 93.2                 | 24800           | 14.9         | 16.4               | -20                                 |
| $\text{CaPr}_4\text{Si}_3\text{O}_{13}$ | 1375/4F                                | 9.5437             | 7.01473            | 5.38                                      | 93.0                 | 17800           | 14.9         | 16.4               | 4                                   |
| $\text{CaNd}_4\text{Si}_3\text{O}_{13}$ | 1325/4F                                | 9.5465             | 7.0337             | 5.44                                      | 94.0                 | 21100           | 14.3         | 15.6               | -23                                 |
| $\text{CaSm}_4\text{Si}_3\text{O}_{13}$ | 1350/4F                                | 9.4336             | 6.9303             | 5.81                                      | 93.5                 | 22000           | 14.2         | 15.4               | -39                                 |
| $\text{CaEu}_4\text{Si}_3\text{O}_{13}$ | 1400/4F                                | 9.4646             | 6.9314             | 5.81                                      | 94.1                 | 20000           | 14.2         | 15.4               | -35                                 |
| $\text{CaTb}_4\text{Si}_3\text{O}_{13}$ | 1625/4F                                | 9.3783             | 6.8645             | 6.15                                      | 89.6                 | 20100           | 13.1         | 15.3               | -12                                 |
| $\text{CaDy}_4\text{Si}_3\text{O}_{13}$ | 1550/4F                                | 9.3784             | 6.8483             | 6.25                                      | 89.8                 | 13300           | 14.0         | 16.3               | 10                                  |
| $\text{CaY}_4\text{Si}_3\text{O}_{13}$  | 1625/4F                                | 9.3863             | 6.8329             | 4.38                                      | 91.8                 | 30500           | 12.8         | 14.4               | -36                                 |
| $\text{CaTm}_4\text{Si}_3\text{O}_{13}$ | 1550/4F                                | 9.3382             | 6.7511             | 6.57                                      | 87.4                 | 17000           | 11.9         | 15.7               | -32                                 |
| $\text{CaYb}_4\text{Si}_3\text{O}_{13}$ | 1625/4F                                | 9.3232             | 6.7249             | 6.72                                      | 91.2                 | 23500           | 13.2         | 15.0               | -13                                 |

**Table 3.9 The optimized sintering temperature, physical and microwave dielectric properties of  $\text{BaRE}_4\text{Si}_3\text{O}_{13}$  [RE = La, Pr, Nd and Sm] ceramics.**

| $\text{BaRE}_4\text{Si}_3\text{O}_{13}$ | ST ( $^{\circ}\text{C}$ ) | Lattice parameter  |                    | Theor. Density ( $\text{g}/\text{cm}^3$ ) | Relative density (%) | $Q_U X F$ (GHz) | $\epsilon_R$ | $\epsilon_{RCORR}$ | $\tau_F$ (ppm/ $^{\circ}\text{C}$ ) |
|---|---------------------------|--------------------|--------------------|---|----------------------|-----------------|--------------|--------------------|-------------------------------------|
|   |                           | A ( $\text{\AA}$ ) | C ( $\text{\AA}$ ) |   |                      |                 |              |                    |                                     |
| $\text{BaLa}_4\text{Si}_3\text{O}_{13}$ | 1325/4F                   | 9.6024             | 7.0888             | 5.78                                      | 87.4                 | 26100           | 14.2         | 17.2               | -38                                 |
| $\text{BaPr}_4\text{Si}_3\text{O}_{13}$ | 1325/4F                   | 9.7250             | 7.2466             | 5.56                                      | 98.7                 | 19700           | 16.8         | 17.2               | -8                                  |
| $\text{BaNd}_4\text{Si}_3\text{O}_{13}$ | 1250/4F                   | 9.6733             | 7.1779             | 5.77                                      | 96.5                 | 16000           | 15.1         | 15.9               | -19                                 |
| $\text{BaSm}_4\text{Si}_3\text{O}_{13}$ | 1325/4F                   | 9.5768             | 7.0827             | 6.09                                      | 94.6                 | 16200           | 15.5         | 16.7               | -27                                 |

THE RELATIVE DENSITY MAXIMA OF BA COMPOSITIONS APPEAR AT A LOWER TEMPERATURE AND CA COUNTERPARTS. IN THE CASE OF COMPOUNDS WITH RE = La, Pr, Nd AND Sm, THE RELATIVE DENSITY MAXIMA OF BA COMPOSITIONS APPEAR AT A LOWER TEMPERATURE AND CA COUNTERPARTS.

SITE ION OCCUPANCIES, THE RELATIVE DENSITY MAXIMA APPEARED AT DIFFERENT TEMPERATURES. THIS INDICATES THAT THE SINTERING BEHAVIOUR OF THESE CERAMICS IS SIGNIFICANTLY AFFECTED BY THE RARE EARTH IONS. IT IS CLEAR THAT SIMILAR TRENDS ARE OBSERVED FOR THE RARE EARTH IONIC RADIUS INCREASES, THE SINTERING TEMPERATURE DECREASES IN THE CASE OF CA AND Y COMPOSITIONS. IN THE CASE OF Ba, THE SINTERING TEMPERATURE REMAINS CONSTANT FOR ALL THE COMPOSITIONS EXCEPT FOR WHERE THE BEST PROPERTIES ARE ATTAINED AT A SINTERING TEMPERATURE OF 1250°C.

FIGURES 3.15 (A) AND (B) SHOW THE MICROSTRUCTURE OF  $\text{CaLa}_4\text{Si}_3\text{O}_{13}$  AND  $\text{CaY}_4\text{Si}_3\text{O}_{13}$  SINTERED AT 1325°C AND 1475°C RESPECTIVELY. BOTH OF THEM REVEALED A UNIFORM SINGLE PHASE AND A WELL PACKED MICROSTRUCTURE. HOWEVER, THE PRESENCE OF SLIGHT POROSITY IS ALSO NOTED. THE  $\text{CaLa}_4\text{Si}_3\text{O}_{13}$  CERAMICS HAS AN AVERAGE GRAIN SIZE LESS THAN 1 μM WHEREAS  $\text{CaY}_4\text{Si}_3\text{O}_{13}$  SHOWS A COMPARATIVELY HIGHER GRAIN SIZE (~ 2-3 μM). FIG. 3.15 (C) SHOWS THE MICROSTRUCTURE OF  $\text{BaLa}_4\text{Si}_3\text{O}_{13}$  SINTERED AT 1325°C. FROM THE SEM IMAGE IT CAN BE INFERRED THAT THE MATERIAL POSSES A HIGHLY DENSE MICROSTRUCTURE. THE RELATIVE DENSITY SHOWS A LOW VALUE OF 87%. ALSO PRESENCE OF SOME UNIDENTIFIED PHASE WHICH IS ABSENT IN THE XRD PATTERN IS ALSO NOTED. THE LOW VALUE OF DENSITY ACHIEVED MAY BE DUE TO THE PRESENCE OF THIS UNEXPECTED PHASE.

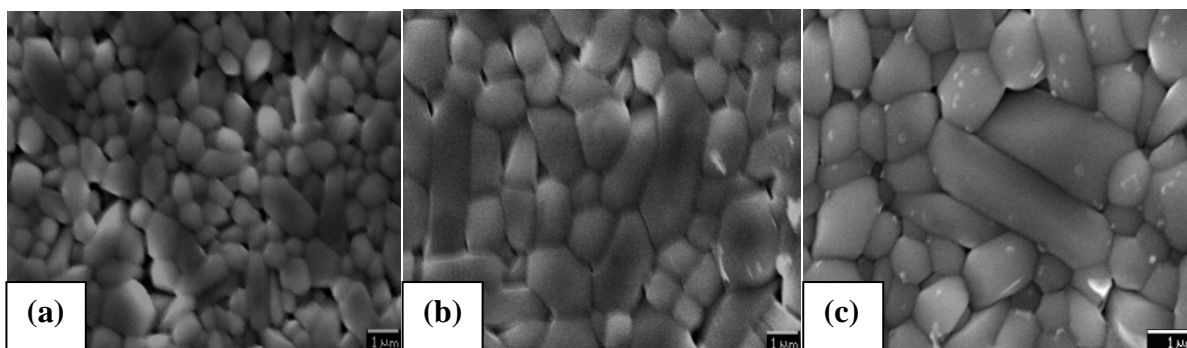


**Fig. 3.15** SEM images of (a)  $\text{CaLa}_4\text{Si}_3\text{O}_{13}$  sintered at 1325°C/2 h, (b)  $\text{CaY}_4\text{Si}_3\text{O}_{13}$  sintered at 1475°C/2 h and (c)  $\text{BaLa}_4\text{Si}_3\text{O}_{13}$  sintered at 1325°C/2 h.

THE MICROWAVE DIELECTRIC PROPERTIES OF  $\text{CaLa}_4\text{Si}_3\text{O}_{13}$  AND  $\text{CaY}_4\text{Si}_3\text{O}_{13}$  SERIES ARE SHOWN IN TABLE 3.8 AND 3.9. NO REGULAR DEPENDENCE OF MICROWAVE DIELECTRIC PARAMETERS WITH IONIC RADIUS IS NOTED FOR CA BASED COMPOSITIONS. GENERALLY, A DECREASE IN IONIC RADIUS PROMOTES SHRINKAGE OF THE TETRAHEDRA AND DECREASES THE IONIC RADIUS.

THIS WILL IN TURN DECREASE THE RELATIVE PERMITTIVITY OF THE MATERIALS. A MAXIMUM PERMITTIVITY VALUE OF 14.9 IS EXHIBITED BY BA AND A MINIMUM VALUE OF 11.9 BY CATM<sub>4</sub>Si<sub>3</sub>O<sub>13</sub>. THIS CAN BE WELL EXPLAINED BY THE RELATIVE DENSITY VALUES OF THESE AS GIVEN IN TABLE 3.8 SINCE RELATIVE PERMITTIVITY IS VERY MUCH DEPENDENT ON THE DENSITY. IN THE CASE OF BA SERIES ONLY FOUR OF THE RARE EARTH BASED SILICATES EXHIBIT RESONANCE AT MICROWAVE FREQUENCY. VERY FEW REPORTS ARE AVAILABLE ON THE EXISTENCE OR FORMATION OF PHASES FOR BAPR SERIES. IT IS SEEN FROM TABLE 3.9 THAT BARE<sub>4</sub>Si<sub>3</sub>O<sub>13</sub> POSSESS A HIGH VALUE OF RELATIVE PERMITTIVITY (CORRECTED FOR POROSITY) COMPARED WITH THAT OF THE RESPECTIVE CA AND SR BASED RARE EARTH SILICATES. THE HIGH IONIC POLARIZABILITY VALUE OF BAA MAXIMUM VALUE OF RELATIVE PERMITTIVITY OF ABOUT 16.8 IS OBTAINED FOR BAPR

THE QUALITY FACTOR OF CA SERIES VARIES FROM 13000-31000 GHZ AS SEEN FROM TABLE 3.8. IT IS A WELL KNOWN FACT THAT APART FROM THE INTRINSIC FACTORS, Q IS AFFECTED BY MANY EXTRINSIC FACTORS SUCH AS THE CONCENTRATION OF DEFECTS, GRAIN SIZE, POROSITY ETC. IT IS CLEAR FROM THE TABLE THAT THE QUALITY FACTOR IS NOT DIRECTLY RELATED WITH THE RELATIVE DENSITY FOR CERTAIN COMPOSITIONS. EVEN AT HIGH CAEU AND MAXIMUM RELATIVE DENSITY, A MAXIMUM QUALITY FACTOR OF NEARLY 30500 GHZ IS OBTAINED BY CA<sub>4</sub>Si<sub>3</sub>O<sub>13</sub>. FROM EARLIER REPORTS IT CAN BE POINTED OUT THAT A LARGE GRAIN SIZE OR A LARGE GRAIN BOUNDARY INDICATES A REDUCTION IN LATTICE IMPERFECTIONS RESULTING IN LOSS MATERIALS [49]. IN THE PRESENT CASE ALSO ONE OF THE REASONS FOR THE HIGH QUALITY FACTOR OF CA<sub>4</sub>Si<sub>3</sub>O<sub>13</sub> MAY BE THE INCREASE IN GRAIN SIZE. ALSO THE IONIC RADII DIFFERENCE BETWEEN CA<sup>2+</sup> AND RE<sup>3+</sup> IONS MAY REDUCE THE LATTICE STRAIN THEREBY INCREASING THE QUALITY FACTOR. HOWEVER, THE LOW QUALITY FACTOR VALUE FOR CATM<sub>4</sub>Si<sub>3</sub>O<sub>13</sub> CAN BE PURELY ATTRIBUTED TO THE LOW VALUE OF RELATIVE DENSITY. CONSIDERING THE BARE<sub>4</sub>Si<sub>3</sub>O<sub>13</sub> IS QUITE SURPRISING TO NOTE THAT WITH A LOW RELATIVE DENSITY EXHIBITS THE MAXIMUM QUALITY FACTOR IN THE SERIES. IN B AND BARE<sub>4</sub>Si<sub>3</sub>O<sub>13</sub> SERIES AS THE RE<sup>3+</sup> IONIC RADII DECREASES, THE QUALITY FACTOR IS FOUND TO DECREASE GRADUALLY DUE TO THE INCREASING IONIC CHARACTER AS OBSERVED IN THE CASE OF SRRE<sub>4</sub>Si<sub>3</sub>O<sub>13</sub> FROM THE TABLES THAT SHOWS VALUE LESS THAN -40 PPM. MAXIMUM VALUE OF -39 PPM IS SHOWN BY CA<sub>4</sub>Si<sub>3</sub>O<sub>13</sub> AND A LOW VALUE OF -94 PPM BY BARE<sub>4</sub>Si<sub>3</sub>O<sub>13</sub>. HOWEVER, THE ATTEMPT TO TERNITHE AND CATI<sub>3</sub>O ADDITION RESULTED IN A NON-

RESONATING OR HIGH DIELECTRIC LOSS COMPOSITION WHICH MAY BE DUE TO THE FORM SECONDARY PHASES. IN THE CASE OF BA-SERIES, A MINIMUM VALUE OF OF ABOUT -8 PPM THE  $\tau_f$  OF A MATERIAL IS VERY MUCH DEPENDENT ON THE STRUCTURE EXPLAINED EARLIER. SINCE IN THE PRESENT CASE NO PHASE TRANSITION IS OBSERVED, STRUCTURAL STUDIES ARE REQUIRED FOR EXPLAINING THE

### 3.5 CONCLUSIONS

- ❖ THE  $\text{RESr}_2\text{I}_3\text{O}_{13}$  [A=CA, SR AND BA; RE=RARE EARTHS] ARE SYNTHESIZED BY SOLID STATE CERAMIC METHOD. THE PHASE AND STRUCTURAL ANALYSIS USING XRD ANALYSIS CONFIRMED A HEXAGONAL SYMMETRY FOR THESE GROUP OF MATERIALS ALL BELONG TO  $P6_3/M$  SPACE GROUP. THE LATTICE PARAMETERS SHOW A DECREASE WITH DECREASED RADIUS OF BOTH A-SITE AND RE-SITE IONS.
- ❖ THE CALCINATION AND SINTERING TEMPERATURES ARE OPTIMIZED AND THE MICROWAVE DIELECTRIC PROPERTIES ARE MEASURED IN THE FREQUENCY RANGE 5-6 GHz.  $\text{SrREI}_3\text{O}_{13}$  CERAMICS SHOWED POOR DENSIFICATION WITH A MAXIMUM RELATIVE DENSITY OF 85% FOR  $\text{SrLaI}_3\text{O}_{13}$ . THE DENSIFICATION OF THE MATERIALS IS IMPROVED BY THE ADDITION OF A SMALL WEIGHT PERCENTAGE OF ZBS GLASS. HOWEVER, THE MICROWAVE DIELECTRIC PROPERTIES ARE NOT IMPROVED MUCH IN THESE COMPOSITIONS ALSO EXHIBIT RELATIVE DENSITY LESS THAN 94%, BUT BETTER IN THE SR-BASED SERIES. THE SR-BA ANALOGUE SHOWS A VERY HIGH DENSIFICATION OF GREATER THAN 95% EXCEPT FOR  $\text{BaLaI}_3\text{O}_{13}$ .
- ❖ THE  $\text{SrREI}_3\text{O}_{13}$  EXHIBITED RELATIVE PERMITTIVITY IN THE RANGE 10-19. A MAXIMUM  $Q_u \times f$  OF ABOUT 26000 GHz IS EXHIBITED BY  $\text{SrLaI}_3\text{O}_{13}$  WITH  $Q_u = 14.2$  AND A RELATIVELY HIGH -46 PPM/C. THE MICROWAVE DIELECTRIC PROPERTIES OF THE COMPOSITIONS ARE CORRELATED WITH THE BOND VALENCE AND BOND STRENGTH. THE  $\tau_f$  OF  $\text{SrLaI}_3\text{O}_{13}$  IS TUNED BY THE ADDITION OF SUITABLE  $\text{BaO}$  AND  $\text{ZnO}$ . IN THE CASE OF THE ADDITION OF NEARLY 8%  $\text{BaO}$ , THE VALUE,  $Q_u \times f$  IS REDUCED TO 13300 GHz WITH AN INCREASE IN  $\tau_f$  OF NEARLY 21.

- ❖ THE BOND VALENCE, BOND STRENGTH AND COVALENCES OF REFINED SRRE COMPOSITIONS ARE CALCULATED AND CORRELATED WITH THE MICROWAVE PROPERTIES. IT IS SEEN THAT AS THE BOND STRENGTH DECREASES, THE RELATIVE AND DIELECTRIC LOSS ARE FOUND TO INCREASE.
- ❖ THE  $\text{CaSi}_3\text{O}_{13}$  AND  $\text{BaSi}_3\text{O}_{13}$  CERAMICS HAVE A RELATIVE PERMITTIVITY LESS THAN 20. THE  $\text{CaSi}_3\text{O}_{13}$  CERAMICS SHOWS A MAXIMUM QUALITY FACTOR OF 30500 GHZ WITH  $Q_r = 12.8$  AND  $D_f = -36 \text{ PPM}^\circ\text{C}$ . THE  $\text{BaSi}_3\text{O}_{13}$  SERIES SHOWS A RELATIVELY HIGH  $Q_r$  AND A LOW  $Q_r f$  VALUE. A MAXIMUM  $Q_r f$  OF 26100 GHZ IS EXHIBITED BY  $\text{BaSi}_3\text{O}_{13}$  WITH  $Q_r = 14.2$  AND  $D_f = -38 \text{ PPM}^\circ\text{C}$ .

## 3.6 REFERENCES

1. M. Z. DONG, Z. X. YUE, H. ZHUANG, S. Q. MENG AND L. TAN, *J. Am. Ceram. Soc.*, **91**, 3981-3985, (2008).
2. M. KONO, H. TAKAGI, T. TATEKAWA AND H. TAMURA, *J. Am. Ceram. Soc.*, **26**, 1909-1912, (2006).
3. M. T. SEBASTIAN, *"Dielectric Materials for Wireless Communication"*, ELSEVIER SCIENCE PUBLISHERS, OXFORD (2008).
4. Y. GUO, H. OHSATO AND K.-I. KAKIMOTO, *J. Am. Ceram. Soc.*, **26**, 1827-1830, (2006).
5. K. P. SURENDRAN, N. SANTHA, P. MOHANAN AND M. T. SEBASTIAN, *J. Am. Ceram. Soc.*, **41**, 301-306, (2004).
6. H. OHSATO, T. TSUNOOKA, T. SUGIYAMA, K. KAKIMOTO AND H. OGAWA, *J. Am. Ceram. Soc.*, **17**, 445-450, (2006).
7. T. S. SASIKALA, M. N. SUMA, P. MOHANAN, C. PAVITHRAN AND M. T. SEBASTIAN, *J. Am. Ceram. Soc.*, **461**, 555-559, (2008).
8. T. JOSEPH, M. T. SEBASTIAN, H. SREEMOOLANADHAN AND V. K. S. NAGESHWARI, *Ceram. Technol.*, **7**, E98-E106, (2010).
9. H. OHSATO, M. TERADA, I. KAGOMIYA, K. KAWAMURA, K. KAKIMOTO AND E. S. KIM, *Trans. Ultrason. Ferroelectr. Freq. Control.*, **55**, 1081-1085, (2008).
10. S. N. RENJINI, S. THOMAS, M. T. SEBASTIAN, S. R. KIRAN AND V. R. K. MURTHY, *Ceram. Technol.*, **6**, 286-294, (2009).
11. S. GEORGE, P. S. ANJANA, V. N. DEEPU, P. MOHANAN AND M. T. SEBASTIAN, *J. Am. Ceram. Soc.*, **92**, 1244-1249, (2009).
12. J. ITO, *Am. Mineral.*, **53**, 890-907 (1968).
13. L. BOYER, J. CARPENA AND J. L. SALGADO, *Solid State Ionics*, **95**, 121-129, (1997).
14. L. BOYER, B. PIRIOU, J. CARPENA AND J. L. SALGADO, *J. Am. Ceram. Soc.*, **311**, 143-152, (2000).
15. J. FELSCH, *Solid State Chem.*, **5**, 266-275 (1972).
16. G. BLASSE, *Solid State Chem.*, **14**, 181-184, (1975).
17. M. J. LAMMERS AND G. BLASSE, *J. Electrochem. Soc.*, **134**, 2068-2072 (1987).
18. J. P. M. VAN VLIET AND G. BLASSE, *Res. Bull.*, **25**, 391-394, (1990).
19. P. J. PANTEIX, I. JULIEN, D. BERNACHE-ASSOLLANT AND P. CHELARD, *J. Am. Ceram. Soc.*, **95**, 313-320, (2006).
20. T. KHARLAMOVA, S. PAVLOVA, V. SADYKOV, O. LAPINA, D. KHABIBULIN, T. KRIEGER, ZAIKOVSKII, A. ISHCHENKO, A. SALANOV, V. MUZYKANTOV, N. MEZENTSEVA, M. CHAIKINA, UVAROV, J. FRADE AND C. ARCO, *Solid State Ionics*, **179**, 1018-1023, (2008).



21. P. J. PANTEIX, E. BÉCHADE, I. JULIEN, P. ABÉLARD AND D. BERNACHE-ASSOLLANT, *Chem. Mater. Res. Bull.*, **43**, 1223-1231, (2008).
22. P. J. PANTEIX, I. JULIEN, P. ABÉLARD AND D. BERNACHE-ASSOLLANT, *Ceram. Int.*, **34**, 1579-1586, (2008).
23. T. J. ISSACS, *Electrochem. Soc.*, **120**, 654-656 (1973).
24. J. LIN AND Q. SUN, *Alloys Compd.*, **210**, 159-163, (1994).
25. G. W. R. R. H. HOPKINS, K. B. STEINBRUEGGE AND W. D. JEFFERSON, *J. Electrochem. Soc.*, **118**, 637-639 (1971).
26. A. YAMANE, T. KUNIMOTO, K. OHMI, T. HONMA AND H. KOBAYASHI, *Solidi C*, **3**, 2705-2708, (2006).
27. S. TAO AND J. T. S. IRVING, *IEEE Trans. Electron Devices*, **36**, 1245-1258, (1989).
28. D. M. IDDLES, A. J. BELL AND A. J. MOUNSON, *Philos. Mag.*, **27**, 6303-6310, (1992).
29. Y. Q. SHEN, A. TOK AND Z. L. DONG, *J. Ceram. Soc. Jpn.*, **93**, 1176-1182, (2010).
30. Y. MASUBUCHI, M. HIGUCHI, H. KATASE, T. TAKEDA, S. KIKKAWA, K. KODAIRA AND S. NAKAYAMA, *Solid State Ionics*, **166**, 213-217, (2004).
31. N. I. SANTHA AND M. T. SEBASTIAN, *J. Ceram. Soc. Jpn.*, **90**, 496-501, (2007).
32. P. S. ANJANA AND M. T. SEBASTIAN, *J. Ceram. Soc. Jpn.*, **92**, 96-104, (2009).
33. Y. MASUBUCHI, M. HIGUCHI, T. TAKEDA AND S. KIKKAWA, *Solid State Ionics*, **177**, 263-268, (2006).
34. C. VINIES, P. K. DAVIES, T. NEGAS AND M. BELLE, *IEEE Trans. Electron Devices*, **31**, 431-437, (1996).
35. R. D. SHANNON, *Appl. Phys. Lett.*, **73**, 348-366, (1993).
36. S. J. PENN, N. M. ALFORD, A. TEMPLETON, X. R. WANG, M. S. XU, M. REECE AND K. SCHRAPER, *J. Am. Ceram. Soc.*, **80**, 1885-1888, (1997).
37. I. D. BROWN, *Acta Crystallogr. Sect. B: Struct. Sci.*, **48**, 553-572, (1992).
38. I. D. BROWN AND R. D. SHANNON, *Acta Crystallogr. Sect. A: Found. Crystallogr.*, **29**, 266-282 (1973).
39. A. FETEIRA, D. C. SINCLAIR AND M. T. LAMAGAN, *J. Mater. Res.*, **20**, 2391-2399, (2005).
40. E. SCHLÖMANN, *Phys. Rev.*, **135**[2A], A413-A419, (1964).
41. P. L. WISE, I. M. REANEY, W. E. LEE, D. M. IDDLES, D. S. CANNELL AND T. J. PRICE, *Mater. Res. Bull.*, **17**, 2033-2040, (2002).
42. H. OHSATO, *J. Ceram. Soc. Jpn.*, **21**, 2703-2711, (2001).
43. M. W. LUFASO, *Chem. Mater.*, **16**, 2148-2156, (2004).
44. A. J. BOSMAN AND E. E. HAVINGA, *Phys. Rev.*, **129**, 1593, (1963).
45. E. L. COLLA, I. M. REANEY AND N. SEIFERT, *Phys. Rev. B*, **74**, 3414-3425, (1993).

46. L. A. KHALAM, S. THOMAS AND M. T. SEBASTIAN, *Ceram. Soc.*, **90**, 2476-2483, (2007).
47. M. T. SEBASTIAN AND H. JANUJUNEN, *Met. Rev.*, **53**, 57-90, (2008).
48. W. D. KINGERY, *Introduction to Ceramics*", JOHN WILEY AND SONS, NEW YORK, (1960).
49. A. E. PALADINO, *Am. Ceram. Soc.*, **54**, 168-169 (1971).
50. N. ICHINOSE AND T. SHIMADA, *Ceram. Soc.*, **26**, 1755-1759, (2006).

## CHAPTER 4

### MICROWAVE DIELECTRIC PROPERTIES OF NOVEL RARE EARTH SILICATE CERAMICS

*The structure and microwave dielectric properties of two novel rare earth silicate based ceramics:  $\text{Sm}_2\text{Si}_2\text{O}_7$  and  $\text{RE}_2\text{Ti}_2\text{SiO}_9$  [RE=La, Pr and Nd] are presented in this chapter. The dielectric properties of these materials are investigated for the first time. The  $\text{Sm}_2\text{Si}_2\text{O}_7$  exhibited a low relative permittivity and dielectric loss which makes it suitable for substrate applications. The influence of several low loss glasses on the sintering temperature, densification and dielectric properties of  $\text{Sm}_2\text{Si}_2\text{O}_7$  ceramics is discussed in detail. Attempts are also made to synthesis and characterize  $\text{Sm}_2\text{Si}_2\text{O}_7$  ceramics by sol-gel method. The microwave dielectric properties of  $\text{RE}_2\text{Ti}_2\text{SiO}_9$  [RE=La, Pr and Nd] ceramics and the effect of solid solution formation on the densification, lattice parameters and microwave dielectric properties are also presented. The results bring out its potential for dielectric resonator applications.*

## 4.1 SYNTHESIS AND MICROWAVE DIELECTRIC PROPERTIES OF $SM_2Si_2O_7$

### 4.1.1 INTRODUCTION

COMMERCIAL INTEREST IN HIGHLY SOPHISTICATED, RELIABLE AND CONVENIENT DEVICES HAS ESTABLISHED A PERMANENT NEED FOR COMPLEX, ROBUST AND MINIATURIZED SUBSTRATES. NEW PACKAGING TECHNOLOGY REQUIRES SUBSTRATES WITH LOW CAPACITANCE INTERCONNECTIONS MADE OF HIGH-CONDUCTIVITY METALS, HIGH WIRING DENSITY AND LOW INDUCTIVE PASSIVE CIRCUIT ELEMENTS. IMPORTANT PROPERTIES OF SUBSTRATE MATERIALS INCLUDE LOW LOSS, HIGH THERMAL CONDUCTANCE, LOW THERMAL EXPANSION AND HIGH INTERFACIAL ADHESION TO THE METAL SURFACES OR OTHER FILMS. IN SEARCH OF NEW HIGH PERFORMANCE MATERIALS FOR MILLIMETER WAVE DEVICES, SILICATES ARE PROPOSED TO BE GOOD CANDIDATES BECAUSE OF THEIR LOW  $\epsilon_r$ . GENERALLY SILICATES ARE FORMED BY A TETRAHEDRAL FRAMEWORK WITH 45% IONIC BOND AND 55% COVALENT BOND. THE COVALENT BOND CAUSES LARGE BOND STRENGTH DUE TO WHICH THE ATOMS CANNOT RATTLE AROUND. [RECENTLY OSHATA ET AL. SUCCESSFULLY DEVELOPED FORSTERITE AND WILLEMITE CERAMICS FOR SUBSTRATE APPLICATIONS. HOWEVER, THE POSSIBILITY OF RARE EARTH BASED SILICATES FOR USE IN MICROELECTRONICS HAS NEVER BEEN INVESTIGATED.

BINARY SYSTEMS CONTAINING OXIDES ARE IMPORTANT IN VARIOUS FIELDS OF TECHNOLOGY, INCLUDING LASER AND OPTICAL FIBRE APPLICATIONS, MICROELECTRONICS AND THE ANALYSIS OF  $SiO_2$  PHASE DIAGRAMS BY FELSCHE [3] SHOWED THAT VARIOUS BINARY SILICATE COMPOUNDS SUCH AS MONOSILICATES AND TREE LIKE COMPOUNDS  $RE_{9.33}(SiO_4)_6O_2$  AND DISILICATES  $RE_2Si_2O_7$  MAY FORM AT NORMAL PRESSURE. CRYSTAL CHEMISTRY OF DISILICATES IS PARTICULARLY COMPLEX, SINCE SEVERAL POLYMORPHIC STRUCTURES ARE REPORTED. THE RARE EARTH SILICATES  $[RE_2Si_2O_7]$  ARE FORMED AS THE MAJOR SECONDARY PHASE IN RARE EARTH HIGH-PERFORMANCE CERAMICS SINTERED WITH RARE EARTH OXIDES AS SINTERING ADDITIVES [4]. DIFFERENT STRUCTURE TYPES (A-L) HAVE BEEN REPORTED FOR THE SINGLE RE DISILICATES [5-7]. THIS DIVERSITY IN STRUCTURE TYPE RESULTS FROM THE MONOTONIC DECREASE IN SIZE OF THE RARE EARTH CATION THROUGH THE LANTHANIDE SERIES AND THE DIFFERENT CRYSTAL CHEMICAL RESPONSE TO CHANGE IN TEMPERATURE AND PRESSURE. IN EACH OF THE STRUCTURE TYPES (A, B, C, D, E, F, G, H AND K) THE  $SiO_4$  TETRAHEDRA ARE ASSOCIATED INTO THE CHAINS OR DIORTHOSILICATE DIMERS, AND THE STRUCTURES ESSENTIALLY REPRESENT DIFFERENT

PACKING DIORTHOSILICATE ANIONS ARE NOT REPRESENT IN THE RATIO 1:2. THE NINTH, TENTH AND ELEVENTH STRUCTURE TYPES ARE NOT DIORTHOSILICATES. INSTEAD, LINEAR TRISILICATE IONS OCCUR WITH ORTHOSILICATE IONS IN THE TYPE B AND L STRUCTURES AND A HORSESHOE SHAPED CATENA-TETRASILICATE OCCURS WITH TWO ORTHOSILICATE IONS PER FORMULA UNIT IN THE TYPE I STRUCTURE. THE TYPE B STRUCTURE HAS BEEN REPORTED FOR THE DISILICATES OF EU, GD, TB, DY, HO AND ER AT THE LOWEST TEMPERATURES INVESTIGATED (1450°C) AT 1 BAR AND FOR TM DISILICATE AT LOW PRESSURE, AS WELL AS FOR THE DISILICATES OF YB AND LU AT HIGHER PRESSURE (7 GPa). PROPOSED THAT THE PHASE TRANSITION SEQUENCE C → X → B IS ACCOMPANIED BY THE CLOSURE OF THE DI(O-Si) BOND ANGLE WITH INCREASE IN PRESSURE. THIS SUGGESTION IS SUPPORTED BY THE HIGH-PRESSURE (10 GPA, 1600 K) TYPE K STRUCTURE FOR THE DISILICATES OF ND, SM, EU AND GD [5], WHERE COMPRESSION IS ACCOMPLISHED MAINLY BY CLOSURE OF THE DI(O-Si) BOND ANGLE TO 123° THROUGH RIGID BODY ROTATION OF THE TETRAHEDRON IN THE DIORTHOSILICATE ION.

THE PHASE RELATIONSHIPS IN THE SYSTEMS HAVE BEEN STUDIED EXTENSIVELY WHERE THE EXISTENCE OF TWO DOUBLE OXIDES WITH COMPOSITIONS AS  $RE_2O_7$  HAS BEEN ALSO INVESTIGATED FROM A STRUCTURAL POINT OF VIEW DUE TO COMPLEX HIGH-T POLYMORPHISM [9]. SO FAR SIX DIFFERENT MODIFICATIONS (I-VI) HAVE BEEN REPORTED. ACCORDING TO ITO AND JOHNSON [10] THE TRANSITION SEQUENCE BETWEEN THE FIRST FOUR FORMS IS AS FOLLOWS:  $\beta \xrightarrow{14450C} \gamma \xrightarrow{15350C} \delta$ . THESE FOUR MODIFICATIONS CAN BE SYNTHESIZED FROM APPROPRIATE REAGENTS BY SOLID STATE REACTIONS IN THE RESPECTIVE STABILITY RANGES. [11] MADE AN ATTEMPT TO IMPROVE THE SINTERING BEHAVIOR AND STRENGTH OF SILICON NITRIDE USING RARE EARTH DISILICATES (WHERE RE: ND, SM, Y AND YB) AS ADDITIVES. WITH THESE IN MIND THE ATTEMPT TO SYNTHESIZE A NEW WAY FOR A NEW LOW LOSS DIELECTRIC MATERIALS MEMBERS SYNTHESIZED IN THIS FAMILY FAILED TO FORM AT ORDINARY CONDITIONS AND EXHIBITED POOR DIELECTRIC PROPERTIES.

IN THIS SECTION THE SYNTHESIS AND DIELECTRIC PROPERTIES DESCRIBED IN DETAIL. A BRIEF DESCRIPTION ON THE SOL-GEL SYNTHESIS OF CERAMICS AND ITS PROPERTIES ARE ALSO DESCRIBED. EFFORTS ARE ALSO MADE TO LOWER THE SINTERING TEMPERATURE OF THE CERAMIC BY THE ADDITION OF VARIOUS LOW LOSS GLASSES.

## 4.1.2 EXPERIMENTAL

### 4.1.2.1 SOLID STATE SYNTHESIS OF $\text{Sm}_2\text{SiO}_7$ CERAMICS

THE  $\text{Sm}_2\text{SiO}_7$  CERAMICS WAS PREPARED BY CONVENTIONAL SOLID STATE CERAMIC PROCESS. HIGH PURITY  $\text{Sm}_2\text{O}_3$  (RE, 99.9%) AND  $\text{SiO}_2$  (ALDRICH CHEMICAL COMPANY, 99.9%) WERE USED AS STARTING MATERIALS FOR THE SYNTHESIS OF SAMARIUM SILICATE. THE CHARGES WERE STOICHIOMETRICALLY WEIGHED AND BALL MILLED IN DISTILLED WATER FOR 24 HOURS USING ZRO<sub>2</sub> BALLS. THE SLURRY WAS DRIED IN HOT AIR OVEN AND CALCINED AT 1150 °C FOR 2 HOURS. CALCINED POWDER WAS GROUND WELL, MIXED WITH POLYVINYL ALCOHOL (PVA), AND PRESSED INTO PELLETS OF 14 MM DIAMETER AND 1-2 MM THICKNESS FOR LOW FREQUENCY MEASUREMENTS. TO STUDY THE DIELECTRIC PROPERTIES IN THE MICROWAVE FREQUENCY RANGE, RECTANGULAR SHEETS OF DIMENSIONS (10x10x1) MM<sup>3</sup> WERE PREPARED AND WERE SINTERED IN THE TEMPERATURE RANGE 1325-1400 °C FOR 2H.

IN ORDER TO STUDY THE EFFECT OF GLASS ADDITION ON THE SINTERING AND DIELECTRIC PROPERTIES OF SAMARIUM SILICATE, VARIOUS LOW LOSS GLASSES (SUCH AS 50ZNO-50B<sub>2</sub>O<sub>3</sub> (ZB), 60ZNO-30B<sub>2</sub>O<sub>3</sub>-10SiO<sub>2</sub> (ZBS), 27B<sub>2</sub>O<sub>3</sub>-35B<sub>2</sub>O<sub>3</sub>-6SiO<sub>2</sub>-32ZNO (BBSZ), 22.2MGO-22.2Al<sub>2</sub>O<sub>3</sub>-55.5SiO<sub>2</sub> (MAS), 35.1Li<sub>2</sub>O-31.7B<sub>2</sub>O<sub>3</sub>-33.2SiO<sub>2</sub> (LBS) AND 20Li<sub>2</sub>O-20MGO-20ZNO-20B<sub>2</sub>O<sub>3</sub>-20SiO<sub>2</sub> (LMZBS) WERE SELECTED. THESE GLASSES WERE PREPARED AS EXPLAINED IN CHAPTER 2 SECTION 2.2. THE CALCINED POWDERS SUBSEQUENTLY MIXED WITH GLASS IN DIFFERENT WEIGHT PERCENTAGE RANGING FROM 0.2 TO 15. THE POWDERS WERE MIXED WITH PVA, GROUND WELL AND PRESSED TO FORM PELLETS AS EARLIER. THE PELLETS WERE SINTERED IN A FURNACE WITH A HEATING RATE OF 10 °C/MIN AND COOLING RATE OF 10 °C/MIN.

### 4.1.2.2 CHEMICAL SYNTHESIS OF $\text{Sm}_2\text{SiO}_7$ CERAMICS

NANO-CRYSTALLINE SAMARIUM SILICATE POWDER WAS SYNTHESIZED BY SOL-GEL PROCESS. THE SOL-GEL PROCESS IS AN EXCELLENT TECHNIQUE FOR NANO POWDER SYNTHESIS. IT OFFERS THE POSSIBILITY OF CONTROLLING THE STOICHIOMETRY AND HOMOGENEITY OF THE RESULTING CERAMICS. MOREOVER, IT OFFERS THE ADVANTAGES OF BOTH OBTAINING FINE GRAINS AND PROCESSING AT LOW TEMPERATURES, WHICH CAN HELP TO ENHANCE THE MICROWAVE DIELECTRIC PROPERTIES OF THE CERAMICS.  $\text{Sm}_2(\text{C}_2\text{H}_3\text{O}_7)_3 \cdot \text{NH}_2\text{O}$  (ALDRICH CHEMICALS, 99.9%), TETRA ETHYL ORTHOSILICATE (TEOS) (98%, ALDRICH CHEMICALS) WERE USED AS STARTING MATERIALS ALONG WITH A

AND ETHYL ALCOHOL (MERCK CHEMICALS, INDIA) AS SOLVENTS. INITIALLY, STOICHIOM OF TEOS WAS REFLUXED IN ETHYL ALCOHOL FOR 30 MIN TO GET A CLEAR S SM(CH<sub>3</sub>COO)<sub>3</sub>.NH<sub>2</sub>O SEPARATELY DISSOLVED IN ACETIC ACID WAS THEN MIXED WITH THE SOLUTION AT ROOM TEMPERATURE UNDER CONSTANT STIRRING TO OBTAIN A STABLE SO HOMOGENEOUS PRECURSOR WAS THEN TRANSFERRED TO A GLASS PETRI DISH AND KEPT ROOM TEMPERATURE FOR ONE WEEK. TRANSPARENT DRY GEL OBTAINED WAS POW SUBJECTED TO CALCINATION. THE PELLETS WERE PREPARED AND SINTERING WA CARRIED OUT AS EXPLAINED ABOVE. THE SPECIFIC SURFACE AREA OF THE SAMPLES WAS NITROGEN ADSORPTION MEASUREMENT (BET) IN MICROMERITICS (GEMINI III 2375) SURFA ANALYZER.

CRYSTALLINE PHASES OF THE SINTERED CERAMICS WERE INVESTIGATED FROM XR THE MICROSTRUCTURES OF THE SINTERED, ETCHED SAMPLES WERE OBSERVED USING ELECTRON MICROSCOPE. THE DENSIFICATION BEHAVIOR OF THE CERAMICS WAS EV DETERMINING THE BULK DENSITY BY ARCHIMEDES METHOD. THE THIN PELLETS WERE EI UNIFORMLY COATING WITH SILVER PASTE ON BOTH SIDES IN THE FORM OF CERAMIC CA THE LOW FREQUENCY (50 HZ - 5 MHZ) DIELECTRIC MEASUREMENTS WERE MADE USING METER. THE MICROWAVE DIELECTRIC PROPERTIES OF THESE CERAMIC COMPOSITES WE AT 9 GHZ AT ROOM TEMPERATURE USING THE CAVITY PERTURBATION TECHNIQUE AS CHAPTER 2 SECTION 2.5.7. THE TEMPERATURE VARIATION OF REAL AND IMAGINARY PERMITTIVITY AT LOW FREQUENCY (1 MHZ) WAS ALSO MEASURED IN THE TEMPERATURE RANGE 25 THE EQUATION:

$$= \frac{1}{\epsilon} \times \frac{\Delta}{\Delta T} \quad (4.1)$$

WHERE  $\epsilon$  IS THE VARIATION IN THE RELATIVE PERMITTIVITY FROM ROOM TEMPERATURE A DIFFERENCE IN TEMPERATURE.

### 4.1.3 RESULTS AND DISCUSSION

#### 4.1.3.1 STRUCTURE AND DIELECTRIC PROPERTIES OF CERAMIC

THE CALCINATION AND SINTERING TEMPERATURES OF THE MATERIAL ARE OPTIMIZ THE TEMPERATURE AT WHICH MAXIMUM DENSITY IS ATTAINED. FOR THIS THE MATERIAL

A TEMPERATURE RANGE OF 1200-1275 AND SINTERED AT AN ARBITRARY TEMPERATURE 1375°C/2H. THE DENSITY VARIATION IS AS SHOWN IN FIG. 4.1 (A). IT IS SEEN THAT THE DENSITY HAS A MAXIMUM AT A CALCINATION TEMPERATURE OF 1250. AT LOWER CALCINATION TEMPERATURES THE COMPOUND FORMATION MAY NOT BE COMPLETED. IT IS ALSO NOTED THAT THE RELATIVE PERMITTIVITY HAS A MAXIMUM VALUE AND DIELECTRIC LOSS EXHIBITED A MINIMUM VALUE (SEE FIG. 4.1 (B)). AT A CALCINATION TEMPERATURE OF 1250 THE CALCINATION TEMPERATURE IS OPTIMIZED AT 1250°C/4H. NOW, IN ORDER TO OPTIMIZE THE SINTERING TEMPERATURE, THE DRY POWDER IS CALCINED AT 1250°C/4H AND SINTERED IN THE TEMPERATURE RANGE 1325-1400

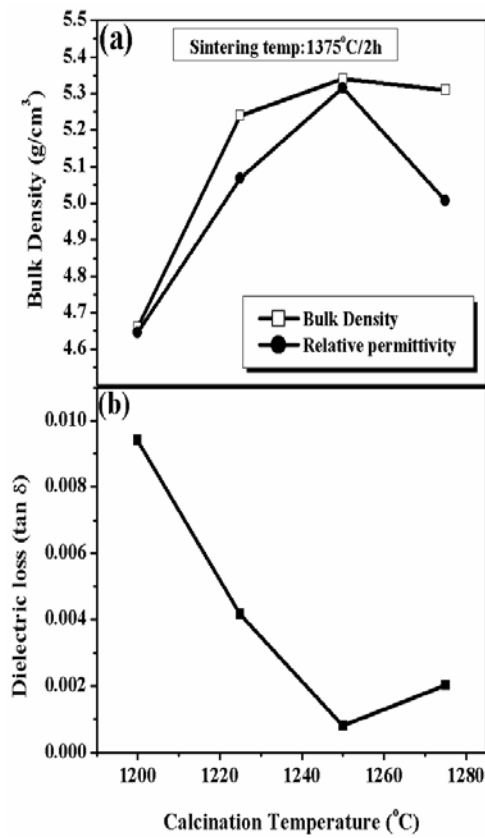


Fig. 4.1 The optimization of calcination temperature.

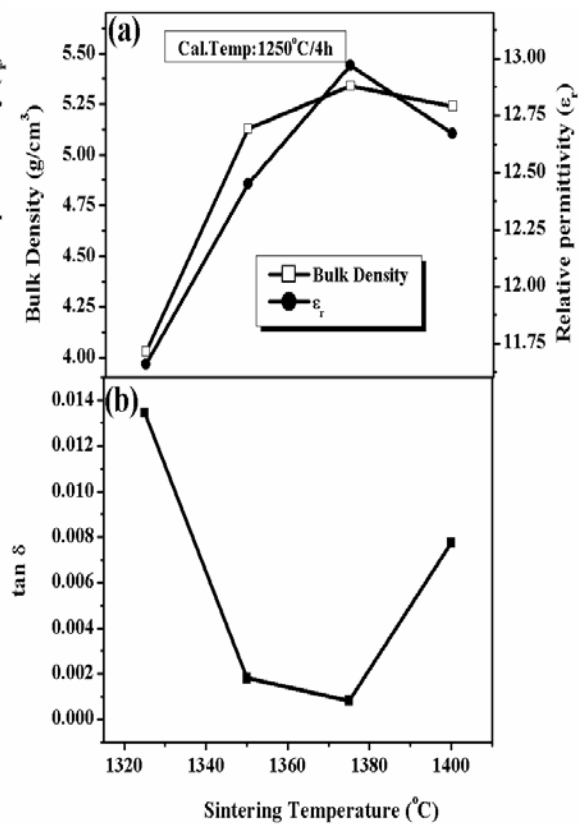


Fig. 4.2 The optimization of sintering temperature.

FIGURE 4.2 (A) SHOWS THE VARIATION OF RELATIVE DENSITY WITH SINTERING TEMPERATURE. THE DENSITY INCREASES GRADUALLY WITH THE SINTERING TEMPERATURE REACHING A MAXIMUM AND THEREAFTER DECREASES. AS A THEORETICAL DENSITY 5.35 G/CM<sup>3</sup> THE RELATIVE DENSITY REACHES TO ABOUT 94 % (5.35 G/CM



OF THE THEORETICAL DENSITY. GENERALLY SILICATES HAVE LOW DENSITY. THE INCREASE IN DENSITY WITH THE SINTERING TEMPERATURE IS DUE TO THE DECREASE IN POROSITY OF THE CERAMIC. THIS IS ALSO DUE TO THE ENHANCED GRAIN GROWTH. HOWEVER, SINTERING AT VERY HIGH TEMPERATURES WOULD CAUSE ABNORMAL GRAIN GROWTH RESULTING IN A DECREASE IN THE DENSITY. IN SOME CASES, IT LEADS TO AN INCREASE IN THE CLOSED POROSITY WHICH ADVERSELY AFFECTS THE DENSITY AND DIELECTRIC PROPERTIES. MOREOVER, INCREASE IN THE SINTERING TIME WOULD ENHANCE GRAIN GROWTH RESULTING IN AN INCREASE IN THE DENSITY. HOWEVER, PROLONGED SINTERING TIMES CAN LEAD TO ABNORMAL GRAIN GROWTH THEREBY REDUCING THE DENSITY AND DIELECTRIC PROPERTIES. IN THE PRESENT CASE THE SINTERING TEMPERATURE IS OPTIMIZED AS 1375

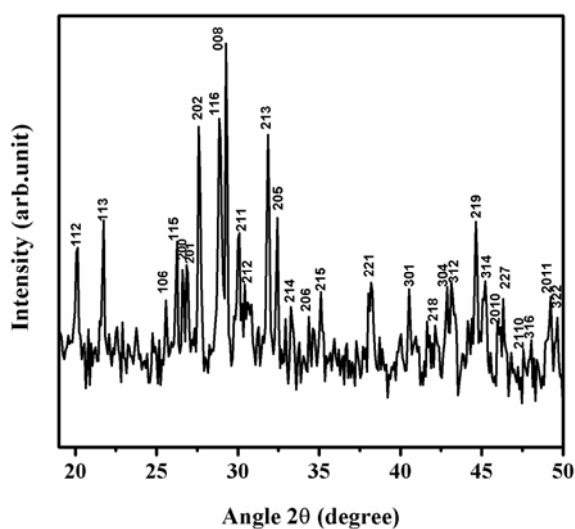


Fig. 4.3 XRD pattern of pure  $\text{Sm}_2\text{Si}_2\text{O}_7$  (CT: 1250°C/4h; ST: 1375°C/2h).

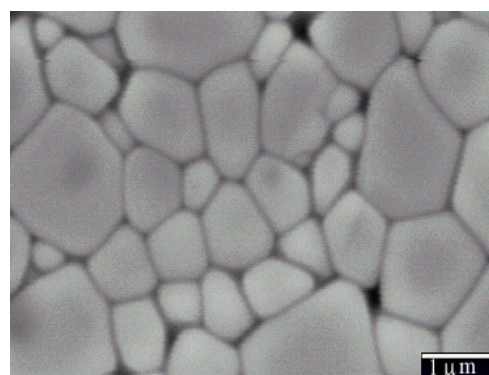


Fig. 4.4 The scanning electron micrographs of pure  $\text{Sm}_2\text{Si}_2\text{O}_7$  calcined at 1250°C/4h and sintered at 1375°C/2h.

FIGURE 4.3 SHOWS THE XRD PATTERN OF CERAMIC CALCINED AT 1250°C/4h AND SINTERED AT 1375°C/2h. THE DIFFRACTION PEAKS ARE INDEXED BASED ON JCPDS FILE NO. 24-711. EARLIER REPORTS SHOWS THAT RARE EARTH BASED DISILICATES ARE FOUND TO EXHIBIT POLYMORPHISM AND ARE DIFFICULT TO FORM UNDER ORDINARY CONDITIONS [6].  $\text{Sm}_2\text{Si}_2\text{O}_7$  HAS A TETRAGONAL CRYSTAL SYMMETRY BELONGING TO  $\text{C}_2\text{H}_2\text{D}_2$  SPACE GROUP. THE LATTICE PARAMETERS CALCULATED FROM THE XRD PATTERNS ARE:  $A = 6.70 \text{ \AA}$  AND  $C = 24.35 \text{ \AA}$ . THEY ARE FOUND TO BE IN GOOD AGREEMENT WITH THE REPORTED VALUES. THE MICROSTRUCTURE OF POLISHED AND ETCHED  $\text{Sm}_2\text{Si}_2\text{O}_7$  CERAMIC SINTERED AT 1375°C FOR 2 HOURS IS SHOWN IN FIG. 4.4. IT INDICATES THAT SAMARIUM SILICATE IS SINGLE PHASE AND HAS A RELATIVELY SMALLER GRAIN SIZE.

AVERAGE Q<sub>MI</sub> THE VARIATIONS IN THE SINTERING CONDITIONS ARE CONSIDERED TO IMPORTANT ROLE IN IMPROVING THE GRAIN-TO-GRAIN CONNECTIVITY OF THE CERAMIC PORES AND ABNORMAL GRAINS ARE OBSERVED WHICH CONFIRMS GOOD DENSIFICATION HOMOGENEOUS MICROSTRUCTURE.

THE DIELECTRIC PROPERTIES OF THE SAMPLES ARE DEFINED BY THE CRYSTALLINE WHICH ARE IN TURN DETERMINED BY THE SINTERING TEMPERATURE. FROM FIG. 4.2 IT IS THE RELATIONSHIP BETWEEN RELATIVE PERMITTIVITY AND SINTERING TEMPERATURE SHOWS SAME TREND AS THAT BETWEEN DENSITY AND SINTERING TEMPERATURE. THE HIGHEST RELATIVE PERMITTIVITY ARE FOUND FOR SAMPLES SINTERED AT OPTIMIZED TEMPERATURE THE RELATIVE PERMITTIVITY IS 12.5 MEASURED AT 1 MHZ. THE VARIATION OF DIELECTRIC LOSS MEASURED AT 1 MHZ WITH SINTERING TEMPERATURE IS ALSO SHOWN IN FIG. 4.2 (B). THE DIELECTRIC LOSS IS FOUND TO DECREASE WITH INCREASE IN THE SINTERING TEMPERATURE. IT REACHES A MINIMUM VALUE OF 0.0008. THIS MAY BE DUE TO THE ESTABLISHED FACT THAT HIGH DIELECTRIC LOSS IS MAINLY CAUSED BY THE INSUFFICIENT DENSIFICATION AND GROWTH AND IMPROVEMENT OF THE GRAIN CONNECTIVITY OF THE CERAMICS WITH TEMPERATURE. IT IS EXPECTED TO DECREASE THE DIELECTRIC LOSS. A UNIFORM GRAIN MORPHOLOGY ALSO CONTRIBUTES TO THE DIELECTRIC LOSS VALUE [12] WHICH IS EVIDENT FROM THE SEM IMAGE.

TABLE 4.1 SUMMARIZES THE MICROWAVE DIELECTRIC PROPERTIES OF SM SAMPLES AT 9 GHz. MICROWAVE FREQUENCY (9 GHz). MEASUREMENTS AT 1 MHz INDICATE THAT SM SAMPLES HAVE A RELATIVE PERMITTIVITY OF 12.5 AND  $\delta = 8 \times 10^{-4}$ . AT THE MICROWAVE FREQUENCY THE VALUES ARE 6.5 AND  $\delta = 6 \times 10^{-3}$ . IT IS SEEN THAT THE RELATIVE PERMITTIVITY HAS A LOW VALUE WHEN COMPARED WITH THAT MEASURED AT 1 MHz. THIS IS DUE TO THE DIFFERENCE IN THE POLARIZATION MECHANISMS AT THESE FREQUENCIES WHICH CONTRIBUTES TO THE RELATIVE PERMITTIVITY. AT LOW FREQUENCIES DIELECTRIC PERMITTIVITY IS ATTRIBUTED TO ALL THE FOUR POLARIZATIONS WHICH ARE ACTIVE AT THESE FREQUENCIES BUT IN THE MICROWAVE FREQUENCY RANGE ONLY ELECTRONIC AND IONIC POLARIZATION CONTRIBUTES TO THE NET RELATIVE PERMITTIVITY AND THEREFORE A REDUCTION IN THE RELATIVE PERMITTIVITY. THE LOSS TANGENT AT 9 GHz IS AN ORDER OF MAGNITUDE HIGHER THAN THAT MEASURED AT 1 MHz. IT MAY BE NOTED THAT AT LOW AND MICROWAVE FREQUENCY RANGE TWO DIFFERENT SAMPLES FOR MICROWAVE MEASUREMENTS WERE LARGE, THIN RECTANGULAR STRIPS AND AT 1 MHz MEASUREMENTS WERE SMALL PELLETS. THE DENSITY AS COMPARED TO THE SMALL PELLETS MADE FOR RADIO FREQUENCY MEASUREMENTS.

MOREOVER, IT MAY BE NOTED THAT THE DIELECTRIC LOSS INCREASES WITH INCREASE IN THE MICROWAVE REGIME [5].

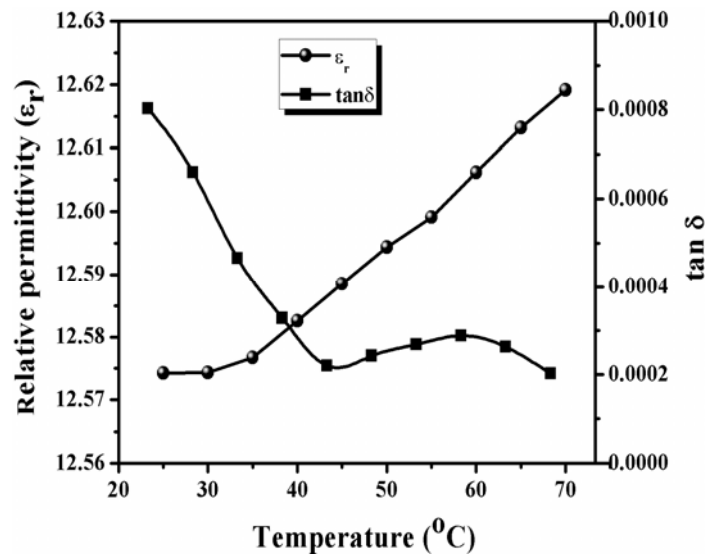


Fig. 4.5 The variation of relative permittivity and dielectric loss (at 1 MHz) of  $\text{Sm}_2\text{Si}_2\text{O}_7$  with temperature.

THE STABILITY OF DIELECTRIC PROPERTIES WITH TEMPERATURE IS THE MAIN CON OF THE PRACTICAL CIRCUITS. FIG. 4.5 SHOWS THE VARIATION OF RELATIVE PERMITTIVITY WITH TEMPERATURE IN THE RANGE. IT IS CLEAR FROM THE FIGURE THAT THE RELATIVE PERMITTIVITY INCREASES IN A REGULAR MANNER WITH RISE IN TEMPERATURE. THE PERMITTIVITY VARIES FROM ABOUT 12.57 TO 12.62 SHOWING A RELATIVE DEVIATION OF 0.5% FOR  $\text{Sm}_2\text{Si}_2\text{O}_7$  HAS A OF +63 PPM/C IN THE MEASURED TEMPERATURE RANGE. THIS IS WELL IN AGREEMENT WITH THE OBSERVATIONS BY BOSMAN AND HAVINGA [13] WHERE THEY NOTED THAT THE TEMPERATURE DEPENDENCE OF RELATIVE PERMITTIVITY IS POSITIVE FOR SMALL CERAMICS WITH ABOUT 20 AND NEGATIVE FOR LARGER CERAMICS. THE VARIATION OF DIELECTRIC LOSS OF THE CERAMICS WITH TEMPERATURE IS ALSO SHOWN IN FIG. 4.5. THE DIELECTRIC LOSS INITIAL VALUE IS 0.0008 AT ROOM TEMPERATURE TO NEARLY 0.0002 WITH A FURTHER RISE IN TEMPERATURE THE DIELECTRIC LOSS ALMOST REMAINS CONSTANT AT THIS VALUE. IT IS CLEAR FROM TABLE 4.1 THAT THE DIELECTRIC PROPERTIES OF  $\text{Sm}_2\text{Si}_2\text{O}_7$  ARE COMPARABLE TO THE CONVENTIONAL CERAMIC SUBSTRATE MATERIALS AND IT IS A PROMISING MATERIAL FOR ELECTRONIC SUBSTRATE

### 4.1.3.2 PROPERTIES OF $\text{Sm}_2\text{Si}_2\text{O}_7$ CERAMIC

THIS SECTION GIVES A BRIEF DESCRIPTION ON THE CHARACTERISTICS OF SOL-GEL  $\text{Sm}_2\text{Si}_2\text{O}_7$  CERAMICS. THE TYPICAL TG CURVES OF DRIED GEL IS SHOWN IN FIG. 4.6. THE RESULT INDICATES THAT THE WEIGHT LOSS BEGAN AT ABOUT 160°C AND ALL CHEMICAL REACTIONS INVOLVING WEIGHT LOSSES, SUCH AS DECOMPOSITION OF POLYMERIC NETWORK WITH THE EVOLUTION OF  $\text{H}_2\text{O}$  AND  $\text{H}_2\text{SiO}_3$  WERE COMPLETED BELOW THIS TEMPERATURE. BEYOND 500°C THE MASS OF THE DRIED GEL EXHIBITED ALMOST NO CHANGE. HOWEVER, THE FORMATION TEMPERATURE OF SOL-GEL  $\text{Sm}_2\text{Si}_2\text{O}_7$  CERAMICS IS 900°C WHICH IS CONFIRMED FROM THE XRD PHASE ANALYSIS SHOWN IN FIG. 4.7. TABLE 4.1 GIVES OPTIMIZED CALCINATION AND SINTERING TEMPERATURES OF  $\text{Sm}_2\text{Si}_2\text{O}_7$  SOLID STATE AND SOL-GEL ROUTE.

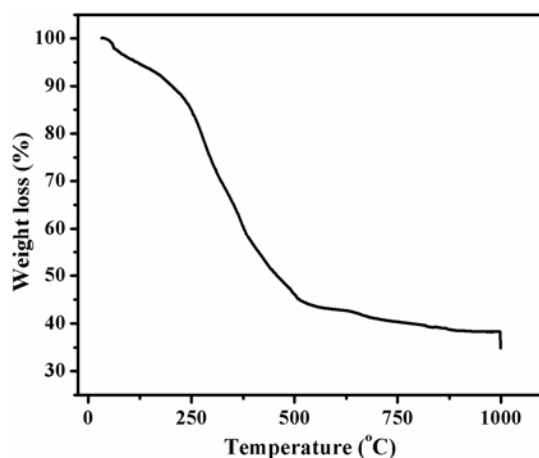


Fig. 4.6 TGA curve of sol-gel synthesized  $\text{Sm}_2\text{Si}_2\text{O}_7$ .

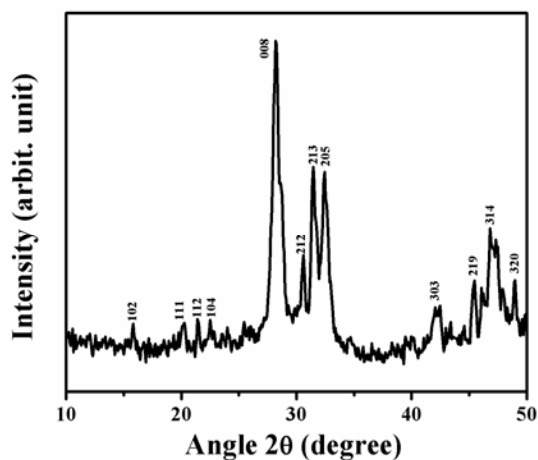


Fig. 4.7 XRD pattern of sol-gel synthesized  $\text{Sm}_2\text{Si}_2\text{O}_7$  calcined at 900°C/4h.

Table 4.1 The physical and dielectric properties of  $\text{Sm}_2\text{Si}_2\text{O}_7$  ceramics synthesized by different methods.

| Synthesis method | CT        | ST        | Relative Density (%) | BET Surface area ( $\text{m}^2/\text{g}$ ) | Dielectric Properties (1 MHz) |              |
|------------------|-----------|-----------|----------------------|--|-------------------------------|--------------|
|                  |           |           |                      |  | $\epsilon_r$                  | TAN $\delta$ |
| SOLID STATE      | 1250°C/4H | 1375°C/2H | 94.02                | 0.15                                       | 12.5                          | 0.0008       |
| SOL-GEL          | 900°C/4H  | 1325°C/2H | 70.50                | 20.94                                      | 7.6                           | 0.0010       |

FIGURE 4.8 SHOWS THE TEM IMAGE OF SOL-GEL SYNTHESIZED POWDER HEATED AT 900°C/4H. THE PARTICLE SIZE VARIES FROM ABOUT 40-70 NM. ALSO THE NANO PARTICLES FOUND TO AGGLOMERATE AND THEY SEEM TO BE INDISTINGUISHABLE. THE LOWER TEMPERATURE WILL RESULT IN A LESS AGGREGATED POWDER. THE SPECIFIC SURFACE AREA MEASUREMENTS SHOW THAT THE MICRO SIZED POWDER HAS A VERY SMALL AVERAGE SURFACE AREA VALUE (0.216 CM<sup>2</sup>/G) AS COMPARED TO THE NANO SIZED ONE (1.094 CM<sup>2</sup>/G). INCREASE THE SINTERING ACTIVITY OF THE POWDER, WHICH WILL IN TURN REDUCE THE SINTERING TEMPERATURE. HOWEVER, IN THE PRESENT CASE EVENTHOUGH A REDUCTION IN CALCINATION TEMPERATURE, THE SINTERING TEMPERATURE IS REDUCED BY 100°C. THESE RESULTS ARE OBSERVED IN THE CASE OF SOL-GEL SYNTHESIZED CERAMICS WHERE AN ADDITIONAL REDUCTION IN THE SINTERING TEMPERATURE IS ACHIEVED WITH THE ADDITION OF TIO<sub>2</sub>.

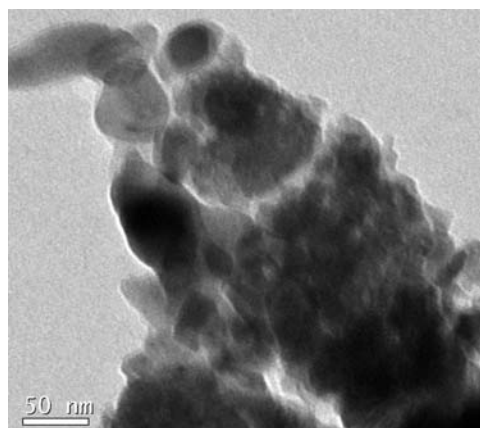


Fig. 4.8 TEM image of  $\text{Sm}_2\text{Si}_2\text{O}_7$  heated at 900°C/4h.

A COMPARISON OF THE DIELECTRIC PROPERTIES OF BOTH THE SAMPLES MEASURED SHOW THAT SOL-GEL SYNTHESIZED CERAMIC EXHIBITS A LOW RELATIVE PERMITTIVITY AND HIGH DIELECTRIC LOSS WHEN COMPARED TO THAT PREPARED THROUGH SOLID STATE METHOD. THIS MAY BE PROBABLY DUE TO THE VERY LOW RELATIVE DENSITY ACHIEVED BY THE FORMER METHOD. AT A TEMPERATURE OF 100°C, IT CAN BE CONCLUDED THAT CERAMIC SYNTHESIZED BY SOLID STATE METHOD POSSESS PROMISING DIELECTRIC PROPERTIES FOR SUBSTRATE APPLICATIONS.

#### 4.1.3.3 EFFECT OF GLASS ADDITION IN SM CERAMIC

THE PURE  $\text{Sm}_2\text{O}_7$  CERAMICS HAS A HIGH SINTERING TEMPERATURE OF ABOUT 1375°C. IT IS IMPERATIVE TO LOWER THE SINTERING TEMPERATURE FOR PRACTICAL APPLICATIONS. ADDITION OF LOW MELTING POINT GLASSES, CHEMICAL PROCESSING AND SMALLER PARTICLES OF THE STARTING MATERIALS ARE THE THREE METHODS TO REDUCE THE PROCESSING TEMPERATURE OF DIELECTRIC AS EXPLAINED IN CHAPTER 1. THE PRESENT SECTION DEALS WITH THE EFFECT OF LOW MELTING GLASSES ON THE SINTERING AND DIELECTRIC PROPERTIES OF SM

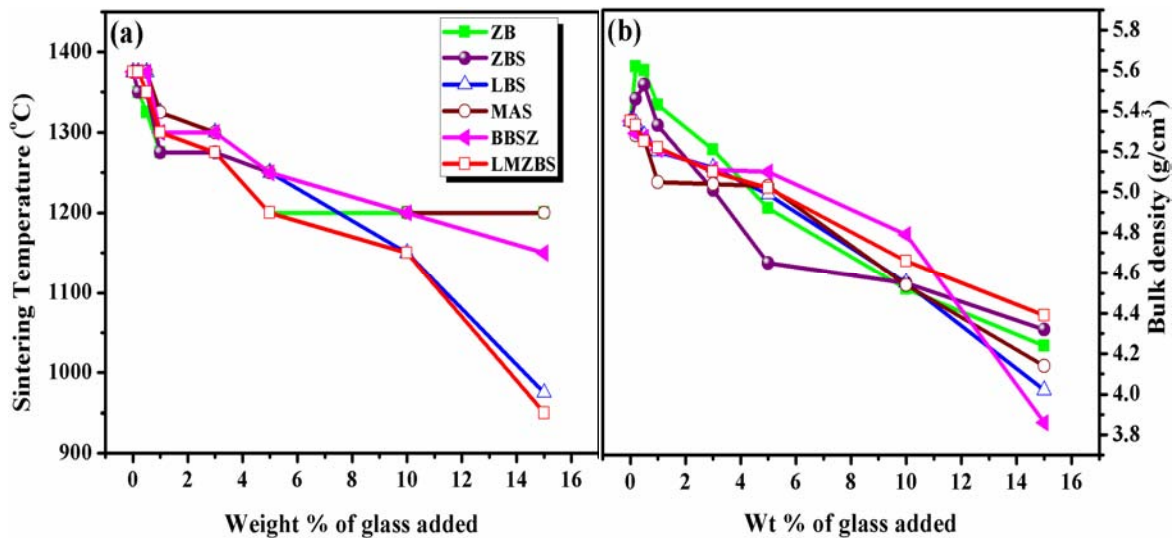


Fig. 4.9 The variation of (a) sintering temperature and (b) bulk density with the amount of glass addition in  $\text{Sm}_2\text{Si}_2\text{O}_7$  ceramics.

FIGURE 4.9 (A) SHOWS THE OPTIMIZED SINTERING TEMPERATURE OF VARIOUS GLASS ADDED IN  $\text{Sm}_2\text{Si}_2\text{O}_7$  CERAMICS. THE SINTERING TEMPERATURES ARE OPTIMIZED FOR THE MAXIMUM DENSITY AND BEST DIELECTRIC PROPERTIES. IT MAY BE NOTED THAT THE ADDITION OF DIFFERENT PERCENTAGE OF VARIOUS GLASSES LOWERS THE SINTERING TEMPERATURE GRADUALLY. THE WELL KNOWN LIQUID PHASE SINTERING TAKING PLACE IN THE CERAMIC-GLASS COMPOSITE IS WELL EXPLAINED IN CHAPTER 2 SECTION 2.1.2.7.2. THESE GLASSES ARE HAVING LOW MELTING POINT AS GIVEN IN TABLE 1.3 IN CHAPTER 1. THE BOROSILICATE GLASSES ARE REPORTED TO BE ADDITIVE TO LOWER THE SINTERING TEMPERATURE FOR MANY DIELECTRIC MATERIALS. THE VARIOUS GLASSES USED IN THE PRESENT STUDY ARE ZB, ZBS, BBSZ, MAS, LBS, AND LMZBS.

LMZBS) REDUCES THE SINTERING TEMPERATURE MUCH EFFECTIVELY. THIS MAY BE DUE THAT ZNO IN THE RESPECTIVE GLASS COMPOSITION ACT AS A MODIFIER OXIDE WHICH NETWORK STRUCTURE OF THE GLASS THEREBY REDUCING THE SOFTENING POINT OF INCREASING ITS FLUIDITY [17]. ~~IT IS ALSO RECOGNIZED AS A TYPICAL GLASS NETWORK FORM THAT HAS A LOW GLASS TRANSITION TEMPERATURE [18].~~ THE SINTERING TEMPERATURE FROM 1375-1275°C WITH THE ADDITION OF 3 WT% OF THE ABOVE GLASSES EXCEPT FOR B. HOWEVER, IT IS INTERESTING TO NOTE THAT ADDITION OF HIGHER WEIGHT PERCENTAGE THESE GLASSES HAS NO EFFECT ON THE SINTERING TEMPERATURE. EVEN WITH THE ADDITION OF THESE GLASSES, THE SINTERING TEMPERATURE IS LOWERED. ~~THIS MAY BE DUE TO~~ THE FORMATION OF SOME HIGH TEMPERATURE STABLE SECONDARY PHASES. A SIMILAR OBSERVED FOR MAS GLASS WHICH MAY BE DUE TO ITS HIGH SOFTENING POINT AS A RESULT OF THE ABSENCE OF THE LITHIUM BASED BOROSILICATE GLASSES IS VERY EFFECTIVE IN LOWERING SINTERING TEMPERATURE. THE LITHIUM BASED GLASSES HAVE A LOW MELTING POINT WHICH IS EFFECTIVE IN LOWERING THE SINTERING TEMPERATURE [19]. IT IS SEEN THAT WITH THE ADDITION OF BOTH LBS AND LMZBS GLASS CONTENT, THERE IS A REGULAR REDUCTION IN THE SINTERING TEMPERATURE OF THE COMPOSITE. HOWEVER, THE LMZBS GLASS IS MORE EFFICIENT IN LOWERING THE TEMPERATURE.

THE THEORETICAL DENSITY OF THE GLASS, ~~ADDED~~ CALCULATED USING EQ. (4.2) [20]:

$$D = \frac{W_1 + W_2}{\frac{W_1}{D_1} + \frac{W_2}{D_2}} \quad (4.2)$$

WHERE W AND V ARE THE WT% OF CERAMIC AND GLASS WITH DENSITIES D<sub>1</sub> AND D<sub>2</sub> RESPECTIVELY. TABLE 4.2 GIVES THE DENSITIES AND OPTIMIZED SINTERING TEMPERATURE FOR VARIOUS GLASS ADDED. ~~THE~~ THEORETICAL DENSITY OF THE CERAMIC-GLASS COMPOSITE DECREASES WITH THE INCREASE IN THE AMOUNT OF GLASS CONTENT. THIS IS DUE TO THE LOWER DENSITY POSSESSED BY THE GLASSES. FIG. 4.9 (B) SHOWS THE DEPENDENCE OF THE BULK DENSITY OF THE COMPOSITE ON THE AMOUNT OF VARIOUS GLASSES ADDED. IT IS FOUND THAT ADDITION OF A SMALL AMOUNT (0.2 WT%) OF ZB, ZBS AND LBS GLASSES IMPROVE DENSIFICATION. A MAXIMUM RELATIVE DENSITY OF ABOUT 99% IS OBTAINED WITH THE ADDITION OF 0.2 WT% OF ZB. ~~THE~~ THE EFFECTIVENESS OF SINTERING AIDS DEPENDS ON SEVERAL FACTORS SUCH AS

TEMPERATURE, VISCOSITY, SOLUBILITY AND GLASS WETTABILITY [21]. THE DENSIFICATION OF THE CERAMIC-GLASS COMPOSITES IS EXPLAINED BY THE VISCOUS FLOW OF THE GLASS PHASE. EARLIER JHOU AND JEAN [22] NOTED THAT THE WETTING BEHAVIOR IS GREATLY IMPROVED BY INCREASING BAO CONTENT IN THE BAO GLASSES SINCE BOTH THE SOFTENING AND MELTING POINTS DECREASES. A COMPLETE WETTING BETWEEN GLASS AND CERAMICS IS NOTED BY CONTACT ANGLE AND IT IS VERY MUCH DEPENDENT ON THE AMOUNT OF SINTERING AID. IN THE CASE OF MAS GLASS ADDITION THE RELATIVE DENSITY IS FOUND TO INCREASE WITH WHICH MAY BE DUE TO THE ABOVE FACT. THE DRIVING FORCE FOR THE DENSIFICATION IS FROM THE CAPILLARY PRESSURE OF THE LIQUID PHASE LOCATED BETWEEN THE FINE PARTICLES. WHEN THE LIQUID PHASE WETS THE SOLID PARTICLES, EACH INTER-PARTICLE SPACE BECOMES A CAPILLARY, IN WHICH A SUBSTANTIAL CAPILLARY PRESSURE DEVELOPS [23]. IT SHOULD BE NOTED THAT DENSIFICATION MAY BE RETARDED DUE TO THE INSUFFICIENT AMOUNT OF GLASS DURING SINTERING. THE INCREASE IN ADDITION OF ZB GLASS DECREASES THE DENSITY AND THE RELATIVE DENSITY REACHES 92% WITH 15 WT% ADDITION OF THE GLASS. THE ZBS GLASS ALSO SHOWS A SIMILAR TREND SHOWING A MAXIMUM RELATIVE DENSITY OF 96% WITH 0.2 WT% ADDITION. THERE IS A FASTER REDUCTION IN THE DENSITY FOR HIGHER WT% OF ZBS GLASS AS COMPARED TO MAS GLASS. IT HAS BEEN REPORTED EARLIER [24-25] THAT ZINC BORATE GLASS IMPROVES THE WETTING OF THE GLASS/CERAMIC COMPOSITES. FOR ALL OTHER GLASSES THE DENSITY SHOWS A DECREASE WITH THE GLASS CONTENT AND THEY DO NOT ASSIST IN DENSIFICATION OF THE COMPOSITES. TO BE NOTED THAT EVEN THOUGH LITHIUM BASED GLASSES LOWER THE SINTERING TEMPERATURE EFFECTIVELY, THE DENSIFICATION IS ADVERSELY AFFECTED. ADDITION OF 15 WT% OF LMZBS GLASSES REDUCES THE RELATIVE DENSITY TO ABOUT 84% AND 88% RESPECTIVELY AT OPTIMIZED SINTERING TEMPERATURES. THIS IS DUE TO THE LOW DENSITY POSSESSED BY THESE GLASSES WHEN COMPARED TO OTHERS (SEE TABLE 1.3 IN CHAPTER 1).



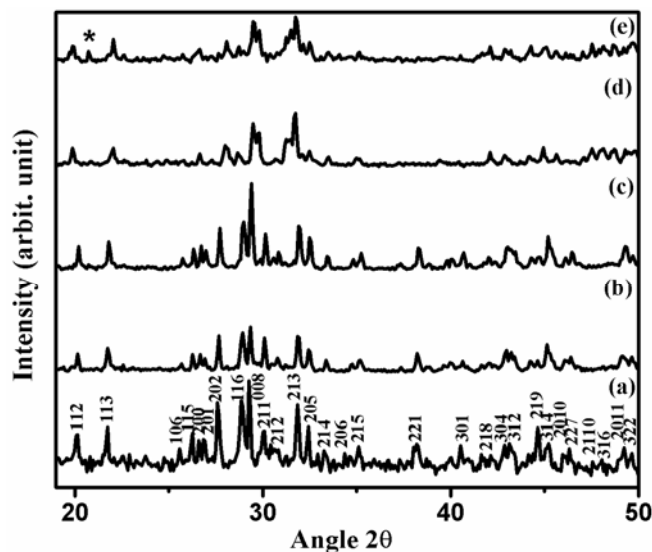
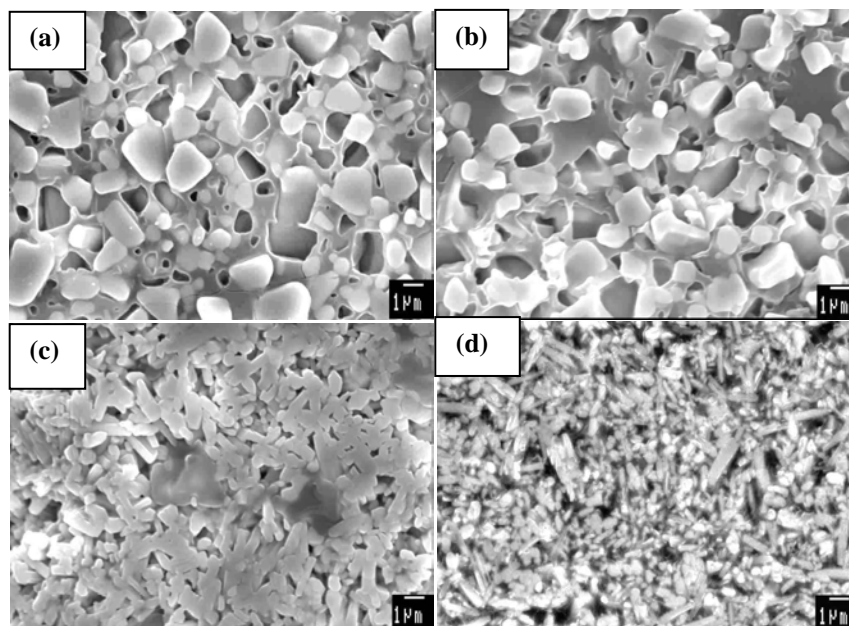


Fig. 4.10 XRD pattern of (a) pure  $\text{Sm}_2\text{Si}_2\text{O}_7$  (ST: 1375 °C), (b)  $\text{Sm}_2\text{Si}_2\text{O}_7$  + 3 wt% LBS (ST: 1300 °C), (c)  $\text{Sm}_2\text{Si}_2\text{O}_7$  + 3 wt% LMZBS (ST: 1275 °C), (d)  $\text{Sm}_2\text{Si}_2\text{O}_7$  + 15 wt% LBS (ST: 975 °C) and (e)  $\text{Sm}_2\text{Si}_2\text{O}_7$  + 15 wt% LMZBS (ST: 950 °C). (\* represents  $\text{SmBO}_3$  phase).

FIGURE 4.10 (B)-(E) SHOWS THE XRD PATTERNS OBTAINED WITH DIFFERENT WEIGHT PERCENTAGE OF LBS AND LMZBS GLASSES. IT IS OBSERVED THAT WITH THE SMALL WEIGHT PERCENTAGE OF BOTH THE GLASSES NO SECONDARY PHASES ARE OBSERVED. OF LARGER AMOUNT (UPTO 15 WT%) OF LBS DOES NOT PRODUCE ANY ADDITIONAL X-RAY DIFFRACTION PEAKS. THIS INDICATES THE NON-REACTIVITY OF LBS GLASS WITH  $\text{Sm}_2\text{Si}_2\text{O}_7$  IN THE ABSENCE OF ADDITIONAL DIFFRACTION PEAKS IN THE XRD PATTERNS OF SAMPLES CONTAINING SMALL AMOUNT OF GLASSES MAY BE DUE TO THE FACT THAT THE GLASS IS IN THE AMORPHOUS STATE. ALTHOUGH, THE SAMPLES ARE SINTERED AND THEN SLOWLY COOLED AT A RATE OF 2°C/MINUTE, LBS LIQUID PHASE IS NOT CRYSTALLIZED RETAINING ITS AMORPHOUS NATURE. IT CAN BE CONCLUDED THAT LBS GLASS EXISTED DURING LIQUID PHASE SINTERING AND DENSIFICATION OF  $\text{Sm}_2\text{Si}_2\text{O}_7$  CERAMIC. HOWEVER, ADDITION OF 15 WT% LMZBS GLASS RESULTS IN AN ADDITIONAL PEAK OF  $\text{SmBO}_3$  (SHOWN IN FIG. 4.10 (E)).

**Table 4.2 Sintering, densification and microwave dielectric properties of pure  $\text{Sm}_2\text{Si}_2\text{O}_7$  and that treated with various glass additives.**

| $\text{Sm}_2\text{Si}_2\text{O}_7$<br>+Glass | Wt %<br>of<br>glass | Sintering<br>Temp.<br>(°C) | Theoretical<br>Density<br>( $\text{g}/\text{cm}^3$ ) | Relative<br>Density<br>(%) | At 9 GHz |              |
|--|---------------------|----------------------------|--|----------------------------|----------|--------------|
|  |                     |                            |  |                            | R        | TAN $\delta$ |
| PUR <br>$\text{Sm}_2\text{Si}_2\text{O}_7$   | 0                   | 1375                       | 5.69   | 94.02                      | 10       | 0.006        |
| ZB   | 0.2                 | 1350/2H                    | 5.67   | 99.12                      | 10.01    | 0.0034       |
|  | 0.5                 | 1325/2H                    | 5.64   | 99.29                      | 9.70     | 0.0031       |
|  | 1                   | 1275/2H                    | 5.60   | 96.96                      | 9.64     | 0.0030       |
|  | 3                   | 1275/2H                    | 5.43   | 95.95                      | 9.05     | 0.0019       |
|  | 5                   | 1200/2H                    | 5.29   | 93.01                      | 8.10     | 0.0019       |
|  | 10                  | 1200/2H                    | 4.97   | 90.95                      | 8.03     | 0.0017       |
|  | 15                  | 1200/2H                    | 4.71   | 90.02                      | 7.58     | 0.0023       |
| ZBS  | 0.2                 | 1350/2H                    | 5.68   | 96.13                      | 9.05     | 0.0039       |
|  | 0.5                 | 1350/2H                    | 5.67   | 97.53                      | 9.07     | 0.0035       |
|  | 1                   | 1275/2H                    | 5.65   | 94.34                      | 8.45     | 0.0029       |
|  | 3                   | 1275/2H                    | 5.59   | 89.62                      | 8.37     | 0.0022       |
|  | 5                   | 1250/2H                    | 5.54   | 83.94                      | 8.10     | 0.0028       |
|  | 10                  | 1200/2H                    | 5.41   | 84.10                      | 8.09     | 0.0022       |
|  | 15                  | 1200/2H                    | 5.29   | 81.66                      | 6.37     | 0.0016       |
| LBS  | 0.2                 | 1375/2H                    | 5.67   | 94.18                      | 9.58     | 0.0043       |
|  | 0.5                 | 1375/2H                    | 5.65   | 93.45                      | 9.08     | 0.0040       |
|  | 1                   | 1325/2H                    | 5.61   | 92.69                      | 8.99     | 0.0036       |
|  | 3                   | 1300/2H                    | 5.46   | 93.77                      | 8.78     | 0.0032       |
|  | 5                   | 1250/2H                    | 5.33   | 93.80                      | 8.35     | 0.0034       |
|  | 10                  | 1150/2H                    | 5.03   | 90.46                      | 6.91     | 0.0022       |
|  | 15                  | 975/2H                     | 4.79   | 83.92                      | 6.06     | 0.0025       |
| MAS  | 0.2                 | 1375/2H                    | 5.67   | 93.12                      | 9.14     | 0.0044       |
|  | 0.5                 | 1375/2H                    | 5.65   | 93.09                      | 8.59     | 0.0037       |
|  | 1                   | 1325/2H                    | 5.61   | 90.02                      | 8.58     | 0.0036       |
|  | 3                   | 1300/2H                    | 5.46   | 92.31                      | 8.72     | 0.0034       |
|  | 5                   | 1250/2H                    | 5.32   | 94.55                      | 8.28     | 0.0031       |
|  | 10                  | 1200/2H                    | 5.02   | 90.44                      | 8.26     | 0.0026       |
|  | 15                  | 1200/2H                    | 4.77   | 86.79                      | 7.07     | 0.0025       |
| BBSZ   | 0.2                 | 1375/2H                    | 5.69   | 92.97                      | 9.07     | 0.0029       |
|  | 0.5                 | 1375/2H                    | 5.68   | 92.78                      | 9.07     | 0.0035       |
|  | 1                   | 1300/2H                    | 5.67   | 91.89                      | 8.92     | 0.0037       |
|  | 3                   | 1300/2H                    | 5.64   | 90.60                      | 8.53     | 0.0030       |
|  | 5                   | 1250/2H                    | 5.61   | 90.91                      | 8.32     | 0.0026       |
|  | 10                  | 1200/2H                    | 5.55   | 86.31                      | 7.79     | 0.0021       |
|  | 15                  | 1150/2H                    | 5.48   | 70.44                      | 6.89     | 0.0022       |
| LMZBS  | 0.2                 | 1375/2H                    | 5.68   | 93.84                      | 12.17    | 0.0038       |
|  | 0.5                 | 1350/2H                    | 5.66   | 92.76                      | 10.10    | 0.0030       |
|  | 1                   | 1300/2H                    | 5.63   | 92.72                      | 9.47     | 0.0031       |
|  | 3                   | 1275/2H                    | 5.52   | 92.39                      | 8.84     | 0.0025       |
|  | 5                   | 1200/2H                    | 5.41   | 92.79                      | 7.75     | 0.0022       |
|  | 10                  | 1150/2H                    | 5.19   | 89.79                      | 7.29     | 0.0033       |
|  | 15                  | 950/2H                     | 4.99   | 87.98                      | 6.91     | 0.0026       |



**Fig. 4.11** The scanning electron micrographs of  $\text{Sm}_2\text{Si}_2\text{O}_7$  (a) doped with 3wt% LBS sintered at  $1300^\circ\text{C}$ , (b) doped with 3wt% LMZBS sintered at  $1275^\circ\text{C}$ , (c) treated with 15wt% LBS sintered at  $975^\circ\text{C}$  and (d) treated with 15wt% LMZBS sintered at  $950^\circ\text{C}$ .

THE COMPOSITIONAL DEPENDENCE OF MICROSTRUCTURE WITH DIFFERENT AMOUNTS FOR  $\text{Sm}_2\text{Si}_2\text{O}_7$  CERAMIC IS SHOWN IN FIG. 4.11 (A)-(D). FIG. 4.11 (A) AND (B) SHOWS THE SEM PICTURES OF  $\text{Sm}_2\text{Si}_2\text{O}_7$  WITH 3 WT% OF LBS AND LMZBS GLASS RESPECTIVELY. THE GLASS MELT AND FORMS A LIQUID PHASE AND THE EXCESS AMOUNT OF GLASS CAN BE CLEARLY OBSERVED IN SEM IMAGES. BOTH THE GLASSES DID NOT REACT WITH THE CERAMIC BUT FORMS A GLASSY PHASE OVER THE GRAIN LEADING TO LIQUID PHASE FORMATION. AS THE AMOUNT OF GLASS INCREASES, PORES APPEAR IN THE MICROSTRUCTURE. FIG. 4.11 (C) AND (D) ILLUSTRATES THE SEM PICTURES OF  $\text{Sm}_2\text{Si}_2\text{O}_7$  DOPED WITH 15 WT% OF LBS AND LMZBS GLASS RESPECTIVELY. IT IS FOUND THAT THE ADDITION OF GLASS REDUCES THE GRAIN SIZE OF THE COMPOSITE INDICATING THAT THE GLASSY SINTERING PROCESS PRODUCES SMALLER GRAIN SIZE THAN SOLID STATE SINTERING. THE DECREASE IN GRAIN SIZE AND INCREASE IN POROSITY ARE DUE TO THE LOWERING OF SINTERING TEMPERATURE BY THE INCREASED GLASS CONTENT. THE PRESENCE OF TRACES OF SECONDARY PHASE IS OBSERVED IN THE CASE OF 15 WT% LMZBS GLASS AS SHOWN IN FIG. 4.11 (D)).  $\text{B}_2\text{O}_3$ -RICH COMPOUNDS GENERALLY HAVE LOW MELTING POINT AND GROW INTO ABNORMALLY LARGE GRAINS DURING SINTERING. IT IS CONSIDERED THAT THE GLASSY SINTERING INTERACTS

WITH OTHER IONS IN THE MATRIX PHASE. THIS SUGGEST THAT, ALTHOUGH AN EXCESSIVE LBS WOULD IMPROVE THE DENSITY OF THE SAMPLES, TOO MUCH LBS WOULD CAUSE A LARGE AMOUNT OF UNWANTED SECONDARY PHASES WHICH COULD DEGRADE THE PHYSICAL PROPERTIES OF THE SAMPLES [26-28].

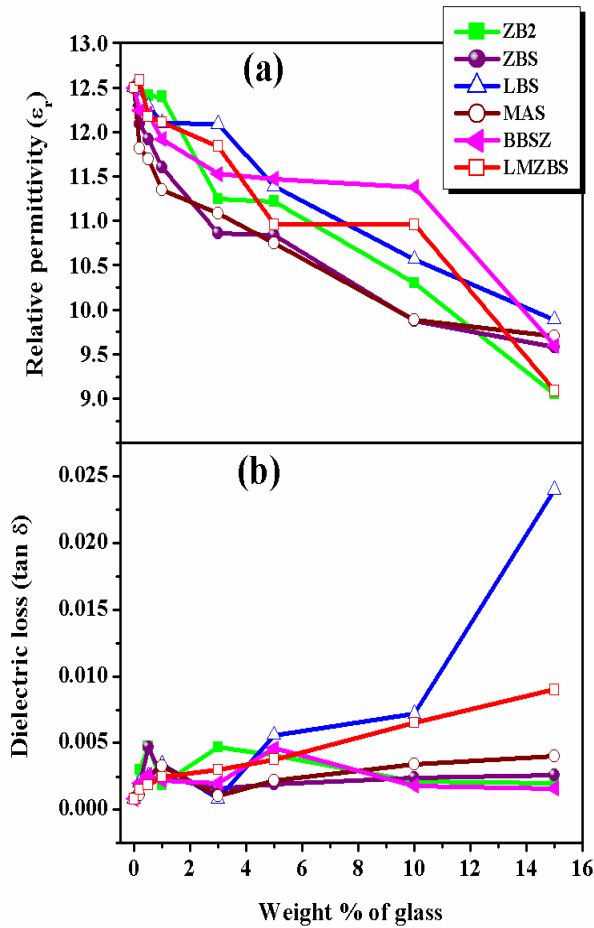


Fig. 4.12 Variation of dielectric properties of  $\text{Sm}_2\text{Si}_2\text{O}_7$  as a function of glass addition.

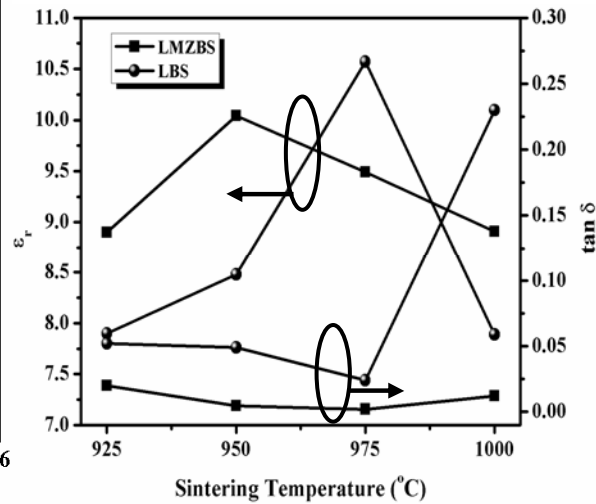


Fig. 4.13 The variation of dielectric properties with sintering temperature for  $\text{Sm}_2\text{Si}_2\text{O}_7$  doped with (a) 15 wt% LBS glass and (b) 15 wt% LMZBS.

ACCORDING TO *et al.* [29] THE MICROWAVE DIELECTRIC LOSS AND THE RELATIVE PERMITTIVITY OF GLASS DEPEND ON THE IONIC SIZE, IONIC DIELECTRIC POLARIZABILITY AND CONCENTRATION OF THE CATION IN THE NETWORK MODIFYING OXIDE IN THE GLASS. FIGURE 4.12 SHOWS THE VARIATION OF RELATIVE PERMITTIVITY MEASURED AT 1 MHz WITH WEIGHT PERCENTAGE OF VARIOUS GLASS ADDED TO CERAMICS. THE RELATIVE PERMITTIVITY GRADUALLY DECREASES WITH INCREASE IN THE AMOUNT OF GLASSES. GENERALLY AN INCREASE IN RELATIVE DENSITY RESULTS IN AN INCREASE IN RELATIVE PERMITTIVITY.

RELATIVE PERMITTIVITY VALUE. HOWEVER, IN THE CASE OF SM WITH LOW WEIGHT PERCENTAGE OF GLASS, EVEN THOUGH AN INCREASE IN THE DENSIFICATION IS NOTED PERMITTIVITY SEEMS TO DECREASE. THIS MAY BE DUE TO THE LOW RELATIVE PERMITTIVITY OF GLASSES. THUS THE PRESENCE OF EXCESS GLASS IN THE MATRIX MAY CONTRIBUTE TO THE DECREASE IN PERMITTIVITY OF THE COMPOSITE. FIG. 4.12 (B) SHOWS THE VARIATION OF DIELECTRIC LOSS AS A FUNCTION OF DIFFERENT GLASS COMPOSITIONS. IT IS OBSERVED THAT THE DIELECTRIC LOSS INCREASES WITH THE ADDITION OF GLASS UP TO ABOUT 10 WT% OF THE GLASSES. HOWEVER, FURTHER ADDITION OF GLASS DOES NOT INCREASE THE

IN ALKALI BORATE GLASS [30], THE OSCILLATION OF THE ALKALI ION WAS LIMITED BY THE STRONG BONDING WHILE IN THE VITREOUS STATE THEY WERE LOOSELY HELD IN THE INTERSTITIAL SITES OF THE NETWORK WHICH WERE RELATIVELY FREE TO OSCILLATE WITH EXTERNAL FIELD, WHICH RESULTS IN EXTENSIVE DIELECTRIC LOSSES. WHEN SUCH LOSSY AMORPHOUS MATERIAL IS INCORPORATED INTO A LOW LOSS MATERIAL, THE DIELECTRIC LOSS OF THE LATTER CAN INCREASE. IN ORDER TO ACHIEVE AN ACCEPTABLE DENSIFICATION AND DIELECTRIC PROPERTIES AT LOW TEMPERATURES, IT IS NECESSARY TO DESIGN GLASS COMPOSITIONS WITH A LOW GLASS TRANSITION TEMPERATURE AND A LOW DIELECTRIC LOSS. IN THE PRESENT INVESTIGATION IT IS OBSERVED THAT AN APPROPRIATE SINTERING AID IS REQUIRED FOR  $\text{SM}_2\text{O}_7$  DIELECTRIC CERAMICS. FIG. 4.13 SHOWS THE VARIATION OF RELATIVE PERMITTIVITY AND DIELECTRIC LOSS WITH SINTERING TEMPERATURE FOR  $\text{SM}_2\text{O}_7 + 15$  WT% LBS AND  $\text{SM}_2\text{O}_7 + 15$  WT% LMZBS GLASSES. IT IS OBSERVED THAT FOR BOTH THE GLASSES THE RELATIVE PERMITTIVITY INCREASES WITH THE SINTERING TEMPERATURE UP TO A PARTICULAR TEMPERATURE AND THEREAFTER DECREASES. THE  $\text{SM}_2\text{O}_7 + 15$  WT% LBS AND  $\text{SM}_2\text{O}_7 + 15$  WT% LMZBS COMPOSITES HAVE A MAXIMUM RELATIVE DENSITY OF 84% AND 88% AT 950°C AND 900°C RESPECTIVELY. BEYOND THESE TEMPERATURES RESPECTIVE TEMPERATURES THE DENSITY IS FOUND TO DECREASE. THE RELATIVE PERMITTIVITY OF THESE COMPOSITIONS ALSO FOLLOW A SIMILAR TREND. IT IS WELL KNOWN [31] THAT SINTERING AIDS CONTAINING BORON OXIDE AND LITHIUM OXIDE PROMOTES DENSIFICATION BY LIQUID PHASE SINTERING UP TO A PARTICULAR TEMPERATURE AND AS THE TEMPERATURE INCREASES THESE OXIDES MAY TAKE PLACE. THIS MAY LEAD TO THE FORMATION OF PORES THEREBY DECREASING THE DENSITY AND THE RELATIVE PERMITTIVITY. FIG. 4.13 ALSO COMPARES THE DIELECTRIC LOSS OF  $\text{SM}_2\text{O}_7 + 15$  WT% LBS AND  $\text{SM}_2\text{O}_7 + 15$  WT% LMZBS MEASURED AT 1 MHZ AS A FUNCTION OF SINTERING TEMPERATURE. FROM THE FIGURE IT IS NOTED THAT THE DIELECTRIC LOSS OF LMZBS ADDED  $\text{SM}_2\text{O}_7$  IS LESS THAN THAT FOR LBS ADDED ONE. THE LMZBS ADDED SAMPLE SHOWS ALMOST A STEADY VARIATION IN THE DIELECTRIC LOSS EXHIBITING A RELATIVE

0.009 AT 95°C WHEREAS THE LBS ADDED COMPOSITE HAS A HIGH LOSS OF 0.024 AT 95°C. THIS MAY BE ATTRIBUTED TO THE FACT THAT THE ADDITIONAL NETWORK FORMER (SMBO) IN THE  $\text{Sm}_2\text{Si}_2\text{O}_7/\text{LMZBS}$  COMPOSITE HAS A LOW DIELECTRIC LOSS IN THE RELATIVE PERMITTIVITY OF 9 [32]. AS THE SINTERING TEMPERATURE INCREASES THE DIELECTRIC LOSS REACHES A MINIMUM AT THEIR RESPECTIVE TEMPERATURES AND THEN INCREASES. THIS IS DUE TO THE INCREASED POROSITY PRODUCED DUE TO THE EVAPORATION OF THE VOLATILE  $\text{B}_2\text{O}_3$  AND  $\text{Li}_2\text{O}$  AT HIGHER TEMPERATURES.

TABLE 4.2 GIVES THE MICROWAVE DIELECTRIC PROPERTIES OF VARIOUS GLASS ADDED  $\text{Sm}_2\text{Si}_2\text{O}_7$  COMPOSITES. A COMPARISON OF THE DIELECTRIC PROPERTIES OF THE COMPOSITES AT DIFFERENT MICROWAVE FREQUENCY POINTS TO THE FACT THAT THE DIELECTRIC LOSS IS IN THE MICROWAVE REGION. ONE OF THE MAIN REASONS MAY BE THAT THE NETWORK FORMERS IN THE REMAINING GLASS CAN PROFOUNDLY ABSORB THE MICROWAVE POWER AT HIGH FREQUENCIES WHICH INCREASES THE DIELECTRIC LOSS OF THE COMPOSITES [33]. THE DIELECTRIC LOSS IS DEPENDENT ON VARIETY OF FACTORS WHICH ARE EXPLAINED IN CHAPTER 1 SECTION 1.1.

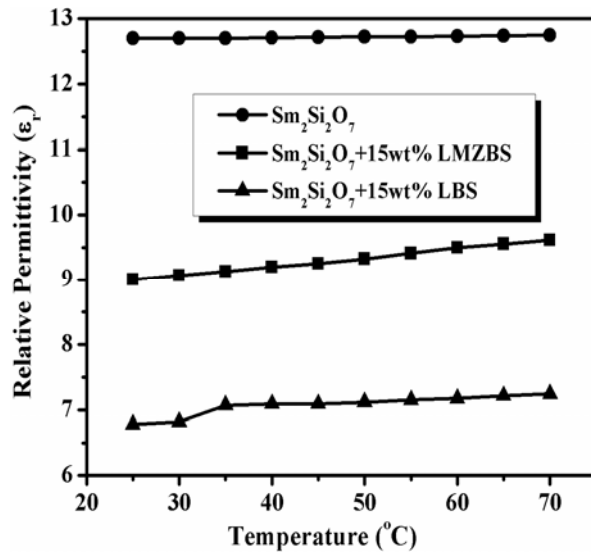


Fig. 4.14 The variation of relative permittivity with temperature of  $\text{Sm}_2\text{Si}_2\text{O}_7$  treated with 15 wt% LBS glass and 15 wt% LMZBS.

FIGURE 4.14 SHOWS THE VARIATION OF RELATIVE PERMITTIVITY WITH TEMPERATURE OF  $\text{Sm}_2\text{Si}_2\text{O}_7$  TREATED WITH 15 WT% LMZBS AND 15 WT% LBS. THE RELATIVE PERMITTIVITY OF  $\text{Sm}_2\text{Si}_2\text{O}_7$  GLASS ADDED COMPOSITE VARIES FROM 9 TO 9.61 IN THE TEMPERATURE RANGE 25-70

VALUE INCREASES TO 793 WITH THE ADDITION OF 15 WT% LMZBS GLASS SHOWING A PERCENTAGE DEVIATION OF NEARLY 0.36%. HOWEVER, A VERSYNOGEDVALTHEOF CASE OF LBS GLASS WHERE THE RELATIVE PERMITTIVITY VARIES FROM 6.78-7.24 IN THE TEMPERATURE RANGE. THE PERCENTAGE DEVIATION FOR THE LBS GLASS IS NOTED AS 0.15. THE ADDITION OF GLASS INCREASES THIS IS DUE TO THE HIGH POSITIVE POSSESSED BY THE GLASSES. THE RESULTS SHOW THAT WITH SUITABLE AMOUNT OF GLASS CAN EFFECTIVELY LOWER THE SINTERING TEMPERATURE AND CAN BE EXPLOITED IN APPLICATIONS.

## 4.2 MICROWAVE DIELECTRIC PROPERTIES OF NOVEL RARE EARTH BASED SILICATES: $RE_2Ti_2SiO_9$ [RE = LA, PR, ND]

### 4.2.1 INTRODUCTION

THE GROWING IMPORTANCE OF CERAMICS DIELECTRICS FOR APPLICATIONS AS MICROWAVE OSCILLATORS, FILTERS ETC HAS LED TO GREAT ADVANCES IN THE MATERIAL RESEARCH OF NEW DIELECTRIC CERAMIC SYSTEMS. MANY MICROWAVE DIELECTRIC MATERIALS HAVE BEEN DEVELOPED AND MODIFIED ACCORDING TO THE NEEDS OF THE SPECIFIC APPLICATIONS. WITH RESPECT TO THE SPECIFIC MICROWAVE APPLICATIONS, THEY SHOULD POSSESS A RANGE OF PROPERTIES, INCLUDING APPROPRIATE RELATIVE PERMITTIVITY, HIGH QUALITY FACTOR, LOW TEMPERATURE COEFFICIENT OF RESONANT FREQUENCY [34]. THE NEED TO PRODUCE THE MATERIALS TO GET CERAMIC MATERIALS HAVING HIGH RELATIVE PERMITTIVITY (>20), HIGH QUALITY FACTOR, SMALL  $Q_f$  VALUE. RECENTLY AVAILABLE OVER THE WORLD WILL EXTEND COMMERCIAL APPLICATIONS OF DIELECTRIC RESONATORS TO MUCH HIGHER FREQUENCIES, BUT FURTHER DEVELOPMENT IS NEEDED.

NOW-A-DAYS, CONSIDERABLE ATTENTION HAS BEEN PAID ON MANY SILICATE MATERIALS FOR USE IN MICROWAVE APPLICATIONS [2, 16, 35-36]. SILICATES GENERALLY EXHIBIT LOW RELATIVE PERMITTIVITY AND ALSO A NEGATIVE VALUE OF TEMPERATURE COEFFICIENT OF RESONANT FREQUENCY. CERAMIC DIELECTRIC MATERIALS BASED ON TITANATES ARE IMPORTANT FOR VARIETY OF APPLICATIONS IN COMMUNICATION SYSTEMS [37]. SEVERAL TITANIUM BASED COMPOSITIONS WERE DEVELOPED. IT SHOWS A LOW  $Q_f$  ALSO FOR CERTAIN LOW LOSS DIELECTRIC MATERIALS SUITABLE AMOUNT OF GLASS ADDITION COULD TUNE TO NEAR ZERO VALUE. IN GENERAL, THESE COMPOSITIONS ARE MUCH EFFECTIVE FOR DEVELOPING MATERIALS WITH TEMPERATURE STABLE DIELECTRIC PROPERTIES.

CONTINUING THE RESEARCH ON SILICATE BASED DIELECTRIC MATERIALS, A STRONG INTEREST IN A NEW CLASS OF MATERIALS- RARE EARTH TITANOSILICATES HAS GROWN OVER THE CRYSTAL STRUCTURE TRIMOUNSITE WITH MONOCLINIC SYMMETRY. IT INCLUDES A NETWORK OF TETRAHEDRA CONNECTED BY TWO TYPES OF OCTAHEDRA [38-39]. AN IDEAL TRIMOUNSITE CRYSTAL STRUCTURE IS SHOWN IN FIG. 4.15.

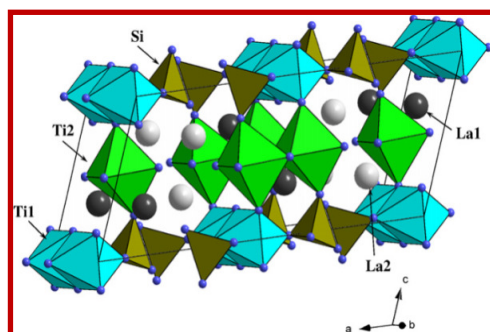


Fig. 4.15 Crystal structure of trimounsite.

UNLIKE PEROVSKITE TYPE STRUCTURES WHERE ALL OCTAHEDRA ARE CORNER SHARED, IN TRIMOUNSITE, POLYHEDRA IN  $\text{RE}_2\text{Ti}_2\text{SiO}_9$  SHARE THEIR EDGES. TWO NON-EQUIVALENT RE SITES EXISTING IN THIS STRUCTURE ARE LOCATED BETWEEN TIS. ALSO, THE LATTICE COMPRISES RELATIVELY LARGE CAVITIES BETWEEN METAL OXYGEN POLYHEDRA, WHICH ARE OCCUPIED BY INTERSTITIAL IONS. EARLIER REPORTS BY SWANSON [38] AND SWANSON [39] INVESTIGATED THREE MIXED VALENCE LA-TITANOSILICATES. HOWEVER, THE DIELECTRIC PROPERTIES OF THESE COMPOUNDS ARE UNKNOWN. THE PRESENT STUDY THROWS LIGHT INTO THE MICROWAVE DIELECTRIC PROPERTIES OF  $\text{RE}_2\text{Ti}_2\text{SiO}_9$  [RE=LA, PR AND ND]. THE EFFECT OF SUBSTITUTION IN THE RE-SITE ON THE STRUCTURE AND PROPERTIES ARE ALSO INVESTIGATED.

## 4.2.2 EXPERIMENTAL

THE  $\text{RE}_2\text{Ti}_2\text{SiO}_9$  [RE = LA, PR AND ND] (NAMED AS LTS, PTS AND NTS RESPECTIVELY) CERAMICS WERE PREPARED BY THE CONVENTIONAL SOLID STATE CERAMIC PROCESS EXPLAINED IN CHAPTER 2, SECTION 2.1.2. THE STARTING MATERIALS WERE HIGH PURITY  $\text{SiO}_2$  (ALDRICH CHEMICAL COMPANY INC., MILWAUKEE, WI; 99.999%),  $\text{TiO}_2$  (ALDRICH INC., ST. LOUIS, MO; 99.9%), RARE EARTH OXIDES,  $\text{La}_2\text{O}_3$ ,  $\text{Pr}_2\text{O}_3$ ,  $\text{Nd}_2\text{O}_3$  (IRE, 99.9 %) CHEMICALS. THE MIXED AND DRIED POWDERS WERE CALCINED AND THEN GROUND WELL IN AN



AGATE MORTAR. AFTER PELLETIZING, SINTERING WAS DONE IN THE TEMPERATURE RANGE FOR 2 HOURS. THE BULK DENSITIES OF THE POLISHED SAMPLES WERE MEASURED USING THE ARCHIMEDIAN METHOD.

THE SINTERED SAMPLES WERE POWDERED AND USED TO ANALYZE THE CRYSTAL STRUCTURE AND PHASE PURITY BY X-RAY DIFFRACTION METHOD AND THE SURFACE MORPHOLOGY OF POLISHED SAMPLES WAS RECORDED USING SCANNING ELECTRON MICROSCOPE. THE DIELECTRIC LOSS ( $\tan \delta$ ) AND  $Q_{uc}$  OF SINTERED AND POLISHED MATERIALS WERE MEASURED IN THE MICROWAVE FREQUENCY RANGE USING RESONANCE TECHNIQUE [42-44] AS DESCRIBED IN CHAPTER 2, SECTIONS 2.5.5.

### 4.2.3 RESULTS AND DISCUSSION

THE CALCINATION AND SINTERING TEMPERATURES OF THE RE- $\text{TiO}_2$  AND ND] DIELECTRIC CERAMICS ARE OPTIMIZED AT THE MAXIMUM DENSITY POINT AS DESCRIBED IN THE PREVIOUS SECTION. THE OPTIMIZED SINTERING TEMPERATURES OF THE RESPECTIVE MATERIALS ARE GIVEN IN TABLE 4.3. FIG. 4.16 SHOWS THE X-RAY DIFFRACTION PATTERNS OF RE- $\text{TiO}_2$  AND ND] SINTERED AT THEIR RESPECTIVE SINTERING TEMPERATURES. THE DIFFRACTION PATTERNS ARE INDEXED BASED ON THE EARLIER REPORTS [JCPDS FILE NO. 82-1490]. THEY BELONG TO THE SPACE GROUP C2/M (12) WITH MONOCLINIC SYMMETRY. THE CRYSTAL STRUCTURE OF RE- $\text{TiO}_2$  HAS BEEN REPORTED BY DIVAKAR. EARLY REPORTS BY KOLITSCH ET AL. INDICATE THAT IT IS DIFFICULT TO SYNTHESIZE, HOWEVER, IN THE PRESENT CASE NO SECONDARY PHASES WERE IDENTIFIED.

FIGURE 4.17 SHOWS THE XRD PATTERNS OF  $\text{La}_{1-x}\text{Nd}_x\text{TiO}_3$  AND  $\text{La}_{1-x}\text{Nd}_x\text{TiO}_3$  CERAMICS SINTERED AT 1275 °C. IT IS NOTED THAT  $\text{La}_{1-x}\text{Nd}_x\text{TiO}_3$  [X=0-2] FORMS A SINGLE PHASE COMPOSITION IN THE WHOLE RANGE. NO ADDITIONAL PHASES ARE DETECTED FROM THE DIFFRACTION DATA. ALL THE PEAKS CAN BE INDEXED BASED ON THE PARENT MATERIAL  $\text{LaTiO}_3$ . IT CAN BE CONCLUDED THAT THESE COMPOSITIONS FORM A SOLID SOLUTION. HOWEVER, IN THE CASE OF ND SUBSTITUTION FOR LA, THE PRESENCE OF ADDITIONAL PHASES OF ND

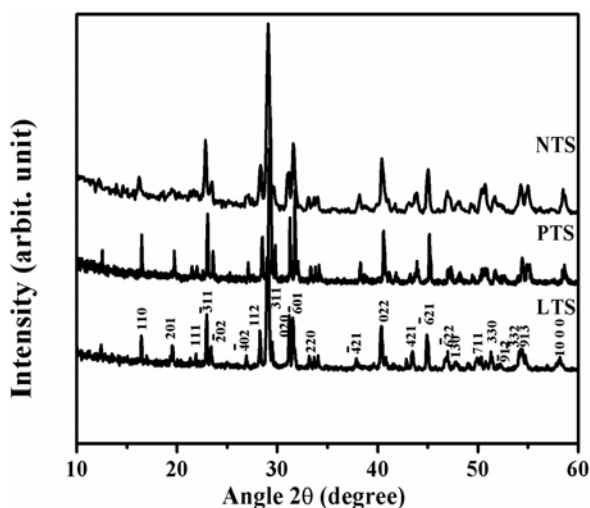


Fig. 4.16 XRD patterns of  $\text{La}_2\text{Ti}_2\text{SiO}_9$ ,  $\text{Pr}_2\text{Ti}_2\text{SiO}_9$ , and  $\text{Nd}_2\text{Ti}_2\text{SiO}_9$ .

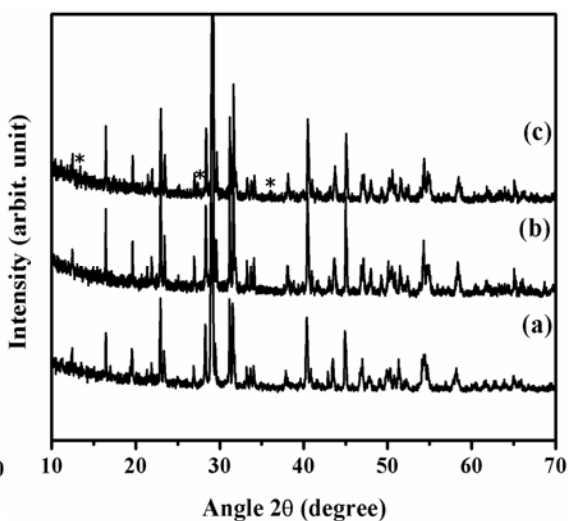


Fig. 4.17 XRD patterns of (a)  $\text{La}_2\text{Ti}_2\text{SiO}_9$ , (b)  $\text{LaPrTi}_2\text{SiO}_9$ , and (c)  $\text{LaNdTi}_2\text{SiO}_9$  (\* represents the  $\text{Nd}_2\text{Si}_2\text{O}_7$  phase).

Table 4.3 The optimized sintering temperatures, lattice parameters and the microwave dielectric properties of  $\text{RE}_2\text{Ti}_2\text{SiO}_9$ , [RE = La, Pr and Nd].

| Material | Sint. Temp            | Theo. density ( $\text{g}/\text{cm}^3$ ) | Lattice parameters |       |       |             | Microwave Dielectric Properties |              |  |
|----------|-----------------------|--|--------------------|-------|-------|-------------|---------------------------------|--------------|--|
|          |                       |  | a (Å)              | b (Å) | c (Å) | $\beta$ (°) | $Q_U X F$ (GHz)                 | $\epsilon_R$ | $\tau_f$ ( $\text{ppm}/^\circ\text{C}$ ) |
| LTS      | 1325 $^\circ\text{C}$ | 5.21                                     | 16.998             | 5.745 | 7.625 | 111.19      | 29500                           | 28.3         | 22.6                                     |
| PTS      | 1325 $^\circ\text{C}$ | 5.36                                     | 16.888             | 5.718 | 7.569 | 111.42      | 33700                           | 29.2         | 19.5                                     |
| NTS      | 1275 $^\circ\text{C}$ | 5.31                                     | 17.029             | 5.737 | 7.638 | 111.23      | 19600                           | 30.1         | 9.6                                      |

THE LATTICE PARAMETERS OF LTS, PTS AND NTS ARE CALCULATED FROM THE PATTERNS USING X'PERT PLUS SOFTWARE PACKAGE AND THE VALUES OBTAINED ARE LISTED IN TABLE 4.3. SINCE THE IONIC RADIUS DECREASES FROM LA TO ND, IT IS EXPECTED THAT THE LATTICE PARAMETERS MUST SHOW A REGULAR VARIATION IE., A DECREASE IN THE LATTICE PARAMETERS. HOWEVER, IN THE PRESENT CASE EVEN THOUGH A DECREASE IS NOTED IN THE CASE OF PTS, THE LATTICE PARAMETERS SHOW AN INCREASE FOR NTS. FIG. 4.18 SHOWS THE VARIATION OF THE LATTICE PARAMETERS OF THE  $\text{RE}_2\text{Ti}_2\text{SiO}_9$ , [A=PR, ND; X=0, 0.5, 1, 1.5, 2] SOLID SOLUTIONS AS A FUNCTION OF X. THE LATTICE PARAMETERS VARY LINEARLY AS THE X VALUE INCREASES.

$\text{La}_{2-x}\text{Pr}_x\text{Ti}_2\text{SiO}_9$  COMPOSITIONS WHICH CONFIRM THAT THE PR SUBSTITUTED SOLID SOLUTION SATISFIES THE VEGARD'S LAW. IT IS SEEN THAT AS PR SUBSTITUTION FOR LA INCREASES, THE LATTICE PARAMETERS (A, B AND C) DECREASE IN A LINEAR FASHION WHICH IS DUE TO THE LOW VALUE OF IONIC RADIUS OF PR WHEN COMPARED WITH THAT OF LA [45-46]. HOWEVER, IN THE CASE OF ND CONTAINING SOLID SOLUTION, A LINEAR VARIATION IN THE LATTICE PARAMETERS IS NOT OBSERVED IN THE RANGE  $0 < x < 1.5$ . THUS UPTO THIS COMPOSITION ( $x = 1.5$ ) VEGARD'S LAW IS OBEYED AND BEYOND THAT AN INCREASE IN THE VALUES ARE NOTED.

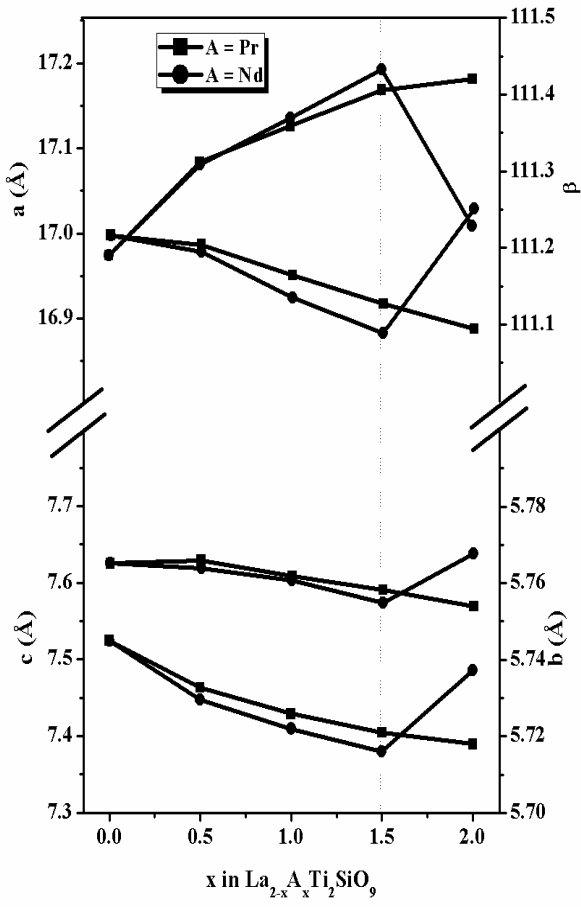


Fig. 4.18 Variation of lattice parameters of  $\text{La}_{2-x}\text{A}_x\text{Ti}_2\text{SiO}_9$  [A= Pr and Nd] with x.

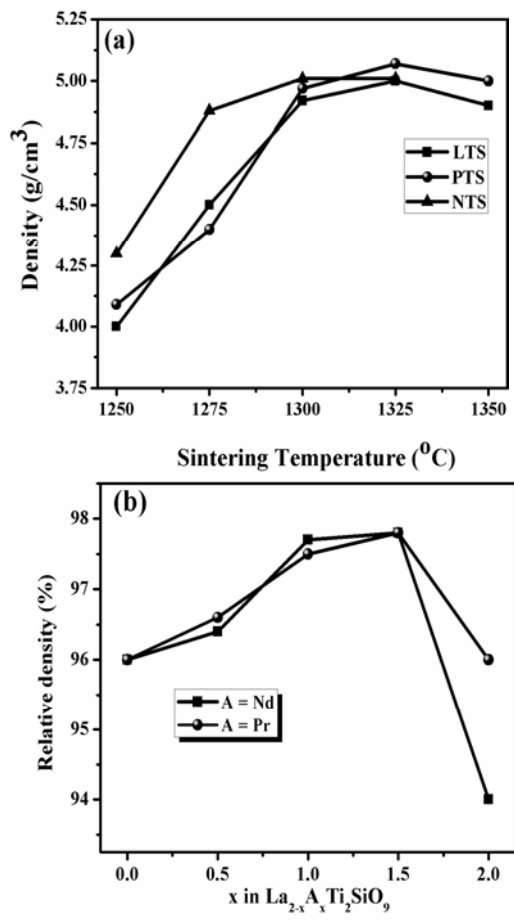


Fig. 4.19 The variation of (a) density of  $\text{RE}_2\text{Ti}_2\text{SiO}_9$  [RE=La, Pr and Nd] with sintering temperature and (b) relative density with composition x.

FIGURE 4.19 (A) SHOWS THE VARIATION OF THE BULK DENSITY OF PR AND ND] CERAMICS WITH SINTERING TEMPERATURE. IT IS SEEN THAT AS THE SINTERING

INCREASES THE DENSITY ALSO INCREASES, REACHES A MAXIMUM AND THEN DECREASES. THIS IS DUE TO THE ELIMINATION OF PORES WITH INCREASE IN THE SINTERING TEMPERATURE. THEORETICAL DENSITIES OF THE MATERIALS ARE GIVEN IN TABLE 4.3. THE SINTERING TEMPERATURES OF THE RESPECTIVE COMPOUNDS ARE OPTIMIZED AT THEIR MAXIMUM DENSITY POINT. THE RELATIVE DENSITY INCREASES TO ABOUT 96%, 95% AND 94% OF THE THEORETICAL DENSITIES FOR LTS, PTS AND NTS CERAMICS RESPECTIVELY AT THEIR OPTIMIZED SINTERING TEMPERATURES. FROM FIGURE 4.20 (B) IT IS SEEN THAT THE RELATIVE DENSITY INCREASES GRADUALLY WITH INCREASE IN X IN PTS AND PR. THE RELATIVE DENSITY INCREASES FROM 96 - 97.8 % IN THE CASE OF BOTH PR AND NTS BASED SOLID SOLUTIONS IN THE RANGE 0 <math>x < 2</math>. HOWEVER, AT  $x = 2$ , FOR PTS AND NTS A SUDDEN DECREASE IN THE RELATIVE DENSITY IS NOTED.

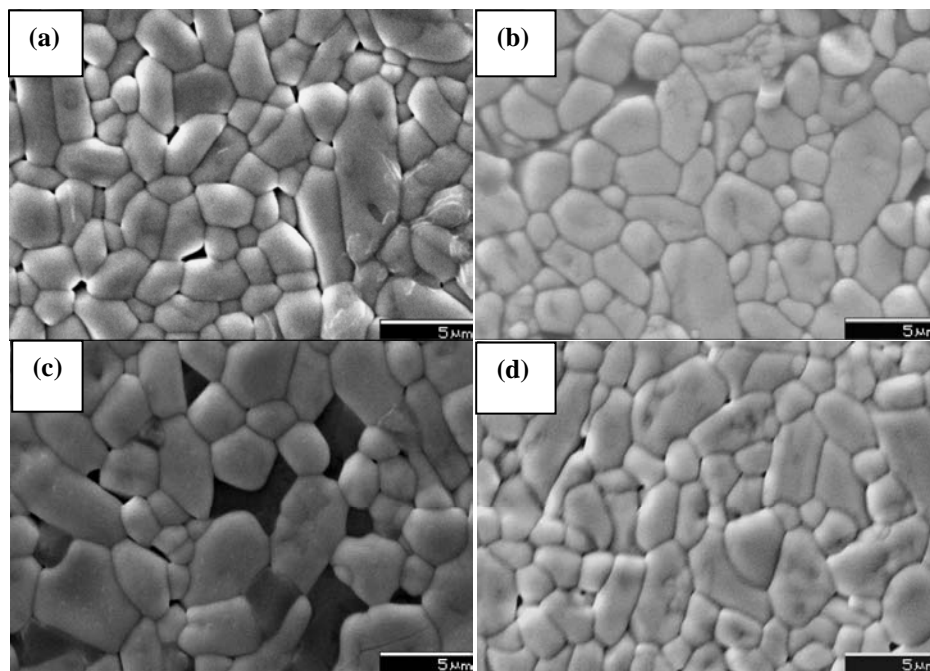


Fig. 4.20 The SEM pictures of (a) LTS, (b) PTS, (c) LNTS and (d) LPTS sintered at 1325°C.

FIGURES 4.20 (A) AND (B) SHOW THE SEM IMAGES OF THE POLISHED AND THERMALLY ETCHED LTS AND PTS RESPECTIVELY SINTERED AT 1325°C. BOTH THE IMAGES SHOW A WELL PACKED SYSTEM WITH GRAIN SIZE VARYING FROM 1-5 μM. NO OBVIOUS PORES AND UNBURNED GRAINS ARE OBSERVED IN THE SEM IMAGES WHICH CONFIRM GOOD DENSIFICATION. FIGURE 4.20 (C) AND (D) RESPECTIVELY SHOWS THE MICROSTRUCTURES OF LNTS AND LPTS SINTERED AT 1325°C.

THE PRESENCE OF SECONDARY PHASE IN LNTS IS EVIDENT FROM THE SEM IMAGE (FIG. 4.20). IT IS ALSO NOTED THAT THE LOW-SMELTING PHASE FORMED APPEARED AS A LIQUID PHASE WHICH IN TURN IMPROVED THE DENSIFICATION OF THE MATERIAL. FIG. 4.20 (D) SHOWS PACKED ARRANGEMENT OF GRAINS FOR THE SOLID SOLUTION LPTS.

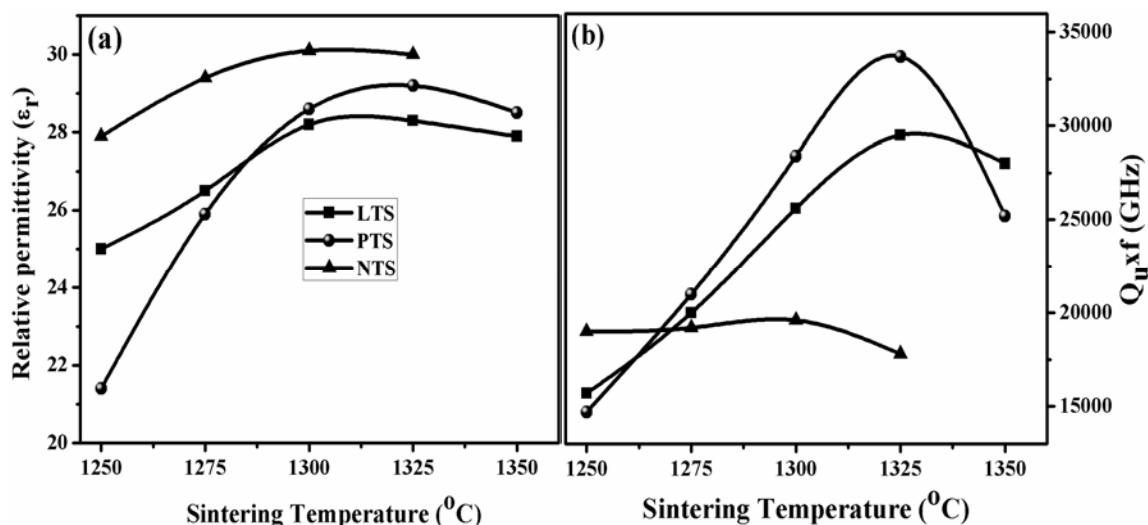


Fig. 4.21 The variation of (a) relative permittivity and (b)  $Q_{uxf}$  of  $\text{RE}_2\text{Ti}_2\text{SiO}_9$  [RE=La, Pr and Nd] with sintering temperature.

FIGURE 4.21 SHOWS THE VARIATION OF THE DIELECTRIC PROPERTIES OF RE [RE=LA, PR AND ND] CERAMICS WITH THE SINTERING TEMPERATURE. THE RELATIVE PERM THE CERAMICS INCREASES WITH INCREASE IN THE SINTERING TEMPERATURES AND SAT FROM FIG. 4.21 (A). THE RELATIONSHIP BETWEEN RELATIVE PERMITTIVITY AND S TEMPERATURES REVEAL THE SAME TENDENCY WITH THAT BETWEEN DENSITY VALUES A TEMPERATURES, BECAUSE HIGHER SINTERING TEMPERATURES WILL CAUSE THE GRAI MINIMUM PORES LEADING TO HIGHER. VALUES OF RELATIVE PERMITTIVITY IS MAXIMUM AT THE TEMPERATURE WHERE THE BULK DENSITY SHOWED A MAXIMUM OR CONSISTENT VA PTS AND NTS RESPECTIVELY SHOW A RELATIVE PERMITTIVITY OF 28.3, 29.2 AND 30.1 AT OPTIMIZED SINTERING TEMPERATURES. SINCE NO ADDITIONAL SECONDARY PHASES ARE XRD, THIS IS CORRELATED WITH THE DECREASE IN DENSITY AT HIGHER TEMPERATURES. SHOWS THE  $Q_{uxf}$  VALUES OF LTS, PTS AND NTS CERAMICS AS A FUNCTION OF SINTERI TEMPERATURES. AS THE SINTERING TEMPERATURE INCREASES, THE QUALITY FACTOR AL

REACHES A MAXIMUM VALUE AND FURTHER INCREASE IN THE SINTERING TEMPERATURE INCREASES THE  $Q$ -FACTOR. THE MICROWAVE DIELECTRIC LOSS IS AFFECTED BY BOTH INTRINSIC AND EXTRINSIC FACTORS [47]. THE MICROWAVE DIELECTRIC LOSS INCREASES DRASTICALLY WHEN THE LATTICE DEFECTS ARE A DISORDERED DISTRIBUTION OF THE CHARGES WHICH DEVIATE FROM PERFECT LATTICE ORDER [48]. A MAXIMUM  $Q$  VALUE OF 33700 GHZ IS SHOWN BY PNTS AT A SINTERING TEMPERATURE OF 1325°C. THE NTS CERAMICS EXHIBITED THE LOWEST QUALITY FACTOR OF 19600 GHZ AT 1275°C.

FIGURE 4.22 SHOWS THE VARIATION OF MICROWAVE DIELECTRIC PROPERTIES OF  $x\text{A}_x\text{Tl}_2\text{SiO}_9$  [A=PR, ND; X=0, 0.5, 1, 1.5, 2] AS A FUNCTION OF X. IT IS CLEAR FROM FIG. 4.22 (A) THAT THE RELATIVE PERMITTIVITY IS LINEARLY DEPENDENT ON THE X VALUE IE., RELATIVE PERMITTIVITY INCREASES WITH INCREASE IN X FOR BOTH PR AND ND. THE RELATIVE PERMITTIVITY INCREASES FROM 28.3 TO 29.2 AND 28.3 TO 30.1 RESPECTIVELY FOR PR AND ND BASED SOLUTIONS. THE RELATIVE PERMITTIVITIES OF THE CERAMICS DEPEND ON THE RELATIVE PERMITTIVITY ALSO ON THE IONIC POLARIZABILITY ACCORDING TO THE IONIC POLARIZABILITY VALUE REPORTED BY VINEIS, THE  $\text{La}^{3+}$  ION (4.82 Å) IS SMALLER THAN THAT OF PR (5.32 Å) AND ND ION (5.01 Å<sup>3</sup>) [49]. THUS WITH THE SUBSTITUTION OF PR OR ND FOR LA, AN INCREASE IN THE RELATIVE PERMITTIVITY IS NOTED WHICH IS DUE TO THE INCREASE IN THE IONIC POLARIZABILITY. RELATIVE PERMITTIVITY OF A CERAMIC IS VERY MUCH AFFECTED BY EXTRINSIC FACTORS LIKE POROSITY. THE RELATIVE PERMITTIVITY IS CORRECTED FOR POROSITY USING EQ. (3.3) IN CHAPTER 3. THE POROSITY CORRECTED RELATIVE PERMITTIVITY CALCULATED USING THE ABOVE EQUATION IS PLOTTED AS A FUNCTION OF X IN FIG. 4.22 (B), WHICH VARIES FROM 30 - 31.7 IN THE CASE OF PR  $x\text{A}_x\text{Tl}_2\text{SiO}_9$  AND FROM 30 - 32.8 FOR ND  $x\text{A}_x\text{Tl}_2\text{SiO}_9$ . THE DIFFERENCE BETWEEN  $\epsilon_r$  AND  $\epsilon_{corr}$  DECREASES WITH X UPTO X=1 AND BEYOND THIS VALUE THE DEVIATION INCREASES SHOWING THE DOMINANT EFFECT OF POROSITY ON THE RELATIVE PERMITTIVITY OF THE CERAMICS.

FIGURE 4.22 (B) SHOWS THE COMPOSITIONAL DEPENDENCE OF QUALITY FACTOR OF  $x\text{A}_x\text{Tl}_2\text{SiO}_9$  [A=PR, ND; X=0, 0.5, 1, 1.5, 2] CERAMICS. IT IS TO BE NOTED THAT AT X = 0.5, THE QUALITY FACTOR DECREASES FOR BOTH A=PR AND ND. IN THE CASE OF LA, THE QUALITY FACTOR GRADUALLY INCREASES AND REACHES A MAXIMUM AT X = 2 WITH A VALUE OF 33700 GHZ. IT IS INTERESTING TO NOTE THAT THE QUALITY FACTOR INCREASES WITH X DESPITE THE FACT THAT A DECREASE IN THE DENSITY IS NOTED AT X=2. HOWEVER, THE LA CERAMICS EXHIBIT ALMOST A CONSTANT  $Q$  IN THE RANGE 0.5 < X < 2. IN VIEW OF THE

CRYSTAL PHASES AND MICROSTRUCTURES, THE VARIATIONS OF THE DIELECTRIC PROPERTIES WITH COMPOSITIONAL CONTENT MAY BE ATTRIBUTED TO THE CHANGE OF PHASE RELATIONS AND MICROSTRUCTURES. THE SUBSTITUTION OF ND FOR LA. THE DIELECTRIC LOSS OF THE PERFECT CRYSTALS AT A GIVEN FREQUENCY IS CONSIDERED TO ORIGINATE FROM THE ANHARMONIC LATTICE FORCES DUE TO THE INTERACTION BETWEEN CRYSTAL'S PHONONS.

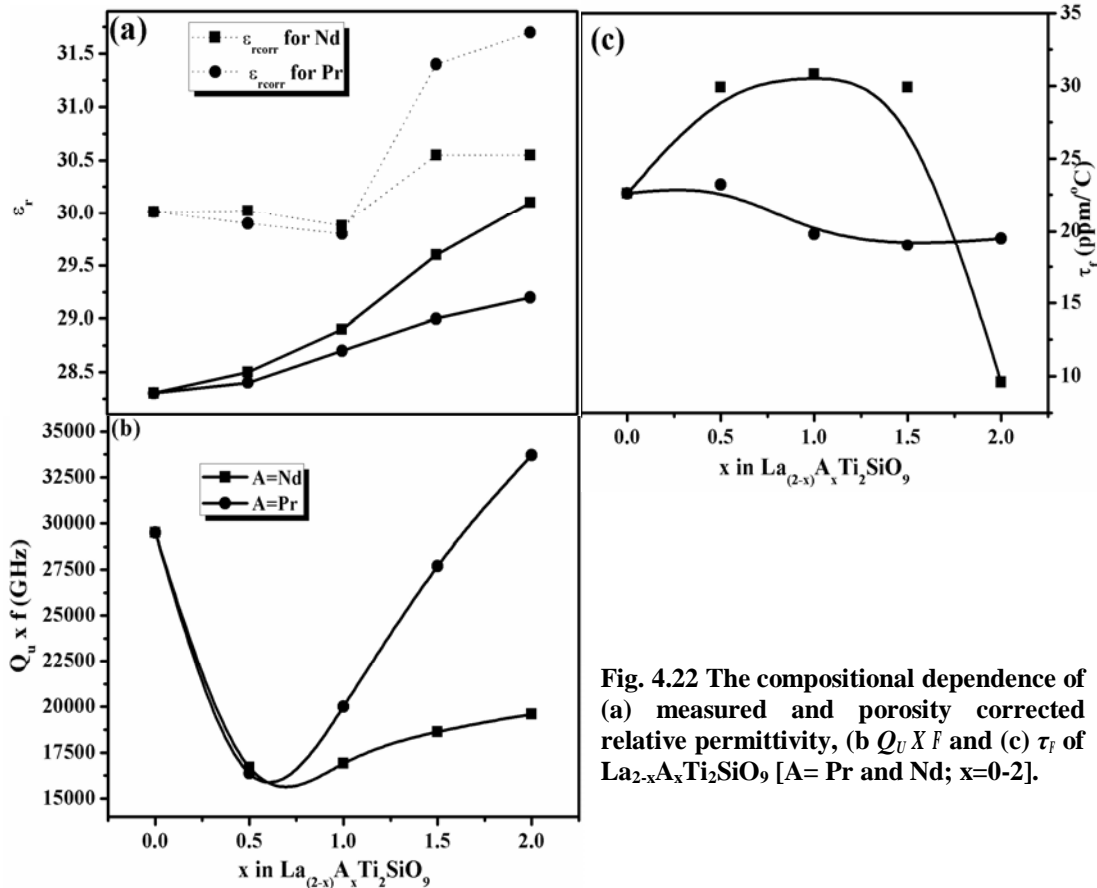


Fig. 4.22 The compositional dependence of (a) measured and porosity corrected relative permittivity, (b)  $Q_u \times f$  and (c)  $\tau_r$  of  $\text{La}_{2-x}\text{A}_x\text{Ti}_2\text{SiO}_9$  [A= Pr and Nd; x=0-2].

FIG. 4.22 (C) SHOWS THE VARIATION OF  $\tau_r$  FOR BOTH PR AND ND SUBSTITUTION FOR LA. IN THE CASE OF PR SUBSTITUTED COMPOSITIONS,  $\tau_r$  REMAINS ALMOST CONSTANT WITH X WHILE FOR ND SUBSTITUTION, A NON-LINEAR REDUCTION IN  $\tau_r$  IS OBSERVED, WHICH IS BEING RELATED WITH THE TEMPERATURE COEFFICIENT OF RELATIVE PERMITTIVITY EXPANSION COEFFICIENT OF WHICH THE VALUE IS APPROXIMATELY 10 PPM/°C. [5] DIELECTRIC CERAMICS [5] HAVE INVESTIGATED THE INTERRELATIONSHIP BETWEEN CRYSTAL STRUCTURE, DYNAMICS AND SUGGESTED THAT  $\tau_r$  OF THESE CERAMICS VARIES LINEARLY AS A FUNCTION OF UNIT CELL VOLUME. THESE CERAMICS HAVE A MINIMUM VALUE OF ABOUT 9.6 PPM/°C.

FOR  $X = 2$ . THUS IT CAN BE CONCLUDED THAT WHILE PR BASED SOLID SOLUTION IMPROVED THE QUALITY FACTOR, THE ND SUBSTITUTION IMPROVED THE

### 4.3 CONCLUSIONS

- ❖ THE SYNTHESIS AND MICROWAVE DIELECTRIC PROPERTIES OF TWO NEW RARE EARTH SILICATES ( $\text{RE}_2\text{SiO}_7$  AND  $\text{RE}_2\text{Ti}_2\text{SiO}_9$  [RE=LA, PR AND ND]) ARE INVESTIGATED IN THIS CHAPTER. THE DIELECTRIC CERAMICS ARE PREPARED BY SOLID STATE CERAMIC ROUTE. THEIR STRUCTURE AND MICROSTRUCTURE ARE DETERMINED USING XRD AND SEM TECHNIQUE RESPECTIVELY. THE  $\text{La}_2\text{SiO}_7$  CERAMICS IS ALSO SYNTHESIZED BY SOL-GEL TECHNIQUE TO OBTAIN NANO POWDERS. THE  $\text{La}_2\text{SiO}_7$  CERAMICS REVEALED A TETRAGONAL SYMMETRY WHEREAS  $\text{Pr}_2\text{SiO}_7$  HAS A MONOCLINIC STRUCTURE.
- ❖ THE DIELECTRIC PROPERTIES OF THESE TWO SILICATE BASED SYSTEMS ARE INVESTIGATED FOR THE FIRST TIME. THE  $\text{La}_2\text{SiO}_7$  CERAMIC POSSESS A RELATIVE PERMITTIVITY OF 12.5 AND DIELECTRIC LOSS OF 0.0008 AT 1 MHZ AT A SINTERING TEMPERATURE OF 1375 °C. AT MICROWAVE FREQUENCY, A LOW RELATIVE PERMITTIVITY OF 10 AND A LOSS FACTOR OF 0.0009 IS OBTAINED.
- ❖ THE SINTERING TEMPERATURES ARE LOWERED BY THE ADDITION OF SEVERAL LOW LOSS GLASSES. IT IS FOUND THAT LBS BASED GLASSES ARE MORE EFFECTIVE IN LOWERING THE SINTERING TEMPERATURE WITHOUT AFFECTING THE DIELECTRIC PROPERTIES. ADDITION OF 15 WT% LBS GLASS REDUCES THE SINTERING TEMPERATURE TO 975 °C WITH  $\epsilon_r$  OF 9.89 AND  $\tan \delta$  OF 0.024 WHEREAS 15 WT% LMZBS GLASS ADDITION DECREASES THE SINTERING TEMPERATURE TO 950 °C WITH  $\epsilon_r = 9.09$  AND  $\tan \delta = 0.009$ .
- ❖ THE SOL-GEL SYNTHESIZED  $\text{La}_2\text{SiO}_7$  CERAMICS RESULTED IN NANO POWDERS WHOSE CALCINATION TEMPERATURE IS MUCH LOWERED TO 900 °C. THE DIELECTRIC PROPERTIES OF NANO  $\text{La}_2\text{SiO}_7$  CERAMICS ARE NOT MUCH PROMISING WHICH IS DUE TO THE LOW DENSIFICATION ACHIEVED.
- ❖ THE  $\text{RE}_2\text{Ti}_2\text{SiO}_9$  [RE = LA, PR AND ND] CERAMICS HAVE A RELATIVE PERMITTIVITY LESS THAN 20 AND RELATIVELY LOW MAXIMUM VALUE OF 33700 GHZ IS SHOWN BY  $\text{Pr}_2\text{Ti}_2\text{SiO}_9$  CERAMICS WITH 29.2 AND  $\tau_f = 19.5$  PPM/°C. THE MICROWAVE DIELECTRIC PROPERTIES OF [RE= LA, ND] CERAMICS ARE



RESPECTIVELY  $f = 29500$  GHZ AND  $19600$  GHZ,  $Q = 28.3$  AND  $30.1$  AND  $Q = 22.6$  AND  $9.6$  PPM.

- ❖ IT IS SEEN THAT PR SUBSTITUTION FOR LA FAVORED THE FORMATION OF SOLID SOLUTIONS IN THE WHOLE RANGE WHILE ND SUBSTITUTION RESULTED IN THE FORMATION OF ADDITIONAL PHASES. AS THE PR CONTENT INCREASES, AN IMPROVEMENT IN THE QUALITY FACTOR IS NOT OBSERVED. THE  $Q$  VALUE IS NOT MUCH AFFECTED.

## 4.4 REFERENCES

1. Y. GUO, H. OHSATO AND K.-I. KAKIMOTO, *Ceram. Soc.*, **26**, 1827-1830, (2006).
2. H. OHSATO, T. TSUNOOKA, T. SUGIYAMA, K. KAKIMOTO AND H. OGAWA, *J. Am. Ceram. Soc.*, **17**, 445-450, (2006).
3. J. FELSCH, *Structure and Bonding*, **13**, 99-197, (1973).
4. U. KOLITSCH, V. IJEVSKII, H. J. SEIFERT, I. WIEDMANN AND J. MAEDINGER, *J. Solid State Chem.*, **161**, 6135-6139, (1997).
5. M. E. FLEET AND X. LI, *Solid State Chem.*, **161**, 166-172, (2001).
6. M. E. FLEET AND X. Y. LI, *Acta Crystallogr., SECT. B: STRUCT. SCIENCE*, **56**, 940-946, (2000).
7. M. E. FLEET AND X. Y. LI, *Am. Mineral.*, **89**, 396-404, (2004).
8. J. LORIER, G. BOCQUILLON, C. CHATEAU AND M. GORAI, *Phys. Rev. B*, **12**, 403-413, (1977).
9. A. I. BECERRO, A. ESCUDERO, P. FLORIAN, D. MASSIOT AND S. ALBAIGES, *J. Solid State Chem.*, **177**, 2783-2789, (2004).
10. H. J. ITO, *Am. Mineral.*, **53**, 1940-1952, (1968).
11. Z. L. HONG, H. YOSHIDA, Y. IKUHARA, T. SAKUMA, T. NISHIMURA AND M. MITOMO, *Ceram. Soc.*, **22**, 527-534, (2002).
12. C.-L. HUANG AND J.-F. TSENG, *Eng. Lett.*, **58**, 3732-3736, (2004).
13. A. J. BOSMAN AND E. E. HAVENBERG, *Phys. Rev.*, **129**, 1593, (1963).
14. M. Z. DONG, Z. X. YUE, H. ZHUANG, S. Q. MENG AND L. TAN, *J. Am. Ceram. Soc.*, **91**, 3981-3985, (2008).
15. Y.-L. CHAI, Y.-S. CHANG, Y.-J. HSIAO AND Y.-C. MIAN, *Res. Bull.*, **43**, 257-263, (2008).
16. S. GEORGE, P. S. ANJANA, V. N. DEEPU, P. MOHANAN AND M. T. SEBASTIAN, *Soc.*, **92**, 1244-1249, (2009).
17. Y. IMANAKA, *Multilayered Low Temperature Cofired Ceramics (LTCC) Technology*, SPRINGER SCIENCE, U.S.A., (2005).
18. J. H. JEAN AND T. K. GUPTA, *Water. Res.*, **10**, 1312-1320, (1995).
19. Y. J. CHOI, J. H. PARK, W. J. KO, I. S. HWANG, J. G. PARK AND S. NAHM, *J. Am. Ceram. Soc.*, **89**, 562-567, (2006).
20. T. TAKADA, S. F. WANG, S. YOSHIKAWA, S. J. JANG AND R. E. NEWNHAM, *J. Am. Ceram. Soc.*, **77**, 1909-1916, (1994).
21. P. LIU, E. S. KIM AND K. H. YOON, *J. Appl. Phys. Part 1*, **40**, 5769-5773, (2001).
22. M. Z. JHOU AND J. H. JEAN, *J. Am. Ceram. Soc.*, **89**, 786-791, (2006).

23. X. CUI AND J. ZHONG, *Mater. Res. Bull.*, **43**, 1590-1597, (2008).
24. O. DERNOVSEK, A. NAEINI, G. PREU, W. WERSING, M. EBERSTEIN AND M. SCHILLER, *Ceram. Soc.*, **21**, 1693-1697, (2001).
25. K. P. SURENDRAN, P. MOHANAN AND M. T. SEBASTIAN, *Chem.*, **177**, 4031-4046, (2004).
26. T. HU, J. JUUTI, H. JANTUNEN AND T. VILKMAN, *Ceram. Soc.*, **27**, 3997-4001, (2007).
27. M. R. JOUNG, J. S. KIM, M. E. SONG, D. S. PAIK, S. NAHM, J. H. PAIK AND B. H. CHOI, *Am. Ceram. Soc.*, **91**, 4165-4167, (2008).
28. S. M. RHIM, S. HONG, H. BAK AND O. K. KIM, *Ceram. Soc.*, **83**, 1145-1148, (2000).
29. J.-M. WU AND H.-L. HUANG, *Non-Crystal. Solids*, **260**, 116-124, (1999).
30. S. N. SALAMA, S. M. SALMAN AND H. DEGRISH, *Int.*, **21**, 159-167, (1995).
31. I. C. HO, *J. Am. Ceram. Soc.*, **77**, 829-832, (1994).
32. T. TAKADA, H. YAMAMOTO AND K. KAGEYAMA, *Appl. Phys. Part 1*, **42**, 6162-6167, (2003).
33. S.-H. WANG AND H.-P. ZHONG, *Mater. Sci. Eng. B*, **99**, 597-600, (2003).
34. M. T. SEBASTIAN, *Dielectric Materials for Wireless Communication*, ELSEVIER SCIENCE PUBLISHERS, OXFORD, (2008).
35. S. THOMAS AND M. T. SEBASTIAN, *Ceram. Soc.*, **92**, 2975-2981, (2009).
36. T. JOSEPH, M. T. SEBASTIAN, H. SREEMOOLANADHAN AND V. K. NAGESHWARI, *Ceram. Technol.*, **7**, E98-E106, (2010).
37. R. J. CAVALLI, *Mater. Chem.*, **11**, 54-62, (2001).
38. U. KOLITSCH, *Ch. J. Mineral.*, **13**, 761-768, (2001).
39. Y. V. PIVAK, V. V. KHARTON, E. N. NAUMOVICH, J. R. FRADE AND F. M. MARQUES, *State Chem.*, **180**, 1259-1271, (2007).
40. S. WANG AND S. J. HWU, *Am. Chem. Soc.*, **114**, 6920-6922, (1992).
41. S. WANG, S.-J. HWU, J. A. PARADIS AND M.-H. WHANGBO, *Chem. Soc.*, **117**, 5515-5522, (1995).
42. B. W. HAKKI AND P. D. COLEMAN, *Trans. Microwave Theory Tech.*, **8**, 402-410, (1960).
43. J. KRUPKA, K. DERZAKOWSKI, B. RIDDLE AND J. BAKER-JARVIS, *Technol.*, **9**, 1751-1756, (1998).
44. W. E. COURTNEY, *IEEE Trans. Microwave Theory Tech.*, **MTT-18**, 476-485 (1970).
45. R. D. SHANNON, *Acta Crystallogr.*, **A32**, 751-757, (1976).
46. Y. KONISHI, *Techn. Rep.*, (1971).

47. W. S. KIM, T. H. KIM, E. S. KIM AND K. H. YOON, *J. Appl. Phys. Part 1*, **37**, 5367-5371, (1998).
48. E. SCHLÖMANN, *Phys. Rev.*, **135**[2A], A413-A419 (1964).
49. C. VINEIS, P. K. DAVIES, T. NEGAS AND S. BELLE, *Met. Res. Bull.*, **31**, 431-437, (1996).
50. A. KAN, H. OGAWA, K. MORI AND J. SUGIMOTO, *Met. Res. Bull.*, **37**, 1509-1518, (2002).
51. H.-J. LEE, K.-S. HONG, S.-J. KIM AND I.-T. KIM, *Met. Res. Bull.*, **32**, 847-855, (1997).

## CHAPTER 5

### **POLYMER-CERAMIC COMPOSITES FOR MICROELECTRONIC APPLICATIONS**

*This chapter describes in detail the synthesis and characterization of various polymer-ceramic composites with  $\text{Sm}_2\text{Si}_2\text{O}_7$  as filler. The polymers used for the present study are Polytetrafluoroethylene (PTFE), Polyethylene (PE) and Polystyrene (PS). These composites are prepared by two different methods:- powder processing and melt mixing methods. The dielectric properties (at 1 MHz and 9 GHz), thermal and mechanical properties of these composites are investigated. The effect of coupling agent and the filler size on these properties are also investigated for PTFE/ $\text{Sm}_2\text{Si}_2\text{O}_7$  composites. Various theoretical models are used to calculate the effective relative permittivities of the composites and are compared with the experimentally observed results.*

## 5.1 INTRODUCTION

THE EVER INCREASING DEMAND FOR HIGH PERFORMANCE ELECTRONIC DEVICES NEEDS NEW MATERIALS TO BE USED AS CIRCUIT BOARD LAMINATES THAT POSSESS SUPERIOR PROPERTIES COMPARED TO THE CONVENTIONALLY USED ONES. THESE MATERIALS SHOULD SATISFY THE REQUIREMENTS SUCH AS LOW RELATIVE PERMITTIVITY TO REDUCE THE SIGNAL PROPAGATION DELAY, DIELECTRIC LOSS FOR BETTER DEVICE PERFORMANCE, HIGH THERMAL CONDUCTIVITY TO REMOVE HEAT GENERATED, LOW OR MATCHING THERMAL EXPANSION COEFFICIENT WITH THE CERAMIC, MOISTURE ABSORPTION RESISTANCE, HIGH DIMENSIONAL STABILITY AND MECHANICAL STRENGTH [2]. IN COMMERCIAL HIGH FREQUENCY SUBSTRATES, BASED ON COMPLEX COMPOSITES OF CERAMIC OR WOVEN QUARTZ FILLERS AND HYDROCARBON RESINS OR GLASS MICROFIBERS MATRIX, IT IS DIFFICULT TO FIND TEMPERATURE COMPENSATING MATERIALS WITH LOW RELATIVE PERMITTIVITY AND LOW DIELECTRIC LOSS [3-4]. THEY ARE BRITTLE AND NEED TO BE SINTERED AT HIGH TEMPERATURES. THESE REASONS, THE APPLICATION OF AN INDIVIDUAL CERAMIC IS GREATLY RESTRICTED IN MANY ASPECTS. POLYMERIC MATERIALS PLAY A VITAL ROLE IN ELECTRONIC PACKAGES AS A RESULT OF EASE OF PROCESSING, LOW COST, LOW RELATIVE PERMITTIVITY, ADHESIVE PROPERTIES AND POOR THERMAL AND MECHANICAL PROPERTIES. THUS THE POLYMER/CERAMIC COMPOSITES WHERE THE CERAMIC FILLERS ARE DISPERSED IN THE POLYMER MATRIX PROVIDE A NEW ROUTE TO COMBINE THE MERITS OF CERAMICS AND THE POLYMERS. THEY UTILIZE THE THERMAL PROPERTIES AND PROCESSABILITY OF POLYMERS.

AMONG THE VARIOUS POLYMERS USED COMMERCIAL POLYETHYLENE TEREPHTHALATE (PET) HOLDS A RELEVANT POSITION DUE TO THE SUPERIOR DIELECTRIC PROPERTIES AND EXCELLENT INERTNESS [2, 5]. PTFE HAS A HIGH VIRGIN CRYSTALLINE MELTING POINT AND EXTREMELY HIGH SHEAR VISCOSITY AT 380°C IN THE MELT [6]. IT HAS A LOW RELATIVE PERMITTIVITY OF NEARLY 2.1 AND EXTREMELY LOW DIELECTRIC LOSS WHICH IS IDEAL FOR A WIDE RANGE OF FREQUENCIES [7]. THE LOW LOSS TANGENT IS A CONSEQUENCE OF THE SINGULAR CONFORMATION OF THE POLYMER BACKBONE, WHICH EFFECTIVELY NEUTRALIZES THE DIPOLE MOMENT OF THE C-F BONDS YIELDING A NET ZERO DIPOLE MOMENT [8]. HOWEVER, THE HIGH VOLUME COEFFICIENT OF THERMAL EXPANSION (CTE), LOW THERMAL CONDUCTIVITY AND POOR STRESS RELIEF RESTRICT THE WIDER USAGE OF PTFE AS SUCH FOR MICROELECTRONIC PACKAGING. MANY STUDIES WERE CONDUCTED TO IMPROVE BOTH THE MECHANICAL AND DIELECTRIC PROPERTIES OF PTFE BY SUITABLE FILLER INCORPORATION [6, 9]. IT IS REPORTED THAT PTFE FILLED WITH

60 WT% SiO<sub>2</sub> FILLER LOWERED THE COEFFICIENT OF THERMAL EXPANSION WITH DESIRABLE PROPERTIES [13]. THE ADDITION OF ZnO-Nb<sub>2</sub>O<sub>5</sub> FILLERS INTO THE PTFE MATRIX SHOWED GOOD FREQUENCY STABILITY OF RELATIVE PERMITTIVITY OVER A WIDE RANGE AND A GOOD AGREEMENT WITH THE PERCOLATION THEORY [14]. IN ORDER TO DEVELOP SUITABLE COMPOSITES FOR HIGH FREQUENCY APPLICATIONS, THE PRIME REQUIREMENT IS A FILLER HAVING LOW RELATIVE PERMITTIVITY, LOW DIELECTRIC LOSS, HIGH THERMAL CONDUCTIVITY AND GOOD THERMAL STABILITY.

ALTHOUGH THE POWDER PROCESSING METHOD FOR THE SYNTHESIS OF PTFE-BASED COMPOSITES IS SIMPLE, THE FINAL DENSITY OF THE COMPOSITES IS RATHER POOR DUE TO THE PRESENT AMOUNT OF POROSITY. THIS CAN BE IMPROVED BY ADOPTING NEW PREPARATION METHODS SUCH AS MOLTEN MELT MIXING OR SIGMA BLENDING TECHNIQUE. HOWEVER, IN ORDER TO FABRICATE PTFE-BASED COMPOSITES, HIGH TEMPERATURES ARE REQUIRED, ALSO PTFE HAS VERY HIGH VISCOSITY COMPARED TO OTHER THERMOPLASTIC POLYMERS LIKE POLYETHYLENE OR POLYSTYRENE. POLYETHYLENE AND POLYETHYLENE ARE NON POLAR POLYMERS WITH A LOW MELTING POINT OF APPROXIMATELY 100°C. THESE POLYMERS POSSESS A LOW RELATIVE PERMITTIVITY OF 2.6 AND 3.2 RESPECTIVELY AND DIELECTRIC LOSS OF 0.0006 AND 0.0004 RESPECTIVELY AT 1 MHZ [18]. EVENTHOUGH STUDIES HAVE BEEN REPORTED ON THE CERAMIC FILLED POLYSTYRENE COMPOSITES [19-21], ONLY A FEW REPORTS ARE AVAILABLE WHICH EXPLORE THE APPLICABILITY OF POLYETHYLENE COMPOSITES FOR HIGH FREQUENCY PACKAGING. POLYETHYLENE IS ALSO A WELL KNOWN POLYMERIC INSULATING MATERIAL WITH HIGH DIELECTRIC STRENGTH, LOW DIELECTRIC LOSS AND GOOD MECHANICAL PROPERTIES. A LARGE NUMBER OF REPORTS [18, 22-24] SHOWING THE DIELECTRIC PROPERTIES OF BOTH METAL AND CERAMIC FILLED POLYETHYLENE COMPOSITES. VARIOUS RESEARCHERS HAVE PUT CONSIDERABLE EFFORT TO IMPROVE THE PROPERTIES OF POLYETHYLENE BY VARYING THE FILLER PARTICLE SIZE, SURFACE COUPLING AGENTS ETC. [25-27]. THE EFFECTS OF BORON NITRIDE CONTENT, PARTICLE SIZE AND TEMPERATURE ON THE THERMAL CONDUCTIVITY OF HDPE-BORON NITRIDE COMPOSITES HAVE BEEN INVESTIGATED BY ZHANG [28]. THERE ARE REPORTS ON THE PROCESSING AND MECHANICAL PROPERTIES OF MULTIWALLED NANOTUBE (MWNT)-HDPE COMPOSITES [29]. THE EFFECTS OF VARIOUS MATERIAL PARAMETERS AND PROCESSING CONDITIONS ON THE FOAM MORPHOLOGIES AND MECHANICAL PROPERTIES OF HDPE-CLAY NANOCOMPOSITES HAVE BEEN STUDIED BY JI [30]. EVEN THOUGH THE MECHANICAL PROPERTIES OF HDPE COMPOSITES ARE WELL STUDIED [31], ATTENTION HAS BEEN PAID TO ITS ELECTRICAL AND THERMAL PROPERTIES.

DUE TO THE DIFFERENCE IN THE SURFACE CHARACTERISTICS BETWEEN THE INORGANIC FILLER AND THE ORGANIC MATRIX, IT IS DIFFICULT TO DISPERSE THE FILLER HOMOGENEOUSLY ESPECIALLY FOR HIGHER VOLUME FRACTION OF FILLER WHICH RESULTS IN HIGH POROSITY AND ABSORPTION LEADING TO UNDESIRABLE CHANGES IN THE DIELECTRIC PROPERTIES AND MECHANICAL INTEGRITY. IN ORDER TO IMPROVE THE PROPERTIES OF FILLED POLYMER COMPOSITES COUPLING AGENTS ARE DEVELOPED [33-34]. COUPLING AGENTS POSSESS SPECIAL STRUCTURE WITH TWO DIFFERENT FUNCTIONAL GROUPS, ONE THAT IS ATTACHED TO THE POLYMER MATRIX AND THE OTHER ONE ATTACHED TO THE INORGANIC FILLER. VARIOUS STUDIES HAVE BEEN REPORTED ON THE EFFECT OF COUPLING AGENTS ON THE THERMAL, MECHANICAL AND DIELECTRIC PROPERTIES OF POLYMER/INORGANIC COMPOSITES [16, 34-36]. EARLIER, CHEN [36] INVESTIGATED THE EFFECT OF PHENYL TRIMETHOXY SILANE CONTENT ON THE THERMAL AND DIELECTRIC PROPERTIES OF POLYMER/INORGANIC COMPOSITES. THE COUPLING AGENT CHANGES THE NATURE BY WHICH POLYMER INTERACTS WITH THE FILLER LEADING TO A DECREASE IN THE POROSITY AND ALSO THE HYDROPHILICITY OF THE SURFACE. THEY ALSO PREVENT THE FORMATION OF FILLER AGGLOMERATION THEREBY PROMOTING A MORE HOMOGENEOUS DISPERSION OF FILLER IN THE MATRIX. THE DIELECTRIC PROPERTIES OF POLYMER/INORGANIC COMPOSITES ARE VERY MUCH DEPENDENT ON THE SIZE AND SHAPE OF THE FILLERS AND THE INTERACTION BETWEEN THE FILLER AND THE POLYMER MATRIX. NOW-A-DAYS POLYMER/NANO COMPOSITES ARE OF GREAT TECHNOLOGICAL INTEREST DUE TO THEIR INTERESTING ELECTRICAL, MECHANICAL AND THERMAL PROPERTIES WHEN COMPARED WITH THAT OF THE CONVENTIONAL MICROMETER SIZE FILLER POLYMER COMPOSITES. WHEN THE FILLER SIZE REDUCES TO NANOMETER LEVEL, THE SURFACE TO VOLUME RATIO INCREASES THEREBY A SIGNIFICANT ENHANCEMENT IN THE ELECTRIC AND THERMAL PROPERTIES OF POLYMER COMPOSITES IS ACHIEVED EVEN AT LOWER FILLER CONTENT. DURING THE LAST FEW YEARS, MANY RESEARCHERS HAVE EXPLORED THE OPTICAL, THERMAL, MECHANICAL AND DIELECTRIC PROPERTIES OF POLYMER/NANO COMPOSITES [23, 35, 37-38]. GOOD AMOUNT OF EFFORT HAS BEEN PUT IN DEVELOPING HIGH K POLYMER/NANO COMPOSITES FOR CAPACITOR APPLICATIONS [39-42]. HOWEVER, A FEW REPORTS ARE AVAILABLE WHICH EXPLOITS THE APPLICABILITY OF POLYMER/NANO COMPOSITES FOR ELECTRONIC PACKAGING APPLICATIONS [37-38, 41-42].

THE PRESENT CHAPTER GIVES A DETAILED INVESTIGATION OF THE THERMAL, MECHANICAL AND DIELECTRIC PROPERTIES OF UNCOUPLED AND COUPLED PTFE, POLYETHYLENE AND POLYSTYRENE POLYMER/INORGANIC COMPOSITES. THE EFFECT OF COUPLING AGENT AND PARTICLE SIZE OF THE FILLER ON THE PROPERTIES OF PTFE/SM<sub>2</sub>SI<sub>2</sub>O<sub>7</sub> COMPOSITES IS ALSO STUDIED. THE EXPERIMENTAL VALUES OBTAINED FOR



PERMITTIVITY, THERMAL CONDUCTIVITY AND COEFFICIENT OF THERMAL EXPANSION WITH VARIOUS THEORETICAL MODELS.

## 5.2 THEORETICAL MODELLING

### 5.2.1 RELATIVE PERMITTIVITY

THE PRECISE PREDICTION OF RELATIVE PERMITTIVITY OF THE COMPOSITE FROM THE PERMITTIVITY OF THE COMPONENTS AND THE VOLUME FRACTION OF THE FILLER IS VERY IMPORTANT IN THE DESIGN OF COMPOSITES FOR ELECTRONIC APPLICATIONS. SINCE THE COMPOSITES ARE MIXTURES OF TWO OR MORE COMPONENTS, THE EFFECTIVE RELATIVE PERMITTIVITY OF THE COMPOSITE BETWEEN THE VALUES OF THE INDIVIDUAL COMPONENTS. THE DIELECTRIC PROPERTIES OF COMPOSITES ARE INFLUENCED NOT ONLY BY THE RELATIVE PERMITTIVITIES OF THE COMPONENTS, BUT ALSO BY OTHER FACTORS SUCH AS THE MORPHOLOGY, DISPERSION AND THE INTERACTION BETWEEN THE TWO PHASES AND HENCE THE PREDICTION OF RELATIVE PERMITTIVITY IS A DIFFICULT TASK. THE FOLLOWING EQUATIONS ARE USED TO CALCULATE THE RELATIVE PERMITTIVITY OF THE COMPOSITE AT LOW FILLER CONTENT:

(a) **Jayasundere-Smith equation** [43]:

$$\epsilon_{eff} = \frac{\epsilon_m(1 - v_f) + \epsilon_f v_f \left[ \frac{3\epsilon_m}{\epsilon_f + 2\epsilon_m} \right] \left[ 1 + \left( \frac{3v_f(\epsilon_f - \epsilon_m)}{\epsilon_f + 2\epsilon_m} \right) \right]}{1 - v_f + v_f \left[ \frac{3\epsilon_m}{\epsilon_f + 2\epsilon_m} \right] \left[ 1 + \left( \frac{3v_f(\epsilon_f - \epsilon_m)}{\epsilon_f + 2\epsilon_m} \right) \right]} \quad (5.1)$$

(b) **Lichtenecker equation** [44] :

$$\ln \epsilon_{eff} = (1 - v_f) \ln \epsilon_m + v_f \ln \epsilon_f \quad (5.2)$$

(c) **Modified Lichtenecker equation** [43]:

$$\ln \epsilon_{eff} = \ln \epsilon_m + v_f \ln \left( \frac{\epsilon_f}{\epsilon_m} \right) \quad (5.3)$$

(d) Maxwell – Wagner equation [45] :

$$\epsilon_{eff} = \epsilon_m \frac{2\epsilon_m + \epsilon_f + 2v_f(\epsilon_f - \epsilon_m)}{2\epsilon_m + \epsilon_f - v_f(\epsilon_f - \epsilon_m)} \quad (5.4)$$

(e) Effective Medium Theory [46] :

$$\epsilon_{eff} = \epsilon_m \left[ 1 + \frac{v_f(\epsilon_f - \epsilon_m)}{\epsilon_m + n(1 - v_f)(\epsilon_f - \epsilon_m)} \right] \quad (5.5)$$

WHERE  $\epsilon_{eff}$ ,  $\epsilon_f$ ,  $\epsilon_m$  ARE THE RELATIVE PERMITTIVITY OF THE COMPOSITES, FILLER AND RESPECTIVELY  $v_f$  AND  $n$  ARE THE VOLUME FRACTION OF FILLER AND AN EMPIRICALLY DETERMINED PARAMETERS IN THE MODIFIED LICHTENECKER AND EMT MODELS RESPECTIVELY.

THE RELATIVE PERMITTIVITY OF COMPOSITES DEPENDS ON THE DISTRIBUTION OF SHAPE AND SIZE OF FILLERS AND INTERFACE BETWEEN CERAMICS AND POLYMERS. RECENTLY [46] PROPOSED AN EFFECTIVE MEDIUM THEORY (EMT) TO PREDICT THE EFFECTIVE RELATIVE PERMITTIVITY OF THE COMPOSITE BY CONSIDERING THESE FACTORS. IN THIS MODEL, THE PROPERTY OF THE COMPOSITE IS TREATED AS AN EFFECTIVE MEDIUM WHOSE RELATIVE PERMITTIVITY IS OBTAINED BY AVERAGING THE PERMITTIVITIES OF THE CONSTITUENTS. EMT MODEL IS A CONSISTENT MODEL WHICH ASSUMES A RANDOM UNIT CELL CONSISTING OF EACH FILLER PARTICLE SURROUNDED BY A CONCENTRIC MATRIX LAYER. THIS RANDOM UNIT CELL WHEN EMBEDDED IN THE MATRIX MEDIUM MUST NOT BE DETECTED IN AN EXPERIMENT USING ELECTROMAGNETIC MEASUREMENTS. THIS MODEL INCLUDES A MORPHOLOGY FACTOR  $n$  DETERMINED EMPIRICALLY. THIS CORRECTION FACTOR  $n$  COMPENSATES FOR THE SHAPE OF THE FILLER USED IN THE POLYMER-CERAMIC COMPOSITE. A VALUE OF  $n$  INDICATES A NEAR SPHERICAL SHAPE FOR THE FILLER, WHILE A HIGH VALUE OF  $n$  INDICATES A LARGELY NON-SPHERICALLY SHAPED PARTICLE. EARLIER REPORTS [46] SHOWED THAT FOR DISPERSED POLYMER CERAMIC COMPOSITES, THE VALUE OF 'N' IS 0.35.

## 5.2.2 COEFFICIENT OF THERMAL EXPANSION (CTE)

THERMAL EXPANSION COEFFICIENTS OF COMPOSITES ARE VERY IMPORTANT IN RELATING TO DIMENSIONAL STABILITY AND THE MECHANICAL COMPATIBILITY WHEN USED WITH OTHER

CONSIDERABLE AMOUNT OF WORK HAS BEEN DONE TO PREDICT THE THERMAL EXPANSION OF COMPOSITES [47-48]. THE RULE OF MIXTURES SERVES AS THE FIRST-ORDER APPROXIMATION OVERALL CALCULATION OF THE CO-EFFICIENT OF THERMAL EXPANSION OF THE COMPOSITE EXPRESSED AS

$$\alpha_c = v_f \alpha_f + (1 - v_f) \alpha_m \quad (5.6)$$

WHERE  $\alpha_c$ ,  $\alpha_m$  AND  $\alpha_f$  ARE COEFFICIENT OF THERMAL EXPANSION OF THE COMPOSITE, MATRIX AND FILLER RESPECTIVELY.

### 5.2.3 THERMAL CONDUCTIVITY

MATERIALS FOR ELECTRONIC PACKAGING REQUIRE HIGH THERMAL CONDUCTIVITY TO DISSIPATE THE HEAT GENERATED IN THE DEVICES. THUS IT IS A NEED TO MODEL AND PREDICT THERMAL CONDUCTIVITY OF THE COMPOSITES IN A NUMBER OF INDUSTRIAL PROCESSES. PREDICTION OF THERMAL CONDUCTIVITY OF THE COMPOSITES COMPRISES A SIGNIFICANT PART OF THE HEAT TRANSFER LITERATURE. MANY REPORTS CONCERNING THE THERMAL CONDUCTIVITY OF COMPOSITES, ASSOCIATED WITH VARIOUS MODELS OR EQUATIONS FOR PREDICTING THERMAL CONDUCTIVITY HAVE BEEN PUBLISHED [49-50]. THEY ARE EITHER THEORETICALLY BASED OR EMPIRICAL WHICH MEANS TO INCLUDE ONE OR MORE EXPERIMENTALLY DETERMINED PARAMETERS. FOR A TWO COMPONENT COMPOSITE, THE SIMPLEST MODEL WITH THE MATERIALS ARRANGED IN EITHER PARALLEL OR SERIES WITH RESPECT TO HEAT FLOW, WHICH GIVE LOWER BOUNDS (ALSO REFERRED TO AS WEINER BOUNDS) OF EFFECTIVE THERMAL CONDUCTIVITY. IN THE PRESENT STUDY, FOLLOWING MODELS ARE USED TO PREDICT THE THERMAL CONDUCTIVITY OF COMPOSITES:

#### 1. Geometric Mean Model:

$$k_c = k_f^{v_f} k_m^{1-v_f} \quad (5.7)$$

WHERE  $k_c$ ,  $k_f$  AND  $k_m$  ARE THE THERMAL CONDUCTIVITIES OF COMPOSITE, FILLER AND MATRIX RESPECTIVELY AND  $v_f$  IS THE VOLUME FRACTION OF THE FILLER IN THE COMPOSITE.

## 2. Agari Model:

AGARI DEVELOPED A MODEL BASED ON THE GENERALIZATION OF MODELS OF SERIES AND PARALLEL CONDUCTION IN COMPOSITES. THE MODEL PROPOSED BY AGARI CONSIDERED THE EFFECT OF DISPERSION STATE BY INTRODUCING TWO FACTORS C<sub>1</sub> AND C<sub>2</sub>

$$k_c = v_f C_2 \left[ \frac{k_f + 2k_m + 2v_f (k_f - k_m)}{k_f + 2k_m - v_f (k_f - k_m)} \right] \quad (5.8)$$

WHERE  $k_c$ ,  $k_m$  AND  $k_f$  ARE THE THERMAL CONDUCTIVITY OF COMPOSITES, POLYMER AND FILLER RESPECTIVELY,  $v_f$  IS THE VOLUME FRACTION OF FILLER.

IN COMPOSITES, EACH PHASE CANNOT BE RESTRICTEDLY ARRANGED IN A BLOCK BUT OF DISCONTINUOUS NETWORK OF FILLER IN THE MATRIX. THESE TWO CONSTANTS DEFINE THE ABILITY OF FORMING CONTINUOUS NETWORK OF FILLER IN THE MATRIX. CONSIDERING THE PREPARATION PROCEDURE OF THE COMPOSITES CAN AFFECT THE CRYSTALLINITY OF THE POLYMER THEREBY THE THERMAL CONDUCTIVITY, IS AFFECTED. ACCORDING TO AGARI, THE VALUES OF C<sub>1</sub> AND C<sub>2</sub> SHOULD BE IN BETWEEN 0 AND 1, THE CLOSER TO 1, THE MORE EASILY CONDUCTIVE CHAINS ARE FORMED IN COMPOSITES.

## 3. Maxwell - Eucken Model

MAXWELL, USING POTENTIAL THEORY [54], OBTAINED AN EXACT SOLUTION FOR THE THERMAL CONDUCTIVITY OF RANDOMLY DISTRIBUTED AND NON INTERACTING HOMOGENEOUS PHASES IN A HOMOGENEOUS MEDIUM AND IS GIVEN BY

$$k_c = k_m \left[ \frac{k_f + 2k_m + 2v_f (k_f - k_m)}{k_f + 2k_m - v_f (k_f - k_m)} \right] \quad (5.9)$$

## 4. Cheng - Vachon Model

BASED ON TSAO'S MODEL WHICH GIVES THE THERMAL CONDUCTIVITY OF TWO PHASE MIXTURE [55], CHENG AND VACHON ASSUMED A PARABOLIC DISTRIBUTION OF THE DISCONTINUOUS PHASE IN THE CONTINUOUS PHASE. THE CONSTANTS OF THIS PARABOLIC DISTRIBUTION WERE DETERMINED BY ANALYSIS AND PRESENTED AS A FUNCTION OF THE DISCONTINUOUS PHASE VOLUME FRACTION. THUS, THE EQUIVALENT THERMAL CONDUCTIVITY OF THE TWO PHASE SOLID MEDIUM WAS DERIVED IN TERMS OF THE DISTRIBUTION FUNCTION, AND THE THERMAL CONDUCTIVITY OF THE CONSTITUENTS. FOR

$$\frac{1}{k_c} = \frac{1}{\sqrt{C(k_m - k_f)[k_m + B(k_f - k_m)]}} \operatorname{LN} \frac{\sqrt{[k_m + B(k_f - k_m)]} + \frac{B}{2} \sqrt{C(k_m - k_f)}}{\sqrt{[k_m + B(k_f - k_m)]} - \frac{B}{2} \sqrt{C(k_m - k_f)}} + \frac{1-B}{k_m} \quad (5.10)$$

WHERE

$$B = \sqrt{3v_f/2} \quad C = -4\sqrt{2/3v_f}$$

### 5. Nielson Model

LEWIS AND NIELSON [56] MODIFIED HALPIN-TSAI EQUATION [57] TO INCLUDE THE EFFECT OF THE SHAPE OF THE PARTICLES AND THE ORIENTATION OR TYPE OF PACKING FOR A POLYMER SYSTEM.

$$k_c = k_m \left[ \frac{1 + ABv_f}{1 - Bv_f} \right] \quad (5.11)$$

WHERE

$$B = \frac{\frac{k_f}{k_m} - 1}{\frac{k_f}{k_m} + A} = 1 + \left( \frac{1 - v_{fm}}{v_{fm}^2} \right) v_f$$

A(-3) IS A FUNCTION OF GEOMETRY OF THE FILLER PARTICLES,  $v_{fm}$  IS THE MAXIMUM FILLER CONTENT.

### 5.3 EXPERIMENTAL

THE  $\text{SM}_2\text{Si}_2\text{O}_7$  CERAMICS WERE PREPARED BY CONVENTIONAL SOLID STATE CERAMIC PROCESSING AS DESCRIBED IN CHAPTER 4, SECTION 4.1.2.1. THE POWDER WAS FINELY GROUND AND SINTERED AT 1375°C. AGAIN THE POWDER WAS FINELY GROUND AND SIEVED USING 100 μM SIEVES. THE PTFE/ $\text{SM}_2\text{Si}_2\text{O}_7$  COMPOSITES WERE PREPARED BY POWDER PROCESSING TECHNIQUE AS EXPLAINED IN CHAPTER 2, SECTION 2.3.1. DIFFERENT VOLUME FRACTIONS OF  $\text{SM}_2\text{Si}_2\text{O}_7$  CERAMICS AND PTFE (HINDUSTAN FLUOROCARBONS, HYDERABAD, INDIA) POWDERS WERE DISPERSED IN ETHYL ALCOHOL USING ULTRASONIC MIXER FOR ABOUT 1 H. A HOMOGENOUS MIXTURE WAS OBTAINED BY REMOVING THE SOLVENT BY EVAPORATION. THE HOMOGENOUSLY MIXED PTFE/ $\text{SM}_2\text{Si}_2\text{O}_7$  POWDERS WERE THEN HOT PRESSED IN THE FORM OF CYLINDRICAL OR RECTANGULAR PELLETS UNDER A UNIAXIAL PRESSURE OF 30 MPa AT 310°C FOR 30 MIN.

IT IS WELL KNOWN THAT GENERALLY THE CERAMIC FILLERS ARE HYDROPHILIC. THIS PROPERTY OF THE FILLER MAY ADVERSELY AFFECT THE PERFORMANCE OF THE COMPOSITE. IT IS RECOMMENDED TO USE SUITABLE COUPLING AGENT TO COAT THE FILLER SURFACE. IN THIS STUDY THE COUPLING AGENT USED WAS PHENYL TRIMETHOXY SILANE (PTMS). IN AN AQUEOUS SOLUTION WAS PREPARED BY ADJUSTING THE PH OF THE WATER TO 3 WITH TRIMETHYL ACETIC ACID. AFTER THAT A VOLUME EQUIVALENT TO 1 WT% OF PTMS WAS ADDED TO THE WATER FOLLOWED BY VIGOROUS STIRRING FOR ABOUT 15 MIN. BEFORE IT HYDROLYSED TO A CLEAR AND HOMOGENEOUS SOLUTION. THE CERAMIC FILLERS WERE MIXED WITH SILANE SOLUTION FOR 24 H. WITHOUT ADDITIONAL SOLVENT. THE RESULTING MIXTURE WAS DRIED AT 120°C TO OBTAIN THE SILANE COATED FILLER.

THE POLYSTYRENE/S<sub>2</sub>O<sub>7</sub> (PS-SM<sub>2</sub>Si<sub>2</sub>O<sub>7</sub>) AND POLYETHYLENE/S<sub>2</sub>O<sub>7</sub> (PE-SM<sub>2</sub>Si<sub>2</sub>O<sub>7</sub>) COMPOSITES WERE PREPARED BY SIGMA-BLEND TECHNIQUE AS EXPLAINED IN SECTION 2.3.2 IN CHAPTER 2. THE POLYMERS WERE FIRST MELTED IN KNEADING MACHINE AT 150°C. DIFFERENT VOLUME FRACTIONS (0 TO 0.5) OF CERAMIC FILLER WERE ADDED TO THE MELT AND BLENDED AT 150°C FOR 30 MINUTES. THUS OBTAINED COMPOSITES WERE THERMO - LAMINATED USING SUITABLE DIE UNDER A PRESSURE OF 200 MPa AND 150°C. AFTER THERMO-LAMINATION, THE COMPOSITES WITH DESIRED SHAPES WERE POLISHED FOR CHARACTERIZATION.

THE DENSITY OF THE COMPOSITES WAS MEASURED USING ARCHIMEDES METHOD. THE MICROSTRUCTURE OF THE COMPOSITES WAS RECORDED USING SEM. THE LOW FREQUENCY DIELECTRIC PROPERTIES AND THE VARIATION IN RELATIVE PERMITTIVITY WITH TEMPERATURE IN THE RANGE 25-60°C WERE MEASURED BY LCR METER (HIOKI 3532-50). THE DIELECTRIC PROPERTIES AT MICROWAVE FREQUENCIES WERE CHARACTERIZED USING HP 8510 VECTOR NETWORK ANALYZER. THE CAVITY PERTURBATION TECHNIQUE WHICH IS DISCUSSED IN DETAIL IN CHAPTER 2, SECTION 2.8.3.

THE FILLER PARTICLE SIZE IS MEASURED USING PHOTON CORRELATION SPECTROSCOPY (CILAS 930 PARTICLE SIZE ANALYZER - FRANCE). THE SPECIFIC SURFACE AREA OF THE FILLER WAS MEASURED BY NITROGEN ADSORPTION MEASUREMENT (BET) IN MICROMERITICS (CONTOUR 2375) SURFACE AREA ANALYZER. THE COEFFICIENT OF THERMAL EXPANSION (CTE) OF THE COMPOSITES WAS MEASURED USING A THERMO - MECHANICAL ANALYZER (TMA - 60H, SHIMADZU). THE THERMAL CONDUCTIVITY IN THE RANGE 25-250°C (PPE) TECHNIQUE [58] (DISCUSSED IN SECTION 2.8.3 IN CHAPTER 2) WAS USED TO DETERMINE THE THERMAL CONDUCTIVITY OF THE COMPOSITES. THERMAL DIFFUSIVITY AND THERMAL EFFUSIVITY WERE ALSO MEASURED FROM PPE SIGNAL.

PHASE AND AMPLITUDE [59]. FROM THE VALUES OF THERMAL CONDUCTIVITY AND SPECIFIC HEAT CAPACITY OF THE SAMPLES WERE OBTAINED.

THE VICKER'S MICROHARDNESS OF PEEK AND PS-SM<sub>2</sub>S<sub>12</sub>O<sub>7</sub> COMPOSITES WERE MEASURED USING MICRO HARDNESS TESTER (CLEMEX 4, GERMANY). BOTH THE SURFACE SAMPLES WERE POLISHED TO HAVE OPTICALLY FLAT SURFACE FOR INDENTATION. THE SAMPLES WERE SUBJECTED TO A LOAD OF 100 G AND DWELL TIME OF 10 S. A TOTAL OF 5 READINGS WERE TAKEN TO GET THE AVERAGE HARDNESS. THE WATER ABSORPTION MEASUREMENTS WERE CONDUCTED ACCORDING TO ASTM D570. THE SAMPLES WERE WEIGHED AND SUBMERGED IN DISTILLED WATER AT 25 °C FOR 24 H. THE SAMPLES WERE REMOVED, WIPED, DRIED AND THE AMOUNT OF WATER ABSORBED WAS CALCULATED BASED ON THE WEIGHT GAIN OF THE SAMPLES.

## 5.4 RESULTS AND DISCUSSION

### 5.4.1 PTFE/SM<sub>2</sub>Si<sub>2</sub>O<sub>7</sub> COMPOSITES

FIGURE 5.1 SHOWS THE PARTICLE SIZE DISTRIBUTION OF PEEK. FROM THE FIGURE IT IS CLEAR THAT PEEK POSSESS A VERY SMALL PARTICLE SIZE WITH AN AVERAGE VALUE OF 1.4 μM.

|                 |        |    |
|-----------------|--------|----|
| Ultrasounds     | : 60   | s  |
| Obscuration     | : 18 % |    |
| Diameter at 10% | : 0.22 | μm |
| Diameter at 50% | : 0.87 | μm |
| Diameter at 90% | : 3.19 | μm |
| Mean diameter   | : 1.44 | μm |

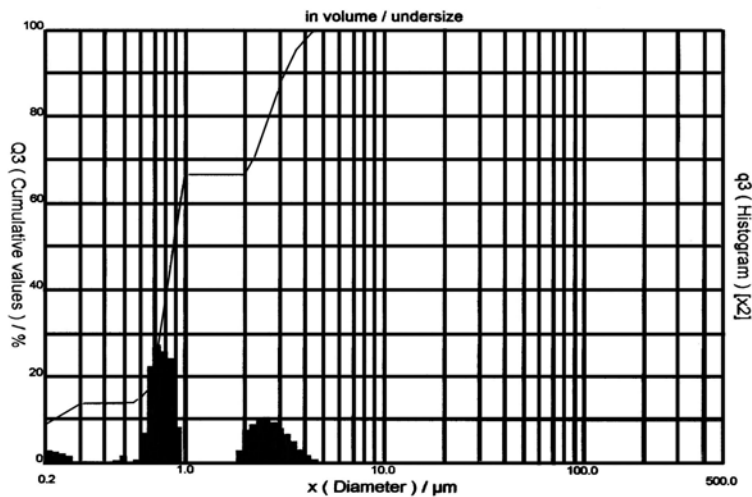


Fig. 5.1 Particle size distribution of Sm<sub>2</sub>Si<sub>2</sub>O<sub>7</sub> filler.

FIGURE 5.2 (A) SHOWS THE SEM IMAGE OF POWDER. FROM THE FIGURE IT CAN BE INFERRED THAT THE CERAMIC SHOWED A PARTICLE SIZE VARYING FROM 1-3  $\mu\text{m}$  WHICH CONFIRMS THE RESULT OBTAINED FROM THE PARTICLE SIZE ANALYSIS. FIGURES 5.2 (B-D) SHOW THE MICRO STRUCTURAL IMAGES OF PTFE/POLYMER – CERAMIC COMPOSITES FOR DIFFERENT VOLUME FRACTION OF CERAMIC LOADING. IT CAN BE SEEN THAT AT LOWER CERAMIC LOADING A GOOD ADHESION IS OBSERVED BETWEEN THE POLYMER AND CERAMIC WITH MINIMUM DEFECTS AND THE  $\text{Sm}_2\text{Si}_2\text{O}_7$  CERAMIC PARTICLES ARE UNIFORMLY DISPERSED THROUGHOUT THE MATRIX. HOWEVER, AS THE FILLER CONTENT INCREASES THE PACKING OF THE PARTICLES LEADING TO PARTICLE AGGLOMERATION. THESE AGGLOMERATES MAY INCREASE THE EFFECTIVE PARTICLE SIZE THEREBY RESTRICTING THE VOID FILLING BETWEEN BIGGER PARTICLES. FROM FIGURE 5.2 (D) IT CAN BE SEEN THAT AS THE CERAMIC CONTENT INCREASES THE POROSITY OF THE COMPOSITES INCREASES WHICH ADVERSELY AFFECTS THE DIELECTRIC, THERMAL AND MECHANICAL PROPERTIES OF THE COMPOSITES.

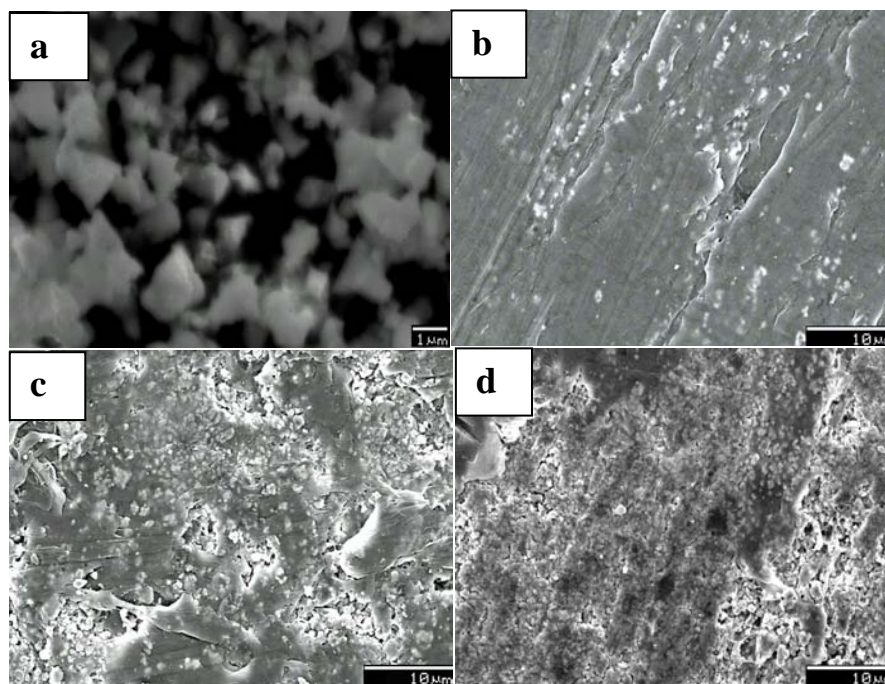


Fig. 5.2 SEM images of PTFE loaded with (a)  $\text{Sm}_2\text{Si}_2\text{O}_7$  powder, (b)  $0.1 v_f \text{Sm}_2\text{Si}_2\text{O}_7$ , (c)  $0.3 v_f \text{Sm}_2\text{Si}_2\text{O}_7$  and (d)  $0.5 v_f \text{Sm}_2\text{Si}_2\text{O}_7$ .

THE THEORETICAL DENSITY OF THE COMPOSITE CALCULATED USING THE MIXTURE RULE [44]:



$$\rho_{comp} = V_1\rho_1 + V_2\rho_2 \quad (5.12)$$

WHERE,  $\rho_2$ ,  $V_1$  AND  $V_2$  RESPECTIVELY ARE THE DENSITY OF THE FILLER, DENSITY OF THE MATRIX, VOLUME OF THE FILLER AND VOLUME OF THE MATRIX. THE DENSITIES OF PTFE AND  $\text{Sm}_2\text{Si}_2\text{O}_7$  MEASURED BY ARCHIMEDES METHOD ARE FOUND TO BE 2.15 AND 7.95  $\text{g/cm}^3$  RESPECTIVELY. TABLE 5.1 GIVES THE RELATIVE DENSITY AND POROSITY OF COMPOSITES WITH VARYING FILLER CONTENT. THE DENSITY OF THE COMPOSITE INCREASES AS THE FILLER LOADING INCREASES DUE TO THE HIGHER DENSITY OF THE CERAMIC. HOWEVER, THE RELATIVE DENSITY GRADUALLY INCREASES IN FILLER CONTENT. THIS BEHAVIOR IS MAINLY DUE TO THE PRESENCE OF PORES PRODUCED DURING THE SYNTHESIS PROCESS WHEN AIR LIBERATION IS RESTRICTED DUE TO THE HIGH VISCOSITY OF THE MATRIX. A MONOTONIC INCREASE IN THE POROSITY IS OBSERVED WITH AN INCREASE IN THE CERAMIC CONTENT. POROSITY GENERALLY ARISES FROM AGGLOMERATION OF CERAMIC SOLVENTS AND ALSO BECAUSE OF THE LOW POLYMER CONTENT WHICH IS INSUFFICIENT TO FORM A PARTICLE NETWORK. THE PRESENCE OF AGGLOMERATION AND PORES IS ALSO EVIDENT IN SEM IMAGES (SEE FIG. 5.2 (C) AND (D)). THE POROSITY REACHES A MAXIMUM VALUE OF 24.7 % AT A FILLER CONTENT OF 0.5 V

**Table 5.1** The density, relative density and porosity of PTFE/ $\text{Sm}_2\text{Si}_2\text{O}_7$  composites.

| Volume fraction filler | Density ( $\text{g/cm}^3$ ) | Relative density (%) | Porosity (%) |
|------------------------|-----------------------------|----------------------|--------------|
| 0.1                    | 2.45                        | 97.8                 | 2.2          |
| 0.2                    | 2.78                        | 97.3                 | 2.7          |
| 0.3                    | 2.95                        | 91.8                 | 8.2          |
| 0.4                    | 2.94                        | 82.4                 | 17.6         |
| 0.5                    | 2.95                        | 75.3                 | 24.7         |

THE VARIATION OF THE DIELECTRIC PROPERTIES OF THE COMPOSITE WITH THE VARYING FILLER DISTRIBUTION AS A FUNCTION OF FREQUENCY IS SHOWN IN FIG. 5.3. THE DIELECTRIC RESPONSE IS STUDIED OVER THE FREQUENCY RANGE 1 KHZ – 1 MHZ. IT IS OBSERVED THAT THE RELATIVE PERMITTIVITY IS ALMOST INDEPENDENT OF FREQUENCY. AS THE CERAMIC CONTENT INCREASES THE RELATIVE PERMITTIVITY ALSO INCREASES DUE TO THE HIGHER RELATIVE PERMITTIVITY OF THE CERAMIC COMPARED TO THE POLYMER. FROM FIG. 5.3 (B) IT IS CLEAR THAT THE DIELECTRIC LOSS TANGENT IS ALMOST INDEPENDENT OF FREQUENCY.

IS VERY MUCH FREQUENCY DEPENDENT. IN THE REGION OF LOW FREQUENCIES, THE DI  
 ATTAINS A HIGH VALUE WHICH DECREASES AS THE FREQUENCY INCREASES. THIS CAN  
 BASED ON THE INTERFACIAL POLARIZATION, KNOWN AS MAXWELL-WAGNER-SILLARS (MWS)  
 WHICH APPEARS IN HETEROGENEOUS SYSTEMS DUE TO THE ACCUMULATION OF CHARGE AT  
 INTERFACES [60]. THIS POLARIZATION IS PREDOMINANT AT THE LOWER FREQUENCIES AND  
 WITH THE FILLER CONTENT. GENERALLY IN POLYMER COMPOSITES INTERFACIAL POLARIZATION IS  
 OPERATIVE AT LOW FREQUENCY, IS ALWAYS PRESENT DUE TO THE PRESENCE OF ADDITIONAL  
 IMPURITIES HAVING LARGER MASSES THAN THE LOW MOLECULAR WEIGHT DIPOLES THAT ARE  
 SYSTEMS HETEROGENEOUS. THE INTERFACIAL POLARIZATION RELATED TO THE LARGE DIELECTRIC  
 INTERFACE IS LESS ACTIVE AS THE ELECTRIC FIELD CHANGES RAPIDLY. HOWEVER, A SLIGHT  
 THE RELATIVE PERMITTIVITY AND AN INCREASE IN DIELECTRIC LOSS IS NOTED BOTH IN THE  
 FREQUENCY REGION (177 KHZ). THIS MAY BE PROBABLY DUE TO CERTAIN RELAXATION MECHANISMS  
 THE POLYMER. SIMILAR RELAXATION MECHANISM WAS OBSERVED AND STUDIED IN DETAIL BY  
*et al.* [61].

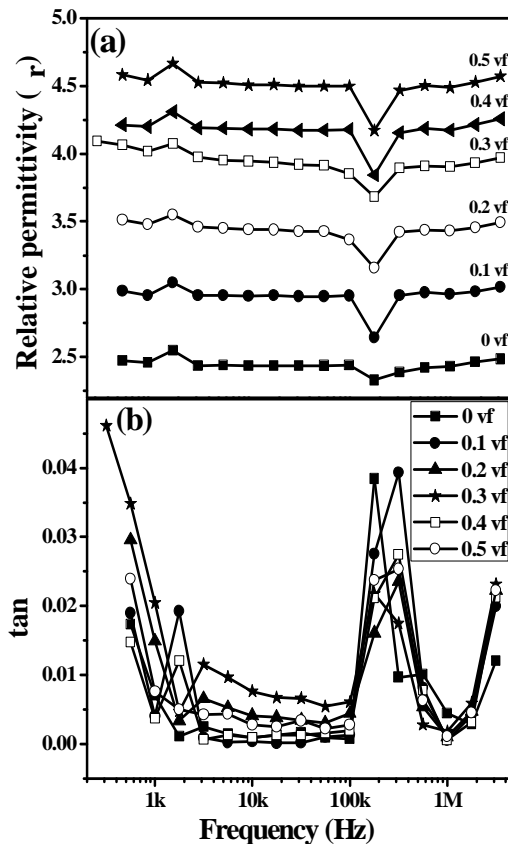


Fig. 5.3 The variation of (a) relative permittivity and (b) dielectric loss with frequency for PTFE/ $\text{Sm}_2\text{Si}_2\text{O}_7$  composites.

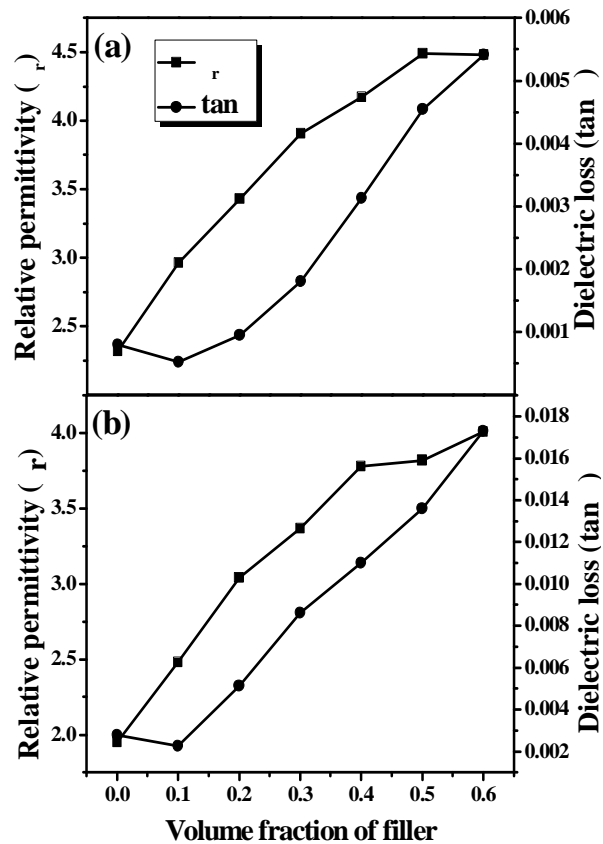


Fig. 5.4 The variation of dielectric properties with filler content for PTFE/ $\text{Sm}_2\text{Si}_2\text{O}_7$  composites at (a) 1 MHz and (b) 9 GHz.

IN A HETEROGENEOUS POLYMER SYSTEM, THE INCLUSION OF FILLER WILL NORMALLY AFFECT THE PROPERTIES OF THE POLYMER MATRIX. FIG. 5.4 GIVES A COMPARISON OF THE DIELECTRIC PROPERTIES OF THE PTFE/SiO<sub>2</sub> COMPOSITES WITH VARYING FILLER CONTENT AT 1 MHZ AND 9 GHZ. AT BOTH THE FREQUENCIES THE RELATIVE PERMITTIVITY INCREASES WITH INCREASE IN THE FILLER CONTENT. THIS IS DUE TO THE RELATIVELY HIGH PERMITTIVITY OF THE FILLER (ε = 10 AT 1 MHZ AND ε = 1.95 AT 9 GHZ) COMPARED TO THAT OF THE MATRIX (ε = 2.1 AT 1 MHZ AND ε = 1.95 AT 9 GHZ). WHEN THE CERAMIC FILLER CONTENT IS SMALL, IT FORMS A DISPERSED PHASE IN THE COMPOSITE. THE DIELECTRIC RESPONSE IS MAINLY CONTRIBUTED BY THE CONTINUOUS MATRIX, DUE TO WHICH THE RELATIVE PERMITTIVITY HAS A LOW VALUE. BUT AS THE FILLER CONTENT INCREASES, THE CERAMIC PARTICLES COME CLOSE TOGETHER LEADING TO AN INCREASE IN THE DIPOLE - DIPOLE INTERACTIONS THEREBY INCREASING THE RELATIVE PERMITTIVITY [62]. THE EFFECTIVE RELATIVE PERMITTIVITY OF THE COMPOSITE MAY BE DEPENDENT ON THE INTERPHASE CHARACTERISTICS. THESE CHARACTERISTICS ARE AFFECTED BY A CHANGE IN THE FILLER PARTICLE SIZE AND / OR BY A CHANGE IN THE CHEMICAL STRUCTURE OF THE INTERPHASE REGION. SINCE THE CHEMICAL STRUCTURE OF THE INTERPHASE REGION IS A FUNCTION OF THE POLYMER AND ITS INTERACTION WITH THE FILLER PARTICLES, A CHANGE OF THE BONDING BETWEEN THESE TWO PHASES WILL AFFECT THE RELATIVE PERMITTIVITY OF THE COMPOSITE. THE DIELECTRIC LOSS WHICH IS THE MEASURE OF THE ENERGY AFFECTING THE FREQUENCY SELECTIVITY OF A MATERIAL IS INFLUENCED BY MANY FACTORS SUCH AS POROSITY, MICROSTRUCTURE AND DEFECTS [63]. FROM THE FIGURE IT IS OBSERVED THAT AS THE FILLER CONTENT INCREASES THE DIELECTRIC LOSS ALSO INCREASES FOR BOTH 1 MHZ AND 9 GHZ. THIS IS ATTRIBUTED TO THE INCREASED POROSITY (SEE TABLE 5.1 OF THE MATERIAL) AND ALSO DUE TO THE INTERFACIAL POLARIZATION BETWEEN THE POLYMER AND CERAMIC AT HIGHER FREQUENCIES. THE DIELECTRIC LOSS VARIES FROM 0.00052-0.00455 AT 1 MHZ WITH THE FILLER ADDITION FROM 0 - 50 VOL %. THIS IS A MUCH SATISFACTORY RESULT WHEN COMPARED WITH SOME OF THE LITERATURE REPORTS ON SEVERAL POLYMER-CERAMIC COMPOSITES [64-65]. AT 9 GHZ, AS THE VOLUME FRACTION OF FILLER INCREASES (0 - 50 VOL%), THE RELATIVE PERMITTIVITY AND DIELECTRIC LOSS INCREASE FROM 1.95 TO 3.82 AND 0.0024 TO 0.0136 RESPECTIVELY. THIS LOW VALUE OF RELATIVE PERMITTIVITY WHEN COMPARED WITH THAT AT 1 MHZ IS DUE TO THE DIFFERENCE IN DIELECTRIC POLARIZATION MECHANISMS. ALL THE FOUR POLARIZATION MECHANISMS (DESCRIBED IN CHAPTER 2) ARE ACTIVE AT LOW FREQUENCIES BUT AS THE FREQUENCY INCREASES ONLY IONIC POLARIZATION DOMINATES. AT LOWER FREQUENCIES, ALL THE FREE DIPOLAR GROUPS

CHAIN CAN ORIENT THEMSELVES RESULTING IN THE HIGHER VALUE OF RELATIVE PERM. THE FREQUENCY INCREASES, THE BIGGER DIPOLES FIND IT DIFFICULT TO ALIGN IN THE RESULTING IN A NET DECREASE IN THE RELATIVE PERMITTIVITY.

THE PTFE MATRIX POSSESSES A LOW VALUE OF THERMAL CONDUCTIVITY OF NEARLY  $0.25 \text{ Wm}^{-1}\text{K}^{-1}$ . THE THERMAL CONDUCTIVITY OF THE FILLER IS MUCH HIGHER IN THE MATRIX AND THEREFORE THERE IS AN EXPECTED INCREASE IN THE THERMAL CONDUCTIVITY WITH FILLER ADDITION. THE INFLUENCE OF THE VOLUME FRACTION OF FILLER ON THE THERMAL CONDUCTIVITY OF PTFE/ $\text{Sm}_2\text{Si}_2\text{O}_7$  COMPOSITES IS SHOWN IN FIG. 5.5. IT IS OBSERVED THAT THE THERMAL CONDUCTIVITY GRADUALLY INCREASES WITH INCREASING FILLER CONTENT. WHEN THE COMPOSITE IS HEATED, THE HEAT WILL FLOW THROUGH THE FILLER PARTICLES, JUST AS ELECTRIC CURRENT FLOWS THROUGH A SMALL RESISTANCE PATH. FOR HIGHER FILLER CONTENT, THE PARTICLES BEGIN TO TOUCH AND FORM CONDUCTIVE CHANNELS IN THE DIRECTION OF HEAT FLOW CAUSING AN EXPONENTIAL INCREASE IN THE THERMAL CONDUCTIVITY. IT IS SEEN THAT FOR A MAXIMUM FILLER CONTENT OF 0.5, THE THERMAL CONDUCTIVITY SHOWS A VALUE AS HIGH AS  $1.764 \text{ Wm}^{-1}\text{K}^{-1}$ .

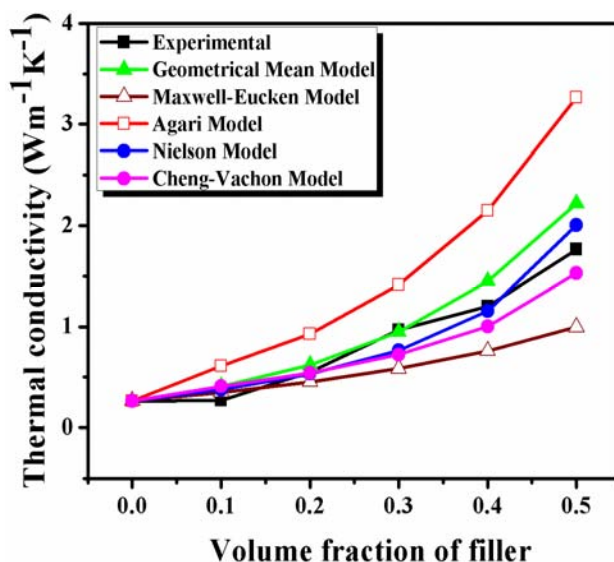


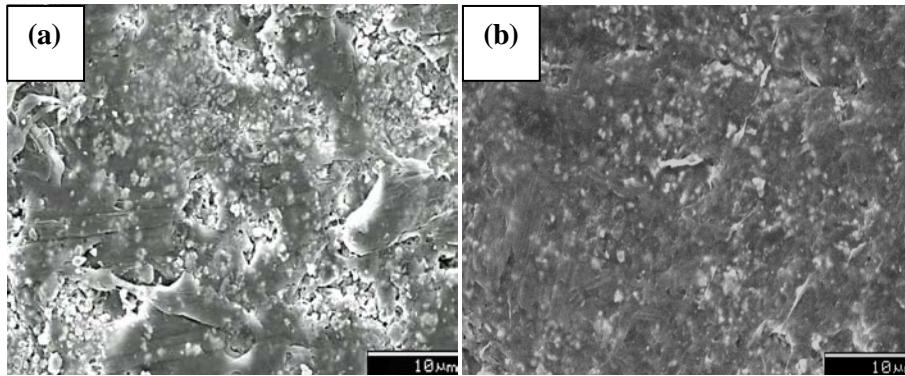
Fig. 5.5 Variation of the thermal conductivity of PTFE- $\text{Sm}_2\text{Si}_2\text{O}_7$  and comparison with the theoretical models.

FIGURE 5.5 ALSO COMPARES THE EXPERIMENTAL THERMAL CONDUCTIVITY WITH THAT PREDICTED USING VARIOUS THEORETICAL MODELS. GENERALLY ALL THE THEORETICAL MODELS ARE VALID ONLY FOR LOWER FILLER CONCENTRATIONS. AS THE FILLER CONTENT INCREASES,

INHOMOGENITY AND DEFECTS IN THE COMPOSITES INCREASES WHICH ARE NOT CONSIDERED IN THE MODELS AND THEREFORE THE DEVIATION FROM THE PREDICTED VALUES ALSO INCREASES. CLEARLY SHOWS THAT THE GEOMETRIC MEAN MODEL AND NIELSON MODEL HOLDS GOOD FOR  $V_f = 0.4$  AND  $0.4V_f$  RESPECTIVELY. EARLIER HASSELMAN AND JOHNSON [66] DEVELOPED A THEORY FOR THE EFFECTIVE THERMAL CONDUCTIVITY OF THE COMPOSITES CONSISTING OF A CONTINUOUS MATRIX WITH DILUTE CONCENTRATIONS OF FILLER, WITH A THERMAL BARRIER RESISTANCE OR K<sub>12</sub> WHICH MAY ARISE FROM POOR MECHANICAL OR CHEMICAL ADHERENCE AT THE INTERFACE. THE NIELSON MODEL ALSO THE COMPOSITE SYSTEM IS CONSIDERED TO BE HOMOGENEOUS AT AN IDEAL INTERFACE. HOWEVER, WITH THE INCREASE IN THE VOLUME FRACTION OF THE FILLER, THE MISMATCH BETWEEN THE MATRIX AND THE FILLER IN THE FORM OF INTERFACIAL GAP BECOMES SERIOUS WHICH ADVERSELY AFFECTS THE HEAT CONDUCTION. THUS THE MODEL NEEDS TO BE MODIFIED BY CONSIDERING THE INTERFACIAL THERMAL RESISTANCE. THE EXPERIMENTAL VALUES ARE HIGHER THAN THAT PREDICTED USING MAXWELL-EUCKEN AND CHENG-VACHON MODELS. THIS MAY BE DUE TO THE FACT THAT THESE MODELS ASSUME THAT THE SHAPE OF THE FILLER IS SPHERICAL. THE DISPERSION STATE OF THE FILLER IN COMPOSITES, IE., FILLER MIXED INTO MELTED MATRIX. THE EFFECT OF POROSITY IS NOT CONSIDERED WHICH WILL AFFECT THE EFFECTIVE THERMAL CONDUCTIVITY OF THE COMPOSITES DUE TO THE POOR THERMAL CONDUCTIVITY OF AIR.

#### 5.4.1.1 EFFECT OF COUPLING AGENT ON THE PROPERTIES OF PTFE/SM COMPOSITES

THE COUPLING AGENTS ARE GENERALLY EMPLOYED TO ENHANCE THE COMPATIBILITY BETWEEN THE POLYMER PHASE AND FILLER PHASE OF THE COMPOSITE SYSTEMS. FIG. 5.6 SHOWS A COMPARISON OF THE SEM MICROGRAPH OF PTFE FILLS WITH AND WITHOUT COUPLING AGENT AND UNTREATED COMPOSITE. IT CAN BE SEEN THAT THE CERAMIC PARTICLES TREATED WITH COUPLING AGENT ARE MORE UNIFORMLY DISTRIBUTED IN THE POLYMER MATRIX AND THERE IS NO AGGREGATION OF PARTICLES IN THE COMPOSITES (ALSO SEE FIG. 5.6 (A)). THUS THE PTMS COUPLING AGENT IS EFFECTIVE IN IMPROVING THE DISPERSION OF FILLER IN THE POLYMER MATRIX.



**Fig. 5.6 SEM images of PTFE loaded with 0.3  $v_f$  (a) untreated and (b) silane treated  $\text{Sm}_2\text{Si}_2\text{O}_7$ .**

TABLE 5.2 GIVES THE RELATIVE DENSITY AND POROSITY OF THE COMPOSITES WITH AMOUNT OF SILANE TREATED FILLER CONTENT. IT IS SEEN THAT THE SILANE TREATMENT IMPROVES THE ADHESION BETWEEN THE MATRIX AND THE FILLER THEREBY IMPROVING THE DENSIFICATION. THIS IS EVIDENT FROM FIG. 5.6. THE SILANE TREATED COMPOSITES SHOW HIGHER RELATIVE DENSITY WHEN COMPARED WITH THAT OF THE UNTREATED ONE. A COMPARISON OF UNTREATED AND TREATED COMPOSITES SHOW THAT THE POROSITY CONTENT IS MUCH REDUCED BY COUPLING. THIS FIGURE SHOWS A HIGH POROSITY OF 24.7 % IN THE CASE OF UNTREATED FILLER WHEREAS THE SILANE TREATED COMPOSITION EXHIBITS A MUCH REDUCED POROSITY OF 18.1 %.

**Table 5.2 The relative density, porosity and microwave dielectric properties of silane treated PTFE/ $\text{Sm}_2\text{Si}_2\text{O}_7$  composites.**

| Volume fraction filler | Relative density (%) | Porosity (%) | Microwave dielectric properties (9 GHz) |             |
|------------------------|----------------------|--------------|---|-------------|
|                        |                      |              | $\epsilon_R$                            | $TAN\delta$ |
| 0.1                    | 99.6                 | 0.4          | 2.55                                    | 0.0040      |
| 0.2                    | 98.5                 | 1.5          | 3.04                                    | 0.0031      |
| 0.3                    | 92.8                 | 7.2          | 3.51                                    | 0.0043      |
| 0.4                    | 86.7                 | 13.4         | 3.92                                    | 0.0054      |
| 0.5                    | 81.9                 | 18.1         | 4.29                                    | 0.0105      |

FIGURE 5.7 SHOWS THE COMPARISON OF THE VARIATION OF THE DIELECTRIC PROPERTIES OF SiO<sub>2</sub> COMPOSITES AT 1 MHz, FOR FILLERS TREATED WITH SILANE COUPLING AGENT AND THAT WHICH IS UNTREATED. IT IS CLEARLY OBSERVED THAT SILANE COATED COMPOSITES SHOWS A HIGHER RELATIVE PERMITTIVITY WHEN COMPARED WITH THE UNTREATED ONE WHICH IS IN AGREEMENT WITH EARLIER STUDIES [33]. THE IMPROVEMENT IN THE DIELECTRIC PROPERTIES IS DUE TO THE ENHANCEMENT IN THE RELATIVE DENSITY OF SILANE TREATED COMPOSITES. ALSO THE SILANE COUPLING AGENT ACT AS A MOLECULAR BRIDGE BETWEEN THE MATRIX AND THE FILLER THEREBY FORMING A COVALENT BOND ACROSS THE INTERFACE. HAVELINE ET AL. [34] HAS EXPLAINED THE ROLE OF COUPLING AGENTS IN DETERMINING THE EFFECTIVE INTERPHASE PERMITTIVITY. THE COUPLING AGENTS EFFECTIVELY CHANGE THE MEANS BY WHICH THE POLYMER PHASE CHEMICALLY INTERACTS WITH THE SURFACE OF THE FILLER PARTICLES. THUS THE DIELECTRIC PROPERTIES ARE CHANGING THE CHARACTERISTICS OF THE INTERPHASE REGION OF POLYMER-CERAMIC COMPOSITES. THE COUPLING AGENT FORMS COVALENT CHEMICAL BONDS WITH THE FILLER SURFACE, THEREBY FORMING THE BOND BETWEEN THE POLYMER MATRIX AND THE CERAMIC FILLER. THIS WILL INCREASE THE MOLECULAR POLARIZABILITY OF THE INTERPHASE THEREBY LEADING TO AN INCREASE IN THE DIELECTRIC PERMITTIVITY. ALSO FROM THE MICROSTRUCTURE A GOOD HOMOGENEOUS DISPERSION OF CERAMIC IN POLYMER IS OBTAINED WHICH ALSO ENHANCES THE DIELECTRIC PROPERTIES. SIMILAR OBSERVATION IS OBSERVED IN THE MICROWAVE FREQUENCY ALSO (SEE TABLE 5.2). FIG. 5.7 ALSO SHOWS THE VARIATION OF DIELECTRIC LOSS OF BOTH THE UNTREATED AND SILANE TREATED COMPOSITES. DIELECTRIC LOSS INCREASES WITH THE FILLER CONTENT AS EXPECTED. THE DIELECTRIC LOSS VALUES ARE RESPECTIVELY FROM 0.00052-0.00455 AND 0.00055-0.00678 FOR THE UNTREATED AND SILANE TREATED COMPOSITES FOR FILLER CONTENTS AS ONE CAN EVIDENTLY SEE FROM THE FIGURE FOR LOWER FILLER (UP TO 10% BY WEIGHT), THE DIELECTRIC LOSS SHOWS NO CLEAR DIFFERENCE BETWEEN THE TWO COMPOSITES. HOWEVER, FOR HIGHER FILLER CONCENTRATIONS THE DIELECTRIC LOSS VALUES EXHIBIT A SIGNIFICANT CONTRAST. THE SILANE COUPLED COMPOSITES POSSESS A HIGHER DIELECTRIC LOSS COMPARED TO THE UNTREATED ONE. SIMILAR OBSERVATION IS REPORTED BY [35] FOR ALUMINIUM/EPOXY COMPOSITES. THIS MAY BE DUE TO THE INCREASE IN THE DIELECTRIC POLARIZATION CAUSED DUE TO THE INTRODUCTION OF ADDITIONAL PHASES. SINCE THE DIELECTRIC LOSS IS QUITE SENSITIVE TO POLAR IMPURITIES OR POLAR OXIDATIVE PRODUCTS FROM POLYMER DEGRADATION DURING COMPOUNDING, THIS INCREMENT IN LOSSES SHOULD BE CONSIDERED CAREFULLY WHEN TARGETING INDUSTRIAL APPLICATIONS. HOWEVER, AT 9 GHz SILANE TREATED COMPOSITES

LOWER DIELECTRIC LOSS WHEN COMPARED WITH THAT OF THE UNTREATED ONE WHICH IS DUE TO THE REDUCED POROSITY. AT 9 GHZ, PTFE LOADS WITH TREATED  $\text{Sm}_2\text{Si}_2\text{O}_7$  HAS  $\epsilon_r = 3.51$  AND  $\tan \delta = 0.0043$ .

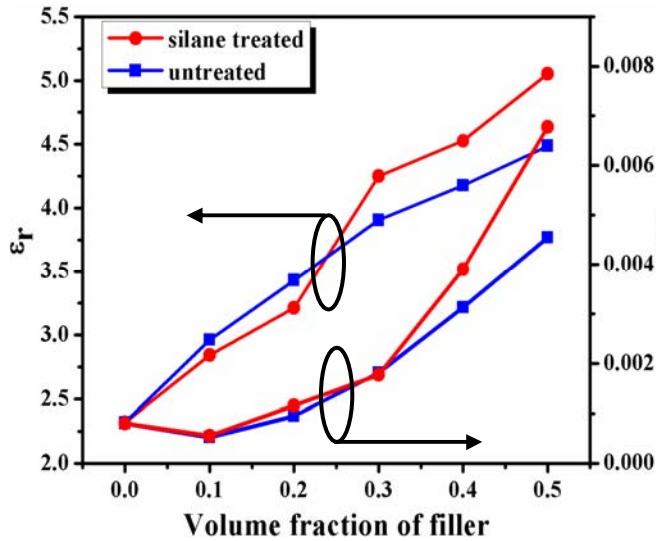


Fig. 5.7 Variation of relative permittivity and  $\tan \delta$  of untreated and silane treated PTFE/ $\text{Sm}_2\text{Si}_2\text{O}_7$  composites with volume fraction of filler at 1MHz.

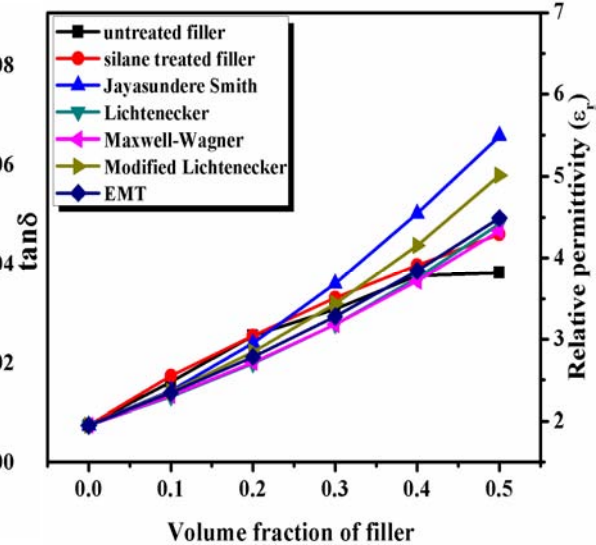


Fig. 5.8 Comparison of experimental and theoretical relative permittivity of PTFE/ $\text{Sm}_2\text{Si}_2\text{O}_7$  composites with volume fraction of filler at 9 GHz.

FIGURE 5.8 SHOWS THE COMPARISON BETWEEN THE EXPERIMENTAL AND THEORETICAL VALUES OF RELATIVE PERMITTIVITY AT 9 GHZ FOR BOTH UNTREATED AND SILANE TREATED PTFE COMPOSITES. THE MEASURED RELATIVE PERMITTIVITIES ARE WELL MATCHED WITH THE PREDICTIONS FOR LOWER FILLER CONTENT ONLY AND DEVIATIONS OCCUR AT HIGHER FILLER CONTENT DUE TO THE IMPERFECT DISPERSION OF CERAMIC PARTICLES AND ALSO DUE TO THE AIR ENCAPSULATION IN THE COMPOSITES WHICH IS NOT CONSIDERED IN THESE PREDICTIONS. AS THE FILLER CONTENT INCREASES ( $> 0.3$ ), THE RELATIVE PERMITTIVITY SHOWS A WIDE VARIATION FROM THE THEORETICAL VALUES. THE MODIFIED LICHTENECKER EQUATION IS REPORTED TO BE WELL SUITED FOR CERAMIC COMPOSITES [13, 67] WHERE A FITTING FACTOR IS INCLUDED WHICH REPRESENTS THE INTERACTION BETWEEN THE FILLER AND THE MATRIX. BUT IN THE PRESENT CASE, A PERCENTAGE DEVIATION OF NEARLY 21% IS NOTED IN THE CASE OF UNTREATED COMPOSITE. THIS IMPLIES THAT THE FITTING FACTOR MUST BE MODIFIED CONSIDERING THE NATURE OF THE



FILLER AND MATRIX. HOWEVER, THE SILANE TREATED COMPOSITES SHOWS GOOD AGREEMENT WITH THE EMT MODEL FOR HIGHER FILLER CONTENT DUE TO THE HOMOGENEITY IN DISPERSION AND ALSO THE RELATIVE PERMITTIVITY WHICH IS EVIDENT FROM TABLE 5.2. IT IS INTERESTING TO NOTE THAT BOTH THE UNTREATED AND SILANE TREATED COMPOSITES HOLD A GOOD MATCH WITH THE EMT MODEL FOR LOW FILLER CONTENT (0.1  $V_f$  TO 0.3  $V_f$ ). IN THE PRESENT CASE THE VALUE OF  $V_f$  IS OBTAINED AS 0.3 WHICH IS IN AGREEMENT WITH THE REPORTED VALUE [46]. HOWEVER, FOR HIGHER FILLER LOADING THE UNTREATED COMPOSITES EXHIBIT A LARGER DEVIATION WHEN COMPARED WITH THE SILANE COUPLED COMPOSITES. IT IS NOTED THAT WHILE THE UNTREATED PTFE/0.5  $V_f$  COMPOSITE SHOW A PERCENTAGE DEVIATION OF 19 % THE SILANE COATED PTFE/0.5  $V_f$  COMPOSITE SHOW ONLY A SMALL DEVIATION OF NEARLY 9 % WHICH IS QUITE ENCOURAGING EVIDENCE FOR THE UNIFORM DISPERSION OF THE CERAMIC FILLER IN THE POLYMER MATRIX WITH THE ADEQUATE COUPLING AGENT.

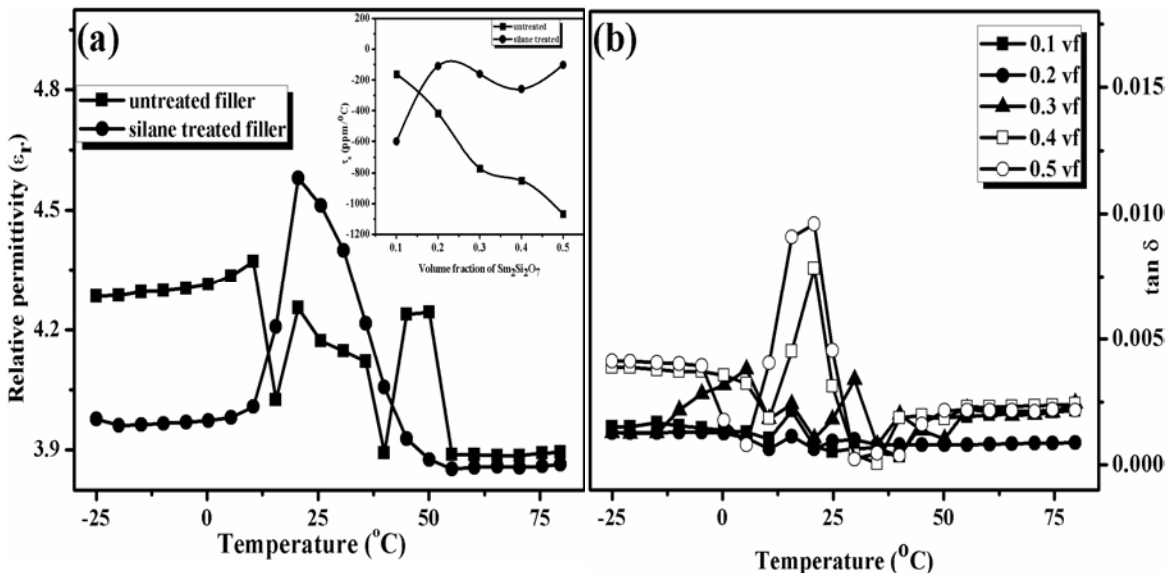


Fig. 5.9 Variation of (a) relative permittivity of untreated and silane coupled PTFE/0.4  $V_f$   $\text{Sm}_2\text{Si}_2\text{O}_7$  composite (b) dielectric loss with temperature for various volume fractions of filler at 1 MHz. Inset of (a) shows the variation of  $\tau_r$  with volume fraction of PTFE/ $\text{Sm}_2\text{Si}_2\text{O}_7$  composites.

THE TEMPERATURE DEPENDENCE OF DIELECTRIC PROPERTIES OF THE COMPOSITE IS AN IMPORTANT FACTOR WHICH JUDGES THE OVERALL PERFORMANCE OF THE MATERIAL. FIGURE 5.9 (B) SHOW THE VARIATION OF DIELECTRIC PROPERTIES OF BOTH UNTREATED AND SILANE TREATED PTFE/0.4  $V_f$   $\text{SM}_2\text{Si}_2\text{O}_7$  COMPOSITE WITH TEMPERATURE IN THE RANGE -25 TO +80  $^{\circ}\text{C}$ . IN BOTH CASES A STEADY INCREASE IN THE RELATIVE PERMITTIVITY AND DIELECTRIC LOSS VALUES

TEMPERATURE AROUND THIS JUMP IS PRESENT IN THE CASE OF ALL THE COMPOSITIONS CONSIDERED IN THE PRESENT STUDY. THIS MAY BE DUE TO THE PHASE CHANGE OF PTFE FROM TRICLINIC TO HEXAGONAL STRUCTURE. BARTHOLOMEW *et al.* [69] HAS ALSO NOTED SIMILAR VARIATION IN THE COMPOSITES.

THE TEMPERATURE COEFFICIENT OF RELATIVE PERMITTIVITY (USING EQ. (4.1) GIVEN IN CHAPTER 4. THE INSET OF FIGURE 5.9 (A) SHOWS THE VARIATION OF FILLER CONTENT FOR UNTREATED AND SILANE COUPLED COMPOSITES. IT IS CLEAR FROM IN THE CASE OF UNTREATED COMPOSITES,  $\tau_f$  BECOMES MORE NEGATIVE WITH THE AMOUNT OF FILLER CONTENT DESPITE THE FACT THAT THE CTE OF PTFE HAS A VALUE OF +63 PPM/°C. [70] ALSO OBSERVED A SIMILAR VARIATION IN THE CASE OF COMPOSITES. GENERALLY, IN COMPOSITES THE DIELECTRIC RESPONSE WITH TEMPERATURE CAN BE EXPLAINED ON THE FOLLOWING TWO COMPETITIVE MECHANISMS [70]. THE SEGMENTAL MOBILITY OF THE POLYMER IS IMPROVED BY THE INCREASE IN TEMPERATURE. THIS WILL ENHANCE THE POLARIZATION OF THE FILLER THEREBY LEADING TO AN INCREASE IN THE RELATIVE PERMITTIVITY. THE OTHER MECHANISM IS RELATED TO THE DIFFERENCE IN THE THERMAL EXPANSION COEFFICIENTS OF THE MATRIX AND THE FILLER. THE LARGE DIFFERENCE IN THESE VALUES MAY PREVENT THE AGGREGATION OF POLAR COMPONENTS AND THIS MIGHT LEAD TO A REDUCTION IN RELATIVE PERMITTIVITY WITH INCREASE IN TEMPERATURE. IN THE PRESENT CASE THE COEFFICIENT OF THERMAL EXPANSION OF PTFE AND  $\text{SM}_2\text{Si}_2\text{O}_7$  ARE 93 PPM/°C AND 1.61 PPM/°C RESPECTIVELY. THUS THE PARTICLE AGGLOMERATION IS DISRUPTED AND SUBSEQUENTLY THE RELATIVE PERMITTIVITY DECREASES.

FIGURE 5.10 SHOWS THE VARIATION OF THE COEFFICIENT OF THERMAL EXPANSION OF PTFE/ $\text{SM}_2\text{Si}_2\text{O}_7$  COMPOSITES WITH DIFFERENT VOLUME FRACTION OF BOTH UNTREATED AND TREATED FILLER. IT IS SEEN THAT WITH THE INCREASE IN FILLER CONTENT THE CTE DECREASES GRADUALLY. THIS IS QUITE EXPECTABLE DUE TO THE LOW VALUE OF CTE POSSESSED BY PTFE WHEREBY THE EXPANSION OF THE MATRIX IS CONSTRAINED [38]. GENERALLY IN COMPOSITES, THE FILLER PARTICLES CAN BE CONSIDERED TO BE SURROUNDED BY TWO TYPES OF POLYMER CHAINS: (I) TIGHTLY BOUND POLYMER OR CONSTRAINED POLYMER CHAIN AND (II) BY LOOSELY BOUND OR UNCONSTRAINED POLYMER CHAIN. WHEN THE FILLER CONTENT INCREASES, THE INTERPOLYMER SPACING DECREASES AND THE UNCONSTRAINED POLYMER CHAINS GET TRANSFORMED INTO CONSTRAINED POLYMER CHAINS. THIS INCREASED CONCENTRATION OF CONSTRAINED PTFE POLYMER CHAINS SUPPRESSES THE THERMAL EXPANSION OF THE COMPOSITES. THE CTE DECREASES FROM

TO 36 PPM/C WITH THE ADDITION OF UNTREATED  $\text{Sm}_2\text{Si}_2\text{O}_7$  CERAMIC. HOWEVER, THE CTE VALUES OF THE COMPOSITES ARE MUCH REDUCED COMPARED TO THE ADDITION OF SILANE COUPLED  $\text{Sm}_2\text{Si}_2\text{O}_7$  CERAMIC INTO THE PTFE MATRIX. THIS IS IN CONTRADICTION WITH EARLIER REPORT BY CHEN [26] WHERE AN INCREASE IN THE CTE VALUE IS NOTED WITH THE ADDITION OF SILANE COATED  $\text{Sm}_2\text{Si}_2\text{O}_7$ . THE DECREASE IN THE CTE VALUE OF SILANE TREATED PTFE/ $\text{Sm}_2\text{Si}_2\text{O}_7$  COMPOSITES IS DUE TO THE INCREASING WETTABILITY AND DISPERSION OF FILLER PARTICLES. THE UNTREATED COMPOSITES CONTAIN TINY GAPS BETWEEN THE FILLER AND THE MATRIX WHICH IS THE REASON FOR THE INCREASED CTE WHEN COMPARED TO THE COUPLED COMPOSITES.

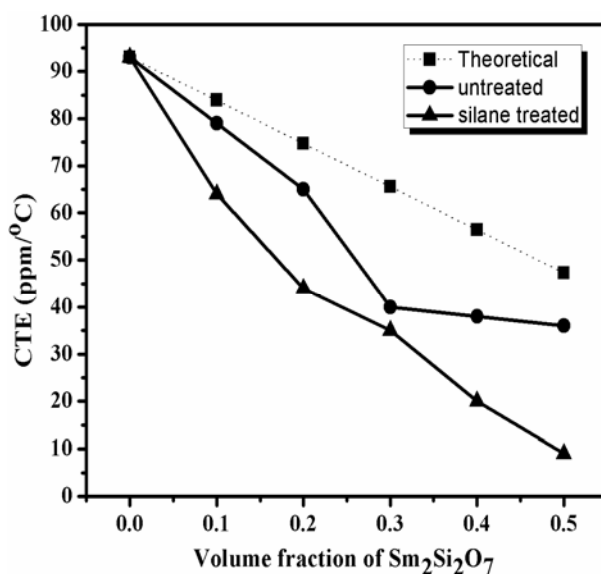


Fig. 5.10 Variation of the coefficient of thermal expansion of PTFE/ $\text{Sm}_2\text{Si}_2\text{O}_7$  composites and comparison using rule of mixtures.

THE EXPERIMENTAL CTE VALUES OF BOTH THE UNTREATED AND THE SILANE TREATED PTFE/ $\text{Sm}_2\text{Si}_2\text{O}_7$  COMPOSITES ARE COMPARED WITH THE THEORETICAL PREDICTION USING THE RULE OF MIXTURES AND ARE SHOWN IN FIG. 5.10. ACCORDING TO THE RULE OF MIXTURES THE CTE OF A TWO PHASE COMPOSITE IS DEPENDENT LINEARLY ON THE VOLUME FRACTION OF THE PHASES. THE EXPERIMENTAL VALUES SHOW A WIDE VARIATION FROM THE CALCULATED ONES. THIS IS DUE TO THE FACT THAT THE EQUATION DOES NOT CONSIDER THE MECHANICAL CONSTRAINTS BETWEEN THE MATRIX DUE TO THE FILLERS.

TABLE 5.3 GIVES THE MICROHARDNESS AND WATER ABSORPTION OF PTFE/SM<sub>2</sub>Si<sub>2</sub>O<sub>7</sub> COMPOSITES WITH FILLER CONTENT VARIATION. THE VICKER'S MICROHARDNESS OF MATRIX IS NEARLY 7  $\text{kg/mm}^2$  AS THE FILLER CONTENT INCREASES, THE MICROHARDNESS INCREASES AS EXPECTED DUE TO THE FACT THAT CERAMICS GENERALLY POSSESS A HIGHER MICROHARDNESS. IT IS SEEN THAT WITH THE INCREASE IN THE FILLER CONTENT THE MICROHARDNESS INCREASES TO VALUE OF 13  $\text{kg/mm}^2$  IN THE CASE OF UNTREATED FILLER AND FOR SILANE COUPLED FILLER.

Table 5.3 The Vicker's hardness and water absorption of PTFE/Sm<sub>2</sub>Si<sub>2</sub>O<sub>7</sub> composites.

| Composite  | Volume fraction of filler ( $v_f$ ) | Vickers microhardness ( $\text{kg/mm}^2$ ) | Water absorption (%) |
|--|-------------------------------------|--|----------------------|
| UNTREATED PTFE/SM <sub>2</sub> Si <sub>2</sub> O <sub>7</sub>      | 0.0                                 | 7  | 0.53                 |
|  | 0.1                                 | 9  | 0.15                 |
|  | 0.3                                 | 10   | 0.22                 |
|  | 0.5                                 | 13   | 13.05                |
| SILANE TREATED PTFE/SM <sub>2</sub> Si <sub>2</sub> O <sub>7</sub> | 0.1                                 | 8  | 0.02                 |
|  | 0.3                                 | 12   | 0.68                 |
|  | 0.5                                 | 16   | 2.17                 |

FROM THE TABLE IT IS ALSO EVIDENT THAT THE WATER ABSORPTION OF THE COMPOSITES INCREASES WITH THE FILLER CONTENT. THIS IS PROBABLY DUE TO THE HYDROPHILIC NATURE OF CERAMICS. A COMPARISON OF THE WATER ABSORPTION OF THE COMPOSITES UNTREATED AND TREATED WITH COUPLING AGENT SHOWS THAT THE SILANE TREATED COMPOSITES POSSESS A LOW WATER ABSORPTION DUE TO THE REDUCED POROSITY (SEE TABLES 5.1 AND 5.2). IN THE CASE OF UNTREATED COMPOSITES THE WATER ABSORPTION SHOWS A VALUE AS HIGH AS 13.05% AT 0.5 VOLUME FRACTION. ON THE OTHER HAND THE ONE TREATED WITH SILANE SHOWS A VERY LOW VALUE OF NEARLY 2.17% AT 0.5 VOLUME FRACTION. THE SILANE COUPLING AGENT REDUCES THE HYDROPHILICITY OF CERAMIC FILLER AND ALSO DISPERSES THE CERAMIC UNIFORMLY IN THE MATRIX THEREBY REDUCING WATER ABSORPTION.

### 5.4.1.2 EFFECT OF PARTICLE SIZE ON THE PROPERTIES OF PTFE/SM COMPOSITES

THE SPECIFIC SURFACE AREA MEASUREMENTS SHOW THAT THE MICRON SIZED POSSESS A VERY SMALL AVERAGE SURFACE AREA AS COMPARED TO THE NANO SIZED ONE (20.94  $\mu\text{m}^2/\text{g}$ ). FIGURES 5.11 (A) AND (B) SHOW THE MICROSTRUCTURAL IMAGES OF P FILLED WITH 0.05 AND 0.25 V<sub>F</sub> OF NANO SIZED  $\text{Sm}_2\text{Si}_2\text{O}_7$  CERAMICS. IT IS TO BE NOTED THAT AT LOWER FILLER CONTENT THE NANO SIZED PARTICLES ARE ALMOST UNIFORMLY DISPERS WHILE HIGHER CERAMIC LOADING FACILITATES THE FORMATION OF CLUSTERS. THE DISP PARTICLES INTO A POLYMER MATRIX IS VERY MUCH DEPENDENT ON THE KINETICS OF PREPARATION. AT LOWER FILLER CONTENT THE ATTRACTIVE VAN DER WAALS FORCES BETWEEN PARTICLES ARE WEAK DUE TO THE LONG INTERPARTICLE DISTANCE. THUS THE AGGLOMERATION CAN BE EASILY BROKEN BY APPLYING THE FORCE PROVIDED BY THE MIXING DEVICE. HIGHER FILLER LOADING THE INTERPARTICLE DISTANCE DECREASES EXPONENTIALLY AND A STRONG FORCE OF ATTRACTION THE PARTICLES GET AGGLOMERATED. THUS IT IS DIFFICULT TO OBTAIN COMPOSITES WITH HIGHER FILLER LOADING OF NANO SIZED POWDER. IN THE PRESENT STUDY MAXIMUM FILLER LOADING OF 0.25 V<sub>F</sub> OBTAINED.

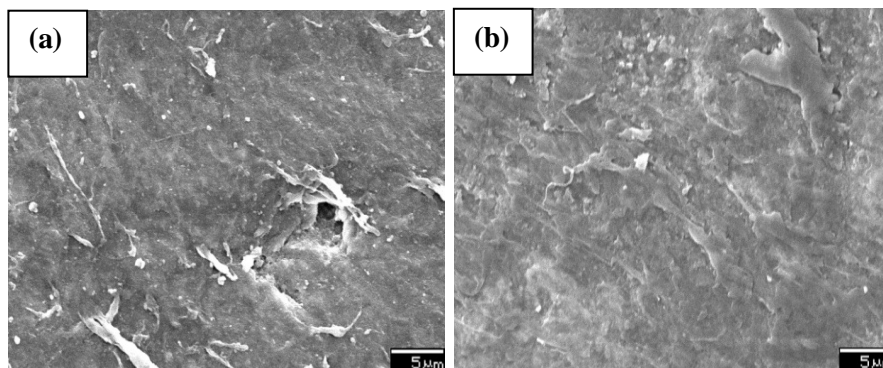


Fig. 5.11 SEM images of PTFE loaded with (a) 0.05 v<sub>f</sub> nano  $\text{Sm}_2\text{Si}_2\text{O}_7$ , (b) 0.25 v<sub>f</sub> nano  $\text{Sm}_2\text{Si}_2\text{O}_7$ .

IN ELECTRONIC PACKAGING APPLICATIONS, THE PROPOSED MATERIAL MUST WITHSTAND TEMPERATURE UP TO 300 °C AND SHOULD MAINTAIN THEIR PROPERTIES [71]. THE THERMAL STABILITY AND WEIGHT LOSS OF THE COMPOSITES ARE ANALYZED USING TGA. FIG. 5.12 SHOWS THE THERMOGRAMS OF PURE PTFE, PTFE LOADED WITH MICRO AND NANO SIZED DISM

DECOMPOSITION OF PTFE STARTS AT 531.9°C AND THE MATERIAL RESIDUE WAS ZERO AT A TEMPERATURE OF 597°C.

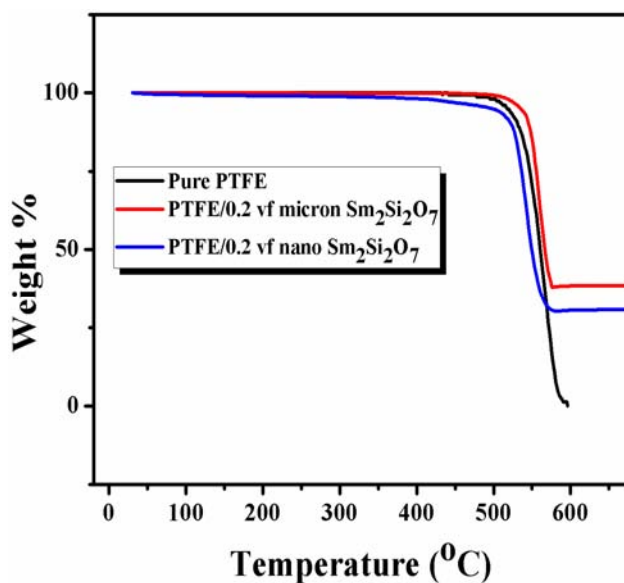


Fig. 5.12 TGA curves of PTFE/ $\text{Sm}_2\text{Si}_2\text{O}_7$  composites.

Table 5.4 TGA parameters of pure PTFE and PTFE loaded with micro and nano  $\text{Sm}_2\text{Si}_2\text{O}_7$ .

| Material                                   | $T_{10}$ ( $^{\circ}\text{C}$ ) | Filler added (wt%) | Filler residue (wt%) |
|--|---------------------------------|--------------------|----------------------|
| PURE PTF                                   | 531.9                           | 0                  | 0                    |
| PTFE/0.2 $V_F$ MSM $\text{Si}_2\text{O}_7$ | 545.7                           | 38.4               | 34.8                 |
| PTFE/0.2 $V_F$ NSM $\text{Si}_2\text{O}_7$ | 522.9                           | 38.4               | 27.9                 |

$T_{10}$  IS THE TEMPERATURE AT WHICH 10% WT OF THE SAMPLE IS LOST AFTER HEATING IN NITROGEN ATMOSPHERE.

TABLE 5.4 GIVES THE PARAMETERS OBTAINED FROM THE TGA CURVE. IT IS SEEN THAT PTFE SHOWS A  $T_{10}$  VALUE OF 531.9°C AND AN INCREASE OF MORE IS NOTED WITH THE ADDITION OF 0.2V<sub>F</sub> MICRON SIZED FILLER. THIS INCREASE IN THE DECOMPOSITION TEMPERATURE MAY BE DUE TO THE INCREASED INTERACTION BETWEEN THE MATRIX AND THE FILLER. SEGMENTAL MOBILITY OF THE POLYMER IS REDUCED. THUS THE THERMAL STABILITY IS INCREASED WITH FILLER ADDITION. THE RESIDUE FILLER IN THE PTFE COMPOSITE AT 600°C

NEARLY CLOSE TO THE AMOUNT INITIALLY ADDED. HOWEVER, IN CONTRAST TO THE EARLIER [72] THE NANO-COMPOSITE SHOWS A LOW DECOMPOSITION TEMPERATURE THAN THE PURE PTFE. IN THE CASE OF NANO FILLER LOADED COMPOSITE, A SLIGHT DECREASE IN WEIGHT LOSS TEMPERATURE IS NOTED WHICH MAY BE DUE TO THE LOSS OF VOLATILE BY-PRODUCTS. FROM TABLE 5.4 WHERE THE RESIDUE FILLER FOR NANO-COMPOSITE IS ONLY 27.9 %.

TABLE 5.5 GIVES THE MICROWAVE DIELECTRIC PROPERTIES OF THE PTFE/SMI COMPOSITES LOADED WITH MICRON AND NANO SIZE FILLERS. IN BOTH CASES IT IS CLEARLY OBSERVED THAT THE RELATIVE PERMITTIVITY INCREASES WITH FILLER CONTENT WHICH IS QUITE EXPECTED. THE INCREASED RELATIVE PERMITTIVITY IS COMPARED WITH THAT OF THE PTFE MATRIX. AN INCREASE IN THE NANO FILLER CONCENTRATION TENDS TO INCREASE THE RELATIVE PERMITTIVITY. THE INCREASE IN THE NUMBER OF NANO PARTICLE FILLERS CONTRIBUTING TO THE EFFECTIVE RELATIVE PERMITTIVITY WHICH OVERHEADS THE EFFECT OF IMMOBILIZATION OF POLYMER CHAINS AT HIGHER FILLER CONTENT WHICH HAS A TENDENCY TO LOWER THE RELATIVE PERMITTIVITY. AT A HIGHER FILLER LOADING LEVEL, THE COMPOSITES FILLED WITH SMALLER PARTICLES WILL HAVE A LARGER INTERFACIAL AREA WHICH PROMOTES THE INTERFACIAL POLARIZATION MECHANISM THEREBY INCREASING THE EFFECTIVE RELATIVE PERMITTIVITY. THE NUMBER OF PARTICLES IN A NANO COMPOSITE IS GREATER THAN THAT IN THE MICRON SIZE COMPOSITES FOR THE SAME FILLER LOADING. SIMILAR OBSERVATIONS WERE EARLIER REPORTED IN THE CASE OF EPOXY/SI COMPOSITES [37]. IT IS ALSO NOTED THAT THE DIELECTRIC LOSS INCREASES WITH THE INCREASE IN FILLER CONTENT FOR BOTH MICRON AND NANO SIZES AND A HIGH DIELECTRIC LOSS IS OBSERVED IN THE NANO FILLED COMPOSITES. THE REASON FOR THIS INCREASE IN DIELECTRIC LOSS IS DUE TO THE LARGE INTERACTION ZONE AND THE INCREASE IN THE LATTICE STRAIN CAUSED BY THE INCREASE IN THE SURFACE AREA. MOREOVER, SEVERAL OTHER FACTORS SUCH AS CRYSTALLINITY, POLYMER MORPHOLOGY, SPACE CHARGE DISTRIBUTION, REDUCTION IN THE INTERNAL POLARIZATION DUE TO THE DECREASE IN THE PARTICLE SIZE AND SCATTERING MECHANISMS MAY ALSO AFFECT THE DIELECTRIC PROPERTIES SIGNIFICANTLY [74].

Table 5.5 The density, microwave dielectric properties and water absorption of PTFE/Sm<sub>2</sub>Si<sub>2</sub>O<sub>7</sub>.

| Volume fraction filler | Density (g/cm <sup>3</sup> ) | Microwave dielectric properties (9 GHz) |              | Water absorption (%) |
|------------------------|------------------------------|---|--------------|----------------------|
|                        |                              | $\epsilon_R$                            | TAN $\delta$ |                      |
| <b>micron</b>          |                              |   |              |                      |
| 0.05                   | 2.21                         | 2.37                                    | 0.0009       | 0.08                 |
| 0.10                   | 2.32                         | 2.48                                    | 0.0023       | 0.15                 |
| 0.15                   | 2.49                         | 2.92                                    | 0.0026       | 0.17                 |
| 0.20                   | 2.79                         | 3.04                                    | 0.0051       | 0.19                 |
| 0.25                   | 2.98                         | 3.49                                    | 0.0057       | 0.23                 |
| <b>nano</b>            |                              |   |              |                      |
| 0.05                   | 2.01                         | 2.33                                    | 0.0046       | 0.05                 |
| 0.10                   | 2.20                         | 2.52                                    | 0.0130       | 0.12                 |
| 0.15                   | 2.40                         | 2.71                                    | 0.0219       | 0.14                 |
| 0.20                   | 2.47                         | 3.06                                    | 0.0161       | 0.54                 |
| 0.25                   | 2.53                         | 3.39                                    | 0.0315       | 0.68                 |

FIGURES 5.13 (A) AND (B) RESPECTIVELY SHOW THE COMPARISON BETWEEN EXPERIMENTAL AND THEORETICAL VALUES OF RELATIVE PERMITTIVITY FOR BOTH MICRON AND NANO SIZE FILLER LOADED PTFE/SM COMPOSITES. IT CAN BE OBSERVED THAT THE NANO FILLED COMPOSITES SHOW A BETTER AGREEMENT WITH THE THEORETICAL PREDICTIONS. FROM IT IS CLEAR THAT NANO COMPOSITES ARE FOUND TO BE IN GOOD AGREEMENT WITH THE LIGHTNECKER EQUATION IMPLYING A GOOD DISPERSION OF THE NANO PARTICLES IN THE TWO-PHASE MODELS, BOTH THE CONSTITUENTS OF THE COMPOSITE SYSTEM ARE CONSIDERED AS DIFFERENT PHASES RATHER THAN CONSIDERING ONE CONSTITUENT OF THE COMPOSITE AS BEING IN A CONTINUOUS PHASE OF ANOTHER. THE RELATIVE PERMITTIVITY OF COMPOSITES ALSO DEPENDS ON THE DISTRIBUTION OF THE FILLER, SHAPE AND SIZE OF FILLERS AND INTERFACE BETWEEN FILLERS AND POLYMERS. THE COMPOSITES WITH LOWER NANO FILLER CONTENT SHOWS A GOOD MATCH WITH THE MIXTURE MODEL WHILE THE HIGHER VOLUME FRACTIONS DEVIATE MORE FROM THE PREDICTIONS. THIS MAY BE DUE TO THE HIGHER AMOUNT OF POROSITY IN THE COMPOSITES. IN THE CASE OF MICRON COMPOSITES MORE PRECISE MODEL WHICH CONSIDERS THE INTERFACIAL CONTRIBUTION TO THE INTERPHASE POWER LAW NEED TO BE CONSIDERED.



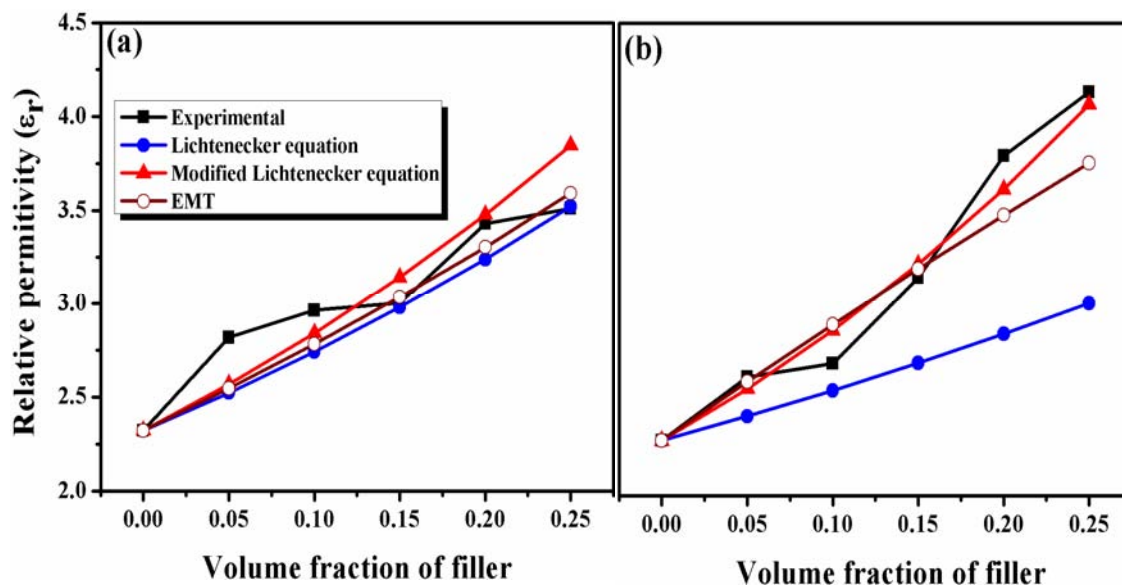


Fig. 5.13 Comparison of experimental and theoretical relative permittivity of (a) PTFE/micro  $\text{Sm}_2\text{Si}_2\text{O}_7$  (b) PTFE/nano  $\text{Sm}_2\text{Si}_2\text{O}_7$  composites with volume fraction of filler at 1MHz.

FIGURE 5.14 SHOWS THE VARIATION OF THE FILLER CONTENT FOR PTFE/SM COMPOSITES. IT IS CLEAR FROM THE FIGURE THAT IN THE CASE OF MICRO-SIZE FILLER,  $\tau_c$  IS MORE NEGATIVE WITH THE AMOUNT OF FILLER CONTENT DESPITE THE FACT THAT THE HAS A VALUE OF +63 PERCENT. FROM THE FIGURE CLEARLY SHOWS THAT THE COMPOSITES WITH MICRO-SIZE FILLER HAVE A LOWER  $\tau_c$  VALUE. IN THE CASE OF NANO-COMPOSITES, THE SEGMENTAL MOBILITY OF THE POLYMER IS MUCH REDUCED SINCE MORE PARTICLES SURROUND EACH CHAIN THEREBY INHIBITING THE FREE MOVEMENT. THE LARGE DIFFERENCE IN THE CTE BETWEEN MATRIX AND THE FILLER MAY PREVENT THE AGGREGATION OF THE POLAR COMPONENTS, LEAD TO A REDUCTION IN RELATIVE PERMITTIVITY WITH INCREASE IN TEMPERATURE. FIGURE 5.14 SHOWS THE VARIATION OF RELATIVE PERMITTIVITY WITH TEMPERATURE IN THE RANGE OF +80°C FOR 0.25 VOLUME FRACTION OF PTFE/NANO  $\text{Sm}_2\text{Si}_2\text{O}_7$  COMPOSITE. IT IS EVIDENT FROM THE FIGURE THAT THE VARIATION OF RELATIVE PERMITTIVITY IS ALMOST REGULAR EXCEPT FOR AN INCREASE IN PERMITTIVITY VALUE AT A TEMPERATURE AROUND 20°C. THIS IS DUE TO THE PHASE CHANGE ASSOCIATED WITH PTFE POLYMER AS DISCUSSED EARLIER.

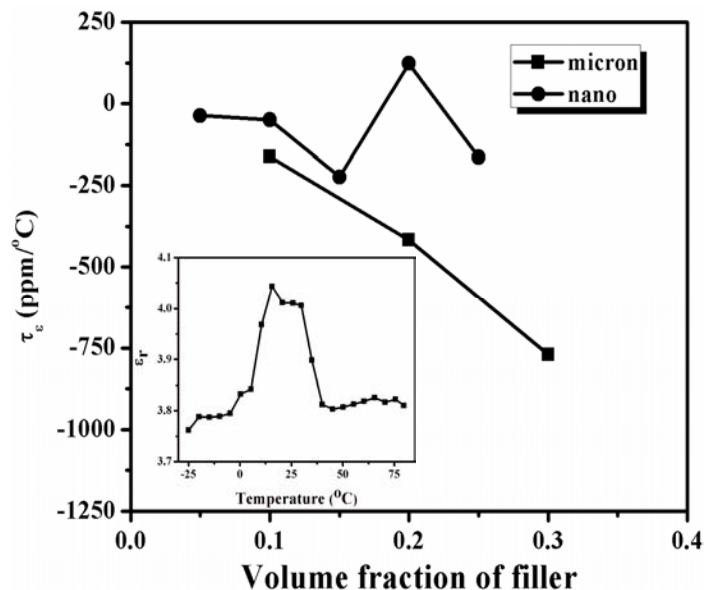


Fig. 5.14 Variation of temperature coefficient of relative permittivity of PTFE/ $\text{Sm}_2\text{Si}_2\text{O}_7$  composites with volume fraction of micron and nano size fillers.

FIGURE 5.15 SHOWS THE VARIATION OF CTE OF PTFE COMPOSITES WITH DIFFERENT VOLUME FRACTION OF BOTH MICRON AND NANO SIZE FILLERS. IT IS FOUND INCREASE IN BOTH TYPE OF FILLER CONTENT, THE CTE DECREASES GRADUALLY. THIS IS EXPECTABLE DUE TO THE LOW VALUE OF CTE POSSESSED BY PTFE (65 PPM/°C) WHEREBY THE EXPANSION OF THE MATRIX IS CONSTRAINED. IT IS TO BE NOTED THAT FOR THE SAME FRACTION OF FILLER, NANO-COMPOSITE EXHIBITS A MUCH LOWER VALUE OF CTE WHEN COMPARED TO THE MICRO COMPOSITES. THE CTE OF MICRO AND NANO LOADED COMPOSITES HAS A CTE VALUE OF 65 PPM/°C AND 40 PPM/°C RESPECTIVELY. THIS MAY BE DUE TO THE FACT THAT, FOR THE SAME FILLER CONTENT, NANO PARTICLES HAVE LARGE SURFACE AREA AND HIGH PARTICLE DENSITY. THIS REDUCES THE FREE VOLUME OF THE MATRIX WHICH IN TURN CONSTRAINS THE MATRIX EXPANSION. ALSO THE NANO PARTICLES ARE WELL DISPERSED IN THE POLYMER MATRIX COMPARED TO THE MICRON SIZED PARTICLES. THIS WILL CREATE GOOD INTERFACIAL AREA BETWEEN NANO  $\text{Sm}_2\text{Si}_2\text{O}_7$  AND PTFE AND REPORTS SHOW THAT COMPOSITES WITH STRONG INTERFACIAL BONDING POSSESS A VERY LOW VALUE OF CTE [75]. IN THE CASE OF NANO-COMPOSITES THE CONCENTRATION OF CONSTRAINED PTFE POLYMER CHAINS IS MUCH HIGHER WHICH SUPPRESSES THE EXPANSION OF THE COMPOSITES.

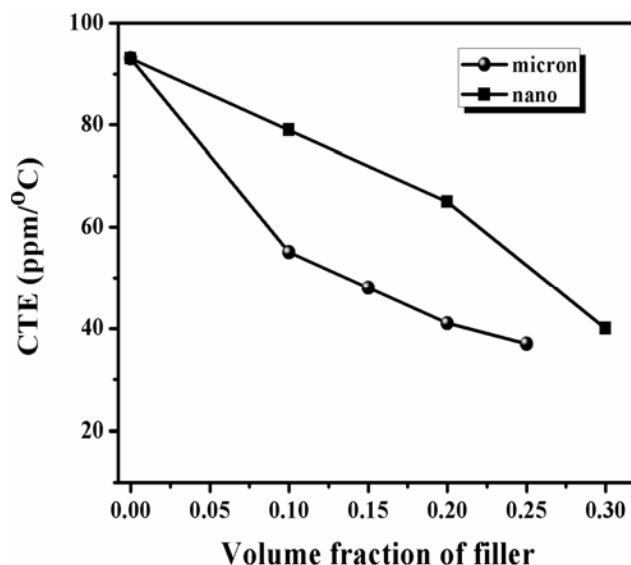


Fig. 5.15 Variation of the coefficient of thermal expansion of micron and nano PTFE/ $\text{Sm}_2\text{Si}_2\text{O}_7$  composites.

TABLE 5.5 ALSO GIVES THE WATER ABSORPTION OF COMPOSITES WITH MICRON AND NANO FILLER CONTENT VARIATION. THE COMPOSITES CONSIST OF TWO MATERIALS, ONE HYDROPHILIC AND THE OTHER HYDROPHOBIC IN NATURE. FROM THE EVIDENT THAT THE WATER ABSORPTION OF BOTH THE COMPOSITES INCREASES WITH THE WHICH IS DUE TO THE HYDROPHILIC NATURE OF THE CERAMICS. A COMPARISON OF ABSORPTION OF THE COMPOSITES WITH VARYING FILLER SIZE SHOWS THAT SMALLER HIGHER IS THE WATER ABSORPTION TENDENCY. IN THE CASE OF PTFE REINFORCED WITH 0.2  $\text{Sm}_2\text{Si}_2\text{O}_7$  SHOWS A WATER ABSORPTION OF 0.19 % WHEREAS ON THE OTHER HAND THAT SAME VOLUME FRACTION OF NANO SHOWS A HIGH VALUE OF 0.54%. THIS IS DUE TO THE HIGHER SURFACE AREA OF NANO CERAMIC FILLER.

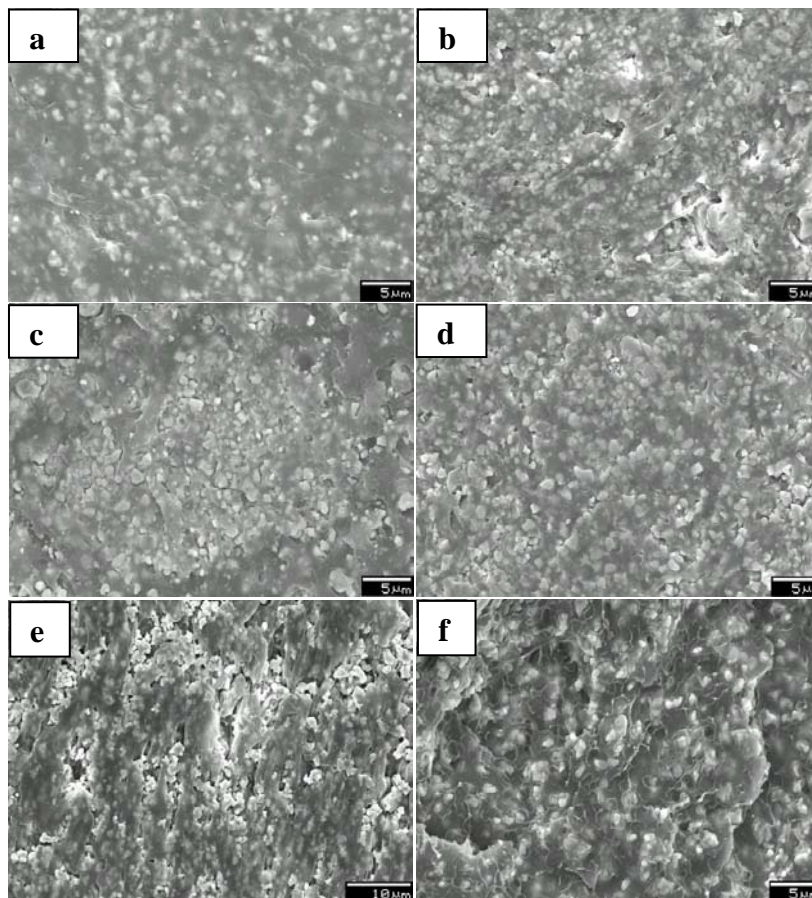
5.4.2  $\text{Sm}_2\text{Si}_2\text{O}_7$  FILLED POLYETHYLENE AND POLYSTYRENE COMPOSITES

Fig. 5.16 SEM images of (a) PE-0.3  $v_f$   $\text{Sm}_2\text{Si}_2\text{O}_7$ , (b) PE-0.5  $v_f$   $\text{Sm}_2\text{Si}_2\text{O}_7$ , (c) PS-0.3  $v_f$   $\text{Sm}_2\text{Si}_2\text{O}_7$ , (d) PS-0.5  $v_f$   $\text{Sm}_2\text{Si}_2\text{O}_7$ , (e) fractured surface of PE-0.3  $v_f$   $\text{Sm}_2\text{Si}_2\text{O}_7$  and (f) PS-0.3  $v_f$   $\text{Sm}_2\text{Si}_2\text{O}_7$ .

FIGURES 5.16 (A)-(D) SHOW THE MICROSTRUCTURAL IMAGES OF PE-SM  $\text{Sm}_2\text{Si}_2\text{O}_7$  POLYMER – CERAMIC COMPOSITES FOR DIFFERENT VOLUME FRACTION OF LOADING. FROM FIG. 5.16 (A) AND 5.16 (B) IT IS CLEAR THAT THE CERAMIC PARTICLES ARE UNIFORMLY DISTRIBUTED IN THE POLYETHYLENE MATRIX. AS THE FILLER CONTENT INCREASES THE CERAMIC PARTICLES GREW DENSER INDICATING EXCELLENT COMPATIBILITY BETWEEN POLYETHYLENE MATRIX. HOWEVER, IN THE POLYSTYRENE COMPOSITES (FIGS. 5.16 (C) AND 5.16 (D)) A HOMOGENEOUS PARTICLE DISTRIBUTION ALONG WITH SMALL TRAILS OF AGGREGATION IS OBSERVED. IT IS ALSO FOUND THAT THE POROSITY OF THESE COMPOSITES INCREASES IN THE FILLER LOADING. FIGS. 5.16 (E) AND (F) SHOW THE FRACTURED SURFACES OF PE-SM

PS-SM<sub>2</sub>Si<sub>2</sub>O<sub>7</sub> FOR 0.3 VOLUME FRACTION OF CERAMIC. THESE MICROSTRUCTURES INDICATE A HOMOGENEOUS DISTRIBUTION OF THE CERAMIC PARTICLES IN BOTH THE POLYMER MELT

**Table 5.6 The physical and dielectric properties (at 1 MHz) of polyethylene-Sm<sub>2</sub>Si<sub>2</sub>O<sub>7</sub> and polystyrene-Sm<sub>2</sub>Si<sub>2</sub>O<sub>7</sub> polymer ceramic composites.**

| Material  | Filler Volume Fraction | Density (g/cm <sup>3</sup> ) | Relative density (%) | Porosity (%) | At 1 MHz     |              |
|---|------------------------|------------------------------|----------------------|--------------|--------------|--------------|
|   |                        |                              |                      |              | $\epsilon_R$ | TAN $\delta$ |
| POLYETHYLENE-SM <sub>2</sub> Si <sub>2</sub> O <sub>7</sub> COMPOSITE | 0.0                    | 0.95                         | 99.6                 | 0.4          | 2.62         | 0.0006       |
|   | 0.1                    | 1.40                         | 98.6                 | 1.4          | 3.17         | 0.0008       |
|   | 0.2                    | 1.87                         | 98.9                 | 1.1          | 3.48         | 0.0014       |
|   | 0.3                    | 2.29                         | 96.6                 | 3.4          | 4.35         | 0.0027       |
|   | 0.4                    | 2.75                         | 96.5                 | 3.5          | 5.02         | 0.0059       |
|   | 0.5                    | 3.14                         | 94.6                 | 5.4          | 5.39         | 0.0091       |
| POLYSTYRENE-SM <sub>2</sub> Si <sub>2</sub> O <sub>7</sub> COMPOSITE  | 0.0                    | 1.04                         | 98.3                 | 1.7          | 3.20         | 0.0017       |
|   | 0.1                    | 1.44                         | 96.0                 | 4.0          | 3.51         | 0.0012       |
|   | 0.2                    | 1.79                         | 90.9                 | 9.0          | 4.19         | 0.0014       |
|   | 0.3                    | 2.21                         | 90.9                 | 9.1          | 4.41         | 0.0034       |
|   | 0.4                    | 2.65                         | 90.9                 | 9.1          | 5.12         | 0.0078       |
|   | 0.5                    | 3.05                         | 90.8                 | 9.2          | 6.11         | 0.0087       |

TABLE 5.6 GIVES THE RELATIVE DENSITY AND POROSITY OF PS-SM<sub>2</sub>Si<sub>2</sub>O<sub>7</sub> AND PS-SM<sub>2</sub>Si<sub>2</sub>O<sub>7</sub> COMPOSITES WITH THE VOLUME FRACTION OF THE FILLER. THE DENSITIES OF POLYETHYLENE AND POLYSTYRENE MEASURED BY ARCHIMEDES METHOD ARE FOUND TO BE 0.95 G/CM<sup>3</sup> AND 1.04 G/CM<sup>3</sup> RESPECTIVELY. IT IS FOUND THAT THE DENSITY OF THE COMPOSITE INCREASES WITH THE FILLER CONTENT AS EXPECTED DUE TO THE HIGHER DENSITY OF CERAMIC. IT IS OBSERVED THAT THE RELATIVE DENSITY IS MORE IN THE CASE OF PE-SM<sub>2</sub>Si<sub>2</sub>O<sub>7</sub> COMPOSITES SHOWING GOOD ADHESION BETWEEN THE POLYMER AND THE CERAMIC PARTICLES. MAXIMUM FILLER LOADING OF SM<sub>2</sub>Si<sub>2</sub>O<sub>7</sub> SHOWS A RELATIVE DENSITY OF 94.6% WHEREAS PS-SM<sub>2</sub>Si<sub>2</sub>O<sub>7</sub> HAS ONLY ABOUT 91% DENSIFICATION. THIS MAY BE DUE TO THE PRES

OF VOIDS INSIDE THE COMPOSITE WITH THE INCREASED FILLER CONTENT. THIS IS A CLEAR EVIDENCE OF THE STRONG ADHESION BETWEEN THE POLYETHYLENE MATRIX AND SMO. THIS IS ALSO CLEAR FROM THE SEM IMAGES.

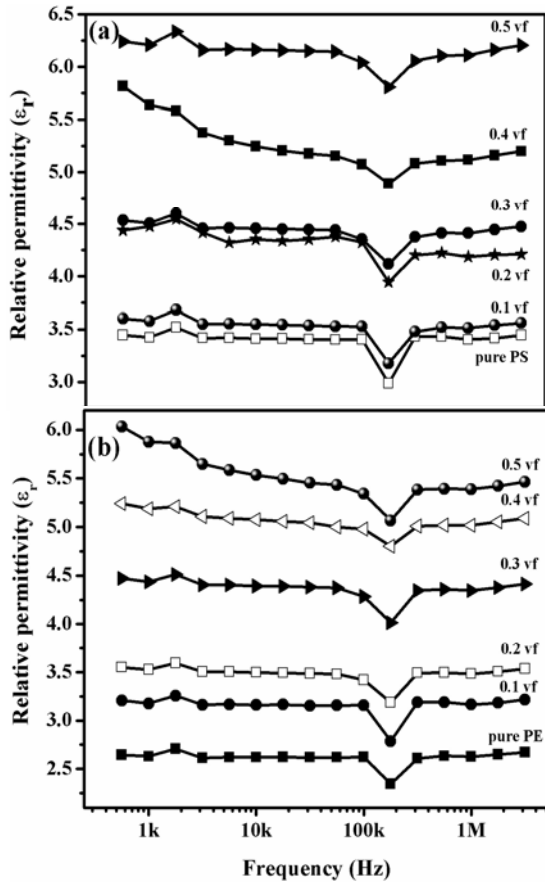


Fig. 5.17 The variation of relative permittivity with frequency for (a) PS/Sm<sub>2</sub>Si<sub>2</sub>O<sub>7</sub> and (b) PE/Sm<sub>2</sub>Si<sub>2</sub>O<sub>7</sub> composites.

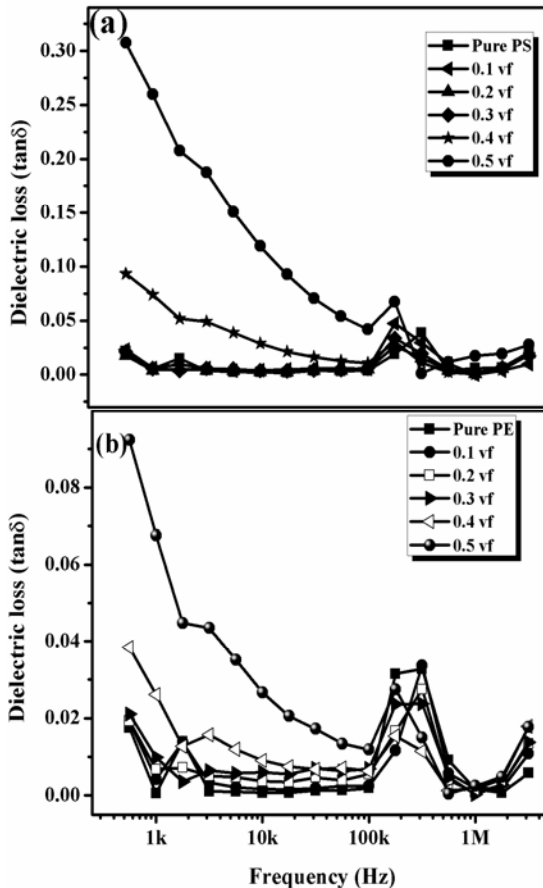


Fig. 5.18 The variation of dielectric loss with frequency for (a) PS/Sm<sub>2</sub>Si<sub>2</sub>O<sub>7</sub> and (b) PE/Sm<sub>2</sub>Si<sub>2</sub>O<sub>7</sub> composites.

THE RELATIVE PERMITTIVITY VARIATION OF THE COMPOSITES WITH THE FILLER D AS A FUNCTION OF FREQUENCY IN THE RANGE 1 KHZ – 1SMOZ AND PE/SMOZ COMPOSITES ARE SHOWN IN FIGS. 5.17 (A) AND (B). IT IS FOUND THAT THE RELATIVE PERM THE COMPOSITES REMAIN NEARLY A CONSTANT IN THE WHOLE MEASURED FREQUO RELATIVE PERMITTIVITY IS FOUND TO BE NEARLY INDEPENDENT OF FREQUENCY LOADING. HOWEVER, FOR HIGHER FILLER CONTENTS IT TENDS TO BE MORE FREQUENCY DEPENDENT. IN POLYMERS THE DIPOLAR ORIENTATION COMES FROM THE MOTION O

GROUPS. BUT THE CROSS LINKING NATURE OF THE POLYMERS HINDERS THE MOLECULAR POLAR GROUPS. THUS THE POLYMER MOLECULES WITHIN THE INTERPHASE REGION ARE FIPOLAR POLARIZATION WHEN COMPARED TO THE MOLECULES IN THE BULK MATRIX RESULTING TO A REDUCTION IN THE RELATIVE PERMITTIVITY.

FIGS. 5.18 (A) AND (B) RESPECTIVELY SHOW THE VARIATION OF DIELECTRIC LOSS TANGENT WITH FREQUENCY. THE DIELECTRIC LOSS INCREASES GRADUALLY WITH THE FILLER CONTENT. HOWEVER, A SLIGHT DECREASE IN RELATIVE PERMITTIVITY IS NOTED FOR BOTH THE COMPOSITES AT 9000 KHZ. THIS MAY BE PROBABLY DUE TO THE DIPOLAR RELAXATION PROCESS ASSOCIATED WITH THE COMPOSITES [41, 76]. AT THE SAME FREQUENCY AN INCREASE IN THE DIELECTRIC LOSS TANGENT IS OBSERVED. IT HAS BEEN REPORTED EARLIER THAT THE POLYSTYRENE AND POLYETHYLENE COMPOSITES SHOW A RELAXATION PEAK IN THE RANGE 1 HZ-100 KHZ AT VERY LOW AND HIGH TEMPERATURES [41, 76]. HOWEVER, IN THE PRESENT CASE THE INCREASE IN THE DIELECTRIC LOSS TANGENT AT ROOM TEMPERATURE MAY BE DUE TO THE NON-ACTIVATED CHARGE MOTION SUCH AS TUNNELLING.

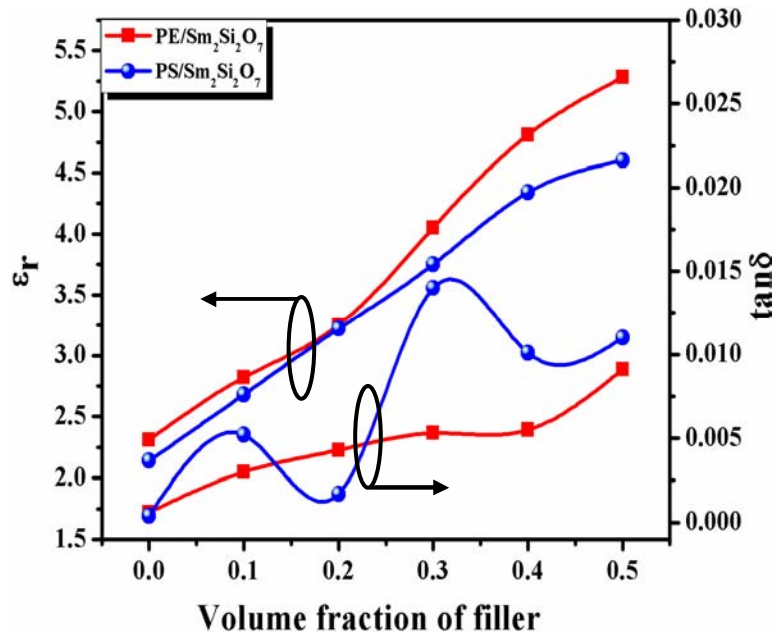


Fig. 5.19 Variation of relative permittivity and  $\tan \delta$  of polystyrene- $\text{Sm}_2\text{Si}_2\text{O}_7$  and polyethylene- $\text{Sm}_2\text{Si}_2\text{O}_7$  composites with volume fraction of filler at 9 GHz.

FIGURE 5.19 SHOWS THE VARIATION OF RELATIVE PERMITTIVITY AND DIELECTRIC LOSS TANGENT WITH VOLUME FRACTION OF  $\text{Sm}_2\text{Si}_2\text{O}_7$  AT 9 GHZ FOR PE- $\text{Sm}_2\text{Si}_2\text{O}_7$  AND PS- $\text{Sm}_2\text{Si}_2\text{O}_7$  COMPOSITES RESPECTIVELY. IN BOTH THE CASES THE RELATIVE PERMITTIVITY INCREASES WITH THE

DUE TO THE HIGH RELATIVE PERMITTIVITY COMPARED WITH THAT OF THE RESPECTIVE MATRICES. FROM THE FIGURE IT IS ALSO OBSERVED THAT AS THE FILLER CONTENT DIELECTRIC LOSS ALSO INCREASES DUE TO THE INCREASED POROSITY OF THE COMPOSITE ALSO DUE TO THE INTERFACIAL POLARIZATION BETWEEN THE POLYMER AND CERAMIC LOADINGS. AT 9 GHZ, A LOW VALUE OF RELATIVE PERMITTIVITY AND DIELECTRIC LOSS ( $\tan \delta = 0.0091$  FOR PE-SM<sub>2</sub>Si<sub>2</sub>O<sub>7</sub> COMPOSITES AND  $\tan \delta = 0.011$  FOR PS-SM<sub>2</sub>Si<sub>2</sub>O<sub>7</sub> COMPOSITES) ARE OBTAINED EVEN FOR A HIGHER FILLER CONTENT (0.5 V

FIGURES 5.20 (A) AND (B) RESPECTIVELY SHOW THE COMPARISON BETWEEN EXPERIMENTAL AND THE THEORETICAL VALUES OF RELATIVE PERMITTIVITY AT 9 GHZ VARIOUS THEORETICAL PREDICTIONS FOR PS/PE/SM<sub>2</sub>Si<sub>2</sub>O<sub>7</sub> COMPOSITES IS SEEN THAT FOR BOTH THE COMPOSITES THE LICHTENECKER AND MAXWELL – WAGNER EQUATION SHOWS A WIDE DEVIATION FROM THE EXPERIMENTAL VALUES. THE PERCENTAGE DEVIATION FROM EXPERIMENTAL VALUES FROM THESE PREDICTIONS IS FOUND TO INCREASE FROM 5.3 % FOR PE-SM<sub>2</sub>Si<sub>2</sub>O<sub>7</sub> TO A MAXIMUM OF 9 % FOR THE FILLER CONTENT OF 0.5 FOR PS-SM<sub>2</sub>Si<sub>2</sub>O<sub>7</sub>. GENERALLY ALL THE THEORETICAL PREDICTIONS ARE VALID FOR LOW FILLER CONTENTS DUE TO THE IMPACT OF CERAMIC PARTICLES AT HIGHER FILLER CONTENTS AND ALSO DUE TO THE AIR ENCAPSULATION IN COMPOSITES. ALSO THESE PREDICTIONS DO NOT CONSIDER THE MATRIX/FILLER INTERACTIONS AND IS VALID FOR COMPOSITES WITH NEAR VALUES OF RELATIVE PERMITTIVITY OF FILLER AND MATRIX. RECENTLY [17] REPORTED THAT MODIFIED LICHTENECKER EQUATION SHOWS A BETTER FIT WITH THE EXPERIMENTAL RESULTS FOR BST-CYCLIC OLEFIN COPOLYMER COMPOSITES BUT EXHIBITED A SIGNIFICANT DISCREPANCY BEYOND A FILLER CONTENT OF 0.5. EARLIER REPORTS [43] SHOW A VALUE OF -0.455352 AND -0.477392 FOR CYANACRYLATE/BATIO POLYMER-CERAMIC COMPOSITES RESPECTIVELY [35]. IN THE PRESENT STUDY OBTAINED A VALUE OF 0.2365 FOR PE-SM<sub>2</sub>Si<sub>2</sub>O<sub>7</sub> AND -0.2272 FOR PS-SM<sub>2</sub>Si<sub>2</sub>O<sub>7</sub> COMPOSITES. THE CALCULATED RELATIVE PERMITTIVITY VALUES USING THE MODIFIED LICHTENECKER EQUATION SHOW GOOD CORRESPONDENCE WITH THE EXPERIMENTAL VALUES FOR BOTH THE COMPOSITES AT A VOLUME FRACTION OF FILLER CONTENT WITH A PERCENTAGE DEVIATION LESS THAN 3 % FOR PE-SM<sub>2</sub>Si<sub>2</sub>O<sub>7</sub> AND 5 % FOR PS-SM<sub>2</sub>Si<sub>2</sub>O<sub>7</sub>. HOWEVER, IT IS FOUND THAT FOR FILLER CONTENT OF 0.5 VOLUME FRACTION PREDICTIONS DEVIATE FROM THE EXPERIMENTAL VALUE SHOWING A VALUE AS HIGH AS 10.5 FOR PS-SM<sub>2</sub>Si<sub>2</sub>O<sub>7</sub> AND NEARLY 20 % FOR PE-SM<sub>2</sub>Si<sub>2</sub>O<sub>7</sub>. THIS LARGE DEVIATION OBSERVED FOR PS-



$\text{Sm}_2\text{Si}_2\text{O}_7$  COMPOSITES MAY BE DUE TO THE SLIGHT INHOMOGENITY IN THE PARTICLE DISTRIBUTION IN THE POLYSTYRENE MATRIX WHEN COMPARED TO THAT OF POLYETHYLENE.

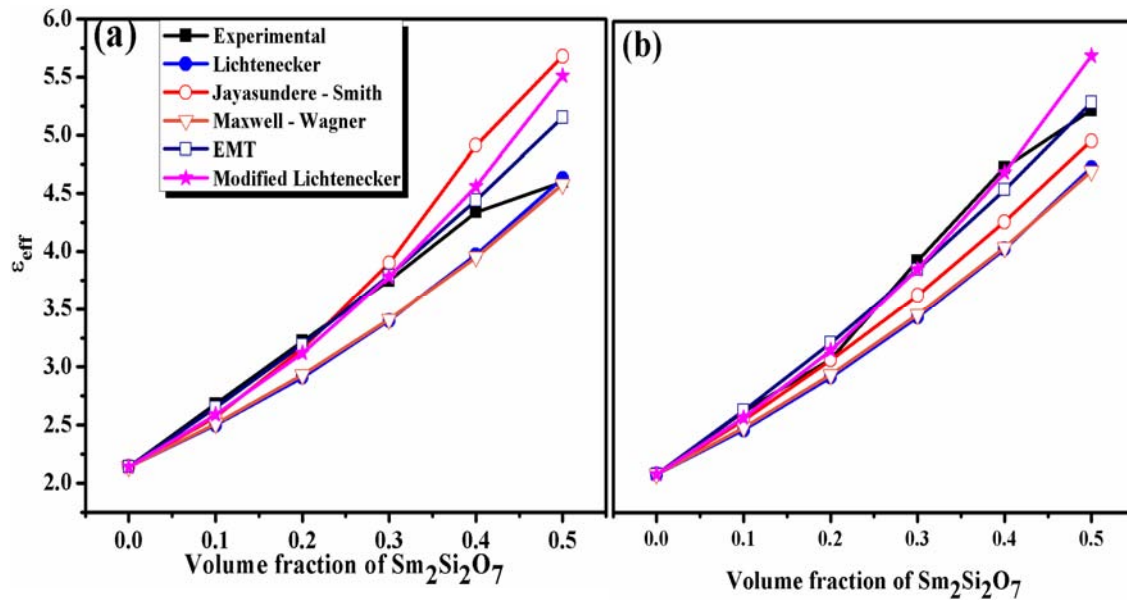


Fig. 5.20 Comparison of experimental and theoretical relative permittivity of (a) polystyrene- $\text{Sm}_2\text{Si}_2\text{O}_7$  and (b) polyethylene- $\text{Sm}_2\text{Si}_2\text{O}_7$  composites at 9 GHz.

THE RELATIVE PERMITTIVITY OF COMPOSITES ALSO DEPENDS ON THE DISTRIBUTION OF FILLER, SHAPE AND SIZE OF FILLERS AND INTERFACE BETWEEN CERAMICS AND POLYMER. IN THE PRESENT WORK WE FOUND THE VALUE OF  $\epsilon_{eff}$  FOR BOTH PE- $\text{Sm}_2\text{Si}_2\text{O}_7$  AND 0.16 FOR PS- $\text{Sm}_2\text{Si}_2\text{O}_7$  COMPOSITES WHICH IS IN AGREEMENT WITH THE EARLIER REPORTS [36]. IT IS OBSERVED THAT THE EMT MODEL HOLDS GOOD FOR PE-SM COMPOSITES EVEN FOR A HIGHER FILLER LOADING OF 0.5. HOWEVER, IN THE CASE OF PS-SM COMPOSITES THE EMT MODEL IS FOUND TO BE WELL MATCHED ONLY FOR LOWER CERAMIC LOADING. FOR A HIGHER FILLER CONTENT OF 0.5 THE MODEL DEVIATES CONSIDERABLY FROM THE EXPERIMENTAL VALUE. COMPARISON OF FIGS. 5.20 (A) AND (B) SHOWS THAT THE PREDICTIONS ARE IN GOOD AGREEMENT WITH EXPERIMENTAL RESULTS FOR PE-SM COMPOSITES THAN FOR PS-SM COMPOSITES. THIS MAY BE DUE TO THE FACT THAT PE-SM SHOWS A BETTER DENSIFICATION THAN THE PS- $\text{Sm}_2\text{Si}_2\text{O}_7$  COMPOSITES AS EVIDENT FROM TABLE 5.6.



THE COMPOSITES DECREASES WITH THE INCREASE IN CERAMIC LOADING. THIS IS DUE TO THE HIGH CTE OF  $\text{Sm}_2\text{Si}_2\text{O}_7$  WHICH WILL CONSTRAINT THE EXPANSION OF THE MATRIX. ALSO COMPOSITES WITH STRONG INTERFACE EXHIBIT AN ADDITIONAL REDUCTION IN CTE [75]. IT IS NOTED THAT THE CTE OF PE- $\text{Sm}_2\text{Si}_2\text{O}_7$  COMPOSITES DECREASES DRASTICALLY FROM 250  $\text{PPM}/^\circ\text{C}$  AT 0% CERAMIC TO 36  $\text{PPM}/^\circ\text{C}$  AT 50% CERAMIC. WHILE FOR PS- $\text{Sm}_2\text{Si}_2\text{O}_7$  COMPOSITES FROM 100  $\text{PPM}/^\circ\text{C}$  TO 36  $\text{PPM}/^\circ\text{C}$ . THE EXPERIMENTAL RESULTS WERE COMPARED WITH THE THEORETICAL PREDICTION USING EQUATION (5.6).

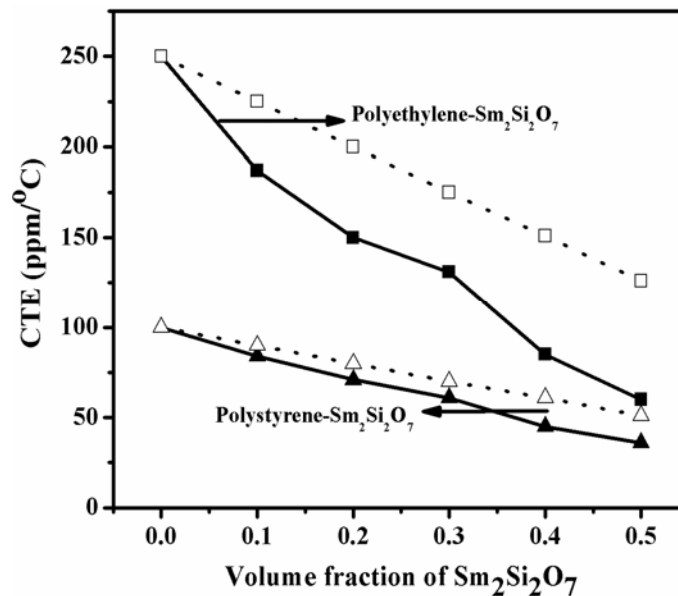


Fig. 5.22 Variation of the coefficient of thermal expansion of polystyrene- $\text{Sm}_2\text{Si}_2\text{O}_7$  and polyethylene- $\text{Sm}_2\text{Si}_2\text{O}_7$  composites and comparison using rule of mixtures.

THE DOTTED LINE REPRESENTS THE CTE VALUES CALCULATED USING THE RULE OF MIXTURES. IT IS OBSERVED THAT THE PREDICTION SHOWS A GOOD AGREEMENT WITH THE OBSERVED CTE VALUES FOR  $\text{Sm}_2\text{Si}_2\text{O}_7$  COMPOSITES WHILE IT SHOWS A WIDE DEVIATION FOR PE- $\text{Sm}_2\text{Si}_2\text{O}_7$  COMPOSITES. IT IS ALSO CLEAR FROM THE FIGURE THAT THE CALCULATED CTEs ARE HIGHER THAN THE OBSERVED CTE RESULTS. THIS MAY BE DUE TO THE DIFFERENCES IN THE MICROSTRUCTURE, BULK MODULUS, AND THERMAL SOFTENING OF THE COMPONENTS WHICH ARE NOT TAKEN INTO ACCOUNT IN THE RULE OF MIXTURES MODEL.

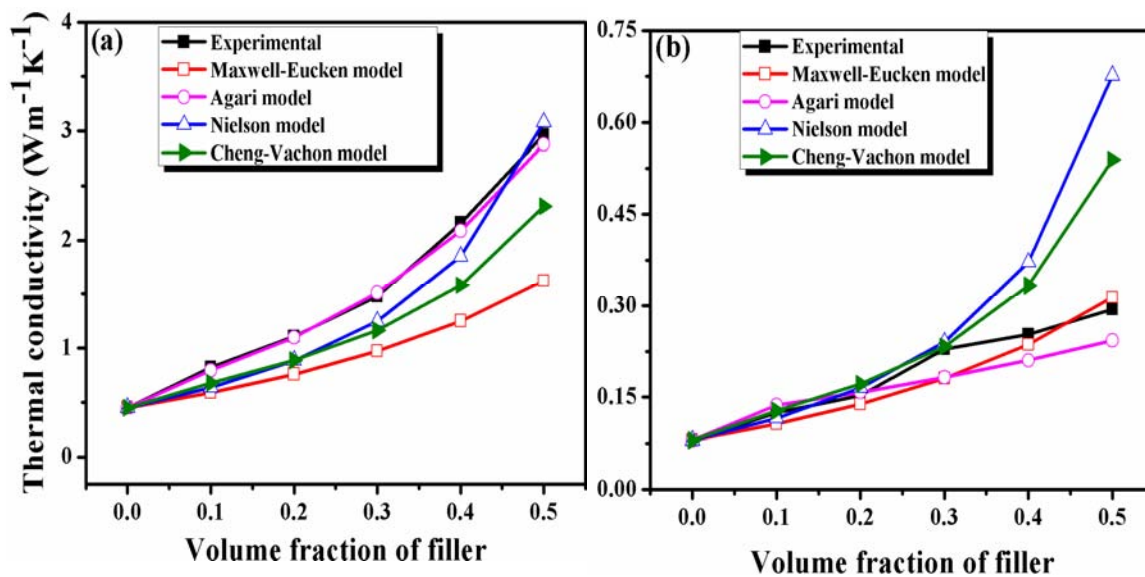


Fig. 5.23 Variation of the thermal conductivity of (a) polyethylene-Sm<sub>2</sub>Si<sub>2</sub>O<sub>7</sub> and (b) polystyrene-Sm<sub>2</sub>Si<sub>2</sub>O<sub>7</sub> composites with the filler content.

FIGURE 5.23 SHOWS THE VARIATION OF THERMAL CONDUCTIVITY OF PE-SM<sub>2</sub>Si<sub>2</sub>O<sub>7</sub> COMPOSITES WITH THE VOLUME FRACTION OF THE FILLER. THE THERMAL CONDUCTIVITY OF BOTH THE POLYMER COMPOSITES INCREASE WITH THE FILLER CONTENT. THE PE-SM<sub>2</sub>Si<sub>2</sub>O<sub>7</sub> COMPOSITES SHOW A HIGH RATE OF INCREASE IN THERMAL CONDUCTIVITY THAN THE PS-SM<sub>2</sub>Si<sub>2</sub>O<sub>7</sub> COMPOSITES WHICH IS DUE TO THE RELATIVELY HIGH THERMAL CONDUCTIVITY OF POLYETHYLENE (0.5 Wm<sup>-1</sup>K<sup>-1</sup>) COMPARED TO THAT OF POLYSTYRENE (0.1 Wm<sup>-1</sup>K<sup>-1</sup>). IN THE CASE OF PE-SM<sub>2</sub>Si<sub>2</sub>O<sub>7</sub> COMPOSITES A SUDDEN INCREASE IN THERMAL CONDUCTIVITY IS NOTED. BEYOND 0.3 VOLUME FRACTION IS DUE TO THE FACT THAT AT HIGHER FILLER CONTENT THE CERAMIC PARTICLES GET CONTACTED AND FORM THERMALLY CONDUCTIVE PATHS IN THE COMPOSITES. FROM SEM IMAGES IT IS CLEAR THAT THE POLYMER PARTICLES (PE AND PS) ARE ESSENTIALLY SURROUNDED BY THE FILLER PARTICLES. THE MOST OF THE SM<sub>2</sub>Si<sub>2</sub>O<sub>7</sub> PARTICLES CAN TOUCH EACH OTHER AND FORM THERMALLY CONDUCTIVE PATHS IN THE COMPOSITES. FOR A FILLER CONTENT OF 0.5 THE THERMAL CONDUCTIVITY OF PE-SM<sub>2</sub>Si<sub>2</sub>O<sub>7</sub> COMPOSITES BECOMES NEARLY 7 TIMES THAT OF PURE POLYETHYLENE (0.5 Wm<sup>-1</sup>K<sup>-1</sup>) WHICH IS 3.5 Wm<sup>-1</sup>K<sup>-1</sup>. THAT OF PS-SM<sub>2</sub>Si<sub>2</sub>O<sub>7</sub> COMPOSITES OF SAME VOLUME FRACTION IS ONLY 0.3 Wm<sup>-1</sup>K<sup>-1</sup>. AGARI AND CO-WORKERS [77] PROVED THAT THE THERMAL CONDUCTIVITY OF THE COMPOSITES IS DEPENDENT ON THE PROCESSING METHOD ADOPTED. THEY FOUND THAT FOR A GIVEN VOLUME FRACTION OF FILLER, THE THERMAL CONDUCTIVITY OF COMPOSITES OBTAINED FROM

DISPERSION METHOD IS HIGHER THAN THAT OBTAINED BY MELT MIXING TECHNIQUE. FIG. 5.23 (A) COMPARES THE EXPERIMENTAL VALUES WITH VARIOUS THEORETICAL PREDICTIONS OBTAINED BY EQUATIONS (5.7) – (5.11). THE AGARI EQUATION IS FOUND TO BE IN GOOD AGREEMENT WITH THE EXPERIMENTAL VALUES IN THE CASE OF PE-SM<sub>2</sub>SI<sub>2</sub>O<sub>7</sub> COMPOSITES WHILE IT SHOWS CONSIDERABLE DEVIATION IN THE CASE OF PS-SM<sub>2</sub>SI<sub>2</sub>O<sub>7</sub>. THIS MAY BE DUE TO THE BETTER DENSIFICATION ACHIEVED BY THE PE-SM<sub>2</sub>SI<sub>2</sub>O<sub>7</sub> COMPOSITES (SEE TABLE 5.6) THEREBY REDUCING THE POROSITY WHICH IMPROVES THE ELECTRICAL CONDUCTIVITY. FIG. 5.23 (B) SHOWS THAT FOR PS-SM<sub>2</sub>SI<sub>2</sub>O<sub>7</sub> COMPOSITES, ALL THE PREDICTIONS HOLD GOOD FOR LOWER CONCENTRATION OF FILLER. AS THE FILLER CONTENT INCREASES THE EXPERIMENTAL VALUES SHOW CONSIDERABLE DEVIATION FROM THE THEORETICAL

**Table 5.7 The Vickers hardness and water absorption of polyethylene-Sm<sub>2</sub>Si<sub>2</sub>O<sub>7</sub> and polystyrene-Sm<sub>2</sub>Si<sub>2</sub>O<sub>7</sub> polymer ceramic composites.**

| Composite   | Volume fraction of filler ( $v_f$ ) | Vicker's microhardness ( $\text{kg/mm}^2$ ) | Water absorption (%) |
|---|-------------------------------------|---|----------------------|
| PE-SM <sub>2</sub> SI <sub>2</sub> O <sub>7</sub> | 0.0                                 | 10  | 0.03                 |
|   | 0.1                                 | 10  | 0.20                 |
|   | 0.3                                 | 14  | 0.25                 |
|   | 0.5                                 | 17  | 0.30                 |
| PS-SM <sub>2</sub> SI <sub>2</sub> O <sub>7</sub> | 0.0                                 | 21  | 0.14                 |
|   | 0.1                                 | 28  | 0.27                 |
|   | 0.3                                 | 33  | 0.30                 |
|   | 0.5                                 | 56  | 0.41                 |

TABLE 5.7 GIVES VICKER'S MICROHARDNESS AND WATER ABSORPTION OF PE-SM<sub>2</sub>SI<sub>2</sub>O<sub>7</sub> AND PS-SM<sub>2</sub>SI<sub>2</sub>O<sub>7</sub> COMPOSITES WITH FILLER VARIATION. THE VICKER'S HARDNESS OF POLYETHYLENE AND POLYSTYRENE ARE FOUND TO BE 10 AND 21 KG/CM<sup>2</sup> RESPECTIVELY. THE MICRO HARDNESS OF THE COMPOSITES IS FOUND TO INCREASE WITH THE FILLER CONTENT. A MAXIMUM OF 56 KG/CM<sup>2</sup> IS OBSERVED FOR PS-SM<sub>2</sub>SI<sub>2</sub>O<sub>7</sub> WHEREAS A MUCH LOWER VALUE OF 17 KG/CM<sup>2</sup> IS OBTAINED FOR PE-SM<sub>2</sub>SI<sub>2</sub>O<sub>7</sub> FOR THE SAME VOLUME FRACTION OF CERAMIC. IT IS EVIDENT FROM THE TABLE THAT AS THE FILLER CONTENT INCREASES

ABSORPTION OF BOTH THE COMPOSITES INCREASES, COMPOSITES EXHIBIT LOW WATER ABSORPTION THAN THE PS COMPOSITES. THIS IS DUE TO THE HIGHER POROSITY OF THE PS-SM<sub>2</sub>Si<sub>2</sub>O<sub>7</sub> COMPOSITES COMPARED TO THAT OF PE COMPOSITES (TABLE 5.6). HOWEVER, THE WATER ABSORPTION IS FOUND TO BE 0.3 FOR PE-SM<sub>2</sub>Si<sub>2</sub>O<sub>7</sub> AND PS-SM<sub>2</sub>Si<sub>2</sub>O<sub>7</sub> COMPOSITES EVEN FOR A HIGHER FILLER CONTENT OF 0.5 V

## 5.5 CONCLUSIONS

- ❖ THE EFFECT OF PS-SM<sub>2</sub>Si<sub>2</sub>O<sub>7</sub> FILLER ON THE DIELECTRIC AND THERMO-MECHANICAL PROPERTIES OF VARIOUS POLYMERS SUCH AS PTFE, POLYETHYLENE AND POLYSTYRENE ARE IN THE INFLUENCE OF COUPLING AGENT AND FILLER PARTICLE SIZE ON THE PERFORMANCE. THE EFFECT OF PS-SM<sub>2</sub>Si<sub>2</sub>O<sub>7</sub> IS ALSO STUDIED IN DETAIL. THE PTFE/S-SM<sub>2</sub>Si<sub>2</sub>O<sub>7</sub> COMPOSITES ARE PREPARED BY POWDER PROCESSING TECHNIQUE AND PE/PS-SM<sub>2</sub>Si<sub>2</sub>O<sub>7</sub> COMPOSITES BY THE MELT MIXING METHOD.
- ❖ THE MICROSTRUCTURE OF THE COMPOSITES SHOWS A UNIFORM DISPERSION FOR ALL FILLER CONCENTRATION AND AS THE FILLER CONTENT INCREASES A SMALL AMOUNT OF AGGLOMERATION IS NOTICED. IT IS FOUND THAT ADDITION OF SILANE TREATED FILLER REDUCED AGGLOMERATION RESULTING IN GOOD HOMOGENEITY IN THE CASE OF PTFE/S-SM<sub>2</sub>Si<sub>2</sub>O<sub>7</sub> COMPOSITES.
- ❖ THE DIELECTRIC PROPERTIES OF THE COMPOSITES ARE MEASURED AT 1 MHZ AND MICROWAVE FREQUENCY RANGE. IT IS SEEN THAT THE RELATIVE PERMITTIVITY AND DIELECTRIC LOSS OF THE COMPOSITES INCREASES WITH INCREASE IN THE FILLER CONTENT. FOR THE FILLER CONTENT OF 0.5 MICROWAVE DIELECTRIC PROPERTIES OF THE COMPOSITES ARE: PTFE COMPOSITE  $\epsilon_r = 3.82$  AND  $\tan \delta = 0.0136$ , PE COMPOSITE  $\epsilon_r = 5.28$  AND  $\tan \delta = 0.0091$  AND PS  $\epsilon_r = 4.60$  AND  $\tan \delta = 0.0110$ . HOWEVER, THE SILANE TREATED AND NANO PTFE/S-SM<sub>2</sub>Si<sub>2</sub>O<sub>7</sub> COMPOSITES SHOWED A HIGHER VALUE OF RELATIVE PERMITTIVITY AND DIELECTRIC LOSS WHEN COMPARED WITH THE UNTREATED ONE.
- ❖ IT IS ALSO OBSERVED THAT THE THERMAL CONDUCTIVITY AND VICKER'S MICROHARDNESS OF THE COMPOSITES IMPROVED WITH FILLER CONTENT WHEREAS THE THERMAL EXPANSION COEFFICIENT DECREASED WHICH IS REQUIRED. ALSO THE ADDITION OF COUPLING AGENT TO THE COMPOSITES IMPROVED THE THERMO-MECHANICAL PROPERTIES OF COMPOSITES. THE

NANO-COMPOSITES EXHIBITED A MUCH LOWER CTE VALUE WHEN COMPARED WITH MICRON COUNTERPART WHEREAS THEY SHOWED A HIGH WATER ABSORPTION VALUE.

- ❖ VARIOUS THEORETICAL PREDICTIONS ARE EMPLOYED TO FIT THE EXPERIMENTAL DATA. RELATIVE PERMITTIVITY, THERMAL CONDUCTIVITY AND THERMAL EXPANSION COEFFICIENTS. EXPERIMENTAL AND THEORETICAL VALUES ARE FOUND TO BE IN GOOD AGREEMENT WITH THEORETICAL VALUES. FILLER CONTENT. THE RESULTS SUGGEST THAT NANOFILLER POLYMER COMPOSITES ARE GOOD CANDIDATES FOR ELECTRONIC PACKAGING APPLICATIONS.

## 5.6 REFERENCES

1. M. B. TIAN, *Substrates for High Density Package Engineering*, TSINGHUA UNIVERSITY PRESS, BEIJING, (2003).
2. R. R. TUMMALA, *Am. Ceram. Soc.*, **74**, 895-908, (1991).
3. E. MOTYL AND B. LOWKIN, *Non-Crystal. Solids*, **305**, 379-385, (2002).
4. P. U. SONJE, K. N. SUBRAMANIAN AND JAALEEM, *J. Mater.*, **36**, 22-29, (2004).
5. S. KOULOURIDIS, G. KIZILTAS, Y. J. ZHOU, D. J. HANSFORD AND IEE. T. VOLAKIS, *Microwave Theory Tech.*, **54**, 4202-4208, (2006).
6. D. M. PRICE AND M. JARROFT, *Chim. Acta*, **392-393**, 231-236, (2002).
7. A. J. BURROUGHS, *Polymer*, **26**, 963-977, (1985).
8. A. WALLACE, *Fluoropolymers*, WILEY INTERSCIENCE, NEW YORK, (1972).
9. G. SUBODH, M. JOSEPH, P. MOHANAN AND M. T. SEBASTIAN, *Am. Ceram. Soc.*, **90**, 3507-3511, (2007).
10. P. S. ANJANA, M. T. SEBASTIAN, M. N. SUMA AND P. MOHAMMAD, *Ceram. Technol.*, **5**, 325-333, (2008).
11. D. C. J. Y. M. WANG AND Y. ZHOU, *J. Electrics and Accoustooptics*, **24**, 225-9 (2002).
12. M. T. SEBASTIAN AND HELI JANTUNEN, *J. Ceram. Soc.*, **7**, 415-434, (2010).
13. S. THOMAS, V. N. DEEPU, P. MOHANAN AND M. T. SEBASTIAN, *Am. Ceram. Soc.*, **91**, 1971-1975, (2008).
14. F. XIANG, H. WANG AND X. YAO, *J. Ceram. Soc.*, **26**, 1999-2002, (2006).
15. G. SUBODH, C. PAVITHRAN, P. MOHANAN AND M. T. SEBASTIAN, *Am. Ceram. Soc.*, **27**, 3039-3044, (2007).
16. K. P. MURALI, S. RAJESH, O. PRAKASH, A. R. KULKARNI AND R. RATHESH, *Mar. Phys.*, **113**, 290-295, (2009).
17. Y. C. CHEN, H. C. LIN AND Y. D. LEE, *J. Polym. Res.*, **10**, 247-258, (2003).
18. S. GEORGE, V. N. DEEPU, P. MOHANAN AND M. T. SEBASTIAN, *J. Phys. Sci.*, **50**, 570-576, (2010).
19. S. YU, P. HING AND X. HU, *J. Appl. Phys.*, **88**, 398-404, (2000).
20. G. PEZZOTTI, I. KAMADA AND S. MIKI, *J. Ceram. Soc.*, **20**, 1197-1203, (2000).
21. D. KHASTGIR, H. S. MAITI AND P. C. BANDYOPADHYAY, *J. Eng., B*, **100**, 245-253, (1988).
22. X. Y. HUANG, P. K. JIANG AND C. U. KIM, *J. Appl. Phys.*, **102**, 124103-8, (2007).
23. X. Y. HUANG, P. K. JIANG, C. N. KIM, Q. Q. KE AND G. L. WANG, *J. Sci. Technol.*, **68**, 2134-2140, (2008).



24. G. SUBODH, V. DEEPU, P. MOHANAN AND M. T. SEBASTIAN, *Appl. Phys. Lett.*, **95**, 062903-3, (2009).
25. Y. DENG, N. LI, Y. WANG, Z. ZHANG, Y. DANG AND M. LIANG, *J. Mater. Sci.*, **64**, 528-530, (2010).
26. J. I. HONG, P. WINBERG, L. S. SCHADLER AND R. W. SEEGEL, *Macromolecules*, **59**, 473-476, (2005).
27. I. KRUPA, I. NOVÁK AND I. CHODÁK, *J. Appl. Polym. Sci.*, **145**, 245-252, (2004).
28. W. ZHOU, S. QI, Q. AN, H. ZHAO AND N. MA, *Chin. Phys. Lett.*, **42**, 1863-1873, (2007).
29. Y. ZOU, Y. FENG, L. WANG AND X. CHEN, *Chin. Phys. Lett.*, **42**, 271-277, (2004).
30. C. JO AND H. E. NAGUBHAY, *Polym. Degrad. Stab.*, **48**, 3349-3360, (2007).
31. G.-W. LEE, M. PARK, J. KIM, J. I. LEE AND H. G. YOON, *Compos. Part A*, **37**, 727-734, (2006).
32. D. KUMLUTAS, I. H. TAVMAN AND M. TURHAN, *Compos. Part B*, **63**, 113-117, (2003).
33. M. G. TODD AND F. G. SHAW, *Appl. Phys.*, **94**, 4551-4557, (2003).
34. L. RAMAJO, M. S. CASTRO AND M. M. REBOREDO, *Compos. Part A*, **38**, 1852-1859, (2007).
35. J. XU AND C. P. WONG, *Compos. Part A*, **38**, 13-19, (2007).
36. Y.-C. CHEN, H.-C. LIN AND Y.-D. LEE, *Polym. Res.*, **11**, 1-7, (2004).
37. S. RAJESH, V. S. NISA, K. P. MURALI AND R. RAJESH, *J. Alloys Compd.*, **477**, 677-682, (2009).
38. R. K. GOYAL, A. N. TIWARI, U. P. MULIK AND Y. S. NEGI, *Sens. Technol.*, **67**, 1802-1812, (2007).
39. S. K. BHATTACHARYA AND R. R. TUMMALAR, *J. Mater. Sci.*, **32**, 11-19, (2001).
40. Z.-M. DANG, D. XIE, Y.-F. YU, H.-P. XU AND Y.-D. HUO, *J. Mater. Chem. Phys.*, **109**, 1-4, (2008).
41. P. GONON, A. SYLVESTRE, J. TEYSSEYRE AND M. PRIOR, *Cat. Mater. Electron.*, **12**, 81-86, (2001).
42. H. HE, R. FU, Y. SHEN, Y. HAN AND X. SONG, *Compos. Sci. Technol.*, **67**, 2493-2499, (2007).
43. A. H. SIHVOLA AND J. A. KONG, *Trans. Geosci. Remote Sens.*, **26**, 420-429, (1988).
44. L. RAMAJO, M. REBOREDO AND M. CASTRO, *Compos. Part A*, **36**, 1267-1274, (2005).
45. Y. SUN, Z. ZHANG AND C. P. WONG, *Polym. Degrad. Stab.*, **46**, 2297-2305, (2005).
46. Y. RAO, J. M. QU, T. MARINIS AND C. P. WONG, *Trans. Compon. Packag. Technol.*, **23**, 680-683, (2000).

47. K. WAKASHIMA, M. OTSUKA AND S. UMEKAWA, *Mater.*, **8**, 391-404, (1974).
48. T. ISHIKAWA, K. KOYAMA AND S. KOBEYASHI, *Mater.*, **12**, 153-168, (1978).
49. R. C. PROGELHOF, J. L. THRONE AND R. R. RUEFELT, *Sci.*, **16**, 615-625, (1976).
50. J. K. CARSON, S. J. LOVATT, D. J. TANNER AND A. C. CHELLEND, *Chellend*, **75**, 297-307, (2006).
51. J. WANG, J. K. CARSON, M. F. NORTH AND D. J. CHELLEND, *Mass Transfer*, **49**, 3075-3083, (2006).
52. Y. AGARI, A. UEDA AND S. NAGAOKA, *Appl. Polym. Sci.*, **43**, 1117-1124, (1991).
53. Y. AGARI, A. UEDA AND S. NAGAOKA, *Appl. Polym. Sci.*, **49**, 1625-1634, (1993).
54. J. C. MAXWELL, *Treatise on Electricity and Magnetism*, DOVER, NEW YORK, (1954).
55. G. T.-N. TSAO, *Ind. Eng. Chem.*, **53**, 395-397, (1961).
56. T. LEWIS, L. NIELSEN, *Appl. Polym. Sci.*, **14**, 1449, (1970).
57. H. JC, *J. Compos. Mater.*, **3**, 732-4, (1969).
58. C. P. MENON AND J. PHILIP, *Appl. Sci. Technol.*, **11**, 1744-1749, (2000).
59. M. T. SEBASTIAN, C. P. MENON, J. PHILIP AND R. W. SCHWARTZ, *Appl. Sci. Technol.*, **94**, 3206-3211, (2003).
60. G. C. PSARRAS, E. MANOLAKAKI AND G. M. TSANIGARIS, *Appl. Sci. Technol. Part A*, **33**, 375-384, (2002).
61. P. GONON AND A. SYLVESTER, *Phys.*, **92**, 4584-4589, (2002).
62. D. H. KUO, C. C. CHANG, T. Y. SU, W. K. WANG AND B. YU, *Chem. Phys.*, **85**, 201-206, (2004).
63. N. G. DEVARAJU, E. S. KIM AND B. IM, *Electron. Eng.*, **82**, 71-83, (2005).
64. S. Z. YU, P. HING AND X. HU, *Appl. Phys.*, **88**, 398-404, (2000).
65. J. ZHANG, H. Q. FAN, S. M. KE, Y. Z. SHI, X. H. ZENG, M. T. BI AND H. T. HUANG, *Compos. Mater.*, **334-335**, 1053-1056, (2007).
66. D. P. H. HASSELMAN AND L. F. JOHNSON, *Compos. Mater.*, **21**, 508-515, (1987).
67. T. HU, J. JUUTI, H. JANTUNEN AND T. VILKMAN, *Chem. Soc.*, **27**, 3997-4001, (2007).
68. J. J. WEEKS, E. S. CLARK AND R. KPEBAYE, *Appl. Phys.*, **22**, 1480-1486, (1981).
69. S. RAJESH, K. P. MURALI, K. V. RAJANI AND R. RAJIVESH, *Ceram. Technol.*, **6**, 553-561, (2009).
70. S.-H. XIE, B.-K. ZHU, X.-Z. WEI, Z.-K. XU AND Y.-Y. XIAO, *Composites Part A*, **36**, 1152-1157, (2005).
71. Y. HE, B. E. MOREIRA, A. OVERSON, S. H. NAKAMURA, C. BIDER AND J. F. BRISCOE, *Thermochim. Acta*, **357-358**, 1-8, (2000).

72. J. JUNG, J. KIM, Y. R. UHM, J.-K. JEON, S. LEE, H. M. LEE AND C. K. TRWEE, *chim. Acta*, **499**, 8-14, (2010).
73. M. G. TODD AND F. G. SM, *Microelectron. J.*, **33**, 627-632, (2002).
74. M. ROY, J. K. NELSON, R. K. MACCRONE, L. S. SCHADLER, C. W. REED, R. KEEFE AND W. ZENGER, *IEEE Trans. Dielectr. Electr. Insul.*, **12**, 629-643, (2005).
75. S. KANG, S. I. HONG, C. R. CHOE, M. PARK, S. RIM AND H. KIM, *Bol. Kim.*, **42**, 879-887, (2001).
76. P. FRUBING, D. BLISCHKE, R. GERHARD-MULTHAUPT AND P. S. D. K. H. A. L. L. E. P. H. Y. S., *Phys.*, **34**, 3051-3057, (2001).
77. Y. AGARI, A. UEDA AND S. NAGA, *Appl. Polym. Sci.*, **42**, 1665-1669, (1991).

## CHAPTER 6

### ALUMINATE BASED COMPOSITES FOR LTCC AND ELECTRONIC PACKAGING APPLICATIONS

*This chapter is divided into two sections. The first section describes the synthesis and properties of aluminate based ceramic glass composites for LTCC substrate applications. The ceramic used for the study is 0.83 ZnAl<sub>2</sub>O<sub>4</sub> - 0.17 TiO<sub>2</sub> (ZAT) with excellent microwave dielectric properties. The effect of various low melting and low loss glasses on the densification, microstructure and microwave dielectric properties of ZAT is discussed in detail. The second section gives a comparative study of PTFE/ZAT and PE/ZAT composites for electronic packaging applications. The dielectric properties of the composites are measured at low and microwave frequencies and the effective relative permittivity obtained are compared with the theoretical predictions.*

## 6.1 SYNTHESIS AND CHARACTERIZATION OF 0.83 ZNA<sub>2</sub>O<sub>4</sub>-0.17 TIO<sub>2</sub>/GLASS COMPOSITES FOR LTCC APPLICATIONS

### 6.1.1 INTRODUCTION

DEVELOPMENT OF VERY LARGE-SCALE INTEGRATION (VLSI) CONTINUOUSLY DEMANDS CERAMIC MANUFACTURERS PROVIDE SUBSTRATE MATERIALS WITH HIGH SIGNAL TRANSMISSION, HIGH WIRING DENSITY, HIGH RELIABILITY AND LOW COST [1-2]. TO MAKE A PACKAGE BECOME SMALLER AND FASTER, LOW RELATIVE PERMITTIVITY CERAMICS CO-FIRABLE WITH HIGHLY CONDUCTIVE METALS SUCH AS AG, PD AND AU ARE DESIRABLE. LOW TEMPERATURE CO-FIRED CERAMIC (LTCC) MULTILAYER SUBSTRATES HAVE RECENTLY BEEN PROPOSED FOR APPLICATIONS IN THE WIRELESS FIELD. THESE SUBSTRATES REQUIRE LOW DIELECTRIC LOSS AND RAPID SIGNAL PROPAGATION AT HIGH FREQUENCIES [3]. A DETAILED DESCRIPTION ON THE LTCC TECHNOLOGY, ITS ADVANTAGES, MATERIAL REQUIREMENTS AND COMMERCIAL APPLICATIONS ARE GIVEN IN CHAPTER 1 SECTION 1.8. GENERALLY SPEAKING, ADDITION OF GLASS TO CERAMICS SOFTENING TEMPERATURE GLASS IS AN EFFECTIVE AND CHEAP APPROACH TO LOWER THE SINTERING TEMPERATURE OF CERAMICS [4]. HOWEVER, IN MANY CASES, THEY MAY INDUCE A SIGNIFICANT DEGRADATION OF DIELECTRIC PROPERTIES BECAUSE OF THE LARGE AMOUNT OF ADDITIVE GLASS WHICH REQUIRE A COMPLICATED PROCESSING. TO WEAKEN THE DESTRUCTIVE EFFECT OF THE GLASS ON THE INTRINSIC MICROWAVE PROPERTIES OF THE CERAMICS, RESEARCHERS HAVE TO FIND A WAY TO REDUCE FLUX WHICH COULD DECREASE THE SINTERING TEMPERATURE GREATLY WITH SMALL AMOUNTS OF GLASS ADDITIVES WITHOUT INFLUENCING THE MICROWAVE DIELECTRIC PROPERTIES OF THE CERAMICS CONSIDERABLY. FOR LTCC, IN ADDITION TO THE LOW SINTERING TEMPERATURE, APPROPRIATE PERMITTIVITY, HIGH QUALITY FACTOR AND A NEAR ZERO TEMPERATURE COEFFICIENT OF RESISTANCE AT HIGH FREQUENCY ARE ALSO CRITICAL REQUIREMENTS FOR COMMERCIAL APPLICATIONS. THUS, THE DEVELOPMENT OF THE NEW MATERIALS WITH INTRINSIC LOW SINTERING TEMPERATURES AND GOOD DIELECTRIC PROPERTIES IS STILL IN RAPID PROGRESS.

A NUMBER OF MATERIAL-RESEARCH LABORATORIES HAVE FOCUSED THEIR EFFORTS ON REDUCING THE SINTERING TEMPERATURES OF FUNCTIONAL MATERIALS. ALTHOUGH SEVERAL RESEARCHERS HAVE REPORTED THE MICROWAVE DIELECTRIC PROPERTIES OF LOW TEMPERATURE SINTERED CERAMICS, THE QUALITY FACTOR OF THE CERAMIC WAS TOO LOW TO USE IN THE MICROWAVE APPLICATIONS AT HIGH FREQUENCY. SEVERAL MICROWAVE DIELECTRIC COMPOSITIONS INCLUDING (ZR,SN)O<sub>3</sub>, (ZR,SN)O<sub>3</sub>-BAMG<sub>1/3</sub>TA<sub>2/3</sub>O<sub>3</sub> [6], BAZN<sub>1/3</sub>TA<sub>2/3</sub>O<sub>3</sub>, BAO-TIO<sub>2</sub>-WO<sub>3</sub> [7], CA[(LI<sub>1/3</sub>NB<sub>2/3</sub>)<sub>1-x</sub>TI<sub>x</sub>]O<sub>3-δ</sub> [8], (ZR,SN)O<sub>3</sub>-CEO<sub>2</sub> [9] AND BAO-BO<sub>3</sub>-TIO<sub>2</sub> [10] SYSTEMS HAVE BEEN STUDIED FOR THE DEVELOPMENT OF

THE MIDDLE-K LTCC BY USING GLASS FRITS. MANY LOW LOSS GLASSES AND LOW MELT HAVE BEEN SUGGESTED AS SINTERING AIDS FOR SEVERAL MATERIALS TO BE USED APPLICATIONS. ZHOU [11] PROPOSED  $0.83\text{Li}_2\text{O} \cdot 0.17\text{V}_2\text{O}_5$  AS AN EFFECTIVE ADDITIVE TO LOWER THE SINTERING TEMPERATURE OF  $\text{TiNb}_2\text{O}_7$  (LNT) CERAMICS, BUT THE INTERACTION BETWEEN V AND AG LIMITED IT FOR LTCC APPLICATIONS. LATER THE SA SUGGESTED  $\text{Li}_2\text{O}$  AND  $\text{CuO}$  AS SUITABLE SINTERING AIDS FOR LNT. THESE WERE ALSO FOUND EFFECTIVE IN REDUCING THE SINTERING TEMPERATURES OF  $(\text{Zn}_{1-x}\text{Bi}_x)_3\text{O}_3$  AND  $\text{BaTiO}_3$  CERAMICS TO BELOW  $900^\circ\text{C}$ .  $\text{ZNO-B}_2\text{O}_3\text{-SiO}_2$  [13] AND  $\text{ZNO}_2\text{-B}_3\text{-Bi}_2\text{O}_3$  [14] BASED GLASS HAVE BEEN REPORTED TO BE EFFECTIVE LOW TEMPERATURE PROMOTERS FOR TITANATE CERAMICS. EARLIER REPORTS [15] SHOWS THAT  $\text{ZNO-LAO}_3$  (BZL) GLASS WHICH IS USED AS OPTICAL GLASS CAN SERVE AS A SINTERING AID FOR  $\text{BaTiO}_3$  LTCC APPLICATION. KIM [16-17] USED  $\text{Bi}_2\text{O}_3$  TO LOWER THE SINTERING TEMPERATURE OF  $\text{Ba}_3\text{Nb}_4\text{O}_{15}$  AND DECREASED  $\text{Q}$  VALUE THROUGH THE FORMATION OF COMPOSITE CERAMICS IN  $\text{Ba}_3\text{Nb}_4\text{O}_{15}$  AND  $\text{Ba}_2\text{Nb}_6$ .

### 6.1.1.1 SPINELS

OXIDE SPINELS COMPRISE A VERY LARGE GROUP OF STRUCTURALLY RELATED MATERIALS, MANY OF WHICH ARE OF CONSIDERABLE TECHNOLOGICAL OR GEOLOGICAL SIGNIFICANCE. SOME OF THEM EXHIBIT A WIDE RANGE OF ELECTRONIC AND MAGNETIC PROPERTIES [19], INCLUDING SUPERCONDUCTIVITY. ON THE OTHER HAND, IRON CONTAINING AND ZINC CONTAINING SPINELS ARE OF GREAT IMPORTANCE PRIMARILY DUE TO THEIR MAGNETIC AND INSULATING PROPERTIES, IN PARTICULAR. AMONG THE VARIOUS SPINEL OXIDES INVESTIGATED, THE MAGNESIUM AND ZINC DIALUMINATE OXIDES HOLDS GREAT IMPORTANCE.  $\text{MgAl}_2\text{O}_4$  HAS ATTRACTED A GREAT DEAL OF ATTENTION AS A TECHNOLOGICALLY IMPORTANT ADVANCED CERAMIC MATERIAL OWING TO ITS HIGH MELTING POINT ( $2135^\circ\text{C}$ ), HIGH MECHANICAL STRENGTH AT ELEVATED TEMPERATURE, LOW ELECTRICAL CONDUCTIVITY, CHEMICAL INERTNESS AND THERMAL SHOCK RESISTANCE. BECAUSE OF THESE PROPERTIES, IT HAS APPLICATIONS RANGING FROM TRADITIONAL REFRACTORIES TO SOME ADVANCED USES SUCH AS THERMAL AND HUMIDITY SENSORS, ARMOUR MATERIALS, EXCELLENT TRANSPARENT MATERIAL FOR LASER ENVELOPES AND ALKALI-METAL VAPOUR DISCHARGE DEVICES. RESEARCHERS HAVE REPORTED THE PREPARATION OF SPINEL BY DIFFERENT CHEMICAL ROUTES LIKE SOL-GEL [20], SPRAY PYROLYSIS, CO-PRECIPITATION, PRECIPITATION FROM ORGANOMETALLIC PRECURSORS, AUTO-IGNITION

MICROWAVE-ASSISTED SYNTHESIS [23] ETC. THESE SPINEL OXIDES ARE WIDE GAP SEMICONDUCORS WITH NUMEROUS OPTICAL, GEOPHYSICAL AND MAGNETIC APPLICATIONS. IT IS ALSO FOUND THAT THESE MATERIALS ARE HIGHLY RESISTANT AT ELEVATED TEMPERATURE AND HIGHLY TRANSPARENT AT SHORT WAVELENGTHS IN UV REGION, WHICH MAKE THEM CANDIDATE MATERIALS FOR REFLECTIVE COATINGS IN AEROSPACE APPLICATIONS.

THE CRYSTAL STRUCTURE OF SPINEL WAS DETERMINED INDEPENDENTLY BY PEARSON AND NISHIKAWA [24-25]. THEY BELONG TO THE FACE CENTERED CUBIC SYMMETRY WITH SPACE GROUP  $Fd\bar{3}m$ . THE CUBIC CELL CONSISTS OF A CLOSE - PACKED ARRAY OF 32 OXYGEN ATOMS WITH 8 TETRAHEDRAL AND 16 OCTAHEDRAL SITES. IN THE NORMAL SPINEL STRUCTURE, THE DIVALENT CATIONS OCCUPY THE TETRAHEDRAL SITES AND THE TRIVALENT CATIONS OCCUPY THE OCTAHEDRAL SITES. A TYPICAL SPINEL STRUCTURE IS AS SHOWN IN FIG. 6.1.

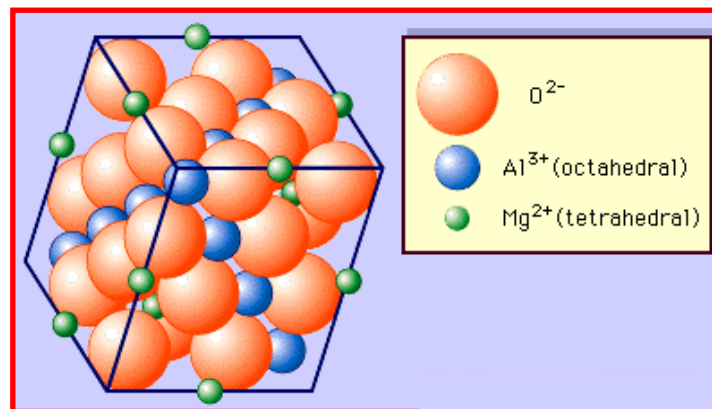


Fig. 6.1 The crystal structure of  $MgAl_2O_4$  spinel. (www.britannica.com)

EARLIER INVESTIGATIONS REVEALED THAT  $ZnAl_2O_4$  [28] ARE POSSIBLE CANDIDATES FOR PACKAGING APPLICATIONS DUE TO THE LOW RELATIVE PERMITTIVITY VALUE. HOWEVER, THE HIGH  $Q$  FACTOR (-79 PPM) OF  $ZnAl_2O_4$  PRECLUDES ITS USE IN PRACTICAL APPLICATIONS. MANY RESEARCHERS HAVE TRIED TO TUNE THESE CERAMICS [29-31]. RECENTLY SURENDRA [27] STUDIED THE EFFECT ON THE DIELECTRIC PROPERTIES OF  $ZnAl_2O_4$  AND TUNED IT TO A NEARLY ZERO VALUE. THEY PROPOSED THE  $ZnAl_xO_4$  [X = 0.17] (NAMED AS ZAT HEREAFTER) AS AN IDEAL COMPOSITION FOR SUBSTRATE APPLICATIONS. HOWEVER THE SINTERING TEMPERATURE OF ZAT WAS HIGH AND NEED TO BE REDUCED FOR LTCC APPLICATIONS. IN THE PRESENT SECTION ATTEMPTS HAVE BEEN MADE TO

SINTERING TEMPERATURE OF  $0.83\text{ZnO}-0.17\text{TiO}_2$  (ZAT) CERAMICS THROUGH SUITABLE GLASS ADDITION FOR LTCC APPLICATIONS.

### 6.1.2 EXPERIMENTAL

THE  $0.83\text{ZnO}-0.17\text{TiO}_2$  (ZAT) CERAMICS WERE PREPARED BY THE CONVENTIONAL SOLID STATE CERAMIC ROUTE. HIGH PURITY ZNO [ALDRICH CHEMICAL COMPANY, 99.9%],  $\text{Al}_2\text{O}_3$  [ALCOA A16SG] WERE TAKEN AS STARTING MATERIALS FOR THE SYNTHESIS OF ZAT. VARIOUS STEPS INVOLVED IN THE SYNTHESIS ARE EXPLAINED IN CHAPTER 2 SECTION 2.1. ZAT WAS CALCINED AT  $900^\circ\text{C}$  IT WAS THEN BALL MILLED WITH  $\text{ZnO}$  ACCORDING TO THE COMPOSITION ( $0.83\text{ZnO}-0.17\text{TiO}_2$ ) FOR 24H. THE SLURRY WAS DRIED AND GROUND WELL. 4 WT% PVA WAS ADDED AS BINDER, MIXED AND AGAIN GROUND INTO FINE POWDER AND PRESSURE FORM CYLINDRICAL DISKS OF 20 MM DIAMETER AND 10 MM THICKNESS UNDER A UNIAXIAL PRESSURE OF ABOUT 100 - 150 MPA. THIN PELLETS OF THE ZAT WITH DIAMETER 14 MM AND THICKNESS 1 MM WERE MADE FOR LOW FREQUENCY MEASUREMENTS. THE GLASSES USED IN THE INVESTIGATION ARE ZB1, ZB2, ZBS, BBSZ, BBS, AS, BB, MBS AND ABS. DIFFERENT WEIGHT PERCENTAGES OF THESE GLASSES WERE ADDED TO THE PURE ZAT. THE PELLETS WERE DESCRIBED ABOVE. THE PURE SAMPLE WAS SINTERED AT  $950^\circ\text{C}$  WHILE THE GLASS ADDED SAMPLES WERE SINTERED AT DIFFERENT TEMPERATURE RANGING FROM  $950^\circ\text{C}$  TO  $1050^\circ\text{C}$ . SINTERED SAMPLES WERE WELL POLISHED AND THEIR BULK DENSITIES WERE CALCULATED BY ARCHIMEDES METHOD. STRUCTURAL, MICROSTRUCTURAL AND MICROWAVE CHARACTERIZATIONS WERE PERFORMED AS EXPLAINED IN CHAPTER 2.

### 6.1.3 RESULTS AND DISCUSSION

THE EFFECT OF NINE DIFFERENT GLASSES (ZB1, ZB2, ZBS, BBSZ, BBS, ABS, MBS, AS AND BB) ON THE SINTERING TEMPERATURE, DENSIFICATION AND MICROWAVE PROPERTIES OF ZAT IS STUDIED. THE PHYSICAL AND ELECTRICAL PROPERTIES OF THE VARIOUS GLASSES USED ARE GIVEN IN TABLE 1.3 IN CHAPTER 2. INITIALLY, A SMALL WEIGHT PERCENTAGE (0.1 WT%) OF THESE GLASSES ARE ADDED TO THE PARENT MATERIAL. TABLE 6.1 GIVES THE OPTIMIZED SINTERING TEMPERATURE AND MICROWAVE DIELECTRIC PROPERTIES OF 0.1 WT% GLASS ADDED COMPOSITES. THE SINTERING TEMPERATURE OF THESE COMPOSITES IS OPTIMIZED FOR MAXIMUM DENSITY AND MICROWAVE DIELECTRIC PROPERTIES. IT IS TO BE NOTED THAT THE ADDITION



OF VARIOUS GLASSES REDUCED THE SINTERING TEMPERATURE CONSIDERABLY. THE PURE ZAT SINTERING TEMPERATURE IS KNOWN [32] THAT BORON BASED GLASSES ARE MORE EFFECTIVE IN LOWERING THE SINTERING TEMPERATURE DUE TO THE LOW SOFTENING POINT (450°C) OF  $\text{B}_2\text{O}_3$ . FROM THE TABLE IT IS CLEAR THAT ZINC BORATE BASED GLASSES ARE MORE EFFECTIVE IN REDUCING THE SINTERING TEMPERATURE WITHOUT AFFECTING THE DIELECTRIC MICROWAVE DIELECTRIC PROPERTIES. THE ZB2, BBSZ AND BBS GLASS LOWERED THE SINTERING TEMPERATURE TO 1400°C WHERE AS ZB1 AND ZBS ARE FOUND TO BE MUCH MORE EFFECTIVE SINCE THE SINTERING TEMPERATURES ARE REDUCED TO 1350°C RESPECTIVELY. WITH THIS VIEW WE HAVE CONSIDERED ONLY FIVE GLASSES (ZB1, ZB2, ZBS, BBSZ AND BBS) FOR FURTHER STUDIES.

**Table 6.1 The optimized sintering temperature and microwave dielectric properties of 0.1 wt% glass added ZAT ceramics.**

| Glass added | Sintering temp: (°C/h) | Microwave Properties |                      |                   |              | Loss at 1MHz |
|-------------|------------------------|----------------------|----------------------|-------------------|--------------|--------------|
|             |                        | Relative Density (%) | $Q_U \times F$ (GHz) | $\tau_f$ (ppm/°C) | $\epsilon_R$ |              |
| PURE ZAT    | 1450/4                 | 97.0                 | 91000                | 1.4               | 11.7         | 0.0010       |
| ZB1         | 1375/4                 | 97.4                 | 71000                | -4.0              | 11.9         | 0.0007       |
| ZB2         | 1400/4                 | 98.3                 | 73200                | 2.6               | 11.9         | 0.0004       |
| ZBS         | 1350/4                 | 97.8                 | 70100                | 2.3               | 11.9         | 0.0016       |
| BBSZ        | 1400/4                 | 97.6                 | 92500                | -3.7              | 11.8         | 0.0019       |
| BBS         | 1400/4                 | 97.3                 | 103000               | -0.7              | 11.8         | 0.0029       |
| AS          | 1425/4                 | 97.1                 | 65000                | 3.0               | 11.7         | 0.0025       |
| BB          | 1400/4                 | 97.0                 | 66300                | 1.8               | 11.8         | 0.0033       |
| MBS         | 1400/4                 | 97.3                 | 68500                | -6.3              | 11.8         | 0.0046       |
| ABS         | 1400/4                 | 97.1                 | 55400                | 2.3               | 11.6         | 0.0050       |

## 6.1.3.1 PHASE ANALYSIS

FIGURE 6.2 (A) SHOWS THE XRD PATTERNS OF PURE ZAT. THE POWDER DIFFRACTION PATTERNS OF ZAT AND TiO<sub>2</sub> ARE INDEXED BASED ON JCPDS FILE CARD NUMBERS 5-669 AND 21-1276 RESPECTIVELY. THE XRD PATTERN OF ZAT SHOWS THAT IT IS A SOLID SOLUTION WITH AS REPORTED EARLIER [31]. FIGS. 6.2 (B), (C), (D) AND (E) SHOW THE XRD PATTERNS OF ZAT SINTERED WITH DIFFERENT WEIGHT PERCENTAGES OF BBSZ GLASS. MOST OF THE CERAMIC GLASS COMPOSITES [33-34] REPORT THE FORMATION OF LOSSY SECONDARY PHASES WHICH ADVERSELY AFFECT THE PHYSICAL AND MICROWAVE DIELECTRIC PROPERTIES. THE PRESENCE OF SECONDARY PHASES IN THE LTCC COMPOSITE SIGNIFICANTLY INCREASES THE POSSIBILITY OF A CHEMICAL REACTION WITH THE METAL ELECTRODE WHICH IN TURN AFFECTS THE PERFORMANCE. IN THE PRESENT CASE NO ADDITIONAL PEAKS ARE OBSERVED FOR ZAT SINTERED WITH 10, 12, 15 WT% OF BBSZ. THIS MAY BE DUE TO THE FACT THAT THE BBSZ DOES NOT REACT WITH THE PARENT MATERIAL TO FORM ADDITIONAL PHASES THEREBY REMAINING AS GLASS AND RETAINING ITS AMORPHOUS NATURE. THIS IS A CLEAR EVIDENCE FOR THE CHEMICAL STABILITY OF THE PARENT MATERIAL.

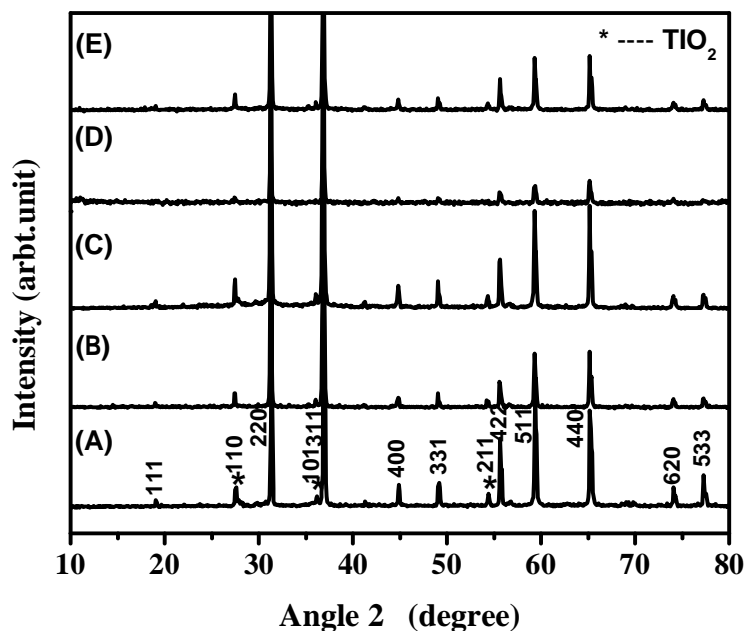


Fig. 6.2 The powder diffraction patterns of (a)  $0.83\text{ZnAl}_2\text{O}_4\text{-}0.17\text{TiO}_2$  (ZAT) (b) ZAT + 10 wt% BBSZ (c) ZAT + 12 wt% BBSZ (d) ZAT + 15 wt% BBSZ (e) ZAT + 10 wt% BBSZ + 0.3 wt% LiF.

### 6.1.3.2 SINTERING AND DENSIFICATION

THE PURE ZAT HAS A SINTERING TEMPERATURE OF 1450°C. IT IS A WELL ESTABLISHED FACT THAT ADDITION OF SMALL AMOUNT OF GLASS TO THE CERAMIC LOWERS THE PROCESSING TEMPERATURE WITH IMPROVED DENSIFICATION AND PROPERTIES. FIGURE 6.3 SHOWS THE VARIATION OF SINTERING TEMPERATURE AS A FUNCTION OF DIFFERENT WEIGHT PERCENTAGE OF ZB1, ZB2, ZBS, BBS AND BBSZ GLASS. THE SINTERING TEMPERATURE GRADUALLY DECREASES WITH INCREASE IN GLASS CONTENT FROM 0.1 WT% - 3 WT% BUT THE RATE OF DECREASE VARIES WITH THE NATURE OF GLASS. GLASSES ZB1 AND ZB2 SHOWS SIMILAR TREND. EVENTHOUGH A SUDDEN DECREASE IS NOTED AT 0.5 WT% ADDITION OF THESE GLASSES, HIGHER GLASS CONTENT SHOWS ONLY A SLIGHT DECREASE IN SINTERING TEMPERATURE. ADDITION OF 3 WT% OF THESE GLASSES REDUCED THE SINTERING TEMPERATURE TO 1325°C.

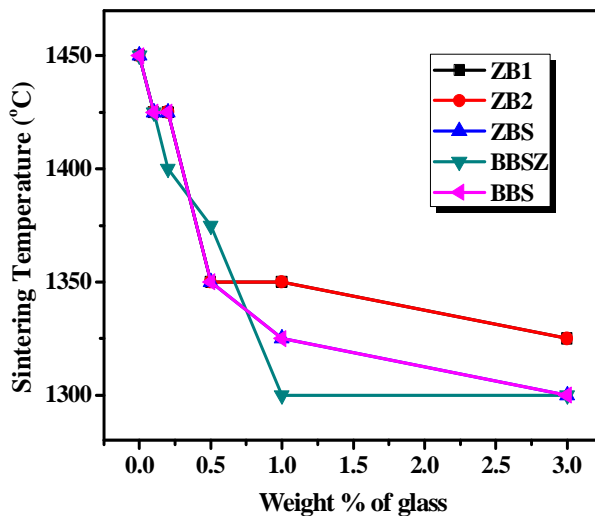


Fig. 6.3 The variation of sintering temperature with weight percentage of various glasses.

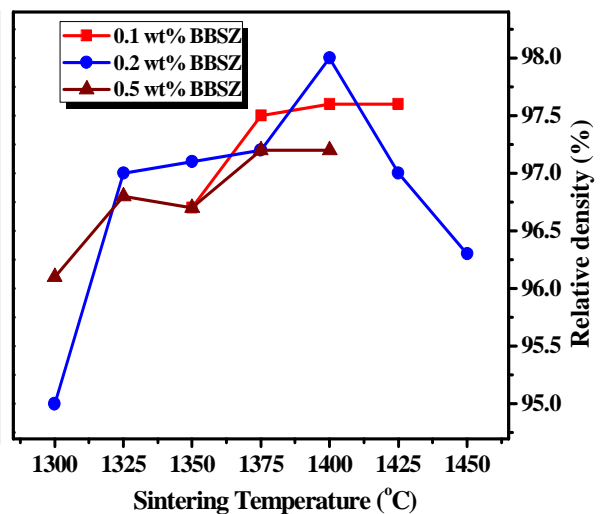


Fig. 6.4 The variation of relative density with sintering temperature with 0.1, 0.2 and 0.5 wt% of BBSZ glass addition to ZAT.

THE THEORETICAL DENSITY OF ZAT MEASURED USING THE MIXTURE RULE IS FOUND TO BE 4.58 G/CM<sup>3</sup>. THE MEASURED DENSITY OF THE SAMPLE SINTERED AT 1450°C IS 4.50 G/CM<sup>3</sup>, WHICH IS 97% OF THE THEORETICAL DENSITY. THE THEORETICAL DENSITY OF ZAT WITH GLASS (ADDED ZAT) IS CALCULATED USING THE EQ. (4.2) IN CHAPTER 4. TABLE 6.1 GIVES THE OPTIMIZED RELATIVE DENSITY OF ZAT WITH 0.1 WT% VARIOUS GLASSES. A SLIGHT IMPROVEMENT IN DENSITY IS NOTED FOR

COMPOSITES WITH 0.1 WT% GLASS ADDITION. FIG. 6.4 SHOWS THE RELATIVE DENSITY DOPED WITH 0.1, 0.2 AND 0.5 WT% BBSZ GLASS AS A FUNCTION OF SINTERING TEMPERATURE. IT IS OBSERVED THAT THE RELATIVE DENSITY INCREASES WITH THE SINTERING TEMPERATURE TO A MAXIMUM AND THEN DECREASES. LOW CONTACT ANGLE, LOW DIHEDRAL ANGLE AND HIGH WETTABILITY OF THE SOLID IN THE LIQUID ARE ESSENTIAL FOR ACHIEVING HIGH SINTERED DENSITY IN CERAMICS. IN SUCH CASES, THE TRANSIENT GLASSY PHASE FORMED AT A LOWER TEMPERATURE CAN ACT AS A SHORT CIRCUIT MEDIUM FOR GRAIN TO GRAIN MATERIALS TRANSPORT [35]. THIS VARIATION IS EXPLAINED BY THE PRESENCE OF SECONDARY PHASES IN SEVERAL SYSTEMS [9, 36]. HOWEVER, THE XRD AND SEM RESULTS CONFIRM THE ABSENCE OF SECONDARY PHASES. THUS THE REASON FOR THE INITIAL INCREASE IN THE DENSITY IS THE ELIMINATION OF PORES AS TEMPERATURE INCREASES. THE TEMPERATURE AT WHICH MAXIMUM DENSITY IS ACHIEVED DEPENDS ON THE GLASS CONTENT. THE LARGER THE AMOUNT OF GLASS, THE LOWER THE SINTERING TEMPERATURE. WHEN THE GLASS ADDITION EXCEEDS 20 WT%, SINTERING IS INITIATED [7]. A MAXIMUM RELATIVE DENSITY OF NEARLY 98% IS REACHED AT A SINTERING TEMPERATURE OF 1400°C FOR 400 WT% BBSZ ADDITION WHICH IS HIGHER THAN THAT FOR 0.1 WT% BBSZ. THIS TEMPERATURE MAY BE THE OPTIMUM FOR THE OCCURRENCE OF LIQUID PHASE SINTERING. FURTHER INCREASE IN THE SINTERING TEMPERATURE MAY FACILITATE THE ELIMINATION OF THE VOLATILE COMPONENTS FROM THE GLASS FRIT FROM GRAIN BOUNDARIES, CAUSING PORE WETTING RESULTING IN TRAPPED POROSITY ASSOCIATED WITH GRAIN GROWTH AT HIGH TEMPERATURE. IT HAS BEEN REPORTED THAT THE SINTERING AIDS CONTAINING BORON OXIDE PROMOTE DENSIFICATION BY LIQUID PHASE SINTERING AND THEN EVAPORATED [37]. IN THE CASE OF 0.1 WT% AND 0.2 WT% BBSZ GLASS ADDITION THE RELATIVE DENSITY INCREASES TO 98% AND 97% RESPECTIVELY AND FURTHER INCREASE IN SINTERING TEMPERATURE DID NOT AFFECT THE DENSIFICATION.

FIGURE 6.5 SHOWS THE VARIATION OF SINTERING TEMPERATURE AND BULK DENSITY OF COMPOSITES WITH WEIGHT PERCENTAGE OF BBSZ GLASS ADDITION. IT IS CLEAR THAT THE SINTERING TEMPERATURE GRADUALLY DECREASES WITH INCREASE IN THE AMOUNT OF GLASS. THE RATE OF DECREASE IS SUDDEN TILL 0.5 WT%, BEYOND THIS LIMIT THE SINTERING TEMPERATURE DECREASES VERY SLOWLY. THE SINTERING TEMPERATURE FOR 0.5 WT % AND 3 WT% BBSZ GLASS ADDITION IS 1600°C AND BEYOND THIS THE TEMPERATURE AGAIN DECREASES TO ABOUT 950°C FOR THE ADDITION OF 10 WT% BBSZ GLASS. ADDITION OF HIGHER AMOUNT OF GLASS (> 10 WT%)

NO EFFECT ON THE SINTERING TEMPERATURE, IE., THE SINTERING TEMPERATURE SATURATED AT 1300°C. THIS IS DUE TO THE FACT THAT THE BBSZ GLASS MELTS AT 950°C.

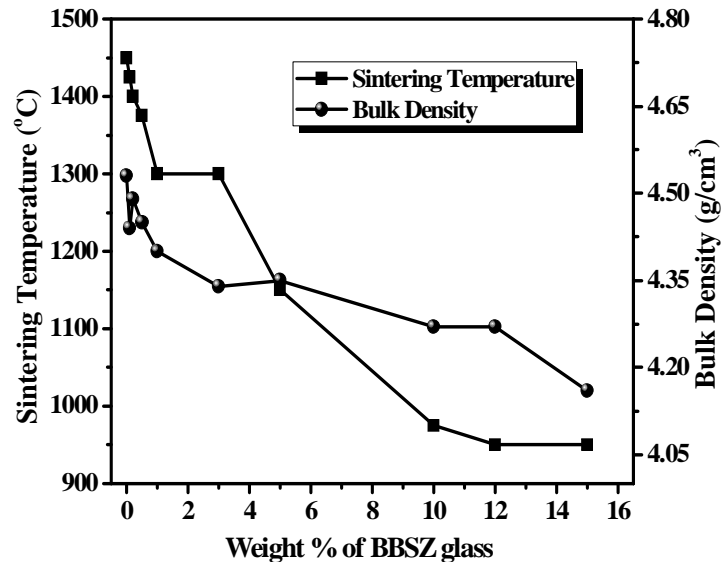


Fig. 6.5 The variation of sintering temperature and bulk density with weight percentage of BBSZ glass.

THE BULK DENSITY ALSO DECREASES WITH THE AMOUNT OF GLASS ADDITION. IT IS NOTED THAT THE 0.2 WT% GLASS ADDED COMPOSITE EXHIBITED A BETTER DENSIFICATION WHEN COMPARED TO THE LOWER WEIGHT PERCENTAGE. THIS MAY BE DUE TO THE FACT THAT AT LOWER WEIGHT PERCENTAGE THE AMOUNT OF MELTED GLASS MAY NOT BE SUFFICIENT ENOUGH TO FILL THE PORES OF THE COMPOSITE. DENSIFICATION. HOWEVER, FURTHER INCREASE IN THE GLASS CONTENT (0.5 WT%) DOES NOT INCREASE RELATIVE DENSITY DUE TO THE LOW DENSITY OF THE GLASS WHEN COMPARED TO THE CERAMIC. FURTHERMORE HIGHER GLASS CONTENT MAY INDUCE POROSITY WHICH ADVERSELY AFFECTS THE DENSITY. THE RELATIVE DENSITY DECREASES FROM 96% TO 91% AS THE BBSZ GLASS CONTENT INCREASES FROM 1 WT% TO 15 WT%.

### 6.1.3.3 MICROSTRUCTURAL ANALYSIS

FIGURE 6.6 (A) SHOWS THE SEM PICTURES OF ZAT SINTERED AT 1300°C. IT INDICATES THAT ZrO<sub>2</sub> AND TiO<sub>2</sub> DO NOT REACT TO FORM ANY SECONDARY PHASE. FIG. 6.6 (B) SHOWS THE SEM PICTURE OF ZAT TREATED WITH 0.2 WT% BBSZ GLASS. SINTERED PARTICLES SEEM TO COALESCE TOGETHER DECREASING THE SURFACE POROSITY. IT IS BELIEVED THAT THE

POINT OF THE BBSZ GLASS PROMOTES LIQUID PHASE SINTERING AND RESULTS IN GOOD DENSIFICATION (SEE ALSO TABLE 6.2). FIG. 6.6 (C) SHOWS THE SEM PICTURE OF ZAT DOPED WITH 10 WT% BBSZ FROM WHICH THE PRESENCE OF SLIGHT POROSITY IS OBSERVED. DUE TO THE MUCH HIGHER SINTERING TEMPERATURE OF THE COMPOSITE, THE GRAIN SIZE IS SMALLER WHEN COMPARED TO HIGH TEMPERATURE SINTERED ZAT. THE GLASS DID NOT REACT WITH ZAT BUT FORMS A COATINGS OVER THE GRAIN LEADING TO EXCESS LIQUID PHASE FORMATION. THE SEM PICTURE OF ZAT DOPED WITH BBSZ AND LIF [FIG. 6.6 (D)] IS SIMILAR TO THAT TREATED WITH 10 WT% BBSZ. FIG. 6.7 (A) SHOWS THE BACK SCATTERED IMAGE OF PURE ZAT AND THAT TREATED WITH 10 WT% BBSZ. FIG. 6.7 (B) CLEARLY SHOWS TWO AREAS (DARK AND LIGHT) INDICATING THE PHASES OF ZAT AND  $\text{TiO}_2$ . IN THE CASE OF BBSZ ADDED COMPOSITE (FIG. 6.7 (C)), THE WHITE AREA SHOWS THE PRESENCE OF UNREACTED GLASS.

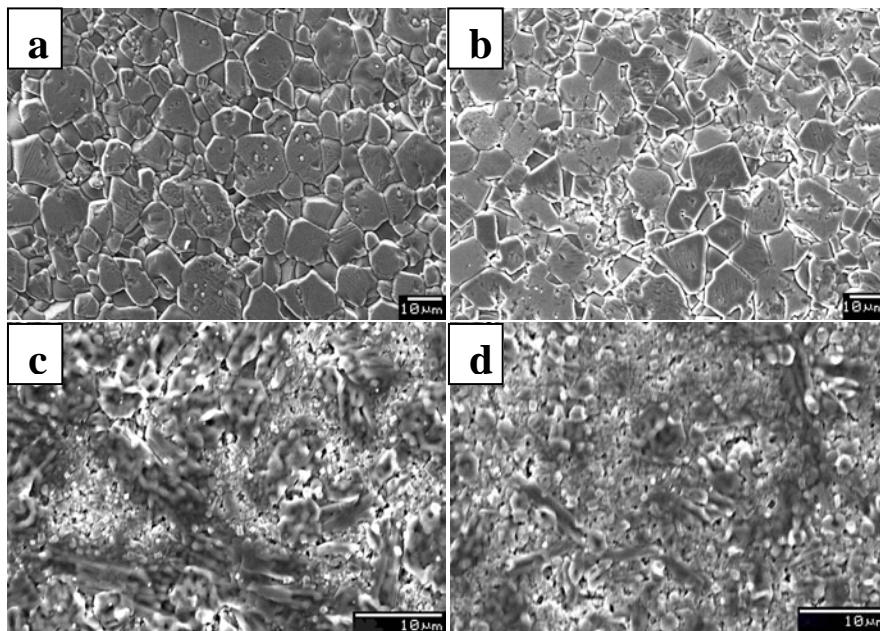


**Fig. 6.6** The scanning electron micrographs of (a) pure ZAT, (b) doped with 0.2 wt% BBSZ sintered at 1400°C, (c) doped with 10 wt% BBSZ sintered at 950°C and (d) doped with 10 wt% BBSZ and 0.3 wt% LiF sintered at 925°C.

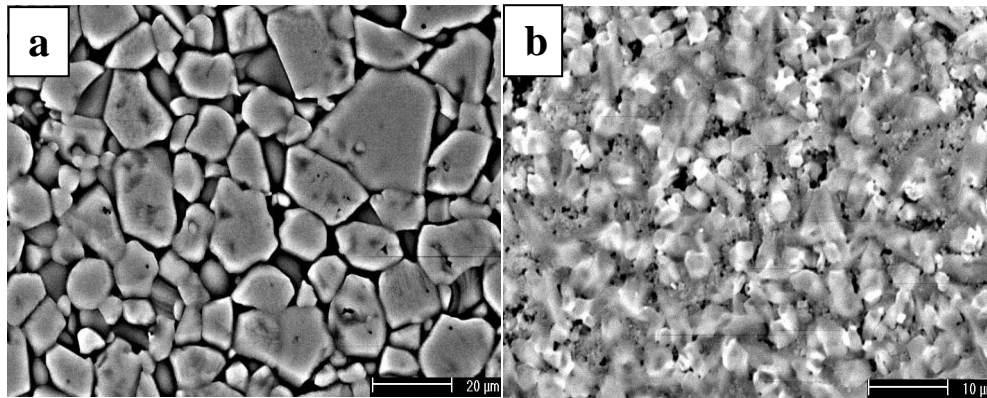


Fig. 6.7 The backscattered electron image of (a) pure ZAT and (b) doped with 10 wt% BBSZ sintered at 950°C.

#### 6.1.3.4 MICROWAVE DIELECTRIC PROPERTIES

THE MICROWAVE DIELECTRIC PROPERTIES OF UNDOPED ZAT SINTERED AT 1450°C  $Q_{uxf}=91000$  GHZ,  $\epsilon_r = 11.7$  AND  $T_f = 1.4$  PPM/°C. THE EFFECT OF GLASS ADDITION ON THE MICROWAVE DIELECTRIC PROPERTIES IS DEPENDENT ON THE CHEMISTRY OF THE GLASS REACTIONS, PHASE CHANGES DURING SINTERING AND FINAL DENSITY. TABLE 6.1 SHOWS THE PROPERTIES OF ZAT DOPED WITH 0.1 WT% OF DIFFERENT LOW LOSS GLASSES. IT IS CLEAR THAT THE GLASSES ARE EFFECTIVE IN IMPROVING THE SINTERABILITY AND THE DIELECTRIC PROPERTIES WITH THE ADDITION OF SMALL WT% OF SOME OF THE GLASSES SUCH AS AS, ABS, MBS AND MBS. THE QUALITY FACTOR IS FOUND TO DECREASE CONSIDERABLY. THIS MAY BE DUE TO THE HIGH DIELECTRIC LOSS EXHIBITED BY THESE GLASSES (SEE TABLE 1.3 CHAPTER 1). DUE TO THE SINTERABILITY AND POOR PROPERTIES EXHIBITED BY THESE GLASS COMPOSITES, THERE IS A NEED FOR FURTHER STUDIES.

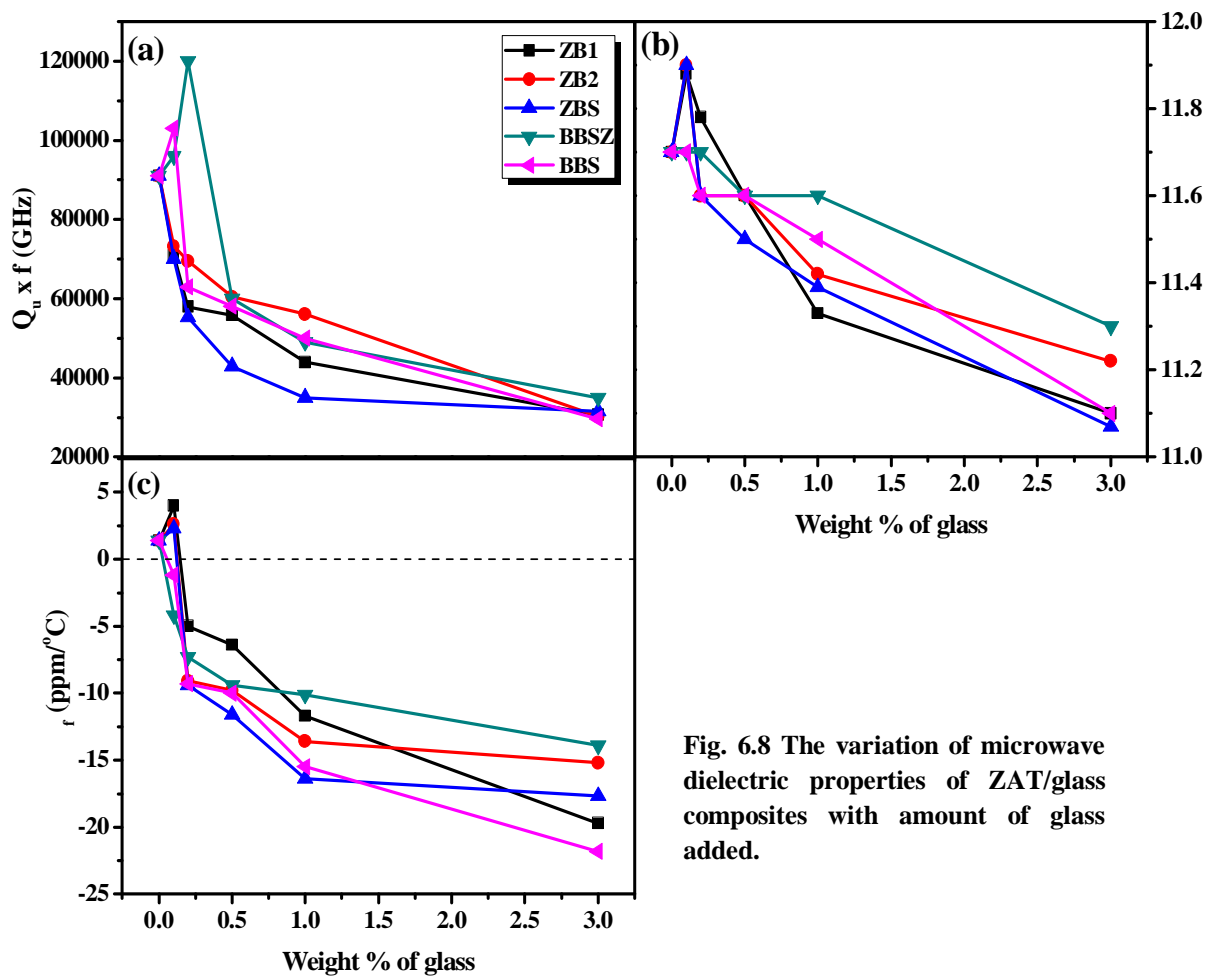


FIGURE 6.8 SHOWS THE MICROWAVE DIELECTRIC PROPERTIES OF VARIOUS GLASS A COMPOSITES. FROM FIG. 6.8 (A) IT IS CLEAR THAT ADDITION OF SMALL WEIGHT PERCENTAGE AND BBS GLASS IMPROVED THE QUALITY FACTOR. THE ADDITION OF BINARY GLASSES (ZB1) SHOWED ALMOST SIMILAR VARIATION IN THE DIELECTRIC PROPERTIES (TABLE 6.1). WITH THE ADDITION OF SMALL AMOUNT (0.1, 0.2 WT%) OF THESE GLASSES INCREASED THE PERMITTIVITY DUE TO THE INCREASE IN RELATIVE DENSITY, THE QUALITY FACTOR IS REDUCED TO 70000 GHZ. THE GLASS IN THE GRAIN BOUNDARY MAY BE RETAINED DURING SINTERING WHICH MAY HAVE INCREASED THE VOLUME WHEN THE EUTECTIC LIQUID FORMATION TOOK PLACE. THE MAIN REASON FOR THE DECREASE IN THE QUALITY FACTOR EVEN THOUGH THE DENSIFICATION IS A SIMILAR TREND IS EXHIBITED BY ZBS GLASS WHERE THE QUALITY FACTOR IS FOUND TO BE 70000 GHZ. IT IS EVIDENT FROM THE FIG. 6.3 THAT THE GLASSES HAVING MORE COMPONENTS ARE USED AS SINTERING AIDS. A COMPARISON OF THE MICROWAVE DIELECTRIC PROPERTIES OF VARIOUS



ADDED ZAT COMPOSITES SHOWED THAT BBSZ AND BBS IMPROVED THE QUALITY FACTOR 96000 GHZ AND 103000 GHZ RESPECTIVELY FOR 0.1 WT % GLASS. HOWEVER, THE ADDITION OF 0.5 WT% OF BBS DECREASED THE QUALITY FACTOR. IN THE CASE OF BBSZ GLASS IT IS FOUND THAT THE ADDITION OF 0.2 WT% IMPROVED THE QUALITY FACTOR TO NEARLY 112900 GHZ WITH  $\tau_f$  OF -7.3 PPM/C. THIS IS DUE TO THE ENHANCED DENSIFICATION DUE TO LIQUID PHASE SINTERING. THE ZNO IN BBSZ GLASS ACTS AS A MODIFIER OXIDE AND THE ADDITIONAL INCREASE OF DENSIFICATION OF CERAMICS WITH SUCH ADDITIVES INCREASE THE DENSIFICATION [22]. ALSO THE LOSS TANGENT OF BBSZ GLASS IS RELATIVELY LOW (0.001) AS COMPARED TO OTHER GLASSES [6] (SEE TABLE 1.1 IN CHAPTER 1). THE VARIOUS LOSS MECHANISMS ASSOCIATED WITH GLASSES IN THE MICROSTRUCTURE ARE ALSO DISCUSSED IN CHAPTER 1, SECTION 1.8.3.3.2. FROM FIG. 6.8 (B) IT IS CLEAR THAT THE QUALITY FACTOR RELATIVE PERMITTIVITY SHOWS AN IMPROVEMENT ONLY FOR LOWER GLASS CONTENT. AS GLASS CONTENT INCREASES, THE RELATIVE PERMITTIVITY GRADUALLY DECREASES WHICH IS DUE TO THE LOW VALUES POSSESSED BY THE GLASSES. IT IS SEEN FROM FIG. 6.8 (B) THAT THE QUALITY FACTOR BECOMES MORE NEGATIVE WITH HIGHER GLASS CONTENT WHICH IS DUE TO THE HIGHER LOSS TANGENT.

THE DIELECTRIC PROPERTIES OF THE MATERIALS ARE DEFINED BY THEIR COMPLEX PERMITTIVITY COMPONENTS WHICH IN TURN ARE DETERMINED BY THE SINTERING TEMPERATURE. FIG. 6.8 (A) SHOWS THE VARIATION OF RELATIVE PERMITTIVITY OF DIFFERENT WEIGHT PERCENTAGE BBSZ AND BBS ZAT COMPOSITE WITH SINTERING TEMPERATURE. THE VARIATION IS SIMILAR TO THE VARIATION WITH TEMPERATURE AS IN FIG. 6.4. THE RELATIVE PERMITTIVITY INITIALLY INCREASES WITH INCREASE IN THE SINTERING TEMPERATURE, ATTAINS A MAXIMUM VALUE AND THEN DECREASES WITH FURTHER INCREASE IN TEMPERATURE. THIS IS BECAUSE THE RELATIVE PERMITTIVITY IS DIRECTLY DEPENDENT ON THE DENSITY. AS THE AMOUNT OF GLASS INCREASES TO 0.2 WT% THE RELATIVE PERMITTIVITY ATTAINS THE MAXIMUM VALUE. ON FURTHER INCREASE IN THE GLASS CONTENT DECREASES THE RELATIVE PERMITTIVITY GRADUALLY DUE TO THE LOW DENSITY OF GLASS AND ALSO DUE TO THE FACT THAT GLASSES HAVE LOW RELATIVE PERMITTIVITY. THE QUALITY FACTOR OF THE COMPOSITE IS STRONGLY DEPENDENT ON BOTH THE SINTERING TEMPERATURE AND GLASS CONTENT. BBSZ GLASS ADDED AS SHOWN IN FIG. 6.9 (B). IN THE CASE OF VARYING GLASS CONTENT WITH SINTERING TEMPERATURE, IT IS FOUND TO INCREASE TO A MAXIMUM VALUE AND THEREAFTER DECREASES. FOR ZAT CERAMICS WITH 0.1, 0.2 AND 0.5 WT% OF BBSZ GLASS ADDITIONS, THE MAXIMUM VALUES ARE 96000, 120000 AND 60000 GHZ RESPECTIVELY AT THEIR OPTIMIZED SINTERING TEMPERATURES. EVENTHOUGH, POROSITY IS ONE OF THE FACTORS AFFECTING THE QUALITY FACTOR.

THE MICROWAVE DIELECTRIC LOSS [38-39], SOME INVESTIGATORS ALSO REPORTED THAT THE FACTOR IS INDEPENDENT OF POROSITY FOR A THEORETICAL DENSITY > 90% [40]. THE INCREASE IN QUALITY FACTOR AT LOW TEMPERATURE IS DUE TO THE INCREASE IN DENSITIES AND WHERE THE MAXIMUM CORRESPONDS TO MAXIMUM DENSIFICATION. THE VARIATION OF  $Q_{\text{eff}}$  WITH SINTERING TEMPERATURE IS SHOWN IN FIG. 6.9 (C). IT SEEMS TO HAVE A NEGATIVE VALUE WITH INCREASE IN TEMPERATURE.

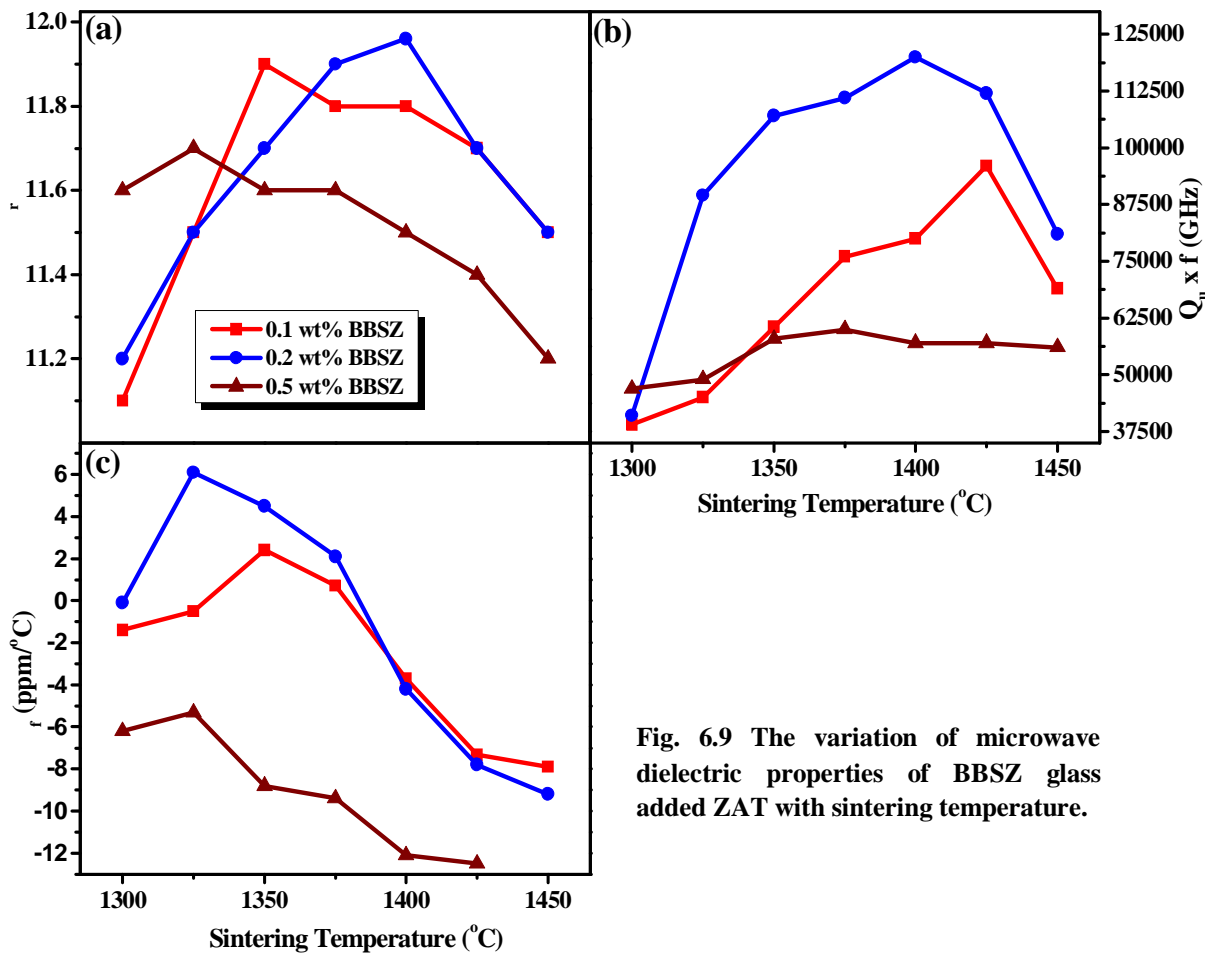


Fig. 6.9 The variation of microwave dielectric properties of BBSZ glass added ZAT with sintering temperature.

**Table 6.2** The sintering temperature, relative density and dielectric properties of ZAT doped with different weight percentage of BBSZ glass.

| Weight % of BBSZ added | Sintering temp. (°C/h) | Microwave Properties |                      |                   |              | Loss at 1MHz |
|------------------------|------------------------|----------------------|----------------------|-------------------|--------------|--------------|
|                        |                        | Relative Density (%) | $Q_U \times F$ (GHz) | $\tau_f$ (ppm/°C) | $\epsilon_R$ |              |
| 0                      | 1450/4                 | 97                   | 91,000               | 1.4               | 11.7         | 0.0010       |
| 0.1                    | 1425/4                 | 97                   | 96,000               | -4.2              | 11.7         | 0.0007       |
| 0.2                    | 1400/4                 | 98                   | 120,000              | -7.3              | 11.9         | 0.0004       |
| 0.5                    | 1375/4                 | 97                   | 60,000               | -9.4              | 11.6         | 0.0016       |
| 1                      | 1300/4                 | 96                   | 49,000               | -10.1             | 11.6         | 0.0019       |
| 3                      | 1300/4                 | 95                   | 35,000               | -13.9             | 11.3         | 0.0029       |
| 5                      | 1150/4                 | 95                   | 21,000               | -19.7             | 11.2         | 0.0035       |
| 10                     | 950/10                 | 93                   | 12,000               | -23.2             | 10.9         | 0.0058       |
| 12                     | 950/10                 | 93                   | 11,500               | -25.2             | 10.9         | 0.0155       |
| 15                     | 950/10                 | 91                   | 9,300                | -29               | 10.6         | 0.0307       |
| 10+0.3LIF              | 925/10                 | 94                   | 14,500               | -28               | 10.5         | 0.0046       |

TABLE 6.2 SUMMARIZES THE PROPERTY OF ZAT/BBSZ GLASS COMPOSITES FOR DIFFERENT WEIGHT PERCENTAGES OF GLASS CONTENT. THE INCREASE IN GLASS CONTENT DECREASES THE QUALITY FACTOR. FOR 5 WT% GLASS ADDITION THE MICROWAVE DIELECTRIC PROPERTIES ARE  $Q_U \times F = 21000$  GHZ,  $\epsilon_r = 11.2$  AND  $\tau_f = -19.7$  PPM/°C. THE QUALITY FACTOR IS REDUCED TO NEARLY 10000 GHZ BY THE ADDITION OF 12 WT% AND 15 WT% BBSZ. SINCE NO SECONDARY PHASE WAS DETECTED IN THE PRESENT SYSTEM, THE VARIATION IN THE QUALITY FACTOR CAN BE ATTRIBUTED TO THE BULK DENSITY OF THE SYSTEM. THE RELATIVE PERMITTIVITY DECREASES TO ABOUT 10.5 AT 15 WT% GLASS ADDITION WHICH IS DUE TO THE REDUCED DENSITY. IN ORDER TO IMPROVE THE DENSIFICATION OF THE MATERIAL A SMALL AMOUNT (0.3 WT%) OF LITHIUM FLUORIDE (LIF) IS ADDED TO THE COMPOSITION ZAT+10 WT% BBSZ. FIG. 6.10 SHOWS THE VARIATION OF QUALITY FACTOR WITH SINTERING TEMPERATURE FOR BOTH ZAT TREATED WITH 10 WT% BBSZ GLASS AND THAT TO WHICH LIF IS ADDED. THE QUALITY FACTOR INCREASED GRADUALLY WITH SINTERING TEMPERATURE FOR BOTH COMPOSITIONS. HOWEVER, ALSO SHIFTED TO MORE NEGATIVE VALUE. IT IS OBSERVED THAT AT A

TEMPERATURE OF 950 A MAXIMUM QUALITY FACTOR IS ABOUT 12000 GHz AND 23 PPM/°C FOR THE COMPOSITION UNTREATED WITH LiF. THE COMPOSITE TREATED WITH LiF DECREASED THE SINTERING TEMPERATURE ALONG WITH AN ENHANCEMENT IN THE DIELECTRIC PROPERTIES. WITH 4500 GHz AND OF 10.5. THE  $\tau$ , HOWEVER, INCREASED TO A VALUE OF -28 PPM/°C. THE LOW RELATIVE PERMITTIVITY OF THE GLASS AND THE PRESENCE OF POROSITY DECREASED THE RELATIVE PERMITTIVITY OF THE CERAMIC-GLASS COMPOSITE. THIS ALSO GIVES THE DIELECTRIC LOSS OF VARIOUS ZAT/BBSZ COMPOSITES AT LOW FREQUENCIES (1 MHz). AT LOW FREQUENCY, THE DIELECTRIC LOSS IS ATTRIBUTED TO THE STRUCTURAL POLARIZATION LOSS WHILE AT THE MICROWAVE FREQUENCIES, THE DECREASE IN THE LOSS MAY BE CAUSED BY THE DISAPPEARANCE OF IONIC POLARIZATION LOSS. IN ADDITION, THE MICROSTRUCTURE ALSO AFFECTS THE DIELECTRIC PROPERTY. THE DIELECTRIC STRUCTURE OF THESE COMPOSITES COMPRISE THE WELL CONDUCTING CRYSTAL GRAINS WHICH ARE SEPARATED BY POORLY CONDUCTING GLASSY PHASE. THE GLASS PHASE OF LOWER CONDUCTIVITY MAY BE EFFECTIVE AT LOW FREQUENCIES WHILE CRYSTAL GRAINS OF HIGH CONDUCTIVITY MAY BE EFFECTIVE AT HIGH FREQUENCIES. THEREFORE, THE HIGHER VALUES OF DIELECTRIC LOSS ARE OBTAINED AT LOWER FREQUENCIES. THE VARIATION OF RELATIVE PERMITTIVITY (MEASURED AT 1 MHz) OF ZAT AND THAT DOPED WITH 10 WT% BBSZ WITH TEMPERATURE IS SHOWN IN FIG. 6.11. IT IS NOTED THAT THE RELATIVE PERMITTIVITY OF ZAT IS ALMOST A CONSTANT IN THE TEMPERATURE RANGE 20-75

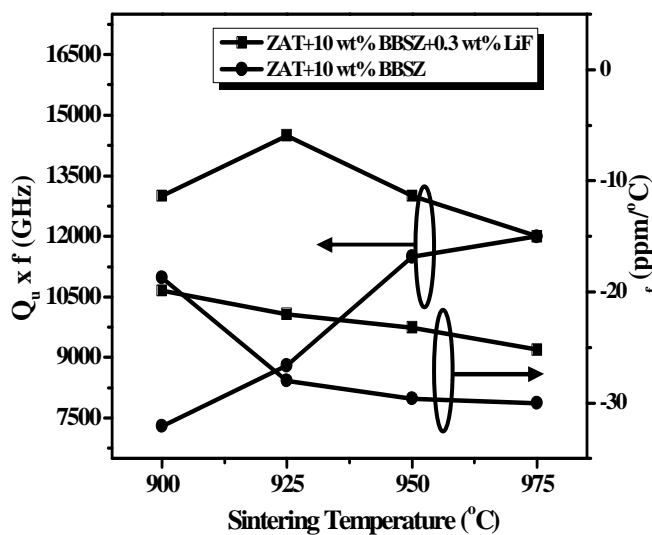


Fig. 6.10 The variation of quality factor and  $\tau$  with sintering temperature for ZAT doped with 10 wt% BBSZ glass.

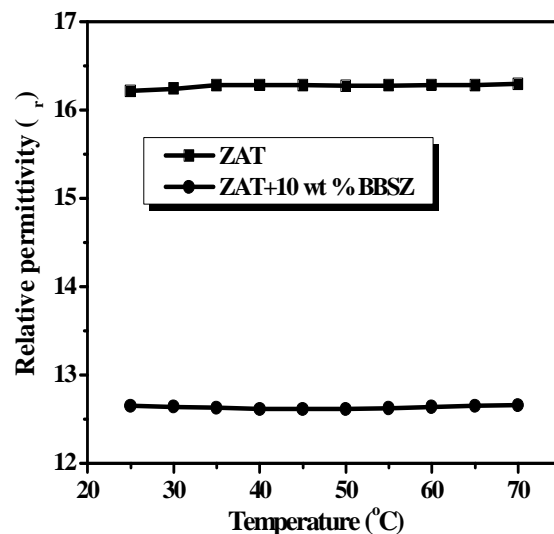


Fig. 6.11 The variation of relative permittivity (1 MHz) with temperature for ZAT and 10 wt% BBSZ added ZAT.

THE SHRINKAGE OF PURE ZAT, ZAT +10 WT% BBSZ AND ZAT +10 WT% BBSZ + 0.3 WT% LiF CERAMICS DURING FIRING PROCESS ARE MONITORED USING DILATOMETRIC METHOD AND THE RESULTS ARE AS SHOWN IN FIG. 6.12. IT IS SEEN THAT PURE ZAT EXHIBITS NO SHRINKAGE IN THE MEASURED TEMPERATURE RANGE. THIS IS BECAUSE THE SINTERING TEMPERATURE OF THE MATERIAL IS AS HIGH AS 1450

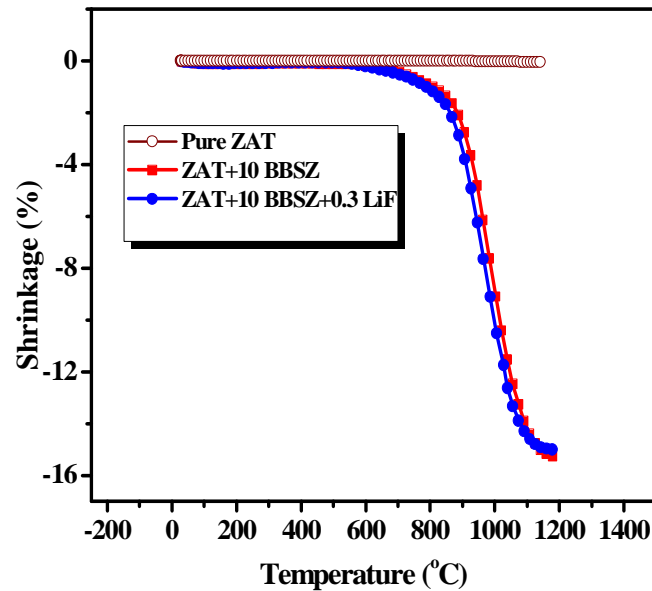
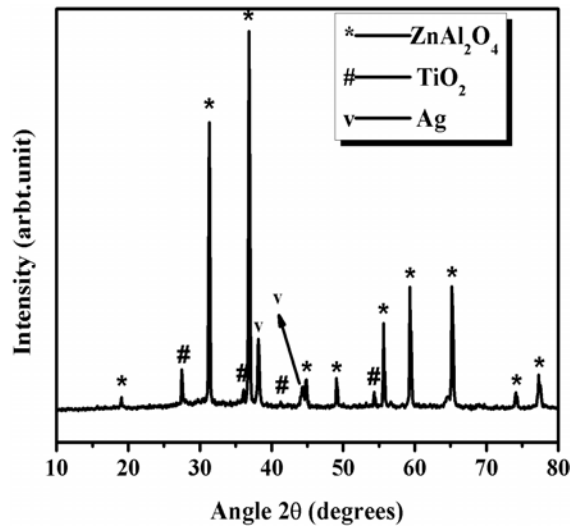
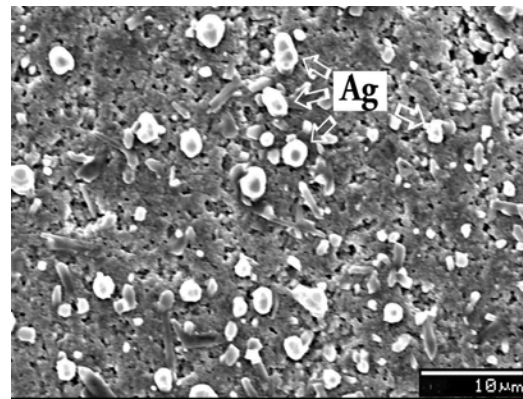


Fig. 6.12 The shrinkage curves of pure ZAT and that doped with 10 wt% BBSZ and 10 wt% BBSZ + 0.3 wt% LiF.

IT IS SEEN THAT WITH THE ADDITION OF 10 WT% BBSZ GLASS THE SHRINKAGE STARTS AT A LOWER TEMPERATURE (THE SAMPLE SINTERED WITH LiF SHRINKS AT A SLIGHTLY LOWER TEMPERATURE THAN THAT ADDED WITH BBSZ GLASS ALONE. HOWEVER, IN BOTH THE SAMPLES SHRINKAGE IS COMPLETE ONLY BEYOND THIS TEMPERATURE BOTH THE COMPOSITES EXHIBIT PERCENTAGE SHRINKAGE OF ABOUT 10 %. HOWEVER, SINTERING AT A LOWER TEMPERATURE DECREASED THE QUALITY FACTOR AS SHOWN IN FIG. 6.10.



**Fig. 6.13** The XRD pattern of 10 wt% BBSZ added ZAT treated with 20 wt% of silver.



**Fig. 6.14** The scanning electron micrograph of ZAT treated with 10 wt% BBSZ glass and 20 wt% silver.

IN ORDER TO USE ZAT/GLASS COMPOSITES FOR LTCC APPLICATIONS, IT IS NECESSARY TO FULLY FULFILL THE REQUIREMENT OF CHEMICAL COMPATIBILITY WITH A METAL ELECTRODE. A COMMON MATERIAL FOR LTCC ELECTRODES IS SILVER. THUS, TO STUDY THE REACTIVITY OF SILVER WITH THE GLASS ADDED CERAMICS, 20 WT% AG IS ADDED TO ZAT + 10 WT% BBSZ COMPOSITION. FIGS. 6.13 AND 6.14 SHOW THE POWDER DIFFRACTION PATTERN AND TYPICAL MICROGRAPH OF THE ABOVE COMPOSITION RESPECTIVELY. THE POWDER DIFFRACTION PATTERNS WERE INDEXED BASED ON JCPDS FILE CARD NUMBER 4-783. IT IS EVIDENT FROM THESE PLOTS THAT SILVER REMAINS UNREACTED WITH THE CERAMIC-GLASS COMPOSITE, WHICH IS IN ACCORDANCE WITH THE REQUIREMENTS OF LTCC.

THIS SECTION GIVES A BRIEF DISCUSSION ON THE DEVELOPMENT OF AN LTCC COMPOSITE BASED ON ZAT AND BBSZ GLASS WITH IMPROVED MICROWAVE DIELECTRIC PROPERTIES AND CHEMICAL COMPATIBILITY. THE NEXT SECTION DEALS WITH THE SYNTHESIS AND CHARACTERIZATION OF ZAT BASED POLYMER – CERAMIC COMPOSITES FOR ELECTRONIC PACKAGING AND APPLICATIONS.

## 6.2 POLYMER/0.83ZNA<sub>2</sub>O<sub>4</sub>-0.17TiO<sub>2</sub> COMPOSITES FOR ELECTRONIC PACKAGING APPLICATIONS

### 6.2.1 INTRODUCTION

THE RECENT DEVELOPMENTS IN ELECTRONICS AND CIRCUIT ASSEMBLY DEMAND PERMITTIVITY MATERIALS FOR THE PACKAGING OF RADIO FREQUENCY, MICROWAVE PRODUCTS [42]. THESE SUBSTRATE MATERIALS MUST POSSESS LOW RELATIVE PERMITTIVITY, DIELECTRIC LOSS TO REDUCE THE SIGNAL PROPAGATION DELAY WHICH IN TURN PROVIDES HIGH PERFORMANCE. THEY SHOULD ALSO HAVE GOOD THERMAL PROPERTIES SUCH AS HIGH THERMAL CONDUCTIVITY TO DISSIPATE THE HEAT GENERATED AND LOW OR MATCHING THERMAL EXPANSION COEFFICIENT WITH SILICON [43-44]. POLYMERS, ESPECIALLY POLYTETRAFLUOROETHYLENE (PTFE) AND POLYETHYLENE (PE), ARE WIDELY USED IN PACKAGING AND SUBSTRATE INDUSTRIES DUE TO THEIR HIGH RELATIVE PERMITTIVITY AND EXCELLENT CHEMICAL INERTNESS [45]. HOWEVER, THE HIGH THERMAL EXPANSION COEFFICIENT OF POLYMERS AND LOW THERMAL CONDUCTIVITY VALENTINELY LIMIT THEIR PRACTICAL USE [46]. THESE DIFFICULTIES CAN BE OVERCOME TO A CERTAIN EXTENT BY THE ADDITION OF INORGANIC FILLERS SUCH AS CERAMIC PARTICLES INTO THE POLYMER MATRIX. CERAMIC POLYMER COMPOSITES CONSISTING OF CERAMIC PARTICLES FILLED IN A POLYMER MATRIX FORM AN IDEAL GROUP OF MATERIALS FOR PRODUCING DEMANDING AND FUNCTIONAL PACKAGES, SINCE THEY COMBINE THE ELECTRICAL PROPERTIES OF CERAMICS AND THE MECHANICAL FLEXIBILITY, CHEMICAL STABILITY AND PROCESSING POSSIBILITY OF POLYMERS. THE KEY PROPERTIES OF THE COMPOSITE VIZ. THERMAL CONDUCTIVITY, PERMITTIVITY, THERMAL CONDUCTIVITY AND COEFFICIENT OF THERMAL EXPANSION ARE DETERMINED BY VARIOUS FACTORS SUCH AS THE NUMBER OF COMPONENTS OR PHASES, VOLUME FRACTION OF EACH PHASE, INDIVIDUAL PROPERTIES OF THE PHASES, PREPARATION METHOD AND THE INTERACTION BETWEEN THE FILLER AND THE MATRIX [47-48]. HOWEVER, HIGH FILLER CONTENT RESULTS IN LOW STRENGTH, LOW THERMAL FLUIDITY, POOR FLEXIBILITY AND DEFECTS IN THE COMPOSITE. THUS WITH THE PROPER DESIGN OF THESE COMPOSITE ONE CAN UTILIZE THE EASE OF PROCESSING AND LOW RELATIVE PERMITTIVITY OF POLYMERS AND HIGH THERMAL CONDUCTIVITY AND THERMAL STABILITY OF CERAMICS.

MANY STUDIES WERE CONDUCTED TO IMPROVE BOTH THE MECHANICAL AND ELECTRICAL PROPERTIES OF PTFE AND PE AS DISCUSSED EARLIER IN CHAPTER 5. ONE OF THE IMPORTANT ASPECTS REGARDING THE DESIGN OF COMPOSITE MATERIALS FOR PRACTICAL APPLICATION IS THE BALANCE BETWEEN RELATIVE PERMITTIVITY. MANY THEORETICAL MODELS HAVE BEEN PROPOSED FOR SUCH

ELECTRICAL AND THERMAL PROPERTIES OF THE COMPOSITES AND SOME OF THE PREDICTIONS OF THE STUDY ARE GIVEN IN CHAPTER 5.

EARLIER STUDIES [31] SHOWED THAT  $0.083\text{ZnO}$  (ZAT) CERAMICS POSSESS GOOD TEMPERATURE STABLE MICROWAVE DIELECTRIC PROPERTIES. IT HAS A RELATIVE PERMITTIVITY 12 AND DIELECTRIC LOSS LESS THAN 0.001 AT 5 GHZ AND A HIGH THERMAL CONDUCTIVITY  $\text{WM}^{-1}\text{K}^{-1}$ . THUS THE ADDITION OF PROPER VOLUME FRACTION OF ZAT AS FILLER INTO THE MATRIX CAN IMPROVE ITS PROPERTY TO CERTAIN EXTENT. THE PRESENT SECTION IS FOCUSED ON THE DIELECTRIC PROPERTIES OF ZAT/PTFE AND ZAT/PE COMPOSITES FOR ELECTRONIC PACKAGING APPLICATIONS.

### 6.2.2 EXPERIMENTAL

THE  $0.83\text{ZnO}$ - $0.17\text{TIO}_2$  (ZAT) CERAMICS WERE PREPARED AS EXPLAINED IN SECTION 6.1.2. ZAT/PTFE (HINDUSTAN FLUOROCARBONS, HYDERABAD, INDIA) AND ZAT/PE COMPOSITES WERE PREPARED BY POWDER PROCESSING METHOD AND MELT MIXING METHOD RESPECTIVELY AS DESCRIBED IN CHAPTER 2. THE POWDERED ZAT WAS MIXED WITH ACETIC ACID SOLUTION FOR 1H AND DRIED. THIS PROVIDED AN ACTIVE SURFACE FOR BINDING WITH POLYMER. ACRYLIC ACID IS A WELL-KNOWN POLYMERIZING AGENT. THE HOMOGENOUSLY MIXED POLYMER/ZAT COMPOSITES WERE THEN COMPACTED USING HOT PRESSURE OF 50 MPA FOR 30 MINUTE.

THE COMPOSITES WERE CHARACTERIZED USING XRD AND SEM. THE THIN PELLETS OF DIAMETER 14 MM AND THICKNESS LESS THAN 1 MM WERE ELECTRODED BY UNIFORMLY COATING SILVER PASTE ON BOTH SIDES IN THE FORM OF CERAMIC CAPACITORS. THE LOW FREQUENCY DIELECTRIC PROPERTIES WERE MEASURED BY LCR METER. THE VARIATION IN RELATIVE PERMITTIVITY WITH TEMPERATURE WAS ALSO INVESTIGATED FOR THE COMPOSITES IN THE TEMPERATURE RANGE 25-100°C. THE MICROWAVE DIELECTRIC PROPERTIES WERE MEASURED BY THE CAVITY PERTURBATION METHOD WHICH IS DISCUSSED IN DETAIL IN CHAPTER 2, SECTION 2.5.6. THE COEFFICIENT OF THERMAL EXPANSION (CTE) OF THE COMPOSITES WAS MEASURED USING A THERMO - MECHANICAL ANALYZER IN THE RANGE 25-200°C. THE WATER ABSORPTION MEASUREMENTS WERE CONDUCTED FOLLOWING ASTM D570 AS DESCRIBED IN CHAPTER 5, SECTION 5.3.



### 6.2.3 RESULTS AND DISCUSSION

FIGURE 6.15 SHOWS THE XRD PATTERNS OF PURE PTFE, ZAT AND THAT FILLED WITH  $V_f$  AND  $0.3V_f$ ZAT RESPECTIVELY. PTFE IS A SEMI-CRYSTALLINE POLYMER AND IT CAN CRYSTALLIZE MORE EASILY AND FASTER THAN ANY OTHER POLYMERS [49]. THE XRD CHARACTERIZATION INDICATES THAT PTFE HAS A STRONG CRYSTALLINE BEHAVIOR OBSERVED EARLIER BY SAJE FROM THE PREVIOUS SECTION IT IS CLEAR THAT IT CAN FORM A SOLID SOLUTION WITH TIO<sub>2</sub> IN THE COMPOSITION  $0.8ZnO/0.2TiO_2$  (ZAT) AND REMAIN AS A MIXTURE. THE POWDER DIFFRACTION PATTERNS OF ZAT AND TIO<sub>2</sub> ARE INDEXED BASED ON JCPDS FILE CARD NUMBERS 5-669 AND 21-1276 RESPECTIVELY. IT IS SEEN THAT AS THE VOLUME FRACTION OF ZAT INCREASES, THE INTENSITY OF PTFE PHASE DECREASES. ALSO NO ADDITIONAL PHASES ARE OBSERVED FOR PTFE/ZAT COMPOSITE INDICATING GOOD CHEMICAL STABILITY.

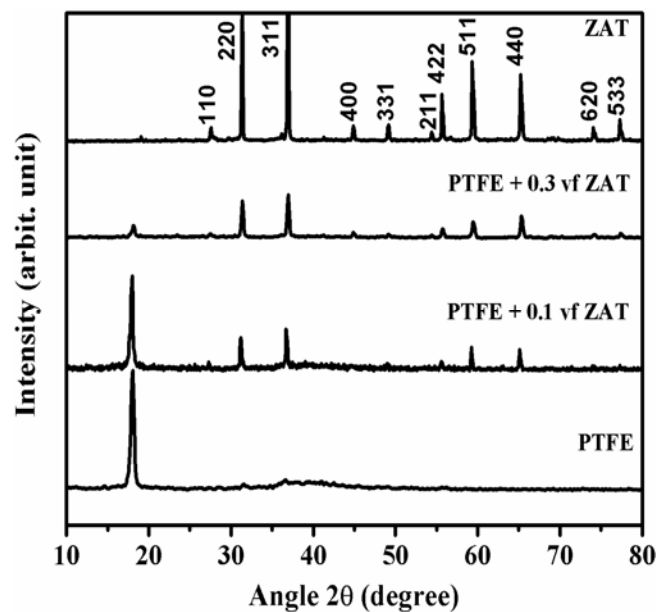
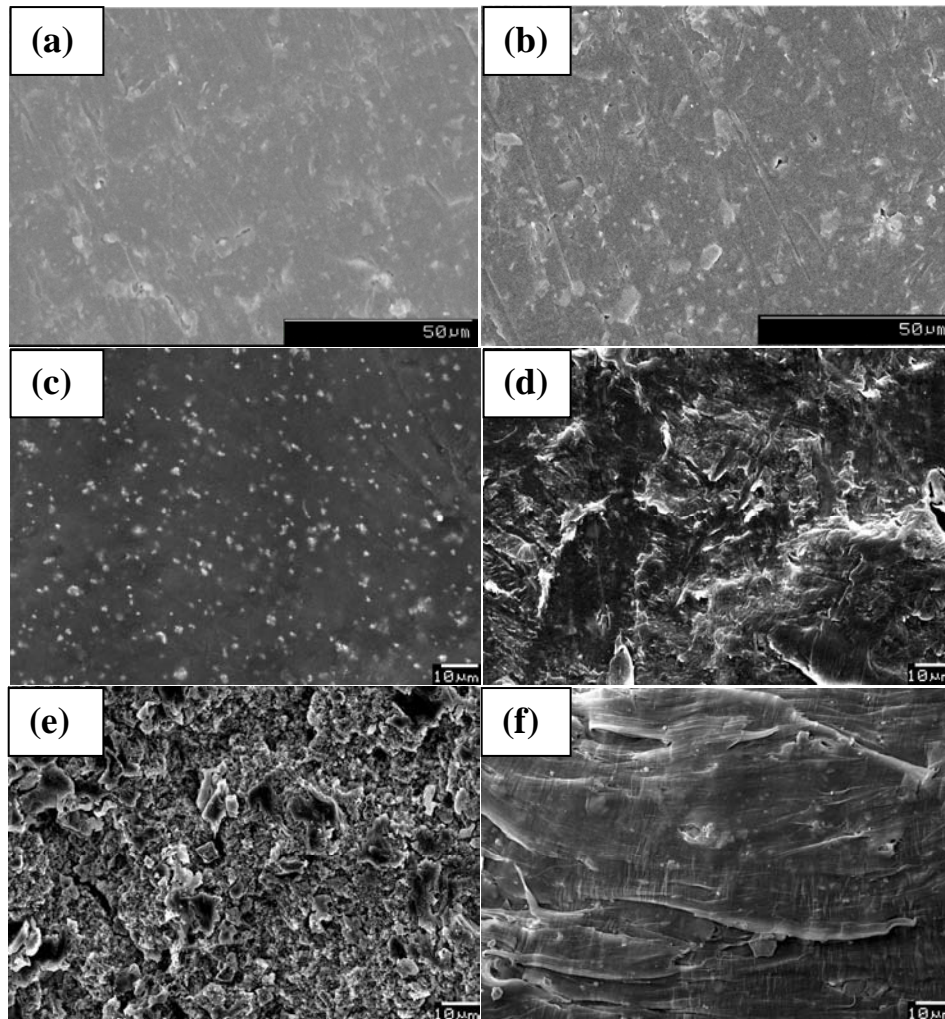


Fig. 6.15 XRD patterns of pure PTFE, ZAT and PTFE/ZAT composites.

THE SURFACE MORPHOLOGIES OF THE DIFFERENT VOLUME FRACTION OF ZAT LOADED IN PTFE AND PE COMPOSITES ARE SHOWN IN FIG. 6.16. IT IS CLEAR FROM THE FIGURES THAT FOR LOWER ZAT CONTENT THE CERAMIC PARTICLES ARE UNIFORMLY DISTRIBUTED IN THE POLYMER MATRIX. AS THE ZAT CONTENT INCREASES, THE CERAMIC PARTICLES ARE DISTRIBUTED THROUGHOUT THE PTFE MATRIX WITH RELATIVELY HIGH SPACING BETWEEN THE PARTICLES. WITH THE INCREASE OF ZAT CONTENT, THE CERAMIC PARTICLES WERE WELL EMBEDDED IN THE MATRIX AND ALSO RESULTED IN THE AGGREGATION OF PARTICLES.

CERAMIC PARTICLES. HOWEVER, A HIGHER DEGREE OF HOMOGENEITY IN DISPERSION IS NOTED IN PE/ZAT COMPOSITES WHICH MAY BE DUE TO THE DIFFERENCE IN THE PROCESSING TECHNIQUE ADOPTED. THE FRACTURED SURFACE OF THE COMPOSITES ALSO CONFIRMS A GOOD BONDING BETWEEN THE MATRIX AND THE FILLER. HOWEVER, PTFE/ZAT COMPOSITE EXHIBITS SOME DEGREE OF PARTICLE AGGLOMERATION AND POROSITY.



**Fig. 6.16 SEM images of (a) PTFE-0.1  $v_f$  ZAT, (b) PTFE-0.3  $v_f$  ZAT, (c) PE-0.1  $v_f$  ZAT, (d) PE-0.3  $v_f$  ZAT and fractured surface of (e) PTFE-0.3  $v_f$  ZAT, (f) PE-0.3  $v_f$  ZAT.**

THE THEORETICAL DENSITY OF BOTH THE COMPOSITES RELATED USING THE MIXTURE RULE GIVEN IN EQ. (5.12) IN CHAPTER 5.

Table 6.3 The physical and dielectric properties of PTFE/ZAT and PE/ZAT composites.

| Volume fraction filler | $\rho$ (%) | $V_{\text{filler}}$ (%) | $V_{\text{matrix}}$ (%) | $V_{\text{air}}$ (%) | Dielectric properties at 1 MHz |             |                          |      |
|------------------------|------------|-------------------------|-------------------------|----------------------|--------------------------------|-------------|--------------------------|------|
|                        |            |                         |                         |                      | $\epsilon_R$                   | $TAN\delta$ | $\tau_\epsilon$ (ppm/°C) |      |
| PTFE/ZAT               | 0.1        | 97.5                    | 9.75                    | 87.75                | 2.5                            | 2.63        | 0.0017                   | -98  |
|                        | 0.2        | 95.0                    | 19.00                   | 76.00                | 5.0                            | 2.79        | 0.0032                   | -120 |
|                        | 0.3        | 94.8                    | 28.44                   | 66.36                | 5.2                            | 3.35        | 0.0063                   | -350 |
|                        | 0.4        | 90.1                    | 36.04                   | 54.06                | 9.9                            | 3.87        | 0.0063                   | -396 |
|                        | 0.5        | 89.3                    | 44.65                   | 44.65                | 10.7                           | 4.22        | 0.0065                   | -580 |
| PE/ZAT                 | 0.1        | 98.9                    | 9.89                    | 89.01                | 1.1                            | 2.96        | 0.0012                   | -38  |
|                        | 0.2        | 97.7                    | 19.54                   | 78.16                | 2.3                            | 3.53        | 0.0033                   | -53  |
|                        | 0.3        | 95.2                    | 28.56                   | 66.64                | 4.8                            | 4.04        | 0.0044                   | -82  |
|                        | 0.4        | 92.3                    | 36.92                   | 55.38                | 7.7                            | 4.63        | 0.0046                   | -187 |
|                        | 0.5        | 91.1                    | 45.55                   | 45.55                | 8.9                            | 5.39        | 0.0052                   | -400 |

THE DENSITIES OF PTFE, PE AND ZAT MEASURED BY ARCHIMEDES METHOD ARE FOUND TO BE 2.15, 0.95 AND 4.58 G/CM<sup>3</sup> RESPECTIVELY. TABLE 6.3 GIVES THE RELATIVE DENSITY AND POROSITY OF THE COMPOSITES WITH VARYING FILLER CONTENT. THE RELATIVE DENSITY IS 97.5 % OF THE THEORETICAL VALUE FOR 0.1 FILLER LOADING WHICH DECREASED GRADUALLY WITH THE INCREASE IN FILLER CONTENT AND REACHED A VALUE OF 89.3% FOR 0.5 FILLER LOADING. THIS INCREASE IN THE RELATIVE DENSITY INDICATES THE PRESENCE OF POROSITY. ON THE OTHER HAND, PE/ZAT COMPOSITES SHOW A BETTER DENSIFICATION AS COMPARED WITH THE PTFE COMPOSITES. IT IS EVIDENT FROM THE SEM IMAGES WHERE A GOOD ADHESION BETWEEN THE PE MATRIX AND ZAT FILLER. EVEN FOR A HIGHER FILLER LOADING, THE RELATIVE DENSITY IS ABOUT 91%. THE POROSITY IS FOUND TO EXHIBIT A MUCH LOWER VALUE (LESS THAN 10%) EVEN FOR A HIGHER FILLER CONTENT. IT SHOULD BE NOTED THAT THE POROSITY HAS A LOWER VALUE AS COMPARED TO THAT REPORTED BY XIAO FOR SRT/PE COMPOSITES [51]. A COMPARISON OF THE POROSITY VALUES OF PTFE/ZAT AND PE/ZAT COMPOSITES SHOW THAT THE FORMER HAS A LOWER POROSITY CONTENT WHICH IS HIGHLY ENCOURAGING.

FIGURES 6.17 (A) AND (B) RESPECTIVELY SHOW THE FREQUENCY DEPENDENCE OF PERMITTIVITY OF THE PTFE/ZAT AND PE/ZAT COMPOSITES WITH DIFFERENT VOLUME FRACTION OF ZAT FILLER IN THE FREQUENCY RANGE 1 KHZ-1 MHZ. IT IS FOUND THAT THE RELATIVE PERMITTIVITY OF THE COMPOSITES REMAIN NEARLY A CONSTANT IN THE ENTIRE FREQUENCY RANGE. THIS SHOWS THE FREQUENCY STABILITY OF THE COMPOSITES. THIS INDICATES THAT THESE COMPOSITES HAVE PROMISING CHARACTERISTICS FOR POTENTIAL APPLICATIONS IN A WIDE RANGE OF FREQUENCIES.

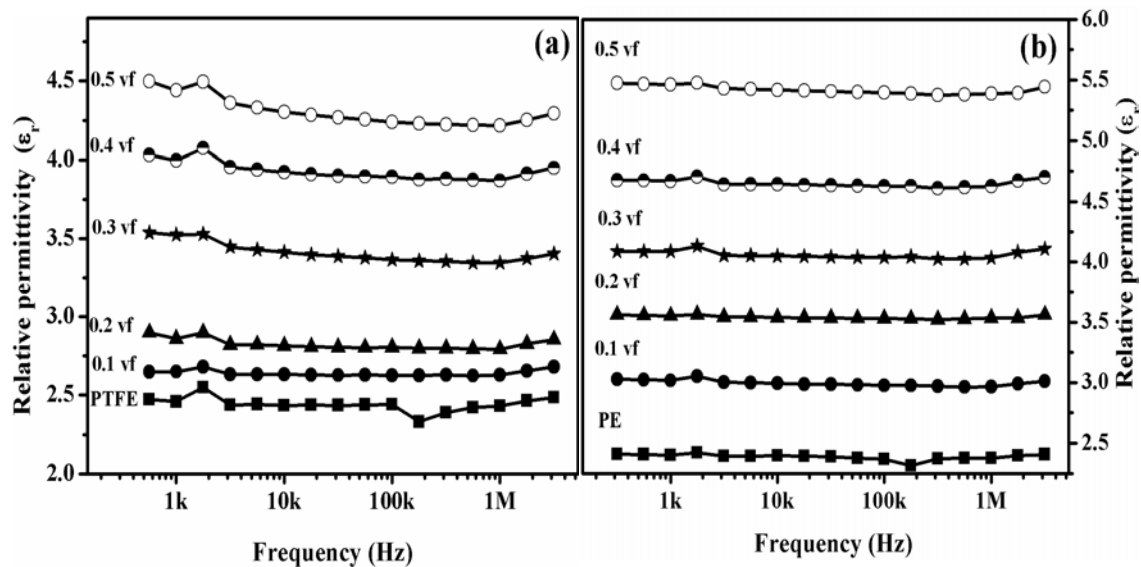


Fig. 6.17 The variation of relative permittivity of (a) PTFE/ZAT and (b) PE/ZAT composites with frequency.

FIGURE 6.18 SHOWS THE VARIATION OF RELATIVE PERMITTIVITY AND DIELECTRIC LOSS TANGENT WITH VOLUME FRACTION OF ZAT FOR BOTH PTFE/ZAT AND PE/ZAT COMPOSITES AT 9 GHZ. FOR BOTH COMPOSITES THE RELATIVE PERMITTIVITY INCREASES WITH INCREASE IN THE FILLER CONCENTRATION. THIS IS DUE TO THE RELATIVELY HIGH PERMITTIVITY OF THE ZAT FILLER (AT 9 GHZ) COMPARED TO THAT OF THE MATRIX. THE DIELECTRIC LOSS ALSO INCREASES WITH INCREASE IN THE FILLER CONTENT. THIS IS DUE TO THE FACT THAT AS THE FILLER CONTENT INCREASES, THE PARTICLES COME CLOSE TOGETHER LEADING TO AN INCREASE IN THE DIPOLE - DIPOLE INTERACTIONS, THEREBY INCREASING THE RELATIVE PERMITTIVITY [52]. THE SAME TREND IS OBSERVED AT 1 MHZ FREQUENCY ALSO. THE DIELECTRIC PROPERTIES OF THE COMPOSITES AT 1 MHZ FOR VARIOUS VOLUME FRACTIONS OF ZAT CONCENTRATION ARE GIVEN IN TABLE 6.3. THE RELATIVE PERMITTIVITY SHOWS A DECREASE

MICROWAVE FREQUENCY WHEN COMPARED WITH THAT AT 1 MHz. IN THE MATRIX A DIPOLE DIPOLAR POLARIZATION MAY BE RESPONSIBLE FOR THIS BEHAVIOR WHEREAS IN COMPOSITES HETEROGENEOUS SYSTEMS, INTERFACIAL OR MAXWELL-WAGNER-SILLARS POLARIZATION IS CONTRIBUTING TO THE DIELECTRIC PROPERTIES. THE DIELECTRIC LOSS WHICH IS THE LOSS OF ENERGY AFFECTING THE FREQUENCY SELECTIVITY OF A MATERIAL IS INFLUENCED BY MANY FACTORS SUCH AS POROSITY, MICROSTRUCTURE AND DEFECTS. IN THIS CASE, THE INCREASED DIELECTRIC LOSS MAY BE ATTRIBUTED TO THE INCREASED POROSITY (SEE TABLE 6.3) OF THE COMPOSITE MATERIAL AND ALSO TO THE INTERFACIAL POLARIZATION BETWEEN THE POLYMER AND CERAMIC AT HIGHER FILLER CONCENTRATIONS. DIELECTRIC LOSS VARIES FROM 0.0017-0.0065 AND 0.0012-0.0052 AT 1 MHz WITH THE FILLER ADDITION FROM 0.1 FOR PTFE/ZAT AND PE/ZAT COMPOSITES RESPECTIVELY. THIS IS A MUCH SATISFACTORY RESULT WHEN COMPARED WITH SOME OF THE EARLIER REPORTED RESULTS FOR POLYMER-CERAMIC COMPOSITES [44, 54-55]. BY COMPARING THE DIELECTRIC PROPERTIES OF THE COMPOSITES, IT CAN BE CONCLUDED THAT THE PTFE/ZAT COMPOSITES EXHIBIT A LOWER PERMITTIVITY WHEN COMPARED TO THAT OF THE PE/ZAT COMPOSITES. HOWEVER, THE DIELECTRIC LOSS OF THE FORMER IS HIGH IN COMPARISON WITH THE PE COUNTERPART.

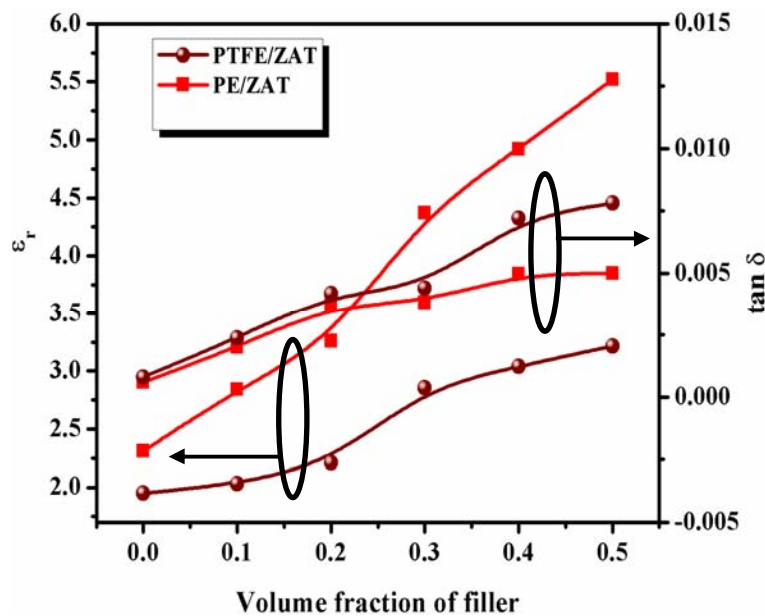


Fig. 6.18 Variation of  $\epsilon_r$  and  $\tan \delta$  (at 9 GHz) of PTFE/ZAT and PE/ZAT composites with volume fraction of filler.

AT 9 GHZ, AS THE VOLUME FRACTION OF FILLER INCREASES, THE RELATIVE PERMITTIVITY AND DIELECTRIC LOSS INCREASES FROM 1.95 TO 3.24 AND 0.0008 TO 0.0089 RESPECTIVELY FOR PTFE/ZAT COMPOSITES. ON THE OTHER HAND, FOR PE/ZAT COMPOSITES THE RESPECTIVE VARIATIONS ARE FROM 2.32 TO 5.52 AND 0.0006 TO 0.005. THE REDUCED DIELECTRIC LOSS FOR PE COMPOSITES CAN BE WELL UNDERSTOOD FROM THE LOW POROSITY VALUE OF THESE COMPOSITES (SEE TABLE 6.3). THE DIELECTRIC LOSS OF THE COMPOSITES AT MICROWAVE FREQUENCIES IS LOWER THAN THAT AT 1 MHZ. AT HIGHER FILLER CONTENT THE LOWER CONNECTION BETWEEN THE FILLER MAY LEAD TO MORE AIR AND MOISTURE CONTENT IN THE COMPOSITES. AT HIGHER FREQUENCY, THERE IS A LARGE DIELECTRIC LOSS DUE TO THE LARGE LOSS FROM THE DIELECTRIC LOSS OF WATER [56].

THE PREDICTION OF RELATIVE PERMITTIVITY OF THE COMPOSITE FROM THE RELATIVE PERMITTIVITIES OF THE CONSTITUENT COMPONENTS AND THE VOLUME FRACTION OF THE FILLER IS AN IMPORTANT FACTOR FOR ELECTRONIC PACKAGING APPLICATIONS. THE EXPERIMENTAL RELATIVE PERMITTIVITY OF BOTH THE COMPOSITES ARE COMPARED WITH THE THEORETICAL PREDICTIONS USING JAYASUNDERE-SMITH, LICHTENECKER, MAXWELL WAGNER, MODIFIED LICHTENECKER AND EMT MODELS GIVEN IN EQS. (5.1) TO (5.5) IN CHAPTER 5.

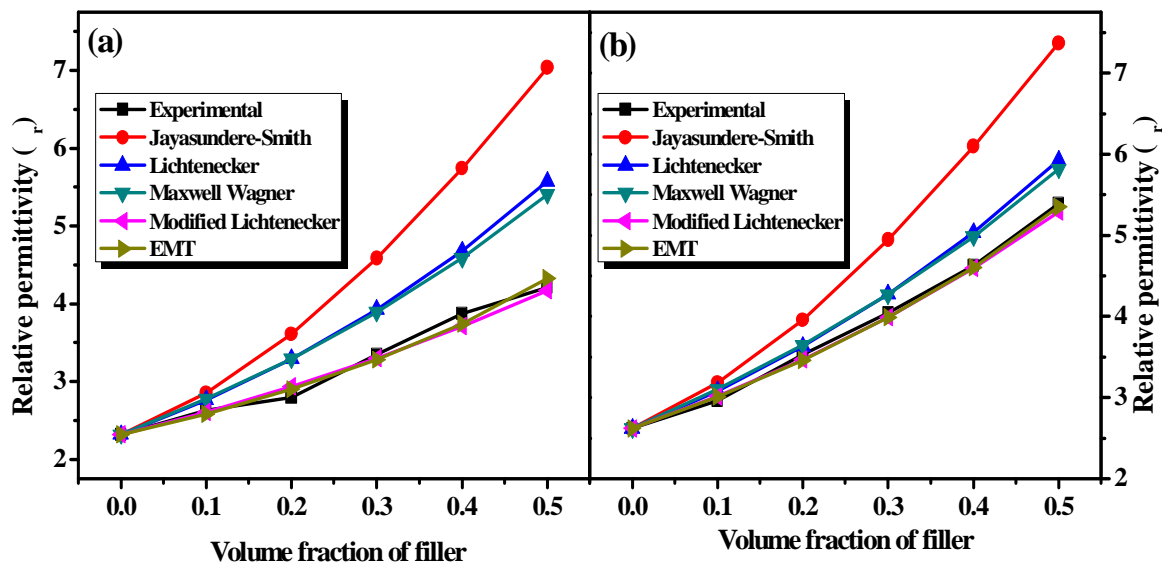


Fig. 6.19 Comparison of experimental relative permittivity with theoretical predictions of (a) PTFE/ZAT and (b) PE/ZAT composites at 1 MHz.

FIGURES 6.19 (A) AND (B) RESPECTIVELY SHOW THE COMPARISON BETWEEN EXPERIMENTAL AND THE THEORETICAL VALUES OF RELATIVE PERMITTIVITY OF PTFE/ZAT COMPOSITES AT 1 MHZ. IT IS CLEAR FROM THE FIGURES THAT FOR PTFE/ZAT COMPOSITES, JAYASUNDERE-SMITH, LICHTENECKER, MAXWELL WAGNER MODELS DEViate FROM THE EXPERIMENTAL VALUES WHEREAS FOR PE/ZAT COMPOSITES THE LICHTENECKER AND MAXWELL WAGNER MODELS ARE FOUND TO BE IN AGREEMENT AT LOWER FILLER CONTENTS ( $V_f$ ). GENERALLY ALL THE THEORETICAL PREDICTIONS ARE VALID FOR LOW FILLER CONTENTS. AS THE AMOUNT OF THE FILLER INCREASES, THE DEVIATION FROM THE PREDICTED VALUE IS OBSERVED DUE TO THE IMPERFECT DISPERSION OF CERAMIC PARTICLES AT HIGHER FILLER CONTENTS. THE AIR ENCLOSED BY THE COMPOSITES WHICH REDUCES THE EFFECTIVE RELATIVE PERMITTIVITY. CLEAR FROM THE FIGURES THAT THE MODIFIED LICHTENECKER EQUATION AND EFFECTIVE MEDIUM THEORY ARE FOUND TO BE IN GOOD MATCH WITH THE EXPERIMENTAL VALUES FOR PTFE/ZAT COMPOSITES. THE FITTING FACTOR OBTAINED IN THE PRESENT STUDY FOR PTFE/ZAT AND PE/ZAT COMPOSITES ARE 0.12 AND 0.14 RESPECTIVELY WHICH IS IN AGREEMENT WITH EARLIER REPORT FOR WELL-DISPersed POLYMER-CERAMIC COMPOSITES [57]. IN THE CASE OF PTFE/ZAT COMPOSITES LICHTENECKER EQUATION EVEN FOR HIGHER VOLUME FRACTION OF THE FILLER, THE DEVIATION FROM PTFE/ZAT AND PE/ZAT ARE 4.1 % AND 1.9 % RESPECTIVELY. THE EFFECTIVE MEDIUM THEORY WHICH ASSUMES THE FILLER AS A RANDOM UNIT CELL EMBEDDED IN THE EFFECTIVE MEDIUM IS FOUND TO BE WELL SUITED FOR A NUMBER OF POLYMER CERAMIC COMPOSITES. THE DEVIATION FROM EMT MODEL IS FOUND TO BE 2.6 % AND A VERY LOW VALUE OF 0.8 % RESPECTIVELY FOR PTFE/ZAT AND PE/ZAT COMPOSITES. THE RELATIVELY LOW PERCENTAGE DEVIATION FOR THE PE/ZAT COMPOSITES IS DUE TO THE LOW POROSITY CONTENT OF THESE COMPOSITES.

THE TEMPERATURE COEFFICIENT OF RELATIVE PERMITTIVITY IS ONE OF THE IMPORTANT PROPERTIES WHICH CONTROL THE OVERALL PERFORMANCE OF THE SUBSTRATE MATERIAL. FIGURE 6.20 (A) AND (B) RESPECTIVELY SHOWS THE VARIATION OF RELATIVE PERMITTIVITY OF PTFE/ZAT AND PE/ZAT COMPOSITES WITH TEMPERATURE AT 1 MHZ. IT IS CLEAR THAT FOR ALL THE COMPOSITES FRACTIONS THE RELATIVE PERMITTIVITY IS NEARLY INDEPENDENT OF TEMPERATURE. THE AVERAGE NEGATIVE PERCENTAGE DEVIATION OF ABOUT 0.46 %. THE TEMPERATURE COEFFICIENT OF RELATIVE PERMITTIVITY OF BOTH ZAT/PTFE AND ZAT/PE COMPOSITES ARE GIVEN IN TABLE 6.3. THE  $\tau_c$  VALUE BECOMES MORE AND MORE NEGATIVE WITH THE INCREASE IN THE FILLER

FOR BOTH THE COMPOSITES. THIS IS QUITE UNEXPECTED SINCE THE FILLER POSSESS A VALUE. THUS THE DECREASE IN RELATIVE PERMITTIVITY WITH TEMPERATURE MAY BE DUE TO THE DIFFERENCE IN THERMAL EXPANSION COEFFICIENT OF POLYMER MATRIX AND THE ZAT FILLER WHICH WOULD DISTURB THE AGGREGATION OF THE POLAR COMPONENTS CAUSING A DECREASE IN RELATIVE PERMITTIVITY [58-59] WHICH HAS BEEN EXPLAINED EARLIER IN CHAPTER 5. ALSO FROM FIG. 6.20 IT IS CLEAR THAT THE PTFE/ZAT COMPOSITES EXHIBIT A VALUE WHICH IS HIGHER COMPARED WITH THAT OF THE PE/ZAT COMPOSITES WHICH MAY BE DUE TO THE POOR ADHESION BETWEEN PTFE AND ZAT FILLER WHEN COMPARED WITH THE LATTER AT HIGHER FILLER CONTENTS.

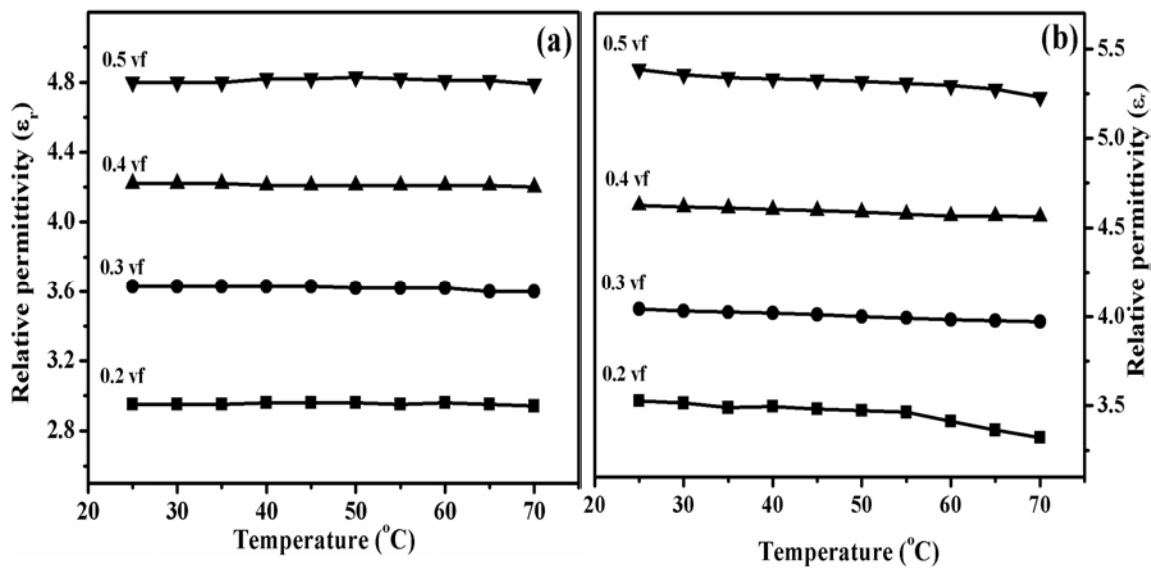


Fig. 6.20 Variation of relative permittivity of (a) PTFE/ZAT and (b) PE/ZAT composites with temperature in the range 25-70°C.

FIGURE 6.21 SHOWS THE VARIATION OF THE COEFFICIENT OF THERMAL EXPANSION OF PTFE/ZAT AND PE/ZAT COMPOSITES AS A FUNCTION OF FILLER CONTENT. IT CAN BE SEEN THAT THE CTE VALUE DECREASES GRADUALLY AS THE FILLER CONCENTRATION INCREASES WHICH IS EXPECTED DUE TO THE VERY LOW CTE VALUE POSSESSED BY THE ZAT FILLER (6.3 PPM/°C) COMPARED WITH THAT OF THE POLYMERS USED. FOR A FILLER CONCENTRATION OF 0.5 VOLUME FRACTION, PTFE/ZAT AND PE/ZAT COMPOSITES EXHIBIT A CTE VALUE OF 28 AND 26 PPM/°C RESPECTIVELY. THE CTE VALUES OBTAINED FOR POLYMER/ZAT COMPOSITES ARE HIGHER WHEN COMPARED WITH POLYMER/SiO<sub>2</sub> COMPOSITES. THE DOTTED LINES IN FIG. 6.21 REPRESENT THE THEORETICAL



CTE VALUES OF BOTH THE COMPOSITES PREDICTED USING THE MIXTURE RULE GIVEN IN LARGE DEVIATION FROM THE PREDICTED VALUE IS NOTED FOR PE/ZAT COMPOSITES. EXPERIMENTAL VALUES ARE IN GOOD AGREEMENT WITH THE THEORETICAL PREDICTION COMPOSITES. THIS IS BECAUSE THE MIXING RULE IS A SIMPLE PREDICTION WHICH CONSIDERS THE CTE VALUES OF THE INDIVIDUAL COMPONENTS AND OTHER FACTORS SUCH AS PORE INTERACTION, STRAINS ETC ARE NOT TAKEN INTO ACCOUNT. HOWEVER, PTFE/ZAT COMPOSITES SHOW A GOOD CORRESPONDENCE WITH THE PREDICTION UPTO A FILLER CONTENT OF 0.4

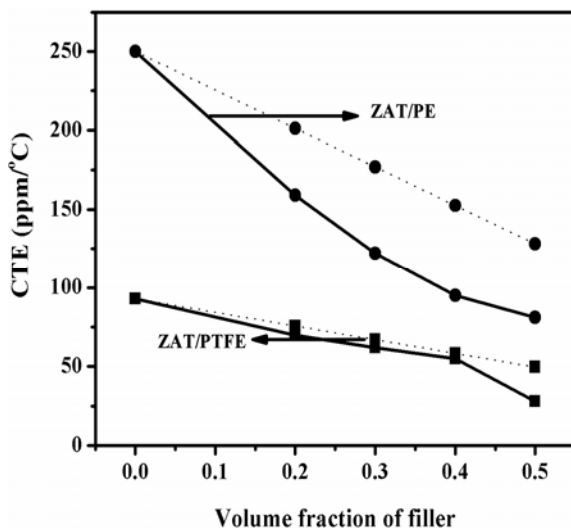


Fig. 6.21 Variation of CTE values of PTFE/ZAT and PE/ZAT composites with filler content.

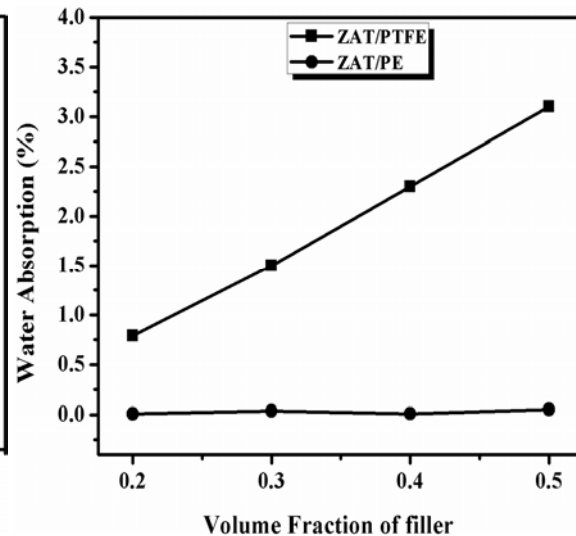


Fig. 6.22 The variation of water absorption of PTFE/ZAT and PE/ZAT composites with filler content.

FIGURE 6.22 SHOWS THE AMOUNT OF WATER ABSORBED BY THE COMPOSITES AS A FUNCTION OF THE FILLER CONTENT. IN BOTH THE CASES, AN INCREASE IN WATER ABSORPTION IS NOTED AS THE FILLER CONTENT INCREASES. A COMPARISON OF THE WATER ABSORPTION VALUES OF ZAT/PTFE AND ZAT/PE COMPOSITES SHOW THAT THE FORMER EXHIBIT A HIGHER VALUE WHICH MAY BE DUE TO THE SURFACE CHARACTERISTICS OF THE MATRIX UNDER CONSIDERATION. IT IS HIGHLY ENCOURAGING THAT EVEN FOR A HIGHER FILLER CONTENT, THE ZAT/PE COMPOSITES HAS A VERY LOW VALUE OF WATER ABSORPTION (0.052 %) WHEN COMPARED WITH ITS ZAT/PTFE COUNTERPART. THIS MAY LEAD TO AN INCREASE IN THE DIELECTRIC LOSS AS OBSERVED IN PTFE/ZAT COMPOSITES.

THE POLYMER CERAMIC COMPOSITES INVESTIGATED IN THIS SECTION HAVE PHYSICAL AND DIELECTRIC PROPERTIES AND CAN BE WELL OPTED FOR ELECTRON APPLICATIONS.

### 6.3 CONCLUSION

#### ➤ ZAT/GLASS COMPOSITES

- ❖ THE EFFECT OF VARIOUS LOW MELTING AND LOW LOSS GLASSES SUCH AS ZB1, ZB2, BBSZ, BBS, ABS, MBS, AS AND BB ON THE SINTERING AND THE MICROWAVE DIELECTRIC PROPERTIES OF  $0.30\text{ZrTiO}_2$  (ZAT) CERAMICS FOR LTCC APPLICATION HAVE BEEN STUDIED.
- ❖ AMONG THE VARIOUS GLASSES STUDIED, BOROSILICATE GLASSES ARE FOUND TO IN LOWERING THE SINTERING TEMPERATURE WITHOUT ADVERSELY AFFECTING PROPERTIES. THE ADDITION OF 10 WT% BBSZ GLASS LOWERED THE SINTERING TEMPERATURE TO ABOUT 1150°C. THE SINTERING TEMPERATURE IS FURTHER REDUCED TO 925°C WITH THE ADDITION OF LIF TO THE ABOVE COMPOSITE.
- ❖ THE XRD AND SEM ANALYSIS INDICATES THE ABSENCE OF ADDITIONAL PHASES IN THE COMPOSITE EVEN FOR HIGHER AMOUNT OF GLASS ADDITION.
- ❖ ADDITION OF 0.2 WT% BBSZ GLASS IMPROVED THE DIELECTRIC PROPERTIES OF ZAT.  $Q_u \times f$  OF 120000 GHZ,  $\Delta_f$  OF -7.3 PPM/°C AND A RELATIVE PERMITTIVITY OF 11.7 AT 1400°C. THE MICROWAVE DIELECTRIC PROPERTIES OF ZAT+10WT% BBSZ ARE  $Q_u \times f$  OF 12000 GHZ,  $\epsilon_r = 10.9$  AND  $\Delta_f = -23$  PPM/°C. THE ADDITION OF 0.3 WT% LIF TO THE ABOVE COMPOSITION SLIGHTLY IMPROVED THE QUALITY FACTOR TO 14000 GHZ AND INCREASED  $\Delta_f$  VALUE TO -28 PPM/°C.
- ❖ THE NON-REACTIVITY OF THE LTCC COMPOSITION WITH AG REVEALED THAT THE COMPOSITION SHOWS EXCELLENT CHEMICAL STABILITY AND CAN BE PROPOSED AS A CANDIDATE FOR LTCC SUBSTRATE APPLICATIONS.

### ➤ ZAT/POLYMER COMPOSITES

- ❖ THE PHYSICAL AND DIELECTRIC PROPERTIES OF PTFE/ZAT AND PE/ZAT COMPOSITE FOR ELECTRONIC PACKAGING APPLICATIONS ARE COMPARED AND STUDIED.
- ❖ THE PTFE/ZAT AND PE/ZAT COMPOSITES ARE PREPARED BY POWDER PROCESSING AND MELT MIXING TECHNIQUES RESPECTIVELY. THE PE/ZAT COMPOSITES EXHIBITED A LOWER LEVEL OF POROSITY AND LOW WATER ABSORPTION VALUE WHEN COMPARED WITH PTFE/ZAT COMPOSITES.
- ❖ THE DIELECTRIC PROPERTIES OF THE COMPOSITES ARE MEASURED AT 1 MHZ AND 9 GHZ. BOTH THE COMPOSITES POSSESS A LOW VALUE OF RELATIVE PERMITTIVITY AND LOSS. AT 9 GHZ, THE PTFE/ZAT AND PE/ZAT COMPOSITE ~~WILLER HAS~~  $\epsilon_r = 2.85$  AND  $4.37$  AND  $\delta = 0.0038$  AND  $0.0044$  RESPECTIVELY. ALSO THEY POSSESS NEARLY STABLE TEMPERATURE VARIATION OF RELATIVE PERMITTIVITY.
- ❖ THE CTE VALUES OF BOTH THE COMPOSITE IS FOUND TO DECREASE WITH INCREASED ZAT CONTENT AND REACHES A MINIMUM VALUE OF ABOUT ~~818 PPM/°C~~  $818$  PPM/°C RESPECTIVELY FOR ZAT WITH PTFE AND PE COMPOSITES. THE RESULTS SUGGEST THAT THE PROPERTIES OF PTFE AND PE CAN BE IMPROVED AND CAN BE USED FOR SUBSTRATE AND ELECTRONIC PACKAGING APPLICATIONS WITH THE AID OF SUITABLE AMOUNT OF ZAT FILLER.

## 6.4 REFERENCES

1. R. R. TUMMALA, *Am. Ceram. Soc.*, **74**, 895-908, (1991).
2. J. H. JEAN AND T. K. GUPTA, *Mater. Sci.*, **27**, 1575-1584, (1992).
3. M. T. SEBASTIAN AND H. JANUJEN, *Thin. Rev.*, **53**, 57-90, (2008).
4. T. TAKADA, S. F. WANG, S. YOSHIKAWA, S. J. JANG AND R. E. NEWNHAM, *J. Am. Ceram. Soc.*, **77**, 2485-2488, (1994).
5. S. X. H. DAI, R. F. HUANG AND D. L. WILCOX, *Ceram. Soc.*, **85**, 828-832, (2002).
6. K. P. SURENDRAN, P. MOHANAN AND M. T. SEBASTIAN, *Chem.*, **177**, 4031-4046, (2004).
7. T. TAKADA, S. F. WANG, S. YOSHIKAWA, S. J. JANG AND R. E. NEWNHAM, *J. Am. Ceram. Soc.*, **77**, 1909-1916, (1994).
8. S. GEORGE AND M. T. SEBASTIAN, *Inorg. Compd.*, **473**, 336-340, (2009).
9. P. S. ANJANA AND M. T. SEBASTIAN, *Ceram. Soc.*, **92**, 96-104, (2009).
10. C. S. CHEN, C. C. CHOU, W. J. SHIH, K. S. LIU AND I. M. LIN, *Chem. Phys.*, **79**, 129-134, (2003).
11. D. ZHOU, H. WANG, L. X. PANG, X. YAO AND X. G. WU, *Ceram. Soc.*, **91**, 4115-4117, (2008).
12. A. CHAOUCHI, S. MARINEL, S. D'ASTORG AND C. ALIOLU, *Ceram. Soc.*, **35**, 939-942, (2009).
13. Q. L. ZHANG, H. YANG, J. L. ZOU AND H. P. WANG, *Lett.*, **59**, 880-884, (2005).
14. H. R. LEE, B. D. LEE AND K. H. YOON, *J. Appl. Phys. Part 1*, **44**, 1333-1336, (2005).
15. E. GUAN, W. CHEN AND L. LUO, *Com. Int.*, **33**, 1145-1148, (2007).
16. D. W. KIM, J. R. KIM, S. H. YOON, K. S. HONG AND C. K. KIM, *Ceram. Soc.*, **85**, 2759-2762, (2002).
17. D.-W. KIM, K. SUN HONG, C. S. YOON AND C. KYUNGKIM, *Ceram. Soc.*, **23**, 2597-2601, (2003).
18. E. J. W. VERWEY AND E. L. HEILMANN, *Ann. Phys.*, **15**, 174-180, (1947).
19. R. KHENATA, M. SAHNOUN, H. BALTACHE, M. RÉRAT, A. H. RESHAK, Y. AL-DOURI AND B. BOUHAFES, *Phys. Lett. A*, **344**, 271-279, (2005).
20. V. K. SINGH AND R. K. SINGHA, *Mater. Lett.*, **31**, 281-285, (1997).
21. Y. SUYAMA AND A. KATO, *Com. Int.*, **8**, 17-21, (2000).
22. S. K. BEHERA, P. BARPANDA, S. K. PRATI HAR AND S. BHARTACHARJEE, *Mater. Lett.*, **58**, 1451-1455, (2004).
23. I. GANESH, B. SRINIVAS, R. JOHNSON, B. P. SAHA AND Y. R. MAHajan, *J. Am. Ceram. Soc.*, **24**, 201-207, (2004).

24. W. H. BRAGG *Philos. Mag.*, **30**, 305-15, (1915).
25. S. NISHIKAWA *Proc. Math. Phys. Soc. Tokyo*, **8**, (1915).
26. K. E. SICKAFUS AND R. HUGHES *Ceram. Soc.*, **82**, 3277-3278, (1999).
27. K. P. SURENDRAN, N. SANTHA, P. MOHANAN AND M. T. SEBASTIAN *Eur. Ceram. Soc.*, **41**, 301-306, (2004).
28. K. P. SURENDRAN, P. V. BIJUMON, P. MOHANAN AND M. T. SEBASTIAN *Eur. Ceram. Soc.*, **81**, 823-826, (2005).
29. C. L. HUANG, T. J. YANG AND C. C. HUANG *Ceram. Soc.*, **92**, 119-124, (2009).
30. W. LEI, W. Z. LU, D. LIU AND J. H. ZHANG *J. Am. Ceram. Soc.*, **92**, 105-109, (2009).
31. K. P. SURENDRAN, M. T. SEBASTIAN, M. V. MANJUSHA AND A. P. PHILLIP *J. Am. Ceram. Soc.*, **98**, (2005).
32. Y. IMANAKA *Multilayered Low Temperature Cofired Ceramics (LTCC) Technology*, SPRINGER SCIENCE, U.S.A., (2005).
33. Y. C. LEE, W. H. LEE AND F. S. SHIUE *J. Appl. Phys. Part 1*, **42**, 1311-1314, (2003).
34. P. S. ANJANA, I. N. JAWAHAR AND M. T. SEBASTIAN *Sci. - Mater. Electron.*, **20**, 587-596, (2009).
35. M. N. RAHAMAN *Ceramic Processing and Sintering*, INT. ED., MARCEL DEKKER INC., NEW YORK, (1999).
36. C.-C. CHIANG, S.-F. WANG, Y.-R. WANG AND W.-C. JIA *J. Appl. Phys.*, **34**, 599-604, (2008).
37. I. C. HO *J. Am. Ceram. Soc.*, **77**, 829-832, (1994).
38. B. D. SILVERMAN *Phys. Rev.*, **125**, 1921, (1962).
39. A. J. MOULSON AND J. M. HERBERT *Ceramics: Materials, Properties, Applications*, 2ND EDITION (1990).
40. C.-L. HUANG AND M.-H. WENG *Cer. Res. Bull.*, **35**, 1881-1888, (2000).
41. M. GONGORA-RUBIO, L. M. SOLÁ-LAGUNA, P. J. MOFFETT AND J. J. SANTIAGO-AVILÉS *Actuators, A*, **73**, 215-221, (1999).
42. H. T. VO AND F. G. SHIUE *Microelectron. J.*, **33**, 409-415, (2002).
43. T. HU, J. JUUTI, H. JANTUNEN AND T. VILKMAN *Ceram. Soc.*, **27**, 3997-4001, (2007).
44. S. YU, P. HING AND X. HU *Appl. Phys.*, **88**, 398-404, (2000).
45. Y. C. CHEN, H. C. LIN AND Y. D. LEE *Polym. Res.*, **10**, 247-258, (2003).
46. Y.-C. CHEN, H.-C. LIN AND Y.-D. LEE *Polym. Res.*, **11**, 1-7, (2004).
47. J. D. BOLT, D. P. BUTTON AND B. AMOS *Sci. Eng., A*, **109**, 207-211, (1989).
48. Z. M. DANG, Y. H. ZHANG AND S. C. TSONG *Met.*, **146**, 79-84, (2004).

49. X. Q. WANG, D. R. CHEN, J. C. HIAN AND S. YI. *J. Appl. Polym. Sci.*, **83**, 990-996, (2002).
50. P. J. RAE AND D. M. DATTELE. *Polymer*, **45**, 7615-7625, (2004).
51. F. XIANG, H. WANG AND X. YAO. *Ceram. Soc.*, **27**, 3093-3097, (2007).
52. D. H. KUO, C. C. CHANG, T. Y. SU, W. K. WANG AND B. YUAN. *Chem. Phys.*, **85**, 201-206, (2004).
53. N. G. DEVARAJU, E. S. KIM AND B. IMIEE. *Electron. Eng.*, **82**, 71-83, (2005).
54. J. ZHANG, H. Q. FAN, S. M. KE, Y. Z. SHI, X. H. ZENG, M. T. BI AND H. T. HUANG, *Compos. Mater.*, **334-335**, 1053-1056, (2007).
55. V. S. NISA, S. RAJESH, K. P. MURALI, V. PRIYADARSINI, S. N. POTTY AND R. RATHEESH, *Compos. Sci. Technol.*, **68**, 106-112, (2008).
56. J. MOLLA, M. GONZALEZ, R. VILA AND A. ABARCA. *Appl. Phys.*, **85**, 1727-1730, (1999).
57. Y. RAO, J. M. QU, T. MARINIS AND C. P. WENGG. *Trans. Compon. Packag. Technol.*, **23**, 680-683, (2000).
58. G. M. TSANGARIS AND G. C. PSARRAS. *Sci.*, **34**, 2151-2157, (1999).
59. M. A. BERGER AND R. L. MCCULLOUGH. *Sci. Technol.*, **22**, 81-106, (1985).

## **CHAPTER 7**

### **CONCLUSIONS AND SCOPE FOR FUTURE WORK**

*This chapter summarizes the results obtained in various chapters in the thesis and suggests the possibility of further extension of the work.*

THE RAPID DEVELOPMENT IN THE MICROELECTRONIC TECHNOLOGIES SUCH AS WIRELESS COMMUNICATIONS, INTELLIGENT TRANSPORT SYSTEM (ITS) AND MICROWAVE INTEGRATED CIRCUITS (MIC) HAS LED TO AN INCREASE IN THE UTILIZED FREQUENCY FROM KILOMETRE WAVE TO MILLIMETRE WAVE. THE DEMAND FOR CERAMICS IN ELECTRONIC EQUIPMENTS IS GROWING RAPIDLY AS A RESULT OF THE ADVANCEMENT OF PHYSICAL AND ELECTRICAL PROPERTIES AND IMMENSE TECHNOLOGICAL APPLICATIONS. THIS BOOK REPORTS THE SYNTHESIS, CHARACTERIZATION AND PROPERTIES OF SOME RARE EARTH DOPED CERAMICS AND ALUMINATE AND THEIR COMPOSITES FOR VARIOUS MICROWAVE APPLICATIONS SUCH AS DIELECTRIC RESONATORS, LOW TEMPERATURE CO-FIRED CERAMICS (LTCC) AND AS ELECTRONIC PACKAGING MATERIALS. THE INVESTIGATIONS PERFORMED ARE DIVIDED INTO SEVEN CHAPTERS.

THE FIRST CHAPTER IS A GENERAL INTRODUCTION TO THE DIELECTRIC RESONATOR, CERAMIC SUBSTRATES, LTCC, ELECTRONIC PACKAGING MATERIALS AND THEIR CURRENT TRENDS. IT ALSO DISCUSSES MATERIAL REQUIREMENTS FOR THE ABOVE APPLICATIONS AND PRESENT CHALLENGES. CHAPTER 2 DISCUSSES IN DETAIL VARIOUS PREPARATION TECHNIQUES USED FOR THE SYNTHESIS OF CERAMICS AND POLYMER CERAMIC COMPOSITES. A BRIEF ACCOUNT OF STRUCTURAL AND MICROSTRUCTURAL CHARACTERIZATION TECHNIQUES LIKE, XRD, ELECTRON DIFFRACTION AND SEM AND ELECTRICAL CHARACTERIZATION METHODS USED ARE ALSO INCLUDED. A DETAILED ACCOUNT OF THE CHARACTERIZATION OF THE CERAMICS AND POLYMER CERAMIC COMPOSITES ARE ALSO GIVEN IN CHAPTER 2.

CHAPTER 3 STARTS WITH A BRIEF INTRODUCTION TO THE APATITE BASED MATERIALS. IT DISCUSSES THE STRUCTURAL ASPECTS AND APPLICATIONS, GIVING SPECIAL EMPHASIS TO THE SILICON DOPED OXYAPATITES. THE CHAPTER DEALS WITH THE SYNTHESIS AND CHARACTERIZATION OF A SERIES OF [A=CA, SR AND BA; RE = RARE EARTHS] CERAMICS. A DETAILED INVESTIGATION ON THE STRUCTURE OF THESE CERAMICS USING XRD REFINEMENTS AND TEM REVEALED THAT THEY BELONG TO THE P6<sub>3</sub>mm SPACE GROUP WITH HEXAGONAL SYMMETRY. HOWEVER, ALL OF THEM EXHIBITED A LOW RELATIVE DENSITY (95%) EXCEPT FOR BA-SR-RE-SR-RE-SR<sub>3</sub>O<sub>13</sub> WHICH EXHIBITED RELATIVE PERMITTIVITY IN THE RANGE 10-19. A MAXIMUM  $\mu_x f$  OF ABOUT 26000 GHZ IS EXHIBITED BY SR-RE-SR-RE-SR<sub>3</sub>O<sub>13</sub> WITH  $\epsilon_r = 14.2$  AND A RELATIVELY HIGH Q-FACTOR OF 46 PPMC. THE MICROWAVE DIELECTRIC PROPERTIES OF THE COMPOSITIONS ARE CORRELATED WITH THE BOND VALENCE AND BOND STRENGTH VALUES.



THAT AS THE BOND STRENGTH DECREASES, THE RELATIVE PERMITTIVITY AND DIELECTRIC LOSS TANGENT INCREASE. THE  $\text{Ba}_2\text{Si}_2\text{O}_7$  IS TUNED BY THE ADDITION OF SUITABLE AMOUNT OF  $\text{TiO}_2$  EVEN THOUGH THE ADDITION OF NEARLY REDUCED THE VALUE, THE  $Q \times f$  IS REDUCED TO 13300 GHz WITH AN INCREASE IN NEARLY 21. THE  $\text{Ba}_2\text{Si}_2\text{O}_7$  AND  $\text{BaSi}_3\text{O}_{13}$  CERAMICS HAVE A RELATIVE PERMITTIVITY LESS THAN 10. THE  $\text{BaSi}_3\text{O}_{13}$  CERAMIC SHOWS A MAXIMUM QUALITY FACTOR OF 30500 GHz WITH  $\tau_f = -36 \text{ PPM}^\circ\text{C}$ . THE  $\text{BaSi}_3\text{O}_{13}$  SERIES SHOWS A RELATIVE PERMITTIVITY AND HIGH  $Q \times f$  VALUE. A MAXIMUM  $Q \times f$  OF 26100 GHz IS EXHIBITED BY  $\text{Ba}_2\text{Si}_2\text{O}_7$  WITH  $\tau_f = 14.2$  AND  $\tau_f = -38 \text{ PPM}^\circ\text{C}$ .

THE SYNTHESIS, CHARACTERIZATION AND MICROPROPERTIES OF TWO NOVEL RARE EARTH BASED SILICATES AND  $\text{RE}_2\text{Ti}_2\text{SiO}_9$  (RE=LA, PR AND ND) CERAMICS ARE DISCUSSED IN CHAPTER 4. THE STRUCTURAL AND MICROSTRUCTURAL STUDIES REVEALED THAT  $\text{Ba}_2\text{Si}_2\text{O}_7$  OF SINGLE PHASE MATERIALS. THE CERAMIC HAS A TETRAGONAL SYMMETRY WHEREAS  $\text{RE}_2\text{Ti}_2\text{SiO}_9$  (RE=LA, PR AND ND) DIELECTRIC CERAMICS POSSESS A MONOCLINIC SYMMETRY. CALCINATION AND SINTERING TEMPERATURES OF THE ABOVE CERAMICS ARE OPTIMIZED. DENSIFICATION AND MICROWAVE DIELECTRIC PROPERTIES OF THE CERAMICS SINTERED AT  $1375^\circ\text{C}/2\text{H}$  EXHIBIT EXCELLENT DIELECTRIC PROPERTIES.  $\epsilon_r = 6 \times 10^3$  MEASURED AT 9 GHz. IN ORDER TO REDUCE THE SINTERING TEMPERATURE OF THE MOST EFFECTIVE METHOD OF GLASS ADDITION IS ADOPTED. SEVERAL LOW LOSS GLASSES SUCH AS  $50\text{B}_2\text{O}_3$  (ZB),  $60\text{ZNO}-30\text{B}_2\text{O}_3-10\text{SiO}_2$  (ZBS),  $27\text{B}_2\text{O}_3-35\text{Bi}_2\text{O}_3-6\text{SiO}_2-32\text{ZNO}$  (BBSZ),  $22.2\text{MGO}-22.2\text{Al}_2\text{O}_3-55.5\text{SiO}_2$  (MAS),  $35.1\text{Li}_2\text{O}-31.7\text{B}_2\text{O}_3-33.2\text{SiO}_2$  (LBS) AND  $20\text{Li}_2\text{O}-20\text{MGO}-20\text{ZNO}-20\text{B}_2\text{O}_3-20\text{SiO}_2$  (LMZBS) ARE ADDED IN DIFFERENT WEIGHT PERCENTAGE TO THE  $\text{Ba}_2\text{Si}_2\text{O}_7$  CERAMICS. IT IS NOTED THAT LITHIUM BASED GLASSES ARE MUCH EFFECTIVE IN REDUCING THE DENSIFICATION TEMPERATURE WITHOUT DEGRADING THE DIELECTRIC PROPERTIES.  $\text{Ba}_2\text{Si}_2\text{O}_7$  CERAMICS TREATED WITH 15 WT% LBS GLASS LOWERED THE SINTERING TEMPERATURE TO  $975^\circ\text{C}$ , WHEREAS THE 15 WT% LMZBS GLASS ADDITION LOWERED SINTERING TEMPERATURE TO  $950^\circ\text{C}$ . THE MICROWAVE DIELECTRIC PROPERTIES OF CERAMICS TREATED WITH 15 WT% LBS GLASS AND THAT TREATED WITH 15 WT% LMZBS GLASS ARE  $\epsilon_r = 2.5 \times 10^3$ ,  $2.2 \times 10^3$  RESPECTIVELY. THE PERMITTIVITY OF CERAMICS AND THAT MIXED WITH 15WT% LMZBS GLASS DID NOT SHOW MUCH VARIATION IN RELATIVE PERMITTIVITY WITH TEMPERATURE.  $\text{RE}_2\text{Ti}_2\text{SiO}_9$  (RE=LA, PR AND ND) CERAMICS EXHIBITED A RELATIVE DENSITY ABOUT OF

THESE MATERIALS HAVE A RELATIVE PERMITTIVITY LESS THAN 20 AND A RELATIVELY LOW MAXIMUM VALUE OF  $\tan \delta$  IS SHOWN BY  $\text{PbTiO}_3$  CERAMICS. IT IS SEEN THAT PR SUBSTITUTION FOR LA FAVORED THE FORMATION OF SOLID SOLUTION IN THE WHOLE RANGE OBEYING WHILE ND SUBSTITUTION RESULTED IN THE FORMATION OF ADDITIONAL PHASES. AS THE INCREASES, AN IMPROVEMENT IN THE QUALITY FACTOR IS NOTED IN  $\text{NiREMSCHHE}$  AFFECTED. A MAXIMUM QUALITY FACTOR OF ABOUT 34000 GHZ IS OBTAINED IN THE  $\text{CaPrTi}_2\text{SiO}_9$  WITH  $\alpha = 29.2$  AND  $\beta = 19.5$  PPM/°C.

CHAPTER 5 DISCUSSES IN DETAIL THE SYNTHESIS AND CHARACTERIZATION OF VARIOUS CERAMIC COMPOSITE USING  $\text{SiO}_2$  CERAMICS AS FILLER FOR ELECTRONIC PACKAGING APPLICATIONS. THE POLYMERS USED IN THE INVESTIGATION ARE PTFE, POLYETHYLENE AND POLYSTYRENE. THE PTFE/ $\text{SiO}_2$  COMPOSITES ARE PREPARED BY POWDER PROCESSING METHOD WHEREAS  $\text{SiO}_2$  LOADED POLYETHYLENE AND POLYSTYRENE COMPOSITES BY MELT TECHNIQUE. THE RELATIVE PERMITTIVITY, DIELECTRIC LOSS ( $\tan \delta$ ) AND VICKERS' MICROHARDNESS INCREASED WITH INCREASE IN FILLER CONTENT. THE THERMAL CONDUCTIVITY INCREASED AND COEFFICIENT OF THERMAL EXPANSION WITH INCREASE IN FILLER LOADING FOR ALL THE COMPOSITES. FOR A FILLER LOADING OF 50%  $\epsilon_r = 3.82$  AND  $\tan \delta = 0.0136$  (AT 9 GHZ),  $k_c = 1.76$  W/M°C,  $\alpha_c = 36$  PPM/°C, MICROHARDNESS OF 13 KGF/MM<sup>2</sup> PE COMPOSITE HAS  $\epsilon_r = 2.28$  AND  $\tan \delta = 0.0091$  (AT 9 GHZ),  $k_c = 2.97$  W/M°C,  $\alpha_c = 60$  PPM/°C, VICKERS' MICROHARDNESS OF 17 KGF/MM<sup>2</sup> COMPOSITE HAS  $\epsilon_r = 56$  AND  $\tan \delta = 0.0110$  (AT 9 GHZ),  $k_c = 0.29$  W/M°C,  $\alpha_c = 36$  PPM/°C, VICKERS' MICROHARDNESS OF 56 KGF/MM<sup>2</sup> THE EFFECT OF COUPLING AGENT AND FILLER PARTICLE SIZE ON THE ABOVE PROPERTIES OF PTFE/ $\text{SiO}_2$  COMPOSITES ARE ALSO STUDIED. THE COMPOSITES MODIFIED USING COUPLING AGENT AND NANO SIZED FILLER COMPOSITES SHOWS AN INCREASED VALUE FOR BOTH PERMITTIVITY AND DIELECTRIC LOSS. HOWEVER, BOTH OF THEM EXHIBITED ENHANCED MECHANICAL PROPERTIES COMPARED WITH THAT OF THE UNTREATED MICRON SIZED COMPOSITES. SEVERAL THEORETICAL MODEL APPROACHES HAVE BEEN EMPLOYED TO PREDICT THE PERMITTIVITY, THERMAL CONDUCTIVITY AND COEFFICIENT OF LINEAR EXPANSION OF THESE SYSTEMS AND THE RESULTS ARE COMPARED WITH THAT OF EXPERIMENTAL DATA. THE THEORETICAL PREDICTIONS ARE FOUND TO BE VALID FOR LOW FILLER CONTENTS.

CHAPTER 6 OUTLINES THE APPLICABILITY OF B.078310 (ZAT) DIELECTRIC CERAMIC BASED GLASS AND POLYMER COMPOSITES FOR LTCC SUBSTRATE AND E PACKAGING APPLICATIONS RESPECTIVELY. THE FIRST SECTION OF THE CHAPTER 6 DISCUSSES THE EFFORTS TAKEN TO REDUCE THE SINTERING TEMPERATURE BY GLASS ADDITION. THE EFFECTS OF GLASSES SUCH AS  $ZNO-BAO-B_2O_3-SIO_2$ ,  $ZNO-B_2O_3-SIO_2$  AND  $B_2O_3-ZNO-B_2O_3-SIO_2$  ON THE MICROSTRUCTURE, DENSIFICATION AND MICROWAVE DIELECTRIC PROPERTIES FOR LTCC APPLICATIONS IS INVESTIGATED. AMONG THE VARIOUS GLASSES ADDED, BBSZ IS FOUND TO LOWER THE SINTERING TEMPERATURE WITHOUT MUCH AFFECTING THE MICROWAVE DIELECTRIC PROPERTIES. THE XRD AND SEM OF BBSZ GLASS ADDED ZAT COMPOSITES SUGGESTED THE EXISTENCE OF NO ADDITIONAL SECONDARY PHASES. THE ADDITION OF 10 WT% BBSZ GLASS TO ZAT REDUCED THE SINTERING TEMPERATURE TO 1000°C WITH REASONABLY GOOD MICROWAVE DIELECTRIC PROPERTIES. THE QUALITY FACTOR IS FOUND TO INCREASE TO A MAXIMUM VALUE OF ABOUT 120000 GHz<sup>2</sup> AT 12000 GHz WITH THE ADDITION OF SMALL WEIGHT PERCENTAGE (0.2 WT%) OF BBSZ GLASS. FURTHER INCREASE IN GLASS CONTENT REDUCED THE SINTERING TEMPERATURE BUT ALSO THE DENSITY AND DIELECTRIC PROPERTIES. THE MICROWAVE DIELECTRIC PROPERTIES OF ZAT+10 WT% BBSZ ARE  $\epsilon_r = 10.9$  AND  $D_f = -23$  PPM/°C. THE ADDITION OF 0.3 WT% LIF TO THE ABOVE COMPOSITION SLIGHTLY IMPROVED THE QUALITY FACTOR TO 14000 GHz<sup>2</sup> BUT ALSO INCREASED THE SINTERING TEMPERATURE. THE COMPOSITES ALSO POSSESSED HIGH CHEMICAL COMPATIBILITY WITH SILVER BRING OUT THE POSSIBILITY OF USING ZAT/10 WT% BBSZ COMPOSITES FOR LTCC SUBSTRATE APPLICATIONS.

THE SECOND SECTION OF THIS CHAPTER COMPARES THE PHYSICAL, DIELECTRIC AND THERMAL PROPERTIES OF ZAT LOADED PTFE AND PE COMPOSITES. THE PE/ZAT COMPOSITES POSSESSED HIGH RELATIVE DENSITY WHEN COMPARED WITH THE PTFE/ZAT COMPOSITES. FOR LOW ZAT CONTENT THE FILLERS ARE UNIFORMLY DISPERSED IN THE MATRIX AND AS THE FILLER CONTENT INCREASES THE AGGLOMERATION ALSO INCREASED AND RESULTED IN POROSITY. THE DIELECTRIC PROPERTIES OF BOTH THE COMPOSITES SHOWS THAT ZAT LOADED WITH PE COMPOSITES EXHIBITED GOOD DIELECTRIC PROPERTIES AND ALSO A VERY LOW WATER ABSORPTION VALUE OF LESS THAN 0.1%. THE THERMAL ANALYSIS SHOWS THAT ZAT FILLER LOADED COMPOSITES HAVE BETTER PROPERTIES THAN THAT OF  $SM_2S_2O_7$  FILLER AND CAN BE USED FOR ELECTRONIC PACKAGING APPLICATIONS.

THE MAJOR RESULTS DRAWN FROM THE THESIS ARE PRESENTED IN THE FOLLOWING TABLES (TABLE 8.1 TO 8.2).

**Table 8.1 The microwave dielectric properties of selected materials proposed for dielectric resonator and LTCC substrate applications.**

| Material   | ST<br>(°C) | $\epsilon_R$ | $Q_U X F$<br>(GHz)/<br>TAN $\delta$ | $\tau_f$<br>(ppm/°C) |
|--|------------|--------------|-------------------------------------|----------------------|
| SRL <sub>4</sub> Si <sub>3</sub> O <sub>13</sub>                           | 1325°C/4H  | 14.2         | 26300                               | -46.0                |
| SRP <sub>5</sub> Si <sub>3</sub> O <sub>13</sub>                           | 1325°C/4H  | 15.6         | 12200                               | -9.0                 |
| SRL <sub>4</sub> Si <sub>3</sub> O <sub>13</sub> + 10 WT% TiO <sub>2</sub> | 1225°C/4H  | 23.4         | 12000                               | 7.5                  |
| CAL <sub>4</sub> Si <sub>3</sub> O <sub>13</sub>                           | 1350°C/4H  | 14.9         | 24800                               | -20.0                |
| CAY <sub>4</sub> Si <sub>3</sub> O <sub>13</sub>                           | 1625°C/4H  | 12.8         | 30500                               | -36.0                |
| CAY <sub>5</sub> Si <sub>3</sub> O <sub>13</sub>                           | 1625°C/4H  | 13.2         | 23500                               | -13.0                |
| BAL <sub>4</sub> Si <sub>3</sub> O <sub>13</sub>                           | 1325°C/4H  | 14.2         | 26100                               | -38.0                |
| LA <sub>2</sub> Ti <sub>2</sub> SiO <sub>9</sub>                           | 1325°C/4H  | 28.3         | 29500                               | 22.6                 |
| PR <sub>2</sub> Ti <sub>2</sub> SiO <sub>9</sub>                           | 1325°C/4H  | 29.2         | 33700                               | 19.5                 |
| ND <sub>2</sub> Ti <sub>2</sub> SiO <sub>9</sub>                           | 1275°C/4H  | 30.1         | 19600                               | 9.6                  |
| 0.83 ZNA <sub>10</sub> O <sub>4</sub> -0.17 TiO <sub>2</sub> (ZAT)         | 1450°C/4H  | 11.7         | 91000                               | 1.4                  |
| ZAT + 0.2 WT% BBSZ   | 1400°C/4H  | 11.9         | 120000                              | -7.3                 |
| ZAT + 10 WT% BBSZ  | 950°C/10H  | 10.9         | 12000                               | -23.2                |
| ZAT + 10 WT% BBSZ + 0.3 LIF  | 925°C/10H  | 10.5         | 14500                               | -28.0                |
| SM <sub>2</sub> Si <sub>2</sub> O <sub>7</sub>                             | 1375°C/2H  | 10.0         | 0.0060                              | -----                |
| SM <sub>2</sub> Si <sub>2</sub> O <sub>7</sub> + 15 WT% LBS                | 975°C/2H   | 6.1          | 0.0025                              | -----                |
| SM <sub>2</sub> Si <sub>2</sub> O <sub>7</sub> + 15 WT% LMZBS              | 950°C/2H   | 6.9          | 0.0026                              | -----                |

**Table 8.2 The physical and microwave dielectric properties of polymer/ceramic composites for substrate and electronic packaging applications.**

| Material   | Relative Density (%) | Water absorption (%) | Dielectric properties (9 GHz) |              | CTE (ppm/°C) |
|--|----------------------|----------------------|-------------------------------|--------------|--------------|
|  |                      |                      | $\epsilon_R$                  | TAN $\delta$ |              |
| PTFE/0.5 V <sub>F</sub> SM <sub>2</sub> SI <sub>2</sub> O <sub>7</sub>                             | 75.3                 | 13.05                | 3.82                          | 0.0136       | 36           |
| PTFE/0.5 V <sub>F</sub> SILANE TREATED <sub>2</sub> SM <sub>2</sub> SI <sub>2</sub> O <sub>7</sub> | 81.9                 | 2.17                 | 4.29                          | 0.0105       | 10           |
| PE/0.5 V <sub>F</sub> SM <sub>2</sub> SI <sub>2</sub> O <sub>7</sub>                               | 94.6                 | 0.30                 | 5.28                          | 0.0091       | 60           |
| PS/0.5 V <sub>F</sub> SM <sub>2</sub> SI <sub>2</sub> O <sub>7</sub>                               | 90.8                 | 0.41                 | 4.60                          | 0.0110       | 36           |
| PTFE/0.5 V <sub>F</sub> ZAT  | 89.3                 | 3.1                  | 3.24                          | 0.0089       | 28           |
| PE/0.5 V <sub>F</sub> ZAT  | 91.1                 | 0.05                 | 5.52                          | 0.0050       | 81           |

THE SCOPE FOR THE EXTENSION OF THE WORK DESCRIBED IN THIS THESIS LIES MAINLY IN THE FOLLOWING AREAS. THE FIRST ONE IS TO IMPROVE THE DENSIFICATION AND MICROWAVE DIELECTRIC PROPERTIES OF THE PROPOSED APATITE SILICATES BY SUITABLE DOPANT ADDITION AND GLASS ADDITION. AS IS SEEN FROM THE RESULTS THAT EVEN THOUGH GLASS ADDITION LOWERS THE SINTERING TEMPERATURE, THE MICROWAVE DIELECTRIC PROPERTIES ARE ADVERSELY AFFECTED. HENCE CHEMICAL MODIFICATION TECHNIQUES LIKE HYDROTHERMAL, CO-PRECIPIATION, CITRATE-GEL, SOL-GEL ETC. WILL BE A CHALLENGING AREA TOWARDS THE DEVELOPMENT OF THESE SILICATES. VARIOUS POLYMER/CERAMIC COMPOSITES DEVELOPED IN THE PRESENT STUDY MAY BE USED TO FABRICATE SUBSTRATE MATERIALS FOR MICROWAVE AND PRINTED CIRCUIT BOARD APPLICATIONS. MOREOVER EFFORTS MAY BE MADE TO IMPROVE THE THERMAL CONDUCTIVITY OF THESE COMPOSITES BY THE ADDITION OF SUITABLE AMOUNTS OF FILLERS. BROADBAND DRAS OF DIFFERENT GEOMETRIES AND DRA ARRAY USING TEMPERATURE SENSITIVE MATERIALS CAN ALSO BE FABRICATED USING THE DEVELOPED DR MATERIALS.

\*\*\*\*\*

## LIST OF PUBLICATIONS

### Publications in SCI Journals

1. L. A. KHALAM **Sherin Thomas** AND M. T. SEBASTIAN, "TEMPERATURE-STABLE AND LOW-LOSS DIELECTRICS IN 'THE ACAB [B' = LANTHANIDES, Y, AND IN] SYSTEM", *Am. Ceram. Soc.* **90**, 2476-2483 (2007).
2. L. A. KHALAM **Sherin Thomas** AND M. T. SEBASTIAN, "TAILORING THE MICROWAVE DIELECTRIC PROPERTIES OF AND BLSB<sub>2</sub>O<sub>9</sub> CERAMICS", *J. Appl. Ceram. Tech.* **4**, 359-366 (2007).
3. **Sherin Thomas** AND M. T. SEBASTIAN, "EFFECT OF CO<sub>3</sub>-DEO<sub>3</sub>-SIO<sub>2</sub>-ZNO GLASS ON THE SINTERING AND MICROWAVE DIELECTRIC PROPERTIES OF BT<sub>0.83</sub>ZN<sub>0.17</sub>", *Mater. Res. Bull.* **43**, 843-851 (2008).
4. **Sherin Thomas**, V. N. DEEPU, P. MOHANAN AND M. T. SEBASTIAN, "EFFECT OF FILLER CONTENT ON THE DIELECTRIC PROPERTIES OF FIBRE COMPOSITES", *Am. Ceram. Soc.* **91**, 1971-1975 (2008).
5. S. RENJIN **Sherin Thomas**, S. R. KIRAN, V. R. K. MURTHY AND M. T. SEBASTIAN, "MICROWAVE DIELECTRIC PROPERTIES AND LOW TEMPERATURE SINTERING OF CERAMIC FOR SUBSTRATE APPLICATIONS", *Ceram. Tech.* **6**, 286-294 (2009).
6. **Sherin Thomas**, V. DEEPU, S. UMA, P. MOHANAN, J. PHILIP AND M. T. SEBASTIAN, "PREPARATION, CHARACTERIZATION AND PROPERTIES OF POLYMER COMPOSITES FOR MICROELECTRONIC APPLICATIONS", *B.* **163**, 67-75 (2009).
7. **Sherin Thomas** AND M. T. SEBASTIAN, "MICROWAVE DIELECTRIC PROPERTIES OF SRRESi<sub>3</sub>O<sub>13</sub> (RE = LA, PR, ND, SM, EU, GD, TB, DY, ER, TM, YB AND Y) CERAMICS", *Am. Ceram. Soc.* **92**, 2975-2981 (2009).
8. JANARDHANAN CHAMESWAR **Sherin Thomas** AND MAILADIL THOMAS SEBASTIAN, "MICROWAVE DIELECTRIC PROPERTIES OF BT<sub>0.83</sub>SIO<sub>2</sub> CERAMICS", *Am. Ceram. Soc.* **93**, 1863-1865 (2010).

9. **Sherin Thomas**, SUJITH RAMAN, P. MOHANAN AND M. T. SEBASTIAN, "EFFECT OF COUPLING AGENT ON THE THERMAL AND DIELECTRIC PROPERTIES OF PTFE/S COMPOSITES" *Composites Part A* **41**, 1148-1155 (2010).
10. RICK UBIC, STEVEN LETOURNEAU, **Sherin Thomas**, G. SUBODH AND M. T. SEBASTIAN, "THE INFLUENCE OF CA SUBSTITUTION ON THE STRUCTURE, MICROSTRUCTURE AND DIELECTRIC PROPERTIES OF (Pb<sub>1-x</sub>Ca<sub>x</sub>)<sub>2</sub>(Zr<sub>1-x</sub>Ti<sub>x</sub>)O<sub>7</sub> DOUBLE PEROVSKITE", *Mater.* **22**, 4572-4578 (2010).
11. **Sherin Thomas**, JITHESH KAVIL AND MAILADIL THOMAS SEBASTIAN, "DIELECTRIC PROPERTIES OF PTFE LOADED WITH MICRO-  $Al_2O_3$  NANOCERAMICS", (COMMUNICATED TO *J. Chem. Phys.*).
12. LII-CHERNG LEE, **Sherin Thomas**, MAILADIL THOMAS SEBASTIAN AND RICK UBIC, "CRYSTAL STRUCTURE OF APATITE TYPE RARE EARTH SILICATE SRRE (COMMUNICATED TO *Ceram. Soc.*)
13. **Sherin Thomas**, B. SAYOOJYAM AND M. T. SEBASTIAN, "MICROWAVE DIELECTRIC PROPERTIES OF NOVEL RARE EARTH BASED  $Y_2SiO_7$  CERAMIC REPR AND ND]" (COMMUNICATED TO *J. Phys. Comp.*).

### Papers to be communicated

14. LII-CHERNG LEE, **Sherin Thomas**, MAILADIL THOMAS SEBASTIAN AND RICK UBIC, "CRYSTAL STRUCTURE AND MICROWAVE DIELECTRIC PROPERTIES OF ARE AND RE=RARE EARTHS]".
15. **Sherin Thomas**, SUJITH RAMAN, P. MOHANAN AND M. T. SEBASTIAN, "THERMAL AND DIELECTRIC PROPERTIES OF EPOXY COMPOSITES".
16. **Sherin Thomas**, SUJITH RAMAN, P. MOHANAN AND M. T. SEBASTIAN, "MICROWAVE DIELECTRIC PROPERTIES OF POLYETHYLENE/ZAT COMPOSITES FOR ELECTRONIC APPLICATIONS".
17. P. S. ANJANA, **Sherin Thomas** AND M. T. SEBASTIAN, "MICROWAVE DIELECTRIC PROPERTIES OF  $Fe_2O_3$  [RE=RARE EARTHS] MICROWAVE DIELECTRIC CERAMICS".

## Publication in National Journal

18. P. S. ANJANA, **Sherin Thomas**, M. T. SEBASTIAN AND J. JAMES, SYNTHETIC MINERALS FOR ELECTRONIC APPLICATIONS, *Science India*, **1** [1], 36-52 (2008).

## International Conference Proceedings

1. P. S. ANJANA, SUMESH GEORGE, **Sherin Thomas**, G. SUBODH, P. MOHANAN AND M. T. SEBASTIAN, EFFECT OF FILLER ON THE MICROWAVE DIELECTRIC PROPERTIES OF PTFE COMPOSITES, INTERNATIONAL CONFERENCE ON ADVANCED MATERIALS AND COMPOSITES, 24-26<sup>TH</sup> OCTOBER, 2007.
2. SUMESH GEORGE, **Sherin Thomas**, S. RENJINI, T. S. SASIKALS, P. S. ANJANA AND M. T. SEBASTIAN, EFFECT OF LITHIUM BOROSILICATE GLASS ADDITION ON THE MICROWAVE DIELECTRIC PROPERTIES OF LOW LOSS CERAMICS, INTERNATIONAL CONFERENCE ON ADVANCED MATERIALS AND COMPOSITES, 24-26<sup>TH</sup> OCTOBER, 2007.
3. G. SUBODH, **Sherin Thomas** AND M. T. SEBASTIAN, "TELLURIUM BASED CERAMICS FOR MILLIMETER WAVE APPLICATIONS", MICROWAVE MATERIALS AND APPLICATIONS – 2007, NOV. 19-21, 2007.
4. M. T. SEBASTIAN, SUMESH GEORGE, P. S. ANJANA, **Sherin Thomas** AND G. SUBODH, "POLYETHYLENE CERAMIC COMPOSITES FOR ELECTRONIC PACKAGING APPLICATIONS", MICROWAVE 2008, NOV. 21-24 JAIPUR.
5. M. V. JACOBS, **Sherin Thomas**, M. T. SEBASTIAN, J. MAZIERSKA, J. HONKAMA AND H. JANTUNEN, "LOW TEMPERATURE MICROWAVE CHARACTERISATION OF GREEN TAPE CERAMIC SPLIT POST DIELECTRIC RESONATOR", APMC-2008, HONG KONG.
6. **Sherin Thomas**, SUJITH RAMAN, P. MOHANAN AND M. T. SEBASTIAN, "PTFE/SM<sub>2</sub>Si<sub>2</sub>O<sub>7</sub> COMPOSITES FOR ELECTRONIC PACKAGING APPLICATIONS", ICE-2008, DELHI UNIVERSITY.
7. **Sherin Thomas**, B. SAYOOJYAM AND M. T. SEBASTIAN, "NOVEL RARE EARTH BASED CERAMIC SILICATES FOR MICROWAVE APPLICATIONS", ISMOT 2009, DEC 16-19, NEW DELHI.



8. M. T. SEBASTIAN, SUMESH GEORGE, SHERIN AND THOMAS, "LOW LOSS LOW PERMITTIVITY SILICATE BASED DIELECTRIC CERAMICS FOR LTCC APPLICATIONS" I. 2009, DEC-16-19, DELHI.

### **Papers in National Conference Proceedings - 3**